General Disclaimer

One or more of the Following Statements may affect this Document

- This document has been reproduced from the best copy furnished by the organizational source. It is being released in the interest of making available as much information as possible.

- This document may contain data, which exceeds the sheet parameters. It was furnished in this condition by the organizational source and is the best copy available.

- This document may contain tone-on-tone or color graphs, charts and/or pictures, which have been reproduced in black and white.

- This document is paginated as submitted by the original source.

- Portions of this document are not fully legible due to the historical nature of some of the material. However, it is the best reproduction available from the original submission.

Produced by the NASA Center for Aerospace Information (CASI)

MSC 00192

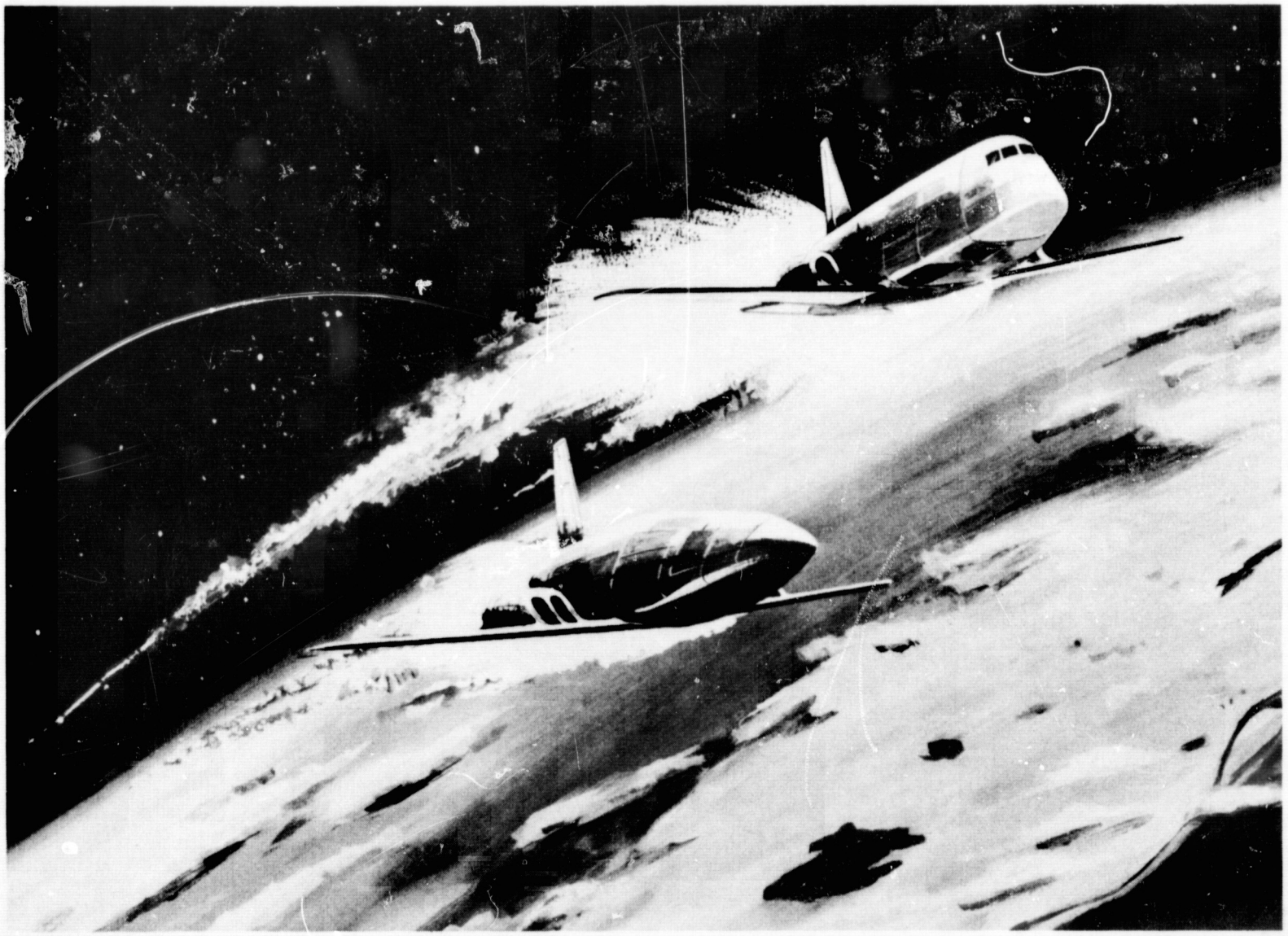

Study of Integral Launch and Reentry Vehicle System

FINAL REPORT

SD 69-573-4

Volume IV • Technical Report — Second Phase
Design and Subsystems Analysis

N70-31835
(ACCESSION NUMBER) (THRU)
586 1
(PAGES) (CODE)
CR-102105 31
(NASA CR OR TMX OR AD NUMBER) (CATEGORY)
FACILITY FORM 602

Space Division
North American Rockwell

SD 69-573-4

MSC 00192

FINAL REPORT

STUDY OF

INTEGRAL LAUNCH AND REENTRY VEHICLE SYSTEM

(Contract NAS9-9205)

VOLUME IV

TECHNICAL REPORT - SECOND PHASE
DESIGN AND SUBSYSTEMS ANALYSIS

DECEMBER 1969

APPROVED:

G.F. Fraser
Study Manager

Space Division
North American Rockwell

PRECEDING PAGE BLANK NOT FILMED.

FOREWORD

This report, containing results of the Study of Integral Launch and Reentry Vehicle System, is submitted in accordance with Contract NAS9-9205 to the NASA Manned Spacecraft Center, Houston, Texas, by the Space Division of North American Rockwell Corporation. The NASA MSC contracting officer's representative directing the study was R.H. Bradley.

This document, Volume IV of a five-volume report, is a summary of design studies of a two-stage reusable logistic shuttle vehicle concept investigated during the second phase of the program.

The volumes of the complete final report are as follows:

STUDY OF INTEGRAL LAUNCH AND REENTRY VEHICLE

Volume	Title	SD Report No.
I	Summary Report	SD 69-573-1
II	Technology Development Requirements	SD 69-573-2
III	Technical Report - Second Phase Environment and Performance	SD 69-573-3
IV	Technical Report - Second Phase Design and Subsystems Analysis	SD 69-573-4
V	Technical Report - Second Phase Operations and Resources	SD 69-573-5

MAJOR STUDY CONTRIBUTORS

The major contributors to the subject contract and their areas of responsibility are listed below. These personnel also were responsible for the material presented in this volume of the final report document.

Name	Title or Function
G. F. Fraser	Study Manager
D. E. Denison	Project Engineer
T. Sackinger	Design
R. Trengove	Design
M. Beer	Weights
J. Joanides	Structures
H. S. Greenberg	Structures
J. Dieter	Materials
L. Crockett	Materials
T. Connors	Thermal Protection
P. Edwards	Propulsion
B. Rosenbaum	Hydraulics
O. T. Stoll	EC/LSS
M. Blaski	Power
D. Engels	Guidance and Control
W. Lee	Guidance and Control
D. Earle	Integrated Electronics

CONTENTS

Section		Page
1.0	INTRODUCTION	1-1
2.0	SUMMARY	2-1
3.0	OBJECTIVES	3-1
4.0	MISSION AND DESIGN REQUIREMENTS	4-1
5.0	SCOPE	5-1
6.0	APPROACH AND STUDY SCHEDULE	6-1
	6.1 Concept Sizing and Performance Analysis	6-1
	6.2 Design Improvement Concepts and Sensitivity Analysis	6-1
	6.3 Conceptual Design	6-2
	6.4 Resource Plans	6-2
	6.5 Technology	6-6
7.0	ENVIRONMENT AND PERFORMANCE SUMMARY	7-1
	7.1 Flight Profile and Vehicle Optimization	7-1
	7.2 Aerodynamics and Design Improvements	7-4
	7.3 Control Concepts	7-6
	7.4 Abort	7-6
	7.5 Thermal Environment	7-7
	7.6 Lateral Ranging Effects and Potential	7-7
	7.7 Approach and Landing	7-10
	7.8 Design Loads	7-10
8.0	DESIGN AND SUBSYSTEM ANALYSIS	8-1
	8.1 Configuration and Design Guidelines	8-2
	8.2 Design	8-4
	8.3 Weight Analysis	8-85
	8.4 Materials	8-142
	8.5 Structures Analysis	8-180
	8.6 Thermal Protection Analysis	8-279

Section		Page
	8.7 Propulsion System	8-304
	8.8 Hydraulic System	8-405
	8.9 Environmental Control/Life Support Systems	8-419
	8.10 Power System	8-450
	8.11 Integrated Electronic Systems	8-466
9.0	CONCLUSIONS	9-1

ILLUSTRATIONS

Figure		Page
2.0-1	Shuttle Vehicle Configuration, 25,000-Pound-Payload, 15-Foot by 30-Foot Cargo Area	2-3
2.0-2	Orbiter General Arrangement	2-5
2.0-3	Booster General Arrangement	2-9
2.0-4	Payload Sensitivity	2-13
5.0-1	Baseline Concept for Phase 2 of Study	5-2
6.0-1	Phase 2 Study Logic	6-3
6.0-2	Phase 2 Study Schedule	6-5
7.1-1	Flight Profile	7-2
7.1-2	Baseline Vehicle Configuration	7-3
7.1-3	Payload Capabilities	7-3
7.2-1	Booster and Orbiter Aerodynamic Configuration Characteristics	7-5
7.5-1	Thermal Environment	7-8
7.6-1	Orbiter Lateral Range Potential	7-9
8.1-1	Shuttle Vehicle Configuration Guidelines	8-3
8.2-1	Baseline 12,500-Pound-Payload Vehicle (Drawing 2234-50)	8-5
8.2-2	Booster Configuration, MSC Concept, for 7,700-Pound-Payload Orbiter (Drawing 2234-65)	8-11
8.2-3	Orbiter Configuration, MSC Concept, for 7,700-Pound-Payload (Internal Cargo) (Drawing 2234-64)	8-13
8.2-4	Booster Configuration, MSC Concept, for 25,000-Pound-Payload Orbiter (Drawing 2234-54A)	8-15
8.2-5	Orbiter Configuration, MSC Concept, for 25,000-Pound Payload (Internal Cargo) (Drawing 2234-56)	8-17
8.2-6	Booster Configuration for 25,000-Pound-Payload Orbiter (15-Foot Diameter by 60-Foot-Length Payload) (Drawing 2234-59)	8-19
8.2-7	Orbiter Configuration, MSC Concept, for 25,000-Pound Payload (Internal Cargo) (Drawing 2234-58)	8-21

Figure		Page
8.2-8	Booster Configuration, MSC Concept, for 5,000-Pound-Payload Orbiter (Drawing 2234-61)	8-23
8.2-9	Orbiter Configuration, MSC Concept, for 50,000-Pound Payload (15-Foot-Diameter by 60-Foot-Length Internal Cargo) (Drawing 2234-60)	8-25
8.2-10	Booster Configuration for 50,000-Pound-Payload Orbiter (22-Foot Diameter by 60-Foot-Internal Cargo) (Drawing 2234-63)	8-27
8.2-11	Orbiter Configuration, MSC Concept, for 50,000-Pound Payload (Internal Cargo) (Drawing 2234-62)	8-29
8.2-12	Cargo Access Evaluation	8-33
8.2-13	Baseline 50,000-Pound-Payload Orbiter (Drawing 2234-68)	8-35
8.2-14	Baseline 50,000-Pound-Payload Booster (Drawing 2234-69)	8-37
8.2-15	50,000-Pound-Payload Orbiter Modified for Center-of-Gravity Balance (Drawing 2234-70)	8-39
8.2-16	Forward-Mounting Turbojet Engine Installation	8-42
8.2-17	Forward Turbojet Engine Installation, Swing-Out Doors	8-43
8.2-18	Baseline 50,000-Pound-Payload Orbiter With Large-Radius Chine (Drawing 2234-72)	8-45
8.2-19	Integral-Tank Orbiter Configuration (Drawing 2234-74)	8-47
8.2-20	Orbiter With Recommended Aerodynamic Body Lines (Drawing 2234-77)	8-49
8.2-21	Orbiter Jet Engine Comparison	8-52
8.2-22	50,000-Pound-Payload Orbiter and Booster in Mated Configuration (Drawing 2234-80)	8-55
8.2-23	50,000-Pound-Payload Orbiter for Detail Design (Drawing 2234-79)	8-57
8.2-24	Typical Orbiter Fuselage and Wing Construction	8-60
8.2-25	Rocket-Engine Thrust-Structure Concept	8-63
8.2-26	50,000-Pound-Payload Booster for Detail Design (Drawing 2234-76)	8-69
8.2-27	Typical Booster Fuselage and Wing Construction	8-72
8.2-28	Booster Thrust-Structure Concept	8-75
8.2-29	25,000-Pound-Payload Vehicle Configuration, 12-Foot-Diameter by 48-Foot-Length Cargo Bay	8-84
8.3-1	Body Structure Weight Factor Comparison	8-87
8.3-2	Wing Structure Weight Factor Comparison	8-87

Figure		Page
8.3-3	Booster Propellant Fraction, Parametric Phase	8-91
8.3-4	Orbiter Parametric Propellant Fraction, T/W = 1.3	8-92
8.3-5	Orbiter Parametric Propellant Fraction, T/W = 1.6	8-93
8.3-6	Orbiter Propellant Fraction, Parametric Phase	8-94
8.3-7	Booster Weight Characteristics With 400,000-Pound-Thrust Rocket Engines	8-97
8.3-8	Orbiter Weight Characteristics With 400,000-Pound-Thrust Rocket Engines	8-97
8.3-9	Vehicle Gross Weight Sensitivity	8-100
8.3-10	Vehicle Payload Sensitivity	8-100
8.3-11	Booster Mass Fraction, Final Configuration Weights	8-123
8.3-12	Orbiter Mass Fraction, Final Configuration Weights	8-124
8.3-13	Orbiter Propellant Fraction, 25,000-Pound Payload	8-141
8.4-1	Typical Properties of ManLabs Zirconium Diboride Hot-Pressed Shapes	8-146
8.4-2	Effect of Temperature on TD NiCr Mechanical Properties (0.015- to 0.040-Inch Sheet)	8-153
8.4-3	TD NiCr Creep Design Limits (Transverse Direction)	8-154
8.4-4	Effect of Temperature on TD NiCr Physical Properties	8-155
8.4-5	Effect of Temperature on Properties of Haynes 188 Cobalt Alloy Sheet and Bar	8-158
8.4-6	Effect of Temperature on Properties of Haynes 188 Cobalt Alloy Sheet (0.020- to 0.080-Inch)	8-159
8.4-7	Effect of Temperature on Properties of Rene′ 41	8-161
8.4-8	Creep Properties of Rene′ 41	8-162
8.4-9	Typical Thermal Conductivity Properties of Insulation Materials	8-167
8.4-10	Typical Properties of Alumina Ceramics	8-174
8.5-1	Baseline Structures Review	8-191
8.5-2	Orbiter Critical Load Conditions	8-194
8.5-3	Booster Critical Load Conditions	8-195
8.5-4	Design Load Intensity	8-196
8.5-5	Maximum Structural Temperatures	8-197
8.5-6	Orbiter Structure and Thermal Protection Trade	8-199
8.5-7	Orbiter Temperatures	8-200
8.5-8	Orbiter Thermal Protection Systems	8-201

Figure		Page
8.5-9	Orbiter Forward Station Structure	8-202
8.5-10	Orbiter Aft Station Structure	8-203
8.5-11	Concepts 1 and 2 and Shortened LH_2 Tank Possibility	8-206
8.5-12	Limit Attachment Loads	8-209
8.5-13	Orbiter Loads for Forward and Aft Attachments	8-212
8.5-14	Drag Attachment Location	8-213
8.5-15	Orbiter Forward Tankage Concepts	8-214
8.5-16	Booster Structure Definition	8-216
8.5-17	Orbiter Structure Definition	8-217
8.5-18	Booster Thrust Structure	8-227
8.5-19	Thrust Structure Longerons	8-228
8.5-20	Skin Stringer Designs	8-231
8.5-21	Crossbeam Design Loads	8-231
8.5-22	Thrust Structure	8-232
8.5-23	Longeron Design Loads	8-233
8.5-24	Wing Frame Loads and Sections	8-235
8.5-25	Typical Heat Shield Construction	8-238
8.5-26	Pressure Distribution on Sides and Bottom of ILRV Booster Fuselage	8-240
8.5-27	Truss Support Structure for Fiberglass-Reinforced Sandwich Panels	8-243
8.5-28	Frame-Extension Beam Section	8-245
8.5-29	Frame Beam Section	8-245
8.5-30	Preliminary Wing Torsional Stiffness Based on Flutter Requirements	8-250
8.5-31	Optimum Shear Webs	8-252
8.5-32	Orbiter Tank Gages	8-256
8.5-33	Orbiter Body Critical Loading Conditions	8-260
8.5-34	Structural Model for Maximum G Condition	8-261
8.5-35	Vertical Tail Support Ring	8-267
8.5-36	Optimum Design Curve for Corrugated Shear Webs	8-270
8.5-37	Orbiter Wing Bending Moment for Maximum $q\alpha$ Condition	8-272
8.5-38	Orbiter Wing Geometry and Loading	8-273
8.6-1	Typical Maximum Orbiter Temperatures for Reentry at High and Low Angles of Attack	8-280
8.6-2	Typical ILRV Maximum Temperatures for Orbiter Wing	8-280
8.6-3	Baseline 12,500-Pound-Payload Vehicle Thermal Protection	8-282
8.6-4	Typical Thermal Protection System Cross Sections	8-290

Figure		Page
8.6-5	Insulation Weight Comparison for Orbiter Underbody Centerline	8-290
8.6-6	Booster Thermal Protection System Definition	8-292
8.6-7	Maximum Temperature Distribution for Booster Sides and Top	8-293
8.6-8	Insulation Requirements for Booster Top	8-293
8.6-9	Maximum Temperature Distribution for Booster Underbody Centerline	8-295
8.6-10	External Insulation Requirements for Booster Underbody Centerline	8-295
8.6-11	Maximum Temperature Distribution for Booster Wing Undersurface	8-296
8.6-12	External Insulation Requirements for Booster Wing Undersurface	8-296
8.6-13	Orbiter Thermal Protection System Definition	8-297
8.6-14	Maximum Temperature Distribution for Orbiter Top	8-298
8.6-15	Insulation Requirements for Orbiter Top	8-298
8.6-16	Maximum Temperature Distribution for Orbiter Sides	8-299
8.6-17	External Insulation Requirements for Orbiter Sides	8-299
8.6-18	Maximum Temperature Distribution for Orbiter Top (Chine and Centerline)	8-301
8.6-19	External Insulation Requirements for Orbiter Underbody	8-301
8.6-20	Internal Insulation Requirements for Orbiter Underbody	8-302
8.6-21	Maximum Temperature Distribution for Orbiter Top (Span)	8-302
8.6-22	External Insulation Requirements for Orbiter Wing Undersurface	8-303
8.6-23	Maximum Temperature Distribution for Orbiter Wing Undersurface	8-303
8.7-1	Booster and Orbiter Rocket-Engine Commonalty	8-305
8.7-2	Booster Configuration With 300,000-Pound Vacuum-Thrust Engines	8-310
8.7-3	Orbiter Configuration With 300,000-Pound Vacuum-Thrust Engines	8-312
8.7-4	Bell-Engine Propellant-Flow Schematic	8-314
8.7-5	400,000-Pound-Thrust Aerospike-Engine Schematic	8-316
8.7-6	Bell and Aerospike Engines Installed Sizes	8-320
8.7-7	Bell and Aerospike Engines Options	8-322
8.7-8	Bell-Engine Configuration Adapted for Aerospike Engine	8-325

Figure		Page
8.7-9	Aerospike-Engine Configuration Adapted for Bell Engine	8-327
8.7-10	Performance Impact of Single-Engine Development	8-329
8.7-11	Orbit Maneuvering Propellant Schedule	8-332
8.7-12	Orbit Maneuvering Propulsion Performance Spectrum	8-333
8.7-13	Booster Thrust Required.	8-342
8.7-14	Pratt & Whitney JT9D-15 Engine Performance, Maximum Continuous and Takeoff Power	8-343
8.7-15	Pratt & Whitney TF33-P-7 Engine Performance, Maximum Continuous and Takeoff Power	8-344
8.7-16	Thrust Versus Altitude for Orbiter	8-345
8.7-17	Pratt & Whitney TF33-P-7 Engine Data	8-346
8.7-18	Pratt & Whitney JT3D-7 Engine Data	8-347
8.7-19	Lightweight Turbojet Engine Data	8-351
8.7-20	Lightweight Turbojet Engine Geometry	8-352
8.7-21	Main Rocket Engine Characteristics	8-354
8.7-22	Booster Main Propulsion System	8-357
8.7-23	Orbiter Main Propulsion System	8-359
8.7-24	Preliminary Propellant Gauging System (Typical for Booster or Orbiter)	8-365
8.7-25	Booster RCS Configuration	8-371
8.7-26	Orbiter RCS Configuration.	8-372
8.7-27	Candidate Thruster Configurations and Materials	8-374
8.7-28	Typical Liquid- and Pump-Fed Propellant Conditioning System	8-376
8.7-29	Typical Gas and Turbo-Compressor Propellant Conditioning System	8-377
8.7-30	RCS System Definition	8-378
8.7-31	Effect of Chamber Pressure on Engine Characteristics	8-379
8.7-32	Optimization of Chamber Pressure	8-381
8.7-33	Orbiter Accumulator Pressure Optimization.	8-382
8.7-34	Turbojet Propulsion System	8-386
8.7-35	Estimated JT9D-15 Turbofan Engine Performance, Thrust Versus Mach Number	8-387
8.7-36	Estimated JT9D-15 Turbofan Engine Performance, SFC Versus Mach Number	8-388
8.7-37	Estimated Pratt & Whitney JT3D-7 Engine Performance, Thrust Versus Mach Number	8-389
8.7-38	Estimated Pratt & Whitney JT9D-7 Engine Performance, TSFC Versus Mach Number	8-390

Figure		Page
8.7-39	Estimated Pratt & Whitney JT3D-7 Engine Performance, TSFC Versus Mach Number	8-391
8.7-40	Typical Turbojet Windmill Start Envelope	8-392
8.7-41	True Vapor Pressure of Aviation Kerosene, Maximum Volatility	8-395
8.7-42	Fuel Data, Aviation Hydrocarbons	8-396
8.7-43	Fuel Flow Versus Mach Number for JT3D-7 and JT9D-15 Engines	8-397
8.7-44	Fuel-System Schematic for Air-Breathing Propulsion Booster With Jet A-1 Aviation Kerosene or JP-5 Fuel	8-398
8.7-45	Predicted Sea-Level Performance of TRW Model 376800 Fuel Booster Pump; Fuel, Mil-T-5624, Grade JP-4, at 60 F (Performance Approximately the Same for Jet A-1 Kerosene)	8-400
8.7-46	Fuel-System Schematic for Air-Breathing Propulsion Orbiter With Jet A-1 Aviation Kerosene or JP-5 Fuel	8-403
8.8-1	Hydraulic System Functions	8-405
8.8-2	Typical Hydraulic System	8-409
8.8-3	Hydraulic System Arrangement	8-410
8.9-1	EC/LSS Systems Concept Options, Orbiter	8-426
8.9-2	Orbiter EC/LSS Schematic	8-436
8.9-3	EC/LSS Equipment Locations	8-438
8.10-1	Comparison of Energy Source Specific Weights	8-455
8.10-2	Electrical Power Subsystem Block Diagram	8-457
8.10-3	Baseline Fuel Cell System	8-458
8.11-1	Master Avionics Program Control	8-472
8.11-2	Interface Units	8-474
8.11-3	Manual Interface	8-474
8.11-4	Memory Access	8-476
8.11-5	Central Computer Organization	8-477
8.11-6	Guidance and Control Hardware and Sensor Locations on Orbiter and Booster	8-504
8.11-7	Relationship of Control Signal Distributor and Signal Coupler	8-513
8.11-8	Control Signal Distributor With Voting Logic	8-514
8.11-9	Input Signal Coupler (Mode-Switching Approach)	8-515
8.11-10	Targeting and Mission Planning	8-516
8.11-11	Prelaunch Calibration and Alignment and Self-Test	8-518
8.11-12	Boost Navigation, Steering, and Control for Orbiter	8-519

Figure		Page
8.11-13	Rendezvous and Docking	8-521
8.11-14	On-Orbit Alignment of IRU's	8-523
8.11-15	Entry Navigation, Steering and Control	8-524
8.11-16	Cruise and Landing Navigation, Steering, and Control for Orbiter and Booster	8-525
8.11-17	Electronically Generated Bar Graph (CRT)	8-528
8.11-18	Contact Analog Display	8-530
8.11-19	Electro-Optical Indicators	8-531
8.11-20	Schematic System Flow Diagram (With Variables)	8-532
8.11-21	Crew Compartment Display Concept	8-533
8.11-22	Time Lines in Orbital Planes	8-534
8.11-23	Docking Display of Range and Velocity	8-535
8.11-24	Docking Display of Azimuth, Elevation, and Roll	8-536
8.11-25	Integration of Crew Into Vehicle Control	8-538
8.11-26	Sensor and Actuator Address Decoder Interface	8-542
8.11-27	Communication Requirements	8-550
8.11-28	Communications System Concept	8-551
8.11-29	On-Board Performance Monitoring and Checkout System	8-555
8.11-30	Systems Flow Diagram of Performance Monitoring Sequence (With BITE)	8-556
8.11-31	On-Board Checkout Sequence Systems Flow Diagram	8-557
8.11-32	Typical Multiplexing Network	8-559
8.11-33	Subsystem Multiplexing Concept	8-561

TABLES

Table		Page
2.0-1	Overall Vehicle Characteristics, Concept Sizing Phase	2-2
2.0-2	General Characteristics of Conceptual Design Vehicle, 50,000-Pound-Payload, 15-Foot by 60-Foot Cargo Bay	2-2
2.0-3	Orbite Description	2-6
2.0-4	Booster Description	2-10
2.0-5	Impact of Burnout Weight Variations	2-12
7.8-1	Structure Design Loads Summary, 50,000-Pound-Payload System	7-12
8.2-1	Initial Baseline Configuration Features	8-7
8.2-2	Various Payload Sizes	8-8
8.2-3	Shuttle Vehicle Configuration Summary	8-31
8.2-4	Baseline 50,000-Pound-Payload Vehicle, 15-Foot by 60-Foot Cargo Bay	8-41
8.2-5	Orbiter General Characteristics	8-54
8.2-6	Booster General Characteristics	8-71
8.2-7	Final 50,000-Pound-Payload Vehicle Description	8-79
8.2-8	Thermal Protection System and Environment	8-83
8.3-1	Baseline 12,500-Pound-Payload Vehicle Projected Weights	8-86
8.3-2	Baseline 12,500-Pound-Payload Vehicle Mass Properties	8-89
8.3-3	Summary Weight Statements, Parametric Phase	8-96
8.3-4	Preliminary 50,000-Pound-Payload Vehicle	8-98
8.3-5	Baseline 50,000-Pound-Payload Vehicle Mass Properties	8-99
8.3-6	Impact of Burnout Weight Variations	8-101
8.3-7	Baseline Vehicle Surface Area	8-102
8.3-8	Baseline Booster Summary Weight Statement	8-103
8.3-9	Baseline Orbiter Summary Weight Statement	8-105
8.3-10	Baseline Configuration Subsystem,Weights	8-107
8.3-11	Final Booster Summary Weight Statement	8-125
8.3-12	Final Orbiter Summary Weight Statement	8-127
8.3-13	Final Configuration Subsystem	8-129
8.4-1	Candidate Structure and TPS Materials	8-143
8.4-2	ILRV Selected Materials	8-144

Table		Page
8.4-3	Design Properties of LI-15	8-148
8.4-4	Alternate External Insulation Concepts	8-149
8.4-5	Approximate Maximum Temperatures for Heat Shield Metals	8-151
8.4-6	Rene'41 (1650 F AGE) Summary of Room Temperature Properties	8-160
8.4-7	Summary of Material Properties of Inconel 718	8-164
8.4-8	Design Mechanical Properties of Ti-6Al-4V (Sheet, Strip, and Plate) (From MIL HDBK 5A)	8-165
8.4-9	Ti-6Al-4V Extrusions (Mechanical Properties - Conditions A, ST, and STA)	8-166
8.4-10	Zicar Product Forms and Properties	8-168
8.4-11	TG 15,000 Properties	8-170
8.4-12	Potential Phase Change Materials	8-171
8.4-13	Typical Properties of Polyurethane Foam	8-172
8.4-14	Approximate Maximum Temperatures for Hot Structure Applications	8-175
8.4-15	Preliminary Numbers for Design Tradeoffs	8-176
8.4-16	Design Mechanical and Physical Properties of Clad 7075 Aluminum Alloy (MIL HDBK 5)	8-177
8.4-17	2219 T87 Properties (0.040- to 0.249-Inch)	8-178
8.4-18	Design Mechanical Properties	8-179
8.5-1a	Materials Properties	8-186
8.5-1b	Materials Properties, Rene'41 1650 F AGE (Preliminary Values)	8-187
8.5-1c	Materials Properties, Inconel 718	8-187
8.5-1d	Materials Properties, Aluminum 2014-T6	8-188
8.5-2	Body Structure Design Loads	8-190
8.5-3	ILRV MSC Configuration Wing Limit Load	8-190
8.5-4	Structural Weight Estimates for Baseline/Orbiter Body and Tankage (12,500-Pound Payload)	8-192
8.5-5	Orbiter Loading Conditions	8-204
8.5-6	Orbiter Critical Design Conditions	8-205
8.5-7	Booster Comparative Loadings for Forward Versus Aft Drag Attach	8-210
8.5-8	Structure Temperatures (F)	8-220
8.5-9	Booster Body Structure Moments and Axial Loads	8-221
8.5-10	Critical Booster Body Structure Loading Intensities	8-222
8.5-11	Booster Tank Sizing	8-223
8.5-12	Study Analytical Relations	8-225
8.5-13	Heat Shield Truss Web Members	8-246
8.5-14	Booster Wing Analysis Data	8-248

Table		Page
8.5-15	Booster Wing Lower Cover Sizes	8-248
8.5-16	Booster Wing Upper Cover Sizes	8-249
8.5-17	Critical Orbiter Tank Design Conditions	8-257
8.5-18	Orbiter Wing Box Analysis Data	8-275
8.5-19	Orbiter Wing Lower Cover Sizes	8-276
8.5-20	ILRV Booster Thrust Structure Weight (Pounds)	8-278
8.7-1	Main Rocket Engine Thrust Requirements for Payload Range	8-305
8.7-2	Rocket Engine Characteristic, Concept Sizing Phase	8-307
8.7-3	Characteristics of 640,000- and 300,000-Pound-Thrust Engines	8-309
8.7-4	Comparison of 300,000-Pound-Thrust Engine System to Baseline System	8-311
8.7-5	Bell and Aerospike Engine Installed Sizes	8-319
8.7-6	Bell Engine and Aerospike Engine Characteristics Comparison	8-323
8.7-7	Orbit Maneuvering Profile	8-330
8.7-8	Orbital Propulsion Requirements and Alternative Characteristics	8-334
8.7-9	Booster LO_2 Pressurization System Weight Trade	8-336
8.7-10	Orbiter LO_2 Pressurization System Weight Trade	8-337
8.7-11	Jet Engine Summary	8-339
8.7-12	Booster Turbojet Engine Summary	8-349
8.7-13	Orbiter Turbojet Engine Summary	8-350
8.7-14	Ascent Propellant Tank Pressure Requirements	8-356
8.7-15	Pressurization System Data and Pressurant Weight	8-361
8.7-16	Booster Propellant and Pressurization System Hardware Weight	8-362
8.7-17	Orbiter ILRV Propellant and Pressurization System Hardware Weight (Main Tank)	8-363
8.7-18	Propellant Management System Weight	8-368
8.7-19	RCS Design Data	8-369
8.7-20	RCS Thruster Sizing	8-373
8.7-21	Orbiter RCS System Weight	8-383
8.7-22	Booster RCS System Weight Estimate	8-384
8.7-23	Turbojet Fuel Properties	8-394
8.7-24	Booster Pump Sizing	8-399
8.7-25	Fuel Pump Drive Trade Study Summary	8-401
8.8-1	Aerodynamic Control Deflection Rates	8-406
8.8-2	Booster Control Surface Hinge Moments	8-406
8.8-3	Orbiter Control Surface Hinge Moments	8-407
8.8-4	Hydraulic Flow Requirements	8-407
8.9-1	EC/LSS Requirements	8-419

Table		Page
8.9-2	Compartment Pressure Requirements	8-443
8.9-3	EC/LSS Weights	8-444
8.9-4	EC/LSS Electrical Power Requirements	8-444
8.10-1	Typical Orbiter Electrical Power Requirements	8-452
8.10-2	Auxiliary Power Subsystem Loads	8-453
8.10-3	Energy Requirements	8-453
8.10-4	Candidate Power System Approaches and Equipment	8-454
8.10-5	Comparison of Candidate Power Sources	8-456
8.10-6	Power Subsystem Equipment Size and Weight	8-461
8.11-1	Projected Guidance and Control Hardware Characteristics (ILRV)	8-503
8.11-2	GN&C Signals to Performance Monitor	8-507
8.11-3	Data Breakdown	8-511

1.0 INTRODUCTION

Future space exploration will be constrained within a limited budget and will benefit from the development of an economical logistic system. NASA, therefore, is directing investigations of reusable logistic vehicles that offer potential major operational cost reductions compared with costs of current systems. Among these investigations is the Study of Integral Launch and Reentry Vehicle System performed by the Space Division of North American Rockwell Corporation for the NASA Manned Spacecraft Center, Houston, Texas, in accordance with Contract NAS9-9205. This document contains results of design, performance, and resource studies accomplished during the second phase of the program. These study results were presented in the final oral review at NASA MSC on 5 November 1969.

The contract was negotiated on 31 January 1969, and activity began on 3 March 1969. The study schedule reflects eight months of technical activity and a subsequent reporting period. The major objective of the study was to define logistic systems that achieve an order-of-magnitude reduction in recurring costs and that advance inherent safety. The program was divided into two phases: the first phase was two months in duration and encompassed comparison of logistic vehicle concepts using expendable boosters. The second phase encompassed investigations of a two-stage reusable vehicle conceived by NASA MSC. In the study, vehicles were configured to deliver 10,000-, 25,000-, and 50,000-pound payloads to a 270-nautical-mile, 55-degree-inclination orbit. Vehicles to deliver 25,000- and 50,000-pound payloads were designed to provide the following cargo bay sizes:

Payload (lb)	Cargo Bay Sizes (ft)
25,000	15 x 30
25,000	15 x 30
25,000	12 x 48
50,000	15 x 60
50,000	22 x 60

Emphasis was placed upon the vehicle designed to deliver the 50,000-pound payload with 15-foot-diameter by 60-foot-length cargo bay. The system has two reusable stages with fixed low-sweep wings and similar aerodynamic shapes. The propulsion system uses LO_2/LH_2 propellants with high-chamber-pressure bell or aerospike engines. The vehicle is

configured for vertical takeoff with the orbiter mounted forward on the booster and the booster and orbiter engines operated sequentially. The forward orbiter location provides a forward center of gravity during the ascent phase of the mission and thus achieves an aerodynamically stable configuration. This arrangement minimizes the thrust-vector control requirement, angle of attack, and aerodynamic loads. Because a major requirement of the logistic vehicle is to minimize operational costs, it becomes necessary to provide a reusable thermal protection system. This objective makes it desirable to limit temperatures experienced on the vehicle during reentry. The approach adopted in the vehicle study was to minimize vehicle heating rate upon reentry by reentering at a high angle of attack with high-lift coefficient and low-lift loading. This reentry mode combined with the large planform area results in a low heating rate and low total heat load.

The booster element of the specified vehicle must cruise back to a land-landing site after separation from the orbiter. For this purpose, turbojets are used for the cruise phase of the mission. The subject vehicle configuration achieves a high subsonic lift-to-drag ratio (L/D) to provide efficient cruise capability and low landing speeds.

The study indicated the feasibility of the two-stage reusable fixed-wing concept. Further design and development of the system and technology advancement are required in certain areas. Areas of development that are critical to establishment of a low-weight reusable system are the external structure and the external and internal thermal protection systems.

Current programs encompass development of a high-chamber-pressure bell engine and an aerodynamic-spike-nozzle engine. The program to develop the main propulsion system must be continued to facilitate development of the subject logistic vehicle. Further development also will be necessary for the oxygen/hydrogen reaction control system. Another major area for technology advancement is demonstration of the reusability of the logistic vehicle with minimum maintenance.

2.0 SUMMARY

The results of the design and subsystem studies performed on a reusable two-stage space shuttle vehicle using LO_2/LH_2 propellants are documented in this volume of the final report. The design and subsystem analysis was directed toward establishing sizes of the shuttle vehicle for a range of payload requirements, identifying design improvements, and defining conceptual design of a selected configuration. Two areas of special study requested by NASA are reported in this volume, propulsion and integrated electronics.

The space shuttle concept used as a basis for vehicle sizing and design studies during the second phase of the program was defined by NASA MSC. The vehicle was configured to contain a payload of 12,500 pounds and provide 2000 cubic feet of cargo volume located aft of the crew. The basic aerodynamic shape and weight-to-planform area relationships for this vehicle were maintained for initial sizing of a vehicle configured to deliver 25,000- and 50,000-pound payloads. Historical aircraft and space vehicle subsystem weight data were used to derive shuttle vehicle parametric weight scaling data. These data were used to derive the sizes and weights of vehicles listed in Table 2.0-1.

The derivation of vehicle sizes and weights was based upon the performance analysis described in Volume III. This performance analysis resulted in the establishment of optimum stage propellant distributions to minimize the vehicle gross weight. A typical configuration developed in the parametric studies is shown in Figure 2.0-1 for a vehicle with 25,000-pound payload capability and a 15-foot-diameter by 30-foot-long cargo bay. The booster and orbiter are similar in shape and have a fixed low-sweep wing with a 7:1 aspect ratio.

The vehicle is launched vertically, with the orbiter located forward to achieve an aerodynamically stable system and to minimize thrust vector control requirements during ascent. Both the booster and orbiter are designed for reentry at a high angle of attack. They each land horizontally. The orbiter has provisions for two crew members, while the booster is unmanned for the normal mission. The payload includes 10 passengers located forward near the crew. A cargo bay is located at the vehicle center of gravity to minimize variation with or without cargo on board, and to prevent a need for significant changes in aerodynamic control surface requirements to trim the vehicle on reentry and during cruise or glide.

Table 2.0-1. Overall Vehicle Characteristics, Concept Sizing Phase

Payload (1000 lb)	Cargo Bay Size		Total Vehicle		Booster		Orbiter	
	Dia (ft)	Length (ft)	Weight (1000 lb)	Length (ft)	Weight (1000 lb)	Length (ft)	Weight (1000 lb)	Length (ft)
7.7	9	35	1664	206	1279	192	385	132
25	15	30	2576	246	2107	207	469	152
25	15	60	2730	261	2204	235	526	177
50	15	60	3480	289	2739	256	741	183
50	22	60	4007	299	3267	268	740	192

Following the concept sizing activity, NASA MSC selected a shuttle vehicle for detail analysis. This vehicle is configured to deliver a 50,000-pound payload and has a 15-foot by 60-foot cargo bay. The general characteristics of this vehicle are presented in Table 2.0-2. The specified weights are based upon a structure and subsystem analysis and include a 10-percent weight contingency.

Table 2.0-2. General Characteristics of Conceptual Design Vehicle, 50,000-Pound Payload, 15-Foot by 60-Foot Cargo Bay

Characteristic	Booster	Orbiter
Weights (1000 lb)		
Launch	3,620	871
Entry	588	257
Landing	532	255
Size		
Body length (ft)	280	202
Planform area (ft^2)	19,770	8,200
Wing span (ft)	244	146
Wing area (exposed) (ft^2)	6,300	2,010
Horizontal area (ft^2)	2,040	1,170
Vertical area (ft^2)	1,590	585
Body wetted area (ft^2)	36,000	17,111
Body volume (ft^3)	320,000	97,690

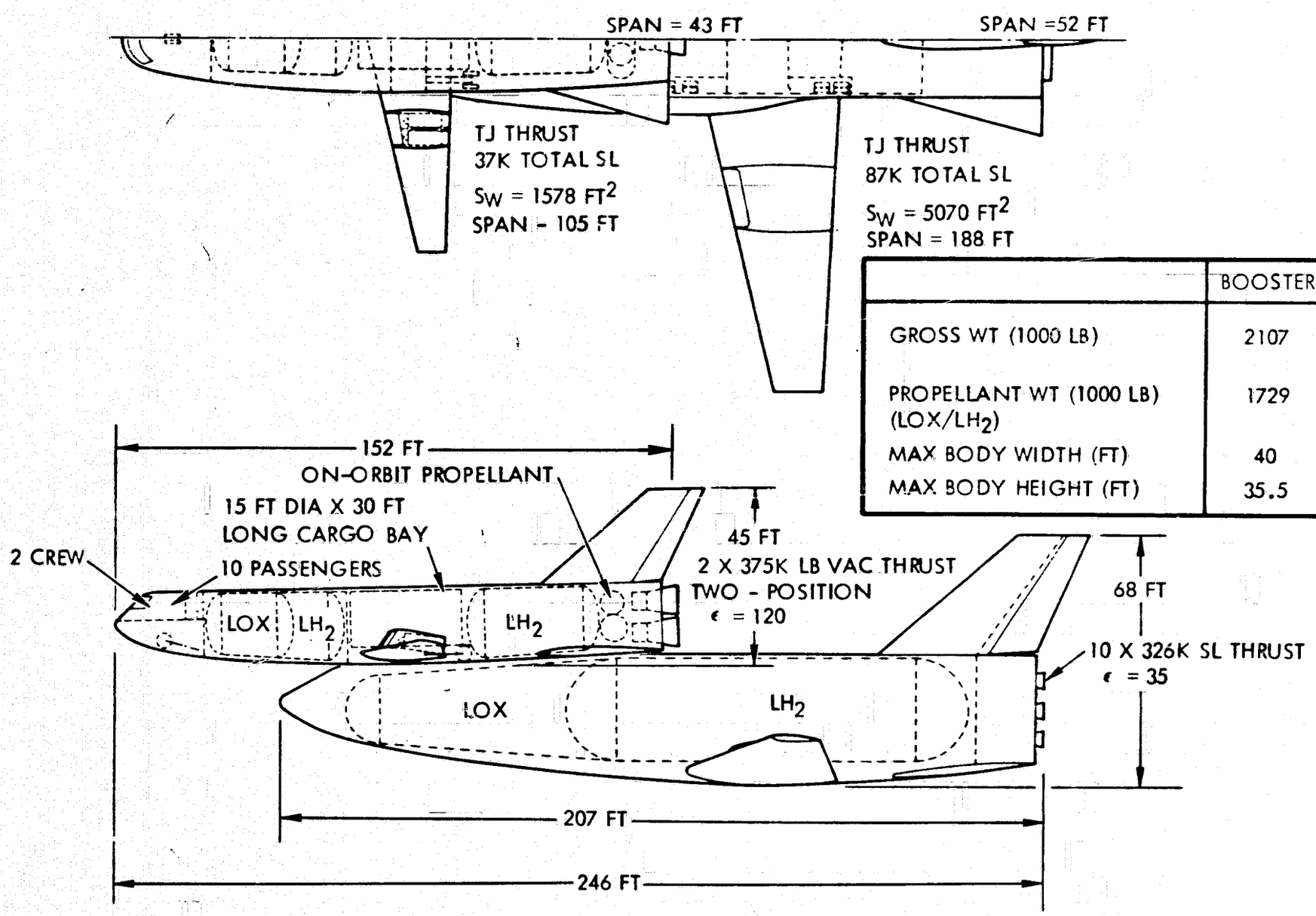

	BOOSTER	ORBITER
GROSS WT (1000 LB)	2107	469
PROPELLANT WT (1000 LB) (LOX/LH_2)	1729	325
MAX BODY WIDTH (FT)	40	26.5
MAX BODY HEIGHT (FT)	35.5	20.5

Figure 2.0-1. Shuttle Vehicle Configuration, 25,000-Pound-Payload, 15-Foot by 30-Foot Cargo Area

Space Division
North American Rockwell

The vehicle selected for detailed analysis has an aerodynamic shape similar to that of the baseline system and retains the same flight mode. The main engines used on the booster and orbiter have the same power head, but different bell nozzles.

The general arrangement of the orbiter is shown in Figure 2.0-2. The two crew members are located forward in an aircraft-type cockpit; provisions for ten passengers are provided in the same general area. Crew and passenger access is provided behind the cockpit area. The ten passengers and their provisions are considered part of the payload. An access tunnel is provided between the crew-passenger compartment and the cargo bay. The cargo bay is centered at the orbiter entry and landing center of gravity to provide a vehicle which can be trimmed on reentry and during cruise with or without cargo on board. The cargo bay can accommodate a 15-foot by 60-foot cargo container. Alternate cargo transfer capability is provided. Small cargo modules can be transferred through a pressurized access door. Non-load-carrying cargo doors can be opened to allow removal of a large payload. The orbiter is designed to allow rotation of a cargo container to provide a docking interface with a space station.

The central cargo bay location requires separation of the ascent propellant tanks. LO_2 and LH_2 tanks are located forward, with a common bulkhead separating the propellants. A second hydrogen tank is located aft of the cargo bay. These aluminum tanks are suspended; therefore, they are not subject to vehicle aerodynamic load. Polyurethane insulation is used on the inside of the LH_2 tank. Separate tanks with superinsulation are used to contain propellant for orbital maneuvers. The primary load-carrying structure is a skin-stiffened titanium shell. To withstand entry thermal environment, the titanium structure is protected on the fuselage bottom and sides by an external densified quartz insulation. Bare titanium is satisfactory on the top of the orbiter because of the mild thermal environment. Glass fiber insulation is used inside the titanium structure to limit the temperature of the tankage and insulation. The orbiter uses fixed, low-sweep titanium wings. Main propulsion is provided by two high-pressure, two-position, bell-nozzle engines that provide both ascent and in-orbit propulsion. The engines are throttled to 10 percent of maximum thrust for orbital maneuvers. Fixed turbofan engines, which provide landing and go-around capability, are mounted above the wings for thermal protection during entry. The reaction control system (RCS) uses gaseous oxygen and hydrogen obtained by vaporizing stored propellants in the on-orbit propellant tanks. The primary features of the orbiter system are summarized in Table 2.0-3.

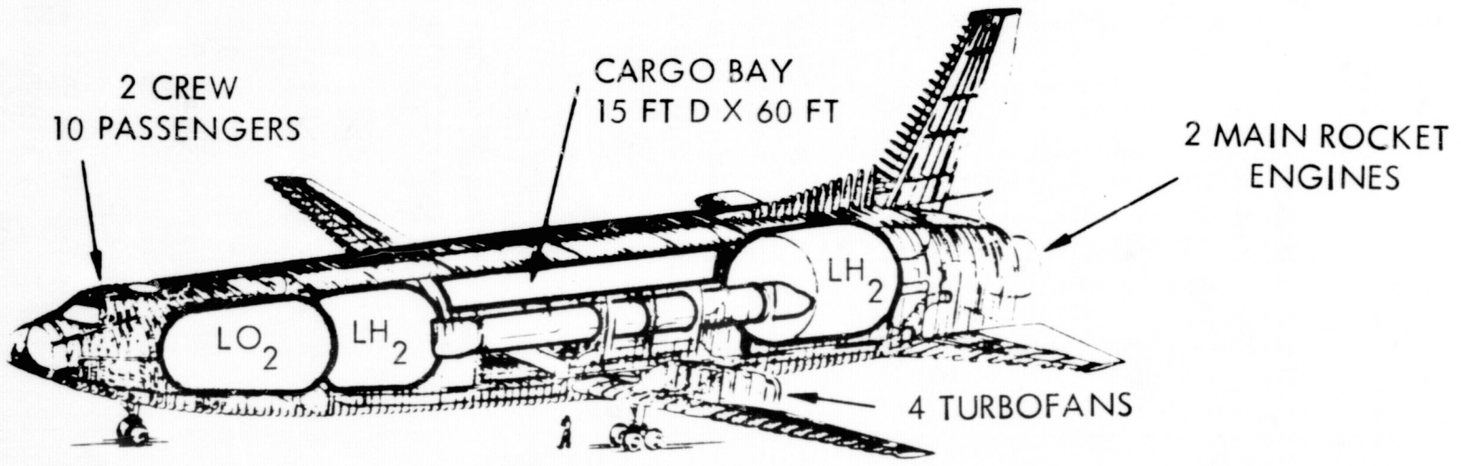

Figure 2.0-2. Orbiter General Arrangement

Table 2.0-3. Orbiter Description

System	Description
Structure and Thermal Protection System	
Primary body structure	6Al-4V titanium, skin stiffened, shell structure Densified quartz (LI-15) external insulation Fiberglass TG-15000 internal insulation
Aerosurfaces	6Al-4V, titanium, two spar Fixed wing, AR = 7, 14-degree sweep Densified quartz (LI-15) external insulation Zirconium diboride leading edges
Ascent tankage	Suspended tanks, pressure design, 2219 Al, Separated by cargo bay, LO_2/LH_2 Forward and LH_2 Aft Double bubble - design tankage, common bulkhead Polyurethane foam internal to LH_2 tank
On-orbit tankage	2219 Al cylindrical tanks High performance insulation, aluminized mylar Polyurethane foam on LH_2 tank, allow N_2 purge
Thrust structure	6Al-4V titanium truss
Main Propulsion	Two 590,000-pound-vacuum-thrust LO_2/LH_2 engine Common engine with booster to $\epsilon \approx 5:1$ Two-position nozzle, ϵ = 58:1/120:1 MR = 6:1, gimbal angle ±7 degrees Throttle to 73 percent for ascent g limitation, 10 percent for on-orbit GO_2 and GH_2 pressurization from main engine for ascent Heated helium pressurization for on-orbit

Table 2.0-3. Orbiter Description (Cont)

System	Description
Turbojet	Four JT3D-7 turbofans, 19,000-lb SLS thrust, 4,650 lb JP fuel
Reaction Control System	O_2/H_2 propellant 28 thrusters, 800-lb thrust, P_C = 300 psia Liquid supply, propellant conditioning, gas storage
Hydraulic System	Four independent systems, 4,000-psi 40-gpm pump, reservoir, N_2 pressurization, filters, relief valve, actuators, titanium lines.
Environmental Control and Life Support System	Thermal and contaminant control with dual-loop water-glycol and water evaporators Cabin pressure supply and control (5 psia), ram-air heat exchanger
Power	Three 5-kw fuel cells, O_2/H_2 Two 80-amp/hr batteries Four 150-hp APU's, O_2/H_2 Four 12-kva alternators
Integrated Electronics	For guidance, navigation, and flight control; data and control management; communications automatic docking and landing Three real-time computers, common equipment Electro-optics displays Multiplex signal distribution Built-in test equipment at subsystem and component level On-board checkout

The general arrangement of the booster is shown in Figure 2.0-3. The primary booster mission is unmanned, but provisions for two crew members are provided for a ferry mission. The booster propellant tanks provide the primary load-carrying structure. The tankage is fabricated from 2219 Al with external stiffened structure. The LO_2 tank is located forward of the LH_2 tank with a common bulkhead separating the propellants. LH_2 tank thermal control requirements are satisfied by polyurethane foam installed internally in the LH_2 tank. An aluminum truss and reinforced phenolic and polyimide honeycomb sandwich substructure is provided to maintain the desired flat base. This structure is also used to bond densified quartz external insulation to the booster bottom and side. The mild thermal environment on the top of the booster is within the capability of honeycomb sandwich material. The booster uses fixed, low-sweep titanium wings. Main propulsion is provided by eleven high-pressure bell-nozzle engines. The same basic engine is used in the orbiter and booster, with altitude and sea-level nozzles attached at an expansion ratio of approximately 5:1. Turbofan engines are provided for cruise, landing, and go-around capability. As in the orbiter, the engines are mounted above the wings for entry thermal protection. The primary features of the booster systems are summarized in Table 2.0-4.

Sensitivity analysis was conducted to establish the impact on vehicle gross weight caused by variations in the predicted orbiter and booster burnout weights. This analysis was conducted on a vehicle to deliver a 50,000-pound-payload system within a 15-foot by 60-foot cargo bay. The results of this analysis are summarized in Table 2.0-5.

Investigations were also performed to determine the payload increment that would be experienced due to variations in system design performance and weight. Investigations encompassed turbojet system changes, system weight variations, specific-impulse degradation, and reduced on-orbit velocity requirement. These data are summarized in Figure 2.0-4. The orbiter and booster configuration previously described used turbojet engines currently available for commercial transports, modified only for the new environment. The figure shows that modification of the booster engine to use hydrogen fuel in place of JP fuel will increase the vehicle payload delivery capability by approximately 10 percent. Current commercial turbojet engines have an engine-thrust-to-engine-weight ratio (T/W) of approximately 4.5:1. The development of a high T/W engine with the lift engine technology being developed by Allison will provide a 20-percent payload gain based on an engine T/W of 15:1. The effect of ±10-percent weight variation is shown. The sensitivity of vehicle gross weight to orbiter weight reductions is apparent. The major potential performance

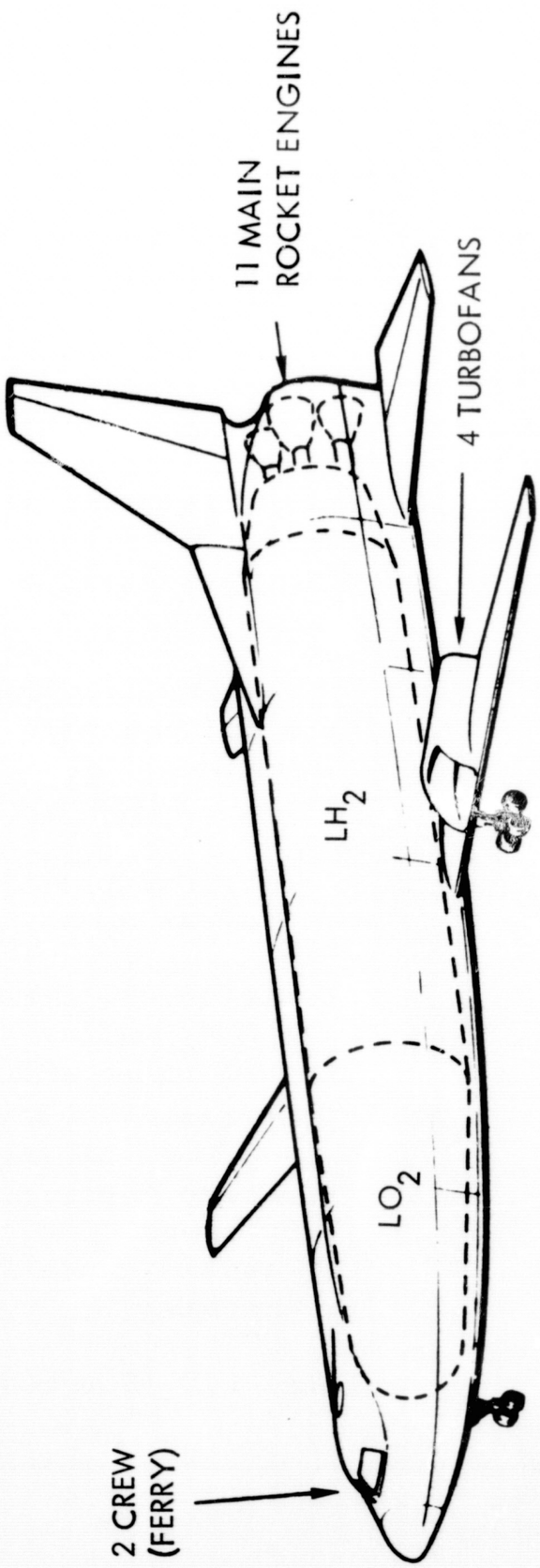

Figure 2.0-3. Booster General Arrangement

Table 2.0-4. Booster Description

System	Description
Structure and Thermal Protection System	
Primary body structure	Propellant tankage, 2219 Al, externally stiffened Circular sections, common bulkhead Polyurethane foam internal to LH_2 tank
TPS substructure	2219 Al truss with phenolic and polyimide honeycomb sandwich panels Densified quartz (LI-15) external insulation Fiberglass TG-15000 internal insulation
Aerosurfaces	6Al-4V titanium, Two Spar Densified quartz (LI-15) external insulation Haynes 188 leading edges
Thrust structure	6Al-4V titanium skin stiffened cone with cross beams
Main Propulsion	Eleven 510,000-pound-sea-level-thrust LO_2/LH_2 engines Common engine with orbiter to $\epsilon \approx 5:1$ Fixed nozzle, $\epsilon = 35:1$ MR = 6:1, gimbal angle ±7 degrees Throttle to 75 percent for ascent g limitation GO_2 and GH_2 pressurization from main engine
Turbojet	Four JT9D-15 turbofans, 57,800 lb JP fuel

Table 2.0-4. Booster Description (Cont)

System	Description
Reaction Control System	O_2/H_2 propellant 24 thrusters, 1800-lb thrust, P_C = 300 psia Liquid supply, propellant conditioning, gas storage
Hydraulic System	Four independent systems, 4000 psi Two 40 gpm pumps, reservoir, N_2 pressurization, filters, relief valve, actuators, titanium lines
Environmental Control System	Thermal control with dual-loop water-glycol and water evaporator, oxygen supply and ram air heat exchanger
Power	Two 80-ah batteries Four 250-hp APUs, O_2/H_2 Four 12-kva alternators
Integrated Electronics	For guidance, navigation, and flight control; automatic docking and landing; data and control management; communications Three real-time computers, common equipment Multiplex signal distribution Built-in test equipment at subsystem and component level On-board checkout

improvement that can then be achieved through structure weight reduction concepts is also apparent. Vehicle performance has been based on nominal performance provided by the engine manufacturer. The importance of achieving the quoted performance is illustrated by the degradation of 15 percent in payload which would be experienced due to a one-percent reduction in engine specific impulse. The orbiter vehicle has an on-orbit velocity capability of 2000 feet per second. This requirement can probably be reduced by 500 feet per second for most missions, and off-loading propellant can provide a 20-percent payload gain.

Table 2.0-5. Impact of Burnout Weight Variations

Burnout Weight Variation (Percent)	Vehicle Gross Weight Change (Percent)
Increase	
+10 (Orbiter)	+12.5
+10 (Booster)	+ 7
+10 (Orbiter and Booster)	+19.5
Decrease	
-10 (Orbiter)	-10
-10 (Booster)	- 5
-10 (Orbiter and Booster)	-15.5

The study has demonstrated the feasibility of the two-stage reusable fixed-wing concept; potential improvements and weight-reduction measures have been identified. Further design and development of the system and technology advancement are required in certain areas. As discussed in Volume III, modification of the vehicle shape may be necessary to minimize buffeting and flow-interference heating effects.

Critical areas for development are the external structure and the external and internal thermal protection system. This effort will be necessary to establish a low-weight reusable system. In the study, the selected external thermal protection concept is based upon the use of densified quartz, which material at the present time has not been fully developed and has certain disadvantages. This material is subject to water absorption and possibly erosion under operating conditions, and it will be necessary to provide an external coating. It is also recognized that current insulation used for the cryogenic propellant tankage does not have extensive reuse capabilities. It will, therefore, be necessary to ensure that the polyurethane insulation materials or their replacements will be capable of reuse with minimum maintenance and without causing hazards to system operation. Present programs encompass the development of high-chamber-pressure bell engines or aerodynamic-spike-nozzle engines. The program to develop the main propulsion system must be continued for development of the logistic vehicle. Further development will also be necessary for the oxygen-hydrogen reaction control system. Another major area for technology advancement will be the reusability of the logistic vehicle with minimum maintenance.

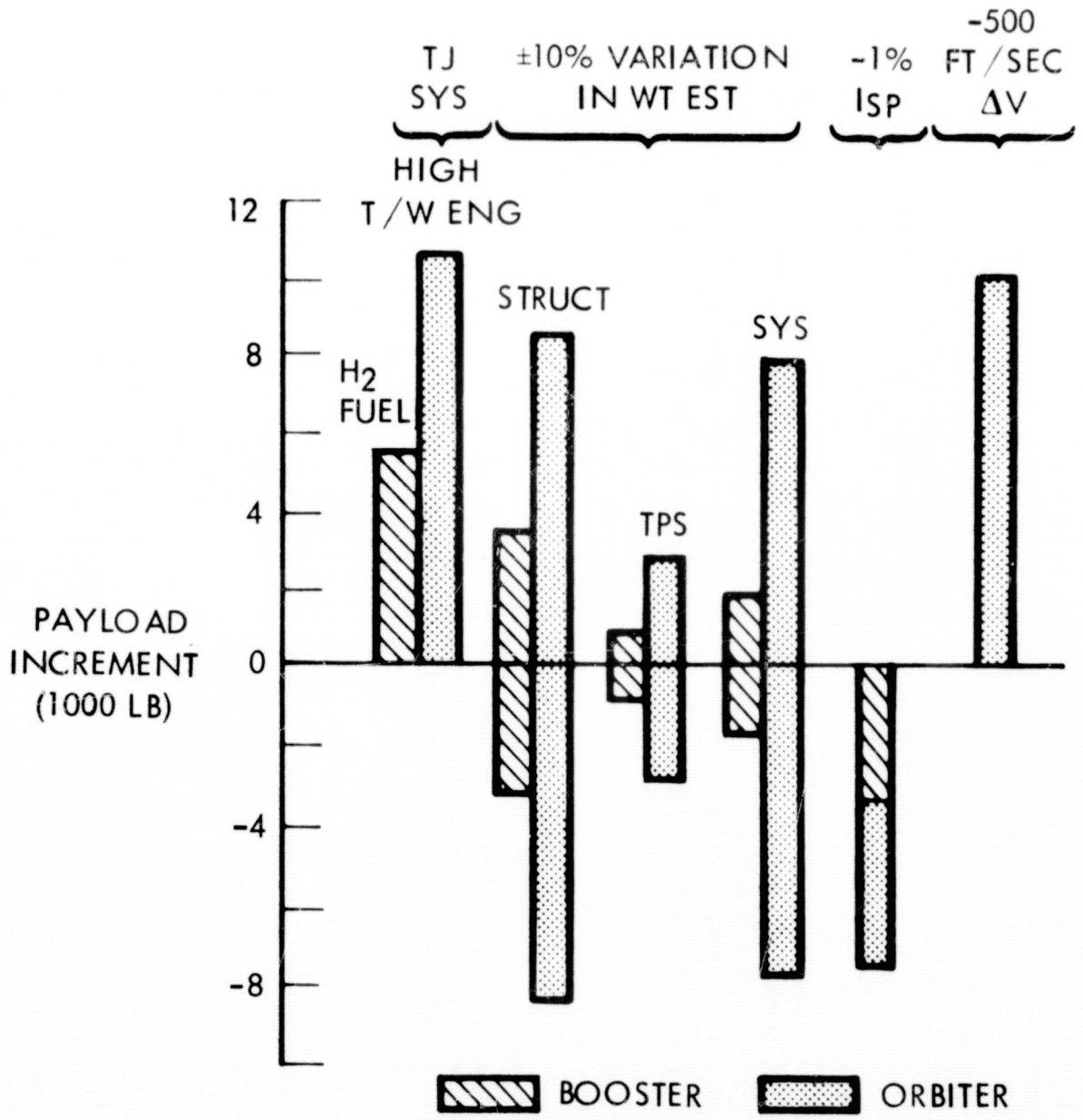

Figure 2.0-4. Payload Sensitivity

3.0 OBJECTIVES

This design study to investigate low-cost space transportation systems is based on the following program objectives:

1. Derive conceptual designs and perform resources analyses to identify the development, manufacturing, procurement, testing, RDT&E, and operations requirements for logistics space vehicle systems to support earth-orbital programs in the post-1974 period. In the major design approaches, attempt to achieve order-of-magnitude reduction in the recurring costs of the total logistic support operational system and to achieve significant advances in the inherent safety of the space vehicle system.

2. Establish requirements for research and technology development; and discuss the potential benefits in terms of systems sensitivities, development risks, etc.

Objectives of the second phase of the study, which is reported in this document, are as follows:

1. Establish sizes and weights of an advanced logistic vehicle concept defined by NASA MSC for payload classes of 10,000, 25,000, and 50,000 pounds.

2. Determine the impact of candidate design improvement concepts for the NASA MSC vehicle.

3. Select vehicle(s) and payload size(s) for conceptual design analysis.

4. Prepare conceptual design definitions of the selected advanced logistic vehicle(s).

5. Define a development approach, and identify technology requirements for the new logistic system.

6. Develop resource plans and cost estimates.

4.0 MISSION AND DESIGN REQUIREMENTS

The following requirements, which are applicable to the shuttle system after it becomes operational, were used during the second phase of the study.

1.	Mission orbit	270-nm, 55-degree inclination.
2.	Launch site	Cape Kennedy.
3.	Payload, up and down	Payload delivered by vehicle with eight 250,000-pound nominal vacuum thrust engines on booster. 25,000-pound payload size, 15-foot diameter by 30-foot length. 25,000-pound payload size, 15-foot diameter by 60-foot length. 25,000-pound payload size, 12-foot diameter by 48-foot length. 50,000-pound payload size, 15-foot diameter by 60-foot length. 50,000-pound payload size, 22-foot diameter by 60-foot length. The payload weight includes ten passengers with provisions and cargo; the payload sizes provide only for cargo. Additional volume will be provided for ten passengers. The weight of two crew members in the orbiter vehicle will be included in the weight of the shuttle vehicle system.
4.	Mission duration	Shuttle vehicle: 30 days on orbit; 7 days active life of systems.

5.	Orbital operations	2,000-foot-per-second velocity capability in excess of that required by the vehicle to obtain a 45- by 100-nm orbit will be provided by the shuttle vehicle.
6.	Launch rate	24 to 50 per year.
7.	Ground mission operations	Conducted from a central facility.
8.	Cargo	Cargo will be self-contained and will provide protective devices or provisions.
9.	Environment	System will be limited to commercial V_n limits; maximum eyeballs-in acceleration for crew will be 3 g; crew and passengers will have shirt-sleeve environment.
10.	Launch and refurbishment sites	Refurbishment site will be the same as launch site.
11.	Communication	Continuous space-to-ground communication will be available; communication will provide for two-day self-validating data transmission.
12.	System failures	System will fail operational after first failure and fail safe after second failure.
13.	Toggle switches	Avoid.
14.	Mission termination and abort	Satisfactory crew and passenger egress shall be made for abort during launch. When necessary, provisions will be made for abort during launch.
15.	Checkout	Shuttle vehicle primary preflight and in-flight checkout systems will be on board the vehicle.

16. Guidance and Navigation	Guidance and navigation functions will be performed on board.
17. Vehicle operation	The vehicle will have a two-man flight crew. It is desirable that it can be flown by a single crewman.
18. Boost stage	The boost stage will be reusable and may be unmanned.
19. Docking	Hard docking is required. Shuttle vehicle atmosphere will be the same as that of the space station base during cargo transfer. Crew transfer will be by IVA. Automatic approach and docking capability will be provided.
20. Orbital insertion	A three-axis translation system is required.
21. Deorbit and reentry	Return opportunity to primary landing site shall be at least once every 24 hours.
22. Landing and go-around	The shuttle vehicle will be capable of go-around with one engine out and more than one landing attempt. Landing visibility will be comparable to that of high-performance aircraft. Zero-zero capability and automatic landing capability should be provided.
23. Self-ferrying	Capability for self-ferry flights between airports will be provided.
24. Onboard provisions	Onboard provisions will be available to ensure postlanding safety.
25. Refurbishment	Minimimum turn-around.
26. Engines	Engines to be considered include high-pressure bell engine and aerospike engine (alternate).

27. Reentry	Vehicles will provide high angle of attack on reentry; RCS will be used.
28. Aerodynamic surfaces for reentry	Aerodynamic surfaces will be fixed for hypersonic velocities.
29. Stability	During boost, vehicle center of gravity will be forward of center of pressure; engine failure will not result in critical design loads.
30. Ranging	Vehicle ranging capability and options to increase lateral ranging will be identified.
31. Margins	A 10-percent weight contingency will be allowed. Performance reserve will be 3/4-percent of the vehicle characteristic velocity with the associated propellant allowance in the terminal stage.

5.0 SCOPE

The basic NASA vehicle concept to be studied is illustrated in Figure 5.0-1. This concept is configured for a crew of two (in orbiter) and the following payloads (which include ten passengers):

1. Payload delivered by vehicle with eight 250,000-pound nominal vacuum thrust engines on booster.

2. 25,000-pound payload, cargo size 15-foot diameter by 30-foot length.

3. 25,000-pound payload, cargo size 15-foot diameter by 60-foot length.

4. 25,000-pound payload, cargo size 12-foot diameter by 48-foot length.

5. 50,000-pound payload, cargo size 15-foot diameter by 60-foot length.

6. 50,000-pound payload, cargo size 22-foot diameter by 60-foot length.

The payload weight includes ten passengers with provisions and cargo; the payload sizes provide only for cargo. Additional volume will be provided for ten passengers. The weight of two crew members in the orbiter vehicle will be included in the weight of the shuttle vehicle system.

Improvement concepts will be investigated, but the following features are mandatory:

1. High angle of attack (approximately 60 degrees) to minimize heating (RCS will be used for control).

2. Fixed wings possibly with adjustable tips; wing shapes may be changed.

3. Fixed turbojets (no swing-out).

Figure 5.0-1. Baseline Vehicle Concept for Phase 2 of Study

SD 69-573-4

Space Division
North American Rockwell

4. No window covers.

5. A flat undersurface and a general cross section shape defined by NASA.

6. Vertical takeoff.

7. Two stages (reusable).

8. Propellant to be LO_2/LH_2.

9. High-pressure pump-fed bell or aerospike engines.

10. No ablative-cooled or transpiration-cooled thermal protection system.

11. Horizontal landing.

6.0 APPROACH AND STUDY SCHEDULE

The logic used in the second phase of the study is illustrated in Figure 6.0-1. The study established sizes and weights of the NASA MSC space shuttle vehicle concept for payloads specified in Section 5.0. Design improvement concepts were evaluated, and vehicle sensitivity to design variables was assessed. Conceptual design definitions of selected vehicles were provided. Resource plans and estimated system nonrecurring and recurring costs were defined. Technology advancement requirements were identified. Vehicle sizing studies and investigations of improvement concepts were performed during the six-week period after formal initiation of the second phase of the study. Data were then submitted to NASA MSC, where selection was made of the vehicle payload sizes and vehicle configurations for conceptual design. Conceptual design data and resource plans were generated for a selected vehicle during the last three months of the second study phase. The schedule for the study activity is presented in Figure 6.0-2.

6.1 CONCEPT SIZING AND PERFORMANCE ANALYSIS

Shuttle vehicle sizes and weights defined by NASA MSC were reviewed to establish system weight-scaling equations. Mandatory features of the shuttle vehicle are defined in Section 5.0. Aerodynamic characteristics of basic NASA MSC concept were investigated to confirm projected environment and performance. Flight trajectory analyses were performed to establish the optimum propellant distribution between the booster and orbiter vehicles to deliver the previously specified payloads. Wing and body sizes were established for the desired wing loading and heat rate on reentry. Methods of increasing vehicle lateral ranging capability were identified, and the impact on vehicle payload return capability or system weight was established.

Design, performance, and program implications for internal and external cargo provisions were identified. Weights and preliminary relative costs were also estimated.

6.2 DESIGN IMPROVEMENT CONCEPTS AND SENSITIVITY ANALYSIS

To establish design features that should be incorporated in the shuttle vehicle, candidate improvement concepts were evaluated to determine their impact on vehicle weight, performance, cost, safety, and technology requirements. Vehicle sensitivity analyses were performed to establish the impact of design criteria, engine performance deviations, system weight growth, and more stringent environments (such as reentry thermal load).

6.3 CONCEPTUAL DESIGN

Based on vehicle sizing and design improvement studies, vehicle configurations selected by NASA MSC were subjected to conceptual design analysis.

Aerodynamic characteristics of the vehicle elements for boost, reentry, flyback, and landing were established; and trajectories were computed for these mission phases. Control requirements and structural and thermal environments were calculated and used in the derivation of of major structure and thermal protection system weights.

System flight characteristics and control requirements for all mission phases were determined and rigid body loads analysis performed to compute structural loads during boost, reentry, and flyback maneuvers.

The effects of aerodynamic characteristics and the approach and landing methods, including manned and unmanned automatic landing, were assessed to establish the desirable approach and landing system.

Subsystem trade studies were performed, and conceptual designs were developed to facilitate estimation of vehicle weights. Preliminary definitions were prepared for vehicle subsystems, and the subsystems were analyzed to determine checkout procedures.

6.4 RESOURCE PLANS

Program requirements for the shuttle vehicle were analyzed to provide direction for design studies.

The possible application of aircraft development and testing approaches to the shuttle vehicle was examined to determine the impact on system development time and cost.

For selected vehicles, a test plan was developed and operations analyses were performed to define procedures and equipment requirements for prelaunch, launch, orbital operations, recovery, transportation, and servicing. Resource plans were developed, and system costs were estimated to Level 5.

6.5 TECHNOLOGY

Technology requirements were identified, and the potential impact of the technology program on the system performance, cost, and schedule was described.

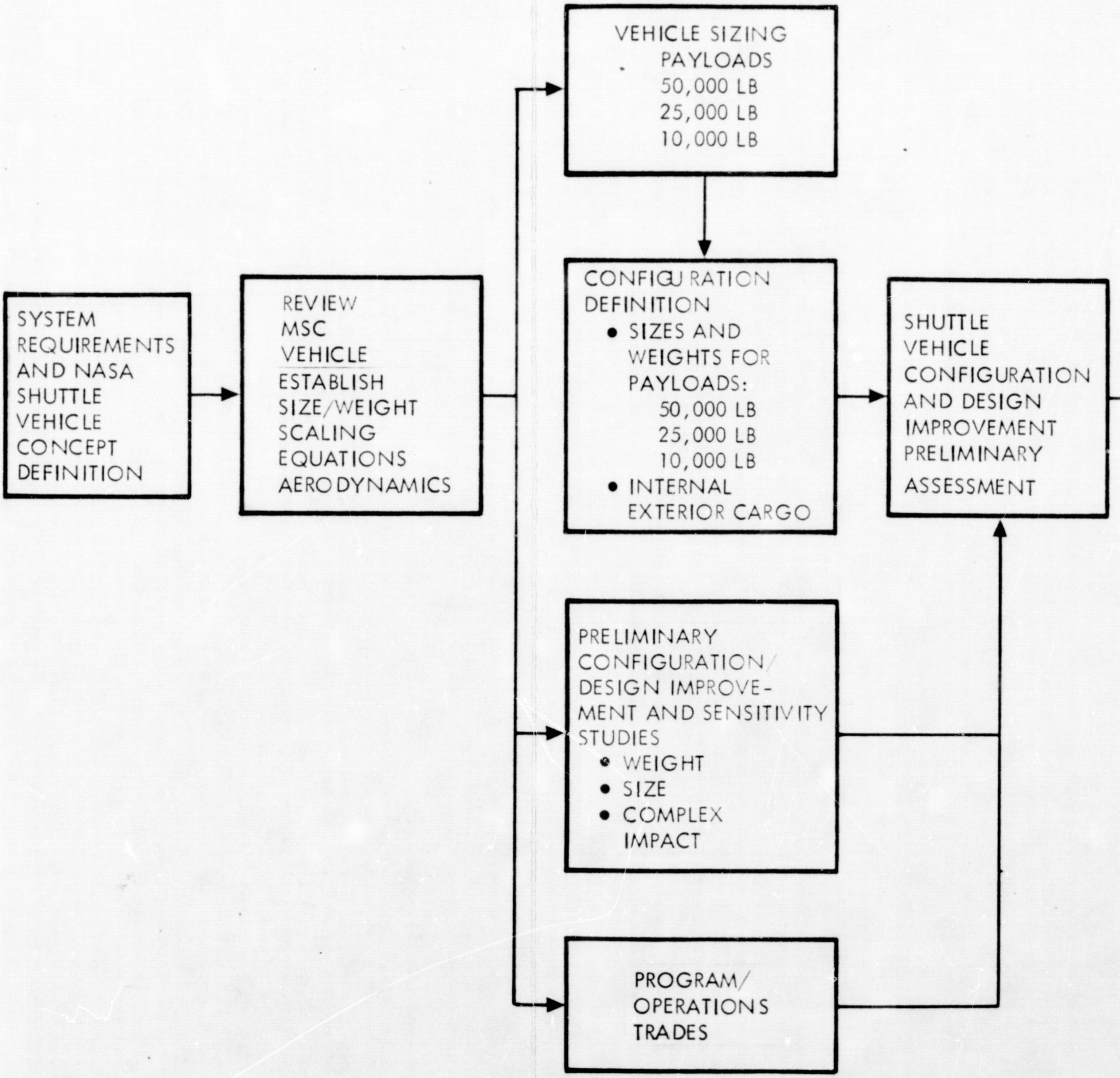

FOLDOUT FRAME 1

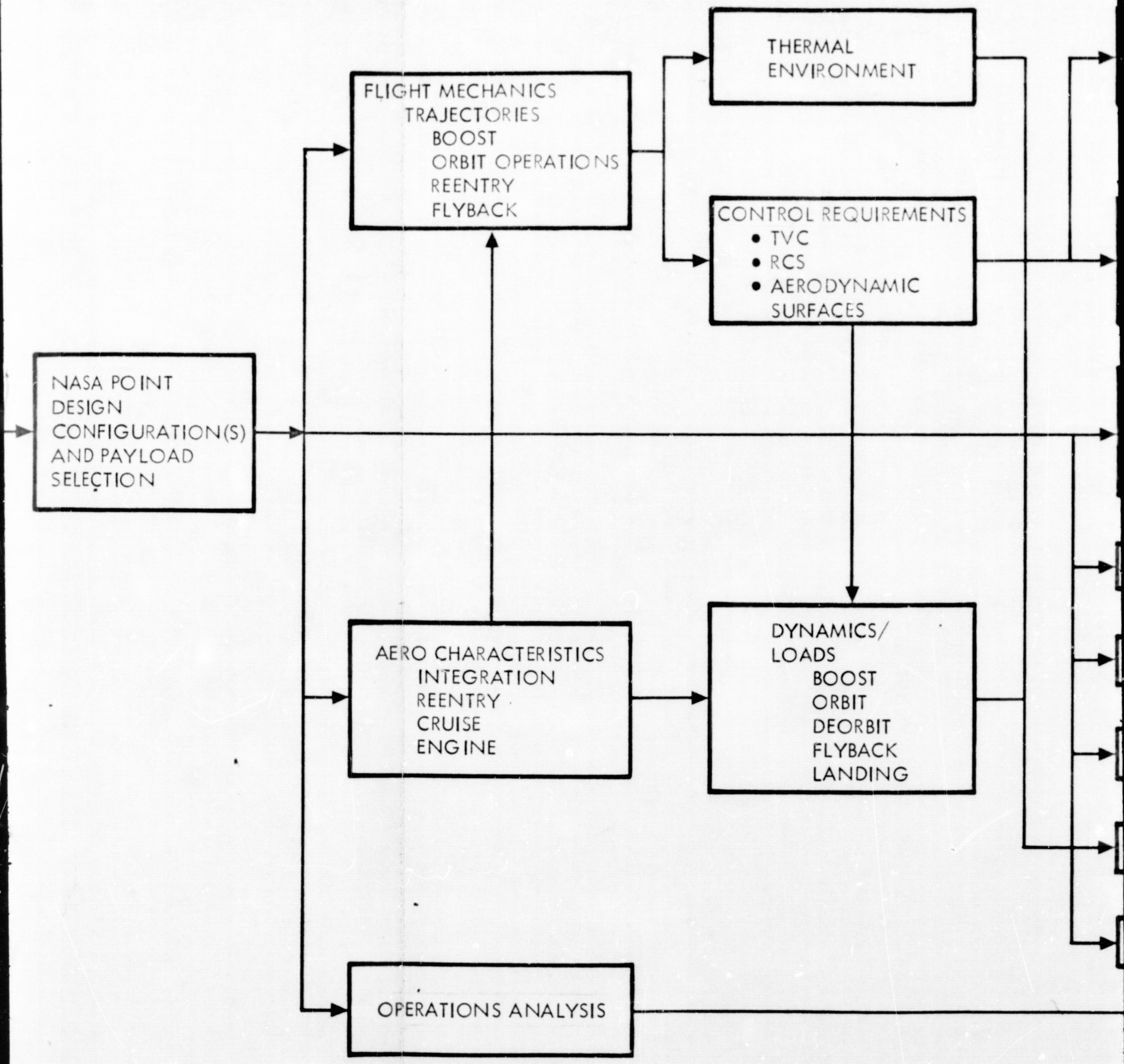

FOLDOUT FRAME 2

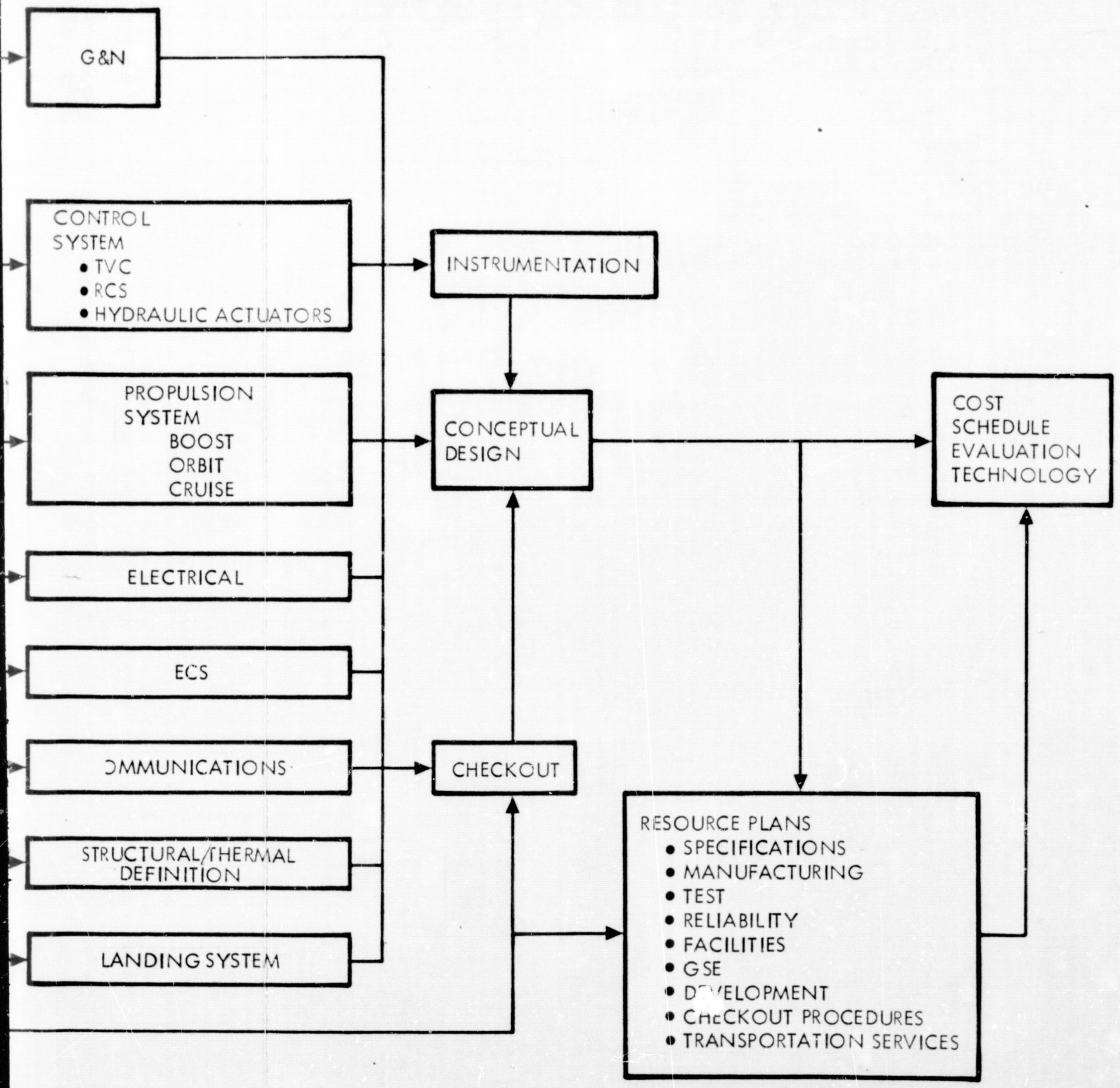

Figure 6.0-1. Phase 2 Study Logic

FOLDOUT FRAME 3

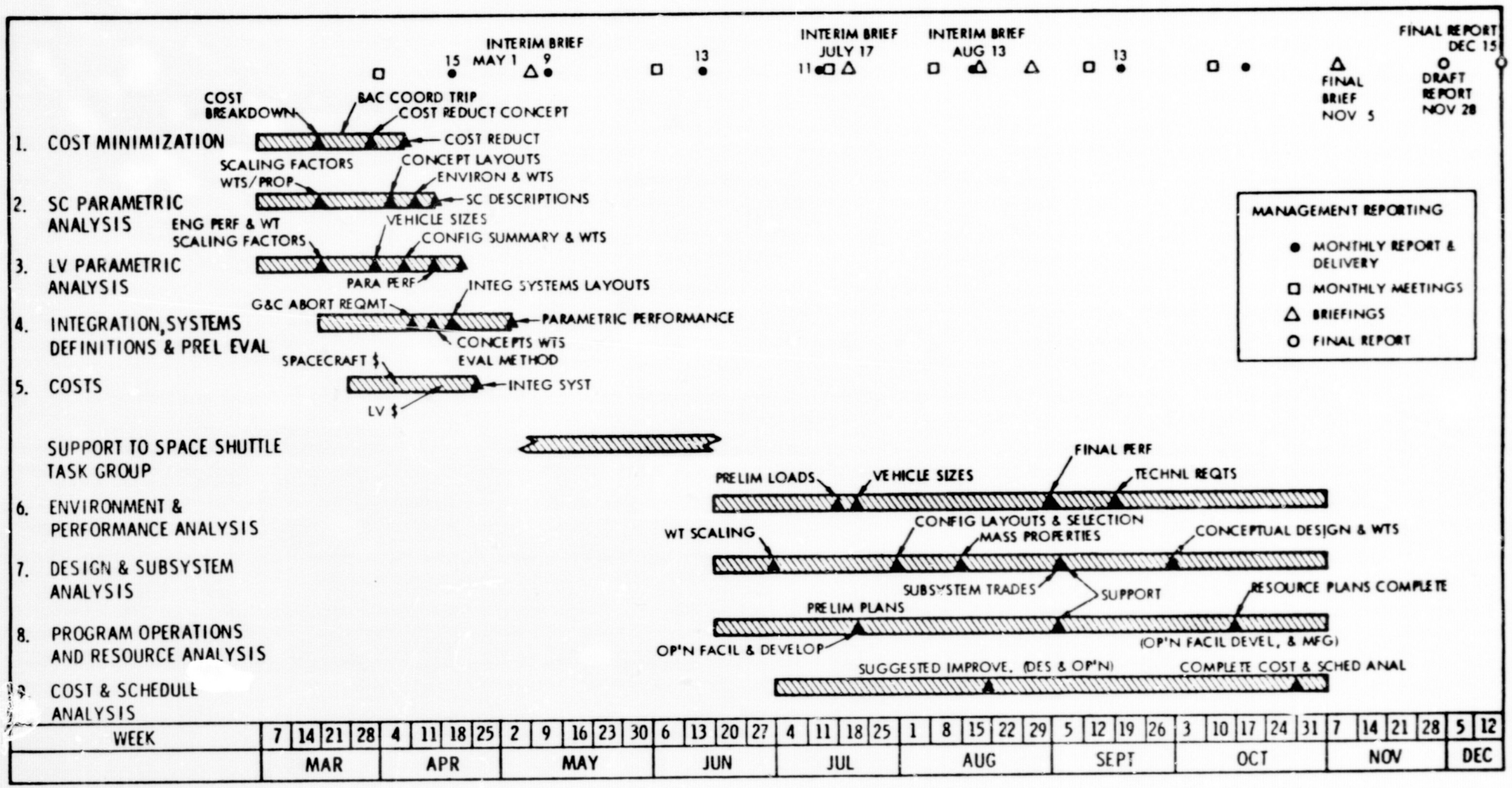

Figure 6.0-2. Phase 2 Study Schedule

6.5 TECHNOLOGY

Technology requirements were identified; and the potential impact of the technology program on the system performance, cost and schedule was described.

7.0 ENVIRONMENT AND PERFORMANCE SUMMARY

The vehicle design was established based on the environment and performance requirements reported in detail in Volume III of this report. The results of the environment and performance analyses are summarized in the following paragraphs.

7.1 FLIGHT PROFILE AND VEHICLE OPTIMIZATION

Flight analyses were performed to establish the optimum propellant distribution between orbiter and booster vehicle to minimize system gross weight. Eleven engines were selected for the booster to provide an optimum vehicle design. This selection was based on the use of two main engines on the orbiter and the same basic engine design on the two vehicle stages.

The flight profile for the selected vehicle is shown in Figure 7.1-1. The two-stage vehicle is launched vertically. Staging occurs at an altitude of 230,000 feet with a velocity of 10,800 fps. Separation is achieved by the use of rockets installed in the orbiter. They displace the vehicle laterally while the attitude of both stages is held constant with the reaction control system. After staging, the booster element rolls with an angle of attack of 52.5 degrees to minimize travel down range. Thus propellant required to cruise back to the landing site is minimized. The orbiter vehicle, after staging, is injected into an orbit of 50 by 100 nautical miles. Then it coasts to an altitude of 100 nautical miles, where the orbit is circularized. A Hohmann transfer is then used to place the orbiter vehicle in a rendezvous orbit of 270 nautical miles and 55 degrees inclination. The orbiter vehicle may remain with the space station from 5 to 30 days. After the orbiter is separated from the space station, a phasing operation is performed. It provides a reentry orbit compatible with location of the landing site. It is noted that the minimum orbital maneuvering velocity required to accomplish the mission is less than the specified design requirement. The orbiter vehicle reenters at a 60-degree angle of attack and maintains this attitude until the vehicle achieves subsonic velocities. After reentry, the orbiter vehicle is pitched over to a glide attitude of approximately 5 degrees to return to the landing site.

The general arrangement of the baseline configuration, sized for a 50,000-pound payload, is illustrated in Figure 7.1-2. Performance capability is summarized in Figure 7.1-3

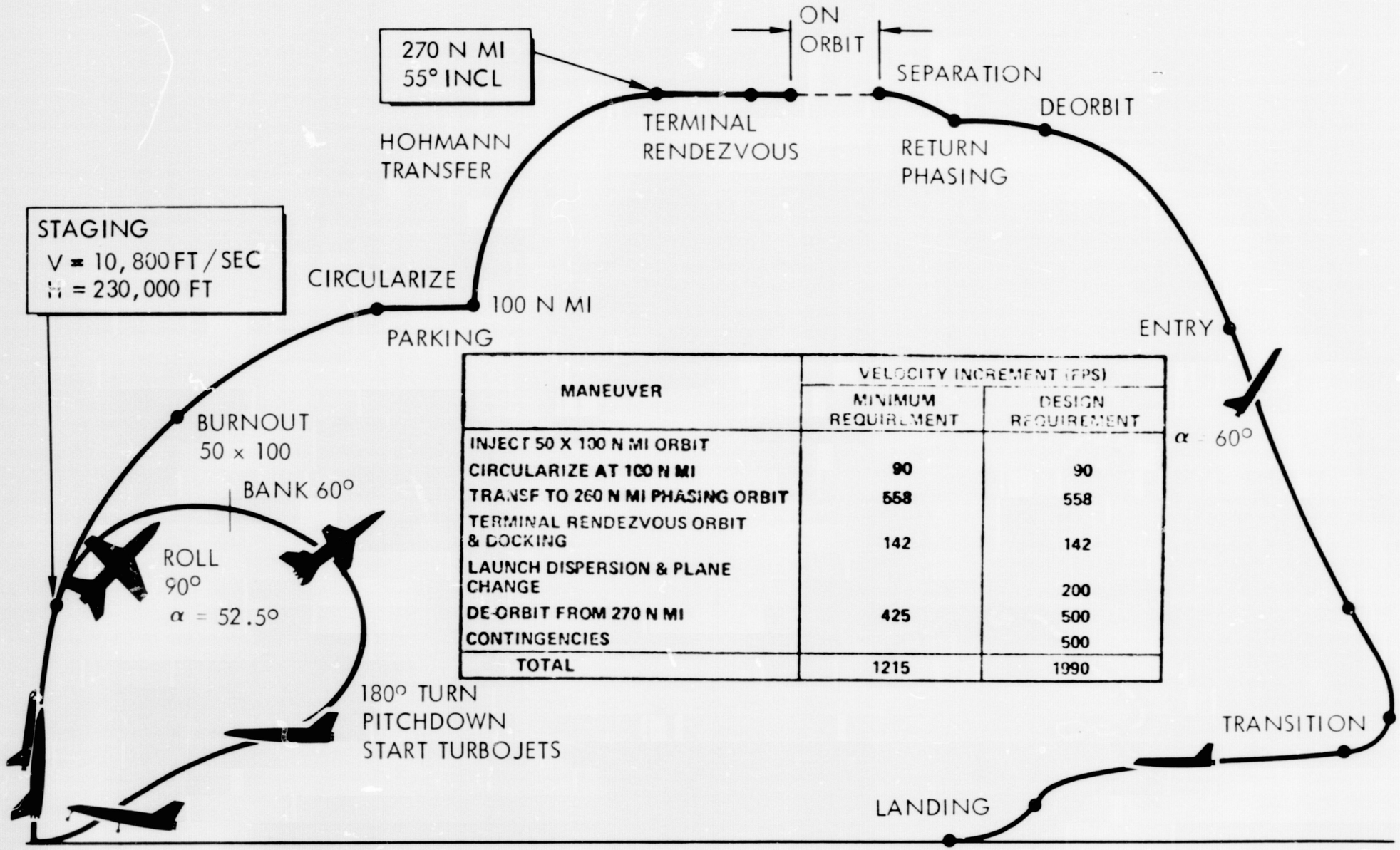

MANEUVER	VELOCITY INCREMENT (FPS)	
	MINIMUM REQUIREMENT	DESIGN REQUIREMENT
INJECT 50 X 100 N MI ORBIT		
CIRCULARIZE AT 100 N MI	90	90
TRANSF TO 260 N MI PHASING ORBIT	558	558
TERMINAL RENDEZVOUS ORBIT & DOCKING	142	142
LAUNCH DISPERSION & PLANE CHANGE		200
DE-ORBIT FROM 270 N MI	425	500
CONTINGENCIES		500
TOTAL	1215	1990

Figure 7.1-1. Flight Profile

Space Division
North American Rockwell

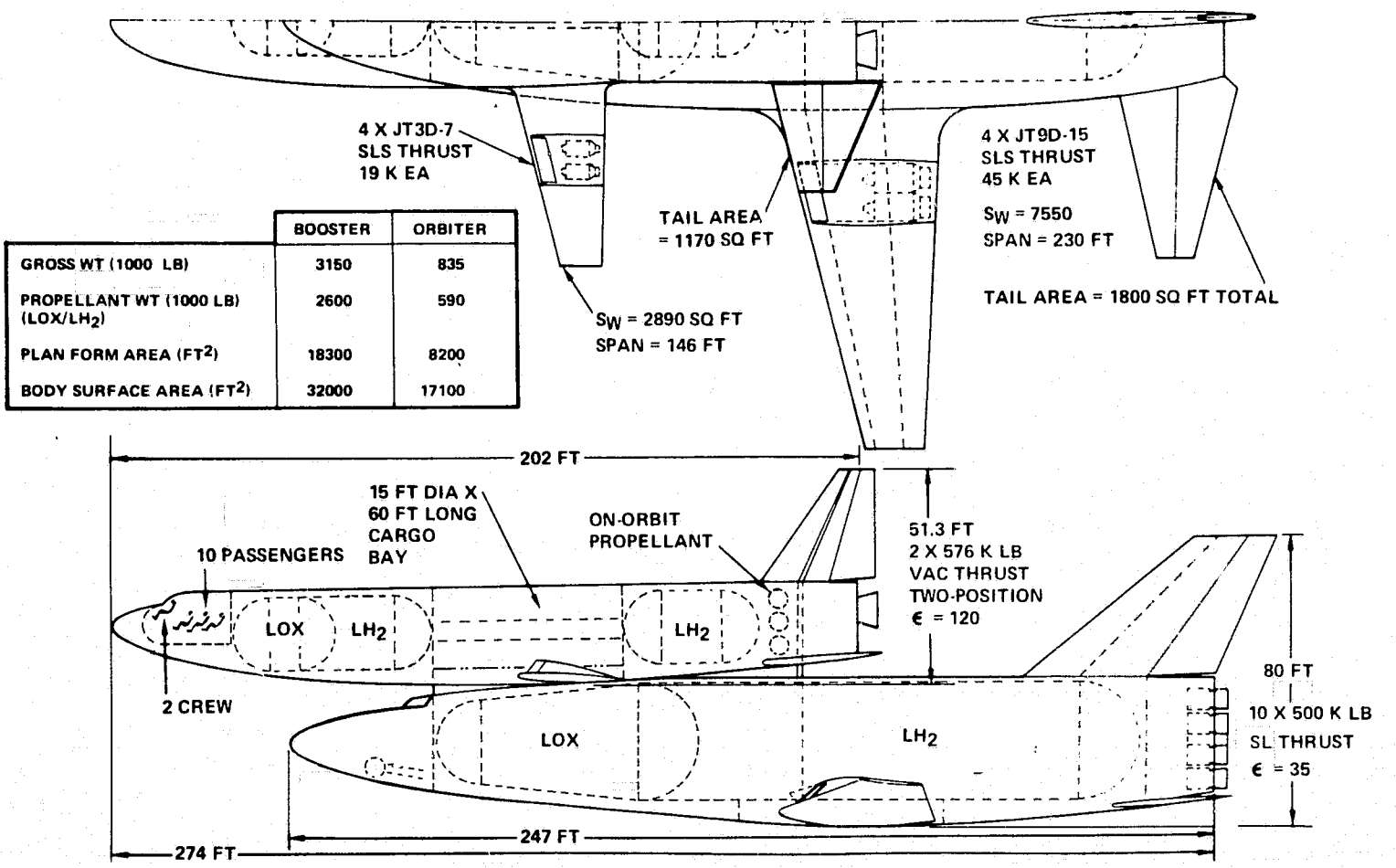

	BOOSTER	ORBITER
GROSS WT (1000 LB)	3150	835
PROPELLANT WT (1000 LB) (LOX/LH_2)	2600	590
PLAN FORM AREA (FT^2)	18300	8200
BODY SURFACE AREA (FT^2)	32000	17100

Figure 7.1-2. Baseline Vehicle Configuration

- KSC LAUNCH
- 50 X 100 N MI INJECTION
- MAX G 3

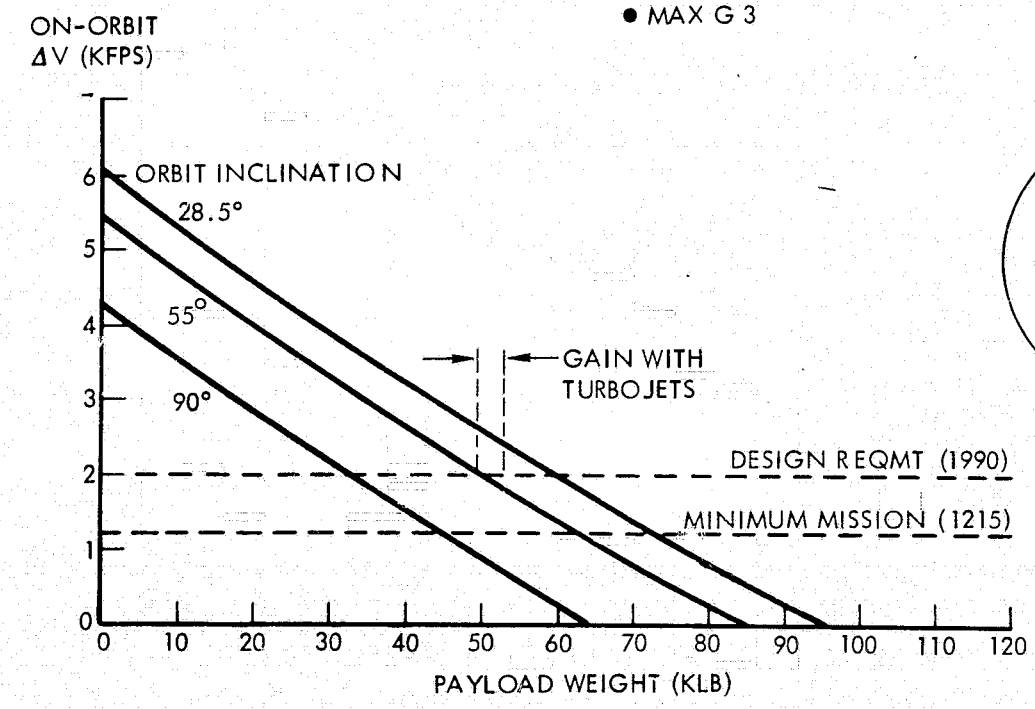

MAXIMUM PAYLOAD (LB)	
28.5° INCL	60,000
55° INCL	50,000
90° INCL	32,700

Figure 7.1-3. Payload Capabilities

7.2 AERODYNAMICS AND DESIGN IMPROVEMENTS

Aerodynamic characteristics of the orbiter and booster vehicles were based on an analysis and wind tunnel tests conducted by NASA. Because the center of gravity is forward during boost, the tandem launch configuration is statically stable from lift-off throughout regions of flight where high aerodynamic loads can be developed. This arrangement results in low thrust-vector deflection angles, a low angle of attack, and low aerodynamic loads.

The flight mode selected for entry and recovery of both stages is similar. Entry is performed at a high angle of attack and maintained until the vehicle decelerates to a low subsonic velocity; then transition to horizontal flight is performed. Test data confirm that the vehicle is stable and trimmable at the high angle of attack at supersonic, transonic, and subsonic speeds. The horizontal tail has been sized to provide a 7-percent static stability margin during subsonic cruise. These data also confirm that elevator effectiveness is sufficient for transition from a high to a low angle of attack.

Aerodynamic characteristics of the booster and orbiter configurations are summarized in Figure 7.2-1. Both vehicles employ a flat bottom on the fuselage. It is cambered to aid in pitch trim and stability at high angles of attack. The flat bottom and sharp corners also promote separation around the sides of the body, which results in low temperatures on the sides and upper surface during entry.

Lateral and directional stability is provided by body shaping. Directional stability is essentially neutral at the high angle of attack during entry. Roll stability is provided by wing dihedral.

Orbiter hypersonic L/D is 0.53 during entry at a 60-degree angle of attack and 7.3 during subsonic glide. The booster entry is performed at a 52.5-degree angle of attack at maximum-lift coefficient to permit life modulation and prevent excessive load factors during the flyback maneuver. L/D at entry is 0.69 and 8.4 during subsonic cruise.

Design improvement investigations indicate that:

1. Use of a radius on the lower body will allow reduced horizontal tail size. Additional effort is required to evaluate impact on thermal protection system and vehicle weight.

2. Directional stability can be improved by use of twin verticals or by use of dihedral on the horizontal surface.

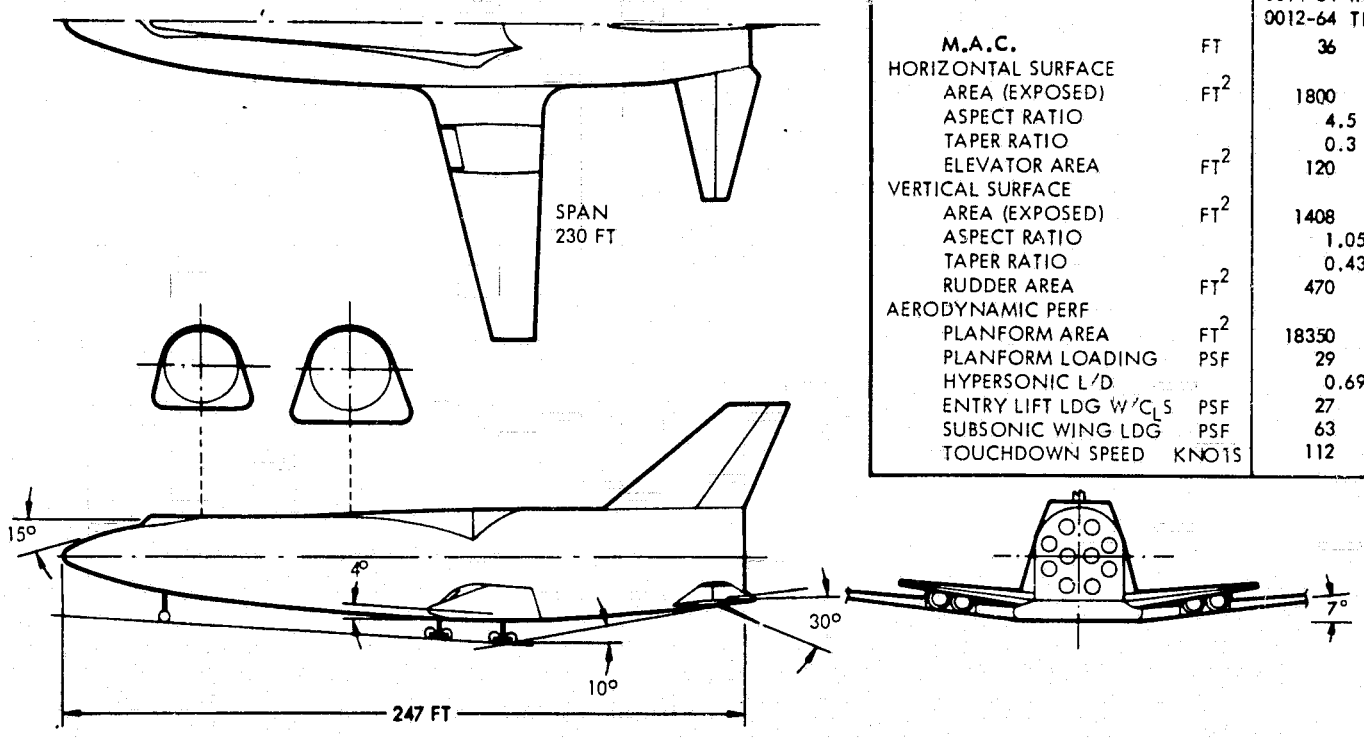

ITEM		
WING		
AREA (TOTAL)	FT^2	7550
ASPECT RATIO		7.0
TAPER RATIO		0.32
AIRFOIL		0014-64 ROOT 0012-64 TIP
M.A.C.	FT	36
HORIZONTAL SURFACE		
AREA (EXPOSED)	FT^2	1800
ASPECT RATIO		4.5
TAPER RATIO		0.3
ELEVATOR AREA	FT^2	120
VERTICAL SURFACE		
AREA (EXPOSED)	FT^2	1408
ASPECT RATIO		1.05
TAPER RATIO		0.43
RUDDER AREA	FT^2	470
AERODYNAMIC PERF		
PLANFORM AREA	FT^2	18350
PLANFORM LOADING	PSF	29
HYPERSONIC L/D		0.69
ENTRY LIFT LDG W/C_LS	PSF	27
SUBSONIC WING LDG	PSF	63
TOUCHDOWN SPEED	KNOTS	112

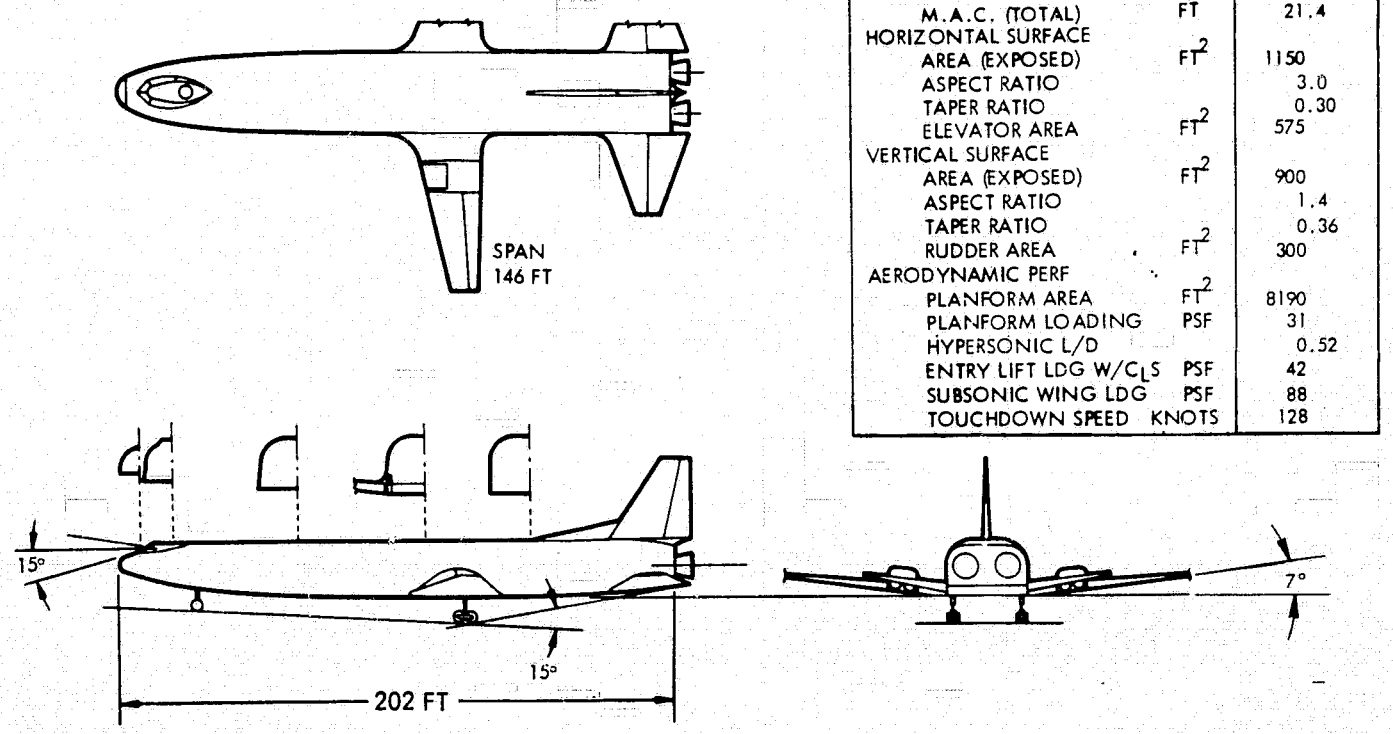

ITEM		
WING		
AREA (TOTAL)	FT^2	2890
ASPECT RATIO		7
TAPER RATIO		0.33
AIRFOIL		0014-64 ROOT 0012-64 TIP
M.A.C. (TOTAL)	FT	21.4
HORIZONTAL SURFACE		
AREA (EXPOSED)	FT^2	1150
ASPECT RATIO		3.0
TAPER RATIO		0.30
ELEVATOR AREA	FT^2	575
VERTICAL SURFACE		
AREA (EXPOSED)	FT^2	900
ASPECT RATIO		1.4
TAPER RATIO		0.36
RUDDER AREA	FT^2	300
AERODYNAMIC PERF		
PLANFORM AREA	FT^2	8190
PLANFORM LOADING	PSF	31
HYPERSONIC L/D		0.52
ENTRY LIFT LDG W/C_LS	PSF	42
SUBSONIC WING LDG	PSF	88
TOUCHDOWN SPEED	KNOTS	128

Figure 7.2-1. Booster and Orbiter Aerodynamic Configuration Characteristics

3. Incorporating roll-out of the body sides aft of the center of gravity is effective in improving directional stability.

4. Increased wing sweep and reduced aspect ratio should be investigated to improve flyback performance.

5. Because of the extreme aft location of the center of gravity on the booster (greater than 60 percent of the body length), the horizontal tail size becomes excessive. Moving the wing aft reduces the tail size. Use of a canard configuration should also be investigated as a way to minimize size of aerodynamic surfaces.

7.3 CONTROL CONCEPTS

The vehicle is controlled through main-engine thrust-vector control (TVC) during the ascent phase of the mission, by use of the reaction control system (RCS) for orbital maneuvers and entry, and by aerodynamic surfaces during subsonic flight.

For the vehicle loading environment to be satisfied, it is necessary to establish the vehicle control characteristics. In the study, the vehicle was analyzed for the ascent phase of the mission, with wind and gust profile based upon a 99-percent probability of nonoccurrence.

With a programmed flight-path angle, control mode, and a 7-degree main engine gimbal limit, the vehicle is subjected to maximum $q\alpha$ of 2970 psf-degree.

A 6-degree-of-freedom control simulation was performed for vehicle reentry. It showed that a control system authority of 0.5 deg/sec^2 acceleration is adequate. A simulation of the transition to cruise maneuver confirmed that pitch-over was smooth and well damped, with use of an elevator command incorporating gain scheduling.

7.4 ABORT

The impact of potential system failures was analyzed. The analysis indicated that failure of a single engine on either the booster or the orbiter will not prevent completion of the primary mission. A system failure requiring premature staging will necessitate action to limit reentry loads on the orbiter. For low-altitude mission termination, the orbiter with two engines operating will remain at low altitude. For high-altitude mission termination, the orbiter engines (one or two) may be used to shape the

trajectory and prevent excessive reentry loads. Failure of two orbiter engines, however, will cause excessive reentry loads and possibly make a water landing necessary. Propellant dumping is required to minimize entry loads in the event both orbiter engines fail.

7.5 THERMAL ENVIRONMENT

For thermal protection system requirements to be established, it was necessary to establish a thermal environment. During ascent, the vehicle is subjected to areas of interference heating on the upper surface of the body. The temperature of 800 F experienced on the upper surface of the orbiter is the critical design temperature condition and is in excess of that experienced during entry.

The most severe thermal environment condition for the under surface of the vehicle occurs during reentry. Figure 7.5-1 illustrates the radiation equilibrium temperature for the orbiter and booster. For reentry, the temperature is illustrated for two locations on the body and for a number of locations on the wing. The temperature is defined as a function of body station or percentage distance across the wing chord. The temperatures are based on vehicle reentry with a lift loading (W/C_LS) of 50 psf.

As shown in the figure, the orbiter experiences temperatures below 1500 F on 90 percent of the body. This thermal environment is based upon reentry at a 60-degree angle of attack. It should be noted, however, that the equilibrium temperatures on wing leading edges during reentry are significantly greater than temperatures experienced generally on the body. Radiation equilibrium temperatures on the wing leading edges are 2800 F to 3200 F without interference effects. Flow interference effects at 20-percent wing span could significantly increase leading-edge temperatures.

As illustrated in the figure, temperatures experienced by the booster during reentry are significantly lower than those experienced by the orbiter and are less than 1400 F on 90 percent of the vehicle.

7.6 LATERAL RANGING EFFECTS AND POTENTIAL

In view of the desire to establish vehicle potential for increased lateral range, investigations were performed to determine the impact of reentering at lower angles of attack. Figure 7.6-1 illustrates orbiter body and wing temperatures and heat load experienced during entry at various angles of attack. As illustrated, the vehicle can achieve approximately 1240 nautical miles of lateral ranging capability at a 20-degree angle of attack without exceeding the temperature limitations of the proposed densified quartz material, except for wing leading edges. The increased heat

REENTRY

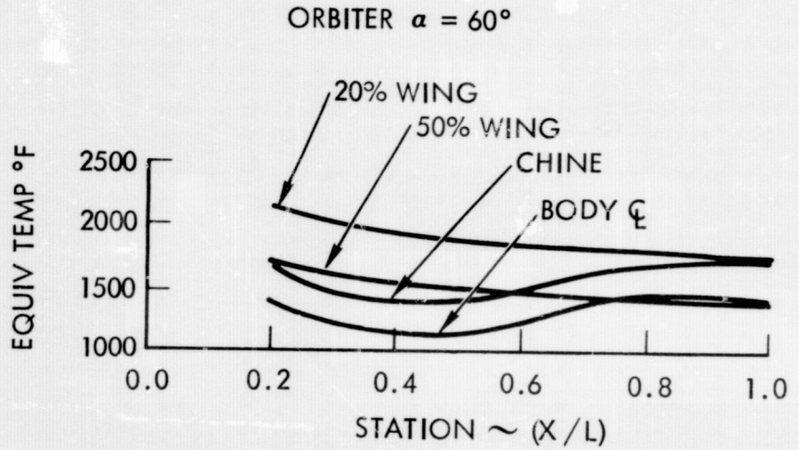

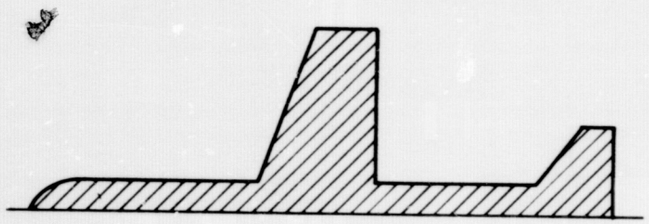

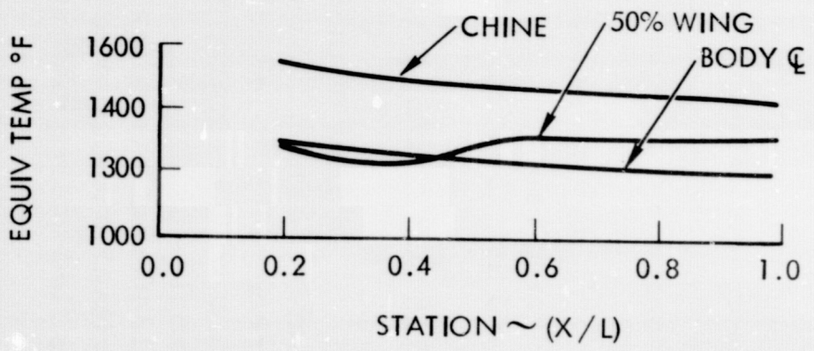

SUMMARY

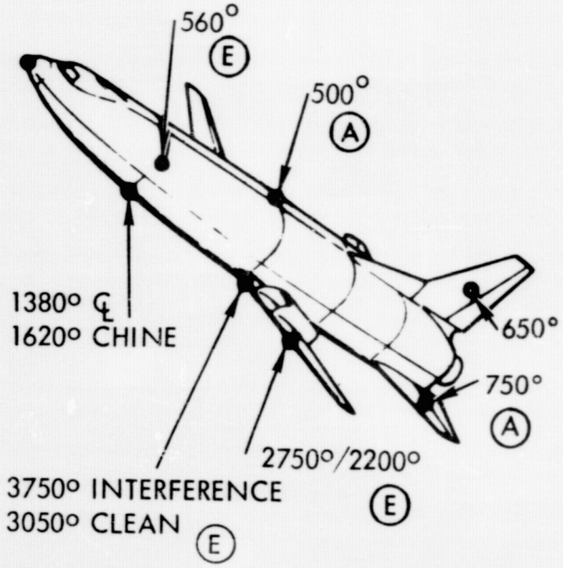

LOCATION	CRITICAL FLIGHT CONDITIONS	RADIATION EQUILIBRIUM TEMPERATURE (°F)	
		BOOSTER	ORBITER
FUSELAGE			
NOSE	ENTRY	1275	1860
LOWER SURFACE 20%	ENTRY	1380	1420
LOWER SURFACE 80%	ENTRY	1220	1450
CHINE	ENTRY	1530	1620
SIDE	ENTRY	540	560
UPPER SURFACE	ASCENT	500	500
WING			
L.E. (NO INTERFERENCE)	ENTRY	2200	3000
LOWER SURFACE 20%	ENTRY	1400	1700
UPPER SURFACE 20%	ASCENT	650	700
HORIZONTAL SURFACE			
L.E.	ENTRY	2020	3450
LOWER SURFACE	ENTRY	1390	1500
UPPER SURFACE	ASCENT	600-650	700
VERTICAL SURFACE			
L.E.	ASCENT	1730	2320
SIDE	ASCENT	600-650	650

Figure 7.5-1. Thermal Environment

Space Division
North American Rockwell

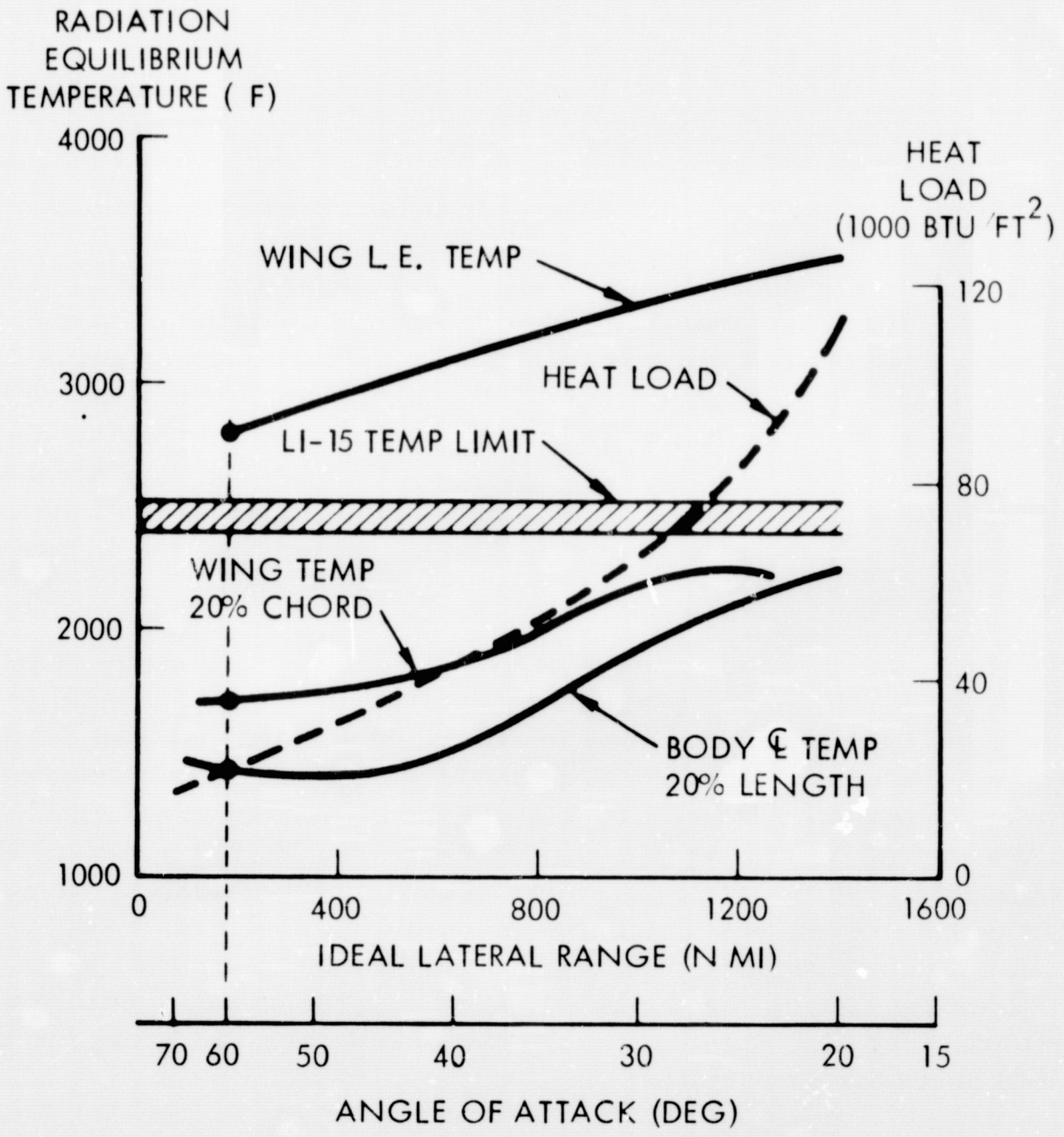

Figure 7.6-1. Orbiter Lateral Range Potential

load, however, with the greater lateral ranging, will require an increase of approximately 22,000 pounds in thermal protection system weight.

The lateral ranging capability of the vehicle can also be increased to 1500 nautical miles by cruising with the turbojet engines and offloading payload and adding turbojet fuel.

7.7 APPROACH AND LANDING

To limit logistics vehicle weight, it becomes extremely important to optimize booster cruise and orbiter landing system weights. Booster descent and turnaround studies were conducted to minimize flyback range. A range of 310 miles was established for the 50,000-pound-payload-class system by developing a banked entry flight mode. This range is 24-percent less than that of a straight-in entry. Optimization of the booster flyback propulsion system resulted in selection of a system employing four JT9D-15 turbojets and flying at Mach 0.38. The system having the lowest weight was that having the fewest engines and cruising at an off-optimum Mach number. The saving in engine weight was greater than the increased fuel weight required for cruise at off-optimum conditions.

The baseline orbiter vehicle, in accordance with study requirements, is configured to provide go-around capability in event of a landing wave-off. Four JT3D-7 turbojets are used in the 50,000-pound-payload orbiter. Total engine and fuel weight is 20,240 pounds, with 82 percent of that weight due to the engines themselves. Deletion of the climb-out capability by eliminating two engines would reduce system weight by 10,120 pounds. Use of high thrust-to-weight ratio turbojets should be investigated. It was estimated that a 9740-pound weight saving could be realized.

Landing speeds for the booster and orbiter are compatible with present transport aircraft. Nominal touchdown speeds are 113 knots for the booster and 128 knots for the orbiter.

7.8 DESIGN LOADS

Design structural loads were defined for the following flight conditions:

1. Prelaunch, with 99.9 percentile ETR ground winds
2. Maximum qo, 2940-psf-degree, with 95 percentile ETR winds aloft
3. Maximum acceleration, 3.0 g's for both stages

4. Booster entry, 4.0 g's maximum

5. Orbiter entry, 2.1 g's maximum

6. Transition to cruise maneuver, 2.5 g's

7. Landing - 10 fps sink speed, 1.4 gear load factor, 1.2 body load dynamic factor

Maximum body loads are summarized in Table 7.8-1 for the 50,000-pound-payload-class system.

Table 7.8-1. Structure Design Loads Summary,
50,000-Pound-Payload System

	Load Station (Inches from booster tail with orbiter attached)	Condition	Limit Loads		
			Axial x 10^{-3} (lb)	Shear x 10^{-3} (lb)	Moment x 10^{-6} (in.-lb)
Booster	2870 (Forward attach)	Max qα	-1865	525	250
	2000 (LOX tank aft bulkhead)	Max qα	-4292	-207	-150
		Max accel	-3872	117	430
	1430 (Aft attach)	Max qα	-4736	-311	-1.10
		Max accel	-4010	459	357
	1350 (Main gear)	Landing	-185	500	-430
	100 (Hold-down)	Prelaunch	-3985	-340	520 (tilt) 740 (no tilt)
Orbiter	2870 (Forward attach)	Max qα	848	484	215
		Max accel	-1552	254	488
	2320 (Main gear)	Max accel	875	270	344
		Landing	-195	-340	-96
	1430 (Aft attach)	Max qα	140	-284	-29
		Max accel	80	334	-0.63

Space Division
North American Rockwell

8.0 DESIGN AND SUBSYSTEM ANALYSIS

Results of the shuttle vehicle design and subsystem analyses and description of the shuttle vehicle conceptual design definition developed to perform the mission requirement are presented in this section. In developing the conceptual design definition, overall vehicle configurations, sizes, general arrangement, and subsystem conceptual definition were established. This detail information provided the necessary base for establishing vehicle weight and cost at the subsystem level.

The study was conducted in two phases: (1) concept sizing phase for various payloads and (2) conceptual design phase for a selected payload. In the concept sizing phase, several payload weights and cargo-bay sizes were considered. A configuration size and weight was established for each payload weight and cargo-bay size. Structures, thermal protection, and propulsion analyses were conducted to support the configuration sizing and weights analysis. These analyses are discussed in subsequent sections. Other system weights were estimated on the basis of historical data and past design study results.

In the conceptual design phase, emphasis was placed on a vehicle to deliver a 50,000-pound payload with a 15-foot-diameter by 60-foot-length cargo bay. Definition of a baseline configuration included a baseline configuration drawing, preliminary weight statement, and mass properties. These data were used to establish the nominal trajectory, vehicle loads, thermal environment, and control requirements and to provide guidance for vehicle design and subsystem analyses. Next, various design improvements to the baseline configuration were studied; and finally, a configuration selection was made for detail weight and vehicle-balance analyses. Based on the detail weight analysis, the booster and orbiter burnout weights were 3.1 percent less and 8.7 percent greater, respectively, than the weights given in the preliminary weight statement; therefore, the vehicle was resized to maintain the 50,000-pound-payload capability. These data are presented as the final weight statement and overall vehicle dimensions.

Limited activity was conducted to size a shuttle vehicle with a 25,000-pound-payload capability and a 12-foot-diameter by 48-foot-length cargo bay based on results of the detail weight study.

8.1 CONFIGURATION AND DESIGN GUIDELINES

Some of the more important configuration and design guidelines utilized during the study are illustrated in Figure 8.1-1 and will be reviewed prior to the detailed system discussions to follow.

The orbiter configuration provides for two crew members and ten passengers located forward with the crew. Access to the cargo bay by the crew and passengers is to be provided. The passengers and their provisions are considered part of the vehicle payload. The booster is unmanned for the primary mission; however, accommodations are provided for two pilots to perform a ferry mission.

The LO_2 propellant, which is the largest weight item at launch, is located forward in both the booster and orbiter. This arrangement provides an aerodynamically stable vehicle during boost by locating the vehicle center-of-gravity forward of the center-of-pressure.

The cargo bay is centered over the orbiter center-of-gravity at landing to provide a balanced configuration with and without cargo on board. Cargo bay design must accommodate transfer of small cargo modules and transfer of a payload approximately equal to the cargo bay dimensions.

Turbojet engines used for cruise, landing, and go-around capability are a fixed installation.

The booster and orbiter utilize a common main rocket engine with two different nozzles. One-engine-out capability is provided for both the booster and orbiter. Total booster thrust must provide an initial thrust-to-weight (T/W) ratio of at least 1.25, and the total orbiter thrust must provide a sea-level T/W ratio greater than 1 (1.125 selected).

The fixed wings used for both the orbiter and booster have dihedral for roll stability. The ratio of the orbiter landing weight to the theoretical wing area is set at approximately 90:1 to provide a low landing speed. The ratio of the booster average cruise-back weight to the theoretical wing area is set at approximately 70:1 to provide efficient cruise and low landing speed.

A flat-bottom planform is provided for both the orbiter and booster. The ratio of the orbiter and booster reentry weight to the planform area (body and aerodynamic surfaces) is set at approximately 30:1 to provide a low-temperature environment.

Hard chines are provided on the lower body to provide hypersonic stability and flow separation at entry. Also, the body forward of the wing is sloped inward, and the lower body is cambered to provide hypersonic stability.

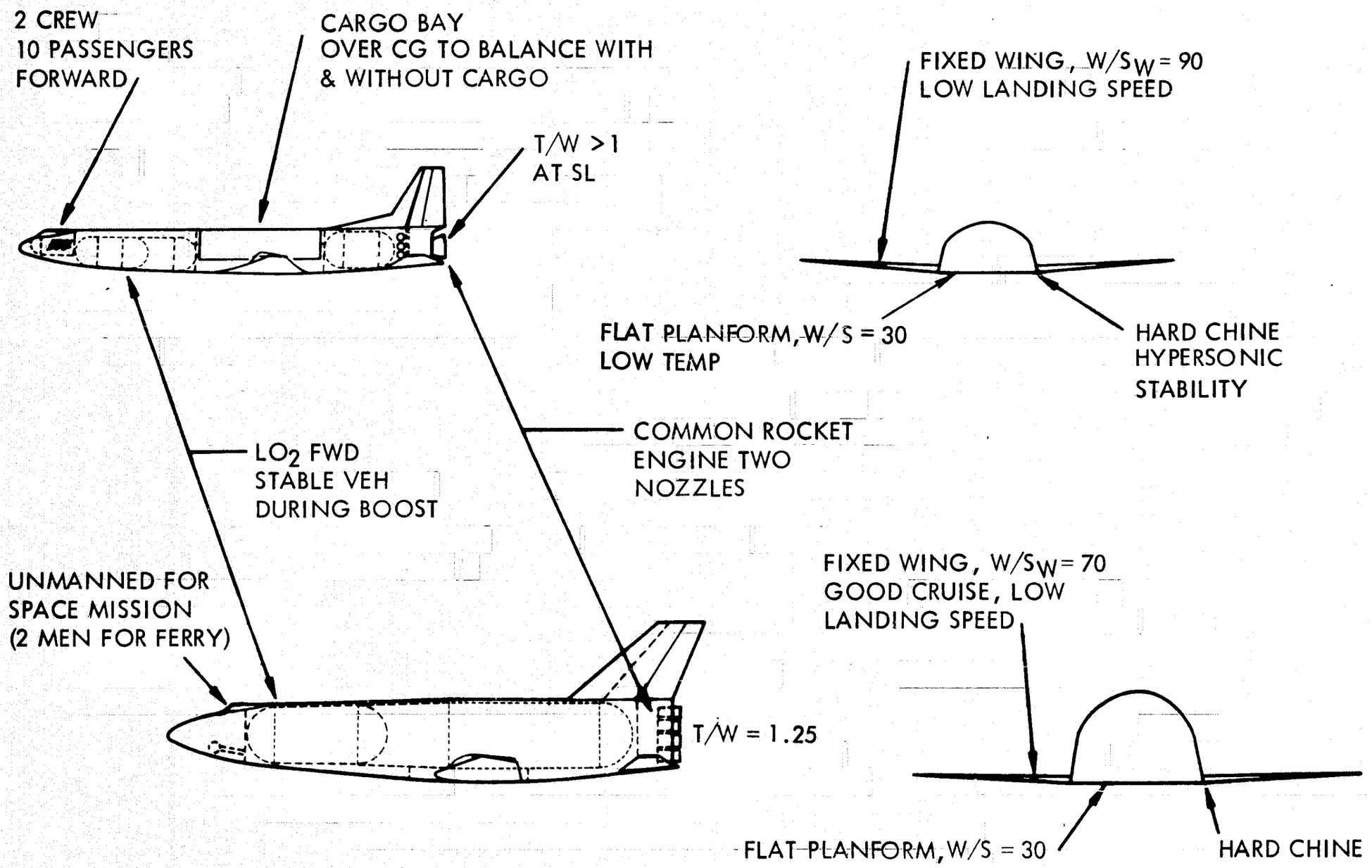

Figure 8.1-1. Shuttle Vehicle Configuration Guidelines

8.2 DESIGN

The following design sections present the baseline configuration established to initiate the contract studies. Vehicle configuration drawings and vehicle sizes developed for a range of payload weights and cargo bay sizes are given; results of configuration and design improvement studies or alternatives are described; and conceptual design of a vehicle with 50,000-pound-payload capability and a 15-foot-diameter by 60-foot-length cargo bay is defined.

Using the final weight scaling relationships obtained from the detail conceptual design activity, the overall configuration size of a shuttle vehicle with 25,000-pound payload capability and a 12-foot-diameter by 48-foot-long cargo bay is established and defined.

8.2.1 Baseline Vehicle Definition

A baseline vehicle configuration drawing was established to initiate the NR contract studies. This configuration drawing aided in the general concept review, weight scaling, mass properties, aerodynamic, thermal environment, structural loads, and control analyses. The vehicle configuration is shown in Figure 8.2-1 (Drawing 2234-50) and is based on information provided by MSC at the beginning of this contract phase. This configuration was designed to contain 12,500 pounds of payload in 2,000 cubic feet of cargo space located aft of the crew. Other pertinent configuration features are presented in Table 8.2-1.

8.2.2 Conceptual Layouts for Various Payloads

During the concept sizing phase of the study, vehicle sizing was conducted for various payload sizes and cargo bay sizes as illustrated in Table 8.2-2. Early in this phase, a series of typical booster and orbiter configurations were prepared to support the generation of parametric weight-scaling data. The vehicle sizing analysis (reported in Volume III) determined the orbiter and booster gross weight and propellant requirements.

Once the vehicle sizes were determined for each payload shown in Table 8.2-2, configuration layouts were prepared to establish overall vehicle size and general arrangement to support vehicle weight estimates and parametric vehicle costing. Pertinent configuration guidelines established for use in preparing the booster and orbiter layouts are as follows.

REPRODUCIBILITY OF THE ORIGINAL PAGE IS POOR.

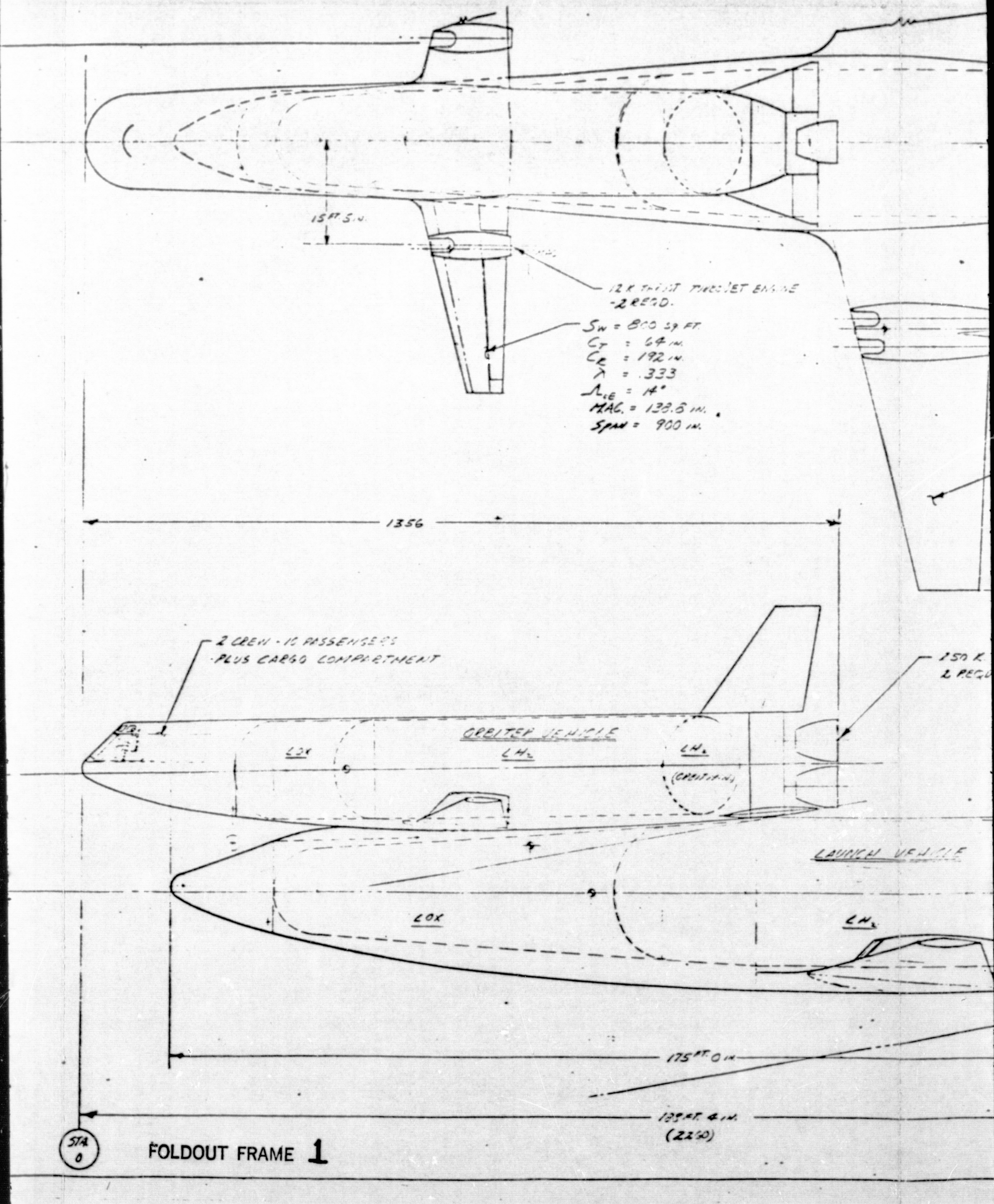

FOLDOUT FRAME 1

REPRODUCIBILITY OF THE ORIGINAL PAGE IS POOR.

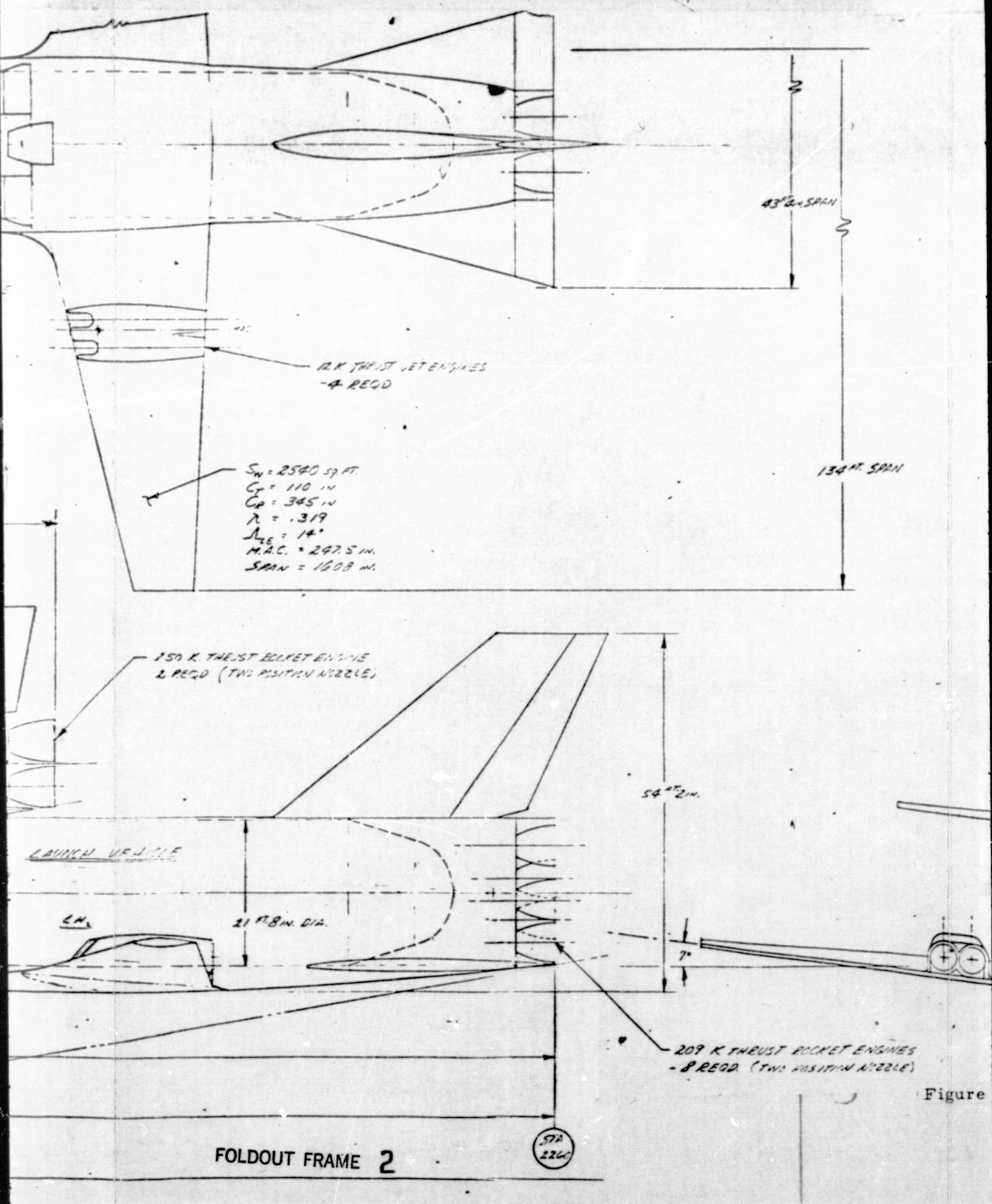

FOLDOUT FRAME 2

Figure

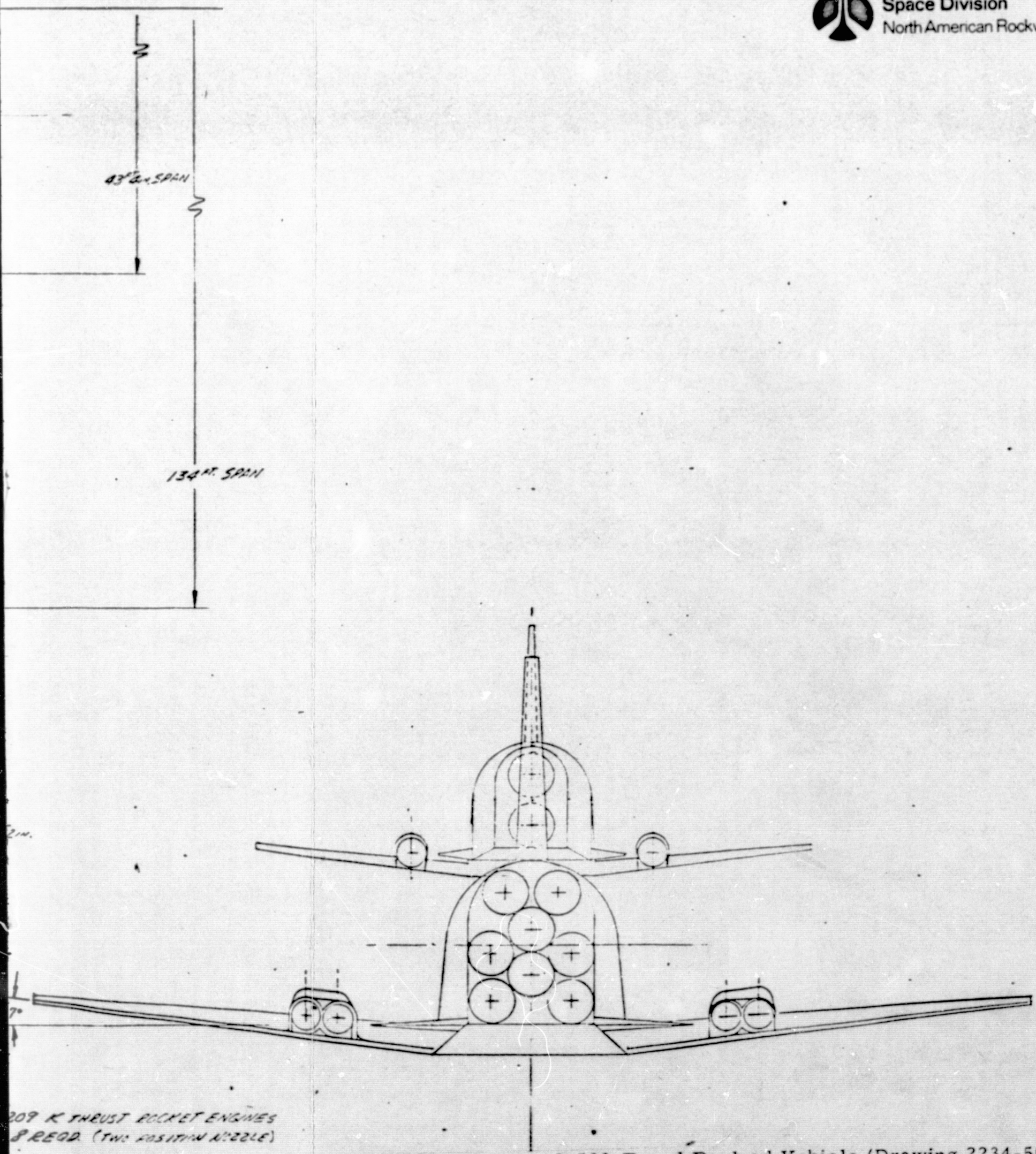

Figure 8.2-1. Baseline 12,500-Pound-Payload Vehicle (Drawing 2234-50)

FOLDOUT FRAME 3

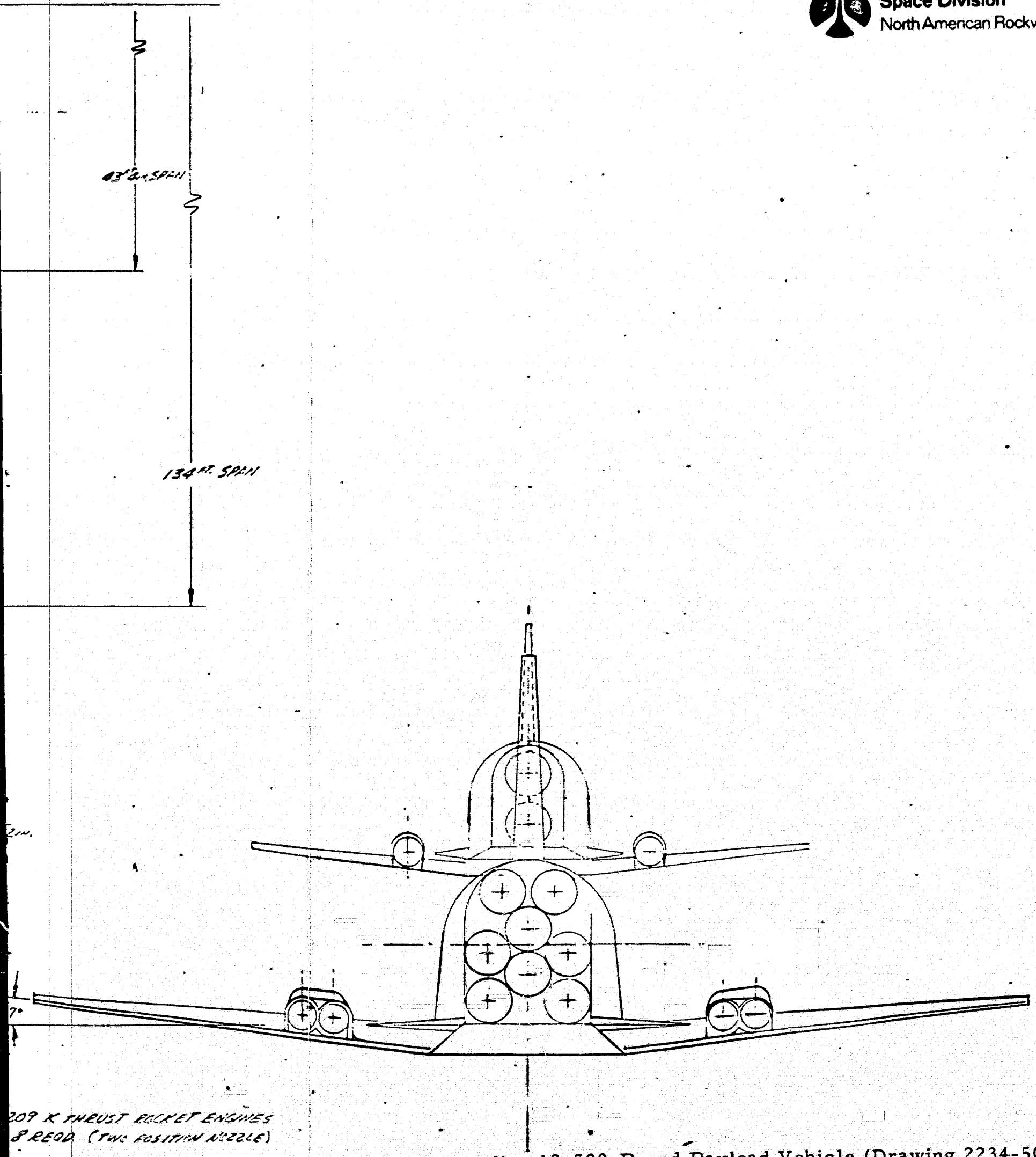

Figure 8.2-1. Baseline 12,500-Pound-Payload Vehicle (Drawing 2234-50)

FOLDOUT FRAME 3

Table 8.2-1. Initial Baseline Configuration Features

Feature	Booster	Orbiter
Weights (1,000 lb)		
Landing	178.8	69.3
Insertion/burnout	199.1	85.0
Ascent propellant	836.7	230.7
Launch	1,035.8	315.7
Size		
Body length, including engine (ft)	175	113
Wing span (ft)	134	75
Wing area, theoretical (ft^2)	2,540	800
Body wetted area (ft^2)	13,500	6,000
Plan area (ft^2)	5,900	2,340
Body volume (ft^3)	76,300	23,810
Propulsion		
Number of rocket engines	8	2
Thrust per engine (1,000 lb)	209 (SL)	250 (vac)
Number of turbojets	4	2
Thrust per engine, SLS (1,000 lb)	12	12

Table 8.2-2. Various Payload Sizes

Payload Class (lb)	Cargo Bay Size (ft)	
	Diameter	Length
10,000*	9	35
25,000	15	30
25,000	15	60
50,000	15	60
50,000	22	60

*Booster and orbiter to use 300,000-pound vacuum-thrust high-chamber-pressure bell engine

1. Weight at entry: stage gross weight less propellant weight

2. Landing weight

   0.982 times the entry weight for orbiter

   0.939 times the entry weight for booster

3. Landing weight/wing area (theoretical)

   90 psf for orbiter

   70 psf for booster

4. Entry weight/planform area (fuselage, wing, and horizontal): 30 psf.

5. Angle of attack at entry: 60 degrees.

6. Wing geometry:

	Orbiter	Booster
Aspect ratio	7	7
Taper ratio	0.333	0.319
Leading edge sweep (degrees)	14	14
Root section depth (percent)	14	14
Tip section depth (percent)	12	12
Angle of incidence (degrees)	4	4
Dihedral (degrees)	7	7
Wing leading edge at body centerline (percent of body length)	42	54.3

Wing located with 38-percent MAC at weight empty c.g.

Wing spars located at 15-percent and 65-percent chord

7. Vertical tail geometry:

	Orbiter	Booster
Leading edge sweep (degrees)	35	50
S_V (exposed)/S_W (theoretical)	0.209	0.20
Aspect ratio	1.5	1.049
Airfoil thickness (percent)	6	6

8. Horizontal tail constructed in plan view by a 15-degree half-angle delta originating at 65.5-percent BL for orbiter and 54.3-percent BL for booster. Horizontal tail trailing edge at end of body.

9. Propellant tankage:

   Volume sized for 1.1 times usable propellant volume

   LO_2 tank located forward

   Maximum diameter, 33 ft

10. Fuselage length determined by iteration considering:

    Fuselage plan area required

    Propellant packaging

    Maximum section width required to enclose payload with 0- to 15-degree sides sloping inward

    Maximum depth of section required to contain cargo, wing carry-through structure, and landing gear.

11. Maximum tail-down line of 10 degrees

12. Ground line at -3.5 degrees

13. Cargo bay centered at estimated orbiter c.g.

14. Same rocket engine used in orbiter and booster with different nozzles

15. Rocket engine expansion ratio

    100:1 to 120:1 for orbiter

    35:1 to 50:1 for booster

16. Jet engines mounted in nacelles on top surface of wing

17. Total turbojet engine thrust is 0.3 times landing weight

Layouts of orbiter and booster vehicles configured to deliver various payloads are shown in Figures 8.2-2 through 8.2-11 (Drawings 2234-65, -64, 54A, -56, -59, -58, -61, -60, -63, and -62). Characteristics of these vehicles are summarized in Table 8.2-3.

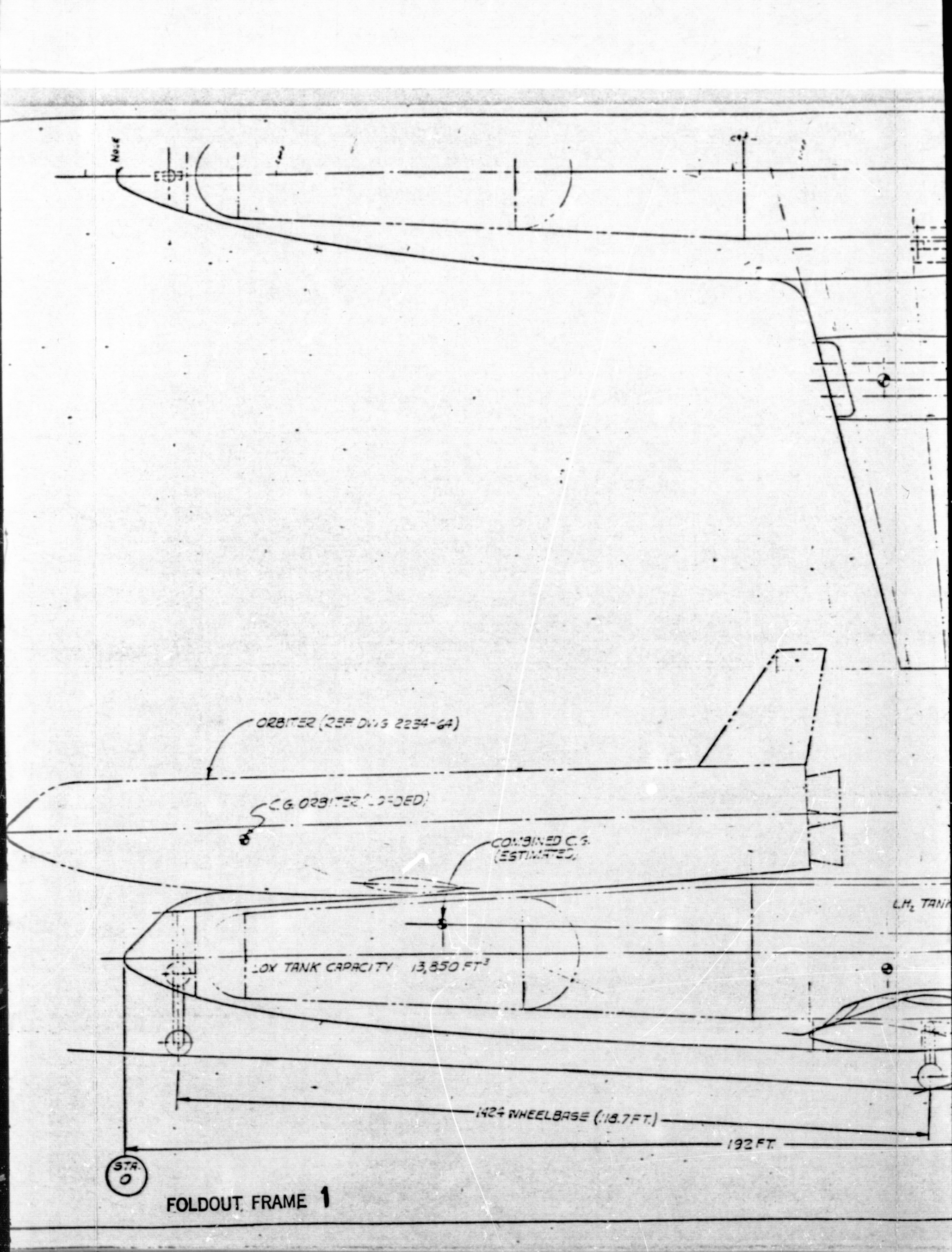

FOLDOUT FRAME 1

REPRODUCIBILITY OF THE ORIGINAL PAGE IS POOR.

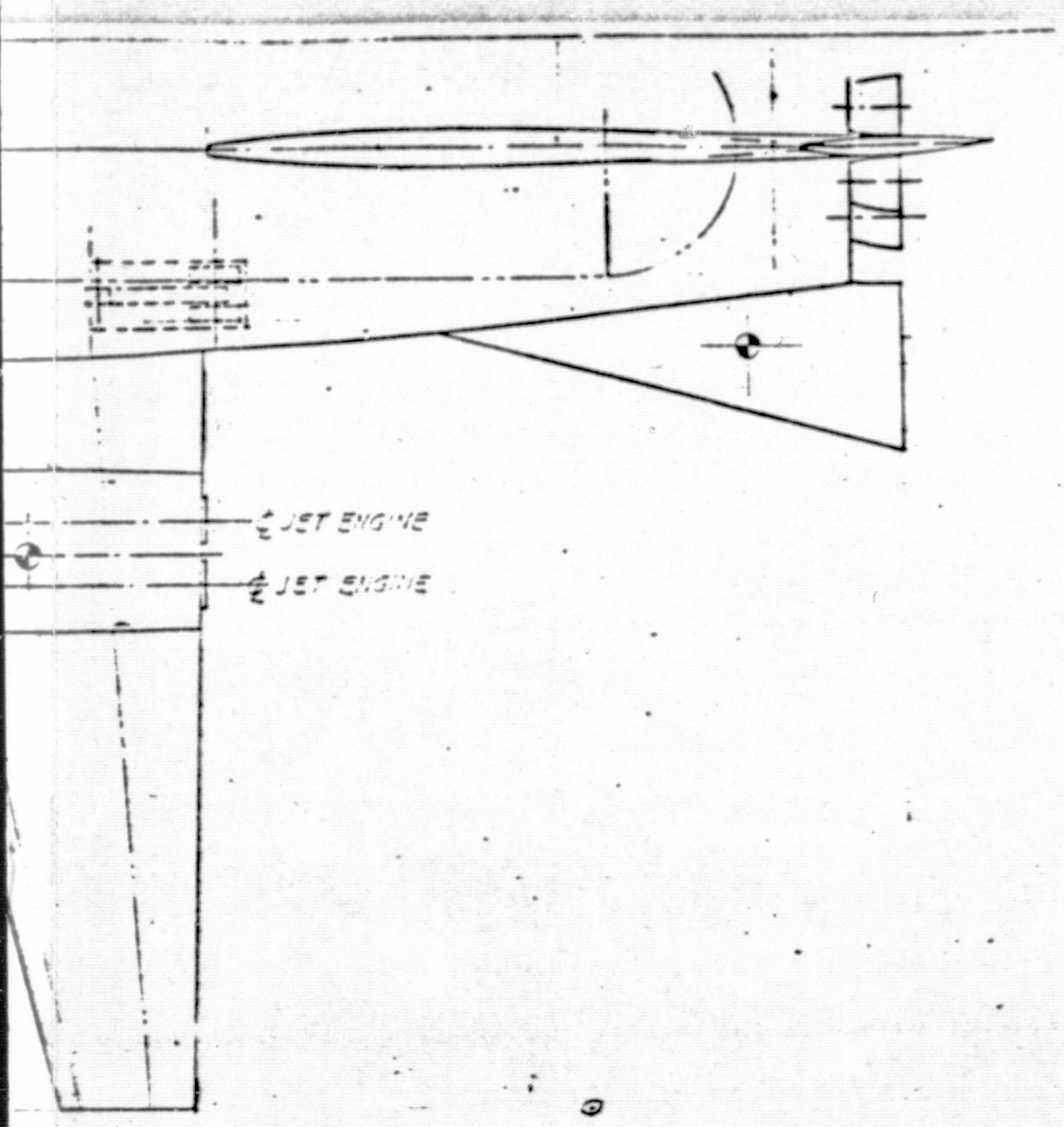

WING GEOMETRY

AREA	3500 FT²
SPAN	157 FT
C_R	33.9 FT
C_T	10.8 FT
Λ_{LE}	14°
λ	.319

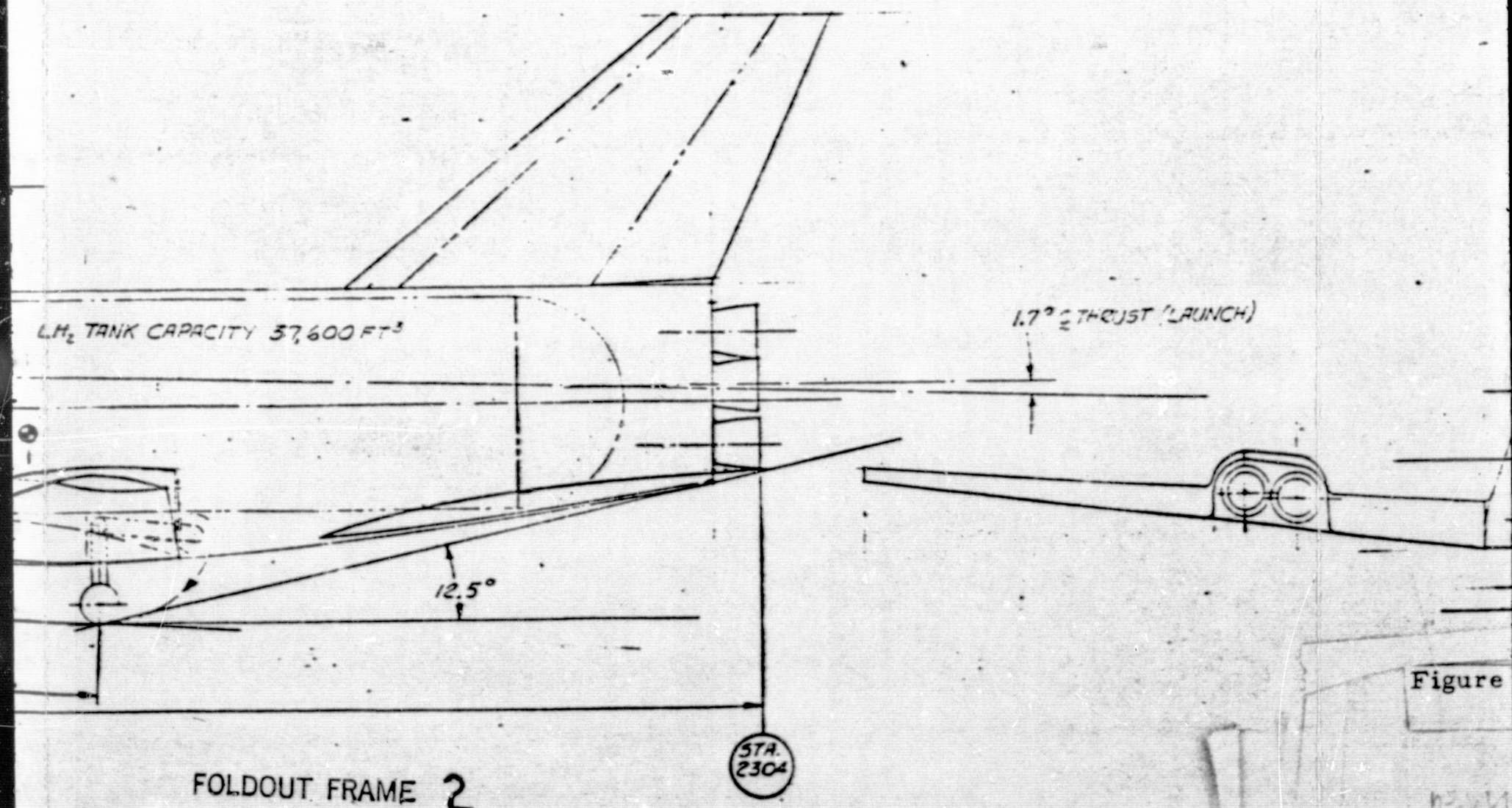

FOLDOUT FRAME 2

Figure

REPRODUCIBILITY OF THE ORIGINAL PAGE IS POOR.

WING GEOMETRY

AREA	3500 FT²
SPAN	157 FT
C_R	33.9 FT
C_T	10.8 FT
Λ-LE	14°
λ	.319

STAGE WEIGHTS, LBS '000

PROPELLANT (LOX & LH₂)	1018
TOTAL LAUNCH	1279
REENTRY	261
LANDING	245

AREAS

S_{WING}	3500 FT²
$S_{FUSELAGE\ BOTTOM}$	5200 FT²
$S_{TOTAL\ (WING+FUSEL.)}$	8700 FT²

8.2-2
SD 69-573-4

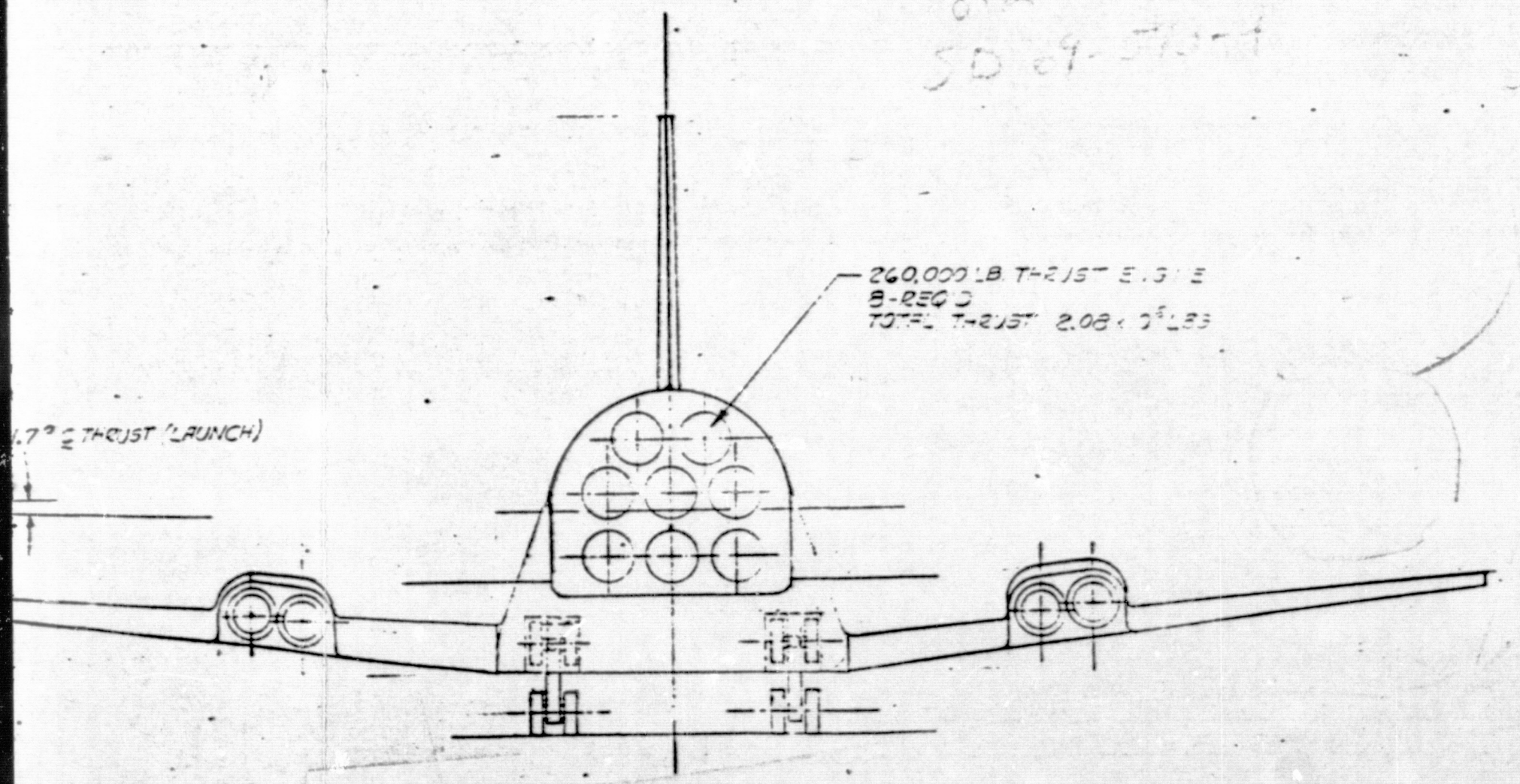

Figure 8.2-2. Booster Configuration, MSC Concept, for 7,700-Pound-Payload Orbiter (Drawing 2234-65)

FOLDOUT FRAME 3

8-11, 8-12

SD 69-573-4

REPRODUCIBILITY OF THE ORIGINAL PAGE IS POOR.

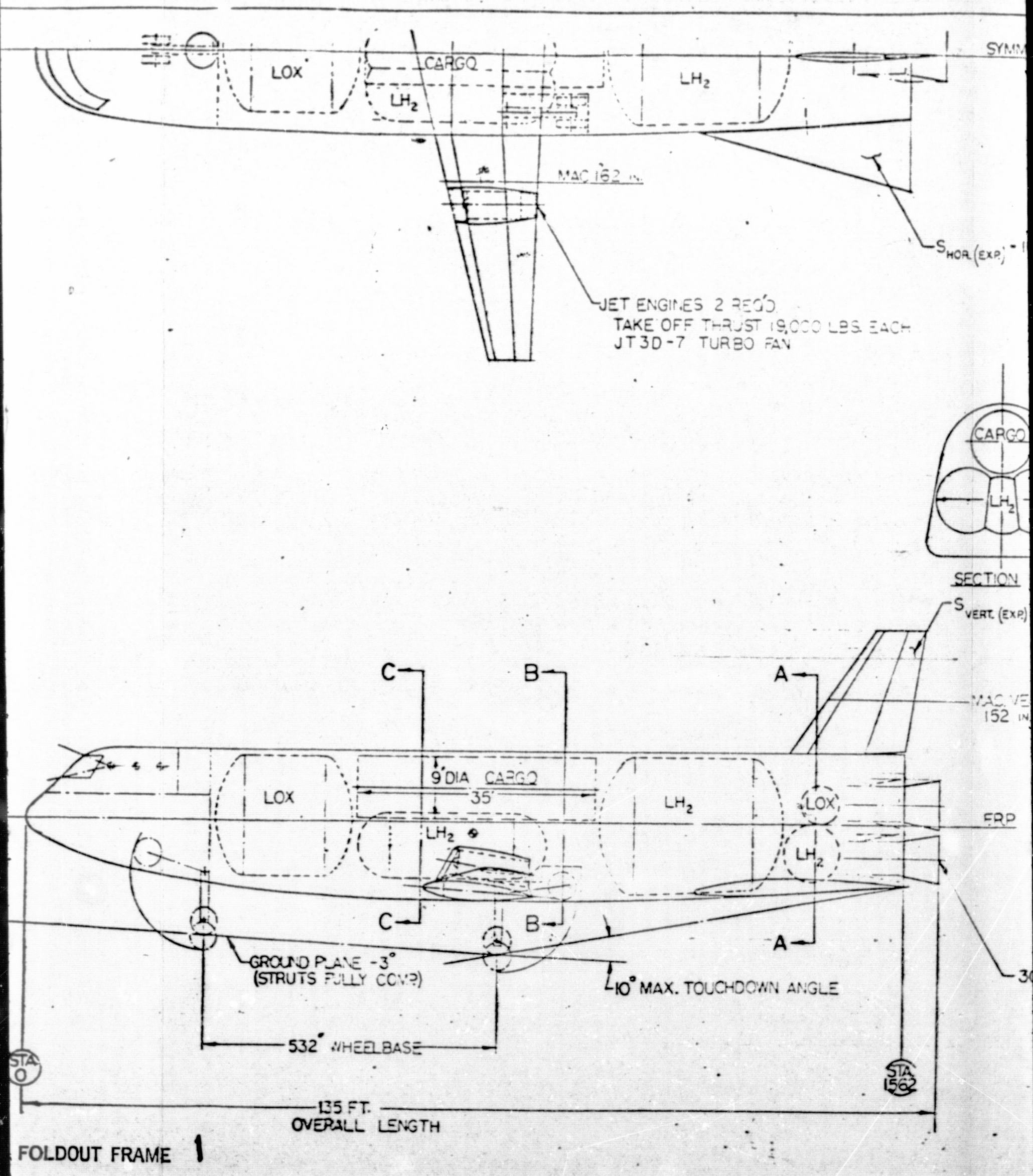

FOLDOUT FRAME 1

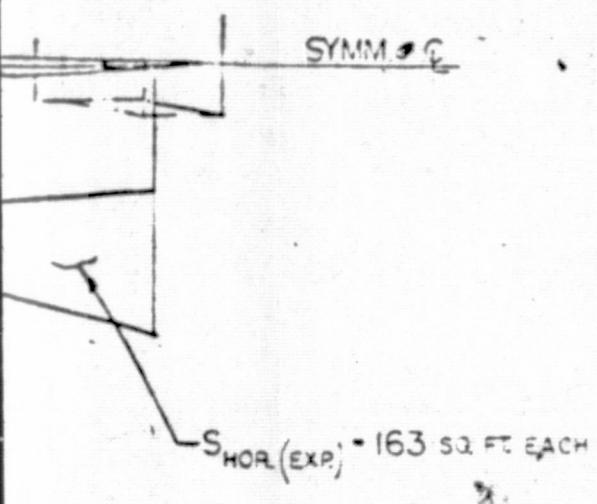

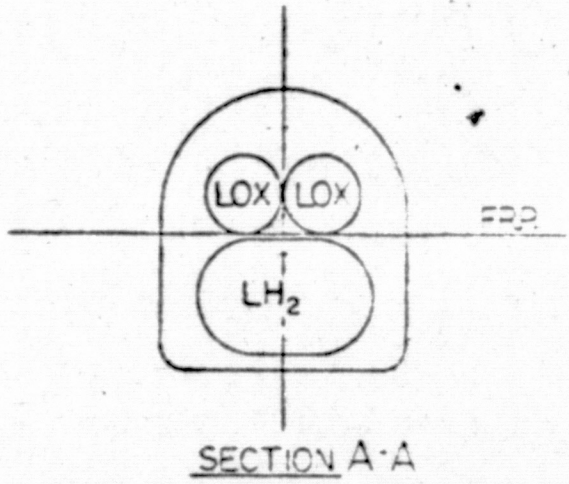

SECTION A-A

WING GEOMETRY

S_W - 1,100 SQ FT
SPAN - 88 FT.
C_R - 18.8 FT.
C_T - 6.3 FT.
Λ_{LE} - 14°
λ - .333
MAC - 162 IN.
A.R - 7

ES. EACH

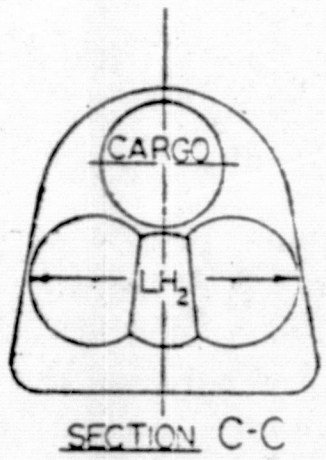

SECTION C-C

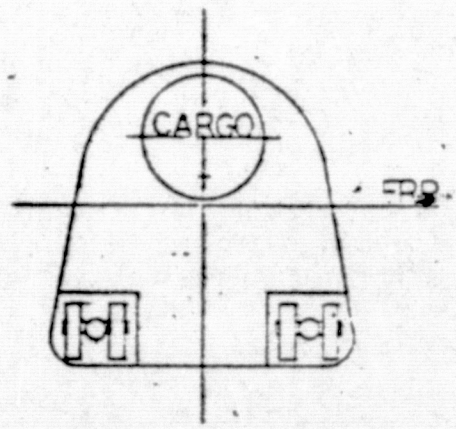

SECTION B-B

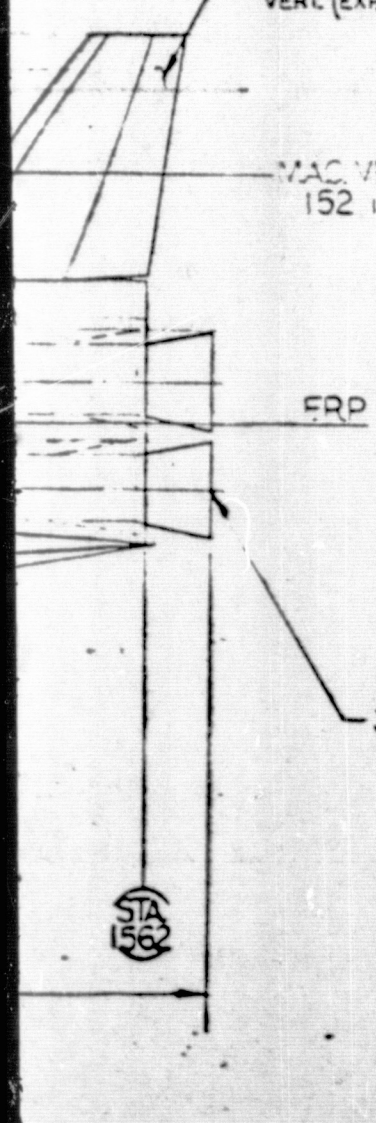

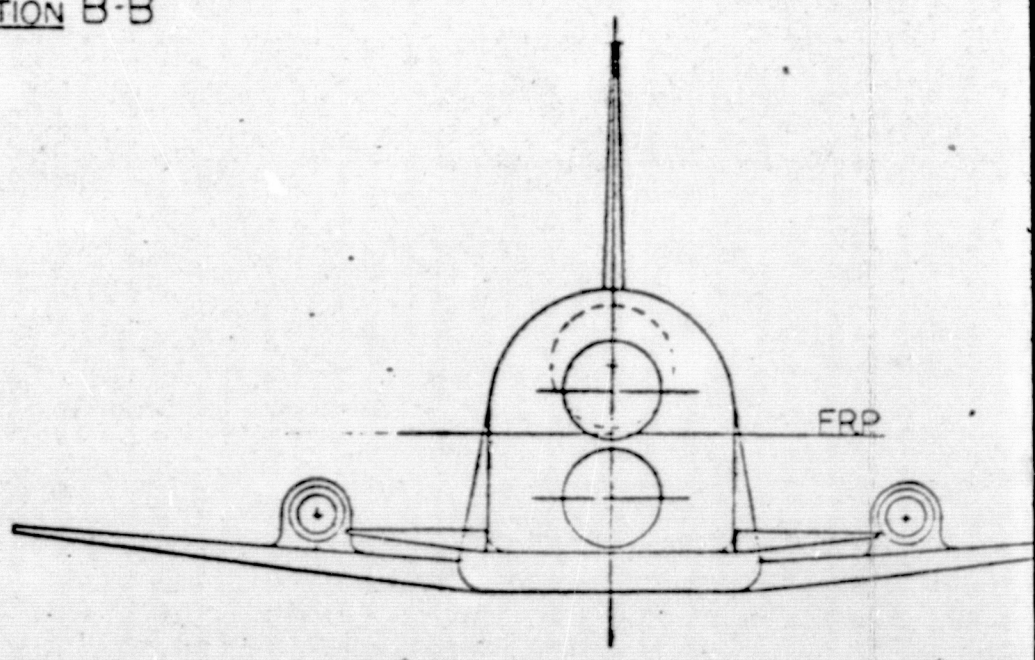

Figure 8.2-3.

FOLDOUT FRAME 2

WING GEOMETRY

S_W - 1,100 SQ FT
SPAN - 88 FT.
C_R - 18.8 FT.
C_T - 6.3 FT.
Λ_{LE} - 14°
λ - .333
MAC - 162 IN.
A.R. - 7

STAGE WEIGHTS

PROPELLANT (LOX & LH_2)	- 284,800 LBS TOTAL
TOTAL LAUNCH	- 385,000 LBS
REENTRY	- 100,200 LBS
LANDING	- 98,600 LBS
PROPELLANT (LOX & LH_2) ON ORBIT	- 14,800 LBS

TOTAL PLANFORM AREAS

S_{WING} - 1,100 SQ FT $\left(\frac{W}{S_W} - 90 \text{ LDG}\right)$
$S_{FUS.}$ - 2,240 SQ FT.
TOTAL - 3,340 SQ FT. $\left(\frac{W}{S}_{TOTAL} - 30 \text{ REENTRY}\right)$

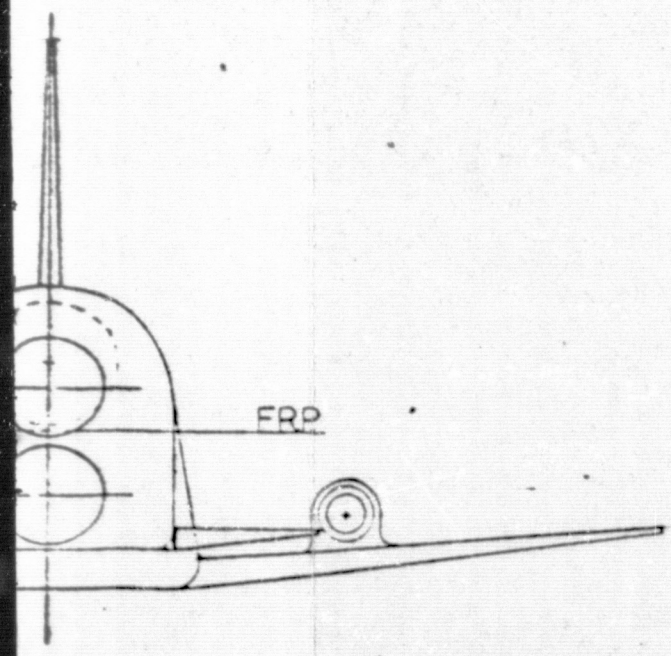

Figure 8.2-3. Orbiter Configuration, MSC Concept, for 7,700-Pound-Payload (Internal Cargo) (Drawing 2234-64)

FOLDOUT FRAME 3

REPRODUCIBILITY OF THE ORIGINAL PAGE IS POOR.

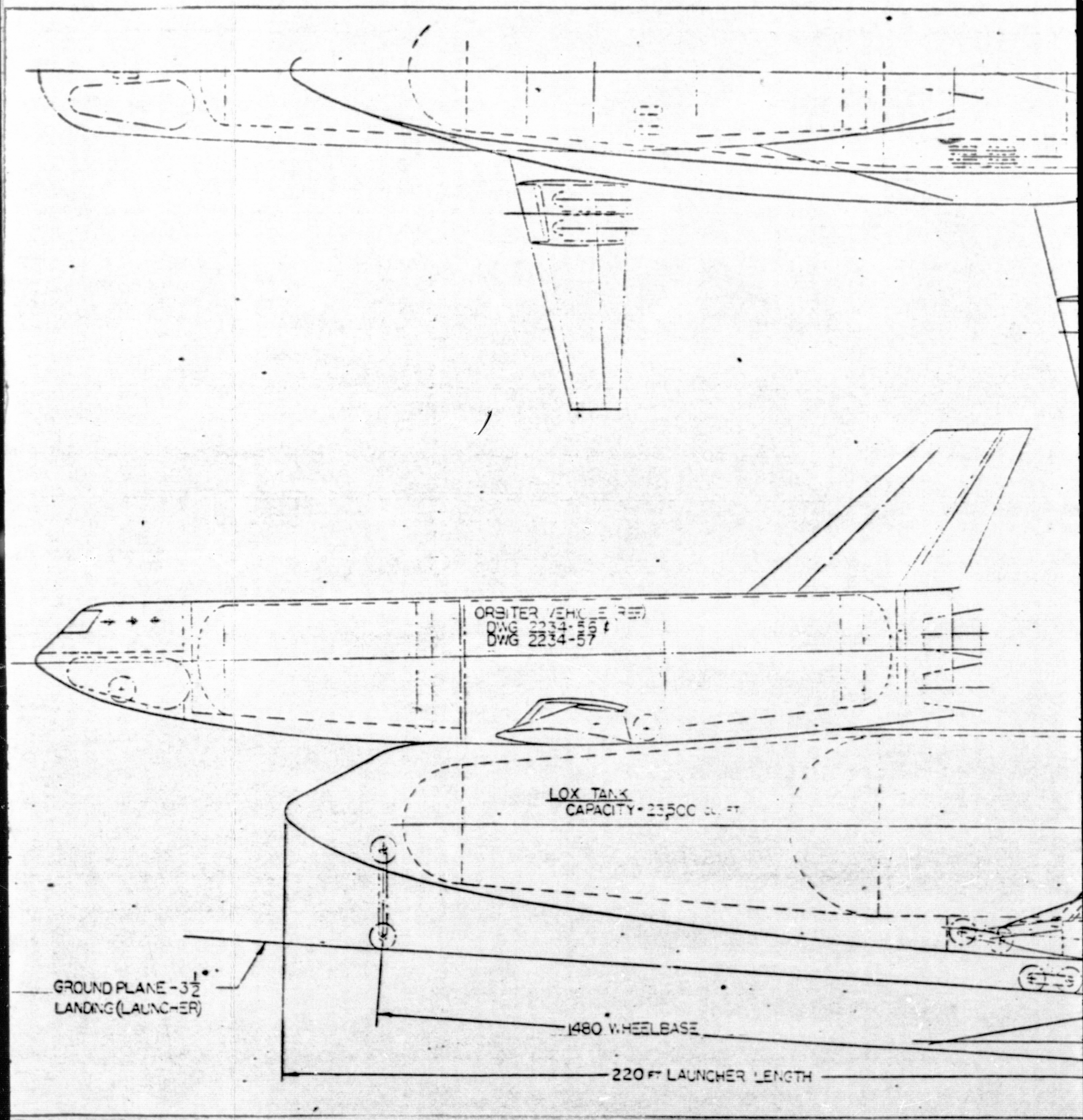

FOLDOUT FRAME 1

REPRODUCIBILITY OF THE ORIGINAL PAGE IS POOR.

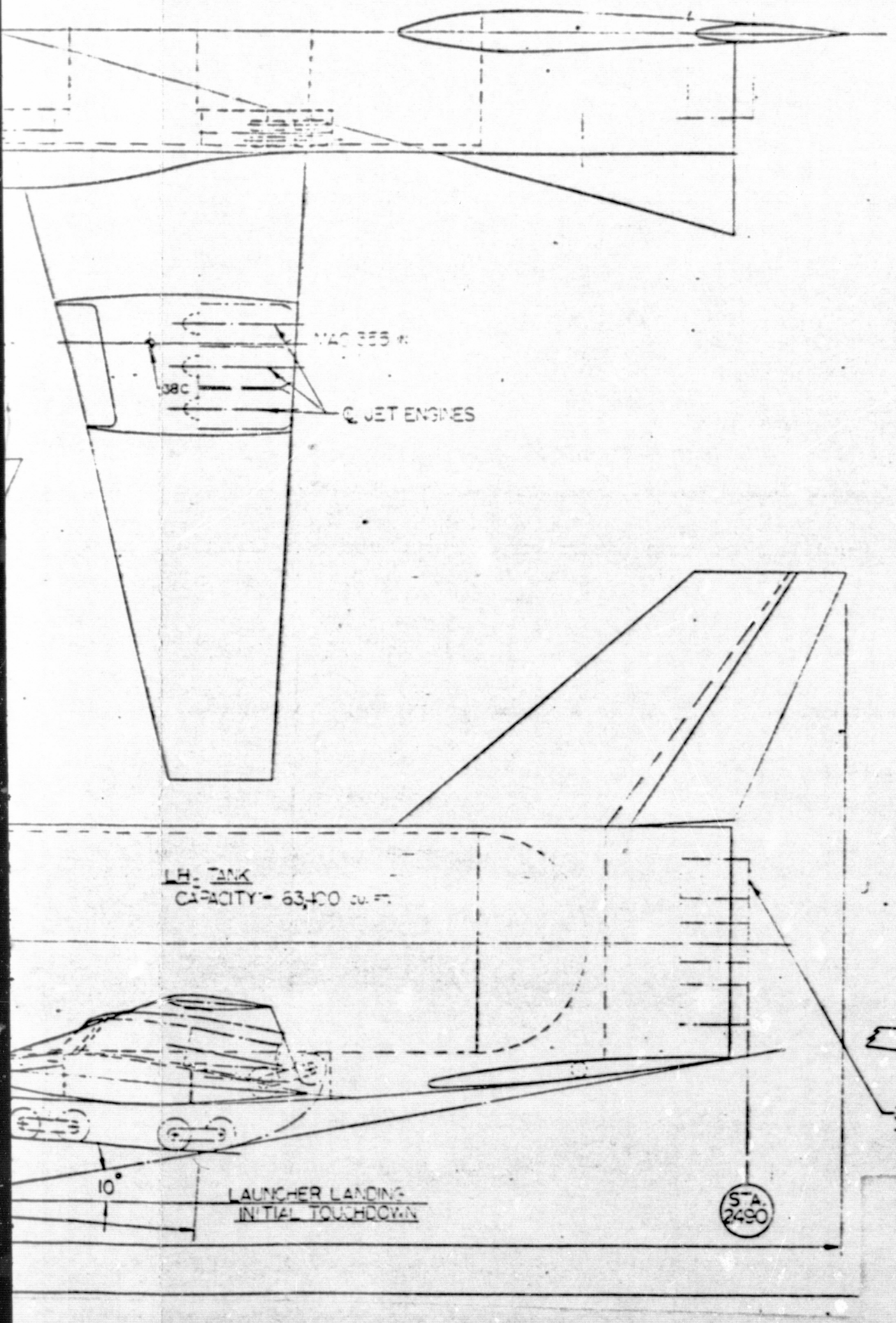

WING

S_W = 5270

SPAN = 186

C_R = 41.7

C_T = 13.1

Λ_{LE} = 45°

λ = .319

TOTAL PL

S_{WING} = 5

S_{FUS} = 7

TOTAL = 12

FOLDOUT FRAME 2

REPRODUCIBILITY OF THE ORIGINAL PAGE IS POOR.

WING GEOMETRY

S_W = 5,070 sq ft
SPAN = 188 ft
C_R = 41.7 ft
C_T = 13.1 ft
Λ_{LE} = 45°
λ = .319

TOTAL PLANFORM AREAS

S_{WING} = 5,070 sq ft $\left(\frac{W}{S_W}$ = 70 LDG$\right)$
S_{FUS} = 7,530 sq ft
TOTAL = 12,600 sq ft $\left(\frac{W}{S_{TOTAL}}$ = 30 REENTRY$\right)$

STAGE WEIGHTS

PROPELLANT ($LOX + LH_2$) = 1,709,000 LBS.
TOTAL LAUNCH = 2,107,000 LBS.
REENTRY = 378,000 LBS.
LANDING = 355,000 LBS.

8.2-4
SD 69-573-4

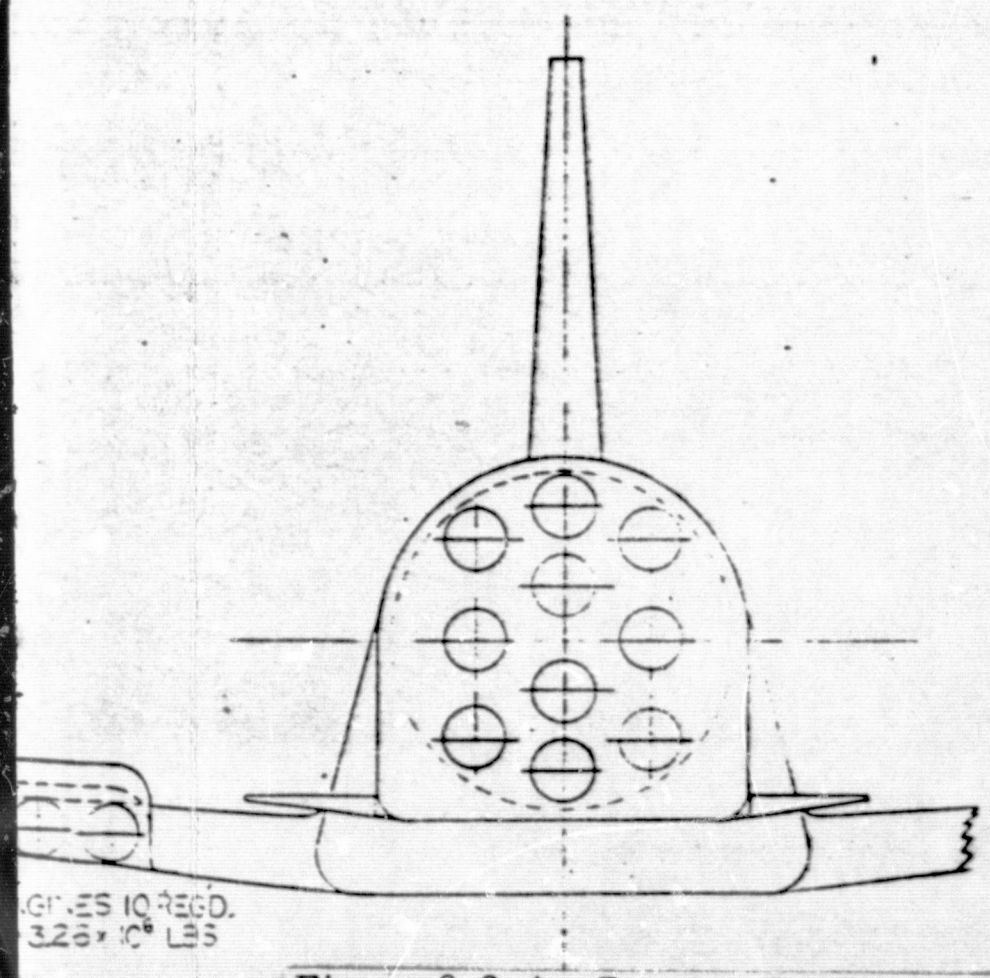

Figure 8.2-4. Booster Configuration, MSC Concept, for 25,000-Pound-Payload Orbiter (Drawing 2234-54A)

REPRODUCIBILITY OF THE ORIGINAL PAGE IS POOR.

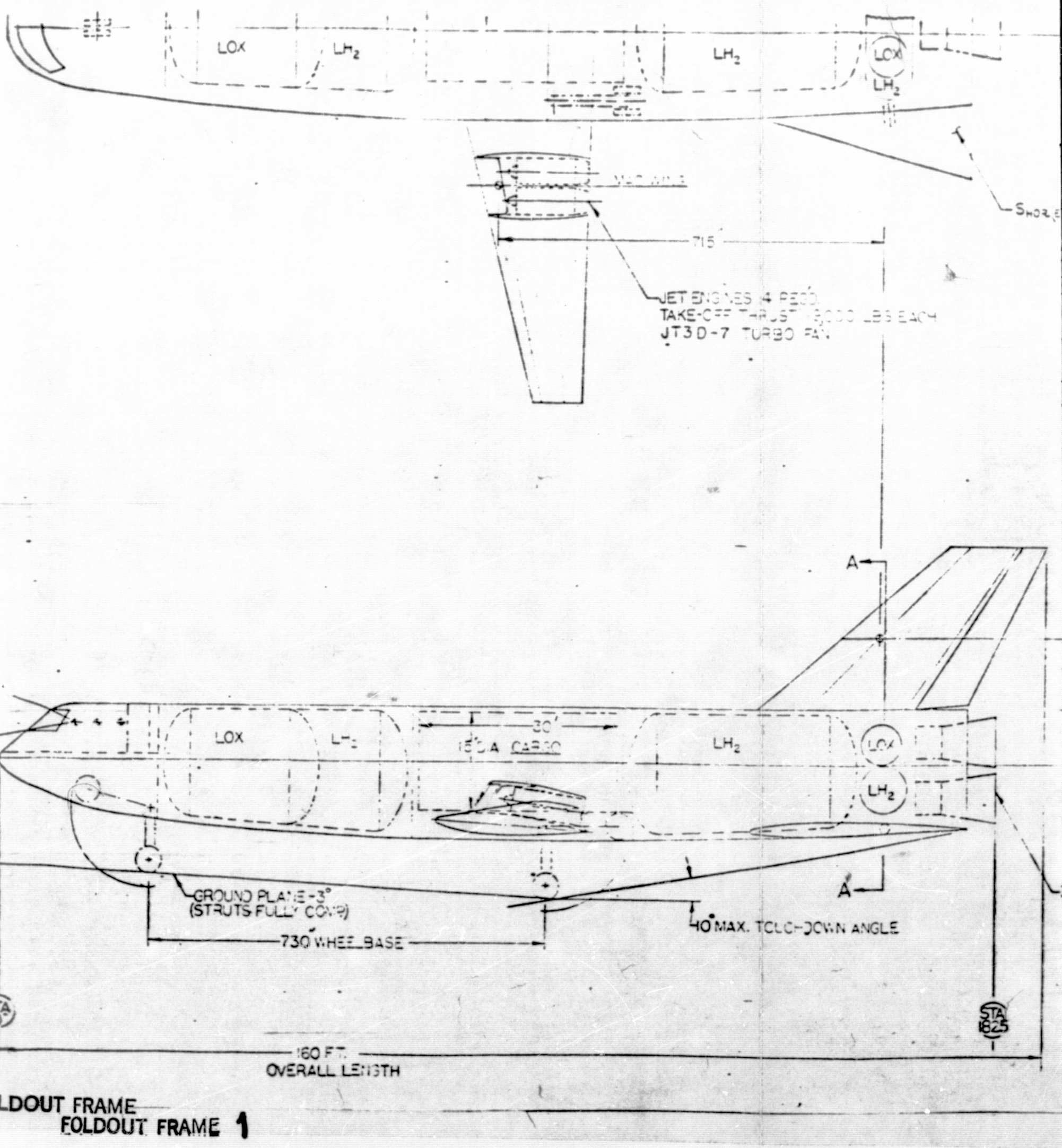

FOLDOUT FRAME

FOLDOUT FRAME 1

REPRODUCIBILITY OF THE ORIGINAL PAGE IS POOR.

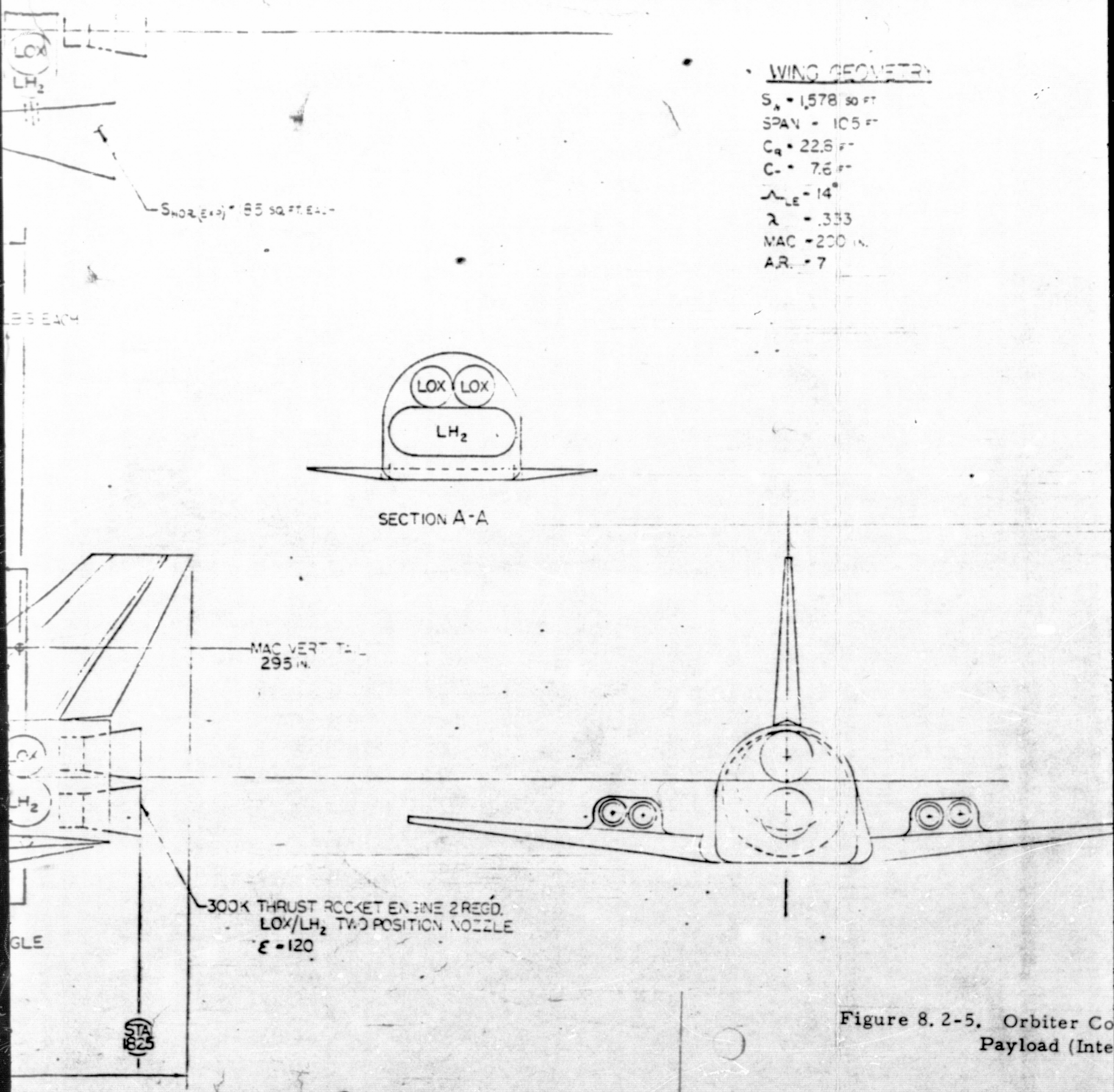

Figure 8.2-5. Orbiter Co
Payload (Inte

FOLDOUT FRAME 2

REPRODUCIBILITY OF THE ORIGINAL PAGE IS POOR.

Space Division
North American Rockwell

WING GEOMETRY

S_A = 1,578 SQ FT
SPAN = 105 FT
C_R = 22.6 FT
C_T = 7.6 FT
Λ_{LE} = 74°
λ = .333
MAC = 200 IN.
A.R. = 7

STAGE WEIGHTS

PROPELLANT (LO_2 & LH_2) = 325,000 LBS TOTAL
TOTAL LAUNCH = 469,100 LBS
REENTRY = 144,100 LBS
LANDING = 142,000 LBS
PROPELLANT (LO_2 & LH_2) ON ORBIT = 21,000 LBS

TOTAL PLANFORM AREAS

S_{WING} = 1,578 SQ FT $\left(\frac{W}{S_A} = 90 LDG\right)$
S_{FUS} = 3,222 SQ FT
TOTAL = 4,800 SQ FT $\left(\frac{W}{S_{TOTAL}} = 30 REENTRY\right)$

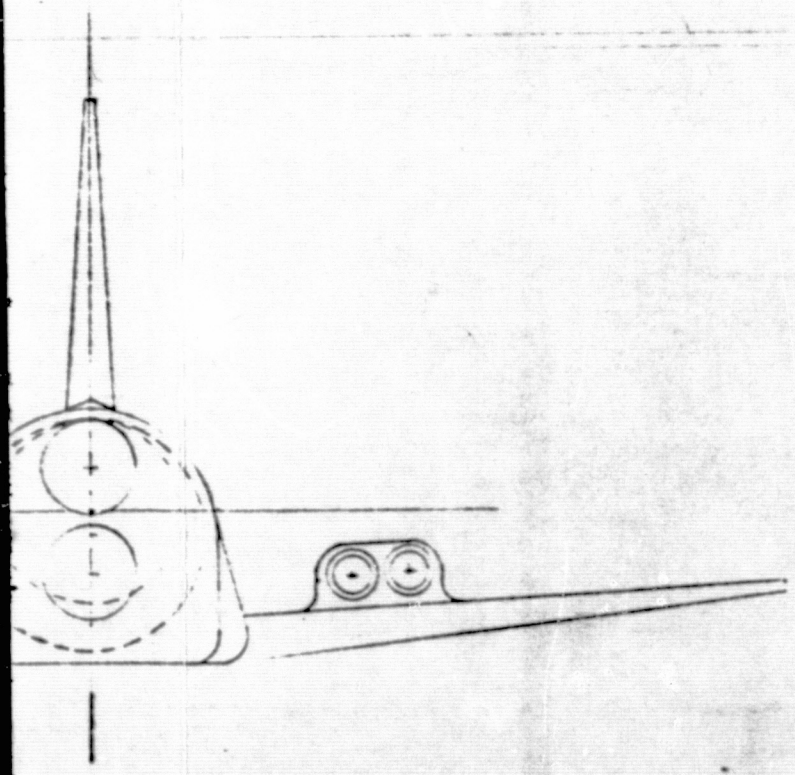

Figure 8.2-5. Orbiter Configuration, MSC Concept, for 25,000-Pound Payload (Internal Cargo) (Drawing 2234-56)

FOLDOUT FRAME 3

REPRODUCIBILITY OF THE ORIGINAL PAGE IS POOR.

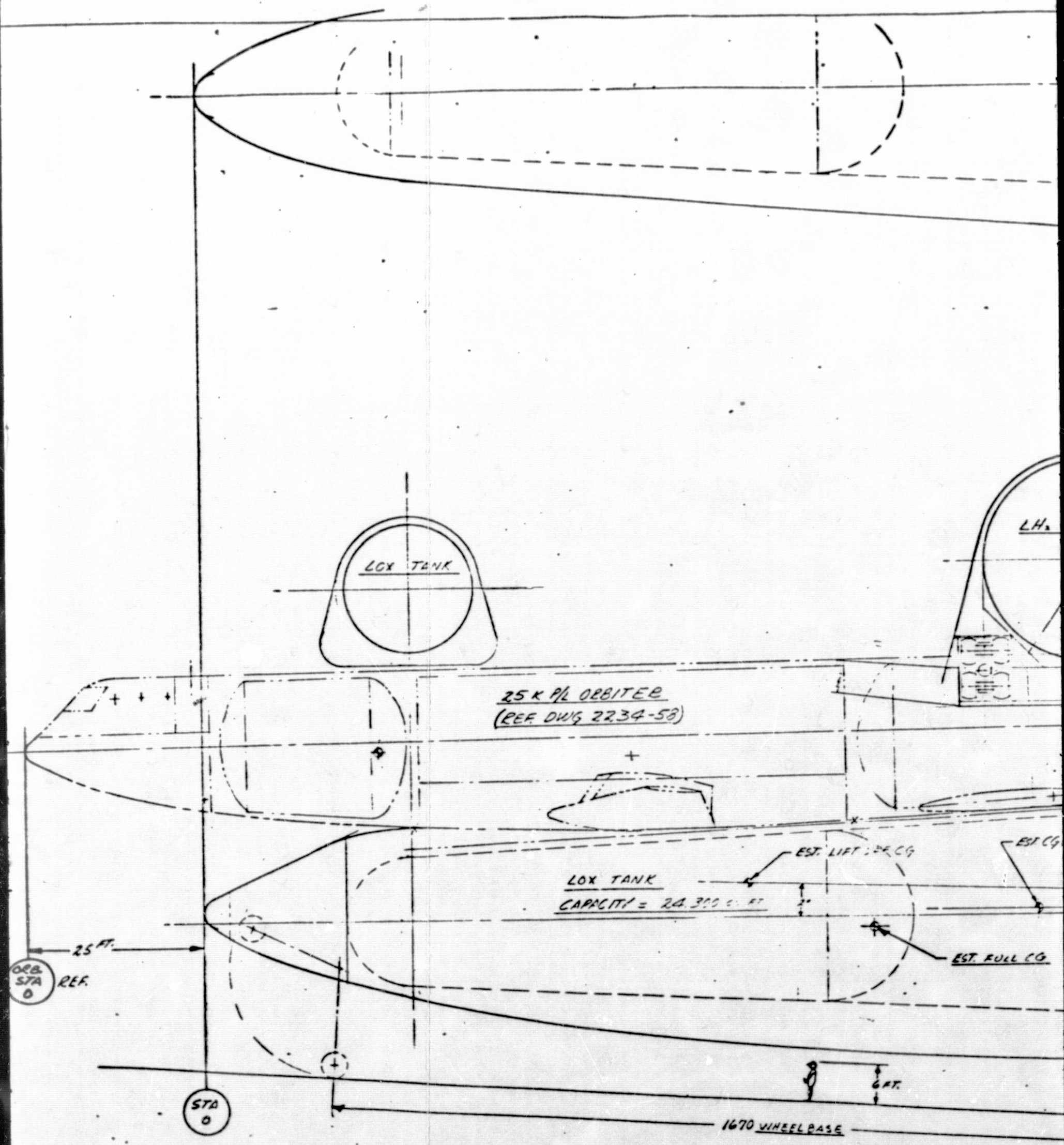

FOLDOUT FRAME 1

REPRODUCIBILITY OF THE ORIGINAL PAGE IS POOR.

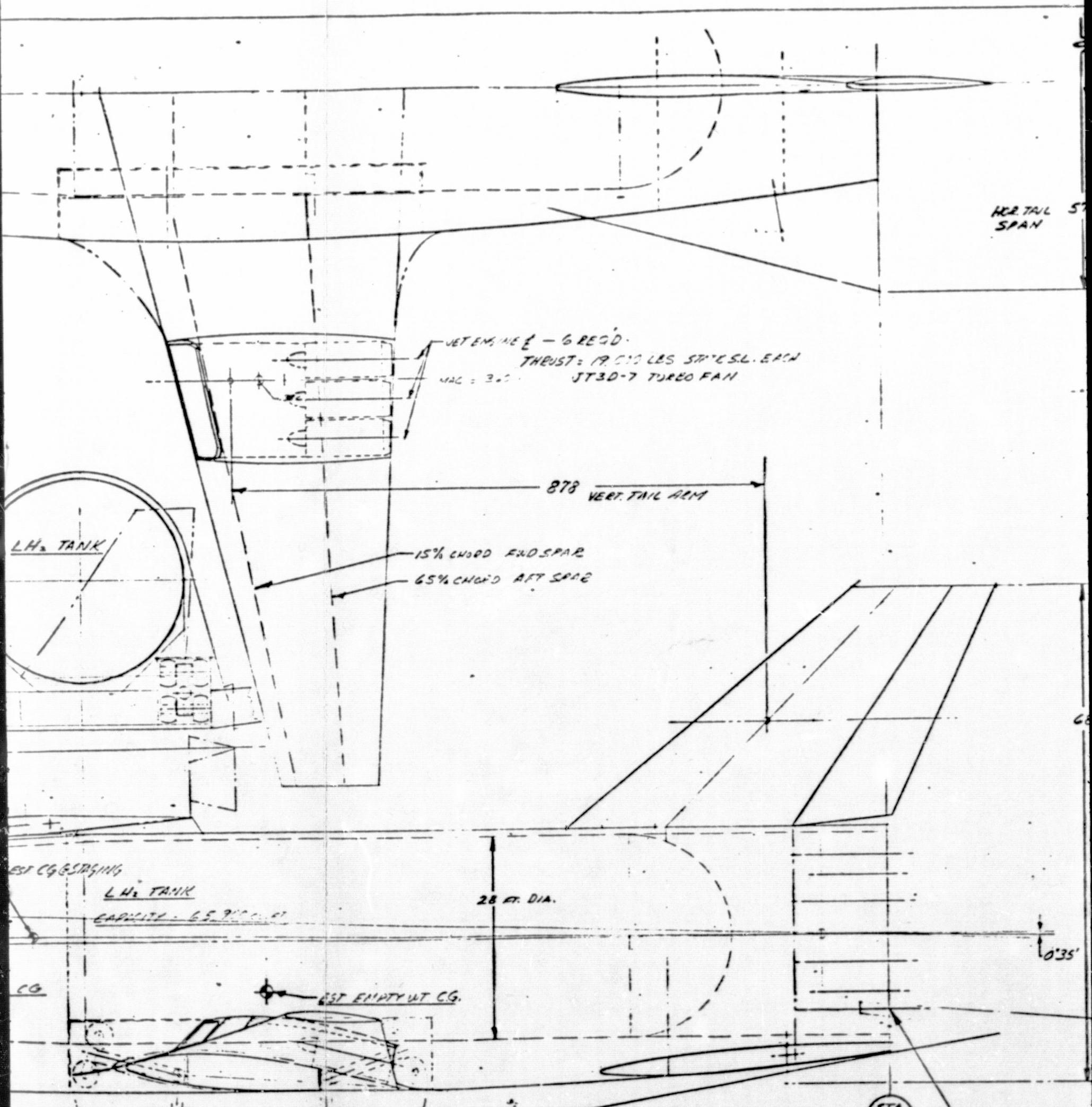

FOLDOUT. FRAME 2

REPRODUCIBILITY OF THE ORIGINAL PAGE IS POOR.

HOR. TAIL SPAN 57.9 FT.

WING GEOMETRY

AREA =	5,240 SQ. FT.
AR =	7
SPAN =	191 FT.
C_{TIP} =	13.3 FT.
C_{ROOT} =	41.7 FT.
λ =	319
Λ_{LE} =	14°

STAGE WEIGHTS

PROPELLANT (LOX/LH_2) =	1,813,000 LBS.
GROSS STAGE WEIGHT =	2,204,000 LBS
RE-ENTRY WEIGHT =	391,000 LBS.
LANDING WEIGHT =	367,000 LBS
JET FUEL WEIGHT =	24,000 LBS.

AREAS

S_{WING} = 5,240 SQ.FT $\quad W/S_W$ = 70 PSF

$S_{FUSELAGE\ BOTTOM}$ = 7800 SQ. FT.

$S_{TOTAL\ BOTTOM}$ = 13,040 SQ FT. $\quad W/S_{TOT.}$ = 30 PSF

68.5 FT.

0°35'

ROCKET ENGINES - 10 REQ'D
THRUST SL. = 375,000 LB. } EACH
VAC = 413,000 LB }
TOTAL THRUST = 3,750,000 LB (SEALEVEL)
= 35

Figure 8.2-6. Booster Configuration for 25,000-Pound-Payload Orbiter (15-Foot Diameter by 60-Foot Payload (Drawing 2234-59)

REPRODUCIBILITY OF THE ORIGINAL PAGE IS POOR.

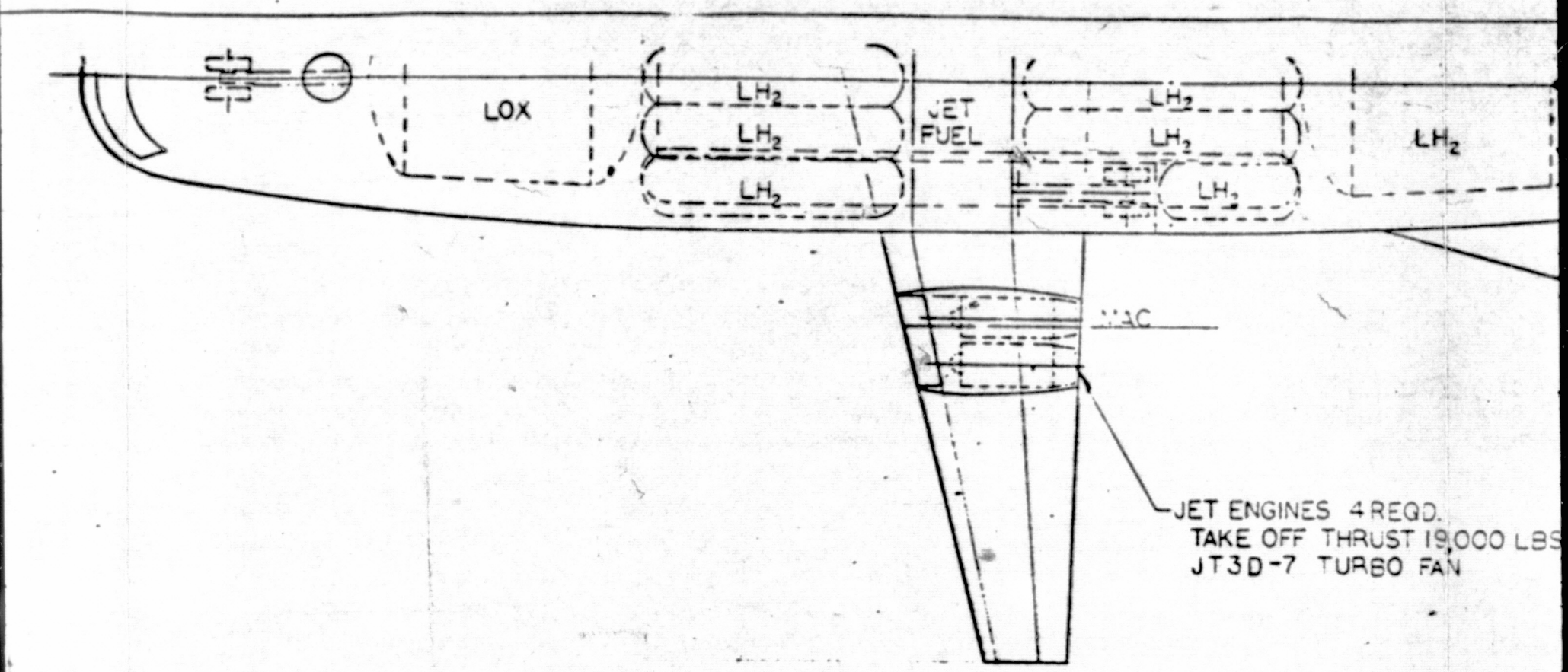

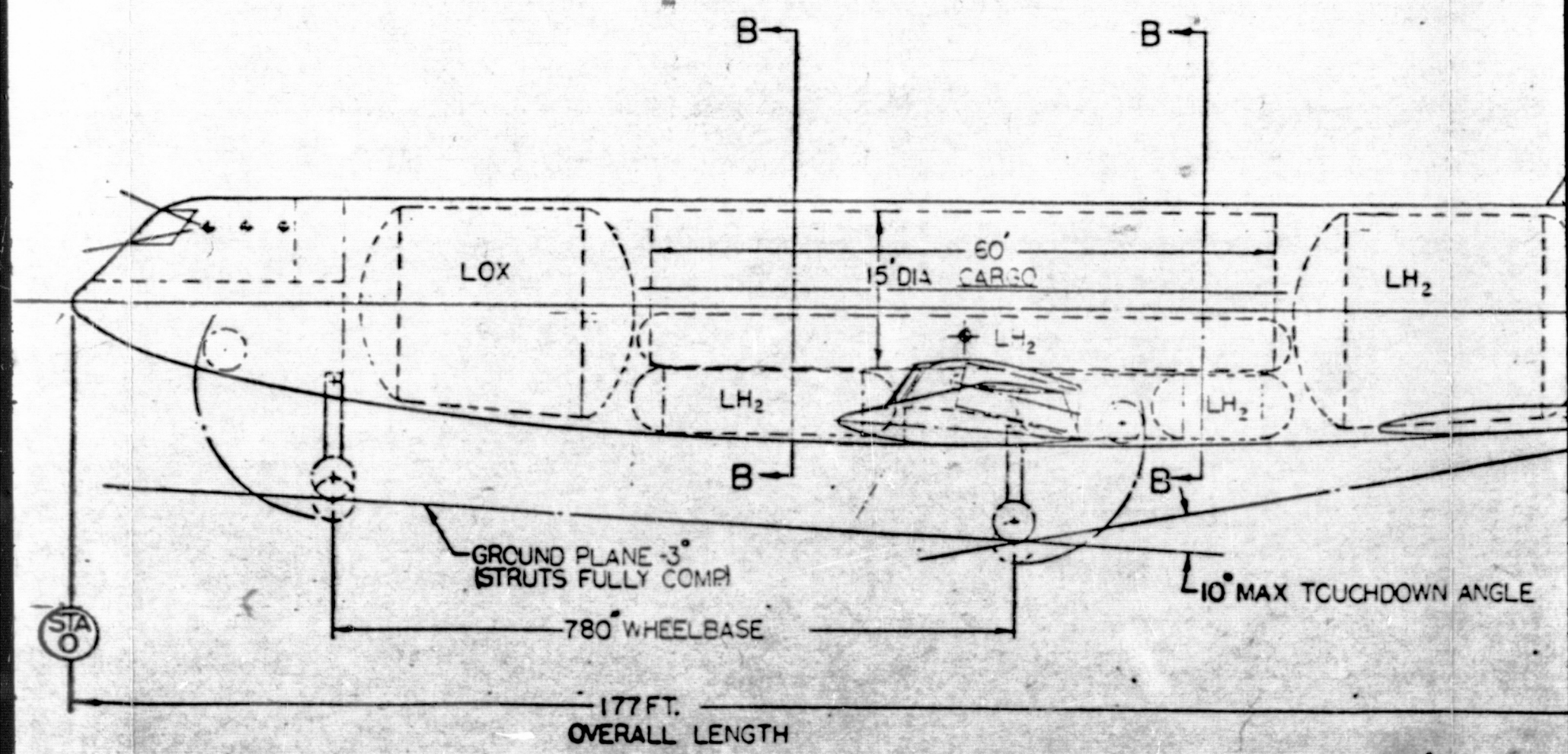

FOLDOUT FRAME 1

REPRODUCIBILITY OF THE ORIGINAL PAGE IS POOR.

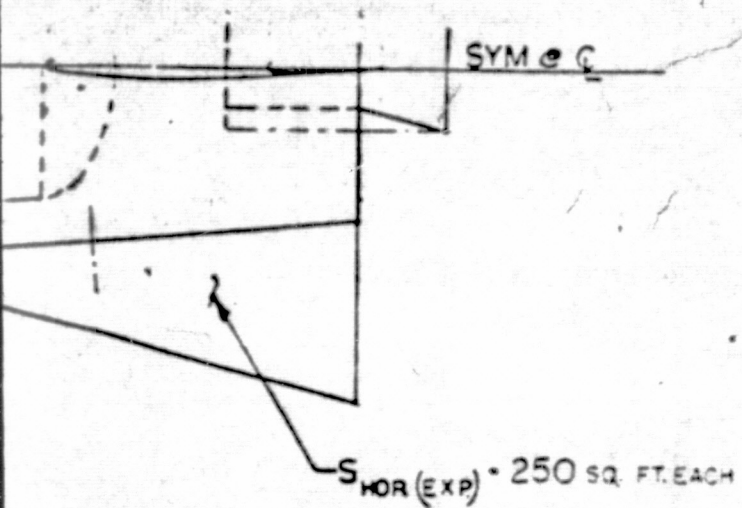

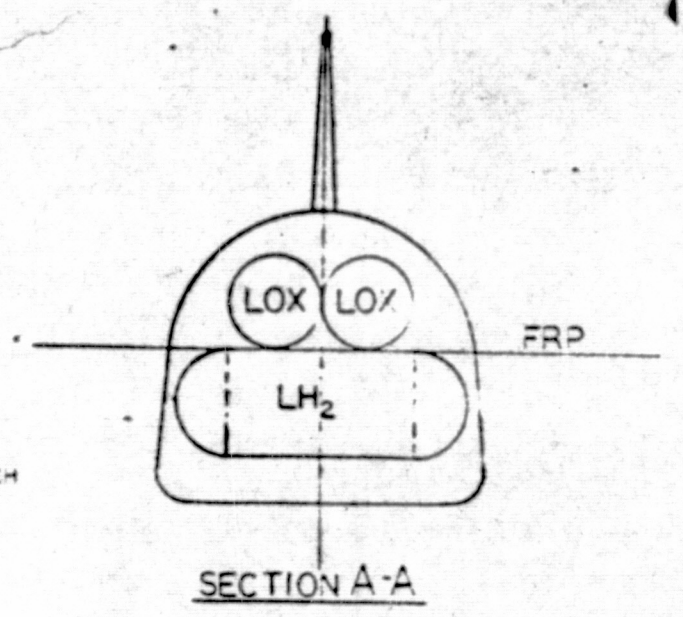

SECTION A-A

WING GEOMETRY

S_W = 1,730 SQ FT
SPAN = 110 FT
C_R = 23.6 FT
C_T = 7.9 FT
Λ_{LE} = 14°
λ = .333
MAC = 208 IN.
AR = 7

BS. EACH

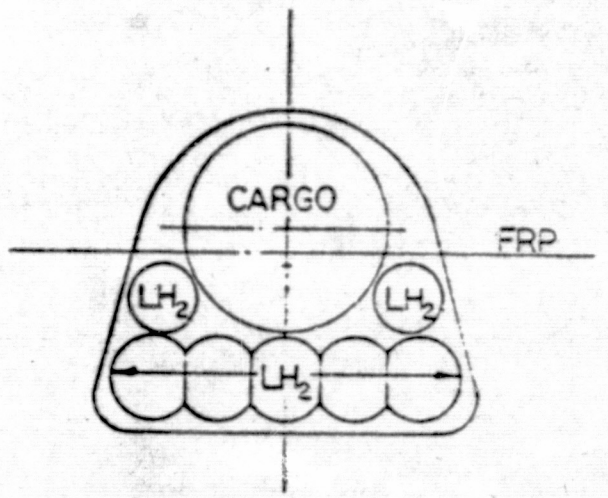

SECTION B-B

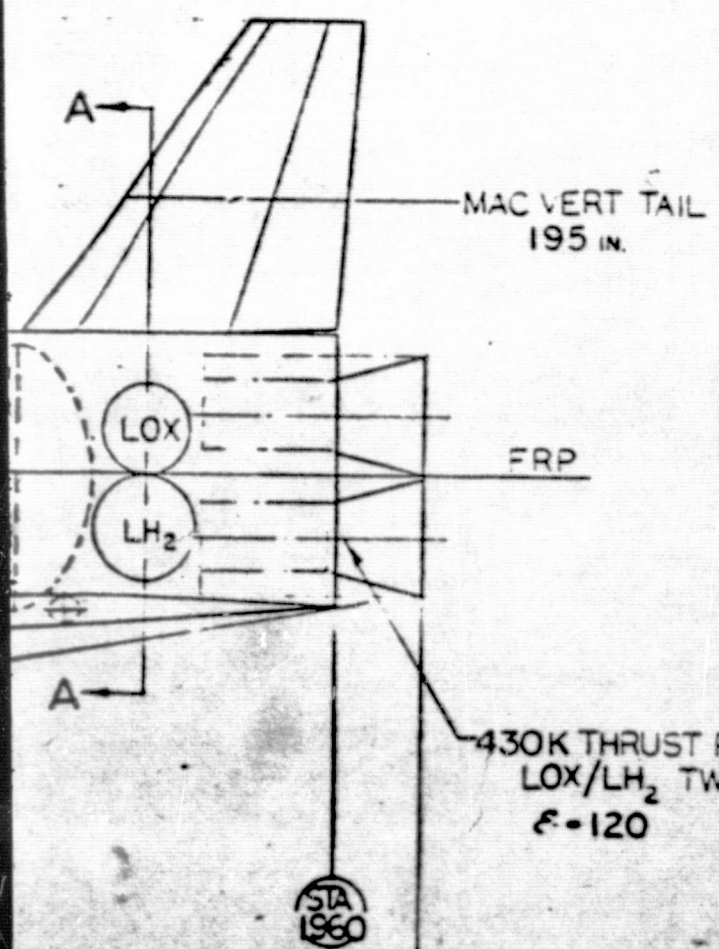

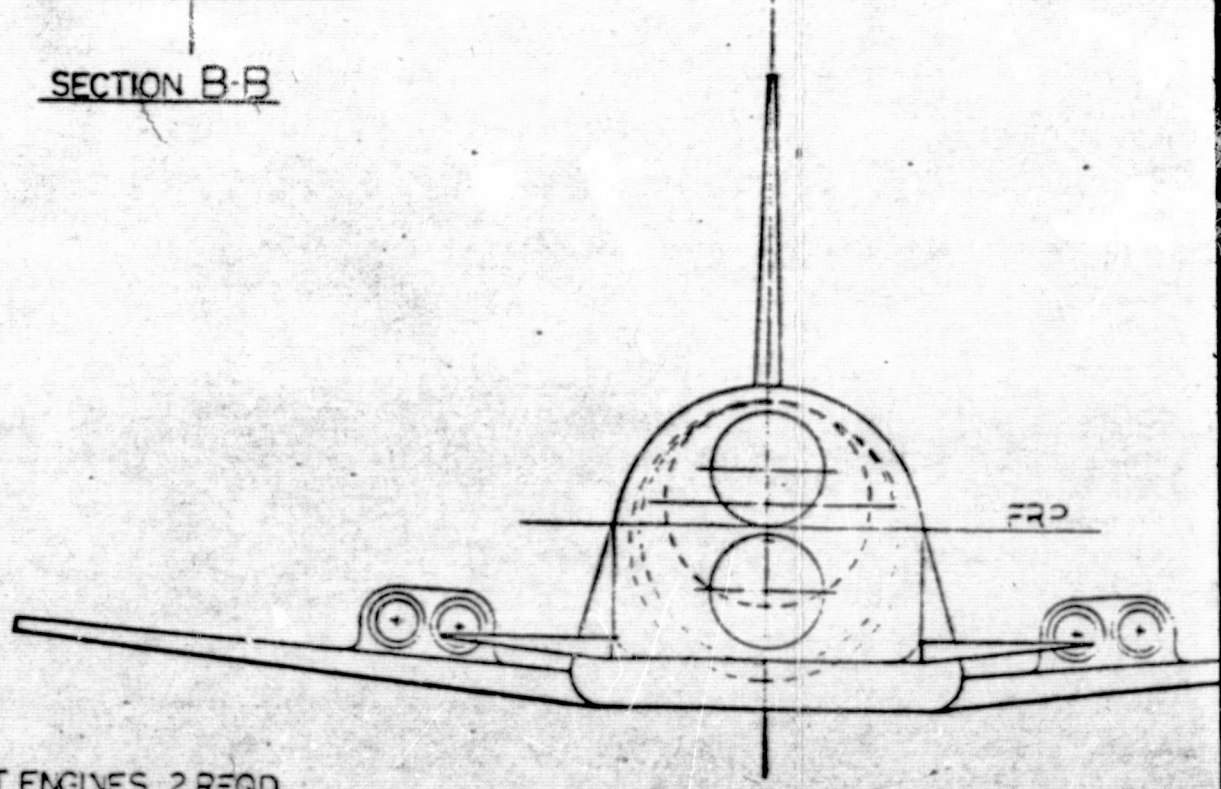

Figure 8.2-7. Orb
Paylo

FOLDOUT FRAME 2

REPRODUCIBILITY OF THE ORIGINAL PAGE IS POOR.

Space Division
North American Rockwell

WING GEOMETRY

S_W = 1,730 SQ FT
SPAN = 110 FT
C_R = 23.6 FT
C_T = 7.9 FT
Λ_{LE} = 14°
λ = .333
MAC = 208 IN
AR = 7

STAGE WEIGHTS

PROPELLANT (LOX/LH_2)	=	368,000 LBS TOTAL
TOTAL LAUNCH	=	526,000 LBS
REENTRY	=	158,000 LBS
LANDING	=	155,500 LBS
PROPELLANT (LOX/LH_2) ON ORBIT	=	23,000 LBS

TOTAL PLANFORM AREAS

S_{WING} = 1,730 SQ FT $\left(\frac{W}{S_W} = 90 \text{ LDG}\right)$
S_{FUS} = 3,530 SQ FT
TOTAL = 5,260 SQ FT $\left(\frac{W}{S_{TOTAL}} = 30 \text{ REENTRY}\right)$

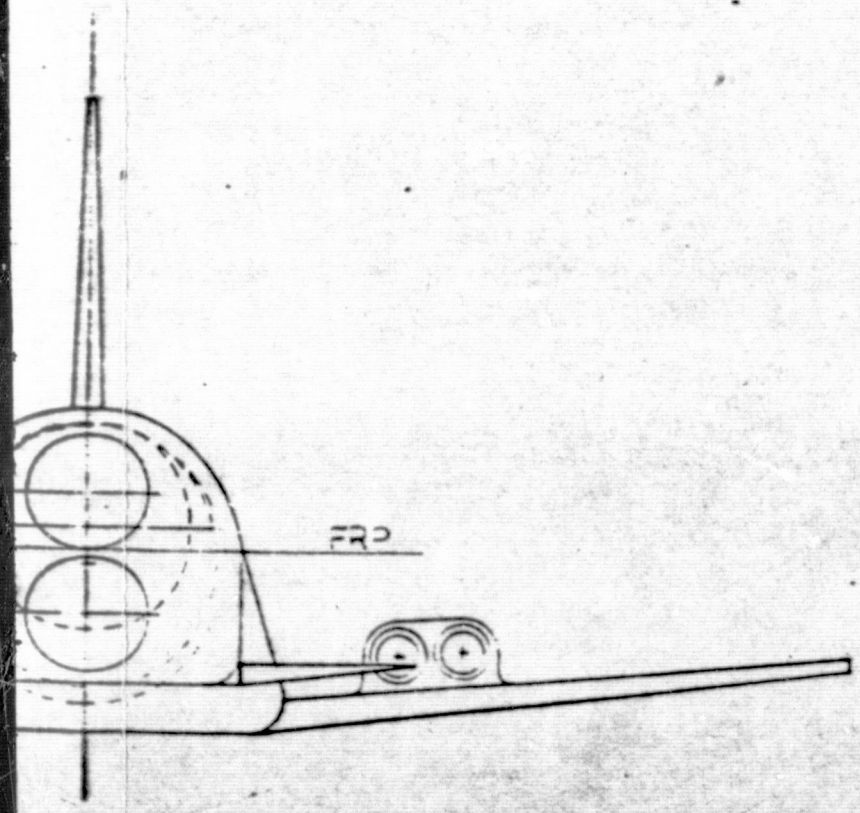

Figure 8.2-7. Orbiter Configuration, MSC Concept, for 25,000-Pound Payload (Internal Cargo) (Drawing 2234-58)

REPRODUCIBILITY OF THE ORIGINAL PAGE IS POOR.

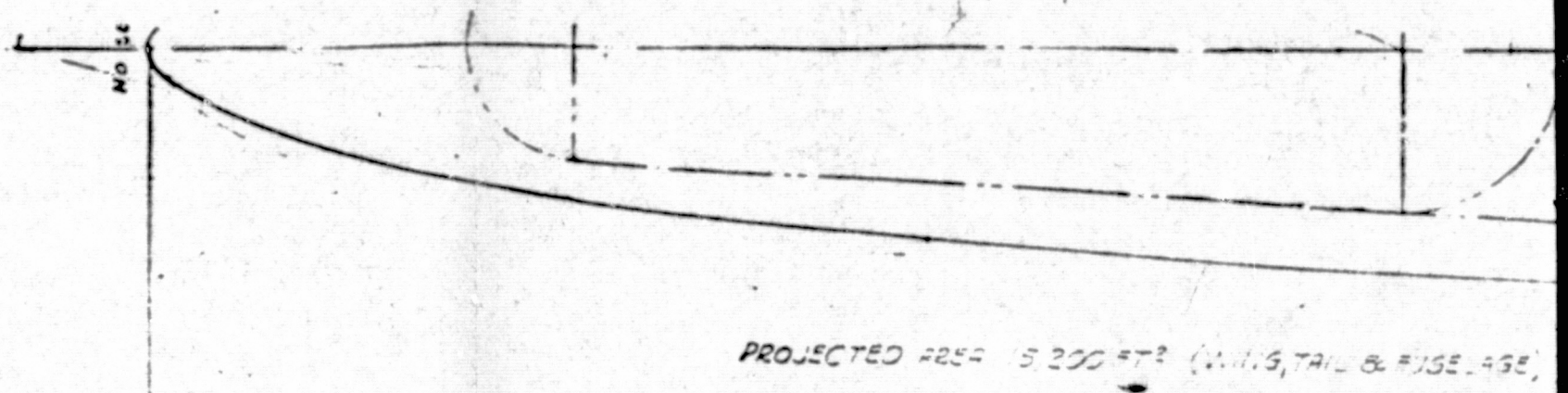

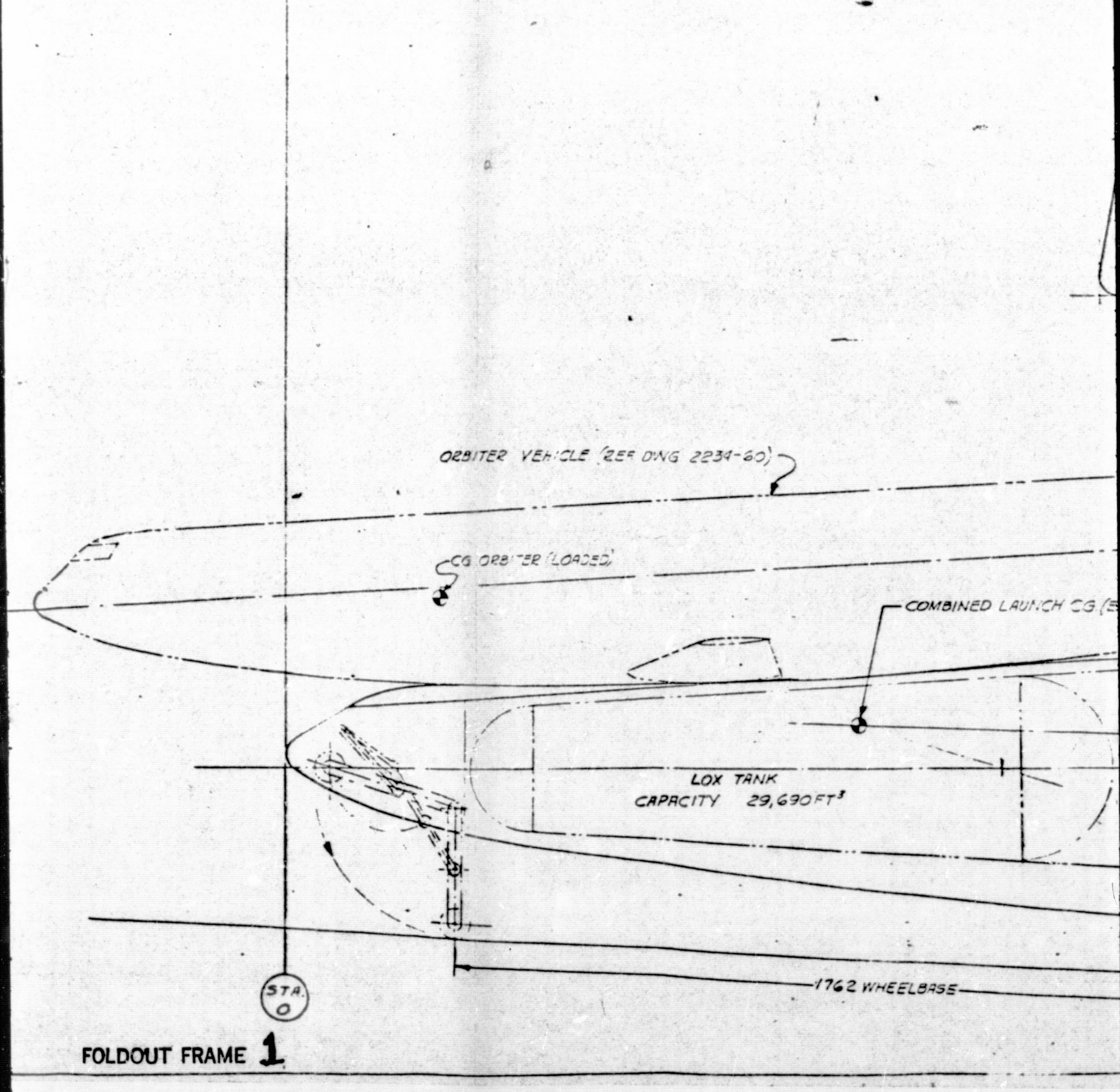

FOLDOUT FRAME 1

REPRODUCIBILITY OF THE ORIGINAL PAGE IS POOR.

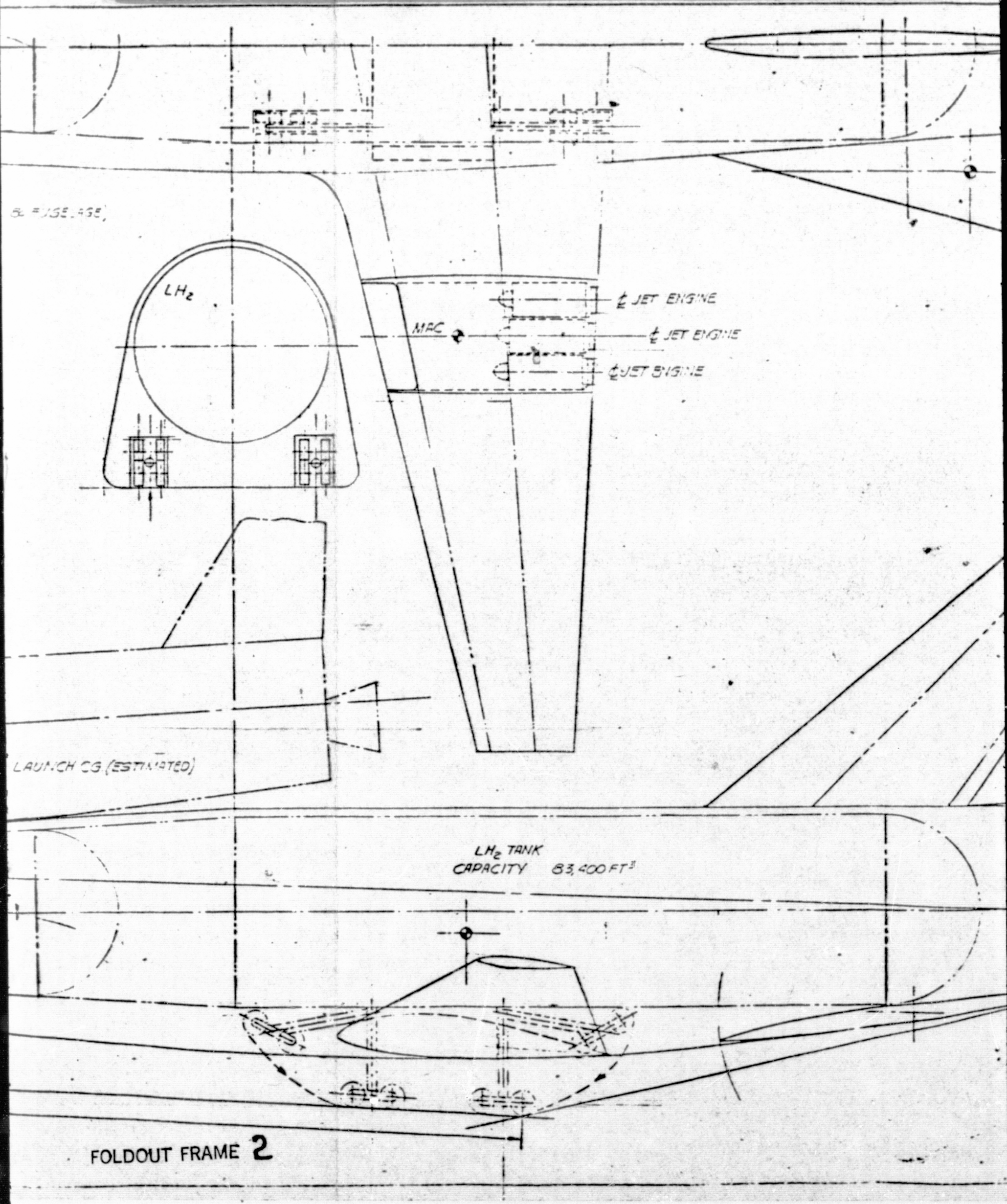

FOLDOUT FRAME 2

REPRODUCIBILITY OF THE ORIGINAL PAGE IS POOR.

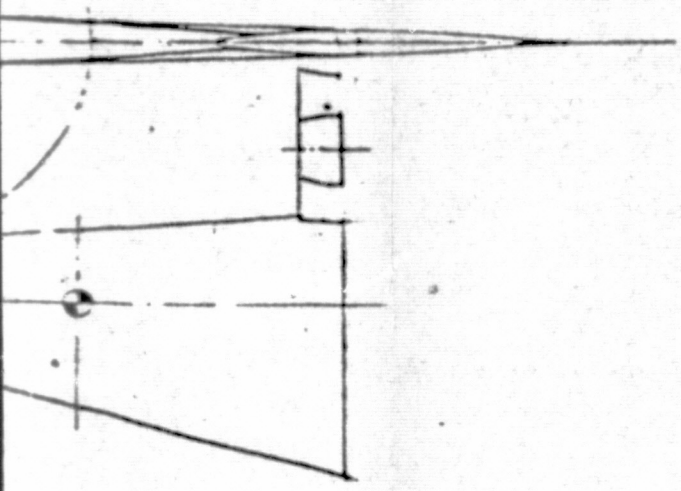

WING GEOMETRY

S_W	6310 FT^2
SPAN	210 FT
C_R	45.6 FT
C_T	14.56 FT.
Λ_{LE}	14°
λ	.319

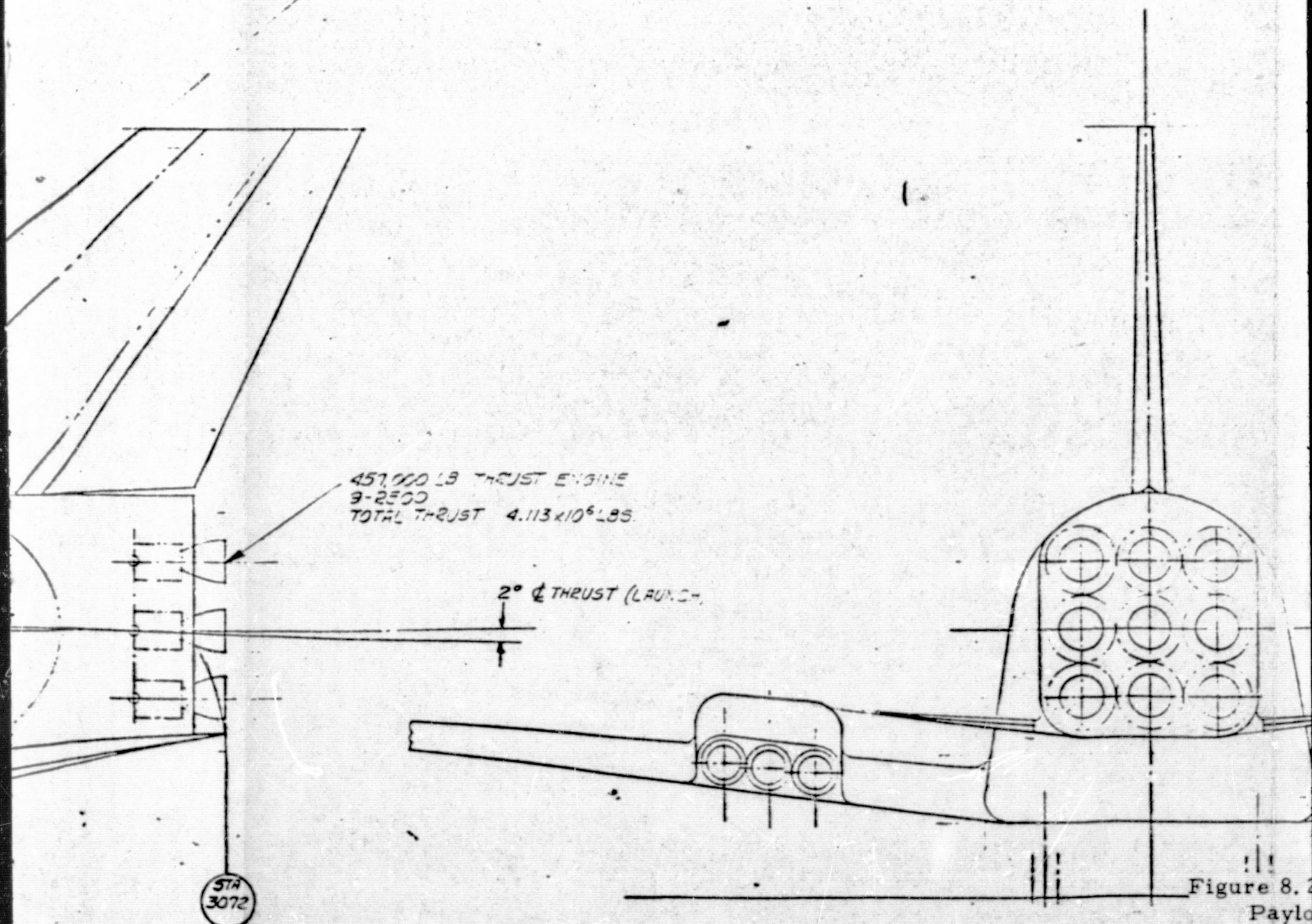

Figure 8. 2
Paylo

FOLDOUT FRAME 3

REPRODUCIBILITY OF THE ORIGINAL PAGE IS POOR.

WING GEOMETRY

S_W	6310 FT²
SPAN	210 FT
C_R	45.6 FT
C_T	14.56 FT.
Λ_{LE}	14°
λ	.319

STAGE WEIGHTS (LBS / 1000)

PROPELLANT (LO_X & LH_2)	2269
TOTAL LAUNCH	2739
RE ENTRY	470
LANDING	441

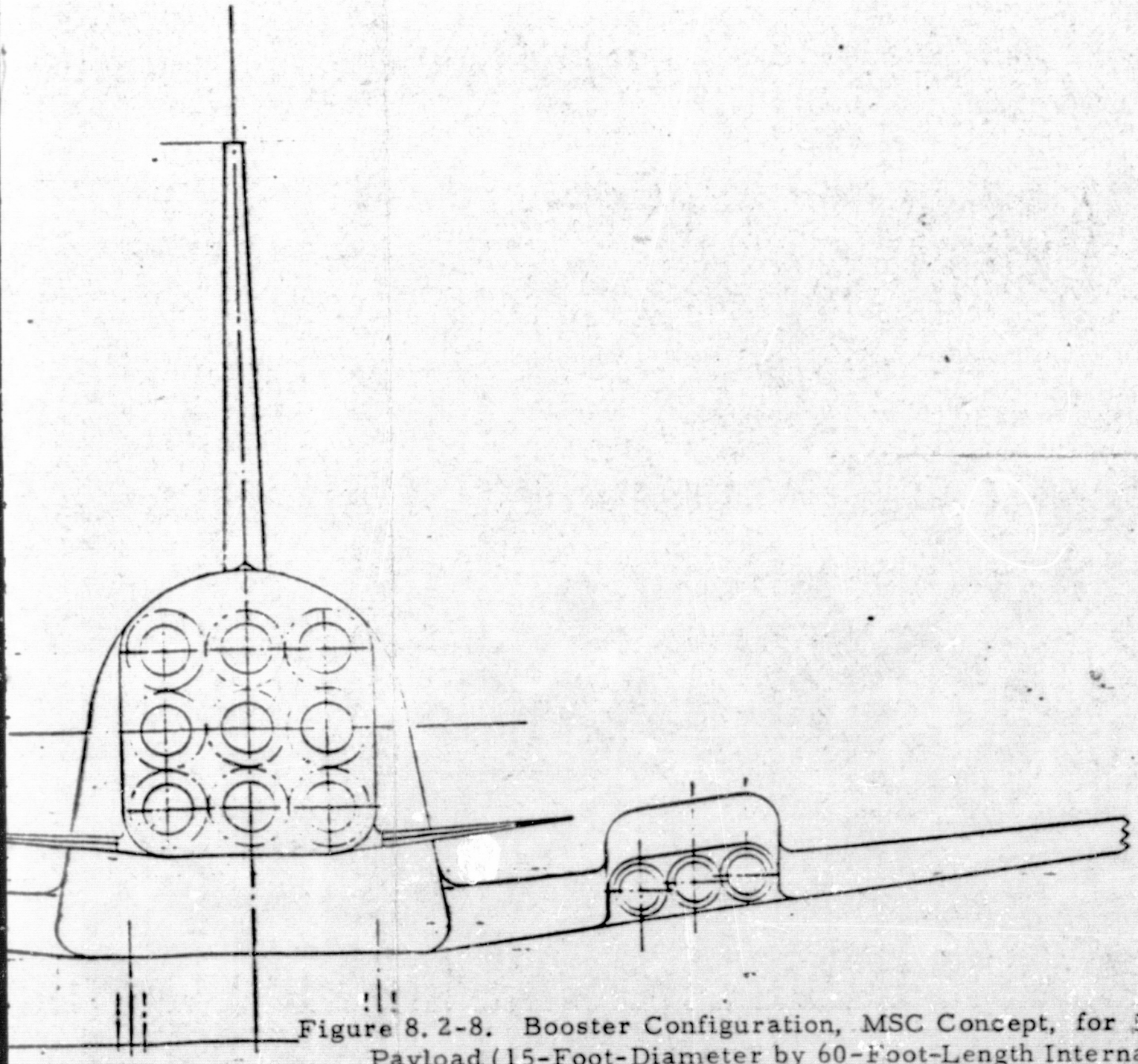

Figure 8.2-8. Booster Configuration, MSC Concept, for 50,000-Pound Payload (15-Foot-Diameter by 60-Foot-Length Internal Cargo)
(Drawing 2234-60)

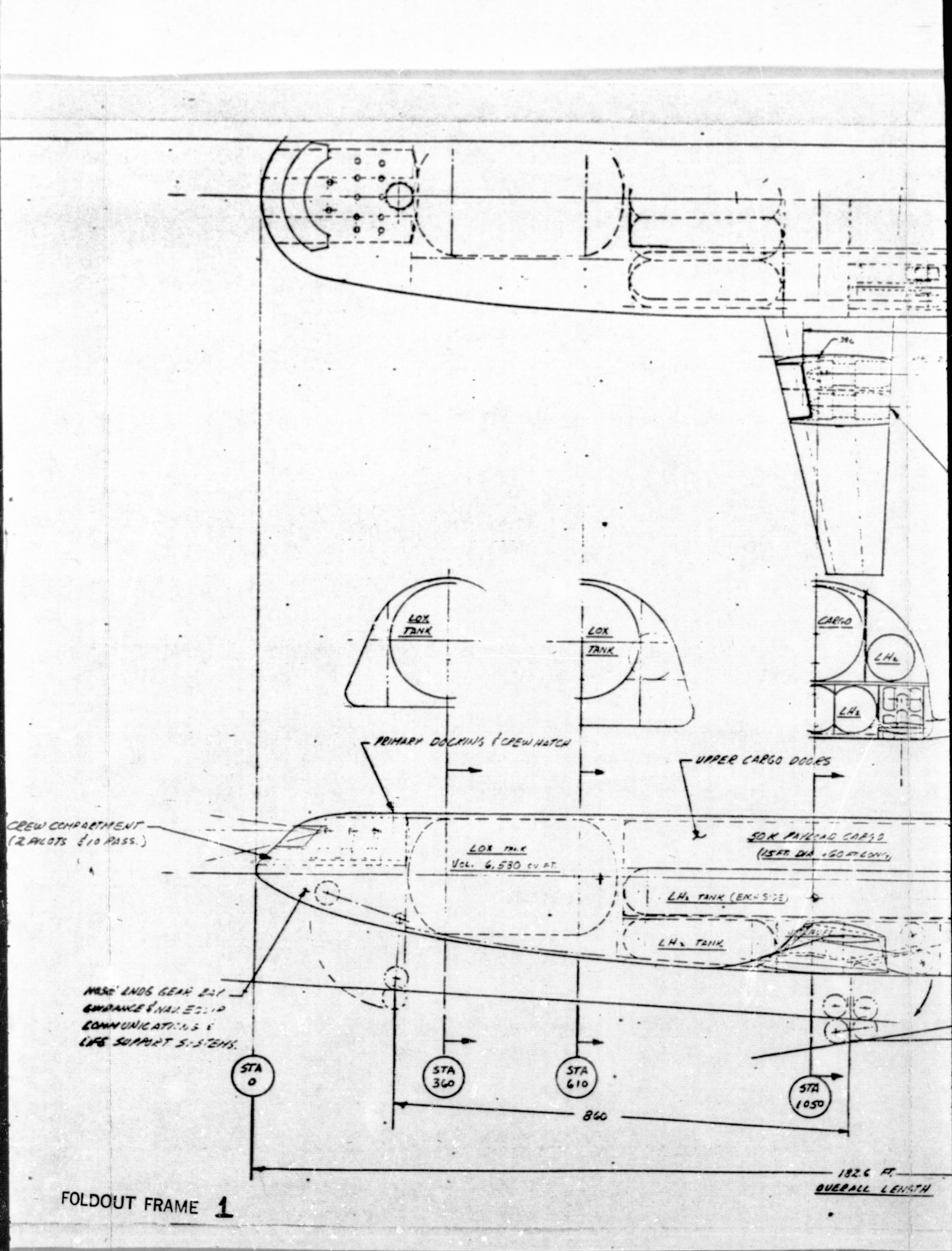

FOLDOUT FRAME 1

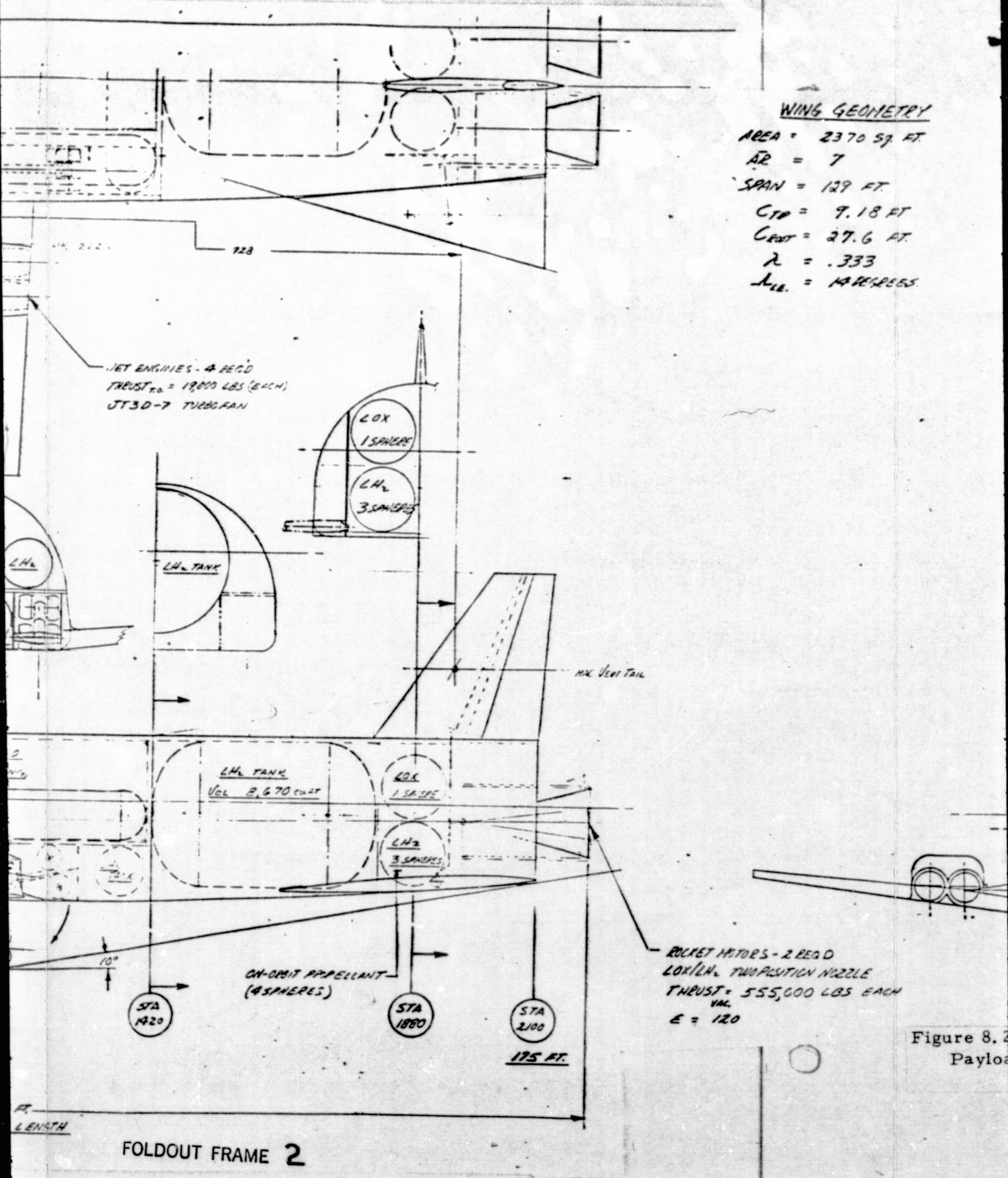

Figure 8.2
Payloa

FOLDOUT FRAME 2

WING GEOMETRY

AREA = 2370 SQ. FT.
AR = 7
SPAN = 129 FT.
C_{TIP} = 9.18 FT
C_{ROOT} = 27.6 FT.
λ = .333
Λ_{LE} = 44 DEGREES

STAGE WEIGHTS

PROPELLANT (LO_2 & LH_2) = 492,000 LBS TOTAL
GROSS STAGE WT. = 741,000 LBS.
RE-ENTRY WT. = 217,000 LBS.
LANDING WT. = 213,000 LBS.
ON-ORBIT PROPELLANT = 32,000 LBS.

TOTAL PLANFORM AREAS

S_{WING} = 2370 SQ. FT. ($W_{LANDING}/S_W$ = 90 PSF)
S_{FUS} = 4860 SQ FT.
S_{TOTAL} = 7230 SQ. FT. ($W_{RE-ENTRY}/S_{TOTAL}$ = 30)

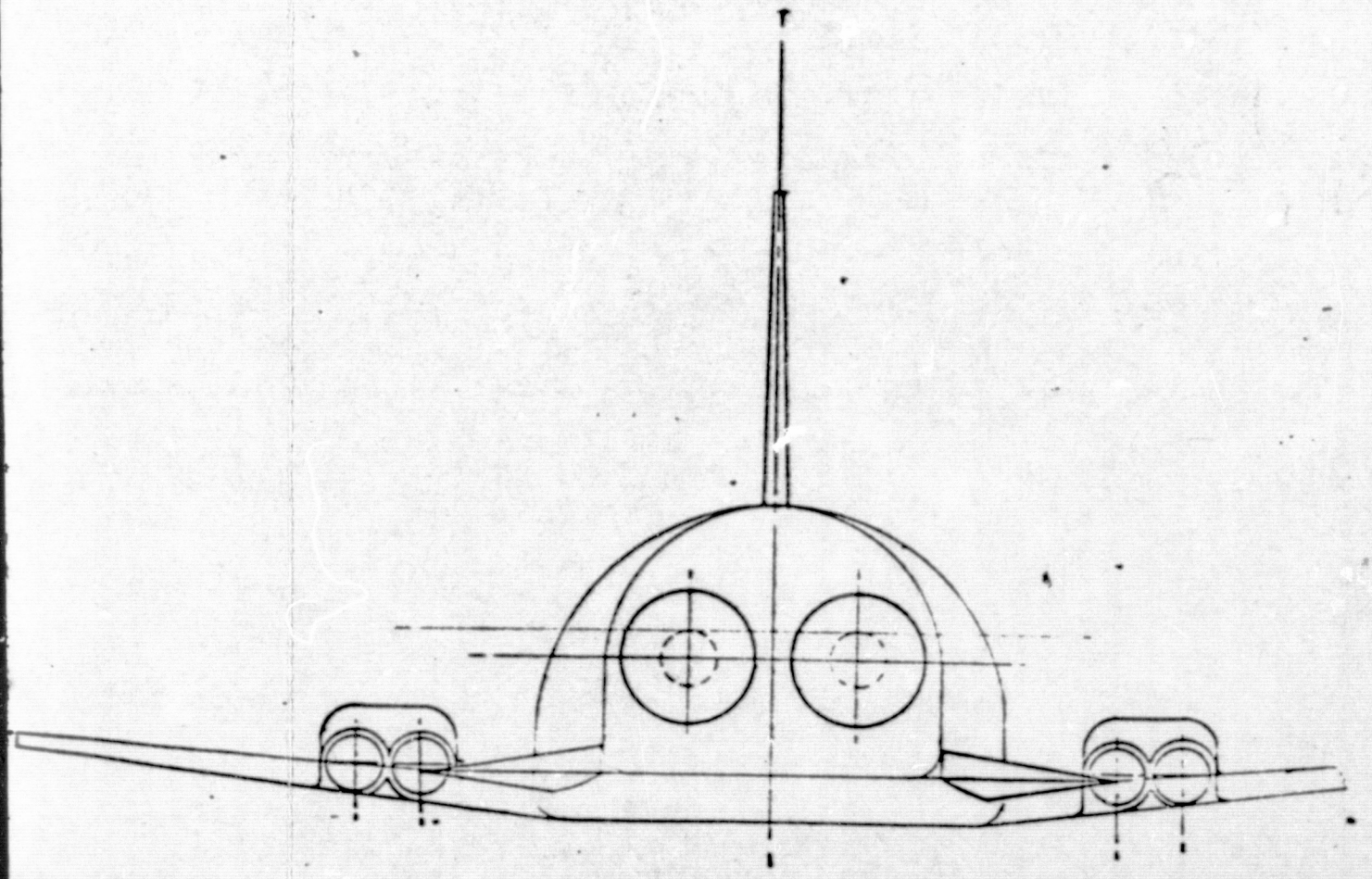

RS - 2 REQ'D
O POSITION NOZZLE
-55,000 LBS EACH

Figure 8.2-9. Orbiter Configuration, MSC Concept, for 50,000-Pound Payload (15-Foot-Diameter by 60-Foot-Length Internal Cargo) (Drawing 2234-60)

REPRODUCIBILITY OF THE ORIGINAL PAGE IS POOR.

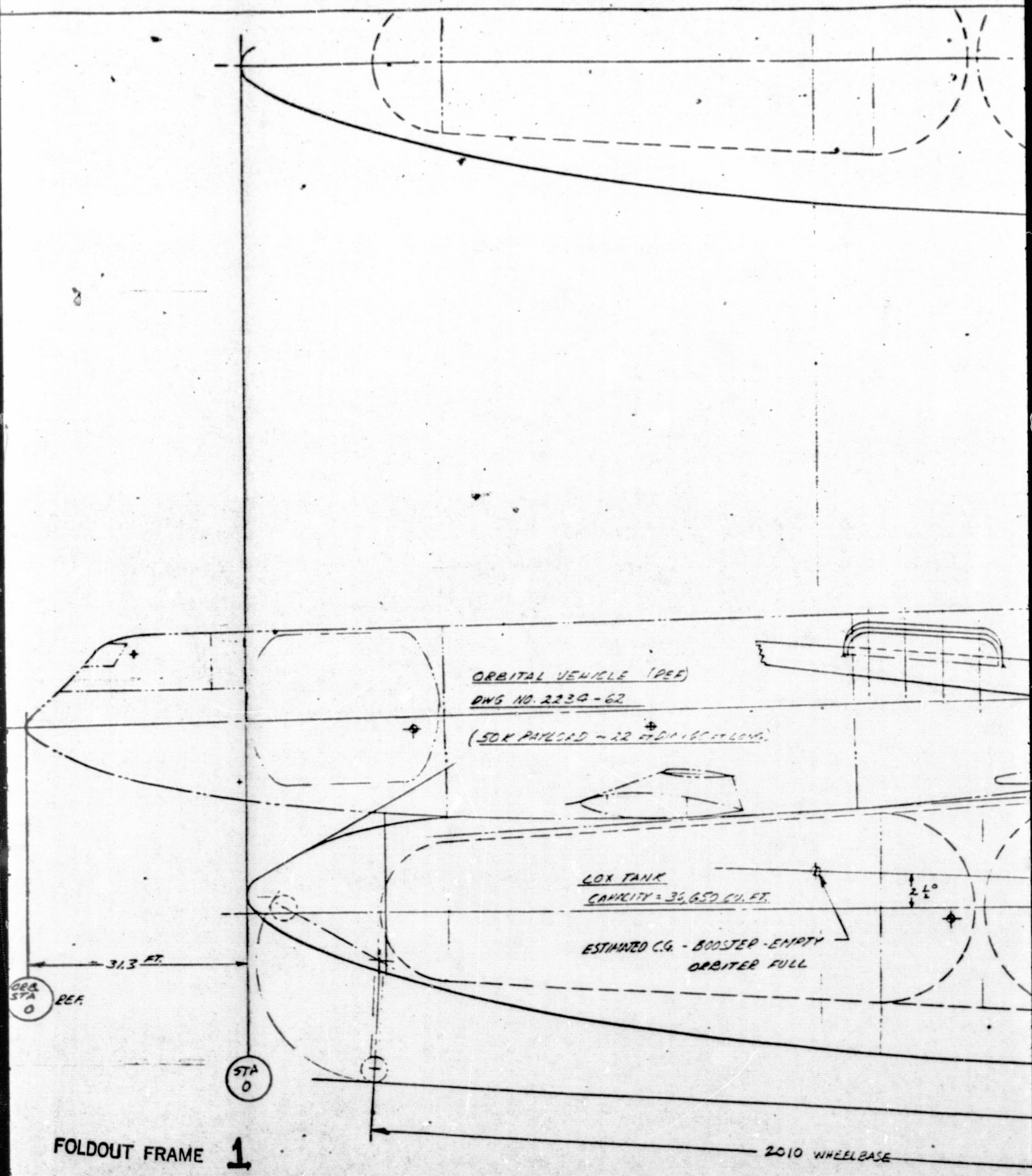

FOLDOUT FRAME 1

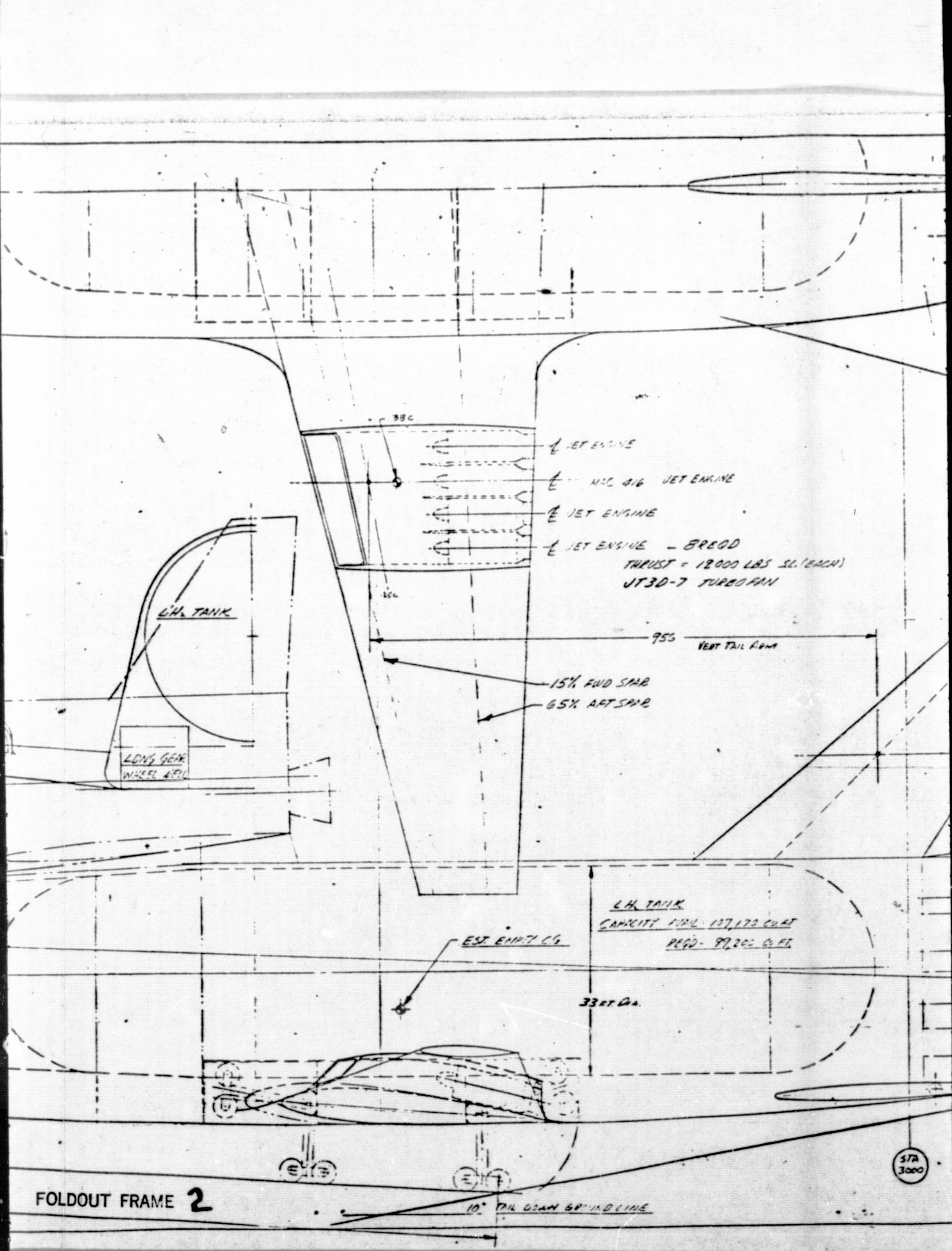

FOLDOUT FRAME 2

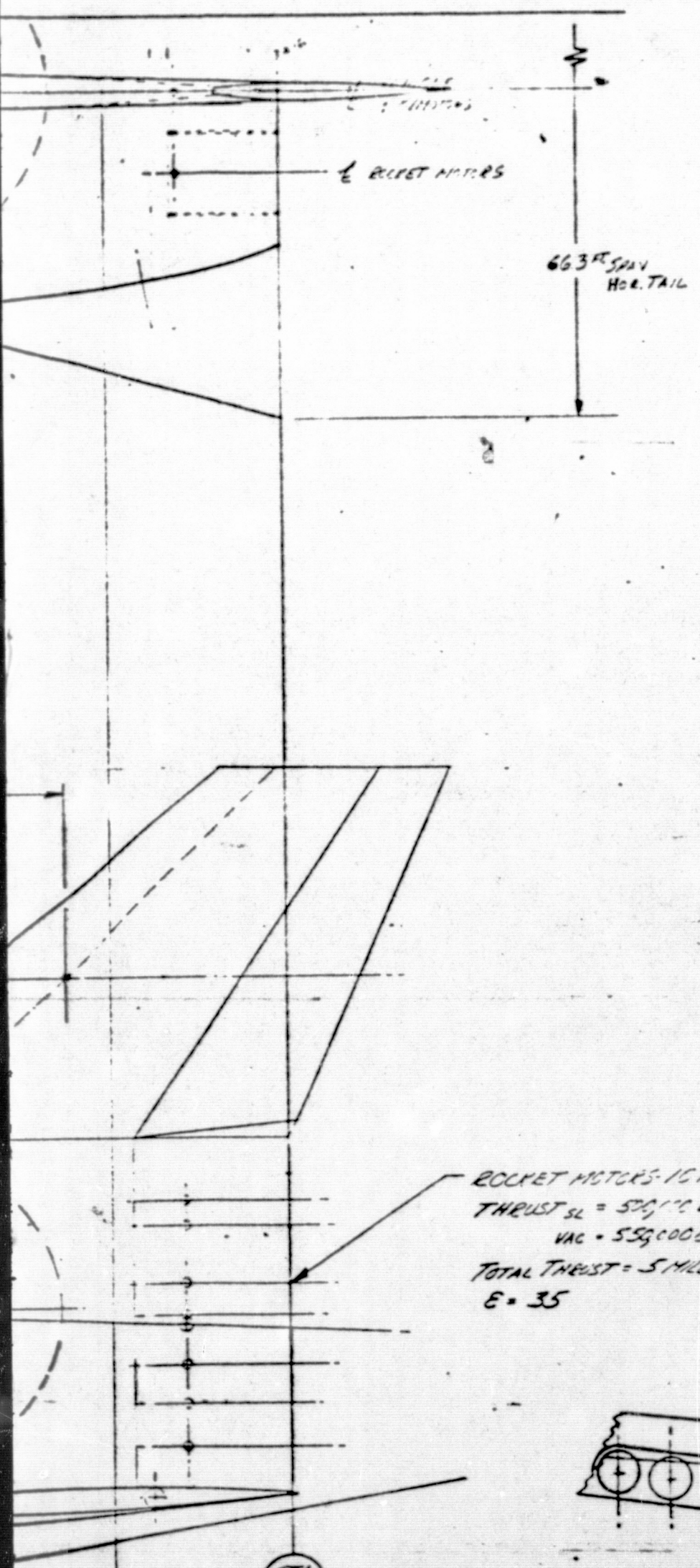

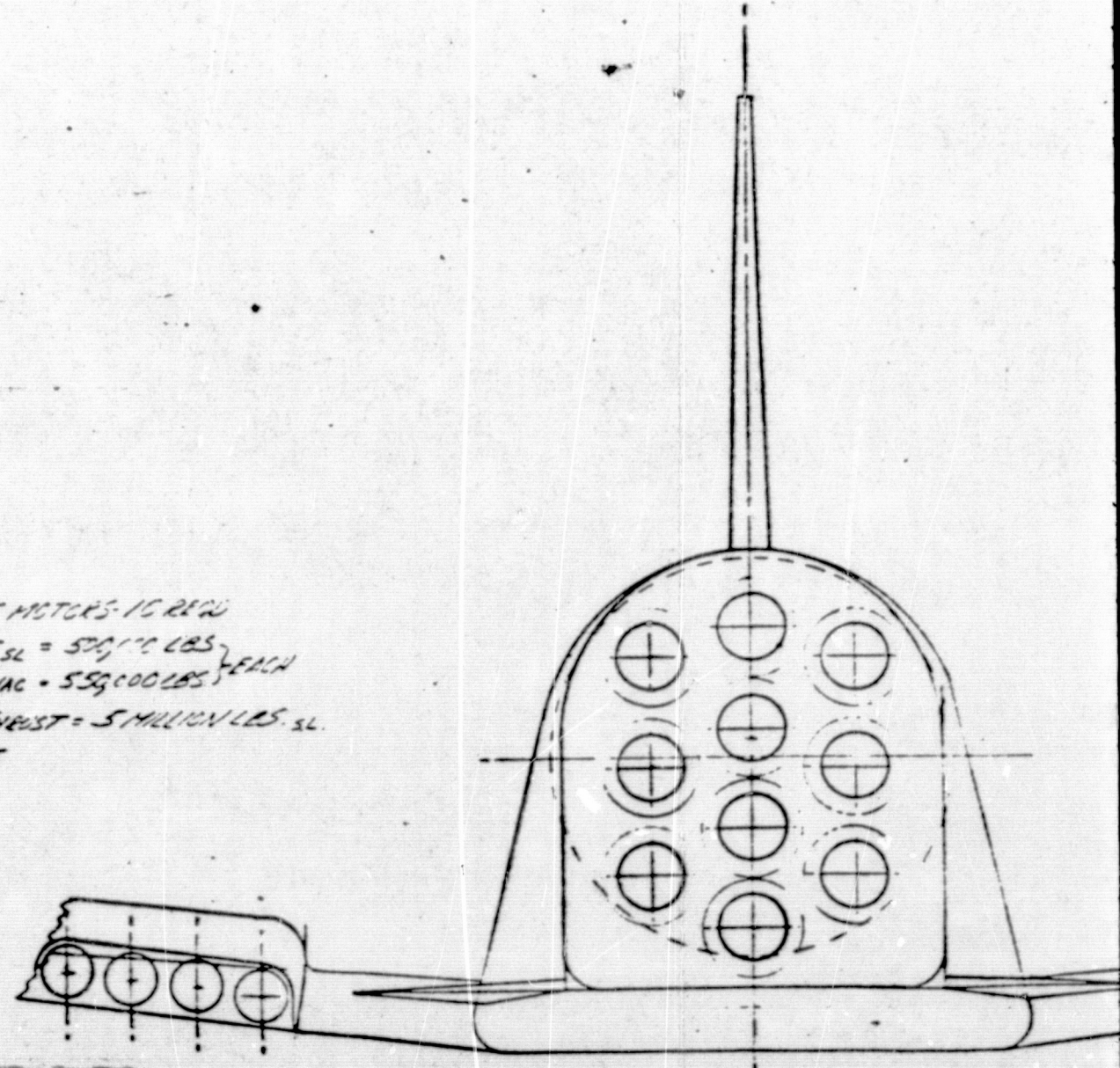

Figure 8.2-10. Booster Configuration f
(22-Foot-Diameter by 60-Foot-
(Drawing 2

FOLDOUT FRAME 3

Space Division
North American Rockwell

WING GEOMETRY

AREA = 7,050 SQ FT
$\bar{AR}$ = 7
SPAN = 222 FT.
C_{TIP} = 15.36 FT
C_{ROOT} = 48.15 FT
λ = .319
Λ_{LE} = 14°

STAGE WEIGHTS

PROPELLANT (LOX/LH$_2$) = 2,731,000 LBS
GROSS STAGE WEIGHT = 3,257,000 LBS.
RE ENTRY WEIGHT = 526,000 LBS.
LANDING WEIGHT = 494,000 LBS.
JET FUEL WEIGHT = 32,000 LBS.

AREAS

S_{WING} = 7050 SQ. FT. $\frac{W}{S_W}$ = 70 PSF
$S_{FUSELAGE\ BOTTOM}$ = 10,480 SQ FT.
$S_{TOTAL\ BOTTOM}$ = 17,530 SQ. FT. $\frac{W}{S_T}$ = 30 PSF

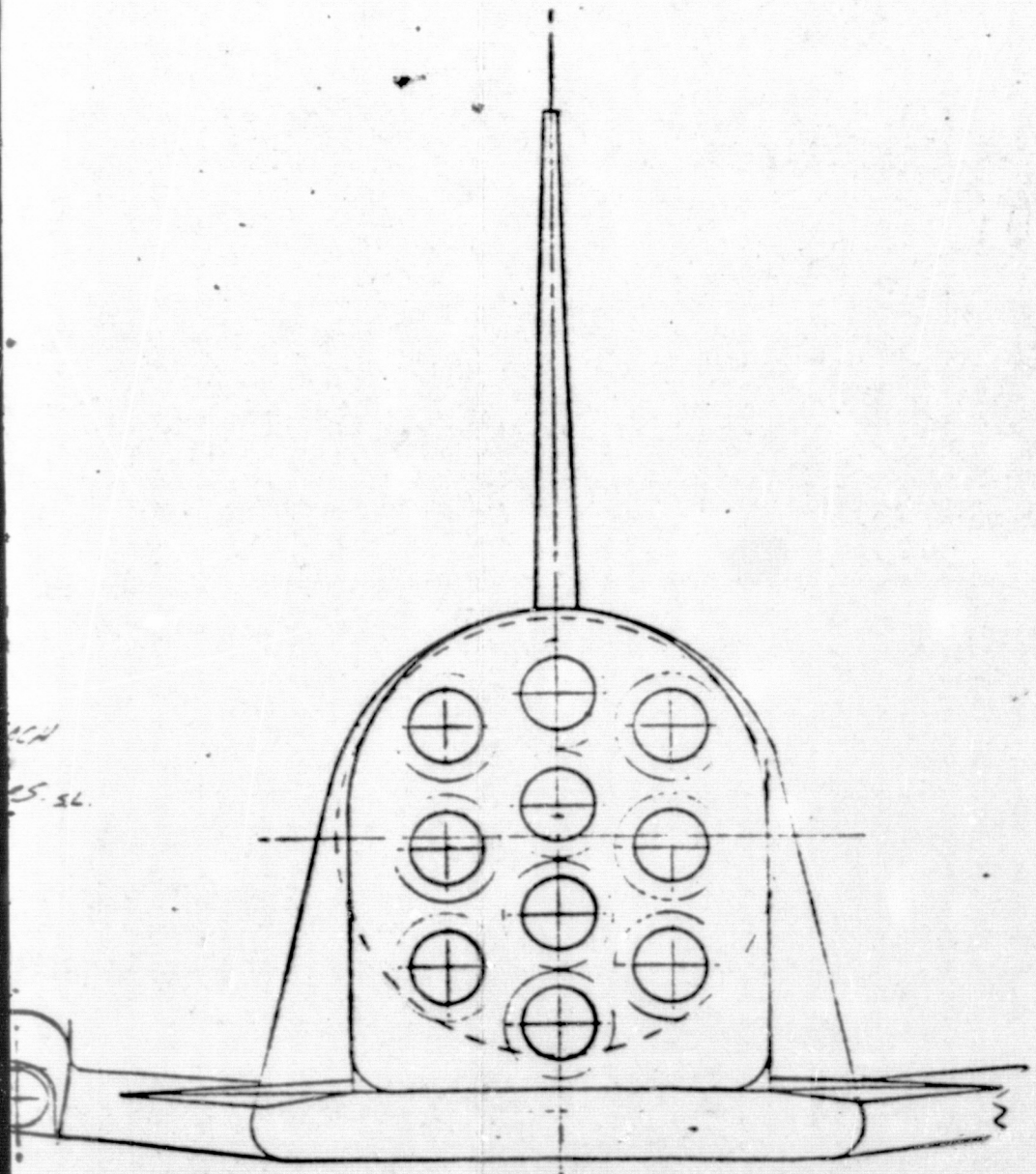

Figure 8.2-10. Booster Configuration for 50,000-Pound-Payload Orbiter (22-Foot-Diameter by 60-Foot-Length Internal Cargo (Drawing 2234-63)

FOLDOUT FRAME 4

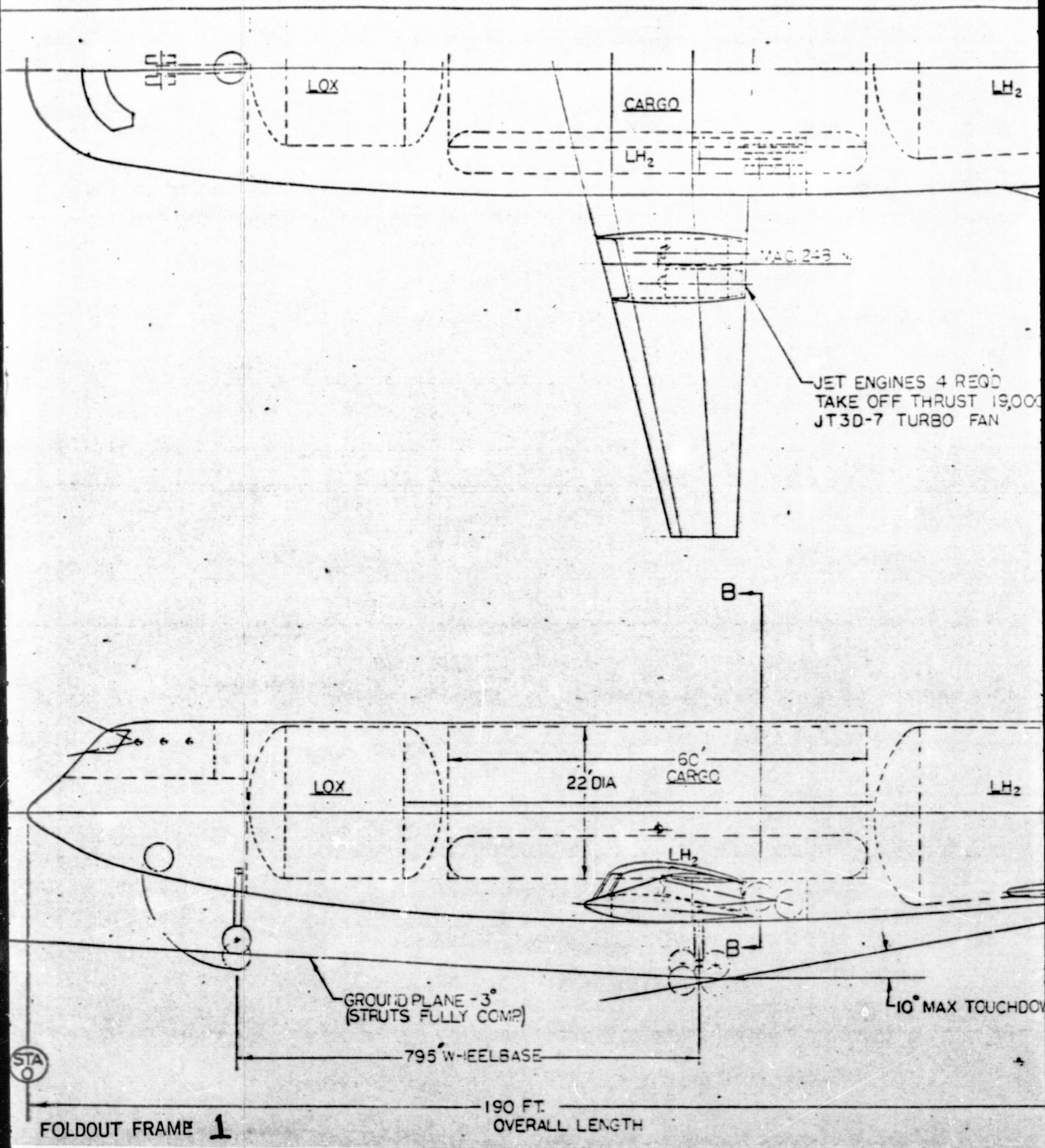

FOLDOUT FRAME 1

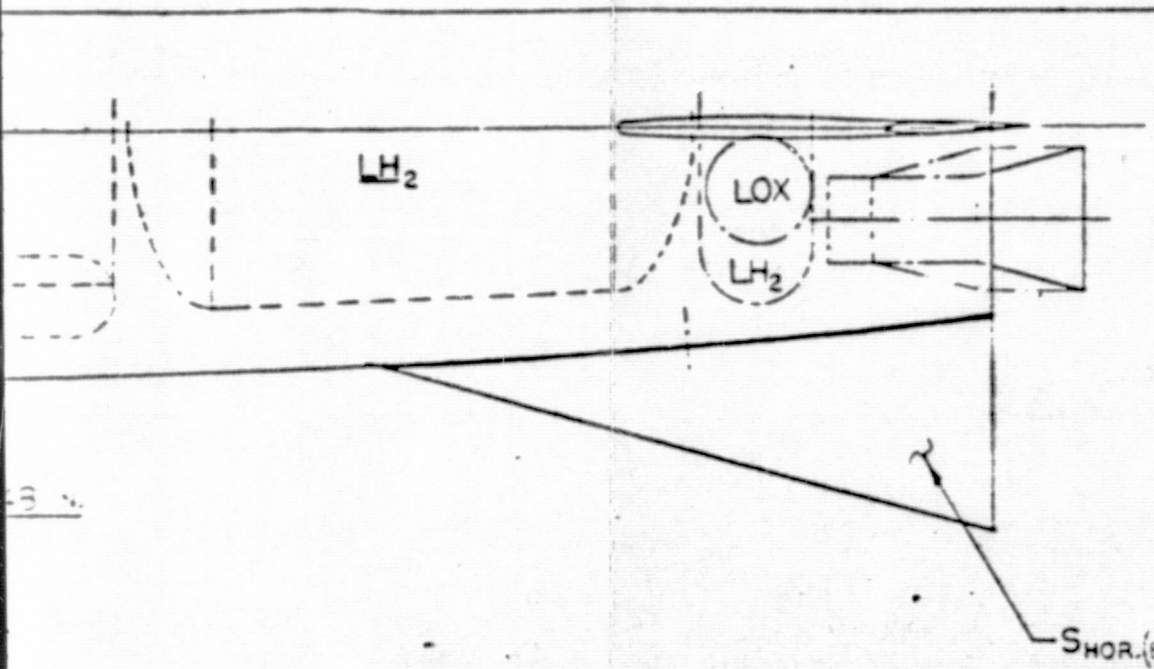

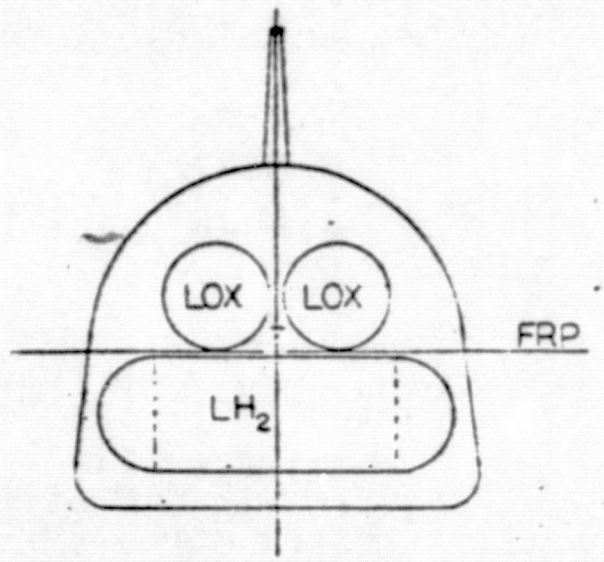

SECTION A-A

JET ENGINES 4 REQD
TAKE OFF THRUST 19,000 LBS EACH
JT3D-7 TURBO FAN

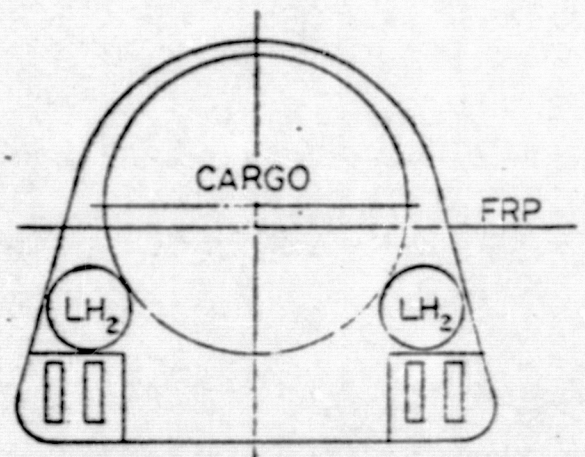

SECTION B-B

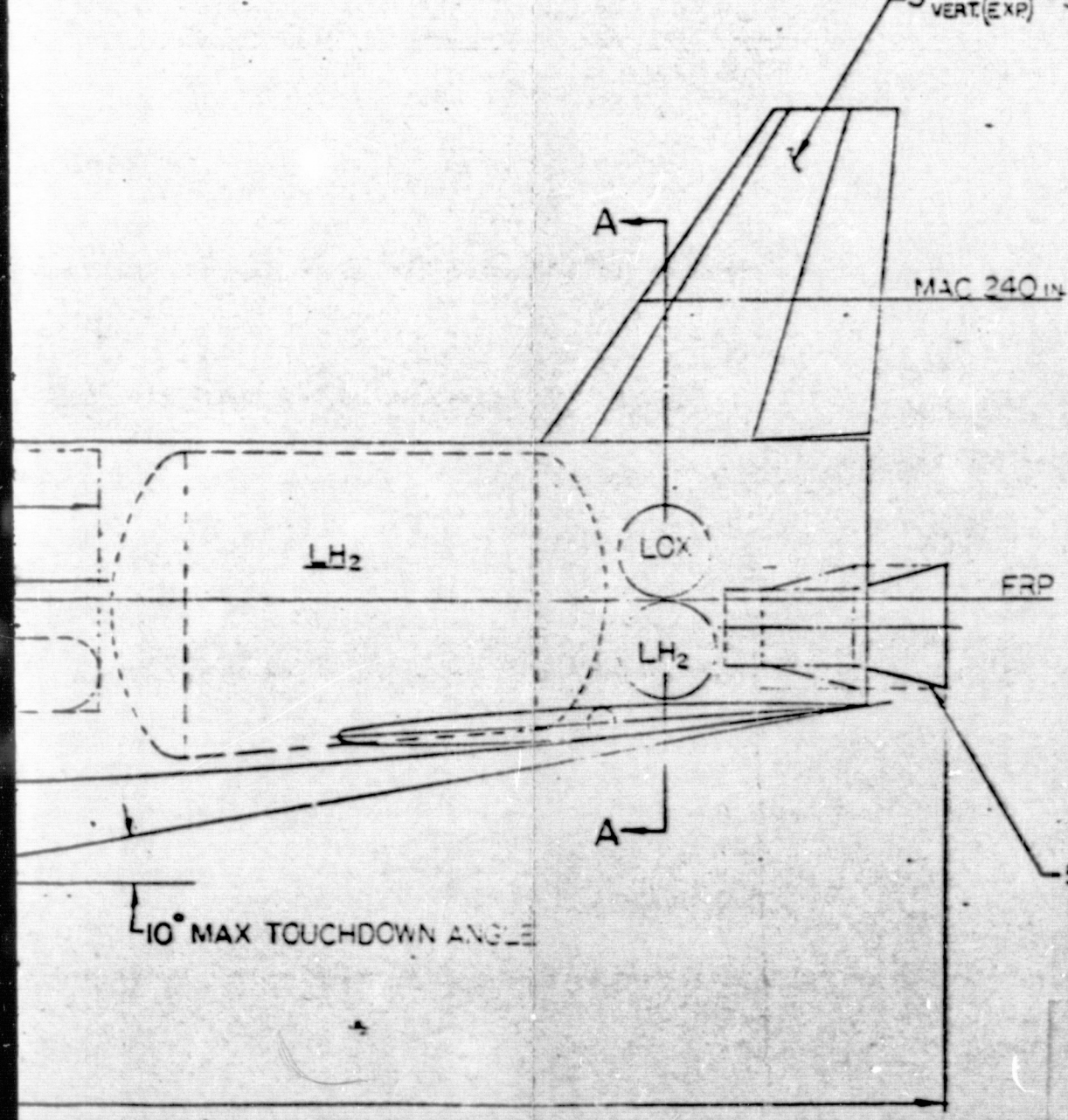

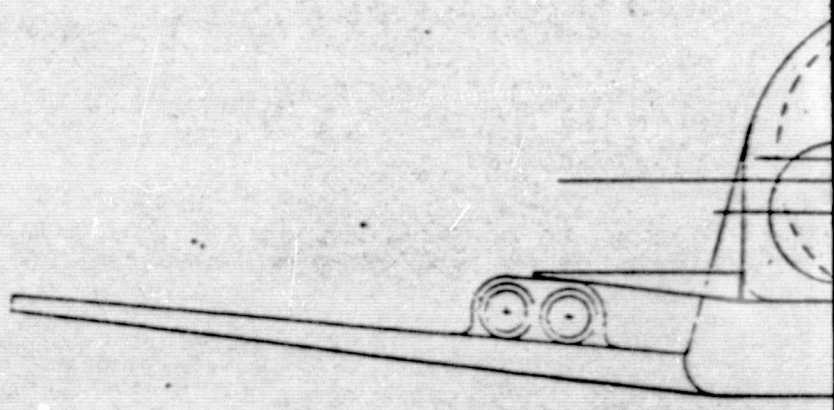

575K THRUST ROCKET ENGINES 2 REQ'D.
LOX/LH_2 TWO POSITION NOZZLE
ε - 120

FOLDOUT FRAME 2

WING GEOMETRY

S_W - 2,540 SQ FT
SPAN - 133 FT
C_R - 28.6 FT
C_T - 9.5 FT
Λ_{LE} - 14°
λ - .333
MAC - 248 IN.
A.R. - 7

STAGE WEIGHTS

PROPELLANT (LOX / LH_2) - 507,000 LBS TOTAL
TOTAL LAUNCH - 740,000 LBS
REENTRY - 233,000 LBS
LANDING - 229,000 LBS
PROPELLANT (LOX / LH_2) ON ORBIT - 34,000 LBS

TOTAL PLANFORM AREAS

S_{WING} - 2,540 SQ FT $\left(\frac{W}{S_W}\right.$ - 90 LDG$)$
S_{FUS} - 5,210 SQ FT
TOTAL - 7,750 SQ FT $\left(\frac{W}{S_{TOTAL}}\right.$ - 30 REENTRY$)$

8.2-11
SD 69-573-4

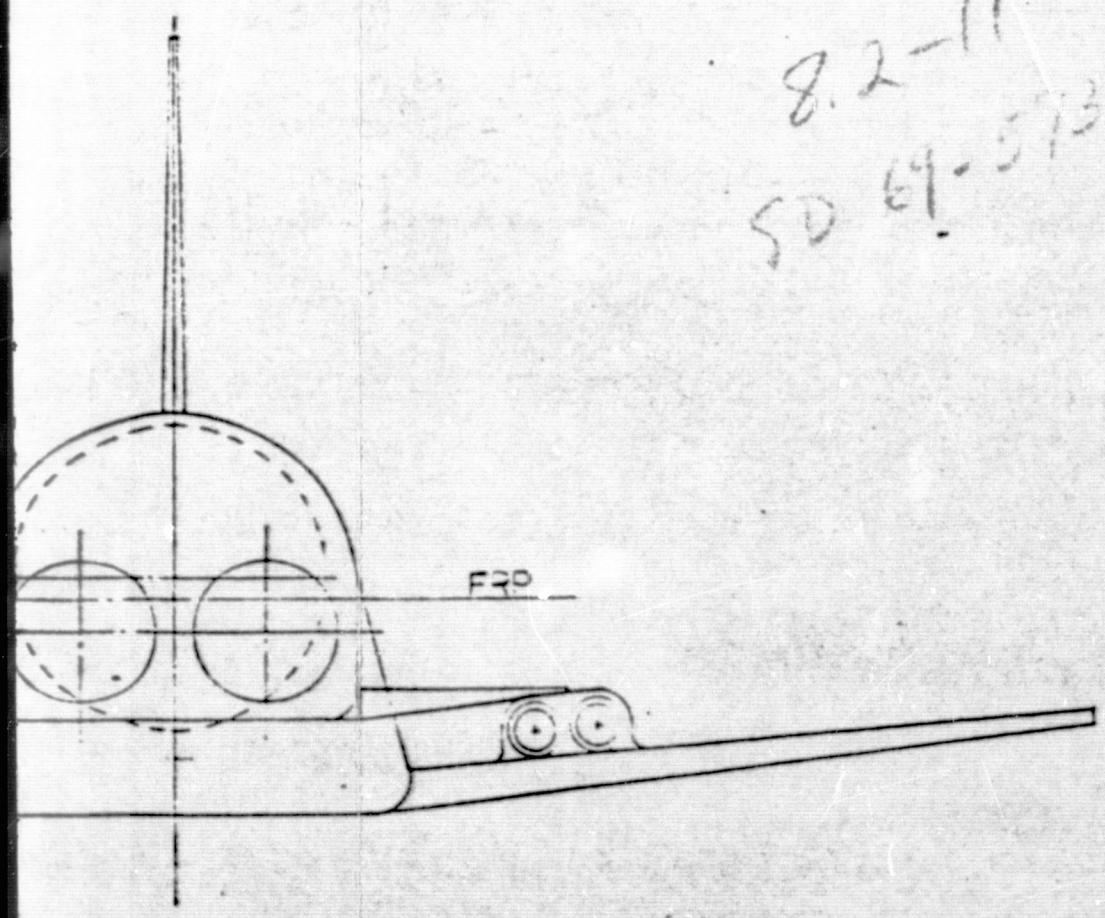

Figure 8.2-11. Orbiter Configuration, MSC Concept, for 50,000-Pound Payload (Internal Cargo) (Drawing 2234-62)

Table 8.2-3. Shuttle Vehicle Configuration Summary

Parameter	7,700-Pound Cargo (2,000 Cubic Ft)		25,000-Pound Cargo				50,000-Pound Cargo			
			15-Ft Diameter by 30-Ft Length		15-Ft Diameter by 60-Ft Length		15-Ft Diameter by 60-Ft Length		22-Ft Diameter by 60-Ft Length	
	Booster	Orbiter	Booster	Orbiter	Booster	Orbiter	Booster	Orbiter	Booster	Orbiter
Gross stage weight (1,000 lb)	1,279	385	2,107	469	2,204	526	2,739	741	3,267	740
Propellant weight (1,000 lb)	1,018	285	1,729	325	1,813	368	2,269	524	2,731	507
Length (ft)	192	132	207	152	235	177	256	182.6	268	192
Wing span (ft)	134	75	188	105	191	110	210	129	222	133
Wing area (ft^2)	3,500	1,100	5,070	1,578	5,240	1,730	6,310	2,370	7,050	2,540
Total plan area (ft^2)	8,700	3,300	12,600	4,800	13,040	5,260	15,670	7,230	17,530	7,750
Number of rocket engines times thrust* (1,000 lb)	8x260	2x300	10x326	2x375	10x375	2x430	9x482	2x555	10x500	2x575
Turbojet thrust (1,000 lb)	60	26	87	37	90	41	108	56	124	60
Overall wehicle length (ft)	206		246		261		289		299	
Gross vehicle weight (1,000 lb)	1,664		2,576		2,730		3,480		4,007	

*Booster thrust shown is at SL; orbiter thrust is in vacuum. Same basic engine is used in booster and orbiter with fixed 35:1 nozzle on booster and two-position 120:1 nozzle on orbiter.

8.2.3 Configuration Improvement and Design Trades

The configuration improvement studies conducted and the evolution of the orbiter and booster configurations subjected to detail design analysis are reported in this section.

Cargo Access

Early in the study, qualitative consideration was given to various methods of cargo access, which is an important design issue because (1) the orbiter must be capable of being trimmed on reentry and during glide/cruise/landing with and without cargo, and (2) the orbiter design must be capable of having a payload the size of the cargo bay removed in orbit. This requirement can have a significant impact on orbiter design and internal arrangement. The impact of top, aft, and forward cargo removal was considered. Top cargo access was selected for this conceptual design phase. Some of the pertinent comments for each concept are shown in Figure 8.2-12.

The top cargo access assumes that the orbiter is docked under the space station. Concepts can include:

1. Rotation of cargo container 180 degrees to form docking interface and interconnect with crew transfer tunnel

2. Raising and translating cargo container forward to form docking interface and interconnect with crew transfer tunnel

3. Lifting container into space station hangar

The aft cargo container access assumes that the aft end of the orbiter is docked to the space station. A cargo container can be removed aft as illustrated in Figure 8.2-12 or the fuselage can be broken aft of the cargo bay. Either approach complicates the orbiter design and internal arrangement. Furthermore, the broken fuselage requires satisfactory relatching for safe entry and also complicates design of the thermal protection system.

The forward cargo container access assumes forward docking with the nose rotated prior to docking. This concept also requires that the fuselage be broken for cargo container removal, satisfactory relatching for safe entry, and sealing of the joint in the thermal protection.

Conceptual Design Configuration Evolution

Following the selection of a 50,000-pound-payload vehicle with a 15-foot-diameter by 60-foot-length cargo bay for conceptual design definition, 50,000-pound-payload baseline orbiter and booster configurations

CARGO ACCESS	COMMENTS
TOP 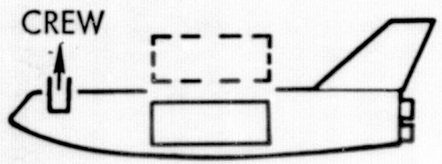 	1. DOCKING IS VISUAL TO PILOT 2. STRUCTURE & LINES NOT BROKEN FOR DOCKING 3. BASIC DESIGN – GOOD AS BASIC STRUCTURE NOT BROKEN. FWD END DIAMETER BASED ON COCKPIT. AFT END DIAMETER BASED ON ENGINES 4. DOCKING – CREW TRAVEL DIRECTLY INTO SPACE STATION 5. LOADING – CARGO EASILY REPLACED ON ORBITER-BOOSTER COMBINATION
AFT 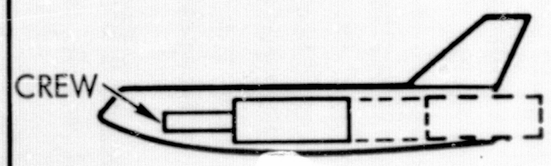 	1. DOCKING NOT VISUAL TO PILOT 2. STRUCTURE & LINES NOT BROKEN FOR DOCKING 3. BASIC DESIGN – VEHICLE DIAMETER AT AFT END BECOMES VERY LARGE DUE TO CARGO HAVING TO GO THROUGH LARGE DIAMETER FOR ENGINES. VOLUME NECESSARY AFT OF CARGO WHICH CANNOT BE USED 4. DOCKING – CREW TRAVEL COMPLETE LENGTH OF VEHICLE 5. LOADING – CARGO NOT READILY REPLACEABLE ON ORBITER-BOOSTER AFTER MATING
FWD 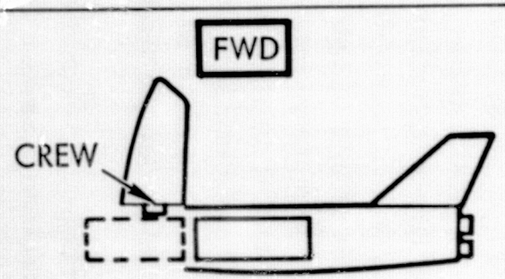 	1. DOCKING NOT VISUAL TO PILOT 2. STRUCTURE, HEAT SHIELD/LINES BROKEN FOR DOCKING 3. BASIC DESIGN – COMPLICATES STRUCTURE, COMPLETE STRUCTURE BROKEN INCLUDING ALL LINES 4. DOCKING – CREW TRAVEL REQUIRED PAST BREAK 5. LOADING – CARGO NOT READILY REPLACEABLE ON ORBITER-BOOSTER AFTER MATING

Figure 8.2-12. Cargo Access Evaluation

reflecting the latest vehicle size requirements were prepared. These baseline configurations are presented in Figures 8.2-13 (Drawing 2234-68) and 8.2-14 (Drawing 2234-69). A summary of the configuration features is given in Table 8.2-4. These baseline configuration layouts provided the basis for generation of mass properties used in structural loads and vehicle control analysis and provided a point of departure for aerodynamic and design studies. In the orbiter, the oxygen is located forward in a single cylindrical tank with a crew access tunnel to the cargo bay. LH_2 is located in two tanks: a pillow-type tank under the cargo bay and forward of the wing carry-through structure and a large cylindrical tank aft of the cargo bay. In the booster, the LO_2 is located forward in a single tank, and the LH_2 is located aft in a single tank. A flat bottom is provided on both the orbiter and booster, and the planform area is sized to provide a weight-to-planform area ratio of 30:1.

The baseline orbiter configuration was prepared assuming a longitudinal center of gravity at X/L = 0.5. Mass properties analysis indicated that the center of gravity would be located at X/L = 0.58. A balanced configuration was prepared with the wing moved aft to locate the center of gravity at the 25-percent MAC and with the cargo bay centered over the center of gravity as shown in Figure 8.2-15 (Drawing 2234-70). This arrangement requires that a portion of the LH_2 be located forward of the cargo bay in addition to the LO_2. The LO_2 was located in a 15-foot-diameter cylindrical tank to provide a good load path to the 15-foot-diameter cargo bay structure. A series of LH_2 pillow tanks is installed under the LO_2 tank and cargo bay. A spherical LH_2 tank is provided aft of the cargo bay.

Other means of moving the orbiter center of gravity forward were investigated. The only system of significant weight that can be moved forward is the turbojet propulsion system. In support of this consideration, the possibility of installing the turbojets in the nose area was grossly evaluated. The four JT3D-7 turbojets can be located within the orbiter mold line at either the cabin area (Station 210) or opposite the LO_2 tank (Station 610) as shown in Figures 8.2-16 and 8.2-17. The cabin area location is preferred because it has the most effect in moving the center of gravity forward and because a fixed installation can be used. The air-induction and nozzle-exhaust systems were not evaluated, but appear to present formidable problems. The effect of the canted installation on vehicle performance, as well as the effect of exhaust heating and interference with aerodynamic surfaces, also requires evaluation. The aft location is shown with swing-out doors, which may provide the better alternative if this location is selected. A decision was made to maintain the top-wing turbojet installation; consequently, the forward-mounted turbojet concepts were not pursued further.

In support of the aerodynamic evaluation to reduce horizontal tail size, a configuration similar to that shown in Figure 8.2-15 was prepared without

REPRODUCIBILITY OF THE ORIGINAL PAGE IS POOR.

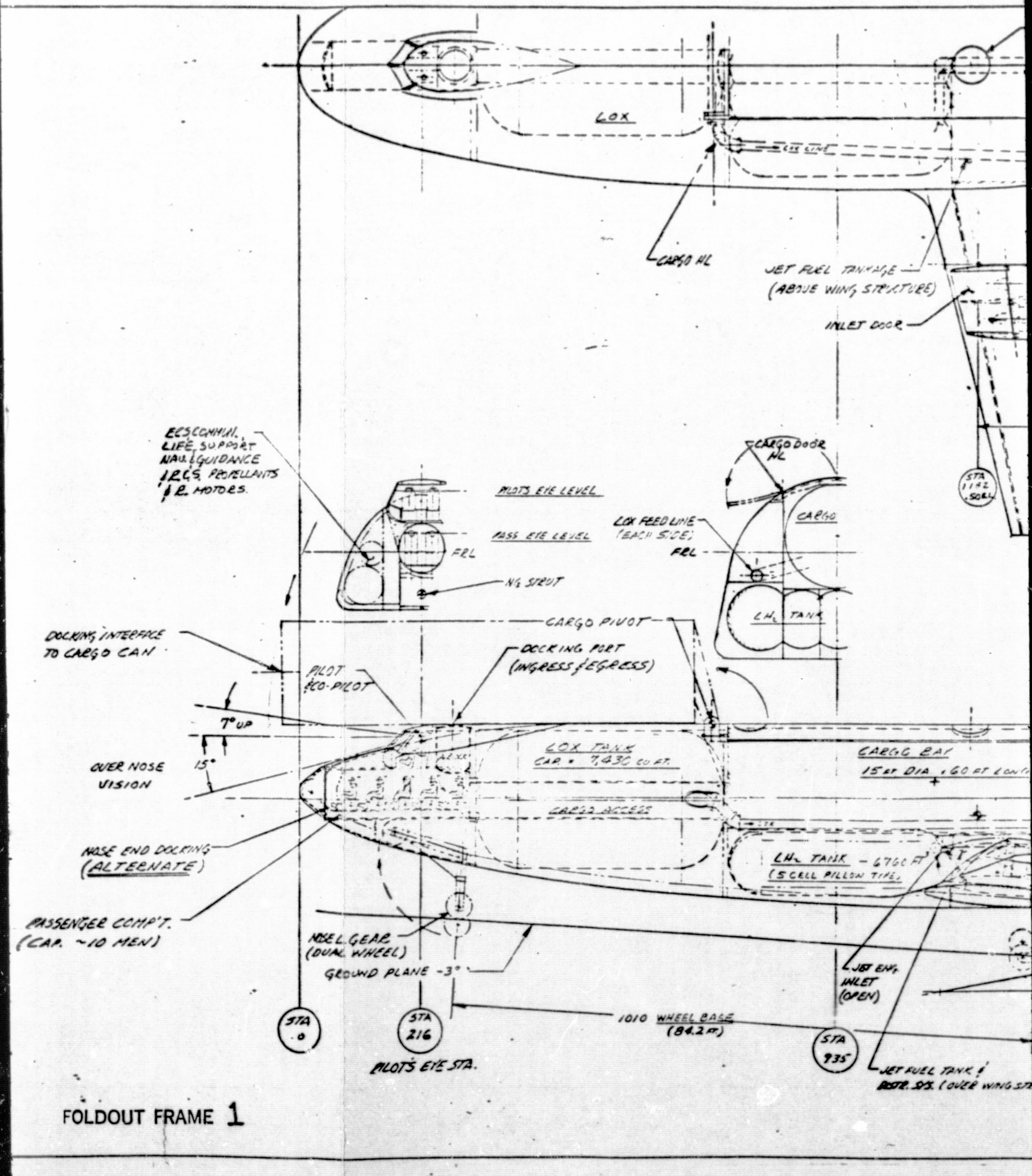

FOLDOUT FRAME 1

SPLIT DOOR HATCH COVER

LH₂ SUMP

℄ VEHICLE

℄ PULSET MOTOR

LH₂

JET ENGINES - 4 REQ'D
TAKE-OFF THRUST = 19,000 LB EACH
UT 3D-7 TURBOFAN

1040

STA 1142 SOR

LOX FEED LINE

LOX SPHERE

℄

LH₂ TANK

LH₂ SPHERE

MAC VERT TAIL 267 IN

FUEL FEED LINE

CRYOGENIC LOX

CARGO DOOR
(SAME - LONG. HL)

CARGO BAY
15 FT DIA x 60 FT LONG

LH₂ TANK
VOL. = 13,601 CU FT

LH₂ FEED LINE (2 SUPPLIES)

ENGINE GIMBAL PT.

10° TOUCH DOWN PLANE

STA 1656

STA 2104

STA 2424
(202 FT)

JET FUEL TANK
RESP. SYS. (OVER WING STRUCTURE)

FOLDOUT FRAME 2

Space Division
North American Rockwell

WING GEOMETRY

AREA (THEOR) = 2620 SQ FT
SPAN = 135.5 FT.
C_{ROOT} = 29 FT.
C_{TIP} = 9.65 FT.
Λ_{LE} (SWEEP) = 14°
λ (TAPER) = .333
M.A.C. = 250 IN.
AR = 7

STAGE WEIGHTS

PROPELLANT (LOX/LH$_2$) = 555,000 LBS.
TOTAL LAUNCH = 835,000 LBS.
REENTRY = 295,000 LBS.
LANDING = 243,000 LBS.
PROPELLANT (ON ORBIT) = 35,000 LBS.

TOTAL PLANFORM AREAS

S_{WING} = 2620 SQ FT (W/S_W = 90 PSF)
$S_{FUS.}$ = 5330 SQ FT.
S_{TOTAL} = 8000 SQ FT. ($W/S_{TOT.}$ = 30)

135.5 FT. WING SPAN

℄ VEHICLE

FRL

35°

ROCKET MOTORS - 2 REQ'D
TWO POSITION NOZZLE
THRUST (VAC.) = 640,000 LBS EACH
ε = 120

FOLDOUT FRAME 3

SCALE: 1" = 100"

0 50' 100' 200' 300' 400' 500'

Figure 8.2-13. Baseline 50,000-Pound-Payload Orbiter (Drawing 2234-68)

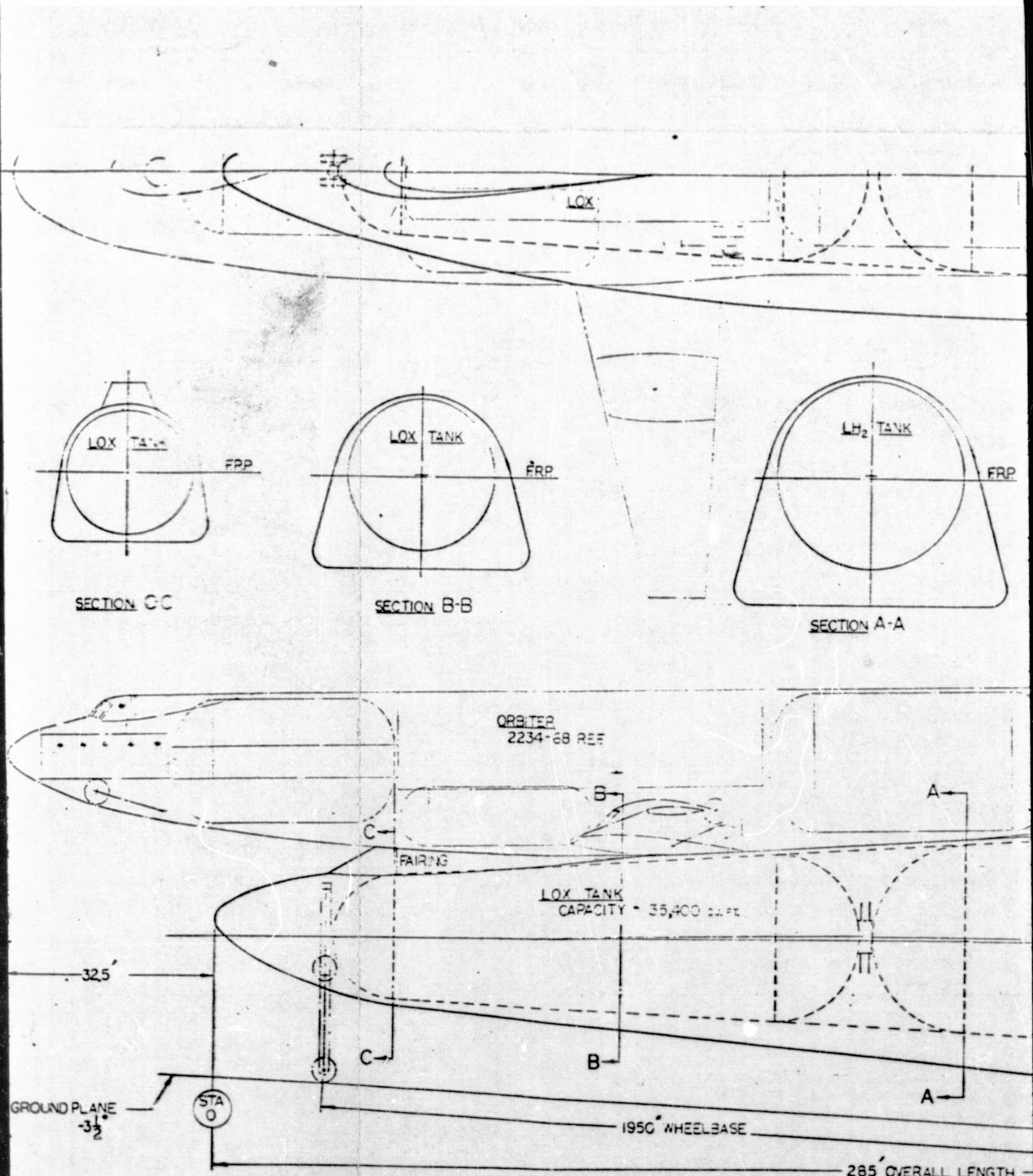

FOLDOUT FRAME 1

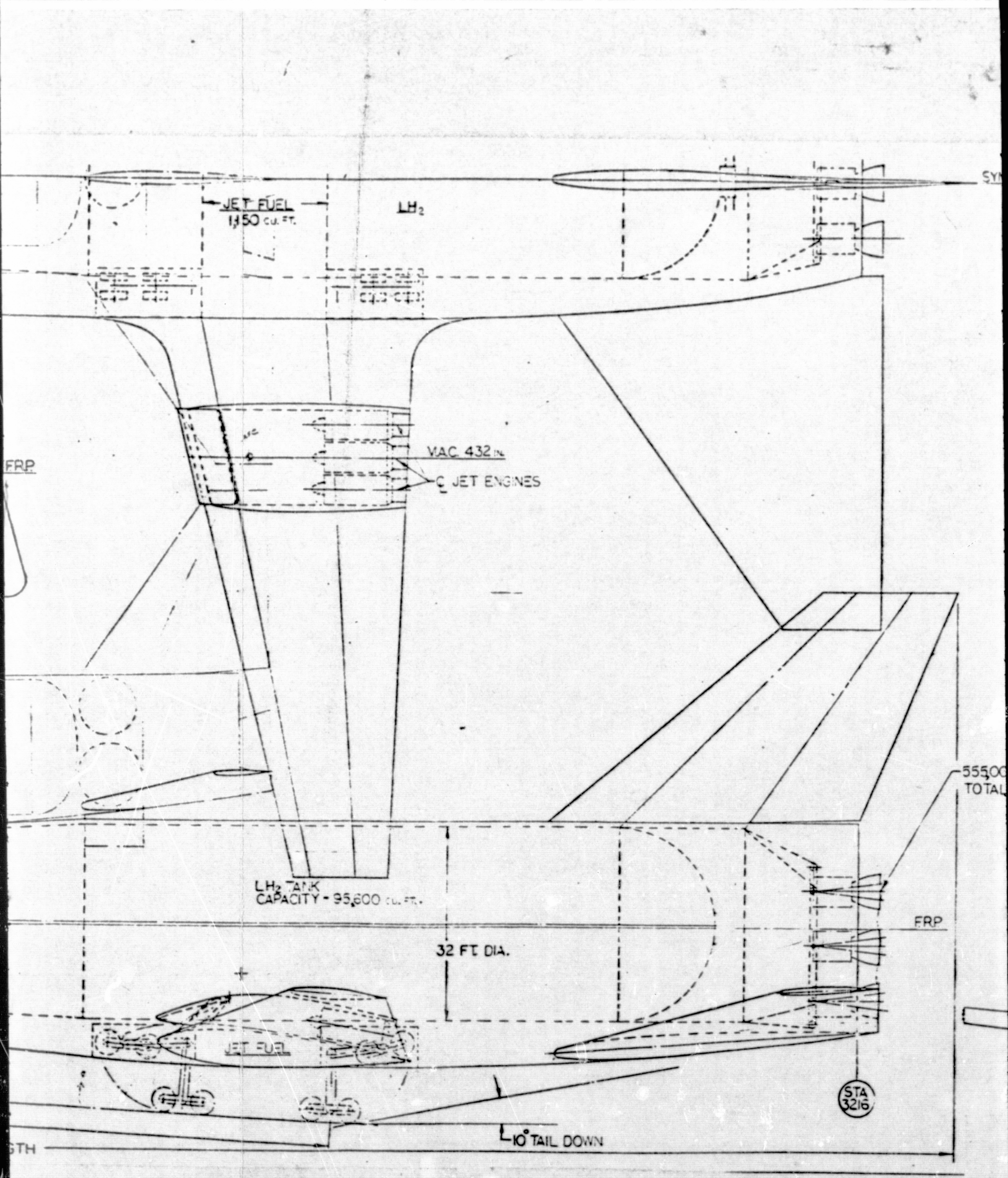

FOLDOUT FRAME 2

SYMM. ℄

WING GEOME

S_W = 7,550 SQ. FT.
SPAN - 230 FT.
C_R = 49.8 FT.
C_T = 15.9 FT.
Λ_{LE} = 14°
λ = .319

555,000 THRUST ROCKET ENGINES 9 REQ'D.
TOTAL THRUST @ SEA LEVEL = 5.55 × 10^6 LBS.

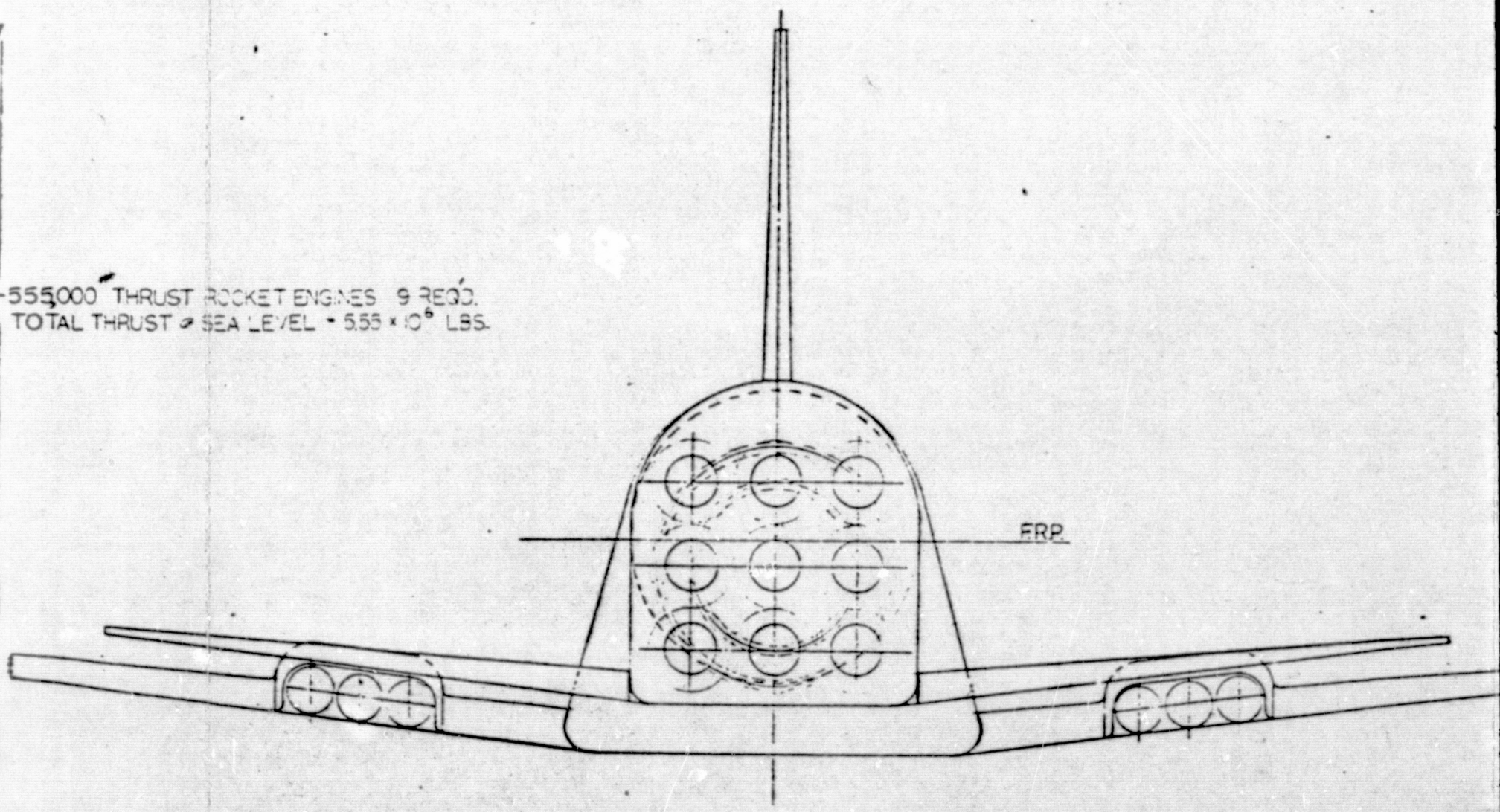

FOLDOUT FRAME 3

WING GEOMETRY

S_W = 7,550 SQ. FT.
SPAN = 230 FT.
C_R = 49.8 FT.
C_T = 15.9 FT.
Λ_{LE} = 14°
λ = .319

STAGE WEIGHTS

PROPELLANT (LOX & LH_2)	=	2,600,000 LBS.
TOTAL LAUNCH	=	3,150,000 LBS.
REENTRY	=	550,000 LBS.
LANDING	=	494,000 LBS.

TOTAL PLANFORM AREAS

S_{WING} = 7,550 SQ. FT. $\left(\frac{W}{S_W} = 70\ LDG\right)$

$S_{FUS.}$ = 11,310 SQ. FT.

TOTAL = 18,860 SQ. FT. $\left(\frac{W}{S}_{TOTAL} = 30\ REENTRY\right)$

8-14

SD 69-

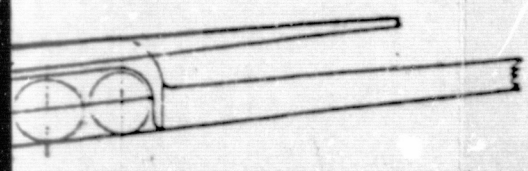

Figure 8.2-14. Baseline 50,000-Pound-Payload Booster (2234-69)

FOLDOUT FRAME 4

SD 69-573-4

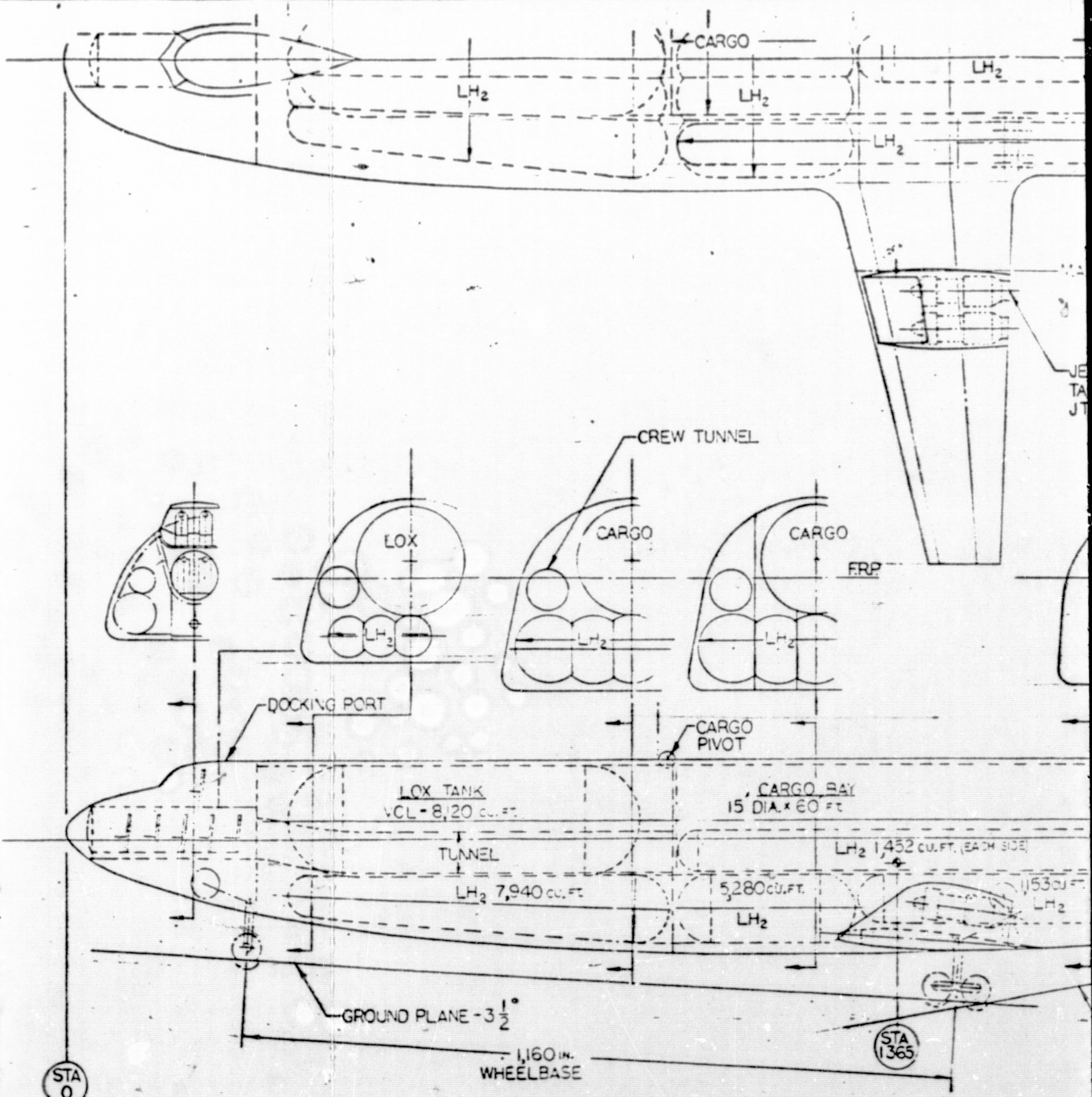

FOLDOUT FRAME 1

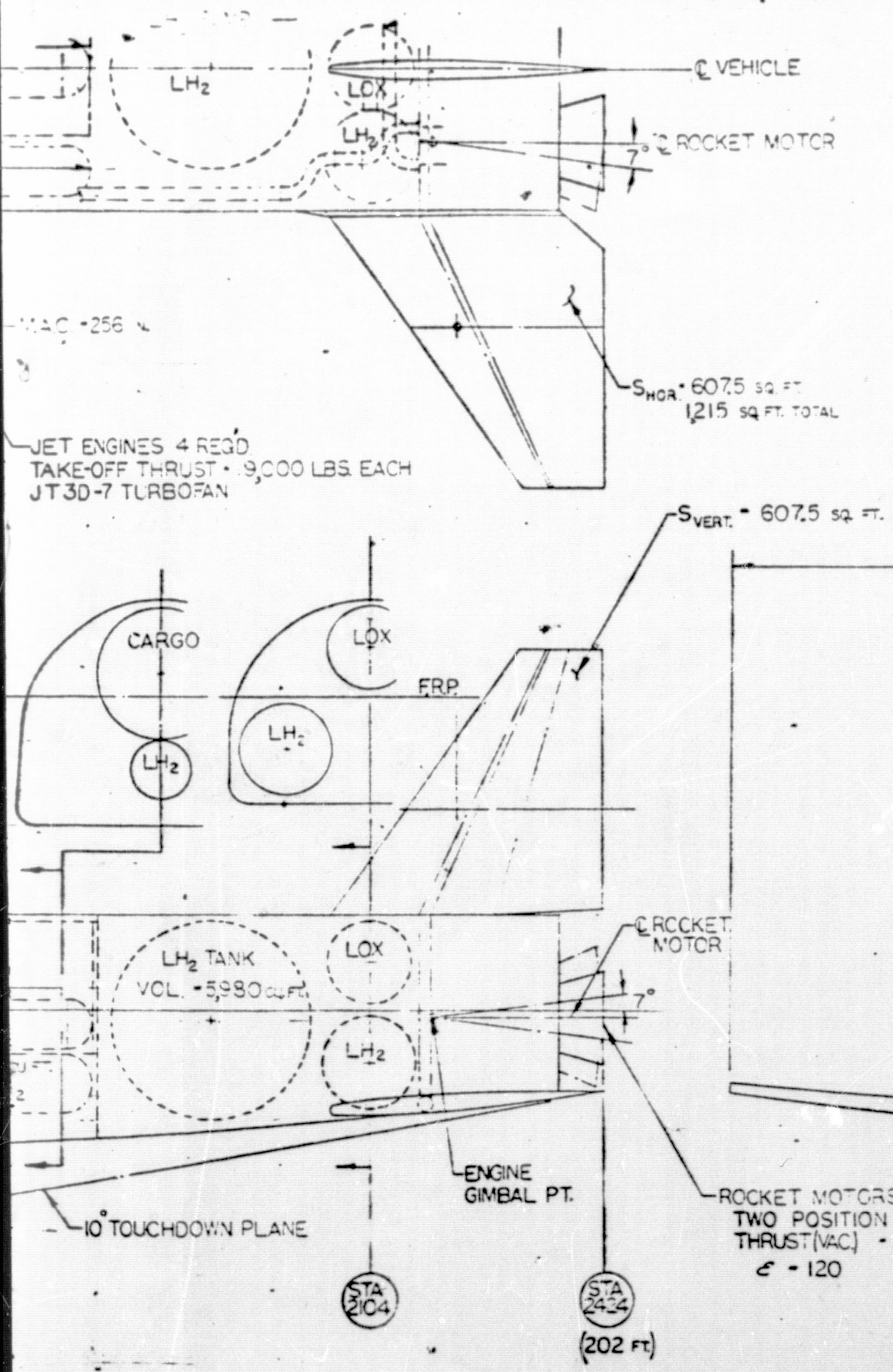

WING GEOMETRY

S_W = 2,680 SQ. FT.
SPAN = 137 FT.
C_R = 29.4 FT.
C_T = 9.8 FT.
Λ = 14°
λ = .333
M.A.C. = 256 IN.
A.R. = 7

SCALE 1" = 100'

0 50' 100' 200' 300' 400' 500'

Figure 8.2-1

FOLDOUT FRAME 2

Space Division
North American Rockwell

WING GEOMETRY

S_W - 2,680 SQ. FT.
SPAN - 137 FT.
C_R - 29.4 FT.
C_T - 9.8 FT.
Λ - 14°
λ - .333
M.A.C. - 256 IN.
A.R. - 7

STAGE WEIGHTS

PROPELLANT (LOX/LH_2) - 555,000 LBS. TOTAL
TOTAL LAUNCH - 835,000 LBS.
REENTRY - 245,000 LBS.
LANDING - 241,000 LBS.
PROPELLANT (LOX/LH_2) ON ORBIT - 35,000 LBS

TOTAL PLANFORM AREAS

S_W - 2,680 SQ. FT. $\left(\frac{W}{S_W} = 90 \text{ LDG}\right)$
$S_{FUS.}$ - 5,480 SQ. FT.
S_{TOTAL} - 8,160 SQ. FT. $\left(\frac{W}{S_{TOTAL}} = 30\right)$

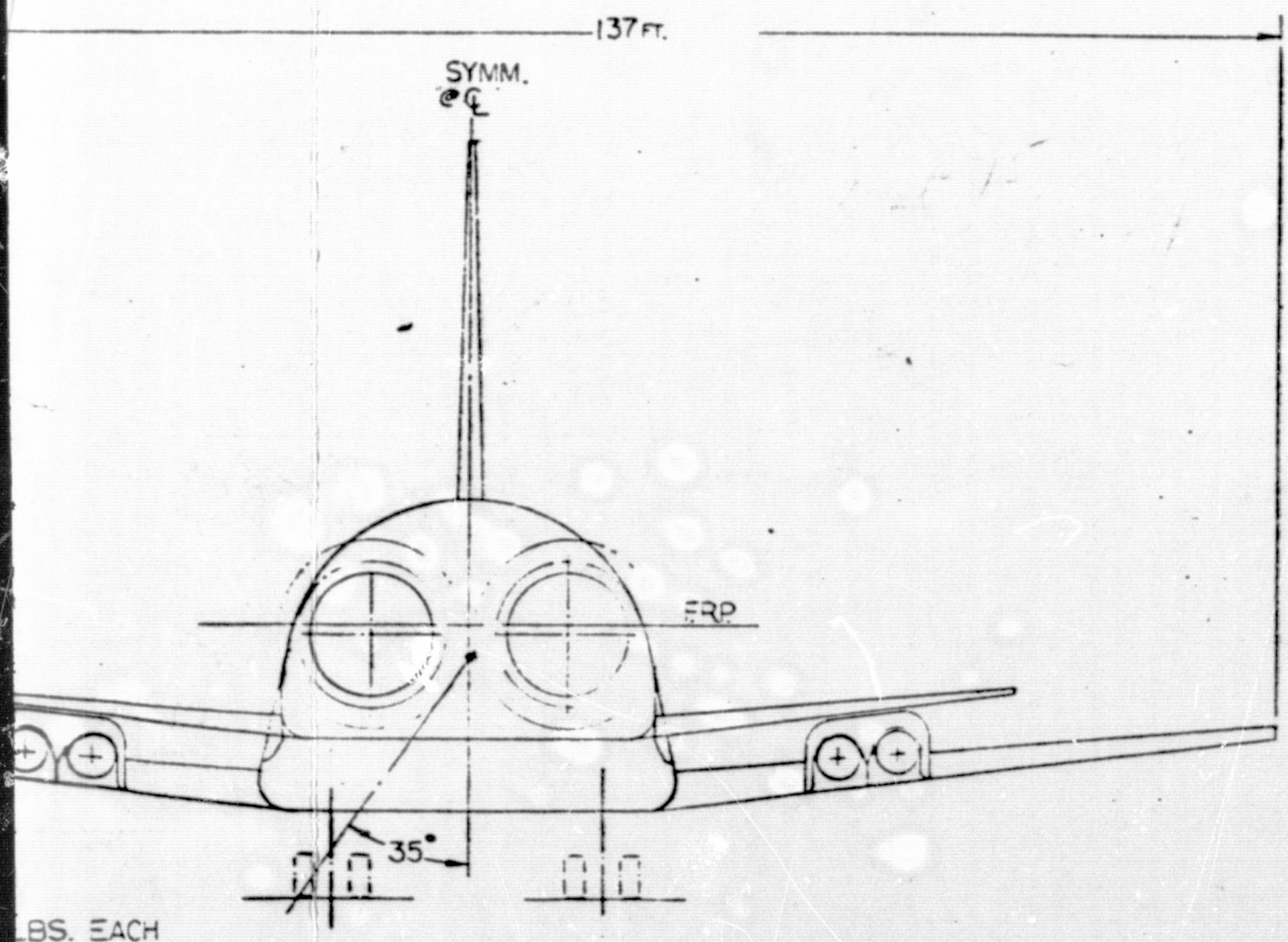

Figure 8.2-15. 50,000-Pound-Payload Orbiter Modified for Center-of-Gravity Balance (Drawing 2234-70)

FOLDOUT FRAME 3

Table 8.2-4. Baseline 50,000-Pound-Payload Vehicle, 15-Foot by 60-Foot Cargo Bay

Feature	Booster	Orbiter
Weights (1,000 lb)		
Landing	494	242
Turbojet fuel	56	3
Burnout and reentry	550	245
On-Orbit propellant	0	35
Ascent propellant	2,600	555
Launch	3,150	835
Size		
Body length (ft)	268	202
Wing span (ft)	230	135.5
Wing area, theoretical (ft^2)	7,550	2,620
Horizontal tail area (ft^2)	3,630	1,215
Vertical tail area (ft^2)	1,408	608
Body wetted area (ft^2)	31,600	19,100
Plan area (ft^2)	18,860	8,000
Propulsion		
Number of rocket engines	9	2
Thrust per engine (1,000 lb)	555	640
Expansion ratio	35	120:1 (Two-position)
Number of turbojets	6	4
Turbojet type	JT3D-7	JT3D-7
Thrust, SLS (1,000 lb)	19	19

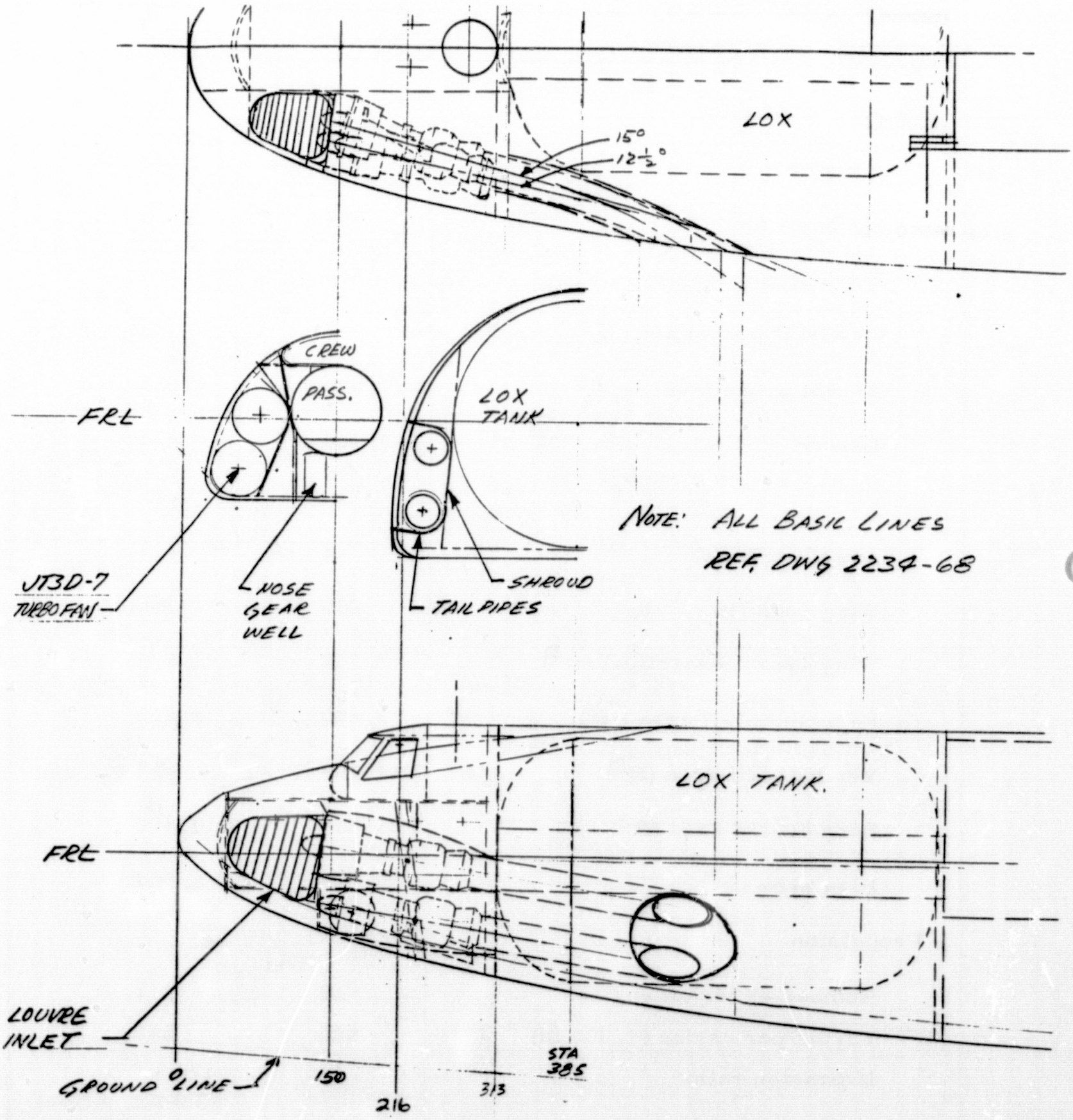

Figure 8.2-16. Forward-Mounted Turbojet Engine Installation

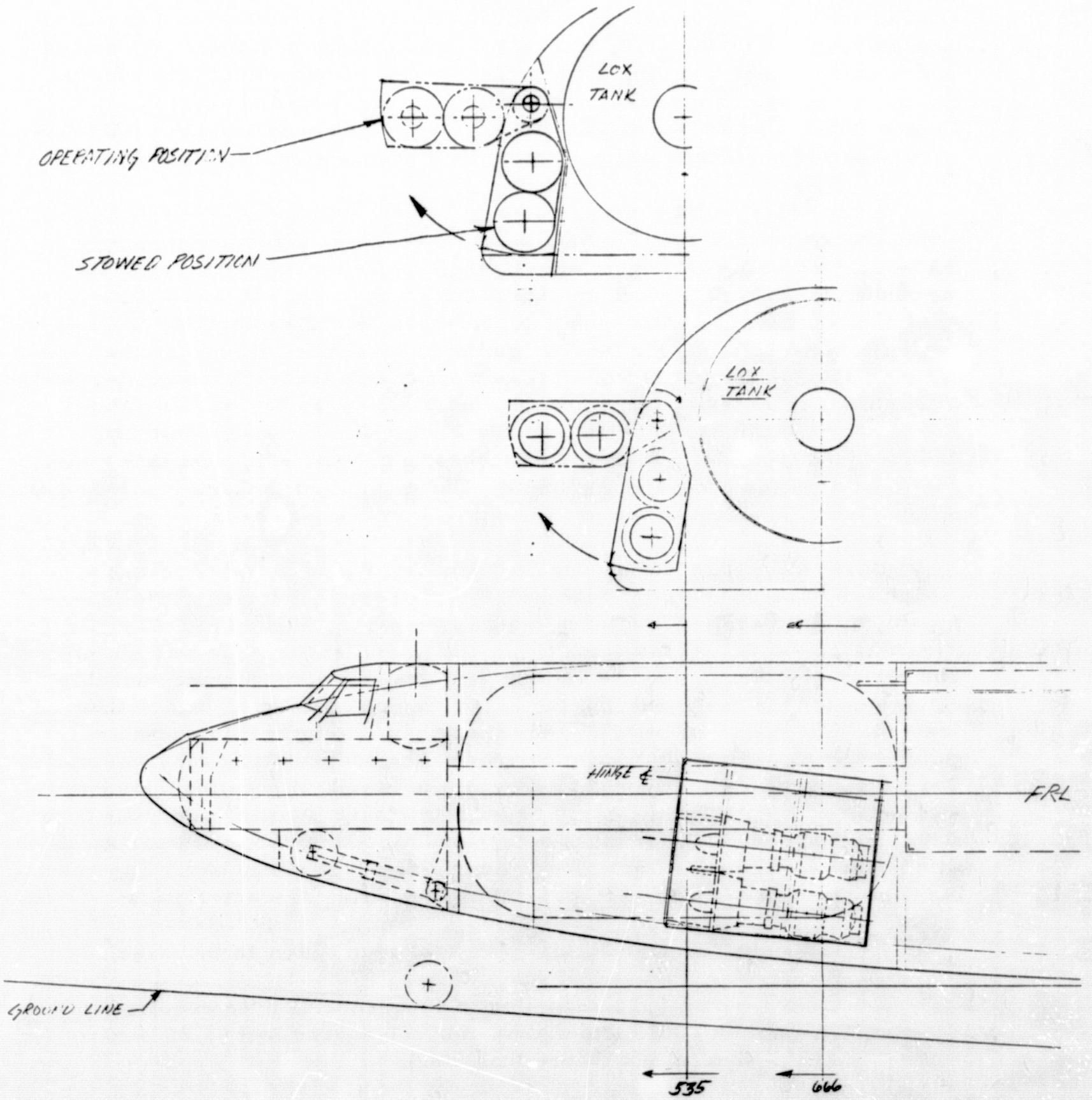

Figure 8.2-17. Forward Turbojet Engine Installation, Swing-Out Doors

the hard chines. The lower body corners have a radius equal to 0.33 of the local body width as shown in Figure 8.2-18 (Drawing 2234-72). A booster configuration with rounded corners was also prepared. Propellant tankage similar to that in the previous design was initially maintained and modified only as required by the outer mold line. In an effort to simplify the propellant tankage design and simplify the distribution of propellant tank inertia loads, it was determined that the modified tankage, also shown in Figure 8.2-18, could be installed within the orbiter body volume. The tanks have separate bulkheads and are a double-bubble design.

A structure and thermal protection system trade was conducted for the orbiter to assess the relative merits of integral tank structure (primary load-carrying structure) and external-shell load carrying structure with suspended tanks. This trade and the results are discussed under Structures Analysis, Section 8.5. Although the previously described orbiter tankage configurations are good for the external structural shell concepts, they are not the best for integral tankage. In support of this tradeoff, an orbiter design with continuous integral tanks passing under the cargo bay was developed and is shown in Figure 8.2-19 (Drawing 2234-74). The body depth had to be increased from 315 inches to 360 inches to provide sufficient tank cross-sectional area for body-bending loads. The propellant tankage is a four-cell pillow tank of constant cross section with a common bulkhead.

Based on new recommended body lines provided by aerodynamics (which are based on current wind tunnel tests being conducted at NASA Ames), another orbiter configuration was prepared, Figure 8.2-20 (Drawing 2234-77). At the same time, the propellant tankage was simplified. The major problem is that the vehicle depth causes considerable unusable volume under the cargo bay and the crew-passenger cabin is higher than desired. The effect of lowering the upper body line to reduce unusable volume was evaluated, and a comparison of the body wetted areas was made. The body shape was configured to provide the lowest silhouette. This design was achieved by placing the cargo bay directly over the wing carry-through structure and providing for tankage fore and aft of the cargo compartment with propellant transfer lines along either side of the cargo bay. The resulting configuration has a longer body and the following characteristics:

1. A gain in fuselage bottom plan area (due to length increase).

2. Item 1 permitted a reduction in exposed wing area required to maintain a total bottom area of 8,200 square feet (3,500- to 2,890-square foot theoretical wing).

3. A significant reduction in body wetted area that would result in reduced structural weight of the vehicle (Δ wetted area of 650 square feet).

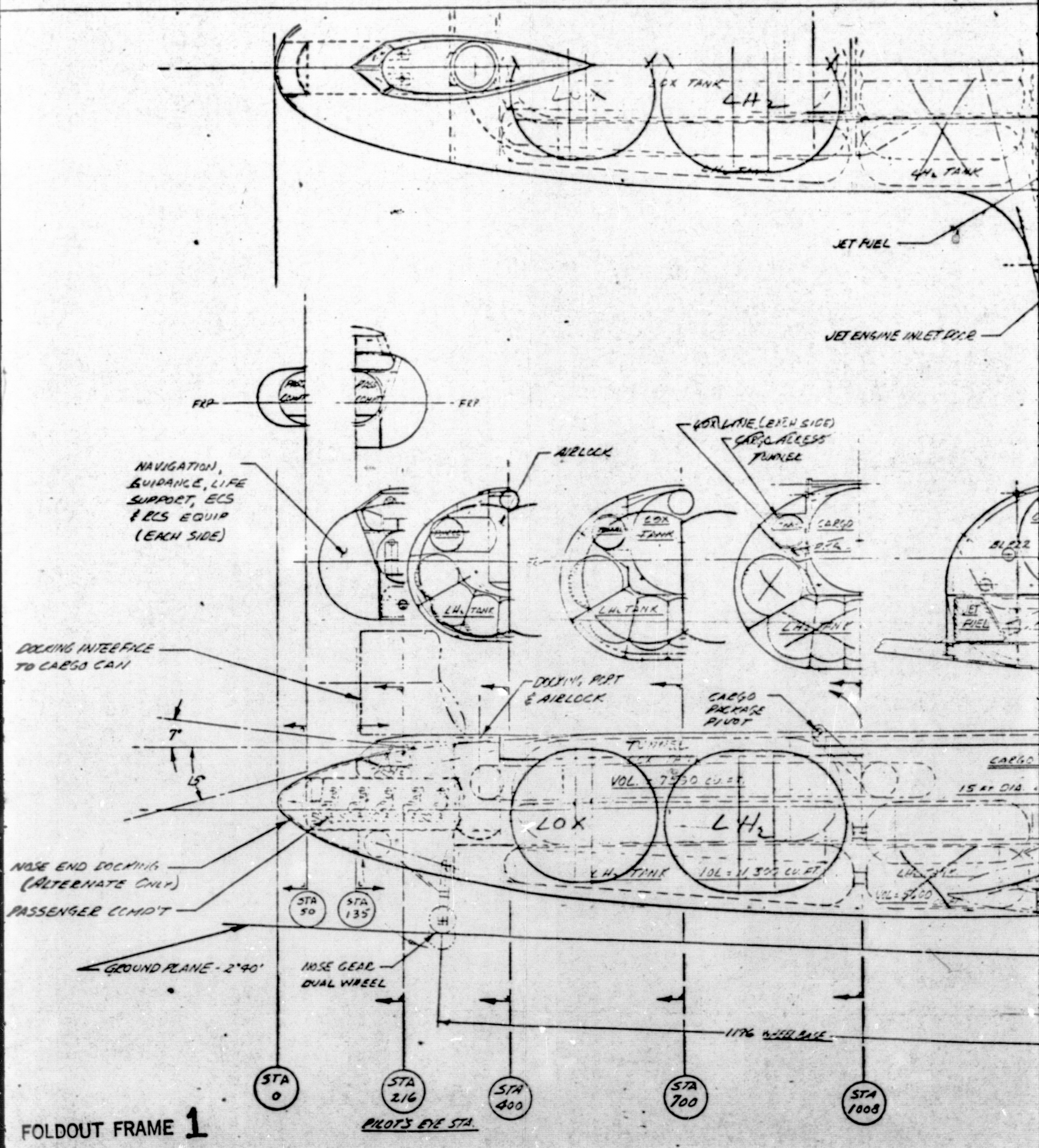

FOLDOUT FRAME 1

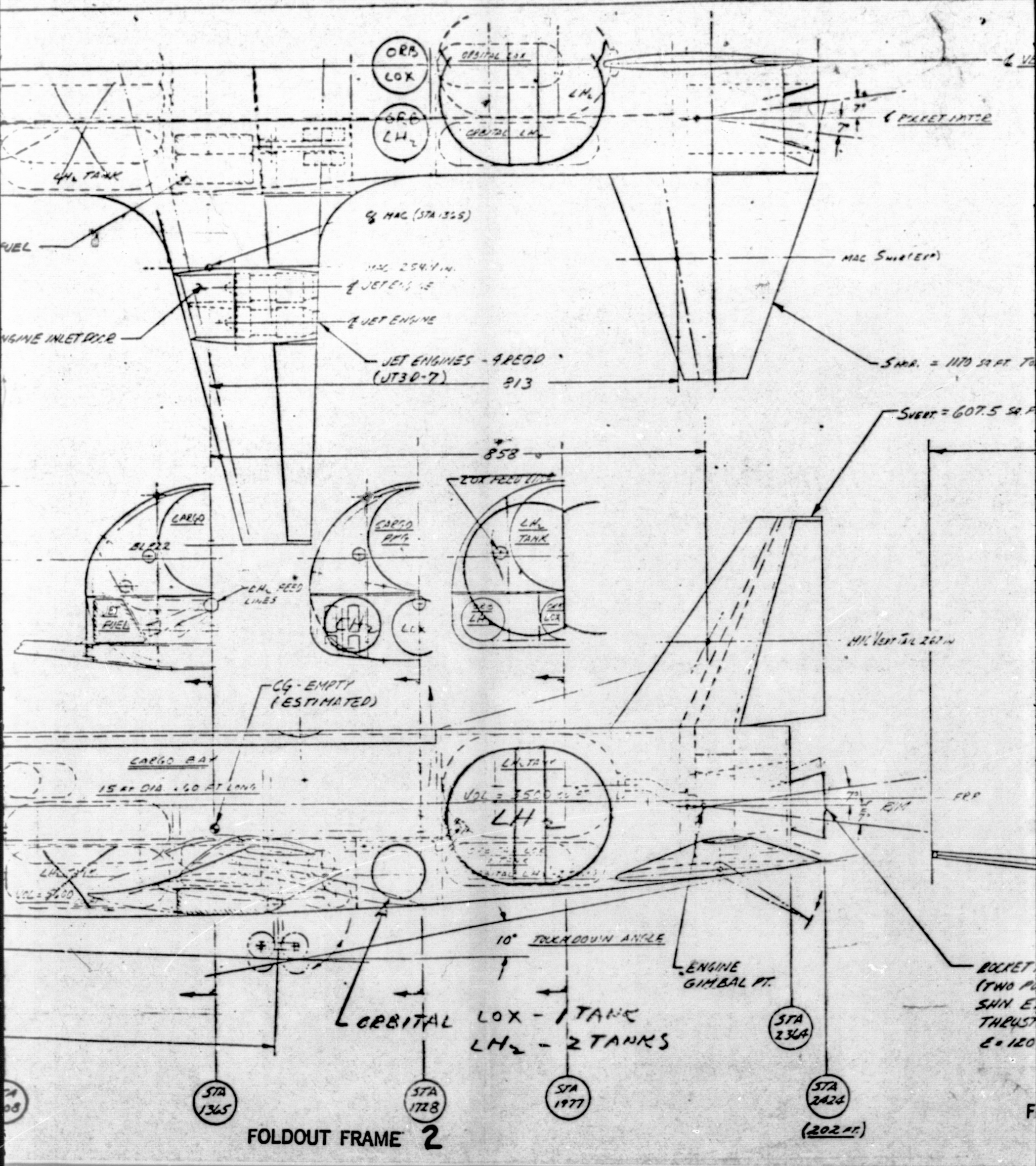

FOLDOUT FRAME 2

WING GEOMETRY

AREA (THEOR) = 2630 SQ FT.
SPAN = 137 FT.
C_{ROOT} = 29.4 FT.
C_{TIP} = 9.8 FT.
$\Lambda_{LE(SWEEP)}$ = 14°
λ (TAPER RATIO) = .333
MAC = 254.4 IN.
AR = 7.0

STAGE WEIGHTS

PROPELLANT (LO. LH.) = 555.000 LBS.
TOTAL LAUNCH = 835.000 LBS.
RE-ENTRY = 245,000 LBS.
LANDING = 241,000 LBS.
ON-ORBIT PROPELLANT = 35,000 LBS.

AREAS

S_{WING} = 2620 SQ FT ($W/S_W \approx 90$ PSF)
S_{FUS} = 5380 SQ FT.
S_{TOTAL} = 8000 SQ FT ($W/S_{TOT} \approx 30$)
$S_{HOR. TAIL}$ = 1170 SQ FT (EXPOSED)
$S_{VERT. TAIL}$ = 607.5 SQ. FT.

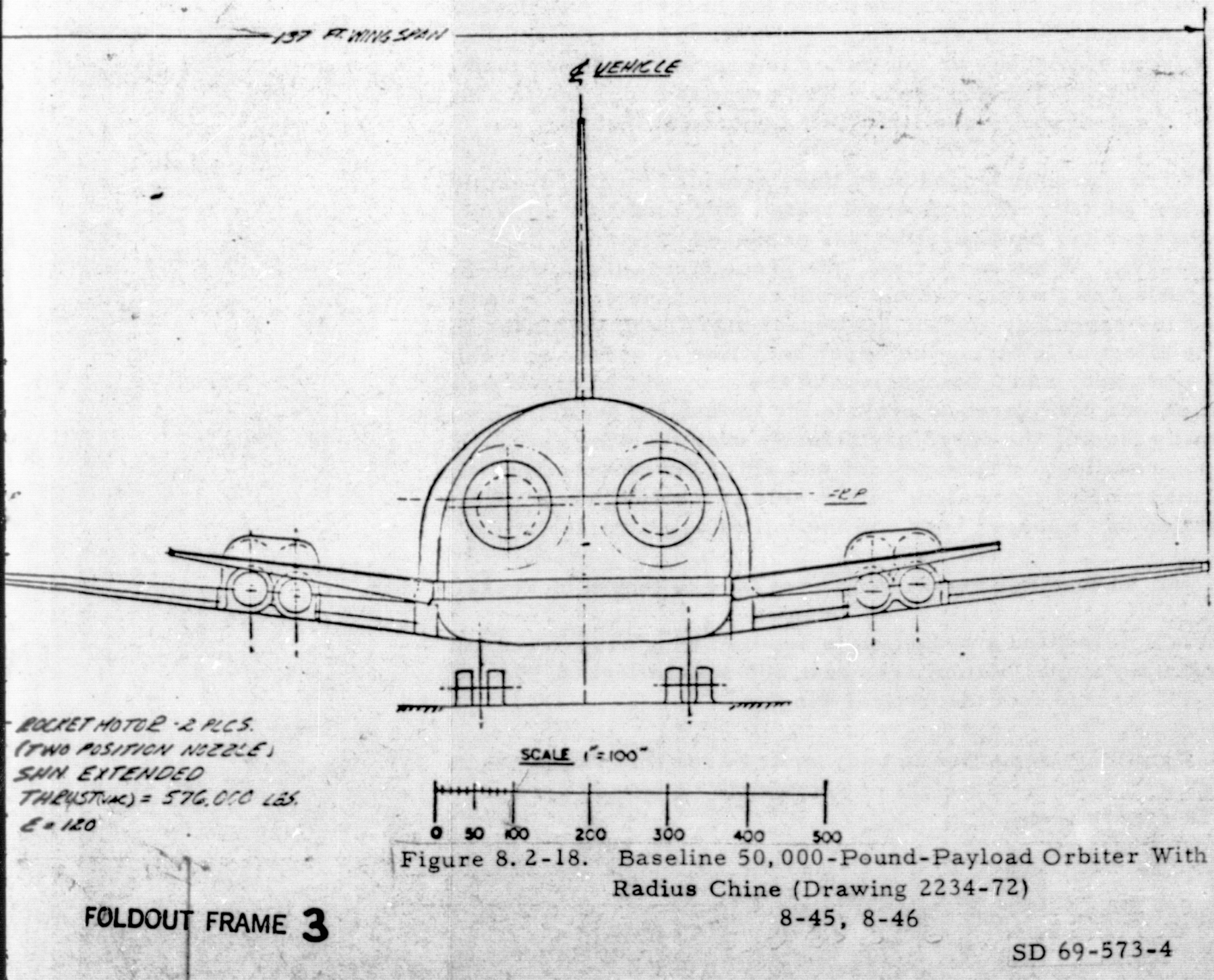

Figure 8.2-18. Baseline 50,000-Pound-Payload Orbiter With Large-Radius Chine (Drawing 2234-72)

FOLDOUT FRAME 3

REPRODUCIBILITY OF THE ORIGINAL PAGE IS POOR.

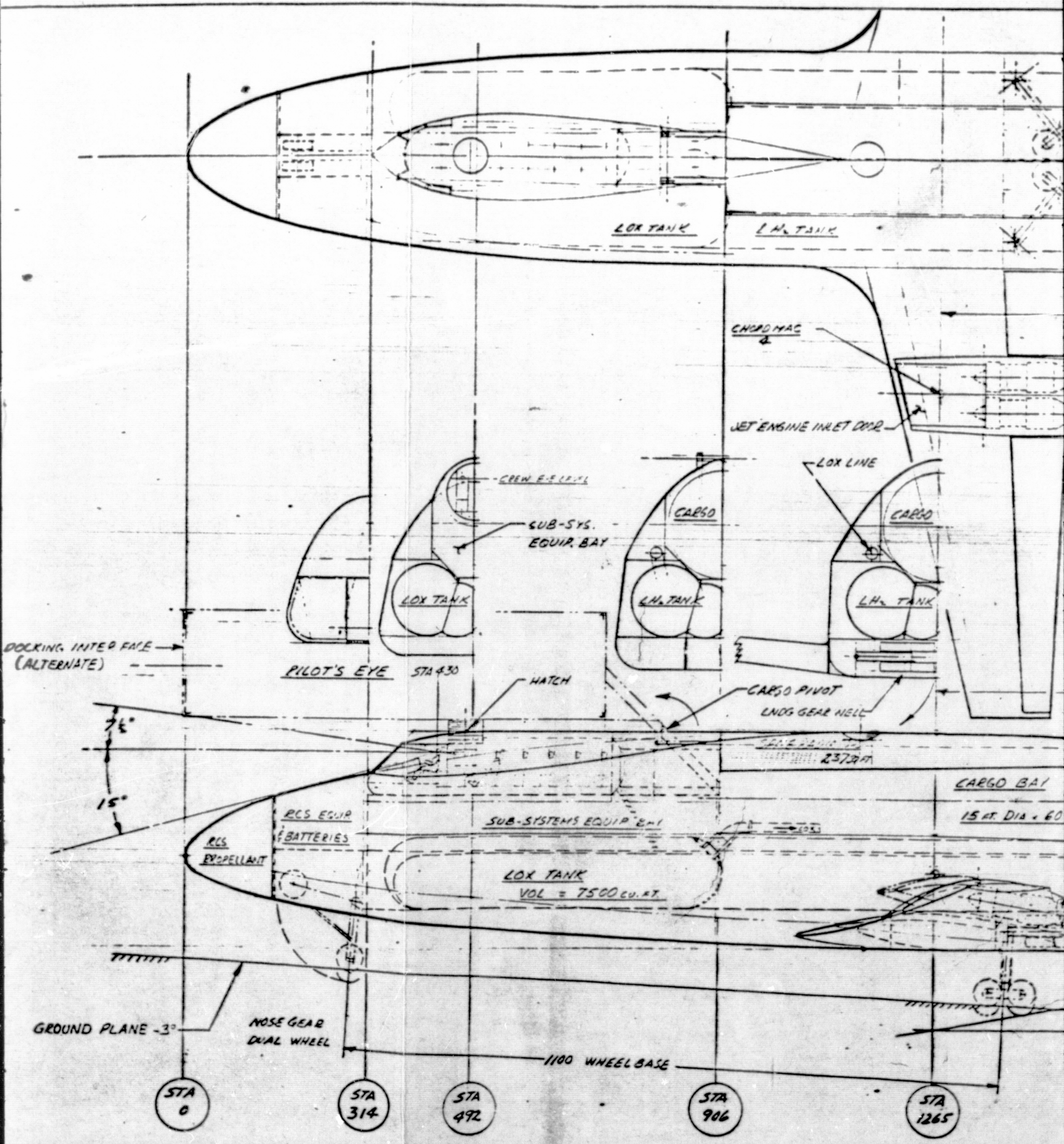

FOLDOUT FRAME 1

WING GEO

AREA (THEOR
SPAN
C ROOT
C TIP
Λ L.E (SWEEP
λ
MAC.
AR

156 FT. SPAN

℄ ROCKET MOTOR

℄-VEHICLE

℄ ROCKET MOTOR

865

MAC HOR TAIL

S_{HOR} = 1170 SQ FT. (EXPOSED)

ET ENGINE
C 2912 IN.
JET ENGINE
30-7)
ACS.

LH₂ TANK ORB. PROP SYS.

LOX LINE
MAIN PROP SYS.

LOX TANK - ORB. PROP SYS.

LH₂

LOX

LH₂ TANK

MAC VERT TAIL

S_V = 607.5 SQ FT.
(EXPOSED)

913

LH₂ - 2 PLCS

LOX - 1 PLC

LOX

H₂ TANK

VOL. = 20,400 CU. FT.

7°

℄ ROCKET MOTORS

7°

10° TOUCH DOWN ANGLE

ENGINE
GIMBAL

ROCKET MOTOR - 2 PLCS.
TWO POSITION NOZZLE
THRUST VAC. = 576,000 LBS
ε = 120

STA 1625

STA 2033

STA 2296

STA 2380

198.5 FT.

FOLDOUT FRAME 2

Space Division
North American Rockwell

WING GEOMETRY

AREA (THEOR)	= 3500 SQ.FT.
SPAN	= 156 FT.
C_{ROOT}	= 33.7 FT.
C_{TIP}	= 11.2 FT.
$\Lambda_{L.E}$ (SWEEP)	= 14°
λ	= .333
MAC.	= 291.2 IN.
AR	= 7.0

STAGE WEIGHTS

PROPELLANT (LO_2/LH_2)	= 555,000 LBS.
TOTAL LAUNCH	= 835,000 LBS.
RE-ENTRY	= 245,000 LBS
LANDING	= 241,000 LBS.
ON-ORBIT PROPELLANT	= 35,000 LBS.

AREAS

S_{WING} = 3500 SQ FT. (THEOR)
$S_{FUSELAGE}$ (PLAN FORM) = 5300 SQ FT.
$S_{HORIZONTAL\ TAIL}$ = 1170 SQ FT (EXPOSED)
$S_{VERTICAL\ TAIL}$ = 607.550 FT (EXPOSED)
TOTAL EFFECTIVE PLANFORM = 8200 SQ.FT.

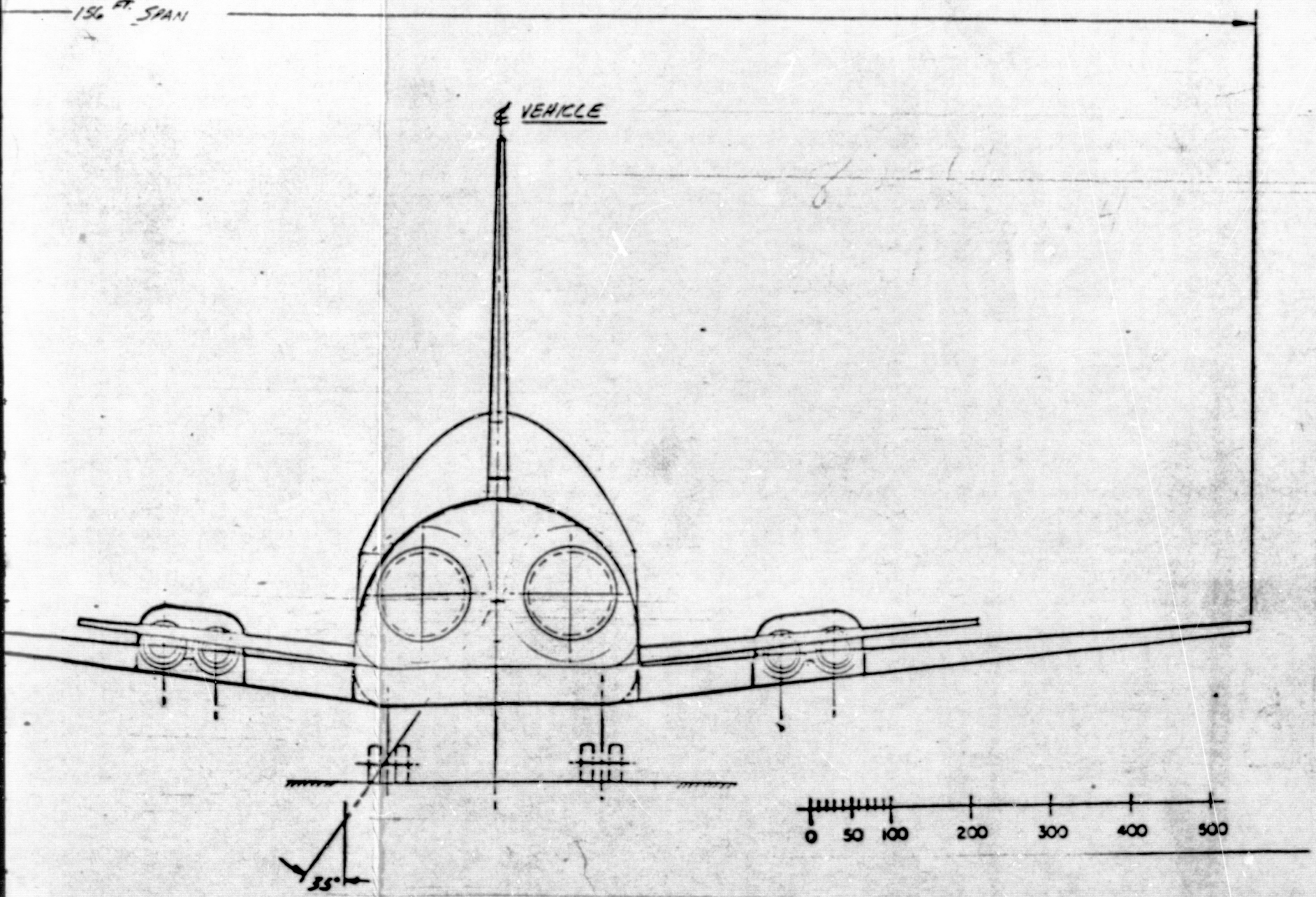

Figure 8.2-19. Integral-Tank Orbiter Configuration (Drawing 2234-74)

FOLDOUT FRAME 3

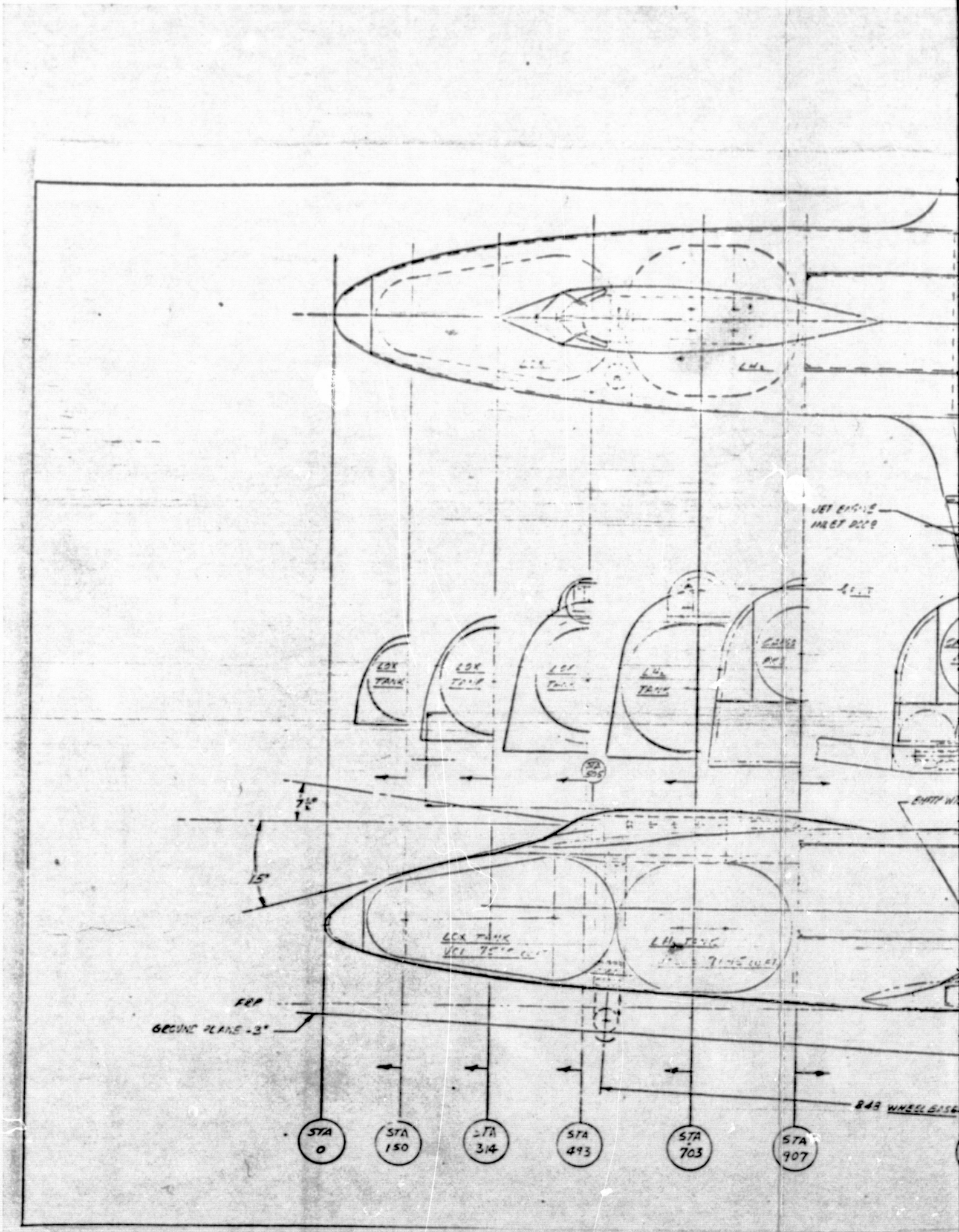

FOLDOUT FRAME

FOLDOUT FRAME 1

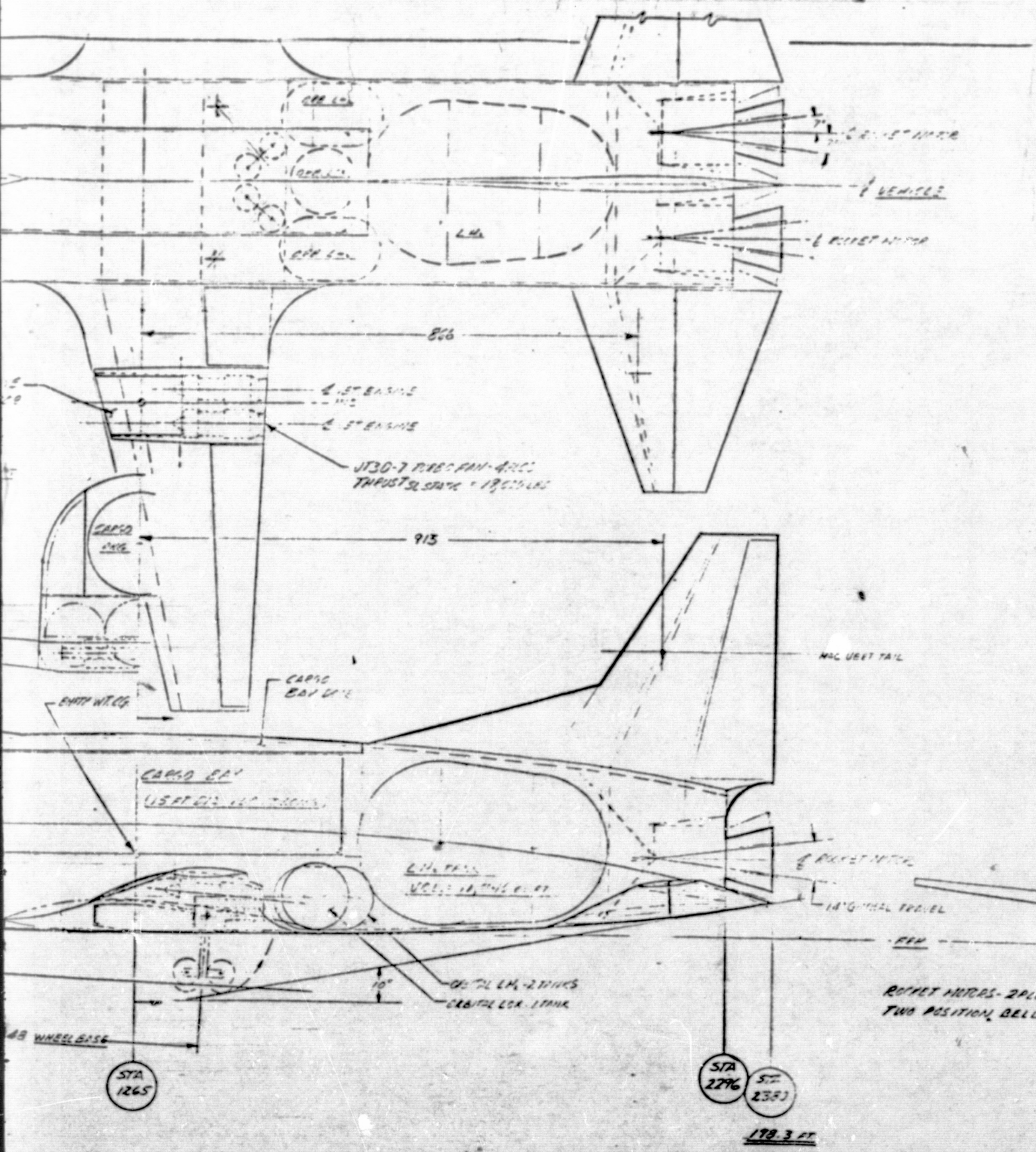

Figure 8.2-20. Orbiter

FOLDOUT FRAME 2

UPSIZE PAGEMAT — 120% KEYLINE IMAGE AREA
BLOW UP CALLOUTS 120% — REDUCE TO 83% OF ORIGINA

Space Division
North American Rockwell

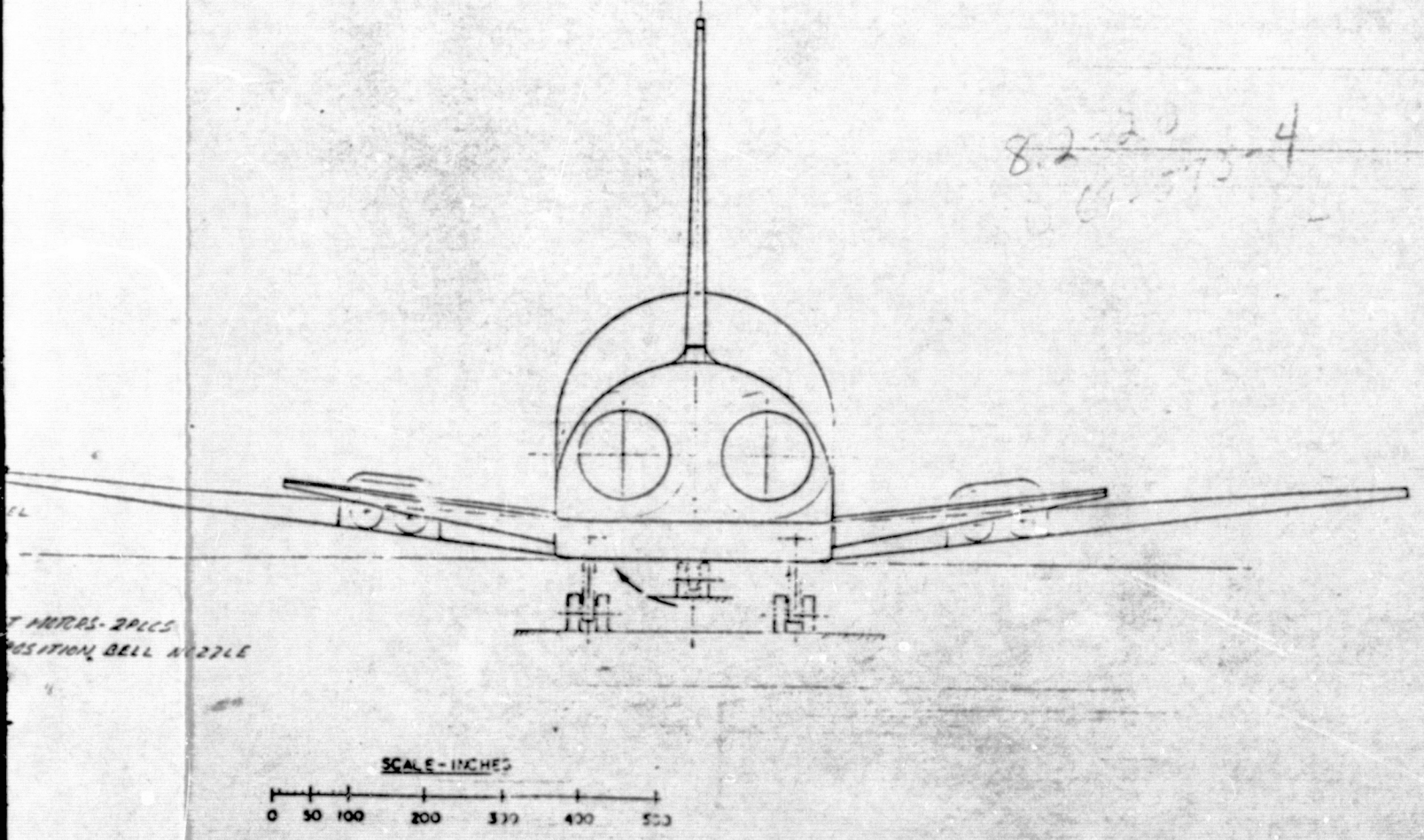

Figure 8.2-20. Orbiter With Recommended Aerodynamic Body Lines
(Drawing 2234-77)

FOLDOUT FRAME 3
8-49, 8-50

SD 69-573-4

REDUCE TO 11 INCHES

UPSIZE PAGEMAT – 120% KEYLINE IMAGE AREA
BLOW UP CALLOUTS 120% – REDUCE TO 83% OF ORIGINAL

PLEASE MAKE CORRECTIONS ON TISSUE OVERLAYS,
OR READING COPY IF AVAILABLE

4. A completely horizontal top mold line (no cockpit protrusion) needed for favorable cargo package handling.

This configuration was selected for the detail design definition described under Conceptual Design Definition, Section 8.2.4 and shown in Figure 8.2-23 (Drawing 2234-79).

Turbojet engines are required for subsonic flight, go-around, and landing. The choice of engine and number of engines is dependent on the thrust requirement, fuel requirement, and installation features. Four P&W JT3D-7 turbofans were selected for the baseline 50,000-pound-payload orbiter; however, vehicle performance studies were considering the use of two JT9D-15 engines. These engines provide twice the thrust of the JT3D and much better specific fuel consumption; nevertheless, from a design point of view, they have twice the frontal diameter. A side-view comparison of the two engines relative to the orbiter wing is shown in Figure 8.2-21. The design problems with the larger JT9D engine mounted on the relatively small orbiter wing can be visualized. Mounting two JT3D engines on each wing requires nacelles approximately 120 inches wide by 60 inches high compared with nacelles approximately 100 inches by 100 inches required for single JT9D engines. The use of four JT3D engines is the preferred installation from a design standpoint.

The 50,000-pound-payload booster baseline configuration layouts are presented in Figure 8.2-14 (Drawing 2234-69). The booster is configured for nine main rocket engines. Two of the same basic engines with higher expansion ratio nozzles are used on the orbiter. The booster was modified to use ten engines since engine thrust and propulsion system weight on the orbiter could be reduced and still meet the minimum thrust requirement. The baseline configuration was prepared with separate propellant tanks; however, the use of a common bulkhead between the LO_2 and LH_2 tanks reduced the booster length and surface area and resulted in an approximately 7,000-pound saving in structure weight. The baseline booster configuration also shows six JT3D turbojets. As the aerodynamic performance studies progressed, it became apparent that the thrust level should be increased. At the same time, use of the JT9D engine (Boeing 747 engine) was being considered because of its low specific fuel consumption. The fuel weight required becomes important for the booster, since it must cruise approximately 300 nautical miles to return to the launch site. Four JT9D engines were selected because they provide the lowest total system weight. Where these large turbojets presented potential installation problems with the orbiter, they can be easily installed on the booster wing.

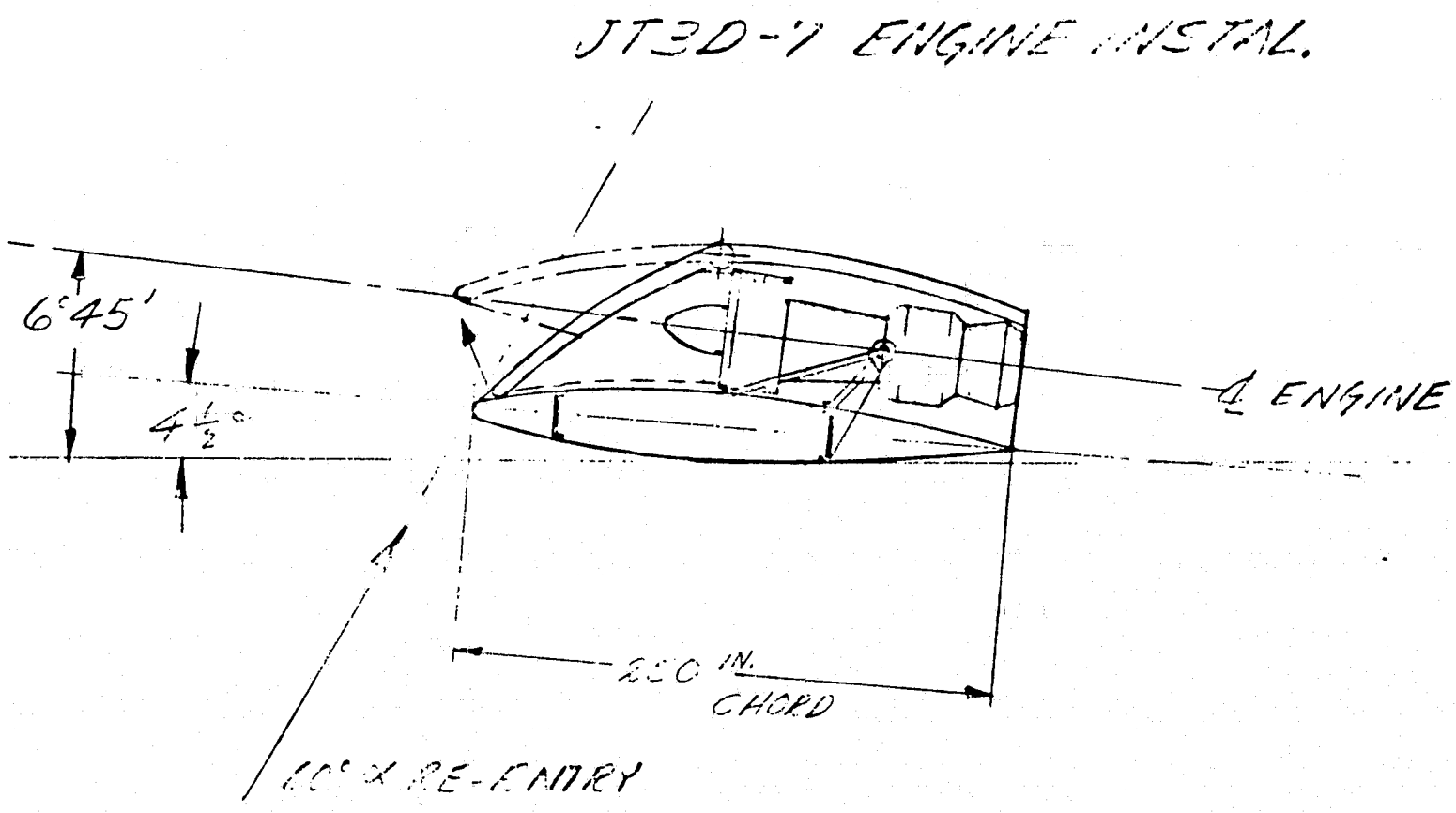

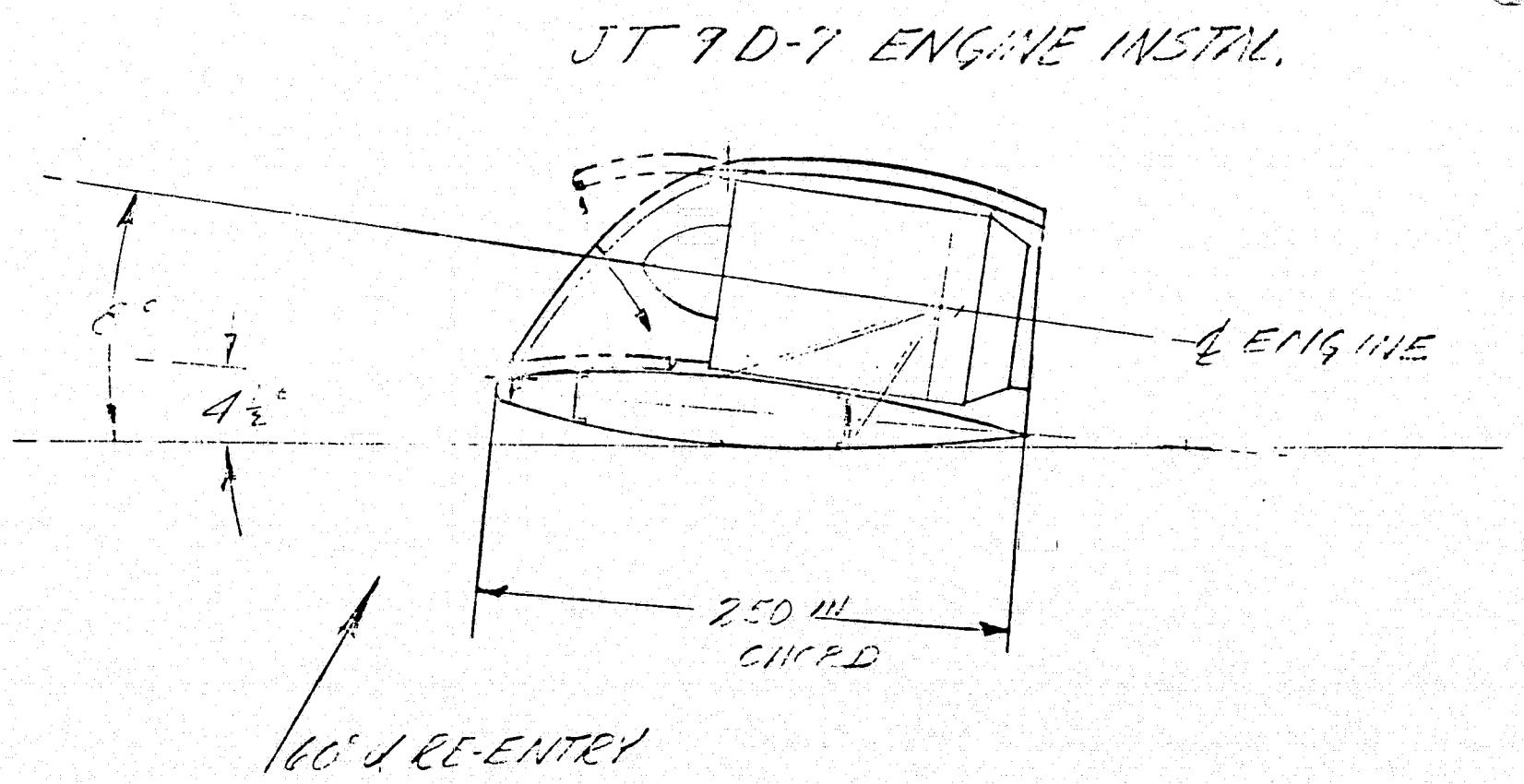

Figure 8.2-21. Orbiter Jet Engine Comparison

8.2.4 Conceptual Design Definition

This section contains a general description of the selected orbiter and booster design in addition to a more detailed discussion and location of the various subsystems within each stage.

The detail weight analysis resulted in booster and orbiter burnout weights that were 3.1 percent less and 8.7 percent greater, respectively, than weights given in the preliminary weight statement; therefore, the vehicle was resized to maintain the 50,000-pound-payload capability. The final configuration definition is presented in this section.

Based on the detail data generated for the 50,000-pound-payload vehicle, a vehicle with 25,000-pound-payload capability and a 12-foot-diameter by 48-foot-long cargo bay was sized. The characteristics of this vehicle are also presented.

Shuttle Vehicle Configuration

The selected configuration is shown in the mated position in Figure 8.2-22 (Drawing 2234-80). The vehicle is launched vertically with the booster and orbiter operated in a sequential mode. Launch provisions on the booster consist of tie-down and support points for the booster on horizontal track-type mobile ground equipment. Actual tie-down is at the nose gear and at the main landing gear support locations. The combined booster-orbiter is moved to the launch site and tilted to a vertical position. The base of the booster is then supported and restrained by hold-down arms on the launch pad. The hold-down arms are released only after sufficient thrust is provided by the booster rocket engines. Details of the launch pad fittings have not been investigated in this study; however, the size and unit loading are similar to those of the current Saturn V vehicle so that existing concepts may be utilized in preparing a detail design of this area.

The orbiter is mated with the booster as shown in Figure 8.2-22. The interface between the two vehicles consists of two launch hooks and two aft tension ties. Orbiter-booster mating and separation fittings are located within a fairing on top of the launcher vehicle. Two reverse-catapult launch hooks are used to transmit longitudinal loads between the booster and the orbiter at Orbiter Station 1040. Two tension-tie fittings (Orbiter Station 2200) are located aft on a major frame in the orbiter that carries the tail surface and thrust structure loads. The orbiter is secured to the booster fittings by means of pyrotechnic operated devices designed to be released simultaneously prior to separation. Separation is achieved by solid rocket motors, RS-V-501 (S-II ullage motors), mounted on each side of the orbiter. The separation motors are mounted in an assembly consisting

of four solid rocket motors and a fairing structure that is jettisoned after separation. A fairing mounted on the top surface of the booster is provided to reduce aerodynamic drag during ascent to the staging altitude.

Orbiter General Description

The 50,000-pound-payload orbiter configuration selected for detail design analysis is presented in Figure 8.2-23 (Drawing 2234-79) and has the general characteristics shown in Table 8.2-5.

Table 8.2-5. Orbiter General Characteristics

Body		**Wing**	
Length	202 ft	Area (theoretical)	2890 sq ft
Width	30 ft	(exposed)	2010 sq ft
Height	21.7 ft	Span	146 ft
Bottom	Flat and cambered	Aspect ratio	7
Planform area	5605 sq ft	Leading edge sweep	14 deg
Wetted area	17,111 sq ft	Taper ratio	0.333
		MAC	257 in.
Horizontal Tail		**Vertical Tail**	
Area (exposed)	1170 sq ft	Area (exposed)	607.5 sq ft
Half span (from ML)	355 in.	Rudder area (30% chord)	182 sq ft
Aspect ratio	3.0	**Cargo Bay**	
Area elevator (50% chord)	585 sq ft	Size	15-ft dia x 60-ft length
Propulsion		**Personnel**	
Number of rocket engines	2	Crew	2
Thrust, vac (ea)	576,000 lb	Passengers	10
Number of turbojets	4	**Weight***	
Type	JT3D-7	Launch	835,000 lb
Thrust, SLS (ea)	19,000 lb	Reentry	245,000 lb
		Landing	243,000 lb
		Propellant (LO_2/LH_2)	555,000 lb
		On-orbit propellant	35,000 lb

*Preliminary weights used in configuration sizing.

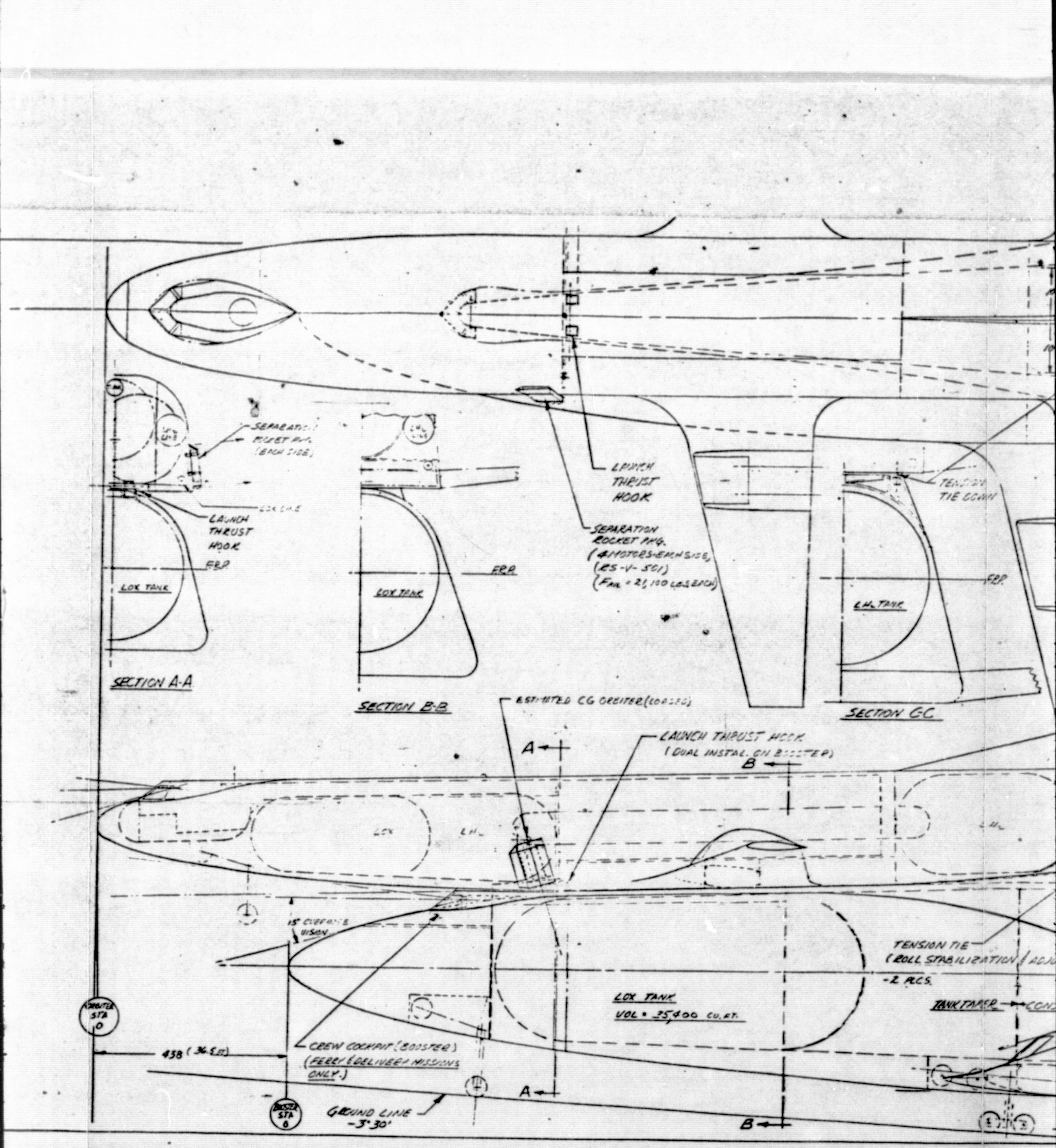

FOLDOUT FRAME 1

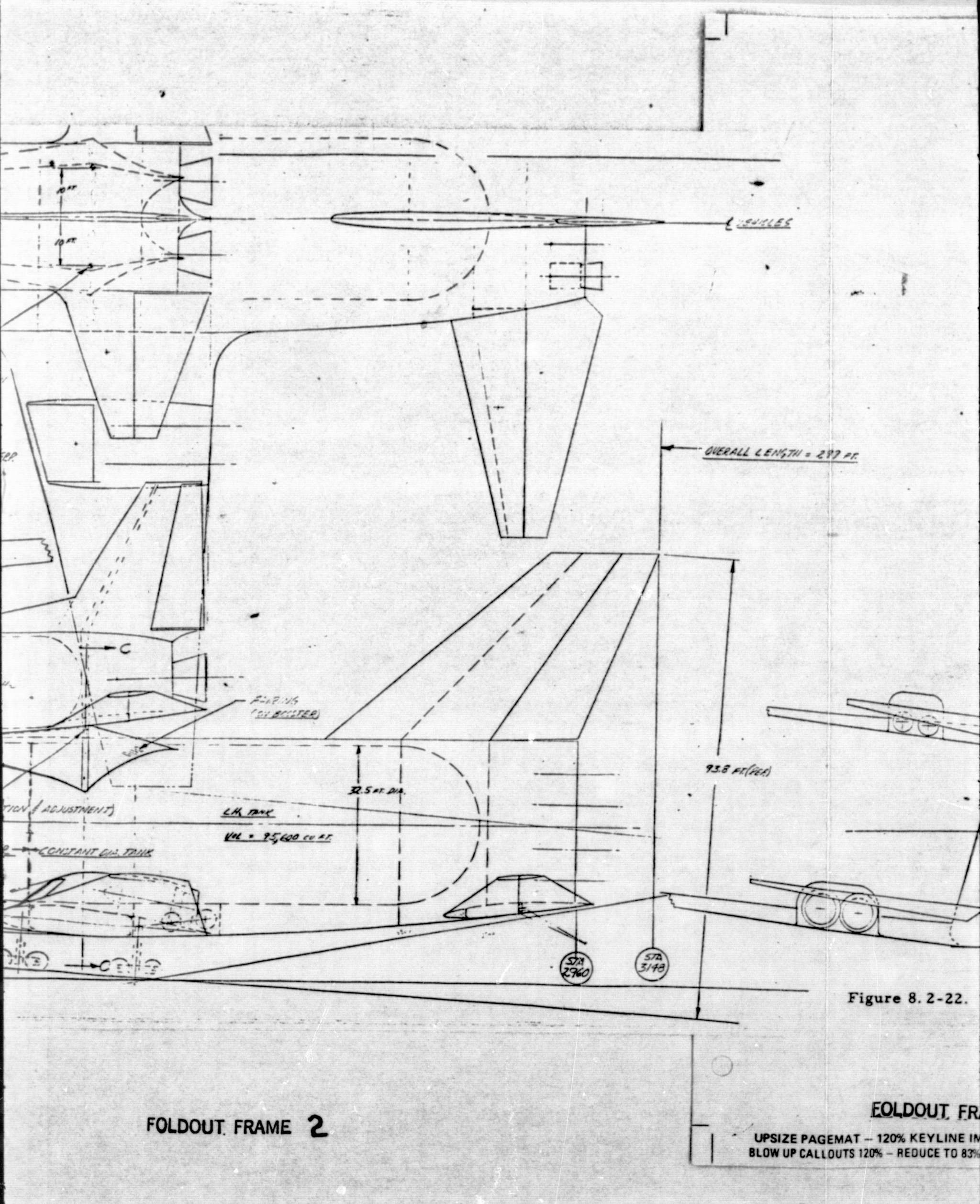

Figure 8.2-22.

FOLDOUT FRAME 2

FOLDOUT FR

UPSIZE PAGEMAT – 120% KEYLINE IN
BLOW UP CALLOUTS 120% – REDUCE TO 83%

Space Division
North American Rockwell

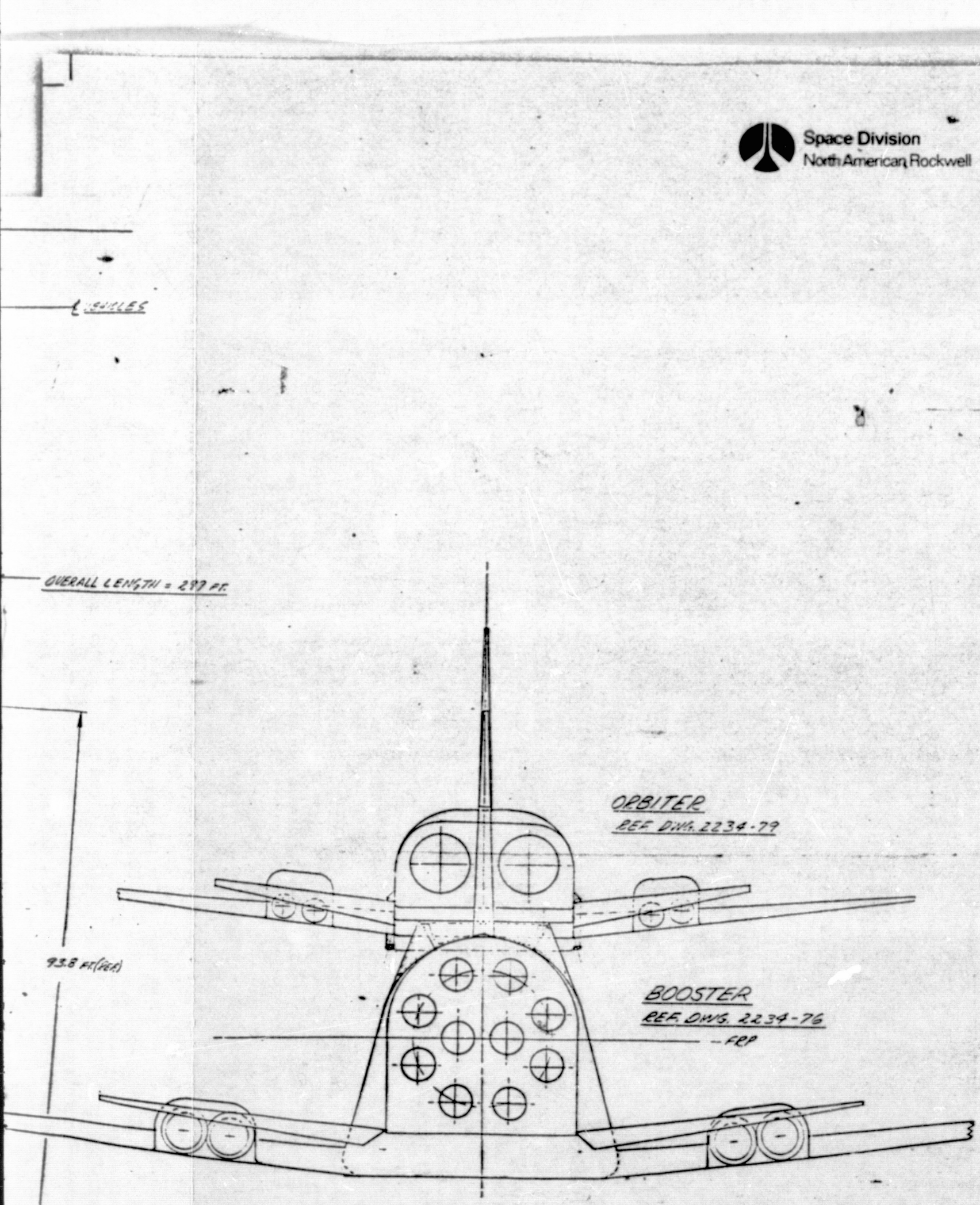

Figure 8.2-22. 50,000-Pound-Payload Orbiter and Booster in Mated Configuration (Drawing 2234-80)

FOLDOUT FRAME 3

UPSIZE PAGEMAT – 120% KEYLINE IMAGE AREA
BLOW UP CALLOUTS 120% – REDUCE TO 83% OF ORIGINAL

REDUCE TO 11 INCHES

PLEASE MAKE CORRECTIONS ON TISSUE OVERLAYS,
OR READING COPY IF AVAILABLE

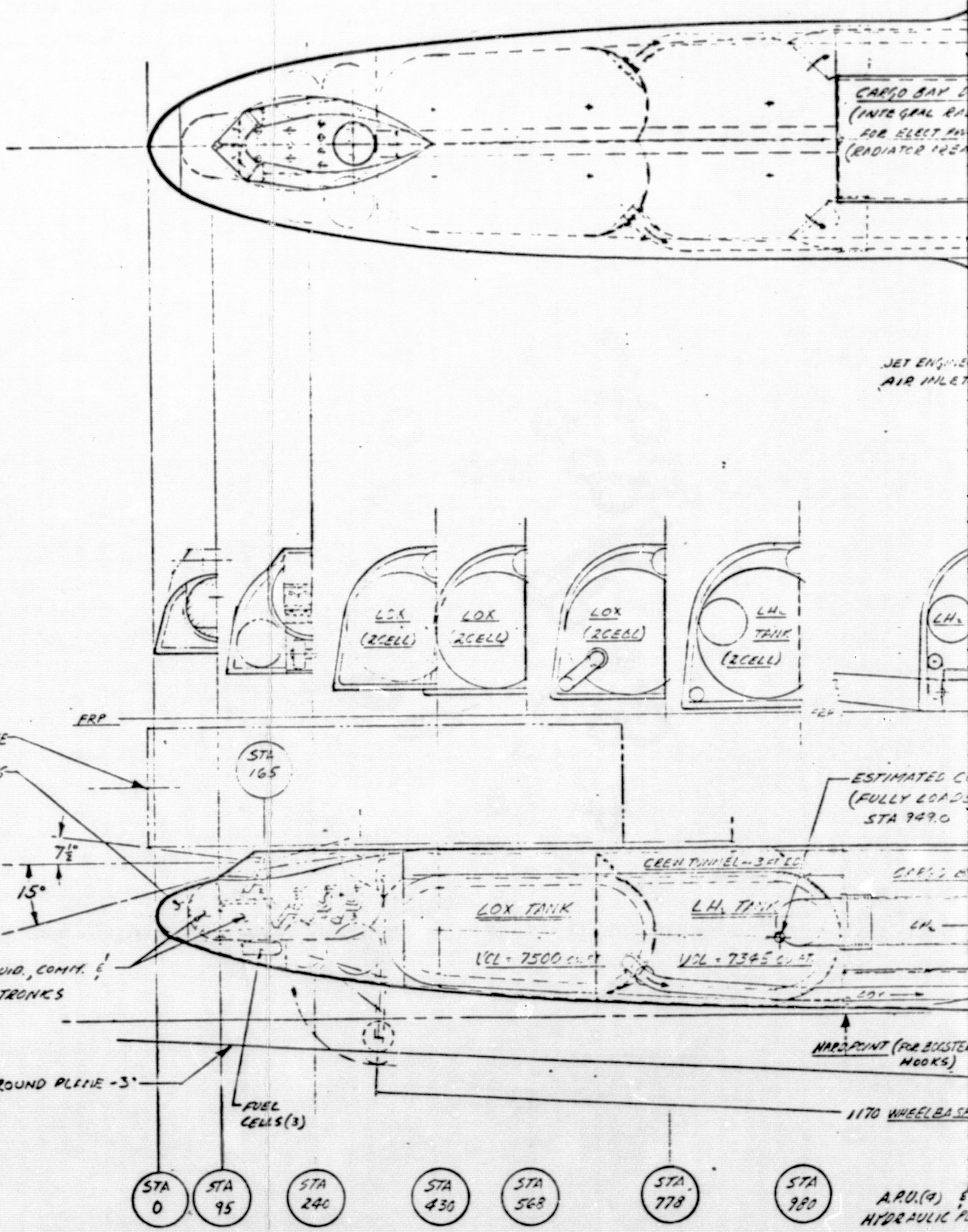

FOLDOUT FRAME 1

CARGO BAY DOORS
(INTEGRAL RADIATORS
FOR ELECT SUB'SYS.)
(RADIATOR AREA TOTAL = 350 SQ FT)

JET ENGINE
AIR INLET

℄ JET ENGINE (JT 30-7)

℄ JET ENGINE (JT 30-7)

RCS THRUSTERS
(ROLL, UP/DN, SIDE FORCE)

CARGO
RMS

LH₂

CARGO
RMS

LH₂

LH₂
TANK
(2 CELL)

ESTIMATED C.G
(FULLY LOADED)
STA 949.0

ESTIMATED C.G
(EMPTY)

LH₂ TANK

VOL = 9744 CU FT

AFT RCS
THRUSTERS

7°

7°

℄ POINT (FOR BOOSTER LAUNCH
HOOKS)

10° TAIL DOWN LINE

1170 WHEELBASE

STA
1333

STA
1403

58% BODY LENGTH

A.P.U.(4) &
HYDRAULIC PUMPS

STA
1792

STA
2084

STA
2202

BOOSTER
ATTACH.
HARD PT.

STA
2420

STA
2500

208.3 FT

FOLDOUT FRAME 2

WING GEOMETRY

S_W (THEOR AREA)	=	2870 SQ FT.
SPAN	=	146 FT.
C_{ROOT}	=	356 IN.
C_{TIP}	=	118.6 IN.
$\Lambda_{L.E}$	=	14°
λ (TAPER)	=	.333
M.A.C.	=	257 IN.
AR	=	7

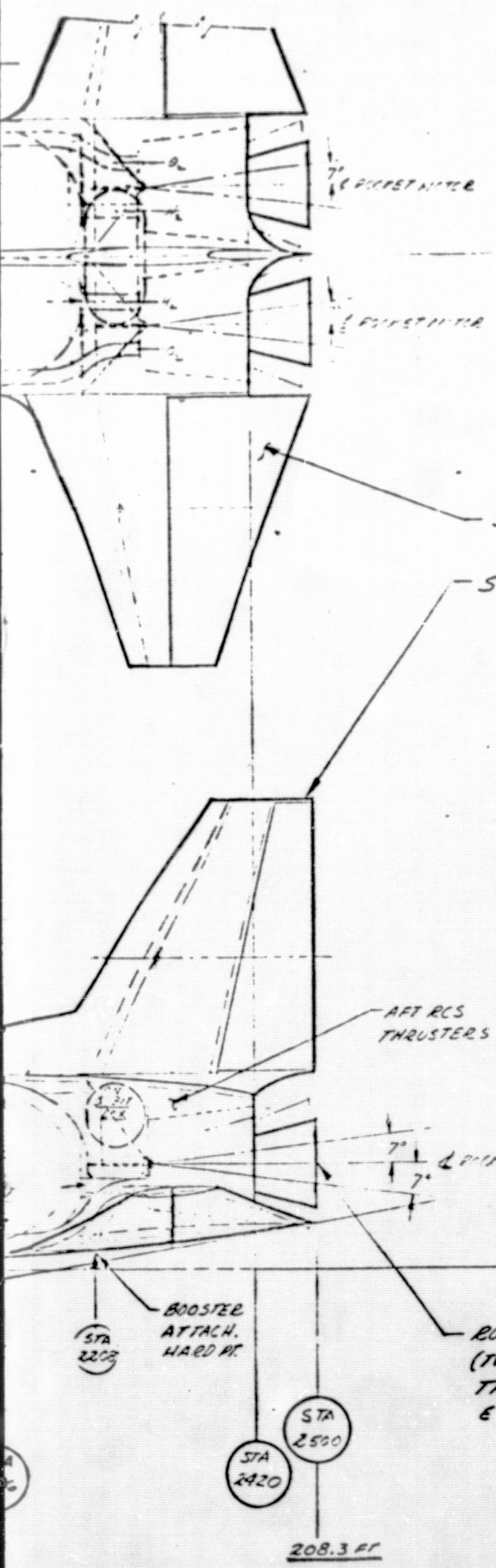

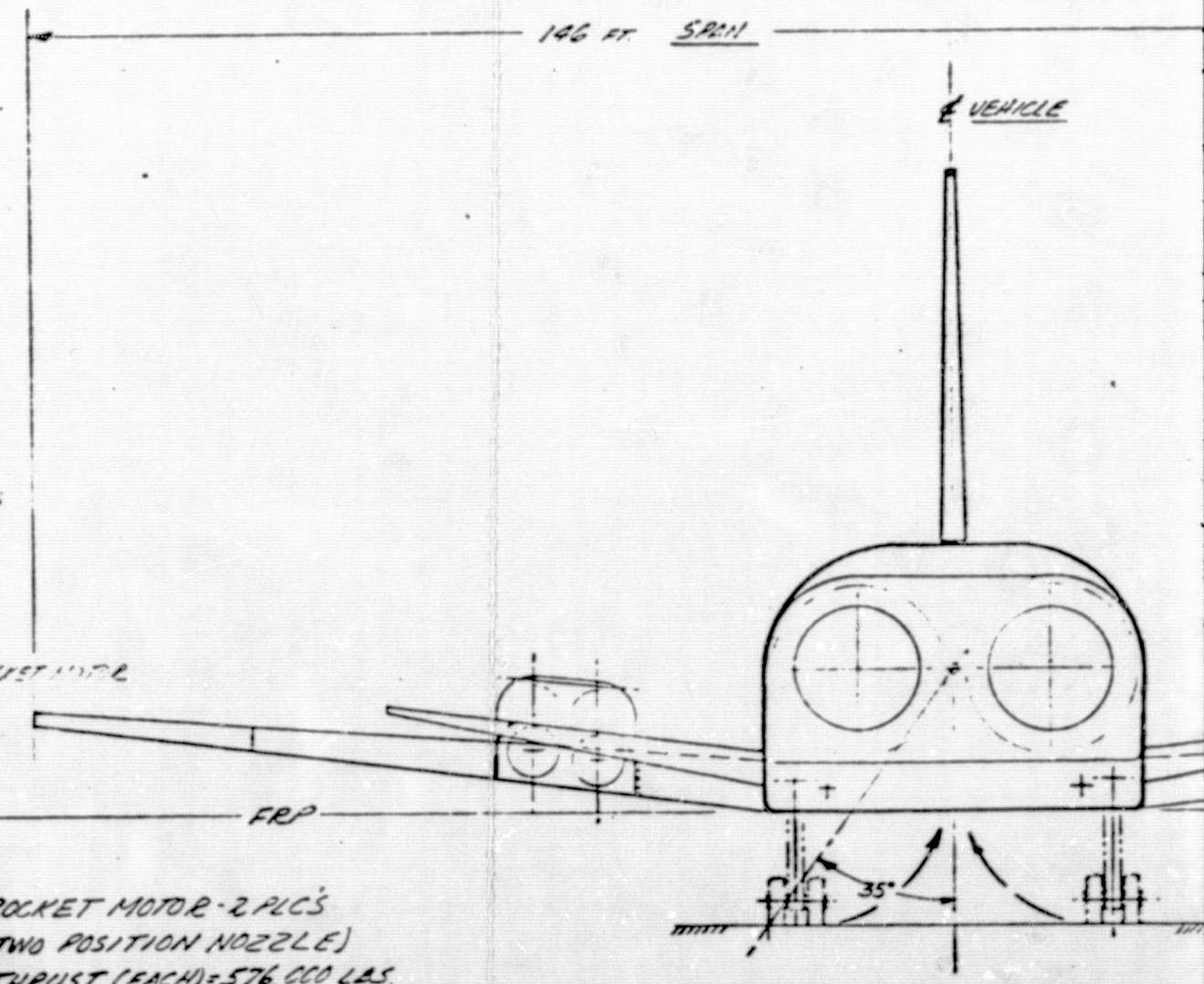

Figure 8.2-23. 50,000-Pound-Pa
(Drawing

SCALE 1 IN = 100 FT.

0 50 100 200 300 400 500

FOLDOUT FRAME 3

WING GEOMETRY

S_W (THEOR AREA)	=	2870 SQ FT.
SPAN	=	146 FT.
C_{ROOT}	=	356 IN.
C_{TIP}	=	118.6 IN.
$\Lambda_{L.E}$	=	14°
λ (TAPER)	=	.333
M.A.C.	=	257 IN.
AR	=	7

STAGE WEIGHTS

PROPELLANT (LOX/LH_2)	= 555,000 LBS
TOTAL LAUNCH	= 835,000 LBS.
RE-ENTRY	= 245,000 LBS
LANDING	= 243,000 LBS

ON-ORBIT PROPELLANT = 35,000 LBS.

PLANFORM AREA

WING (EXPOSED)	=	2010 SQ.FT.
FUSELAGE	=	5605 SQ.FT.
HOR. TAIL (50% CHORD)	=	585 SQ FT
TOTAL	=	8200 SQ.FT.

146 FT. SPAN

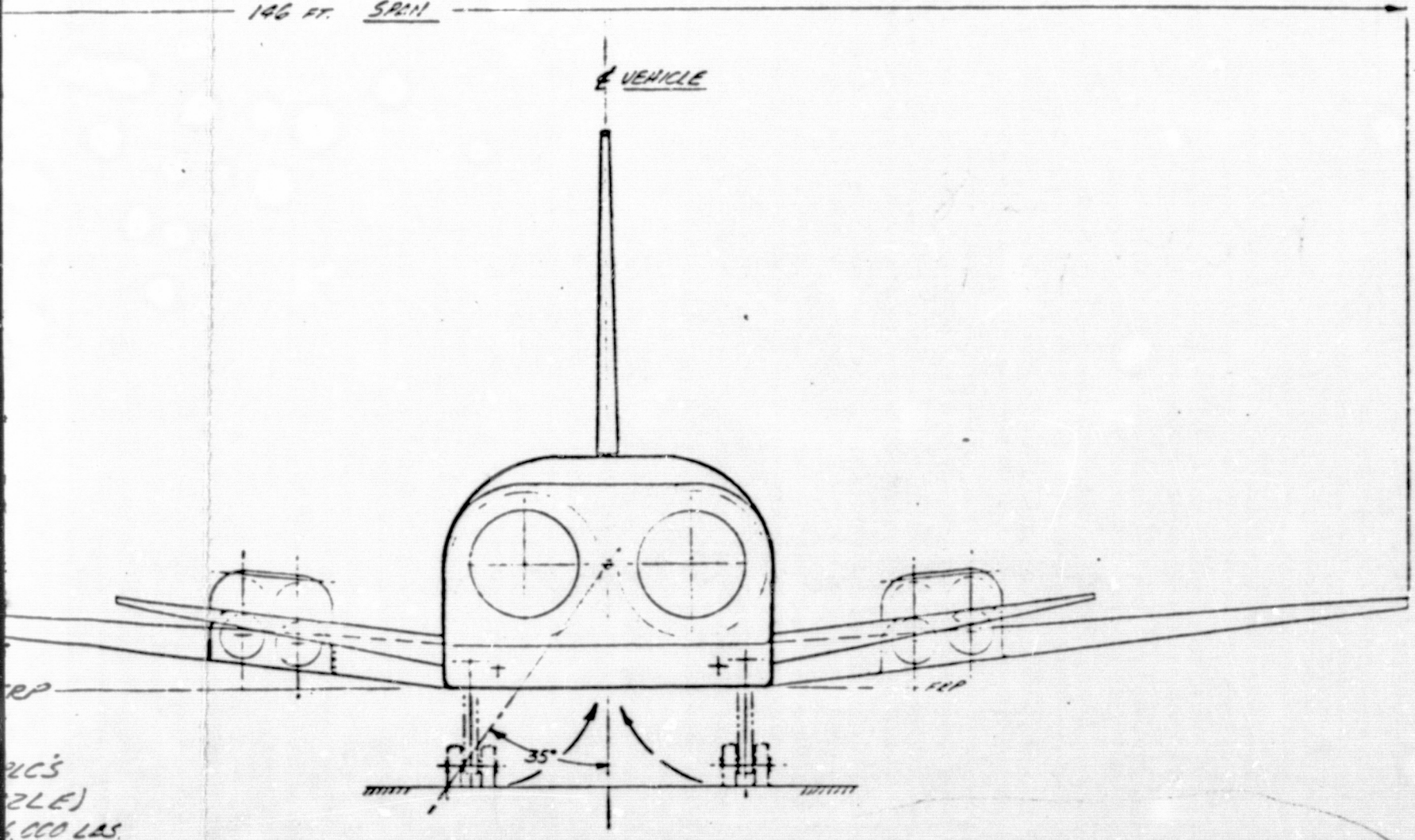

Figure 8.2-23. 50,000-Pound-Payload Orbiter for Detail Design (Drawing 2234-79)

SCALE 1 IN=100 FT.

0 50 100 200 300 400 500

FOLDOUT FRAME 4

8-57, 8-58

SD 69-573-4

The main propulsion system is used for orbiter injection into a 50- by 100-nautical-mile orbit and subsequent transfer to the space station orbit of 270 nautical miles. The orbiter is designed for an on-orbit life of seven days active systems and with up to thirty days maximum in orbit. Provisions are made for performing deorbit, reentry, and horizontal landing using runways suitable for conventional jet aircraft. The orbiter vehicle has provisions for subsonic flight in a typical ferry mission from the manufacturing or refurbishment site to a launch site.

Fuselage and Aerodynamic Surfaces. The orbiter fuselage provides a major portion of the aerodynamic surface by employing a flat bottom over the entire length of the body resulting in an area of 5,605 square feet. To minimize the body surface area, the height is set at the minimum allowable to accommodate the cargo bay. The orbiter body shell is the primary load-carrying structure. The basic structural material is 6Al-4V STA titanium. The body construction consists of hat-section stiffened skin mounted on fuselage frames as illustrated in Figure 8.2-24. The hat-section stiffeners are internal providing a smooth outer skin for heat-shield attachment and a smooth surface where the structure is exposed. Frame spacings vary from 20 to 40 inches, and frame depths vary from 6 to 12 inches. Major bulkheads are located for propellant tank support, wing carry-through attachments, tail-group attachments, thrust-structure attachments, and landing-gear fittings. Three major body longerons are provided. A keel longeron runs along the orbiter bottom from the LO_2 tank bulkhead area to the aft LH_2 tank area. Two upper-shoulder longerons are provided along the cargo-bay cutout structure. Provisions are made for top-loading of the cargo by employing nonstructural doors along the upper side of the fuselage. As illustrated in Figure 8.2-24, a major bulkhead is provided to shear body loads around the cargo bay cutout. To withstand the entry thermal environment, the titanium structure is protected on the bottom and sides of the fuselage by external densified quartz insulation panels bonded to the titanium structure. Bare titanium is satisfactory on the top of the orbiter because of the mild thermal environment. Fiberglass insulation is used inside the titanium structure to limit the temperature of the tankage and insulation interface for long-life consideration of the polyurethane foam used in the LH_2 tanks.

The wing and tail group structures are similarly constructed of 6Al-4V STA titanium alloy with the primary structure formed by a torque box assembly. Leading-edge assemblies are attached to the front spar; and the flaps, ailerons, and trailing edges are attached to the rear spar. The wing main structural box extends from the 15-percent chord plane to the 65-percent chord plane. Typical wing construction is also shown in Figure 8.2-24. Spars are beaded webs, and 20-inch rib spacing is used.

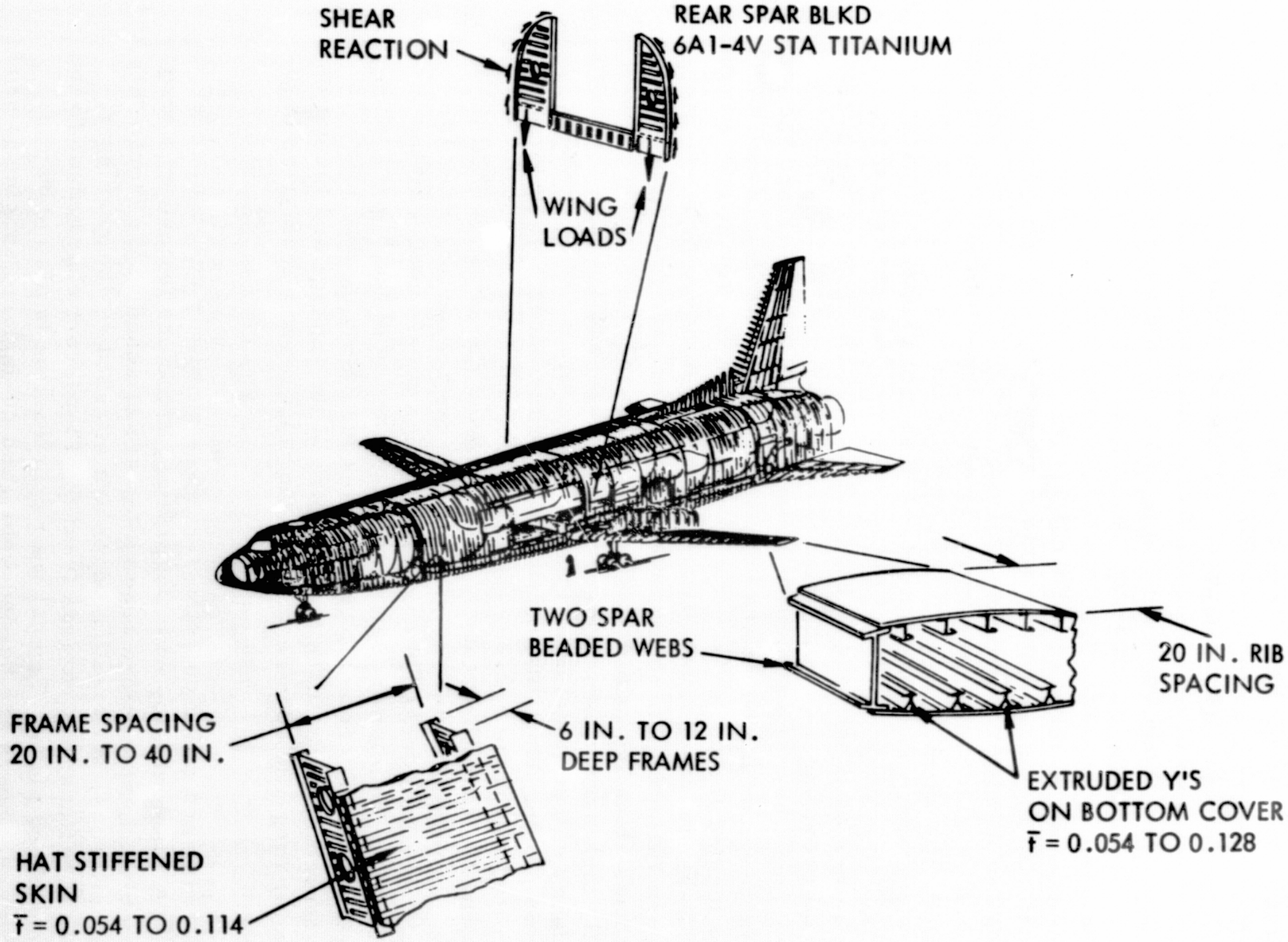

Figure 8.2-24. Typical Orbiter Fuselage and Wing Construction

Maximum wing load is provided by negative lift. The bottom cover uses extruded Y sections for stiffners because of the high loads. The top cover uses Z sections for stiffness.

The wing has a thermal protection system utilizing LI-15 insulation panels bonded to the titanium wing surface, except for the high heating area at the leading edge. This area is protected with zirconium diboride sections attached to the leading edge surface by means of tantalum fasteners imbedded in the zirconium sections. The thickness of the LI-15 insulation varies to satisfy the temperature profiles about the wing.

The horizontal tail surface provides a means of varying the surface area to satisfy the pitching moment requirements for the hypersonic, and subsonic flight profiles. The horizontal surface has a 50-percent elevator that can be positioned in a 60-degree-up attitude to reduce the tail surface during the reentry phase and to provide a satisfactory pitch moment for transition to low angle of attack. During the pitch-down and subsonic flight, the elevator is lowered to the normal position to provide pitch trim for the remainder of the flight.

The total planform area is 8,200 square feet with a body area of 5,605 square feet, a horizontal tail area of 585 square feet and an exposed wing area of 2,010 square feet

Landing Gear. The landing gear consists of two main landing gears and a nose gear assembly. The main gear consists of hydraulic struts with a four-wheel bogey on each. The nose gear has a slightly longer strut with dual wheels. The main gear is located aft of the rear wing spar and provides a maximum tail-down angle of 10 degrees. This position is consistent with present large aircraft requirements. The landing weight played a major part in the preliminary sizing of the gear. First, the landing weight was assumed to have a 20- to 80-percent nose-main gear weight distribution. This distribution defined the weight allowable for each tire or wheel. The main gear wheels were sized to have a nominal 30,000-pound load per tire, which is less than the loading per tire on current commercial aircraft. The effects of temperature and space environment led to the conservative selection of tire loading which resulted in eight tires of 48-inch diameter for the main gear and two tires of 48-inch diameter for the nose gear.

The main gear is designed to retract inward underneath the cargo bay compartment just aft of the rear wing spar. The gear is powered by hydraulic actuators. A systems weight saving may be realized by considering a retraction system for the ferry mission flights only. This retraction mode would only be used for ferry flights and could conceivably

limit the hydraulic system required for the primary mission. The retraction feature is not mandatory for space operations since the gear may be stowed manually prior to stacking for launch.

Figure 8.2-23 locates the relative position of each landing gear, the full-down and retracted positions, and the possible support points that could be used for this type of gear. Adequate turnover angle is provided for normal operation.

Main Rocket Propulsion. The orbiter main propulsion system utilizes two bell-nozzle rocket engines mounted side by side with each providing 576,000-pound vacuum thrust. The two-position bell-type nozzle is used to provide an expansion ratio of 120 during thrusting and is retracted by use of jack screws into the base of the body during reentry and landing to provide the necessary environmental protection and ground clearance. The extended engine length is 220 inches and the stowed engine length is 127 inches. The orbiter engines are the same as the booster engines, except for the two-position nozzle. Clearance between engines is provided with a ±7-degree gimbal angle in all directions.

The thrust structure for the orbiter engines consists of a titanium truss arrangement with provisions for an engine mount pad that interfaces with the forward mount on each rocket engine. The forward end of the truss terminates at the intersection of a main body frame and fore and aft longerons. The main body frame accommodates loading from the vertical and horizontal tail surfaces and the aft booster attach fittings. The fore and aft longerons distribute the engine thrust loads into the body shell. The thrust structure concept is illustrated in Figure 8.2-25.

The central cargo bay location requires separation of the ascent propellant tanks. LO_2 and LH_2 tanks are located forward of the cargo bay, and a second LH_2 tank is located aft of the cargo bay. These tanks are suspended and, therefore, are not subjected to vehicle aerodynamic loads. The forward tank is a single two-cell pillow tank structure with a common bulkhead locating the LO_2 forward and the LH_2 aft. The shape of the tank results in a valley on the centerline to provide tunnel access between the crew compartment and the cargo bay. The two-cell pillow tank provides the most efficient use of the present body cross-section area. Capacity of the forward tank is 7,500 cubic feet of LOX and 7,345 cubic feet of LH_2. The tank is supported from the body structure with tank attachments located at the common bulkhead. Stabilizing supports are provided at the forward end of the tank to allow for differential thermal expansion between the body structure and tank. The aft LH_2 tank, installed between the cargo bay and rocket engine bay, is also a two-cell pillow tank, sized to efficiently use the available cross-sectional area and to allow passage of a LOX feed line along

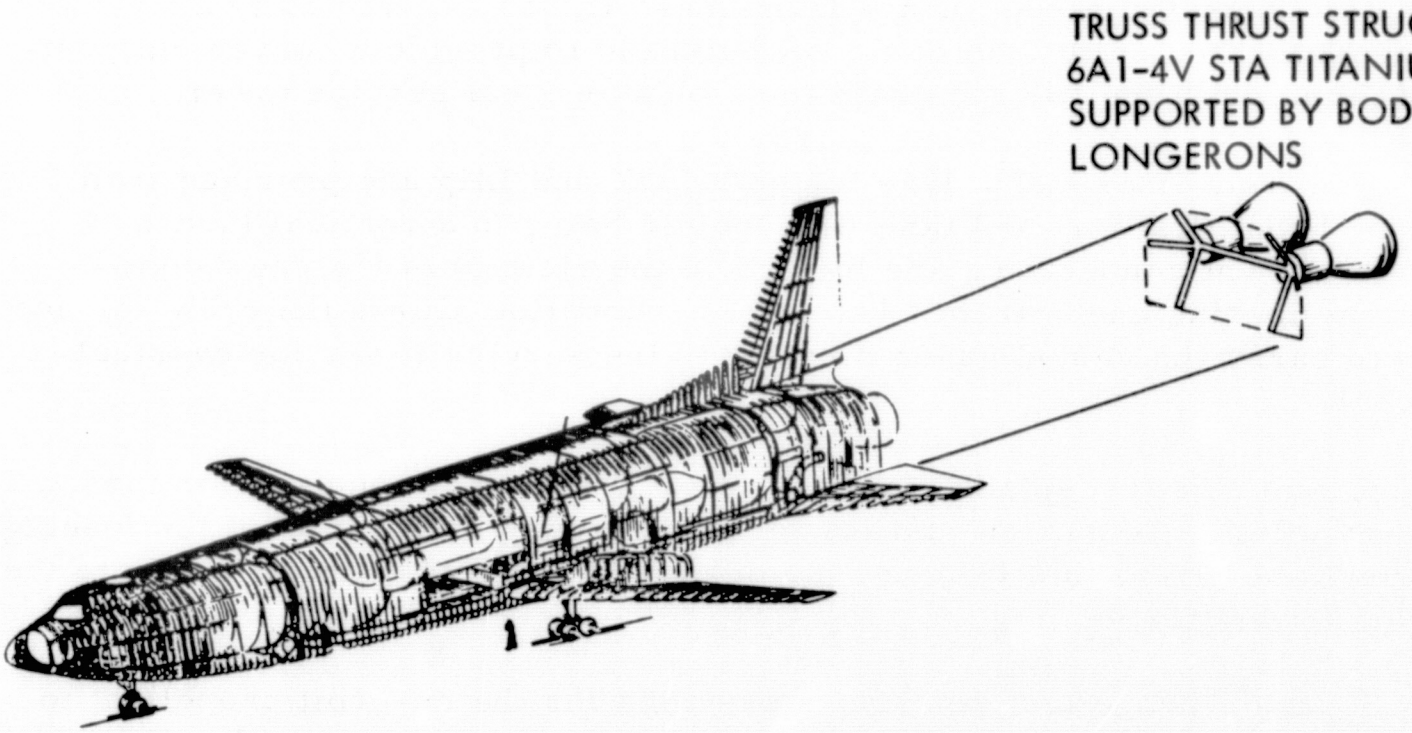

Figure 8.2-25. Rocket Engine Thrust Structure Concept

each lower corner near the hard chines. The capacity of this tank is 9,745 cubic feet. Two large-diameter tank interconnects furnish the remaining capacity of 1,655 cubic feet on each side of the cargo bay and provide propellant transfer from the forward tank to the aft tank. Total LH_2 capacity for the orbiter is 20,400 cubic feet.

Simplicity of the feed system for the rocket motors is maintained by direct LH_2 feed lines to the rocket motors, one from each cell of the two aft-tank bubble cells. The lines are 16-inch-diameter vacuum-jacketed lines with prevalves and expansion joints. The LOX feed lines are located low and outboard near the hard chines and have minimum bends to the LOX inlet of the rocket motors. Two 14-inch vacuum-jacketed feed lines, as well as prevalves and expansion joints are provided.

The LH_2 tanks have polyurethane foam installed internally for thermal protection. The LH_2 tanks and interconnects may be inspected internally to determine the condition of the internal insulation following flight. A single entrance to the LH_2 system is required to inspect the complete LH_2 tankage.

Propellant fill and drain lines on the orbiter are located at the bottom or aft end of the LH_2 tank. A fill-and-drain valve is installed in each feed line to the rocket motors. Lines from these valves are routed to a fly-away umbilical located on the top of the aft bulkhead to provide a convenient position to mate with the fill and drain lines on a vertical service tower.

Dual vent lines and valves for both LOX and LH_2 are provided from the top of the most forward tank (the orbiter being in a vertical launch attitude). Vent connections are located in the vicinity of the crew compartment docking and entrance hatch. This location allows the crew service boom tc carry the vented gases directly to the service tower for eventual disposal.

A vent line (receptacle on the side of the orbiter) required for the APU installation is located just forward of the wing on the side of the fuselage. Exhaust gases from this vent are plumbed to the erection tower (opposite the service tower) for venting.

Separate propellant tankage is provided for the on-orbit propellant to be used after insertion of the orbiter into the 50- by 100-nautical-mile orbit. This propellant provides for transfer to the space station altitude, gross rendezvous, and deorbit. The separate tankage is provided to simplify propellant orientation, to minimize prestart pressurization, and to maintain propellant for up to 30 days in orbit. Two LH_2 tanks are located behind the wing spar and under the cargo bay. These tanks contain 5,000 pounds of LH_2. Thermal protection is provided by an external layer of polyurethane foam (to allow an N_2 purge) and by high-performance multilayer aluminized mylar insulation. The feed lines are connected into the main LH_2 feed lines downstream of the prevalve. A single LO_2 tank with a capacity of 30,000 pounds is located just forward of the main engines. Thermal protection is provided by high-performance insulation. Similar to the LH_2 system, the feed lines are connected into the main LO_2 feed line downstream of the prevalve.

A system of purging the interior of the orbiter is required for the thermal protection system and for safety reasons. Pockets of oxygen or hydrogen cannot be present during fueling and during the mission. This purge operation uses gaseous nitrogen, which is introduced through a port near the crew entrance hatch and is distributed from a point forward in the nose of the orbiter. The nitrogen is allowed to purge the interior of the orbiter until liftoff. Exhaust of this gas is through the aft bulkhead. The exhaust ports in the bulkhead are sealed during the reentry phase of the flight.

Turbojet Propellant. Turbojet engines are provided on the orbiter for the subsonic cruise or go-around operation as well as for ferry flights. Air-breathing propulsion is provided by P&W JT3D-7 turbofan engines, installed on the upper side of the wing to afford maximum thermal protection during the reentry phase of flight. The four engines are mounted in single two-engine nacelles on each wing. The nacelle is designed with a retractable inlet that provides thermal protection when closed and becomes an inlet duct when extended. The nacelle divider provides the structural support and housing for the inlet actuation system. The engines are located with the exhaust exit plane at the trailing edge of the wing. The center of gravity of the engine is located in the vicinity of the aft spar and is structurally supported at the aft spar and a center beam of the nacelle.

The turbojet engine fuel is contained in a bladder-type tank located in the wing carry-through structure. This volume is from the front spar (15-percent chord) and the rear spar (65-percent chord) and extends across the vehicle body. Internal, electrically driven pumps and plumbing distribute the JP fuel outboard to the engine nacelles. Additional capacity for fuel may be installed in the cargo bay for ferry missions with the extra tanks plumbed into the basic fuel distribution system as on conventional drop-tank installations.

Reaction Control System. An O_2/H_2 reaction control system is installed to provide rotation and translation in all orbiter axes. Twenty-eight 800-pound RCS motors are provided. Pitch and yaw rotation is provided by eight motors located in the nose area and eight motors located in the tail area. The pitch motors located near the bottom of the orbiter are canted out the side of the lower fuselage to prevent penetration of the heat shield. Two -x translation motors are also located in the nose, and two +x translation motors are located in the tail. Roll is provided by eight motors located in the engine nacelle area of the wing. RCS propellants are stored as liquids in the on-orbit tankage. RCS propellant conditioning equipment is located near the on-orbit tankage to pump the liquid to high-pressure and to vaporize the liquid propellants. The gaseous propellants are supplied to accumulators located in the forward, center, and aft fuselage near the RCS motor modules.

Other Systems. The items of navigation, guidance, communications, control panels, and displays are located within the pressurized crew compartment. Their installation will be normally on the pilot-copilot display panel, forward of the panel, and below the floor ahead of the passenger compartment. The orbiter is designed to be controlled by a two-man crew on both orbital and ferry flights. Electrical power control is from the right side of the cockpit; however, the power generation equipment is located in unpressurized areas of the orbiter.

The orbiter contains three 5-kw fuel cells located below the forward portion of the crew compartment ahead of the nose gear well. This location provides access to these critical units for replacement, even in the awkward position of the orbiter when mated to the booster in a vertical launch attitude. The three fuel cells may be removed through the nose gear well when the nose gear is lowered.

Four auxiliary power units are located in the bottom fuselage bay forward of the wing front spar. This location was chosen because of the critical hydraulic power and weight involved and because it is centrally located with respect to the actuators of the wing control surfaces, elevator, rudder, rocket motor gimbal, and the main landing gear.

Access to the APU bay is normally through the cargo bay floor when the cargo is not in place. This area is also accessible through the cargo bay floor when the orbiter and booster are mated. Oxygen and hydrogen supplies for the fuel cells are in separate tanks located on each side of the nose landing gear wheel well. The APU's are supplied from the RCS accumulators.

The environmental control system is located on both sides of the passenger compartment. The radiators for heat rejection are assumed to be on the top surface of the nonstructural cargo bay doors. This location is chosen so that a system of shutters may be built into the doors and so that doors can be opened in orbit to direct the heat radiation away from the orbiter or any mating vehicle. The radiator lines from both the ECS and electrical power system (fuel cells) are located along each side of the crawl tunnel from the passenger compartment to the cargo bay.

Crew Systems and Passenger Accommodations. A pressurized crew and passenger compartment is provided in the forward end of the orbiter. A side-by-side crew arrangement is provided with an over-the-nose vision of 15 degrees by locating the crew seating on a level higher than the passenger seating arrangement. The compartment is essentially a hemispherically ended pressure cylinder with an integral canopy opening, a docking-entrance hatch , and a crew-to-cargo-tunnel entrance on the top surface of the cylinder. The forward end of the compartment is reserved for the highest density systems, such as navigation, guidance, electronics, batteries, and communications. Entrance to the crew compartment is through the docking port on the top centerline. Access to each seat, in a launch position, is by a ladder mounted on the crew floor to the aft bulkhead. Standing headroom is provided for all passengers when the orbiter is in a horizontal position. Adequate headroom is provided for crew and passengers as shown in the horizontal landing position similar to conventional jet aircraft accommodations.

Docking Provisions and Cargo Transfer. The orbiter may be docked to a space station by using one of the following methods:

1. Vertical translation to the crew-passenger hatch located in the cockpit area

2. Vertical translation to a docking ring designed into the cargo bay doors (Docking loads are taken out through the large fuselage frames in the vicinity of the wing-fuselage junction.)

3. End docking to a 15-foot-diameter by 60-foot-length cargo container that has been rotated out of the cargo bay (Full 180-degree rotation places the docking interface ahead of the nose of the orbiter but still within view of the docking operator.)

Vertical maneuvers associated with Items 1 and 2 may be visually monitored by means of a closed-circuit TV system mounted in the top surface of the orbiter. When the cargo canister is utilized as a docking interface, the docking operator (the copilot) has a visual means of performing the maneuver.

These docking provisions permit crew transfer in an IVA environment when docking to a space station with an empty cargo hold, docking to a space station without prepositioning of cargo canister, and docking to a space station with the cargo canister positioned for docking and cargo transfer.

The selected cargo transfer design utilizes top removal of the cargo and pivoting of the cargo container 180 degrees with crew access through the roof of the cockpit to the cargo container. Primary docking to the orbiter may be accomplished at the crew and passenger entrance hatch, at the docking ring contained in the cargo bay doors, or at the end of a cargo container when in position (rotated out of the cargo bay 180 degrees). For any selected position of docking, it is possible to have the passengers transfer to the space station by IVA means. When the cargo container is used, transfer may take place in a shirt-sleeve environment with the proper procedure of pressurization being used.

The simple 180-degree pivot mechanism located on each side of the crawl tunnel just forward of the cargo bay is powered by an electric motor gear drive direct to the pivot point. Structural arms are provided from the pivot to the forward end of the cargo can. When a cargo canister is installed, the aft end is mounted to the aft cargo bay bulkhead during boost operations. The nonstructural doors on the top of the fuselage are operated by separate electric driven actuators on each end.

General Booster Description

The booster provides an initial velocity increment to the orbiter. The booster is also capable of reentry, cruise back to the launch site, and landing in a conventional aircraft mode. For initial delivery and repeated use of this vehicle, a ferry-type mission is also a requirement. The ferry mode employs two pilots, while the normal space mission is unmanned and automatically controlled through launch, reentry, and landing phases.

The 50,000-pound-payload booster configuration selected for detailed analysis is shown in Figure 8.2-26 (Drawing 2234-76) and has the general characteristics listed in Table 8.2-6.

Fuselage and Aerodynamic Surfaces. The booster primary fuselage structure varies considerably from that selected for the orbiter in that integral propellant tanks are used to serve the dual function of propellant containment and primary-body load-carrying structure. This approach is the normal practice for current launch vehicles. The tanks are modified cylinders with circular cross sections to provide a minimum weight structure pressure vessel. The tanks are of integral skin and stringer design using 2219 T-87 aluminum alloy. The stringers and ring frames are located outside of the tank to simplify the installation of polyurethane foam insulation inside the LH_2 tank. Typical structure concepts are shown in Figure 8.2-27. The tank skin gauge varies from 0.082 to 0.170 inches. Frame spacing varies from 24 to 36 inches and stringer spacing varies from 3 to 6 inches.

The tank has a maximum diameter of 32.5 feet. Constant diameter is maintained for approximately 91 feet, at which point the forward tapered section is continued forward. The tapered tank section, including the hemispherical dome, is approximately 98.5 feet long. These two tank sections are mated at the bulkhead on the fuselage that corresponds with the forward spar of the wing. The forward end of this 188.5 foot tank is separated by a common bulkhead resulting in a LO_2 tank of 7,500 cubic feet capacity. Load distribution bulkheads are mounted to the tank at points of concentrated loads to accommodate launch fittings, the common bulkhead, the forward and aft wing spars, the engine thrust structure joint, and the vertical stabilizer mount located at the beginning of the aft hemispherical dome.

Secondary structure is required outside the integral tankage to provide the desired external mold lines (flat bottom with hard chines) and provide a thermal protection system substructure. This secondary structure uses 2219 aluminum alloy truss and grid configuration mounted to the integral tank. Reinforced phenolic and polyimide honeycomb sandwich panels are

REPRODUCIBILITY OF THE ORIGINAL PAGE IS POOR.

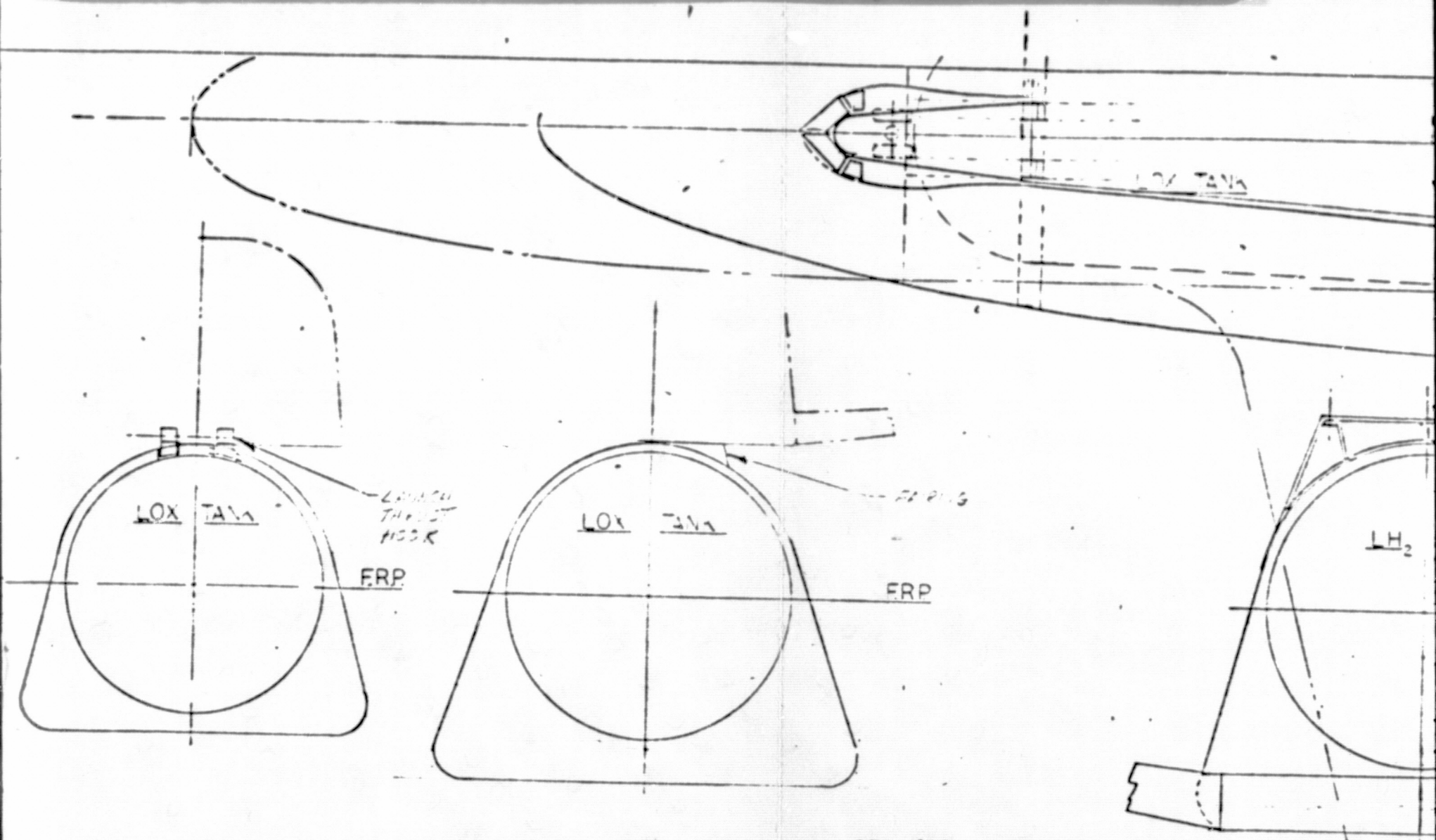

FOLDOUT FRAME 1

JET FUEL
1,150 CU. FT.

LH_2 TANK

FAIRING
(BRAKE SIDE)

LH_2 TANK

FRP

SECTION C-C

JET ATTACK-2 REQ'S

VAC 432 IN.

JET ENGINES 4 REQ'D.
55,500 THRUST EACH

B

B

C

C

FAIRING

FAIRING

CU. FT.

LH_2 TANK
CAPACITY - 95,000 CU. FT.

32.5 DIA.

+4°

JET FUEL

4°

10° TAIL DOWN STRUTS COMPRESSED

FOLDOUT FRAME 2

263' OVERALL LENGTH

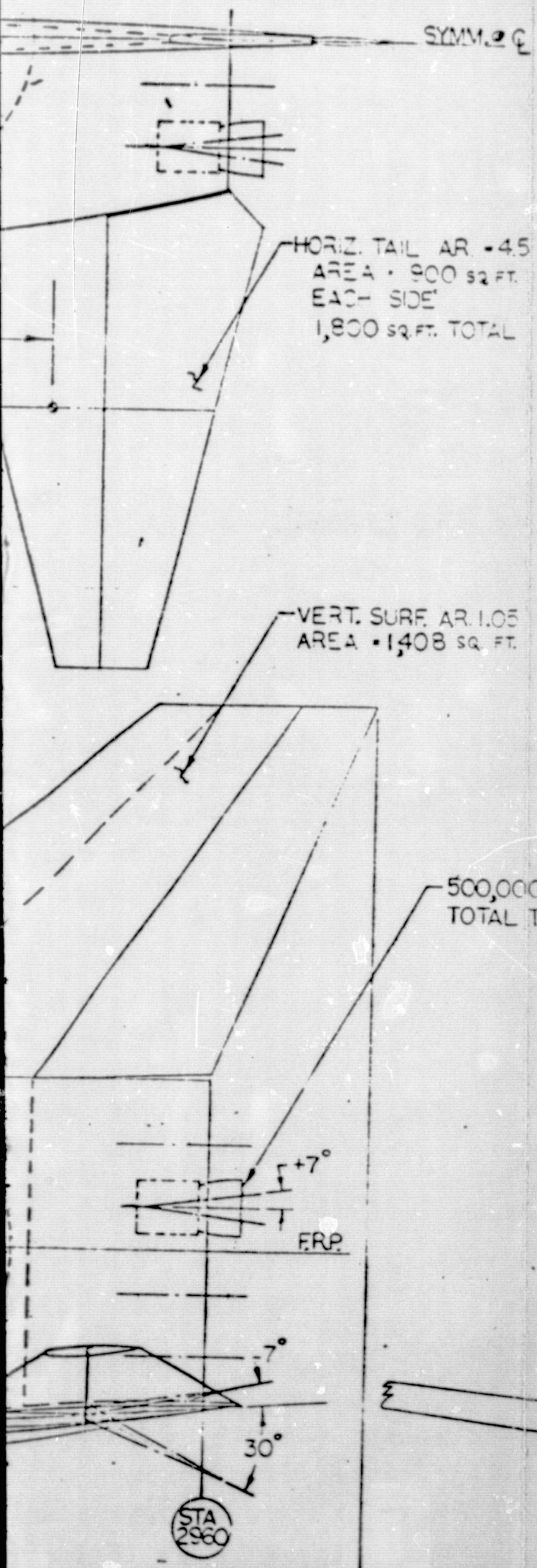

500,000 THRUST ROCKET ENGINES 10 REQD.
TOTAL THRUST SEA LEVEL = 5.00×10^6 LBS.

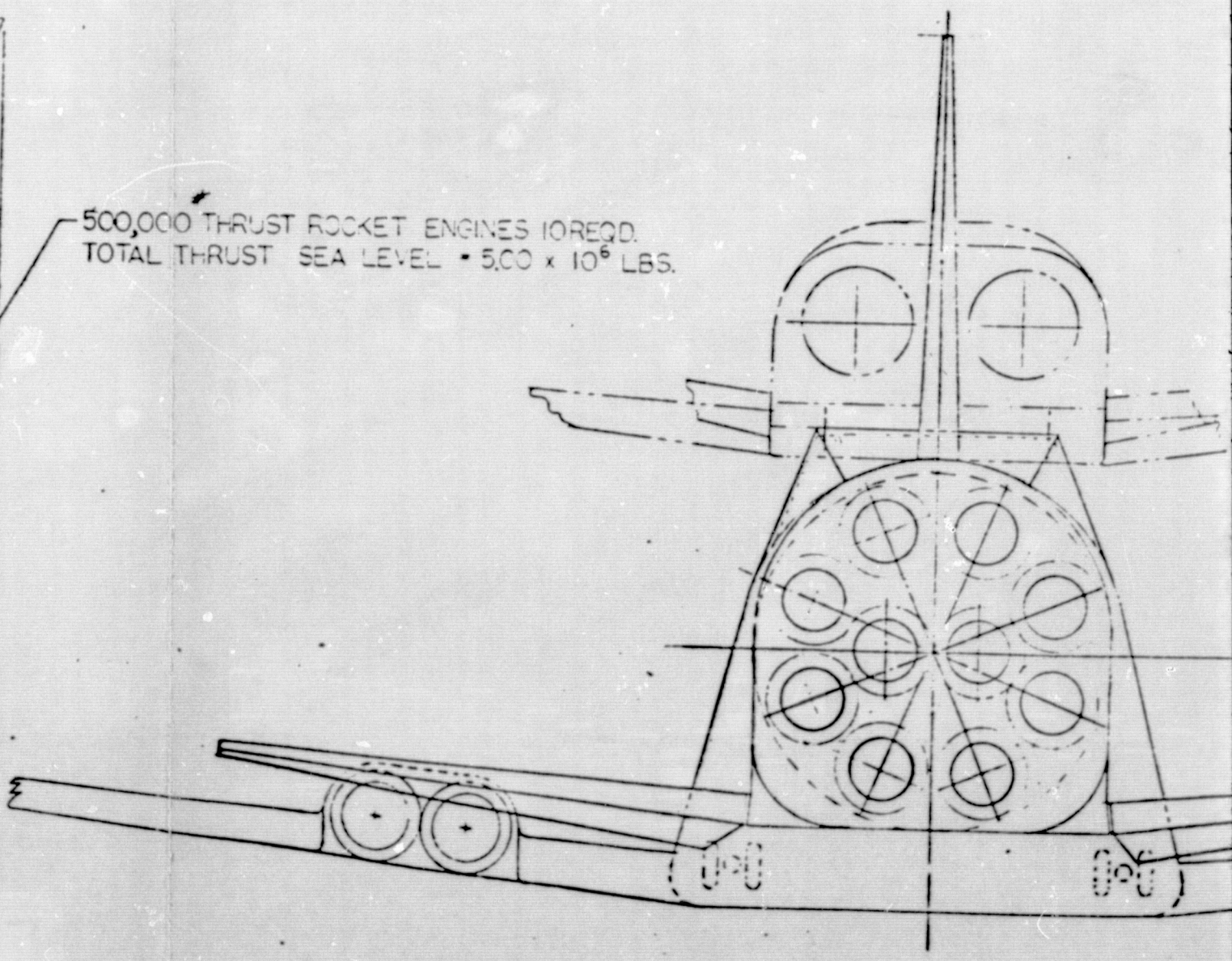

FOLDOUT FRAME 3

Space Division
North American Rockwell

WING GEOMETRY

S_W = 7,550 SQ FT.
SPAN = 230 FT.
C_R = 49.8 FT.
C_T = 15.9 FT.
$\Lambda_{LE.}$ = 14°
λ = .319
MAC = 432 IN.
A.R. = 7

STAGE WEIGHTS

PROPELLANT (LOX & LH_2)	=	2,600,000 LBS
TOTAL LAUNCH	=	3,150,000 LBS.
REENTRY	=	550,000 LBS.
LANDING	=	494,000 LBS.

TOTAL PLANFORM AREAS

S_{WING} = 7,550 SQ FT. $\left(\frac{W}{S_A}\right.$ = 70 LDG.)

$S_{FUS.}$ = 10,800 SQ FT.

TOTAL = 18,350 SQ FT $\left(\frac{W}{S_{TOTAL}}\right.$ = 30 REENTRY)

F.R.P.

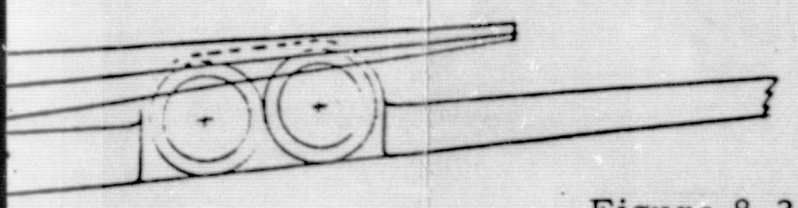

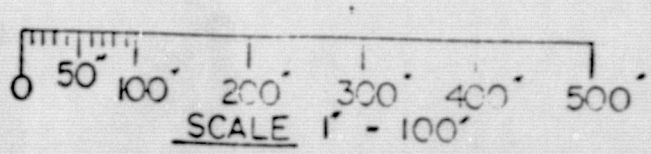

Figure 8.2-26. 50,000-Pound-Payload Booster for Detail Design (Drawing 2234-76)

FOLDOUT FRAME 4

Table 8.2-6. Booster General Characteristics

Body	
Length	247 ft
Width	46.7 ft
Height	41 ft
Bottom	Flat and cambered
Planform area	12,960 ft^2
Wetted area	32,000 ft^2
Wing	
Area (theoretical)	7,550 ft^2
(exposed)	5,430 ft^2
Span	230 ft
Aspect ratio	7 deg
Leading edge sweep	14 deg
Taper ratio	0.319
Mean aerodynamic chord	432 in.
Horizontal Tail	
Area (exposed)	1800 ft^2
Area elevator	900 ft^2
Aspect ratio	4.5
Vertical Tail	
Area exposed	1408 ft^2
Propulsion	
Number rocket engines	10
Thrust, SL (ea)	500,000 lb
Turbojets	4
Type	JT9D-15
Thrust, SLS (ea)	45,500 lb
Weights*	
Launch	3,150,000 lb
Entry	550,000 lb
Landing	494,000 lb
Propellant (LO_2/LH_2)	2,600,000 lb

*Preliminary weights used in configuration sizing.

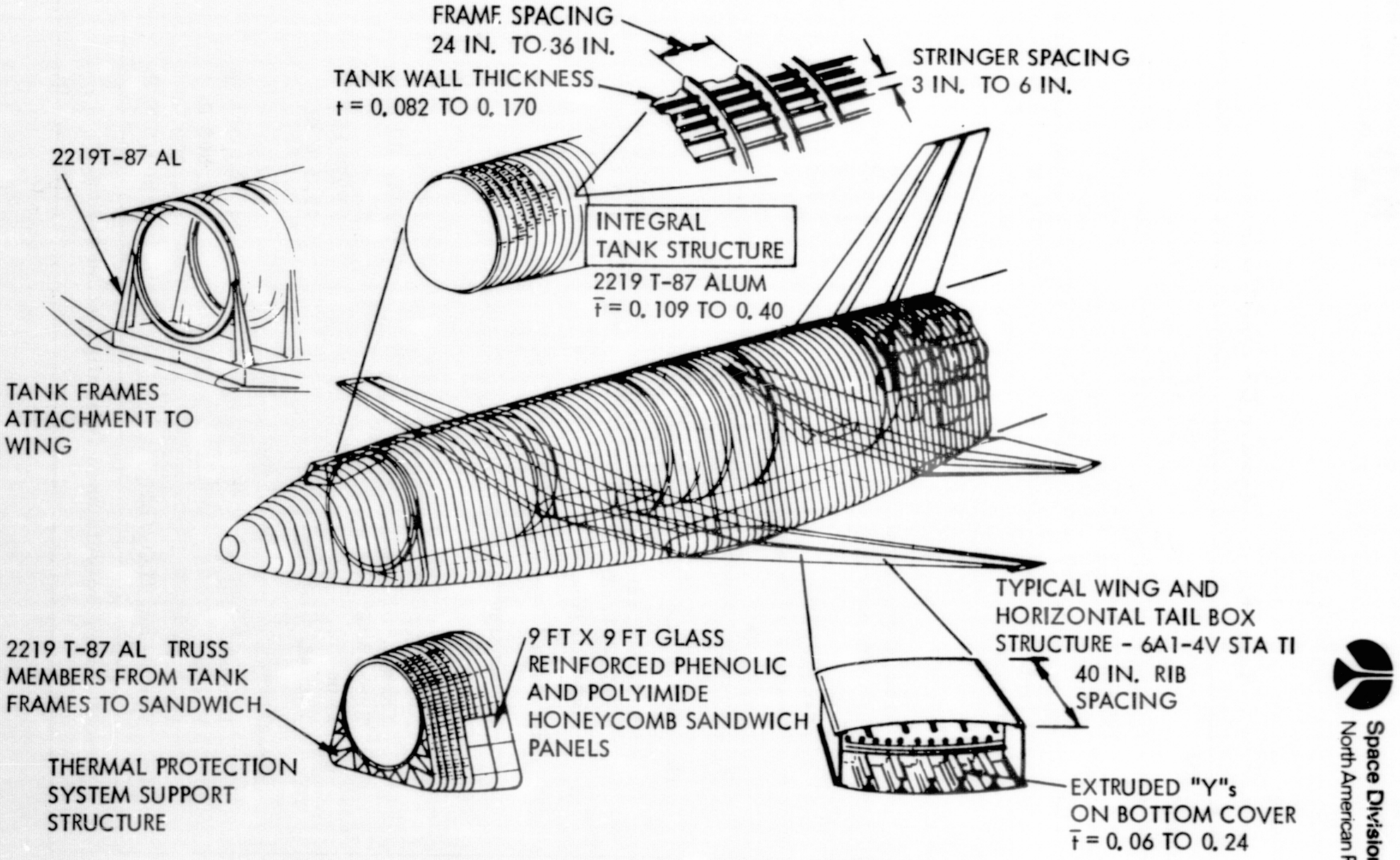

Figure 8.2-27. Typical Booster Fuselage and Wing Construction

mechanically attached to the aluminum substructure. Similar to the orbiter, the bottom and lower sides of the fuselage are protected during reentry by densified quartz (LI-15) external insulation panels bonded to the honeycomb sandwich panels. Fiberglass insulation (TG-15000) is installed between the substructure and tankage to limit the tankage polyurethane foam temperature to 175 F for multiple reuse of the foam.

The wing is attached to the body at two main frames that are integral parts of the LH_2 tank. The aft section of the body is skin and stringer construction with major frames located coincident with the main spars of the tail surfaces. The wing is designed as a two-spar, center-torque box fabricated of 6Al-4V STA titanium alloy. The leading and trailing edges are similarly fabricated and attached to the front spar (15 percent chord plane) and rear spar (65 percent chord plane), respectively. The trailing edge consists of flaps that extend from the body half breadth to approximately 70 percent of the span. The ailerons are the outboard section of the trailing edge. Similar to the orbiter, the spars are beaded construction. The rib spacing is 40 inches. The bottom cover also uses extruded Y sections, and the upper cover uses Z sections. The thermal protection system (TPS) consists of a Haynes 188 leading edge with LI-15 on the lower surface only. TPS is not required on the upper surface.

Landing Gear. The high landing weight of 494,000 pounds for the launcher presented a design condition similar to that for the present day heavy-duty jet cargo aircraft (the C-5A landing weight is approximately 640,000 pounds). Therefore, a main gear with four, four-wheel bogeys is used to provide reasonable tire and wheel loading and more even load distribution to satisfy existing runway designs. The design shown in Figure 8.2-26 allows for installation of two main gears forward of the forward wing spar and two main gears aft of the aft wing spar. The nose gear is shown as a single strut with dual wheels. A more detailed analysis of the nose gear loads may result in additional wheels and tires on the same nose gear axle.

The landing gear is designed to be operated by hydraulic actuators. At the present time, full cycling capability is required for all landing gear when used in the ferry mode. An ultimate concept that may offer considerable weight-saving may be the use of a pneumatic operating system for limited operation of the gear, since retractions in flight occur only during the ferry missions.

The present landing gear system contains the following major components:

1. Four main struts
2. Four wheels to each main strut(a total of 16 wheels for the main landing gear system)
3. A nose-landing-gear strut
4. A dual-wheel arrangement on the nose gear

Figure 8.2-26 shows the relative position of each landing gear, the full down and retracted positions, and the possible support points for the gear.

Main Rocket Propulsion. The booster main rocket propulsion system consists of 10 high-chamber-pressure rocket engines with fixed bell-nozzles having a 35:1 expansion ratio. Each rocket engine provides 500,000-pound sea-level thrust. The rocket engine is basically the same as that used in the orbiter. The engine has the same power head and an expansion ratio of approximately 5:1 where the booster nozzle is attached. The ten engines are arranged with eight engines in a circular pattern and two engines side by side inside the circle. The eight outside engines are gimbaled ±7 degrees to provide vehicle control during boost. The engine spacing provides clearance in the event engines are gimbaled towards each other. The center engines are not required to gimbal, but sufficient engine clearance is available to allow inner engine gimbal.

A preliminary design of the booster thrust structure has been performed and is shown in Figure 8.2-28. The thrust structure must transmit the load from ten 550,000-pound vacuum-thrust engines to the booster body structure perimeter. It must also sustain the load conditions that occur with one engine out, or all engines gimbaled concurrent with the applied engine gimbal actuator loads. The thrust structure must also provide structural rigidity compatible with the actuator engine control system. To transmit these loads to the perimeter of the booster body structure, a skin stringer frame conical shell is provided. The eight outboard-engine thrust loads are applied directly through the individual gimbal blocks attached to eight longerons. The two inboard-engine thrust loads are applied to four cross-beams through compatible deflection of a rigid octagonal structure. The four cross-beams transfer the total thrust of these two engines to the eight longerons. The cross-beams also react the horizontal force component of the engine thrust load at the longerons. The total thrust loads are in turn sheared into the skin stringer shell. A total of six frames is provided on the

THRUST
STRUCTURE
6Al-4V STA Ti

Figure 8.2-28. Booster Thrust-Structure Concept

shell at equal intervals to stabilize the skin stringer column designs, to react longerons kick loads, and to shear lateral forces into the shell. A system of compression ties and lateral supports are provided to transfer side forces into the aftmost frame, efficiently and to stabilize the cross-beam compression cap. The preliminary design stress analysis of this configuration is based upon the foregoing strength requirements and the use of 6Al-4V titanium throughout the design. A titanium 6Al-4V design is expected to be lighter than an aluminum design in view of the high loading intensities.

Each engine has an independent 16-inch LH_2 feed line from the tank bottom to the engine feed line interface. The feed line includes a normally open prevalve and expansion joint. Each engine also has an independent 16-inch LO_2 manifold located in the engine compartment. The LO_2 lines also include prevalves and expansion joints. The LO_2 manifold is supplied by two 30-inch feed lines routed from the LO_2 tank along the lower outboard corners of the fuselage.

Propellant fill and drain lines on the launcher are located at the aft end of the LH_2 tank. The LO_2 fill line leads directly to the outer manifold, outside of the thrust structure; the LH_2 fill line is located in one of the feed lines between the engines and the hemispherical bulkhead. Jettisonable umbilicals are located on the aft face of the rear bulkhead at each side of the vertical fin.

Vent lines for both LO_2 and LH_2 are installed within the booster to vent the tanks as they are filled in a vertical and launch attitude. External connections are located on the side of the launch vehicle in the vicinity of the ferry cockpit. Vent lines are also required for the combustion gases given off by the APU installation. High-temperature lines run directly from the side of the fuselage to an overboard vent located on the rail structure of the mobile erection tower.

Turbojet Installation and Jet Fuel Location. The booster has four JT9D turbofan engines, two in each nacelle mounted on the top surface of the wing. This position was chosen because the entire nacelle would be in the shadow, or wake region, caused by the high angle of attack during entry. Turbojet engines are used for return from a downrange position after launch to a landing site near the original launch site. These engines are also used to deliver the booster to the launch site by a series of ferry flights. The nacelle has been designed with a center structural beam with the engines supported from this beam and the aft spar of the wing. The forward part of the nacelle is designed to open after reentry to become the air inlet for two engines. The inlet fairing door is sloped off approximately 45 degrees

to assure proper clearance of the shock wave from the leading edge during reentry and to limit the heating input into the nacelle structure. The inlet nacelle door has been designed to open upward with the hinge above the inlet face of the engines. Capture area is compatible with the inlet area of the two JT9D engines in the flight speed range for the flyback and ferry missions. The jet fuel is located within the wing carrythrough structure in a bladder type cell. Fuel boost pumps and plumbing are contained in the wing structural box between the 15 and 65 percent spar locations and extend outboard to the engine nacelles. The total volume required for jet fuel within this center wing box area is 1,150 cubic feet. Additional tankage may be desired for ferry flights; tanks can be temporarily installed between the main landing gears in the body area.

Reaction Control System. An O_2/H_2 reaction control system is installed in the booster to provide pitch, yaw, and roll control during separation and entry maneuver. Twenty-four, 1800-pound-thrust RCS motors are provided. Pitch and yaw motors are located in the nose section; roll motors are located in the turbojet engine nacelle area. RCS propellants are stored as liquids and conditioned to high pressure gases for use in the RCS motors. RCS propellant conditioning equipment is located forward of the wing to pump the liquid to high pressure and vaporize the liquid propellants. The gaseous propellants are supplied in accumulators located in the forward portion of the vehicle.

Other Systems. The primary mode of launcher operation is unmanned, with provisions for manned operations for ferry or flight testing. The guidance, navigation, and control system equipment is located in the nose section, arranged to accommodate a pilot and co-pilot for the manned mission operations, and provide proper arrangement for all automatic flight operations.

Hydraulic and electrical power is provided by an auxiliary power unit (APU) installation located just forward of the wing front spar. The APU's are designed to operate on gaseous hydrogen and oxygen during the launch, reentry, and return portions of the mission.

Crew Systems. The crew systems and provisions are used only for the ferry mode of operation. A cockpit enclosure of the same geometry as the orbiter has been provided as an extension of the top fairing on the booster. The cockpit will contain minimum instrumentation and controls to deliver the booster to the launch site. Pilot and co-pilot accommodations may be removed at the launch site; automatic flight control and systems equipment will be used for the remainder of the mission.

Final 50,000-Pound-Payload Configuration Definition

Following the detailed analysis conducted on the booster and orbiter, it was determined that the booster weight was 3.1 percent less than the preliminary weight statement and that the orbiter was 8.7 percent heavier than the preliminary weight statement. The vehicle was therefore resized to maintain the 50,000-pound-payload capability. The vehicle description is presented in Tables 8.2-7 and 8.2-8.

25,000-Pound-Payload Configuration

Using the weight scaling data obtained from the detailed 50,000-pound system analysis, a shuttle vehicle with 25,000-pound-payload capability and a 12-foot by 48-foot cargo bay was sized (Figure 8.2-29).

The system descriptions are similar to those in the previous sections. The main rocket engine thrust level is less because of the reduced vehicle weight. The booster requires ten 414,000-pound-sea-level-thrust engines, and the orbiter requires two 482,000-pound-vacuum-thrust engines. The booster and orbiter body length are reduced to 230 feet and 175 feet, respectively.

Table 8.2-7. Final 50,000-Pound-Payload Vehicle Description

	Booster	Orbiter
Vehicle Weights		
Gross weight (lb)	3,619,872	870,977
Entry weight (lb)	587,522	256,515
Landing weight (lb)	532,002	254,807
Wing Geometry		
Span (ft)	244	146
Sweep (deg)	14	14
Taper ratio	0.319	0.333
Exposed area (sq ft)	6300	2010
MAC (ft)	37	21.4
Leading edge radius (in.)	7.1	4.05
Vehicle Dimensions		
Length (ft)	280	202
Planform area (ft^2)	19,770	8,200
Body wetted area (ft^2)	36,000	17,111
Wing wetted area (ft^2)	12,600	4,020
Horizontal tail wetted area (ft^2)	4,080	2,340
Vertical tail wetted area (ft^2)	3,180	1,170
Body mold-line volume (ft^3)	320,000	97,690
Volumetric efficiency ($V^{2/3}/A$)	0.13	0.124
Main Propulsion		
Propellant type	LO_2/LH_2	LO_2/LH_2
Mixture ratio	6:1	6:1
Engine thrust (1,000 lb)	510 (sl)	590 (vac)
Expansion ratio	35:1 (sl)	58:1 (sl)/120:1 (vac)
Number of engines	11	2
Firing sequence	1	2

Table 8.2-7. Final 50,000-Pound-Payload Vehicle Description (Cont)

	Booster	Orbiter
Turbojet Propulsion		
Engine type	JT9D-15	JT3D-7
Number of engines	4	4
Engine-out capability	Yes	Yes
Engine thrust, SLS (1,000 lb)	45.5	19
SFC (lb/hr/lb)	0.364	0.55
Launch Data		
T/W (initial)	1.25	1.36
Engine-out capability	Yes	Yes
Maximum acceleration (g)	3	3
Burnout time, from lift-off (sec)	220	440
Burnout velocity (fps)	10,866	25,855
Burnout altitude (ft)	245,000	303,806
Burnout range (nm)	98	680
Burnout flight path angle (deg)	6.9	0
On-Orbit Data		
Inclination (deg)		55
Injection conditions (nm)		50 x 100
Station altitude (nm)		270
Maneuver ΔV (total) (fps)		2,000
Entry Data		
Reentry angle (deg)	6.5 (Staging)	-1.5
Reentry velocity (fps)		25,134
Lateral range, (nm) $\alpha = 60$	48	190
Longitudinal range (nm)	310 (Flyback)	2,545
Lateral range, T_{MAX}(nm)		1,240
Maximum acceleration (g)	4.0	2.08

Table 8.2-7. Final 50,000-Pound-Payload Vehicle Description (Cont)

	Booster	Orbiter
Recovery Data		
Flyback range (nm)	310	0
Landing speed (knots)	113	128
Touch down angle of attack (deg)	8	8
Aerodynamic Parameters		
Hypersonic (L/D) maximum (inviscid)	2.05	1.53
Hypersonic (L/D)design	0.69	0.53
Subsonic (L/D) maximum	8.40	7.30
Entry planform loading (psf)	30	31
Landing planform loading (psf)	27	31
Landing wing loading (psf)	67	88
Reserves		
RCS (lb)	460	950
ECS (lb)	0	50
Power (lb)	200	880
Turbojets, go-arounds (lb)	10,600	3,900
Orbit man system 500 fps (lb)	---	9,600
Primary propulsion, FPR (lb)	0	4,700
Safety Factors		
Crew compartment	2	2
Primary structure	1.5	1.5
Secondary structure	1.5	1.5
Pressure tanks (propellant)	1.5	1.5
(pneumatic)	2.0	2.0
Payload Definition		
Weight (lb)		50,000
Size, diameter x length (ft x ft)		15 x 60

Table 8.2-8. Thermal Protection System and Environment

Vehicle Region	Maximum Equilibrium Temperature (deg F)		Heat Load (Btu/ft^2)		Area (ft^2)		Weight (lb)*	
	Booster	Orbiter	Booster	Orbiter	Booster	Orbiter	Booster	Orbiter
Body								
Nose region	1,275	1,860	306	6,450	--	--	--	--
Lower surface (20 percent L)	1,380	1,420	224	2,080	12,900	5,667	5,594	6,846
Side wall	540	560	36.5	207	8,800	4,222	3,760	2,390
Top surface	500	500	32	32	14,300	7,222	--	--
Wings (straight)								
Upper surface (20 percent C)	650	700	55.6	65.5	--	2,010	--	402
Lower surface (20 percent C)	1,400	1,700	260	3,652	6,300	2,010	2,801	2,852
Leading edge	2,200	3,000	1,530	22,460	--	124	--	888
Stabilizers								
Horizontal								
Upper surface	650	700	55.6	65.5	--	585	--	468
Lower surface	1,390	1,500	351.0	2,330	1,020	585	512	760
Leading edge	2,020	3,450	1,210	35,900	--	67	--	478
Vertical								
Sides	650	650	55.6	55.6	--	--	--	--
Leading edge	1,730	2,320	358	2,160	--	34	--	242
Other								
Cryogenic tanks (LH_2)	175	175			16,600	9,275	3,704	2063
Internal	500	500			36,000	17,110	6,304	9,372

*These weights do not include 10 percent contingency.

PRECEDING PAGE BLANK NOT FILMED.

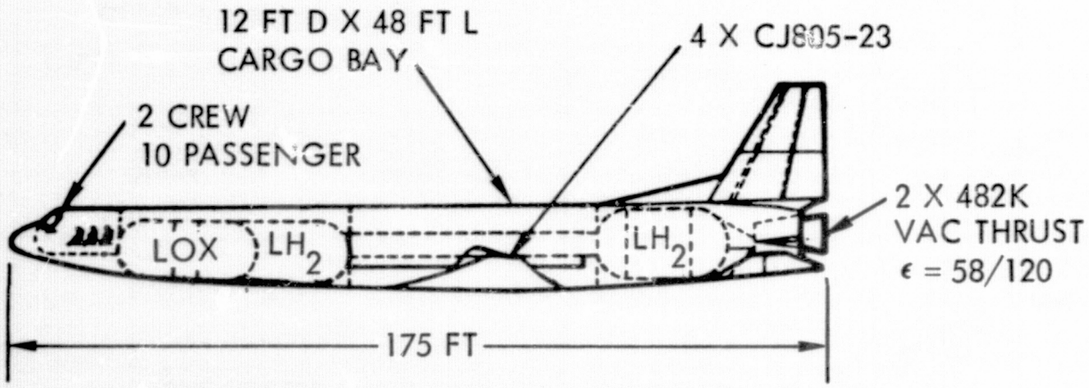

- WING SPAN = 127 FT
- WING AREA = 1555 FT^2 (EXPOSED)
- PLAN FORM AREA = 6330 FT^2

WEIGHT (1000 LB)

ITEMS	BOOSTER	ORBITER
PAYLOAD	-	25
BURN OUT	482	190
ON-ORBIT Wp	-	25
ASCENT Wp	2179	434
GROSS STAGE	2661	649
LAUNCH	3310	

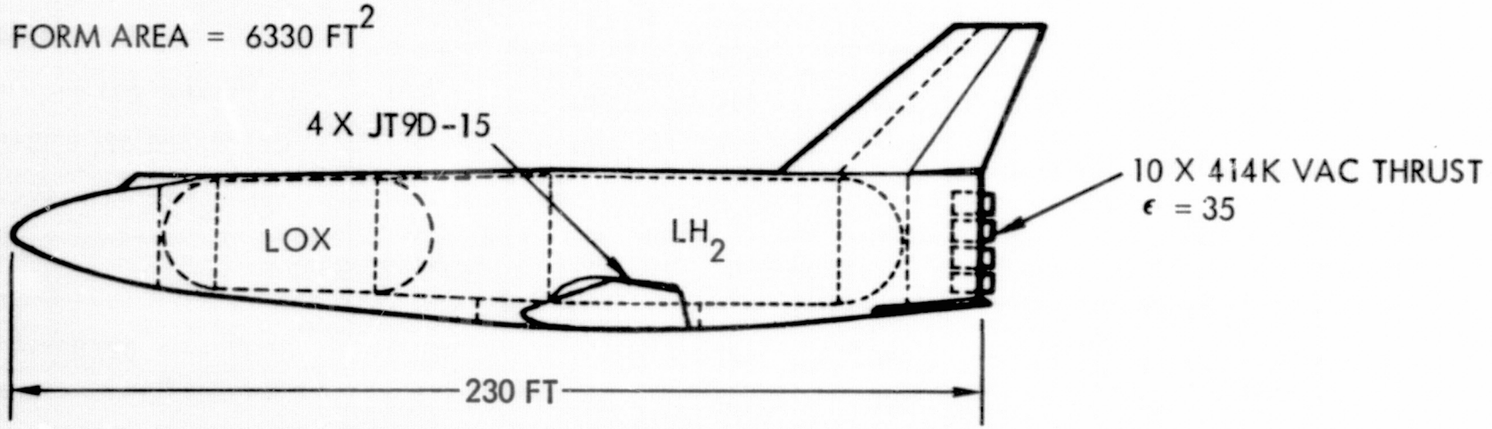

- WING SPAN = 221 FT
- WING AREA = 5,000 FT^2 (EXPOSED)
- PLAN AREA = 16,000 FT^2

Figure 8.2-29. 25,000-Pound Payload Vehicle Configuration, 12-Foot Diameter by 48-Foot Cargo Bay

Space Division
North American Rockwell

8.3 WEIGHT ANALYSIS

The weight analysis conducted was directed toward:

1. Review of the 12,500-pound-payload baseline configuration weight and development of mass characteristics for loads, control, and design analysis

2. Preparation of gross weight statements for the range of payloads and cargo bay sizes

3. Weight sensitivity studies

4. Preparation of mass properties for the 50,000-pound-payload baseline system selected for detail analysis

5. Detail weight analysis of orbiter and booster stages of a shuttle vehicle providing 50,000-pound-payload capability and 15-foot-diameter by 60-foot-length cargo bay

The following sections present the results of these studies.

8.3.1 Baseline Configuration Review, 12,500-Pound Payload

Since NASA MSC had recently conducted studies of the shuttle vehicle concept that NR was beginning to study, the available MSC weight data were reviewed and compared with subsystem weight scaling data being used in other NR studies. The data available were for a vehicle with 12,500-pound-payload capability. The projected weights are summarized in Table 8.3-1. The only apparent significant differences were in the orbiter body structure weight factor and aerodynamic surfaces weight factor.

A comparison of the orbiter and booster average body structure weight factor with aircraft and booster stages is shown in Figure 8.3-1. The orbiter and booster structure weight factors obtained from the body and tank structure weight shown in Table 8.3-1 and the external body envelope area are shown as solid circles in Figure 8.3-1. These values appear to be low compared with those of previous systems; however, external body envelope area is significantly greater than the primary structure wetted area because of the flat-bottom configuration. When the structure weight factor is based on the primary structure area (dashed circles in Figure 8.3-1), the weight factors are in general agreement with past systems. These structural weight factors and the slope determined from historical data were applied to the parametric data presented in the next section.

Table 8.3-1. Baseline 12,500-Pound-Payload Vehicle Projected Weights

Item	Weight (lb)	
	Orbiter	Booster
Aerodynamic surfaces	7,500	25,500
Body and tank structure	17,900	56,200
Induced environment protection	10,000	20,000
Systems	26,100	66,000
Two crew, 10 passengers plus 3,000-pound return cargo	5,400	--
Trapped propellants (rocket)	700	2,100
Reserve jet fuel and expendable	1,700	9,000
Normal landed weight	69,300	178,800
Net payload and fluids	15,700	20,300
Insertion and burnout	85,000	199,100
Ascent propellant	230,700	836,700
Launch weight	315,700	1,035,800
Combined liftoff weight	1,351,500	

A comparison of wing weight factors as a function of theoretical wing area is shown in Figure 8.3-2. The factor determined from the MSC data and used in the generation of parametric weight data is 7 pounds per square foot. This value appears to be optimistic, but was accepted until a detail analysis could be performed.

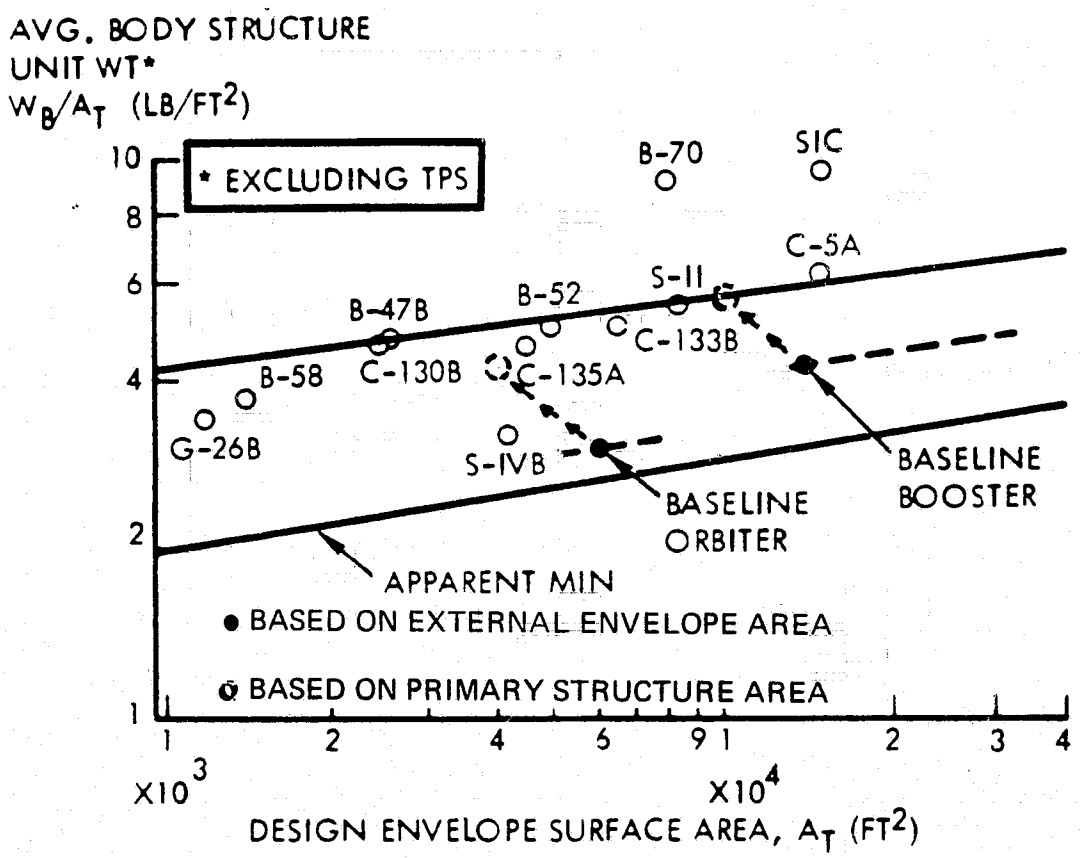

Figure 8.3-1. Body Structure Weight Factor Comparison

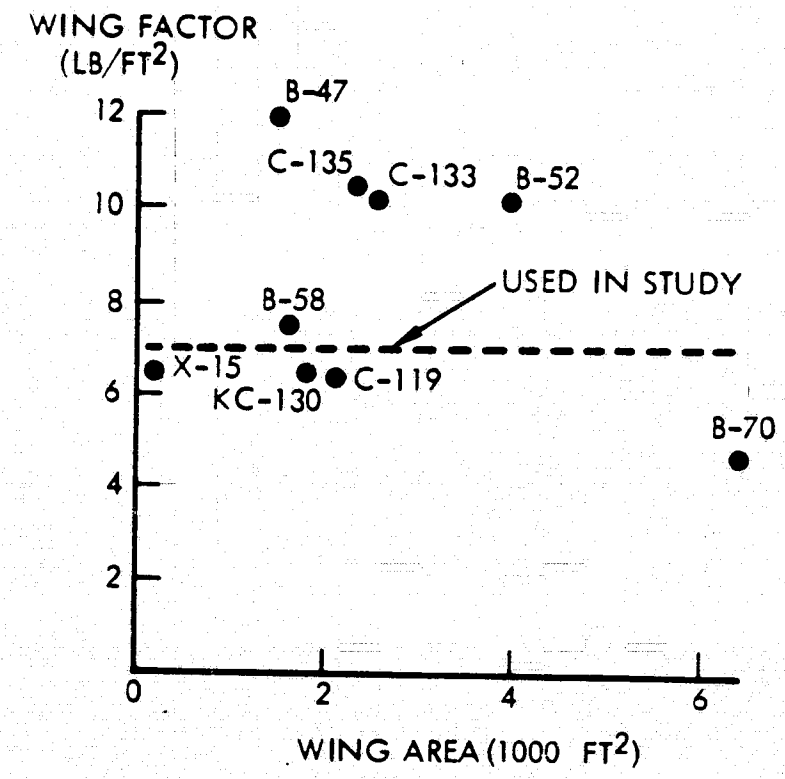

Figure 8.3-2. Wing Structure Weight Factor Comparison

8.3.2 Baseline 12,500-Pound-Payload Vehicle Mass Properties

Mass properties for the baseline 12,500-pound-payload vehicle were established for use in the vehicle control and loads analysis. Mass properties were determined for the following operational conditions:

1. Launch
2. Maximum dynamic pressure
3. Maximum acceleration
4. Preseparation
5. Postseparation
6. Entry
7. Landing

The mass properties were established by reviewing the baseline configuration drawing (Figure 8.3-1) presented in Section 8.2., Design, and estimating equipment location and structure and thermal protection system weight distribution. The mass properties are presented in Table 8.3-2.

8.3.3 Concept Sizing For Various Payloads

Parametric weight data were prepared for use in shuttle vehicle sizing, which is presented in Volume III of this report. Data were generated for the following payloads:

1. 10,000 pounds with 2,000-cubic-foot cargo volume
2. 25,000 pounds with 15-foot-diameter by 30-foot-length cargo bay
3. 25,000 pounds with 15-foot-diameter by 60-foot-length cargo bay
4. 50,000 pounds with 15-foot-diameter by 60-foot-length cargo bay
5. 50,000 pounds with 22-foot-diameter by 60-foot-length cargo bay

The parametric data also reflected variation in propellant mixture ratio and orbiter and booster thrust levels.

Table 8.3-2. Baseline 12,500-Pound-Payload Vehicle Mass Properties

Condition	Vehicle Configuration	Weight (1,000 lb)	Center of Gravity* (in.)			Moment of Inertia (slug $ft^2 \times 10^{-6}$)		
			X	Y	Z	I_{xx}	I_{yy}	I_{zz}
Prelaunch/ Liftoff	Booster and orbiter	1,351	804	0	228	5.8	70.9	71.3
Max Q (t = 72 sec)	Booster and orbiter	1,048	869	0	224	6.0	59.2	57.2
Max G (t = 180 sec)	Booster and orbiter	587	883	0	272	5.3	50.6	49.4
Pre-separation (t = 201 sec)	Booster and orbiter	506	856	0	293	5.0	47.2	46.3
Postseparation entry (t = 201 sec)	Booster	190	1346	0	102	2.2	11.7	13.0
Landing	Booster	179	1349	0	102	2.3	11.6	13.0
Postseparation/ orbiter ignition	Orbiter	316	464	0	208	0.34	5.3	5.4
Entry	Orbiter	73	649	0	185	0.32	2.5	2.5
Landing	Orbiter	72	648	0	187	0.32	2.5	2.5

*C.G. Reference

BOOSTER AND ORBITER

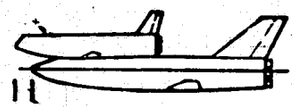

FRL, Z = 200

X = 0 X = 160

BOOSTER AND ORBITER SEPARATED



FRL, Z = 200

X = 0

The parametric weight data were developed with the aid of a weight-synthesis computer program that sizes the booster and orbiter stages and calculates the stage weight, size, volume, and propellant fraction. Inputs to the program are subsystem weight-scaling factors, vehicle geometry relationship, configuration requirements, and rocket-engine performance.

The body weight factor varies as a function of wetted area; however, to give the approximate value used, the orbiter and booster structure weight factor values are 3 and 4.1 pounds per square foot at 6,000 and 13,600 square feet of external body area, respectively. Note that the structural weight factors used are based on the external body area, which is the area calculated in the vehicle geometry routine. A factor of 7 pounds per square foot was used for aerodynamic surfaces. Thermal protection system weight factors used are 1.6 and 1.4 pounds per square foot for the orbiter and booster. These values are based on the MSC weight statement. Other system weight factors used computed system weights very close to those predicted by MSC. A 10-percent contingency factor was applied to each subsystem to account for unknowns.

Vehicle geometry parameters relating length, volume, wetted surface area, and planform area were established from the 12,500-pound-payload baseline configuration drawing.

The configuration requirements recognized by the weight synthesis program are as follows:

1. Entry weight to planform area, 30:1

2. Landing weight to wing area, 90:1 for the orbiter and 70:1 for the booster

Booster parameter data are shown in Figure 8.3-3. The propellant fraction, $W_P/W_{BO} + W_P$, is shown as a function of gross stage weight, booster thrust, and propellant mixture ratio. For comparison, the value obtained from the 12,500-pound-payload baseline data provided by MSC is shown. If a 10-percent growth factor is applied, as was done in this study, the MSC value compares favorably with the parametric data.

Orbiter parametric data are presented in Figures 8.3-4, -5, and -6. Figure 8.3-4 presents the propellant fraction as a function of orbiter gross weight (excluding payload weight) for 25,000- and 50,000-pound-payload orbiters with two cargo bay sizes each. These data are for a propellant mixture ratio of 6:1 and engine thrust-to-orbiter-weight ratio (T/W) of 1.3:1. Figure 8.3-5 contains the same data, but for a T/W of 1.6:1. Performance

PRECEDING PAGE BLANK NOT FILMED.

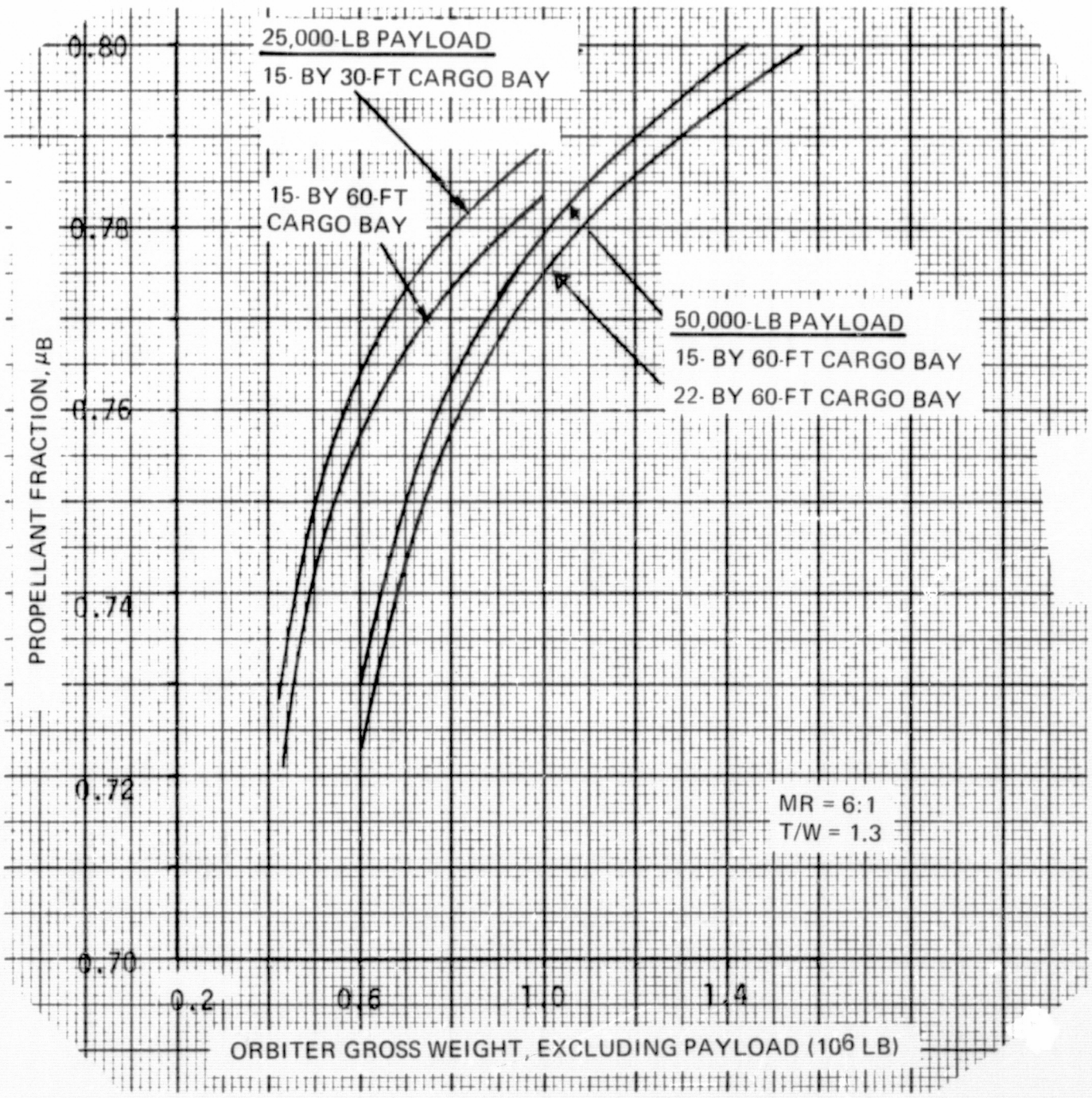

Figure 8.3-4. Orbiter Parametric Propellant Fraction, T/W = 1.3

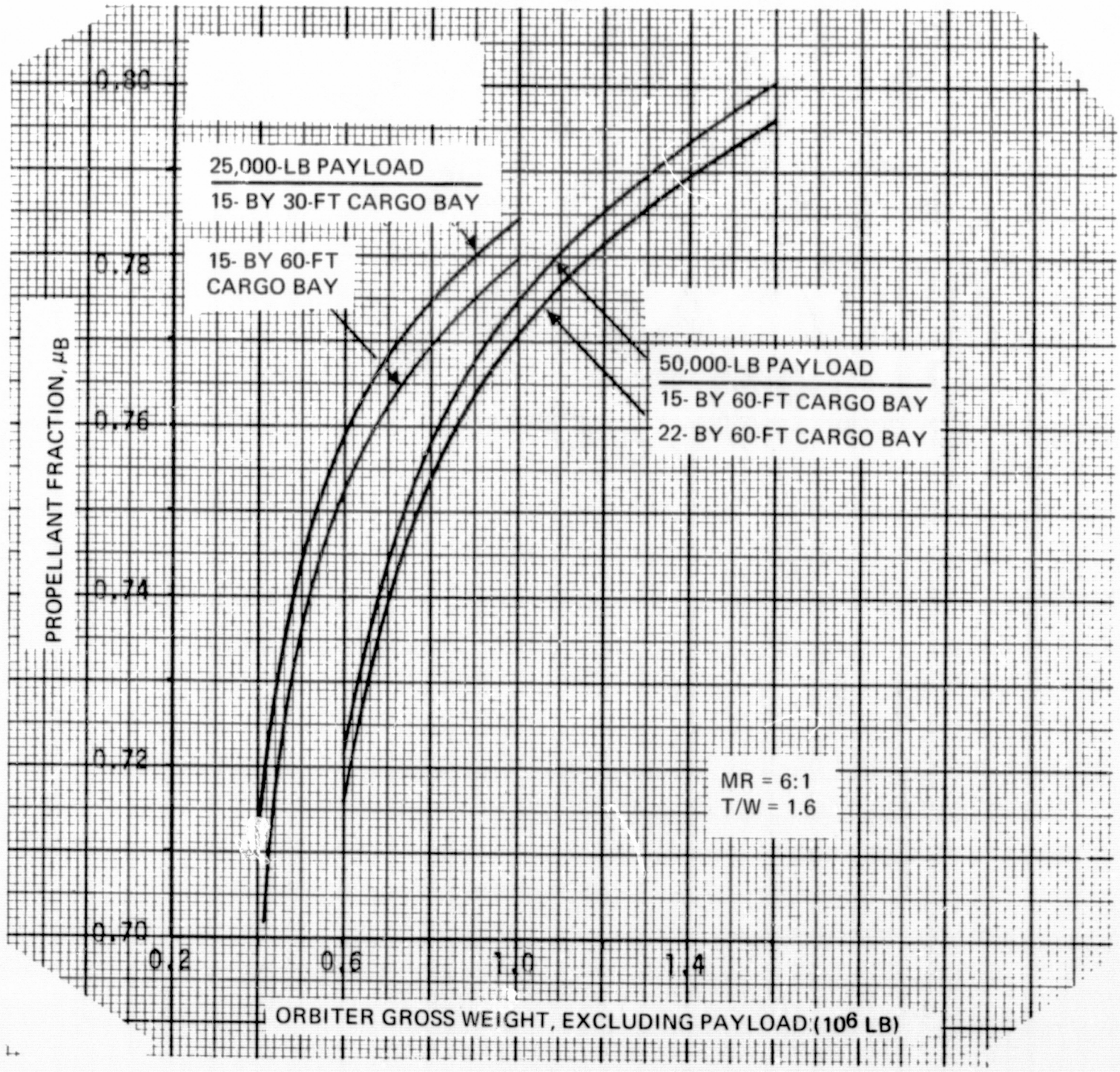

Figure 8.3-5. Orbiter Parametric Propellant Fraction, T/W = 1.6

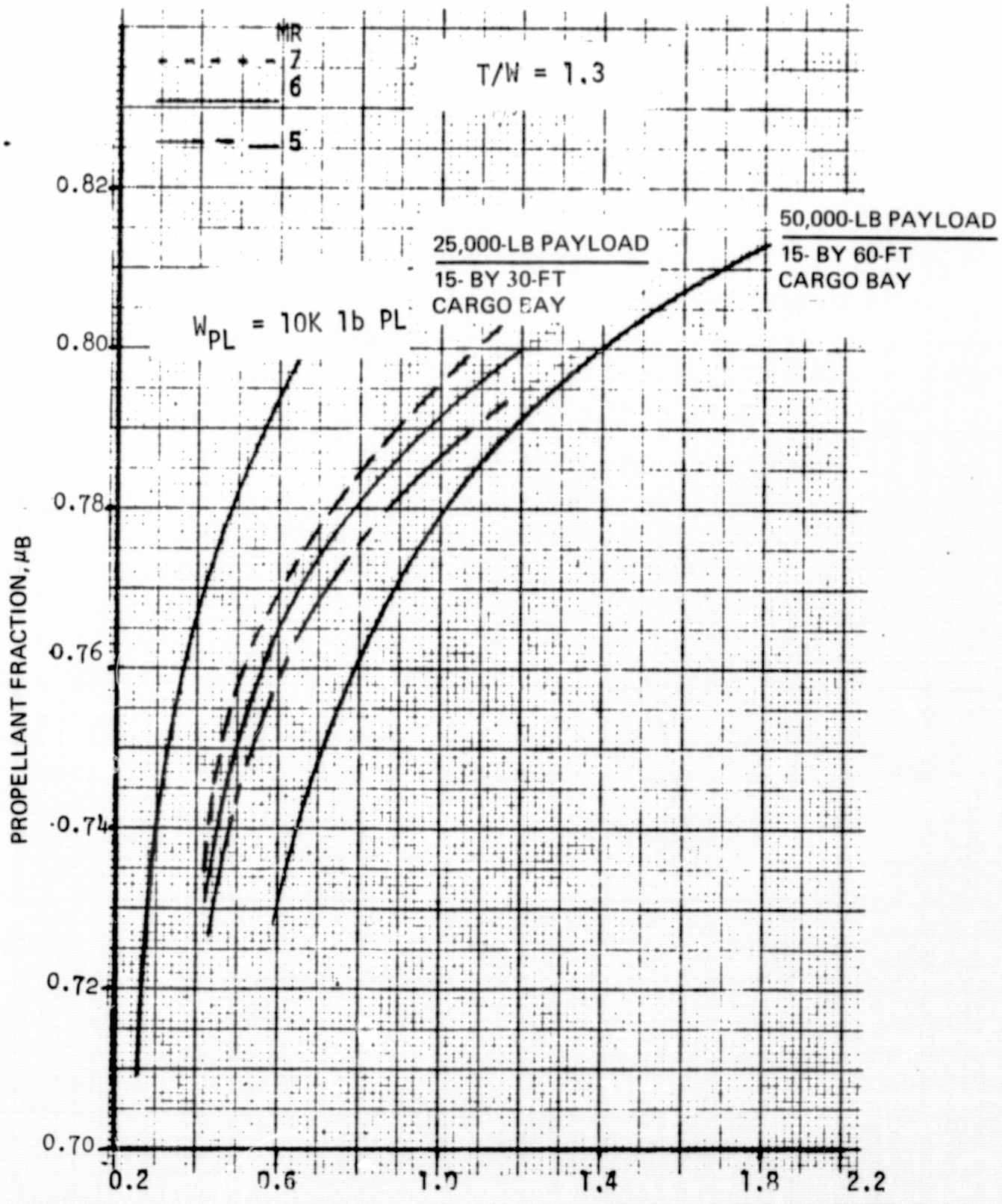

(Excluding Payload)

Figure 8.3-6. Orbiter Propellant Fraction, Parametric Phase

analysis determining the effect of propellant mixture ratio was conducted for a 25,000-pound-payload system with a 15-foot-diameter by 30-foot-length cargo bay. Parametric weight data for this vehicle are presented in Figure 8.3-6. The data for a 10,000-pound-payload system with 2,000-cubic-foot cargo volume is also shown. As indicated in the curves, the predicted propellant fraction is very sensitive to stage gross weight.

These parametric data were used in the vehicle flight performance analysis documented in Volume III of this report. Based on the vehicle sizing analysis to establish vehicle gross weight and weight distribution between orbiter and booster, summary weight statements were prepared for the various vehicles. These summary weight statements are presented in Table 8.3-3.

8.3.4 Special Study

A special study was requested by NASA to establish the payload capability of shuttle vehicles with 3,000,000- and 3,500,000-pound gross weights and rocket propulsion consisting of 400,000-pound-sea-level-thrust engines. Parametric weight curves were prepared for the vehicle sizing analysis and are presented in Figure 8.3-7 and 8.3-8 for the booster and orbiter, respectively.

8.3.5 Baseline Configuration, 50,000-Pound Payload

Following the parametric phase, NASA MSC selected a shuttle vehicle for detail design analysis. The selected vehicle was to have a 50,000-pound-payload capability with a 15-foot-diameter by 60-foot-length cargo bay.

Prior to initiating the more detailed analysis of the 50,000-pound-payload shuttle vehicle, the vehicle weight developed during the parametric analysis was reviewed and updated to reflect the best current estimate of structure weight factors, aerodynamic surfaces sizes, and subsystem weights. The baseline vehicle gross weight is estimated to be 3,985,000 pounds, compared with 3,480,000 pounds at the end of the parametric phase. A preliminary weight statement was prepared, and the booster and orbiter summary weight is shown in Table 8.3-4.

Using the baseline vehicle configuration and weights, vehicle mass properties, center of gravity, moment of inertia, and weight distribution were determined for use in the vehicle loads, control, aerodynamic, and design analysis. The center of gravity and inertia data are presented in Table 8.3-5.

Table 8.3-3. Summary Weight Statements, Parametric Phase

Code	System	Weights (lb)									
		Payload (1,000 lb), Cargo Bay Size (ft x ft)									
		7.7, 9 x 35		25, 15 x 30		25, 15 x 60		50, 15 x 60		50, 22 x 60	
		Booster	Orbiter	Booster	Orbiter	Booster	Orbiter	Booster	Orbiter	Booster	Orbiter
1.0	Aerodynamic surfaces	40,547	11,622	59,952	17,642	64,641	17,842	75,381	23,832	84,301	25,313
2.0	Body structure	73,373	25,414	106,819	37,564	112,214	40,456	133,253	55,902	155,506	65,116
3.0	Induced environmental protection	28,995	15,278	42,256	22,508	45,329	23,986	53,279	32,682	61,360	38,539
4.0	Launch recovery and docking	8,596	3,176	13,531	4,306	13,580	4,771	16,132	5,859	18,174	6,662
5.0	Main propulsion system	67,384	17,999	96,988	20,709	101,169	22,480	132,325	34,840	151,584	33,900
6.0	Orientation control, separation and ullage	2,517	2,281	7,700	2,971	6,185	3,816	7,777	2,990	7,757	2,741
7.0	Prime power source	1,990	1,990	1,990	1,990	1,990	1,990	1,990	1,990	1,990	1,990
9.0	Guidance and navigation	584	584	584	584	584	584	584	584	584	584
11.0	Communications	474	474	474	474	474	474	474	474	474	474
12.0	Environmental control	1,518	1,518	1,518	1,518	1,518	1,518	1,518	1,518	1,518	1,518
14.0	Personnel provisions	245	245	245	245	245	245	245	245	245	245
15.0	Crew station controls and panels	290	290	290	290	290	290	290	290	290	290
	Weight dry	226,513	80,871	332,047	110,821	348,219	118,943	332,047	161,206	483,783	177,372
17.0	Personnel	491	491	491	491	491	491	491	491	491	491
18.0	Cargo/personnel		7,700		25,000		25,000		50,000		50,000
	Operating weight empty	227,004	89,062	332,538	136,312	348,710	143,943	423,739	211,697	484,274	227,863
22.0	Go-around propellant and service items	22,603	3,697	36,493	5,116	36,805	5,069	43,796	5,238	49,499	7,909
	Burnout weight	249,607	92,759	369,031	141,428	385,515	149,012	467,535	216,935	533,773	235,772
25.0	RCS and ECS requirements	5,882	2,285	4,877	2,285	5,255	2,298	5,816	2,895	6,457	3,084
	Gross weight less propellant	255,429	95,044	373,908	143,713	390,770	151,311	473,351	219,833	540,230	238,856
25.0	Rocket propellant	1,018,200	284,800	2,106,908	325,000	1,813,000	368,000	2,269,000	523,700	2,731,000	506,800
	Gross flight weight	1,273,629	379,844	2,106,908	468,713	2,203,770	519,311	2,742,351	743,533	3,271,230	745,656

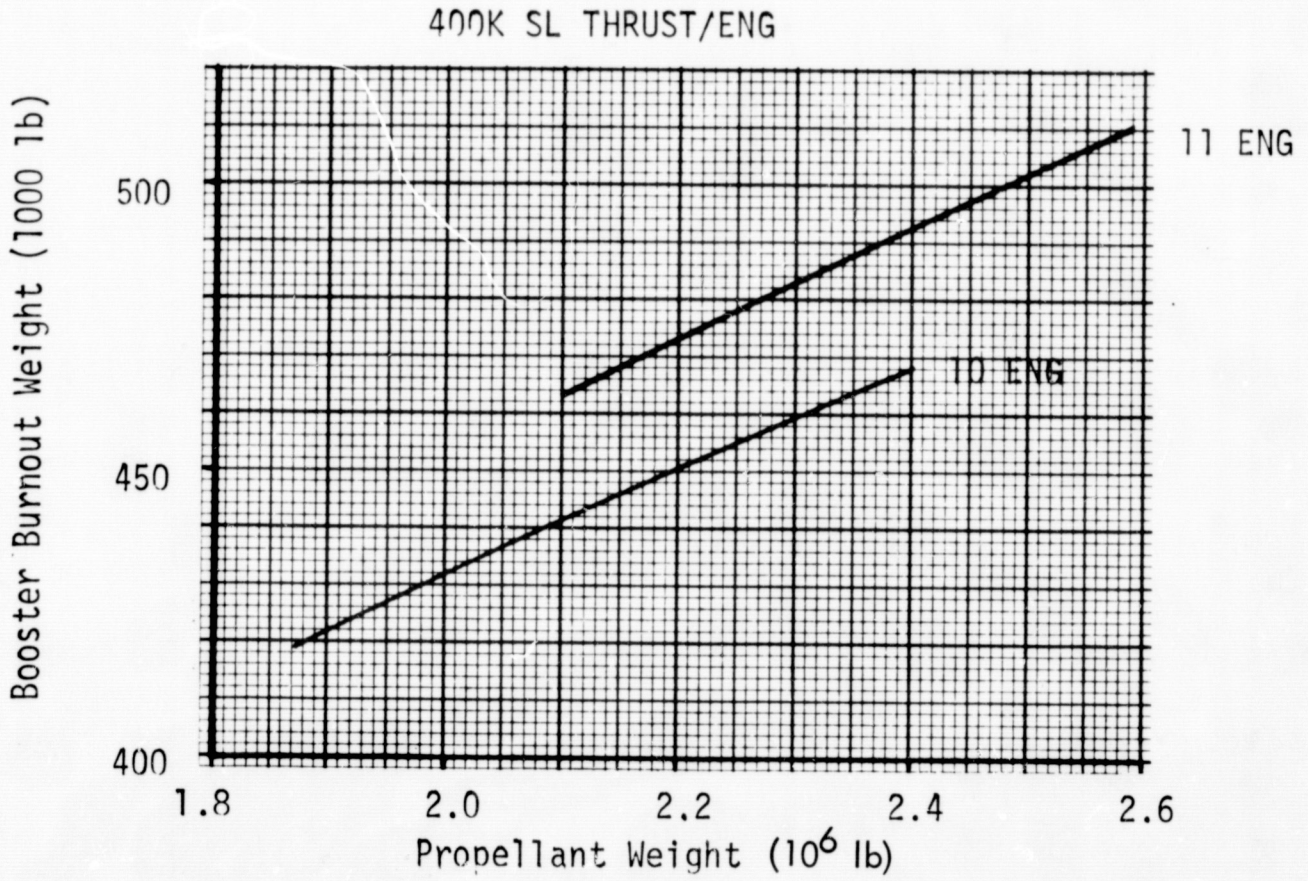

Figure 8.3-7. Booster Weight Characteristics With 400,000-Pound Rocket Engines

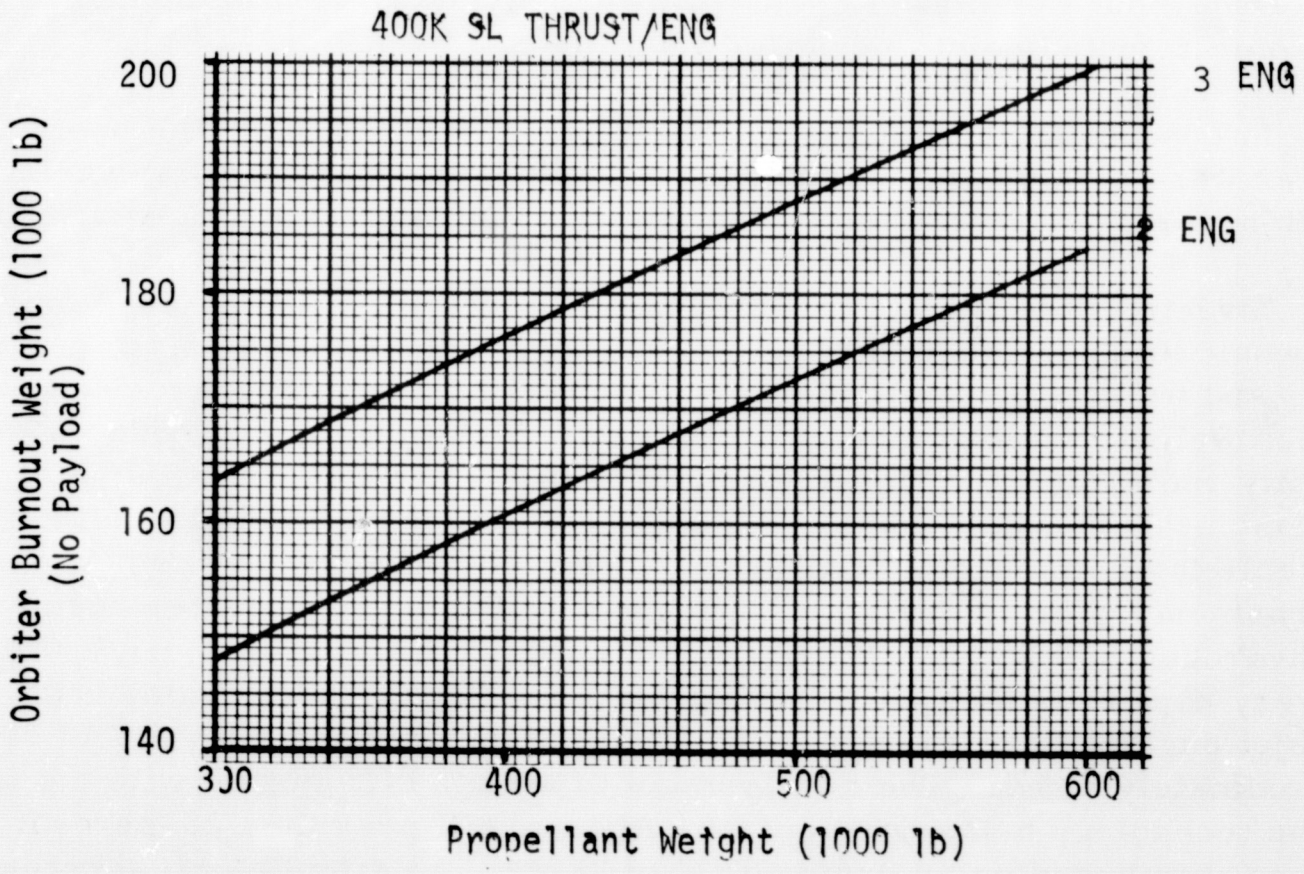

Figure 8.3-8. Orbiter Weight Characteristics With 400,000-Pound Rocket Engines

Table 8.3-4. Preliminary 50,000-Pound-Payload Vehicle

Item	Weight (lb)	
	Booster	Orbiter
Dry weight	472,100	182,719
Cargo	---	50,000
Residuals, reserves, and service items	77,900	12,281
Burnout weight	550,000	245,000
Rocket propellant	2,600,000	590,000
Gross weight	3,150,000	835,000

Sensitivity analysis was conducted to establish the impact on vehicle gross weight that would be caused by variations in the predicted orbiter and booster burnout weights. Results of this analysis are shown in Figure 8.3-9, and some selected points tabulated in Table 8.3-6.

In conducting this analysis, the velocity increment for the booster and orbiter were maintained constant. Stage propellant fraction was varied as a function of stage size as illustrated in the previous parametric weight data.

Investigations were also performed to determine the payload increment that would be experienced because of variations in system design, performance, and weight. Investigations encompassed turbojet system changes, system weight variations, specific impulse degradation, and reduced on-orbit velocity requirement. These results are presented in Figure 8.3-10. The baseline orbiter and booster configuration turbojet engines currently available for commercial transports were modified only for the new environment. The figure shows that modification of the booster engine to use hydrogen fuel in place of JP fuel will increase the vehicle payload delivery capability by approximately 10 percent. Current commercial turbojet engines have an engine-thrust-to-engine-weight ratio (T/W) of approximately 4.5:1. The development of a high T/W engine with the lift engine technology being developed by Allison will provide a 20-percent payload gain based on an engine T/W of 15:1. The effect of ±10-percent weight variation to various systems is shown. The sensitivity of vehicle

Table 8.3-5. Baseline 50,000-Pound-Payload Vehicle Mass Properties

Condition	Vehicle Configuration	Weight (1000 lb)	Center of Gravity* (in.)			Moment of Inertia (slug-ft^2 x 10^{-6})		
			X	Y	Z	I_{xx}	I_{yy}	I_{zz}
Prelaunch/liftoff	Booster and orbiter	3,985	1419	0	355	37	301	292
Max Q (t = 72 sec)	Booster and orbiter	2,955	1550	0	375	36	286	281
Max G (t = 180 sec)	Booster and orbiter	1,730	1590	0	427	34	303	300
Preseparation (t = 210 sec)	Booster and orbiter	1,385	1541	0	459	32	280	279
Postseparation/ reentry	Booster	550	2035	0	207	17	85	95
Postseparation/ orbiter ignition	Orbiter	835	959	0	274	3	29	31
Orbiter reentry	Orbiter	245	1368	0	260	3	16	18

*C.G. Reference

Booster and Orbiter

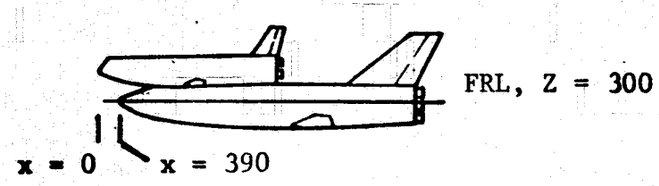

Booster and Orbiter Separated

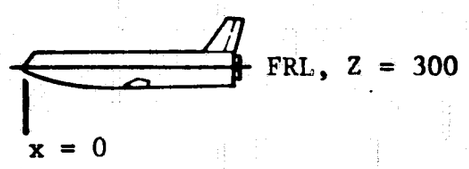

Space Division
North American Rockwell

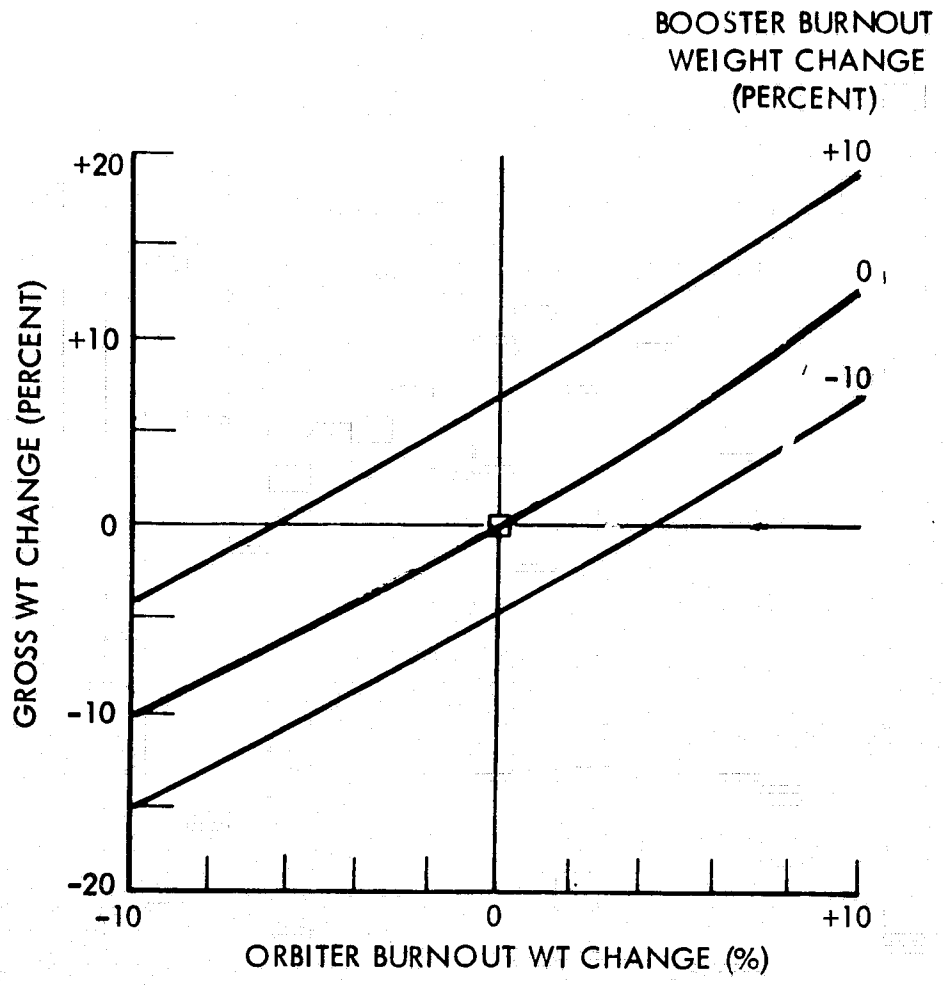

Figure 8.3-9. Vehicle Gross Weight Sensitivity

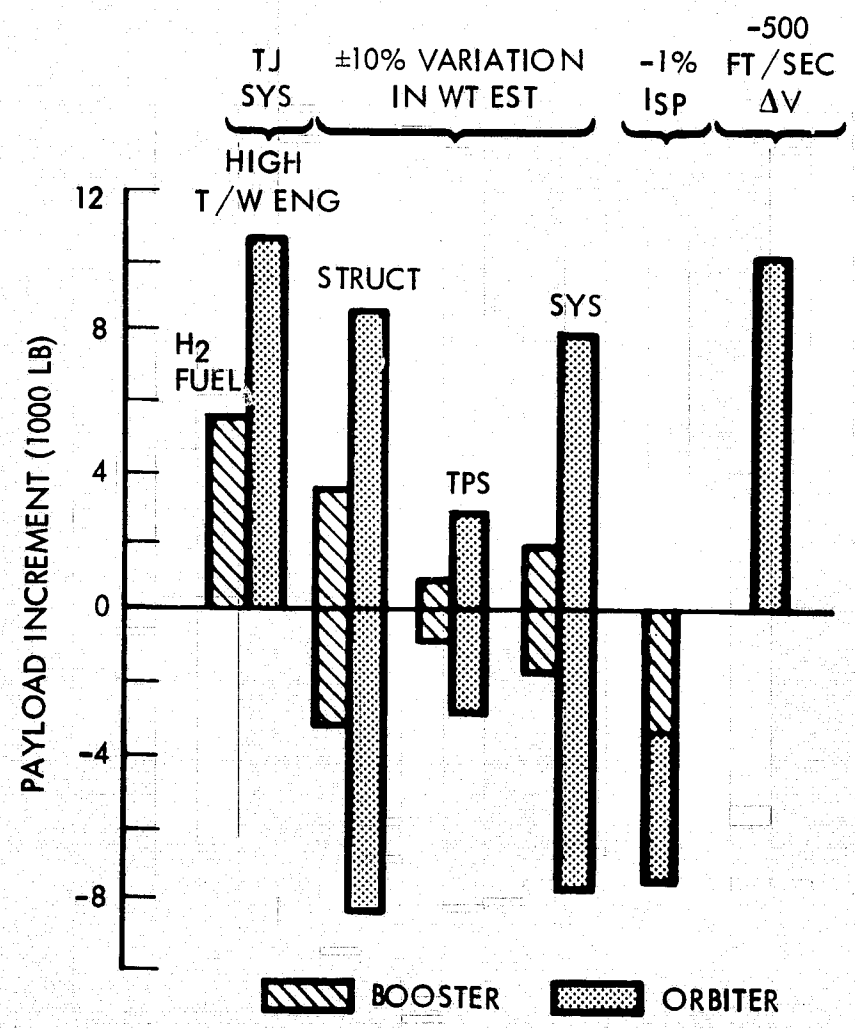

Figure 8.3-10. Vehicle Payload Sensitivity

Table 8.3-6. Impact of Burnout Weight Variations

Burnout Weight Variation	Vehicle Gross Weight Change (percent)
Weight increase	
+10 percent, orbiter only	+12.5
+10 percent, booster only	+ 7.0
+10 percent, orbiter and booster	+19.5
Weight decrease	
-10 percent, orbiter only	-10.0
-10 percent, booster only	- 5.0
-10 percent, orbiter and booster	-15.5

gross weight to orbiter weight reductions is apparent. The major potential performance improvement attainable through structure weight-reduction concepts is also apparent. Vehicle performance is based on nominal performance provided by the engine manufacturer. The importance of achieving the quoted performance is illustrated by the 15-percent degradation in payload that would be experienced following a 1-percent reduction in engine specific impulse. The orbiter vehicle has an on-orbit velocity capability of 2,000 feet per second. This requirement can probably be reduced by 500 feet per second for most missions, and off-loading propellant can provide a 20-percent payload gain.

8.3.6 Detail Weight Analysis, 50,000-Pound-Payload Vehicle

The booster and orbiter configurations selected for detail weight analysis were previsouly presented in the Design Section as Figures 8.2-26 (Drawing 2234-76) and 8.2-23 (Drawing 2234-79). The baseline vehicle surface areas are shown in Table 8.3-7. A comprehensive analysis of these configurations was conducted in conjunction with the subsystem analysis to provide accurate system weight estimates commensurate with a Phase A study. The baseline booster and orbiter summary weight statements are

Table 8.3-7. Baseline Vehicle Surface Area

Vehicle Surface	Area (ft^2)	
	Booster	Orbiter
Body wetted area	32,220	17,111
Wing exposed plan area	5,430	2,010
Horizontal tail exposed plan area	1,800	1,170
Vertical tail exposed plan area	1,408	585

presented in Tables 8.3-8 and 8.3-9 for four conditions, launch, boost burnout, entry, and landing. Second - and third-generation subsystem weights are presented in Table 8.3-10. A discussion of each of the subsystems is presented in the following paragraphs.

Aerodynamic Surfaces

The aerodynamic surfaces were structurally analyzed. The structural material is 6AL-4V titanium. The wing torque box was structurally analyzed, and 27 percent was added to the weight, based on Los Angeles Division (LAD) preliminary design experience to achieve a realistic wing torque box weight. The leading and trailing structural weights were derived from structure weight factors developed by LAD. The results of the detail analyses indicate that the booster and orbiter wing weight factor is 8.20 pounds per square foot, based on the exposed wing area.

The same procedure, as used on the wing, was employed in evaluating the tail surfaces. The result is a booster horizontal stabilizer weight factor of 7.46 lb/ft^2 and an orbiter weight factor of 5.29 lb/ft^2. Similarly the booster and orbiter vertical surface weights result in 7.03 lb/ft^2 and 8.13 lb/ft^2 vertical tail weight factors.

Body Structure

The booster and orbiter fuselage sections were structurally analyzed. The booster propellant tanks are the basic load-carring structure. The tanks are a skin/stringer/ring frame design and are fabricated from aluminum with the $\bar{t}$ ranging from 0.051 to 0.326 inches. This tank structure, along with the truss sections (to support the heat shield substructure), longerons, external frames and some secondary structure constitute

Table 8.3-8. Baseline Booster Summary Weight Statement

Code	System	Weight (lb) A	B	C	D
1.0	Aerodynamic surfaces	84,433	84,433	84,433	84,433
2.0	Body structure	199,606	199,606	199,606	199,606
3.0	Induced environment protection	22,038	22,038	22,038	22,038
4.0	Launch, recovery, and docking	18,996	18,996	18,996	18,996
5.0	Main propulsion	108,702	108,702	108,702	108,702
6.0	Orientation control, separation and ullage	8,100	8,100	8,100	8,100
7.0 and 8.0	Prime power source; Power conversion and distribution	4,734	4,734	4,734	4,734
9.0	Guidance and navigation	682	682	682	682
10.0	Instrumentation	583	583	583	583
11.0	Communication	440	440	440	440
12.0	Environmental control	337	337	337	337

A Gross launch weight
B Boost burnout weight
C Entry weight
D Landing weight

Table 8.3-8. Baseline Booster Summary Weight Statement (Cont)

Code	System	Weight (lb) A	B	C	D
14.0	Personnel provisions	-	-	-	-
15.0	Crew station control and panel	149	149	149	149
	Subtotals (dry weight)	448,800	448,800	448,800	448,800
17.0	Personnel	-	-	-	-
18.0	Cargo	-	-	-	-
21.0	Residual propellant and service items	24,129	24,129	11,129	11,129
	Subtotals (inert weight)	472,929	472,929	459,929	459,929
22.0	Reserve propellant and service items	13,169	13,004	12,954	10,800
25.0	Full-thrust propellant	2,647,000	47,000	47,000	-
	Total weight	3,133,098	532,933	519,883	470,729

A Gross launch weight
B Boost burnout weight
C Entry weight
D Landing weight

Table 8.3-9. Baseline Orbiter Summary Weight Statement

Code	System	Weight (lb)			
		A	B	C	D
1.0	Aerodynamic surfaces	26,177	26,177	26,177	26,177
2.0	Body structure	60,666	60,666	60,666	60,666
3.0	Induced environment protection	29,438	29,438	29,438	29,438
4.0	Launch, recovery, and docking	10,382	10,382	10,382	10,382
5.0	Main propulsion	51,704	51,704	51,704	51,704
6.0	Orientation control, separation and ullage	8,582	7,414	7,414	7,414
7.0 and 8.0	Prime power source; Power conversion and distribution	5,197	5,197	5,197	5,197
9.0	Guidance and navigation	770	770	770	770
10.0	Instrumentation	589	589	589	589
11.0	Communications	588	588	588	588
12.0	Environmental control	1,463	1,463	1,463	1,463

A Gross launch weight
B Boost burnout weight
C Entry weight
D Landing weight

Table 8.3-9. Baseline Orbiter Summary Weight Statement (Cont)

Code	System	Weight (lb) A	B	C	D
14.0	Personnel provisions	364	364	364	364
15.0	Crew station control and panel	275	275	275	275
	Subtotals (dry weight)	196,195	195,027	195,027	195,027
17.0	Personnel	660	660	660	660
18.0	Cargo*	50,000	50,000	50,000	50,000
21.0	Residual propellant and service items	6,120	6,120	3,155	3,155
	Subtotals (inert weight)	252,975	251,807	248,842	248,842
22.0	Reserve propellant and	12,337	9,468	7,188	4,000
25.0	Full-thrust propellant	590,650	35,650	650	-
	Total weight	855,962	296,925	256,680	252,842

A Gross launch weight
B Boost burnout weight
C Entry weight
D Landing weight

*Because of orbiter weight growth, the baseline vehicle does not have 50,000-pound-payload capability.

Table 8.3-10. Baseline Configuration Subsystem Weights

Item	Weight (lb)	
	Booster	Orbiter
1.0 AERODYNAMIC SURFACES		
Wing	(44,577)	(10,996)
Carry-through torque box	31,728	5,922
Section forward of box	3,169	1,694
Section aft of box	9,680	3,380
Horizontal aft surface	(13,430)	(6,195)
Carry-through torque box	7,920	2,438
Section forward of box	880	832
Section aft of box	4,630	2,925
Vertical tail	(9,902)	(4,756)
Carry-through torque box	5,086	2,395
Section forward of box	2,418	1,302
Section aft of box	2,398	1,059
Wing carry-through body structure	(16,524)	(4,230)
Wing	11,460	2,030
Horizontal aft surface	5,064	2,200
Total aerodynamic surfaces	*84,433	*26,177
2.0 BODY STRUCTURE		
Primary structure	(132,505)	(51,066)
Skin and stringers	-	23,683
Frames and bulkheads	15,356	21,281
Longerons	8,020	1,598
Joints, splices, etc.	4,771	2,207

*Leading edge and trailing edge were based on statistical data. The structural box was based on design area requirements and converted to realistic weight when multiplied by 1.27

Table 8.3-10. Baseline Configuration Subsystem Weights (Cont)

Item	Weight (lb)	
	Booster	Orbiter
2.0 BODY STRUCTURE (Cont)		
Truss and miscellaneous structures	18,564	-
LO_2/LH_2 tank	85,794	-
Secondary structure	(41,080)	(5,309)
Heat shield substructure	33,831	-
Miscellaneous structure	873	2,461
Joints, splices, etc.	4,404	551
Doors and closeouts	1,972	2,297
Thrust structure	(16,846)	(3,830)
Contingency	(9,175)	(2,758)
Total body structure	199,606	60,666
3.0 INDUCED ENVIRONMENTAL CONTROL		
Aerosurfaces	(2,973)	(6,090)
Wing		
Underside and leading edge	2,521	3,740
Topside	-	402
Horizontal aft surfaces		
Underside and leading edge	452	1,238
Topside	-	468
Vertical tail	-	242
Fuselage external	(8,400)	(9,236)
Underbody	5,048	6,846
Sides and top	3,352	2,390

Table 8.3-10. Baseline Configuration Subsystem Weights (Cont)

Item	Weight (lb)	
	Booster	Orbiter
3.0 INDUCED ENVIRONMENTAL CONTROL (Cont)		
Fuselage internal	(5,296)	(9,372)
Underbody	1,733	1,134
Sides and top	2,918	4,816
Supporting and attaching structure	645	3,422
LH_2 tank insulation	(3,364)	(2,063)
Contingency	(2,005)	(2,677)
Total induced environmental control	22,038	29,438
4.0 LAUNCH RECOVERY AND DOCKING		
Landing gear and systems	(18,283)	(9,917)
Forward gear	*6,002	*3,242
Main gear	*11,148	*6,022
Hydraulic actuation		
Actuators and controls	705	465
Plumbing	428	188
Docking		(364)
Separation system	(545)	-
Contingency	(168)	(101)
Total launch, recovery and docking	18,996	10,382

*These weights are derived from statistical data and carry no contingency.

Table 8.3-10. Baseline Configuration Subsystem Weights (Cont)

Item	Weight (lb) Booster	Orbiter
5.0 MAIN PROPULSION		
Liquid rocket engine system	(66,532)	(28,804)
Engines	*50,000	*10,800
Propellant feed		
Prevalves	3,000	600
LH_2 lines	1,200	240
LOX lines	8,500	1,920
Fill and drain valves and disconnects	400	200
LH_2 fill and drain lines	150	75
LOX fill and drain lines	50	25
Pressurization system		
Vent valves	200	200
Pressure manifold	450	185
Pressure lines	100	20
Pressure regulator and check valves	180	100
Heat exchanger	400	80
Lines, fittings, etc.	500	100
Orbital maneuvering feed system		
Tank shutoff, vent valves and press. regulator	-	125
Helium supply tankage	-	1,000
Helium supply lines	-	100
Engine hydraulic actuation		
Actuators and controls	672	224
Plumbing	730	100
Propellant tanks		
LOX/LH_2 tank		6,259
LH_2 tank interconnector		2,093
LH_2 tank		3,404
Orbital tanks		954

*Engine manufacturers weights. Did not add contingency.

Table 8.3-10. Baseline Configuration Subsystem Weights (Cont)

Item	Weight (lb) Booster	Orbiter
5.0 MAIN PROPULSION (Cont)		
Turbojet engine system	(39,629)	(20,367)
Engines	*33,500	*17,050
Propellant feed		
Pumps, heaters and feed lines	280	131
Vent, port, bleed, and other valves	40	35
Sensors and wiring	100	80
Tank seal	285	151
Air induction system		
Pressure duct and nacelles	5,424	2,920
Fuel management system	(250)	(364)
Sensors and wiring	250	364
Contingency	(2,291)	(2,169)
Total main propulsion	108,702	51,704
6.0 ORIENTATION CONTROLS, SEPARATION, ETC.		
Attitude control system	(2,060)	(3,660)
Engine installation		
Engines	*360	*168
Propellant storage		
O_2 tanks	892	2,163
H_2 tanks	324	786
Valving	44	90

*Engine manufacturers weights. Did not add contingency.

Table 8.3-10. Baseline Configuration Subsystem Weights (Cont)

Item	Weight (lb) Booster	Orbiter
6.0 ORIENTATION CONTROLS, SEPARATION, ETC. (Cont)		
Propellant feed and control		
Turbines and gas generators	68	62
Pumps, O_2 and H_2	38	34
Isolation valves	46	44
Pressure regulators	200	225
Check valves	40	48
Heat exchangers	48	40
Aerodynamic surface hydraulic control	(5,336)	(3,095)
Actuators and controls	3,750	2,147
Plumbing	1,586	948
Separation rocket propellant case	(-)	*(1,168)
Contingency	(704)	(659)
Total orientation controls, separation, etc.	8,100	8,582
7.0 and 8.0 PRIME POWER SOURCE, CONVERSION, AND DISTRIBUTION		
Electrical power	(915)	(2,766)
Fuel cells	-	630
Hydrogen tank	-	339
Oxygen tank	-	393
Plumbing and valves	-	120
Battery	130	130
Inverter	-	156
Power control and distribution module	125	125
Battery charger	-	16
Distribution wiring	320	240
Remote distributors	320	320
Radiators	-	100

*Engine manufacturers weights. Did not add contingency

Table 8.3-10. Baseline Configuration Subsystem Weights (Cont)

Item	Weight (lb)	
	Booster	Orbiter
7.0 and 8.0 PRIME POWER SOURCE, CONVERSION, AND DISTRIBUTION (Cont)		
Supports	20	197
Reactants	-	*
Auxiliary power	(2,136)	(1,180)
Auxiliary power unit	920	600
Hydrogen tank	359	139
Oxygen tank	417	161
Plumbing and valves	100	60
Distribution wiring	120	80
Power control and distribution module	50	50
Supports	170	90
Reactants	*	*
Hydraulic power	(1,252)	(779)
Pumps	192	96
Reservoir	160	110
Plumbing and valves	774	447
Nitrogen pressuration	126	126
Contingency	(431)	(472)
Total prime power source, conversion and Distribution	4,734	5,197
9.0, 10.0, AND 11.0 INTEGRATED ELECTRONIC SYSTEMS		
Guidance and navigation (Code 9.0)	(620)	(700)
Integrated computer system	75	100
Inertial reference units and electronics	180	180
Horizon sensors	-	20
Telescope and navigation base	-	35
Air data sensors	24	24
Sensor signal couplers	20	20

*Reactants listed under Code 21.0.

Table 8.3-10. Baseline Configuration Subsystem Weights (Cont)

Item	Weight (lb)	
	Booster	Orbiter
9.0, 10.0, AND 11.0 INTEGRATED ELECTRONIC SYSTEMS (Cont)		
RCS driver package	40	40
Cabling	200	200
Supports	81	81
Instrumentation (Code 10.0)	(530)	(530)
Multiplexing (signal distribution)	100	100
Central timing	20	20
Recorder/playback	25	25
Printout unit	15	15
Multiplexer wiring and connectors	350	350
Supports	20	20
Communications (Code 11.0)	(400)	(535)
Voice command		
VHF antenna	25	25
S-band PA	-	32
USBE	32	32
Up-data link	21	21
Premodulator processor	15	15
S-band antenna	10	10
Audio center	8	8
TV	-	5
Tracking and ranging		
Multimode radar	50	50
Digital ranging generator, antennas, and contingencies	70	70
Laser	-	50
Navigation aids		
Tacan	20	20
Distance measuring equipment	14	14
Radar altimeter	15	15

Table 8.3-10. Baseline Configuration Subsystem Weights (Cont)

Item	Weights (lb)	
	Booster	Orbiter
9.0, 10.0, AND 11.0 INTEGRATED ELECTRONIC SYSTEMS (Cont)		
Landing aids		
Glide scope	5	5
Localizer	4	4
Marker beacon	4	4
Supports and wiring	55	85
Redundancy, 15 percent	52	70
Contingency total systems	(155)	(182)
Total integrated electronic systems	1,705	1,947
12.0 ENVIRONMENTAL CONTROL SYSTEM		
Environmental control system	(306)	(1,285)
Humidity and CO_2 control system	-	190
Electronic cold plate network	85	85
Cabin cooling system	59	149
Cooling pump package	63	91
Radiator system	-	187
Evaporators	-	91
Ramair heat exchanger	36	43
GSE heat exchanger	35	43
Oxygen system, emergency, and pressure control	-	56
Portable water system	-	73
Evaporator water system	-	56
Urine and fecal system	-	26
Evaporator water	-	54
Oxygen	-	14
CO_2 absorber elements	-	27
Structure	28	100
Contingency	(31)	(178)
Total environmental control system	337	1,463

Table 8.3-10. Baseline Configuration Subsystem Weights (Cont)

Item	Weights (lb) Booster	Orbiter
14.0 PERSONNEL PROVISIONS		
Accommodations for personnel	(-)	(265)
Seats and restraints		163
Supports		30
Shock absorbers		72
Fixed life support equipment	(-)	(40)
Galley equipment		6
Containers restraints		30
Urine transfer		4
Contingency	(-)	(59)
Total personnel provisions	(-)	(364)
15.0 CREW STATION CONTROLS AND PANELS		
Controls and panels	(135)	(250)
Contingency	(14)	(25)
Total crew station controls and panels	149	275
17.0 PERSONNEL		
Crew	(-)	(377)
Crew		*360
Constant wear garments		7
Coveralls		7
Headsets		1
Electrical umbilical		2
Personal gear	(-)	(18)
Fecal collection		10
Tissue		1

*No contingency used for crew.

Table 8.3-10. Baseline Configuration Subsystem Weights (Cont)

Item	Weights (lb)	
	Booster	Orbiter
17.0 PERSONNEL (Cont)		
Towels		1
Urine hose and filter		6
Life support	(-)	(129)
Food		16
Water drinking device		5
Survival kit		96
Medical kit		12
Crew accessories	(-)	(66)
Fire extinguisher		36
Tool kit		10
Flight data file		20
		(70)
Total personnel		660
18.0 CARGO		
Environmental control (Code 12.0)	(-)	(497)
CO_2 absorbers		296
Oxygen		156
Evaporator water		45
Personnel provisions (Code 14.0)	(-)	(1,752)
Seats and restraints		1,452
Containers		290
Galley equipment		4
Urine transfer		6
Personnel (Code 17.0)	(-)	
Crew		(2,271)
Crew		1,800
Constant-wear garments		77

Table 8.3-10. Baseline Configuration Subsystem Weights (Cont)

Item	Weights (lb)	
	Booster	Orbiter
18.0 CARGO (Cont)		
Coveralls		60
Headsets		7
Electrical umbilical		20
Personal gear		
Tissue		3
Towels		2
Fecal collection		10
Urine hose and filter		6
Life support		
Food		170
Survival kit		116
Cargo (not systems) (Code 18.0)	(-)	(45,480)
Total cargo	-	50,000
21.0 RESIDUAL PROPELLANT AND SERVICE ITEMS		
Residuals	(13,090)	(3,165)
Trapped rocket propellant	13,000	2,965
Trapped attitude control propellant	90	200
Service items	(11,039)	(2,955)
Gaseous hydrogen	3,400	600
Gaseous oxygen	5,725	1,220
Hydraulic fluid	1,914	1,025
Pressurant	-	110
Total residual propellant and service items	24,129	6,120

Table 8.3-10. Baseline Configuration Subsystem Weights (Cont)

Item	Weights (lb)	
	Booster	Orbiter
22.0 RESERVE AND SERVICE PROPELLANT		
Reserve propellant	(10,800)	(4,000)
Turbo propellant	10,800	4,000
Service propellant	(2,369)	(8,337)
Attitude control propellant	1,710	3,800
Electrical power LH_2	-	132
Electrical power LO_2	-	1,458
Auxiliary power LH_2	366	143
Auxiliary power LO_2	293	115
Separation rocket propellant	-	2,689
	13,169	12,337
25.0 FULL-THRUST PROPELLANT		
Full-thrust propellant	(2,647,000)	(590,650)
Turbojet fuel	47,000	650
Orbit maneuver propellant		35,000
Ascent propellant	2,600,000	555,000
Total full-thrust propellant	2,647,000	590,650

the body. The heat shield substructure is phenolic and polyimide honeycomb sandwich weighing 1.05 lb/ft^2. The booster thrust structure is fabricated from titanium and is a stiffened cone with cross-beam design.

The orbiter fuselage is fabricated from titanium and is a stiffened skin and frame design. The propellant tanks are not integral with this structure and are subsequently classified under main propulsion. The titanium primary structure construction is skin and stringer with $\bar{t}$ ranging from 0.054 to 0.114 inch. The frame spacing varies from 20 to 40 inches and the cross sectional area of these frames range from 0.70 to 1.08 square inch. The orbiter thrust structure is also fabricated from titanium and is a truss design.

Induced Environmental Protection

The thermal protection system thickness and weights are based on thermal analysis. External insulation, densified quartz (LI-15), is used on the body and wings. Fiberglass insulation (TG-15,000) is used internally to further limit the temperature of the LH_2 tank and other structure. Polyurethane foam is used internally in the LH_2 tankage. Zirconium diboride is used on hot leading edges.

The booster wing environment requires insulation of the underside with varying thicknesses of densified quartz (LI-15) averaging 0.46 lb/ft^2. The orbiter, because of its more critical environment, has 1.42 lb/ft^2 of LI-15 insulation on the exposed wing underside. The orbiter wing topside carries 0.20 lb/ft^2 of LI-15. Leading edge insulation uses zirconium diboride and required 6.83 lb/linear ft.

The booster horizontal stabilizer underside requires that the under section up to the control surface hinge point be protected. This application results in a weight of 0.50 lb/ft^2, and the leading edge requires 7.5 lb/linear ft.

The booster fuselage underbody structural thermal protection varies in thickness, being heaviest at the nose and thinnest at the aft end. Side protection is uniform throughout. The top does not require protection. The protected area is 60 percent of the total wetted area. Orbiter protection is similar to that of the booster and covers 58 percent of the total wetted area.

Booster internal insulation and supporting structure between the skin and tankage averages 0.164 lb/ft^2. The orbiter requires 0.548 lb/ft^2 of which 0.348 lb/ft^2 is insulation and the remainder supporting structure.

Insulation is required to prevent excessive hydrogen boiloff. Polyurethane foam is placed inside the tanks to facilitate inspection. The weight is 0.223 lb/ft^2 of tank wetted area, and the thickness is 1.0 inch.

Launch, Recovery, and Docking

In this system, the landing gear was statistically evaluated as 4 percent of the vehicle landing weight. To produce a lighter gear, fabrication from titanium was projected; and the overall weight was reduced by ten percent. The total booster landing gear weight is 17,150 pounds and the orbiter is 9,264 pounds. At a later date, Cleveland Pneumatic Tool submitted a landing gear weight study. Their weights for the booster gear are 16,120 pounds and for the orbiter, 9000 pounds. If 5 percent is added to these weights for attach fittings, the result is 16,926 and 9,450 pounds for booster and orbiter, respectively. These resulting weights justify NR's statistical prediction.

Main Propulsion

Systems applicable to main propulsion were studied, and a detail weight statement was supplied by the subsystem analysts. The rocket and turbojet engine weights were derived from manufacturers available engine data. Orbiter propellant tanks are fabricated from 2219 aluminum and are not primary body structure. The tanks are required to withstand tank pressure and inertia loads only. Skin gages vary from 0.048 to 0.096 inch.

Orientation Controls, Separation

The reaction control system weight was determined by system analysis. An O_2/H_2 system is used with 28 RCS motors in the orbiter and 24 motors in the booster. The system includes propellant-conditioning equipment to pump and vaporize liquid propellants and store gaseous propellants.

The aerodynamic surfaces hydraulic control system was analyzed, and detail weights were provided by the system analysts. Necessary actuators, controls, and trunk plumbing are included in the weights.

Prime Power Source, Conversion, and Distribution

The power system weights were determined by system analysis. The orbiter electrical power system includes three, 5-kilowatt fuel cells and associated equipment, two, 80-ampere-hour batteries and chargers, and a power distribution system. The booster electrical power system includes two 80-ampere-hour batteries and a power distribution system.

Booster and orbiter auxiliary power is provided by four O_2/H_2 APU's. Booster and orbiter APU power levels are 250 and 150 horsepower, respectively. A 12-kva alternator is included in each APU power unit weight.

Hydraulic power is provided by four independent systems. The booster has two 40-gpm pumps and equipment per system. The orbiter has one 40-gpm pump and equipment per system.

Integrated Electronics

The integrated electronic weights were determined by system analysis. The weights are shown for guidance and navigation, instrumentation, and communication.

Environmental Control System

ECS system weight was determined by system analysis. Systems are provided for thermal control of both manned and equipment areas and for contaminant control of the manned area. A dual-loop water glycol system and associated equipment are used for thermal control.

8.3.7 Center of Gravity Prediction

Centers of gravity of the baseline configurations were calculated to determine if the location is satisfactory for the aerodynamic surfaces used in the orbiter and booster design. Critical conditions are entry and landing.

The baseline orbiter has a gross weight of 855,962 pounds. A longitudinal center of gravity (X_{CG}) is at Body Station 949 (X/L = 0.39) and the vertical center of gravity (Z_{CG}) is at 126 inches above the fuselage reference plane (FRP). The landing weight is 252,842 pounds. The X_{CG} is at Station 1415 (X/L = 0.585), and the Z_{CG} is 109 inches above the FRP. These two centers of gravity satisfy the flight and landing modes requirements.

The baseline booster has a gross weight of 3,133,098 pounds with an X_{CG} at Station 1238 (X/L = 0.42) and a Z_{CG} 16 inches below the FRP. The landing weight is 470,729 pounds with the X_{CG} at Body Station 1975 (X/L = 0.667), and the Z_{CG} is 79 inches below the FRP. The relationship between the wing, landing gear and the landing center of gravity does not present an acceptable configuration. To design an acceptable configuration, portions of several subsystems and their fluids were relocated forward. These systems were attitude control, hydraulic and auxiliary power, and turbojet propellant and tankage. The result was a shift of the X_{CG} to Station 1820 (X/L = 0.615) during entry and to Station 1926 (X/L = 0.65) during landing. These conditions represent a workable configuration. Althrough a workable C.G. solution was identified, this area requires considerably more work to identify the best method of balancing the booster.

8.3.8 Final Weight Statement

Comparing the baseline booster and orbiter weights with the preliminary baseline weights shows that the booster burnout weight decreased 3.1 percent while the orbiter burnout weight increased 8.7 percent. These weight changes resulted in a decrease in payload capability; therefore, the vehicle was resized to maintain 50,000-pound-payload capability. Parametric weight curves were prepared so that vehicle sizing analysis could be conducted. These data are presented in Figures 8.3-11 and 8.3-12. The resized orbiter is very close to the baseline; however, the booster is considerably heavier. The final configuration summary weights are presented in Tables 8.3-11 and 8.3-12 for the booster and orbiter. Using the detail weight breakdown developed for the baseline configuration as a guide, a detail weight breakdown is presented for the final configuration (Table 8.3-13).

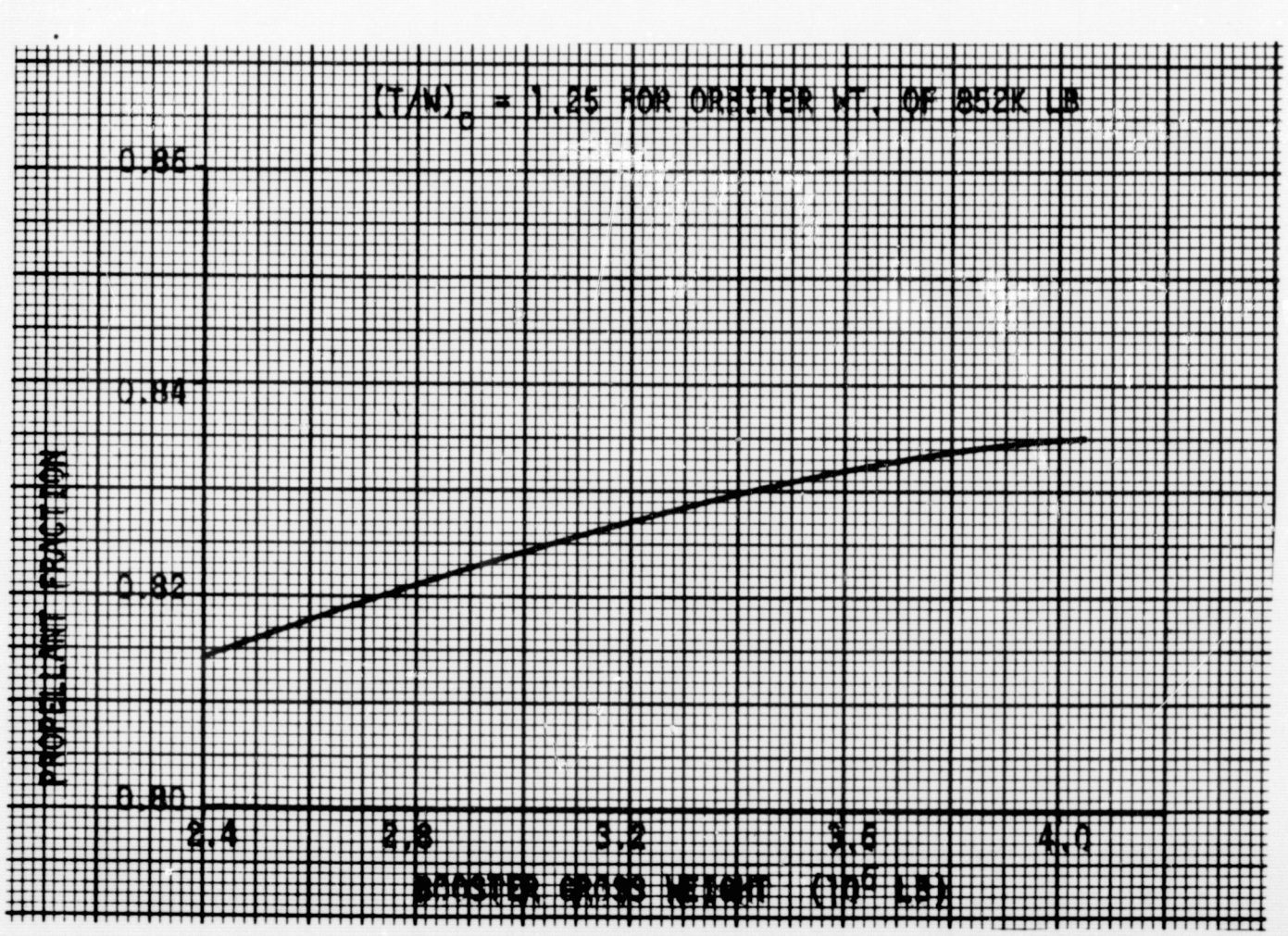

Figure 8.3-11. Booster Mass Fraction, Final Configuration Weights

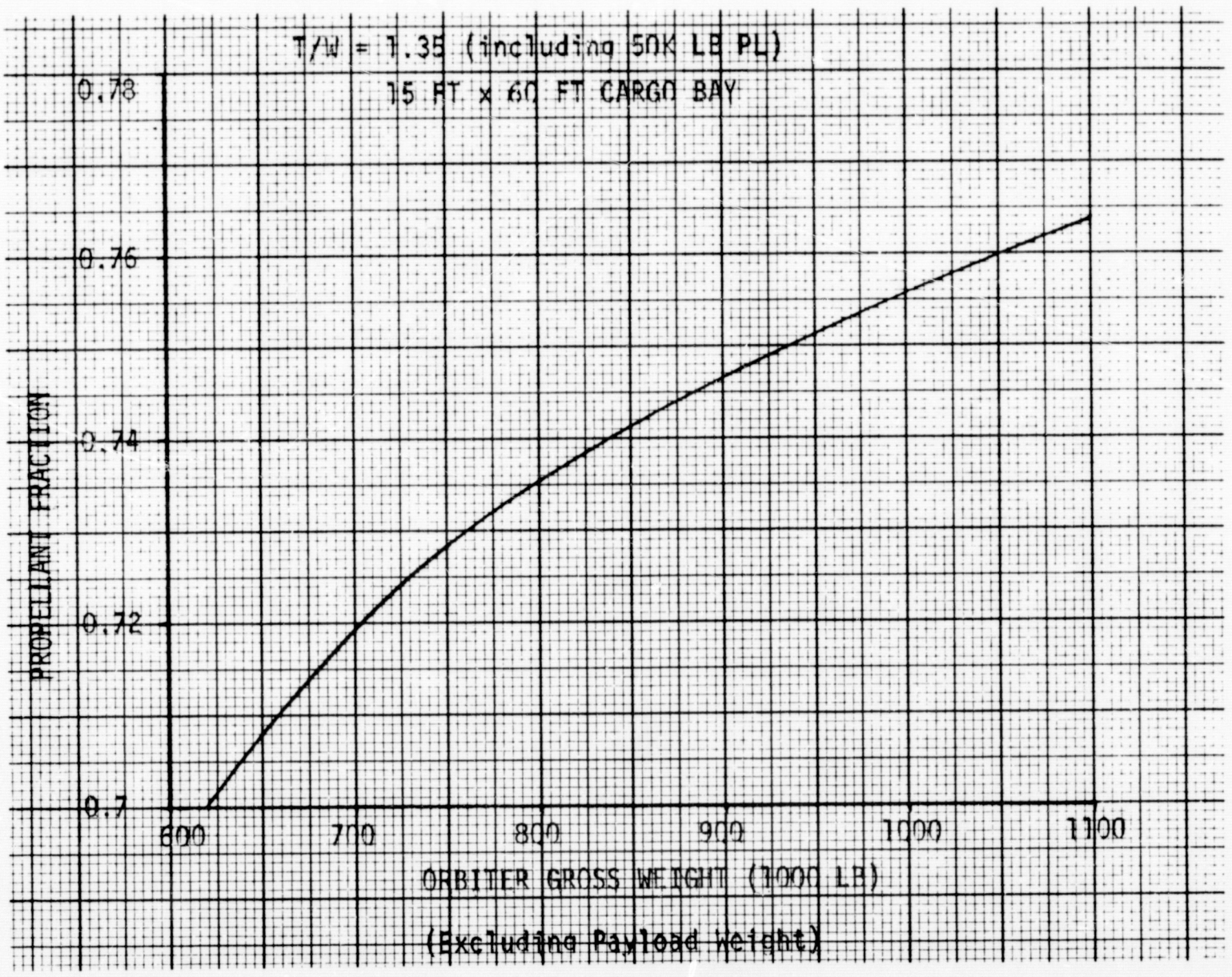

Figure 8.3-12. Orbiter Mass Fraction, Final Configuration Weights

8.3.9 25,000-Pound-Payload Vehicle

A shuttle vehicle was being sized to provide 25,000-pound-payload capability with a 12-foot-diameter by 48-foot-long cargo bay. Using the knowledge gained from the detail weight analysis previsouly described, parametric data were prepared for the sizing of this vehicle. The booster propellant fraction curve (Figure 8.3-11) is satisfactory for this sizing with minor modification for charge in engine thrust to maintain the lift of thrust-to-weight ratio of 1.25:1. Orbiter propellant fraction data are presented in Figure 8.3-13.

Table 8.3-11. Final Booster Summary Weight Statement

Code	System	Weight (lb) A	B	C	D
1.0	Aerodynamic surfaces	95,400	95,000	95,400	95,400
2.0	Body structure	229,642	229,642	229,642	229,642
3.0	Induced environment protection	25,572	25,572	25,572	25,572
4.0	Launch, recovery, and docking	21,500	21,500	21,500	21,500
5.0	Main propulsion	118,887	118,887	118,887	118,887
6.0	Orientation control separation, and ullage	9,150	9,150	9,150	9,150
7.0 and 8.0	Prime power source; Power conversion and distribution	5,350	5,350	5,350	5,350
9.0	Guidance and navigation	682	682	682	682
10.0	Instrumentation	583	583	583	583
11.0	Communication	440	440	440	440
12.0	Environmental control	337	337	337	337

A Gross launch weight
B Boost burnout weight
C Reentry weight
D Landing weight

Table 8.3-11. Final Booster Summary Weight Statement (Cont)

Code	System	Weight (lb) A	B	C	D
14.0	Personnel provisions	-	-	-	-
15.0	Crew station control and panel	149	149	149	149
	Subtotals (dry weight)	507,692	507,692	507,692	507,692
17.0	Personnel	-	-	-	-
18.0	Cargo	-	-	-	-
21.0	Residual propellant and service items	28,600	28,600	13,510	13,510
	Subtotals (inert weight)	536,292	536,292	521,202	521,202
22.0	Reserve propellant and service items	13,480	13,271	13,220	10,800
25.0	Full-thrust propellant	3,070,100	53,100	53,100	-
	Total weight	3,619,872	602,663	587,522	532,002

A Gross launch weight
B Boost burnout weight
C Reentry weight
D Landing weight

Table 8.3-12. Final Orbiter Summary Weight Statement

Code	System	Weight (lb)			
		A	B	C	D
1.0	Aerodynamic surface	26,177	26,177	26,177	26,177
2.0	Body structure	61,658	61,658	61,658	61,658
3.0	Induced environment protection	29,438	29,438	29,438	29,438
4.0	Launch recovery and docking	10,382	10,382	10,382	10,382
5.0	Main propulsion	52,632	52,632	52,632	52,632
6.0	Orientation control, separation, and ullage	8,582	7,414	7,414	7,414
7.0 and 8.0	Prime power source; Power conversion and distribution	5,197	5,197	5,197	5,197
9.0	Guidance and navigation	770	770	770	770
10.0	Instrumentation	589	589	589	589
11.0	Communications	588	588	588	588
12.0	Environmental control	1,463	1,463	1,463	1,463

A Gross launch weight
B Boost burnout weight
C Reentry weight
D Landing weight

Table 8.3-12. Final Orbiter Summary Weight Statement (Cont)

Code	System	Weight (lb) A	B	C	D
14.0	Personnel provisions	364	364	364	364
15.0	Crew station control and panel	275	275	275	275
	Subtotals (dry weight)	198,115	196,947	196,947	196,947
17.0	Personnel	660	660	660	660
18.0	Cargo	50,000	50,000	50,000	50,000
21.0	Residual propellant and service items	6,215	6,215	3,200	3,200
	Subtotals (inert weight)	254,990	253,822	250,807	250,807
22.0	Reserve propellant and service items	12,337	9,468	7,188	4,000
25.0	Full-thrust propellant	603,650	43,650	650	-
	Total weight	870,977	306,940	258,643	254,807

A Gross launch weight
B Boost burnout weight
C Reentry weight
D Landing weight

Table 8.3-13. Final Configuration Subsystem

Item	Weight (lb)	
	Booster	Orbiter
1.0 AERODYNAMIC SURFACES		
Wing	(51,029)	(10,996)
Carry-through torque box	35,186	5,922
Section forward of box	4,048	1,694
Section aft of box	11,795	3,380
Horizontal aft surface	(15,035)	(6,195)
Carry-through torque box	8,507	2,438
Section forward of box	1,072	832
Section aft of box	5,456	2,925
Vertical tail	(11,157)	(4,756)
Carry-through torque box	5,531	2,395
Section forward of box	2,802	1,302
Section aft of box	2,824	1,059
Wing carry-through body structure	(18,179)	(4,230)
Wing	12,590	2,030
Horizontal aft surface	5,589	2,200
Total aerodynamic surfaces	*95,400	*26,177
2.0 BODY STRUCTURE		
Primary structure	(151,070)	(49,591)
Skin and stringers		24,505
Frames and bulkheads	16,808	21,281
Longerons	9,400	1,598
Joints, splices, etc.	5,474	2,207
Truss and miscellaneous structures	20,508	-
LO_2 and LH_2 tank	98,880	-

*Leading edge and trailing edge were based on statistical data. The structural box was based on design area requirements and converted to realistic weight when multiplied by 1.27. The final weight is derived by scaling the baseline configuration.

Table 8.3-13. Final Configuration Subsystem (Cont)

Item	Weight (lb)	
	Booster	Orbiter
Secondary structure	(47,199)	(5,309)
Heat shield substructure	38,941	-
Miscellaneous structure	993	2,461
Joints, splices, etc.	5,053	551
Doors and closeouts	2,212	2,297
Thrust structure	(20,846)	(4,000)
Contingency	(10,527)	(2,758)
Total body structure	229,642	61,658
3.0 INDUCED ENVIRONMENTAL CONTROL		
Aerosurfaces		
Wing	(3,313)	(6,090)
Underside and leading edge	2,801	3,740
Topside	-	402
Horizontal aft surfaces		
Underside and leading edge	512	1,238
Topside	-	468
Vertical tail	-	242
Fuselage external	(9,926)	(9,236)
Underbody	5,594	6,846
Sides and top	4,332	2,390
Fuselage internal	(6,304)	(9,372)
Underbody	2,093	1,134
Sides and top	3,531	4,816
Supporting and attaching structure	680	3,422
LH_2 tank insulation	(3,704)	(2,063)
Contingency	(2,325)	(2,677)
Total induced environmental control	25,572	29,438

Table 8.3-13. Final Configuration Subsystem (Cont)

Item	Weight (lb) Booster	Orbiter
4.0 LAUNCH RECOVERY AND DOCKING		
Landing gear and systems	(20,783)	(9,917)
Forward gear	*6,864	*3,242
Main gear	*12,750	*6,022
Hydraulic actuation		
Actuators and controls	728	465
Plumbing	441	188
Docking	(-)	(364)
Separation system	(545)	-
Contingency	(172)	(101)
Total launch, recovery, and docking	21,500	10,382
5.0 MAIN PROPULSION		
Liquid rocket engine system	(76,365)	(29,693)
Engines	**57,300	**11,300
Propellant feed		
Prevalves	3,300	600
LH_2 lines	1,500	254
LOX lines	9,900	2,000
Fill and drain valves and disconnects	400	200
LH_2 fill and drain lines	150	75
LOX fill and drain lines	50	25
Pressurization system		
Vent valves	240	200
Pressure manifold	520	194
Pressure Lines	183	26

*These weights derived from statistical data and carry no contingency.
**Engine manufacturers weights. Did not add contingency

Table 8.3-13. Final Configuration Subsystem (Cont)

Item	Weight (lb)	
	Booster	Orbiter
Pressure regulator and check valves	200	100
Heat exchanger	470	80
Lines, fittings, etc.	580	100
Orbital maneuvering feed system		
Tank shutoff, vent valves, and pressure regulator	-	125
Helium supply tankage	-	1,000
Helium supply lines	-	100
Engine hydraulic actuation		
Actuators and controls	812	224
Plumbing	760	100
Propellant tanks		
LOX/LH_2 tank		6,414
LH_2 tank interconnector		2,128
LH_2 tank		3,494
Orbital tanks		954
Turbojet engine system	(39,669)	(20,367)
Engines	*33,500	*17,050
Propellant feed		
Pumps, heaters, and feed lines	320	131
Vent, port, bleed valves, etc.	40	35
Sensors and wiring	100	80
Tank seal	285	151
Air induction system		
Pressure duct and nacelles	5,424	2,920
Fuel management system	(300)	(364)
Sensors and wiring	300	364
Contingency	(2,553)	(2,208)
Total main propulsion	118,887	52,632

Table 8.3-13. Final Configuration Subsystem (Cont)

Item	Weight (lb)	
	Booster	Orbiter
6.0 ORIENTATION CONTROLS, SEPARATION, ETC.		
Attitude control system	(2,197)	(3,660)
Engine installation		
Engines	*396	*168
Propellant storage		
O_2 tanks	957	2,163
H_2 tanks	354	786
Valving	44	90
Propellant feed and control		
Turbines and gas generators	68	62
Pumps, O_2 and H_2	38	34
Isolation valves	46	44
Pressure regulators	200	225
Check valves	40	48
Heat exchangers	54	40
Aerodynamic surface hydraulic control	(6,153)	(3,095)
Actuators and controls	4,352	2,147
Plumbing	1,801	948
Separation rocket propellant case	(-)	*(1,168)
Contingency	(800)	(659)
Total orientation controls, separation, etc.	9,150	8,582
7.0 AND 8.0 PRIME POWER SOURCE, CONVERSION AND DISTRIBUTION		
Electrical power	(977)	(2,766)
Fuel cells		630
Hydrogen tank		389
Oxygen tank		393

*Engine manufacturers weights. Did not add contingency.

Table 8.3-13. Final Configuration Subsystem (Cont)

Item	Weight (lb)	
	Booster	Orbiter
Plumbing and valves		120
Battery	150	130
Inverter		156
Power control/distribution module	125	125
Battery charger		16
Distribution wiring	360	240
Remote distributors	320	320
Radiators		100
Supports	22	197
Reactants		*
Auxiliary power		
Auxiliary power unit	(2,603)	(1,180)
Hydrogen tank	1,040	600
Oxygen tank	454	139
Plumbing and valves	529	161
Distribution wiring	136	60
Power control/distribution module	180	80
Supports	50	50
Reactants	214	90
	*	*
Hydraulic power		
Pumps	(1,284)	(779)
Reservoir	208	96
Plumbing and valves	160	110
Nitrogen pressurization	790	447
	126	126
Contingency	(486)	(472)
Total prime power source, conversion and distribution	5,350	5,197
9.0, 10.0, AND 11.0 INTEGRATED ELECTRONIC SYSTEMS		
Guidance and Navigation (Code 9.0)	(620)	(700)
Integrated computer system	75	100
*Reactants listed under Code 21.0		

Table 8.3-13. Final Configuration Subsystem (Cont)

Item	Weight (lb)	
	Booster	Orbiter
Inertial reference units and electronics	180	180
Horizon sensors	-	20
Telescope and navigation base	-	35
Air data sensors	24	24
Sensor signal couplers	20	20
RCS driver package	40	40
Cabling	200	200
Supports	81	81
Instrumentation (Code 10.0)	(530)	(530)
Multiplexing (signal distribution)	100	100
Central timing	20	20
Recorder/playback	25	25
Printout unit	15	15
Multiplexer wiring and connectors	350	350
Supports	20	20
Communications (Code 11.0)	(400)	(535)
Voice command		
VHF antenna	25	25
S-band PA	-	32
USBE	32	32
Updata link	21	21
Premodulator processor	15	15
S-band antenna	10	10
Audio center	8	8
TV	-	5
Tracking and ranging		
Multimode radar	50	50
Digital ranging generator antennas, and controls	70	70
Laser	-	50
Navigation aids		
Tacan	20	20
Distance measuring equipment	14	14
Radar altimeter	15	15

Table 8.3-13. Final Configuration Subsystem (Cont)

Item	Weight (lb)	
	Booster	Orbiter
Landing aids		
Glide scope	5	5
Localizer	4	4
Marker beacon	4	4
Supports and wiring	55	85
Redundancy, 15 percent	52	70
Contingency total systems	(155)	(182)
Total integrated electronic systems	1,705	1,947
12.0 ENVIRONMENTAL CONTROL SYSTEM		
Environmental control system	(306)	(1,285)
Humidity and CO_2 control system	-	190
Electronic cold plate network	85	85
Cabin cooling system	59	149
Cooling pump package	63	91
Radiator system	-	187
Evaporators	-	91
Ram-air heat exchanger	36	43
GSE heat exchanger	35	43
Oxygen system, emergency, and pressure control	-	56
Portable water system	-	73
Evaporator water system	-	56
Urine and fecal system	-	26
Evaporator water	-	54
Oxygen	-	14
CO_2 absorber elements	-	27
Structure	28	100
Contingency	(31)	(178)
Total environmental control system	337	1,463

Table 8.3-13. Final Configuration Subsystem (Cont)

Item	Weight (lb)	
	Booster	Orbiter
14.0 PERSONNEL PROVISIONS		
Accommodations for personnel	(-)	(265)
Seats and restraints		163
Supports		30
Shock absorbers		72
Fixed life support equipment	(-)	(40)
Galley equipment		6
Containers restraints		30
Urine transfer		4
Contingency	(-)	(59)
Total personnel provisions	(-)	(364)
15.0 CREW STATION CONTROLS AND PANELS		
Controls and panels	(135)	(250)
Contingency	(14)	(25)
Total crew station controls and panels	149	275
17.0 PERSONNEL		
Crew	(-)	(377)
Crew		*360
Constant wear garments		7
Coveralls		7
Headsets		1
Electrical umbilical		2
*No contingency used for crew.		

Table 8.3-13. Final Configuration Subsystem (Cont)

Item	Weight (lb)	
	Booster	Orbiter
Personal gear	(-)	(18)
Fecal collection		10
Tissue		1
Towels		1
Urine hose and filter		6
Life support		(129)
Food		16
Water drinking device		5
Survival kit		96
Medical kit		12
Crew accessories		(66)
Fire extinguisher		36
Tool kit		10
Flight data file		20
		(70)
Total personnel		660
18.0 CARGO		
Environmental control (Code 12.0)	(-)	(497)
CO_2 absorbers		296
Oxygen		156
Evaporator water		45
Personnel provisions (Code 14.0)	(-)	(1,752)
Seats and restraints		1,452
Containers		290
Galley equipment		4
Urine transfer		6
Personnel (Code 17.0)	(-)	
Crew		(2,271)
Crew		1,800
Constant wear garments		77

Table 8.3-13. Final Configuration Subsystem (Cont)

Item	Weight (lb)	
	Booster	Orbiter
Coveralls		60
Headsets		7
Electrical umbilical		20
Personal gear		
Tissue		3
Towels		2
Fecal collection		10
Urine hose and filter		6
Life support		
Food		170
Survival kit		116
Cargo, not systems (Code 18.0)	(-)	(45,480)
Total cargo	-	50,000
21.0 RESIDUAL PROPELLANT AND SERVICE ITEMS		
Residuals	(15,190)	(3,215)
Trapped rocket propellant	15,090	3,015
Trapped attitude control propellant	100	200
Service items	(13,410)	(3,000)
Gaseous hydrogen	4,249	615
Gaseous oxygen	7,151	1,250
Hydraulic fluid	2,010	1,025
Pressurant	-	110
Total residual propellant and service items	28,600	6,215
22.0 RESERVE AND SERVICE PROPELLANT		
Reserve propellant	(10,800)	(4,000)
Turbo propellant	10,800	4,000

Table 8.3-13. Final Configuration Subsystem (Cont)

Item	Weight (lb)	
	Booster	Orbiter
Service propellant	(2,680)	(8,337)
Attitude control propellant	1,845	3,800
Electrical power LH_2		132
Electrical power LO_2		1,458
Auxiliary power LH_2	463	143
Auxiliary power LO_2	372	115
Separation rocket propellant		2,689
Total reserve and service propellant	13,480	12,337
25.0 FULL THRUST PROPELLANT		
Full-thrust propellant	(3,070,100)	(603,650)
Turbojet fuel	53,100	650
Orbit maneuver propellant	-	43,000
Ascent propellant	3,017,000	560,000
Total full-thrust propellant	3,070,100	603,650

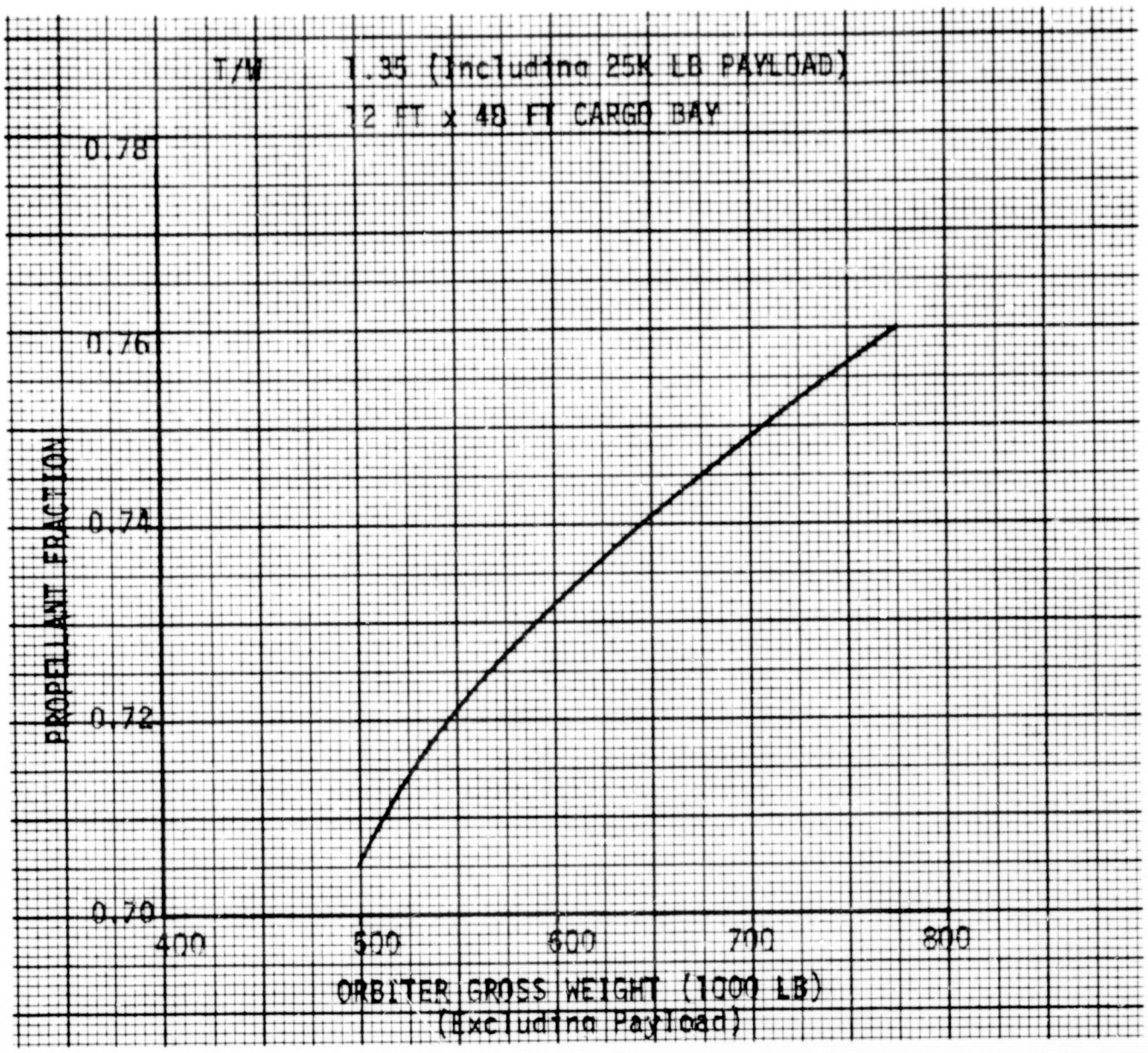

Figure 8.3-13. Orbiter Propellant Fraction, 25,000-Pound Payload

8.4 MATERIALS

The materials investigations were directed toward definition of material properties for use in the selection and design of ILRV thermal protection and structural systems. Material selection for the ILRV thermal protection system (TPS) and the basic structure is dictated primarily by structural load requirements, calculated maximum operating temperatures, heat load, and relative weights. Consideration must also be given to methods of installing the thermal protection so it can withstand the vehicle flexing and vibration environment. Thermal and loading environments for the ILRV orbiter and booster are defined in Volume III of this report.

A critical factor influencing selection of the thermal protection material is the reentry thermal environment. Since the baseline vehicle is designed to minimize reentry heating rates by providing low lift loading, the temperatures on the underside of the orbiter vehicle are generally less than 1500 F. Temperatures on the wing leading edges, however, are approximately 3000 F without flow interference or shock effects. As expected, the leading edges will be subjected to the highest temperatures, followed by the nose cap, under-body section, the upper body, the inner structure, and the main cryogenic tanks. Candidate materials (Table 8.4-1) were studied for each of these critical areas and are described and characterized in this section in order of descending temperature capabilities. The weight saving capability of advanced composites and the fracture mechanics techniques to be utilized are also discussed.

Table 8.4-2 summarizes the materials selected for the ILRV booster and orbiter.

8.4.1 Ceramics - Leading Edges

Diborides

The maximum operating temperature on the ILRV orbiter will be generated at the leading edges of the wing and horizontal stabilizer of the vehicle. In these areas, materials must be selected to operate reliably in the 3000 to 3600 F temperature regime. While tantalum alloys have acceptable properties to 3000 F, the problem of an adequate oxidation-resistant coating for a reentry-type environment has not been resolved. Graphites will function with an adequate margin of mechanical strength up to 3600 F, but they must also be coated like tantalum to prevent oxidation and extend service life. Unlike tantalum, graphites have a single use over-temperature ablation mode capability as an emergency backup, should the coating fail or temperatures exceed projected operational limits. The

Table 8.4-1. Candidate Structure/TPS Materials

Heat Shield/Structure		Deg F	Insulation
Very difficult to meet shuttle goals	Ablators	5000	Foamed graphite (Pyrofoam Grafoil)
	Ceramics		Carbon cloth and felt
	Graphites	4000	Foamed ceramic (Zirconia)
			Ceramic fibers (Zirconia)
	Reinforced pyrolyzed plastic	3000	
Good potential	Refractory metals - tantalum, columbium		Ceramic fibers (Dynaflex Dynaquartz)
	Densified quartz (LI-15)		
	Super alloys - TD NiCr	2000	Ceramic fibers (Microquartz)
Shuttle goals can be met	Haynes 188 René 41 Hastelloy X Inconel 718	1000	Glass fibers (TG 15000) Reflective film
	Titanium alloys		Phase change materials
	Aluminum alloys		Polyurethane foam
		0	

Table 8.4-2. ILRV Selected Materials

Location	Booster Material	Orbiter Material
Wing/tail leading edge	Haynes 188	Zirconium diboride
Wing lower surface thermal protection	Densified quartz LI-15	Densified quartz LI-15
Wing upper surface thermal protection	None	Densified quartz LI-15
Wing load carrying structure	Titanium 6Al-4V STA	Titanium 6Al-4V STA
Nose	Densified quartz LI-15	Densified quartz LI-15
Fuselage lower surface external thermal protection	Densified quartz LI-15	Densified quartz LI-15
Fuselage external thermal protection	Densified quartz LI-15	Densified quartz LI-15
Fuselage upper surface thermal protection	None	None
Fuselage structure	Reinforced phenolic and polyimide honeycomb panels with aluminum standoff structure	Titanium 6Al-4V STA
Fuselage internal insulation	Fiberglass TG-15000	Fiberglass TG-15000
Propellant tank structure	Aluminum 2219-T87	Aluminum 2219-T87
LH_2 tank internal insulation	Polyurethane foam	Polyurethane foam
LO_2 tank insulation	None	None
On-orbit propellant tank insulation	---	Multilayer HPI and polyurethane

most promising candidate leading edge materials are hafnium and zirconium diboride base refractory ceramics, which both have good oxidation resistance to about 4000 F and should be reusable according to published data (Figure 8.4-1). These ceramics were developed under an AFML contract.

The diboride refractories are based on zirconium or hafnium diboride, with additives of silicon carbide and, in some compositions, carbon, to improve oxidation and thermal-shock resistance and to make hot pressing of dense fine grain material practical. The materials have high melting points, and are hard and relatively brittle. The brittleness requires design concepts applicable to ceramics, i.e., avoidance of stress raisers and minimization of tensile loading. Hot press forging of the diborides is reportedly possible, but the practical limitations of the process have not been defined.

Diffusion bonding (hot press forge bonding) of the diborides can be done if the geometry of the parts to be bonded is suitable. Provisions for generous radii at changes of section must be made. Joining with mechanical fasteners is subject to special design consideration of thermal expansion, stress concentrations, capability and compatibility of the fastener material, and associated problems. Tantalum inserts can be included in the material when it is pressed but the exposed surface of these inserts require an oxidation protective coating which limits the maximum operating temperatures of those surfaces to 2500 F.

The zirconium diboride refractories are available from ManLabs in the compositions described, with a six-week leadtime required for cylindrical shapes. Special shapes requiring die manufacture and large sizes would require more time. Sizes are primarily dependent on press capability and stroke. Cost of the basic powder material is approximately $10 to $12 per pound, with pressing and machining costs additional.

8.4.2 Heat Shield

Exposed Radiative Insulation

LI-15. This material, developed by Lockheed, is a quartz fiber held together and densified with a proprietary silica binder. The external insulation concept, utilizing a nonablating, low thermal conductivity material on vehicle aerodynamic surfaces, has been selected for the baseline vehicle.

Of primary interest is the ability of such a system to reradiate entry heating energy with lower backface temperatures than radiative metal panel systems. The consequent reduction in attachment complexity, insulation, and insulation support provisions result in significant weight advantages for external insulation.

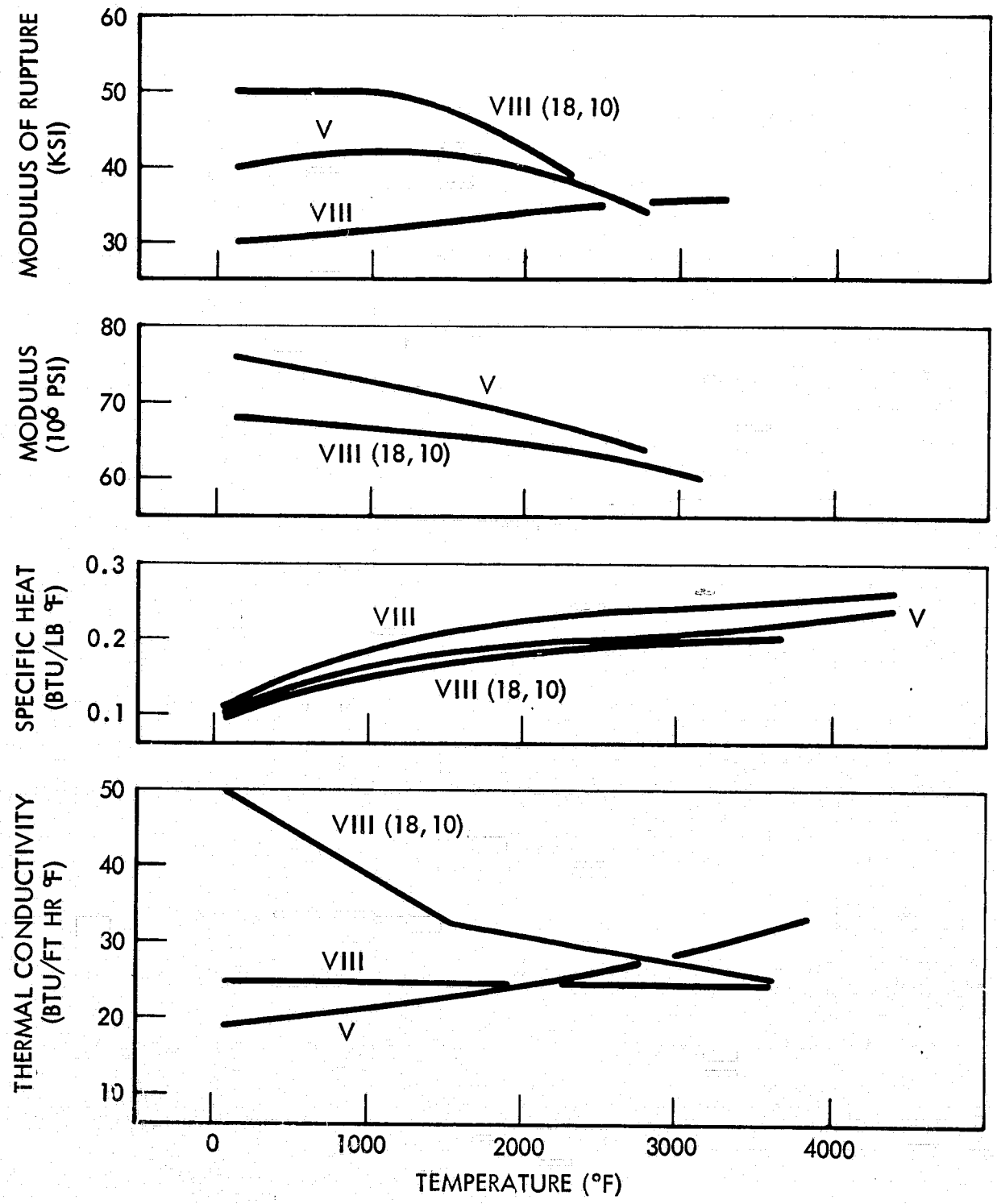

ROOM TEMPERATURE PROPERTIES	COMPOSITION		
	ZIRCONIUM BORIDE V	ZIRCONIUM BORIDE VIII	ZIRCONIUM BORIDE VIII (18, 10)
ρ (LB/CU IN.)	0.20	0.16	0.19
ELONGATION (PERCENT)	0	0	0
F_{cu} (KSI)	400	300	300
α (MICRO-IN./IN. °F) (80 TO 2540 F)	4.2	3.2	4.1

Figure 8.4-1. - Typical Properties of ManLabs Zirconium Diboride Hot-Pressed Shapes

In addition, such a thermal protection system should be simple to analyze thermally and structurally because of its homogeneity, its ruggedness compared to thin metal radiative panels, and its simplicity to repair. Additionally, the material may respond to over-temperature exposure by ablating without catastrophic failure as opposed to radiative panels which might fail under the same overstress condition.

Obviously, then, external insulation is a highly desirable system on portions of the vehicle with radiation equilibrium temperatures too high for the primary structure materials but lower than the ablation temperature of the insulation. The baseline TPS system has external insulation on both booster and orbiter lower fuselage and lower wing surfaces and on the orbiter upper wing surface. The baseline TPS was sized utilizing the LI-15 data presented in Table 8.4-3. Though the data have not been verified by NR testing and cost/availability is unknown, the data were utilized in vehicle sizing studies.since no other data were available.

The unknowns indicated in Table 8.4-3 must be resolved if TPS systems are to utilize LI-15. Since it is the NR assumption that NASA will furnish the detail design parameters for LI-15, that material is not included in the list of concepts (Table 8.4-4) which NR plans to include in a preliminary screening test program on external insulation.

Other Candidate Materials. Other candidate materials, their source, and proposed packaging techniques are listed in Table 8.4-4.

To make an external insulation feasible, the materials used must have certain properties: low thermal conductivity, low density, high surface emissivity, no surface recession at radiation equilibrium temperature, low thermal expansion, thermal shock resistance, and sufficient strength to withstand the entire loads spectrum from launch through landing. In addition, sufficient toughness to withstand normal handling, rain erosion, etc., and reasonable LOX compatibility are necessary.

It would be highly desirable if the materials had high in-plane thermal conductivity to eliminate local hot spots, low solar absorptivity-to-emissivity ratio, high strength, and low modulus of elasticity at all temperatures.

Four basic types of materials seem capable of performing in such a role:

1. Fibers with binders (organic or inorganic)

2. Fibers in containers

Table 8.4-3. Design Properties of LI-15

Property	Design Value		
Density (PCF)	15		
Maximum operating temperature for multiple use	2500 F		
	Mean Temp (°F)	C_p (Btu/lb °F)	K Btu-in. / hr-ft^2 °F
Specific heat and thermal conductivity (at 1 atmosphere)	200	0.20	0.41
	600	0.25	0.51
	1000	0.27	0.63
	1400	0.29	0.74
	1800	0.29	0.88
Emissivity	0.8		
Moisture absorption	10 percent without additional coating		
Rain erosion aerodynamic shear resistance	Unknown - overcoating anticipated		
Shrinkage	Unknown - preheating to operating conditions possible		
Thermal expansion	3×10^{-7} in. /in. °F		
Cost availability	Unknown		
Tensile/compressive ultimate at 75 F	100 psi		
Tensile modulus at 75 F	17,000 psi		

Table 8.4-4. Alternate External Insulation Concepts

Description	Source	Detail Configuration
Vycor foam	Corning	10 PCF density, 0.020 full density skin 20 PCF density, 0.020 full density skin 30 PCF density, 0.020 full density skin
Zirconia textiles	Union Carbide Research	2 PSF blanket ZYW-30 fabric bag containing 14 PCF ZYF-100 felt 2 PSF blanket 2 ply ZYW-15 fabric (laminated with zirconia) pan containing ZYF-100 felt
Boron nitride textiles	Carborundum R&D	2 PSF blanket boron nitride fabric (~ 1.5 pounds per sq yd) bag containing 4 to 6 PCF boron nitride fibers 2 PSF blanket 1 ply boron nitride fabric (as above) laminated with boron nitride pan containing 4 to 6 PCF boron nitride fibers
Quartz fabric (no binder)	Avco	2 PSF blanket quartz fabric bag containing quartz felt 2 PSF blanket quartz fabric bag containing low density 3D quartz weave
Silica fabric (with binder)	GE	2 PSF slab of converted silicone resin reinforced with random fibers 2 PSF slab of converted silicone resin reinforced with quartz fiber omni-weave

3. Less than full density ceramics

4. Full density ceramics

Of these, the last may be eliminated immediately since both conductivity (K) and density (ρ) are so high that the Kρ product is beyond feasible range.

The less than full density ceramics, as represented by refractory foam firebricks (zirconia, alumina, etc.), have been evaluated in other studies and shown to be prone to thermal shock damage. Impregnation with organics alleviates the problem but violates the concept of mission life without planned major maintenance. Foamed glasses glazed with full density silica may meet the Kρ product and thermal shock resistance requirements but the design complexities of attaching such a brittle material make its use dubious.

The class of silica foams produced by converting silicone resins is attractive in that fibrous or 3D fabric reinforcements could be incorporated for strength. However, no detail design data are available though exploratory work has been done by Avco, GE, and McDonnell Douglas.

Refractory fibers (glass, silica, zirconia, etc.) are thermally attractive if they can be processed in low density forms stable under flight vibrations and loads.

Thus, fibers in "bags" of refractory fabric or metal analogous to aircraft insulation blankets must be considered along with constructions utilizing refractory laminates (zirconia reinforced zirconia) containers. Either of these systems can be made thermally acceptable but may not be capable of sustaining loads without excessive weight penalties.

In the final class, fibers bonded in a stable shape with organics (ablators) have been successfully flown on numerous entry vehicles but the minimum maintenance philosophy would be violated. Therefore, the use of inorganically bonded fibers as typified by LI-15 (Lockheed Missile and Space Division, LMSD) seems to hold maximum promise.

Metallic Materials

Metallic materials for heat shield application cover the temperature range up to 2500 F. To negate the necessity of repeating material properties in the Structures section (paragraph 8.4.4), material properties in this section will cover the complete temperature range from cryogenic to maximum as applicable to the specific metal.

Table 8.4-5 shows the maximum operating temperature for heat shield (low stress) application.

Columbium. The diborides may extend to areas where temperature will not exceed 2400 to 2500 F. Coated columbium alloys can be operated to approximately 2500 F but are creep and coating limited to about 2400 F for multiple reuse. Because columbium oxidizes rapidly in air above about 1200 F, it must be protected with coatings that are basically silicides or aluminides. These coatings are usually formed on the surface of the alloy by pack cementation or slurry coating and fusing in an inert gas atmosphere or vacuum. Coating failure can result from mechanical damage, imperfections in coating, and loss of silicon caused by low oxygen pressure and high temperature. Diffusion of the coating elements into the columbium alloy substrate can also result in coating failure, or alternatively, can degrade the properties of the alloy by embrittlement. Creep can cause failure by embrittlement. Creep can cause failure by change in geometry or by exceeding the capability of the coating to conform. In addition, a change of emittance of the coating to a lower value, because of high-temperature exposure at low oxygen pressure, is a possible source of failure resulting from the corresponding temperature increase. It is anticipated that inspection of all coated columbium details would be routine between flights, at least until a history of coating performance would permit longer periods between inspection.

Table 8.4-5. Approximate Maximum Temperatures for Heat Shield Metals

Metal	Maximum Temperature (F)
Coated columbium	2500
TD NiCr.	2000
Haynes 188	2000
Rene 41	1700
Inconel 718	1300
Ti 6 Al 4V	1000

A columbium alloy such as C129Y can be cold formed by normal forming operations. Minimum bend radius of 2T is feasible. Joining can be accomplished by tungsten inert gas (TIG) or electron beam (EB) with typical weld joint efficiency approaching 100 percent. Resistance welding is possible, but involves more difficulty in coating the faying surfaces after welding. Coating is also a problem at brazed joints. Mechanical joints require special attention to reduce coating failure.

The fused slurry silicide coatings are more uniform as applied and are the most reliable of the currently available oxidation protective coatings for columbium. The coating is applied as a slurry of the powders of the constituent elements (silicon plus others) in a lacquer vehicle, either by dipping or spraying. After drying, the coating is fused in a vacuum or inert gas atmosphere. The molten silicon is an active flux, wetting and dissolving up to 1-1/2 mils from the columbium alloy surface in addition to the other powder constituents of the slurry. The resulting coat is about 3 to 4 mils thick, and will protect the columbium alloy to about 2600 F under reentry conditions.

TD Nickel-Chromium. Oxidation control coatings not only complicate the use of columbium, but also reduce reliability. It is, therefore, desirable, when body temperatures permit, to use a material such as thoria dispersion strengthened nickel-chromium alloy (TD NiCr). Typical properties are presented in Figures 8.4-2 through 8.4-4. TD NiCr has excellent oxidation resistance in air to 2200 F without a coating; however, NR feels that the alloy still has many problems to be resolved and that 2000 F is a more realistic upper temperature limit for multiple-use applications. This temperature limit is based on the fact that many promising materials have failed to achieve projected temperature capabilities. Supporting this conservative temperature limit is the expectation that TD NiCr will lose some chromium at high temperatures and at pressure below 1 torr (such as during the initial phases of reentry). Some data indicate as much as a 15 percent reduction in strength after 100 hours at 2000 F in a hard vacuum. There may also be an effect on the emittance of the oxidized surface. Insufficient data exist to determine if this latter phenomenon will be a life-limiting factor.

The high-temperature strength (especially creep) of TD NiCr is dependent on grain size, which is subject to the working-annealing history of the material. Any severe forming operation must be followed by a high-temperature anneal (2400 F for 1 hour) to restore creep strength.

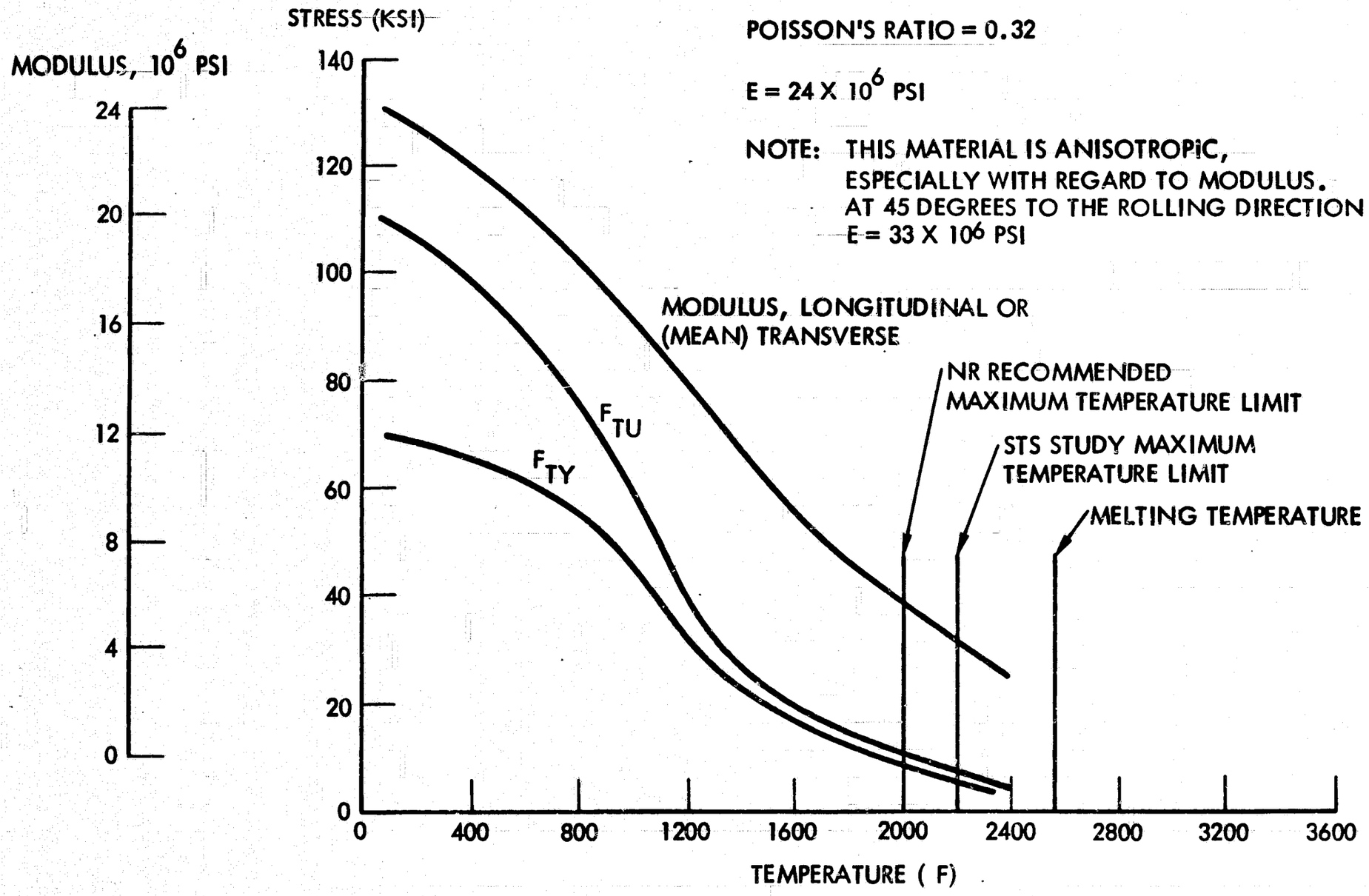

Figure 8.4-2. Effect of Temperature on TD NiCr Mechanical Properties (0.015- to 0.040-Inch Sheet)

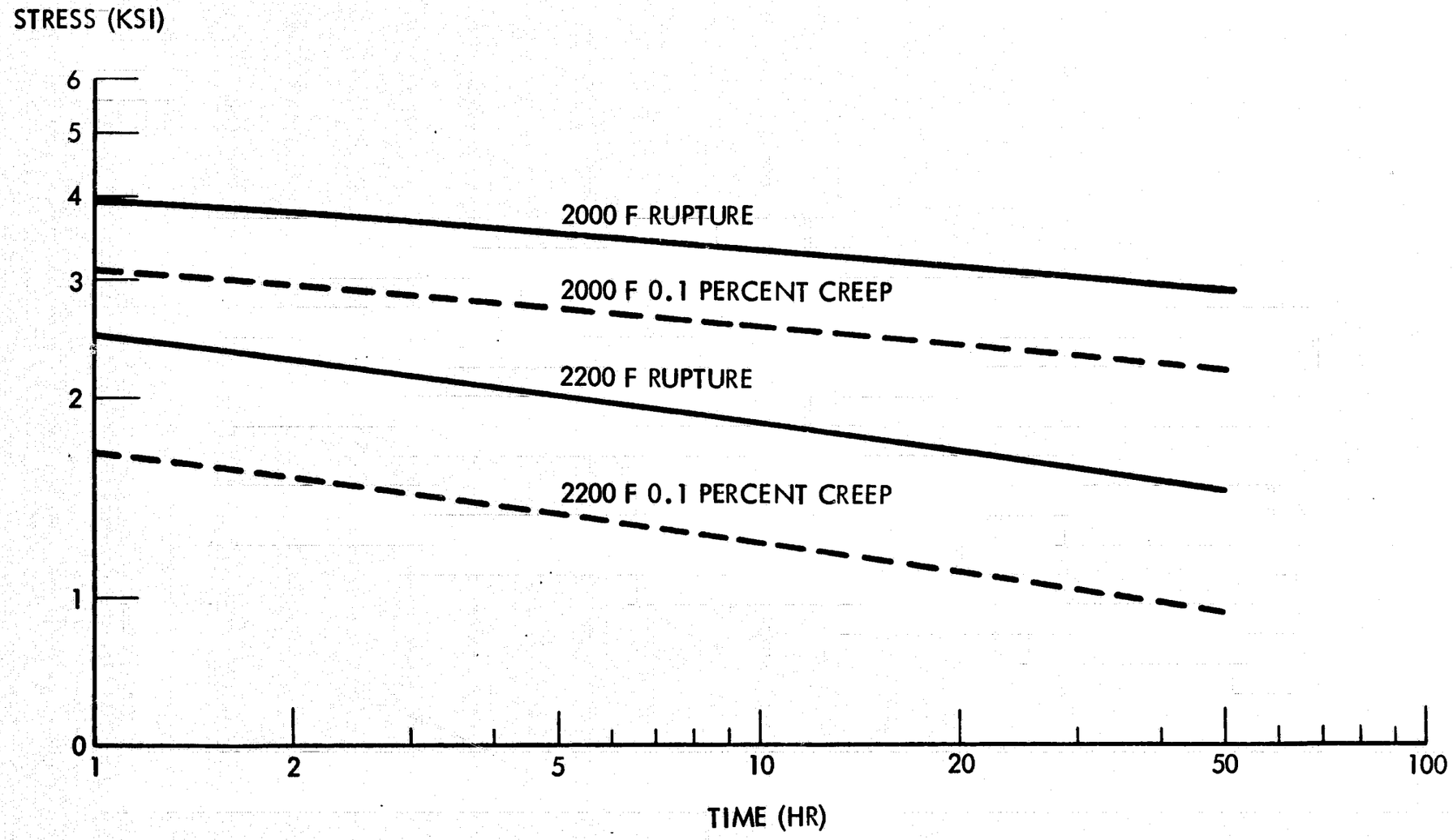

Figure 8.4-3. TD NiCr Creep Design Limits (Transverse Direction)

Space Division
North American Rockwell

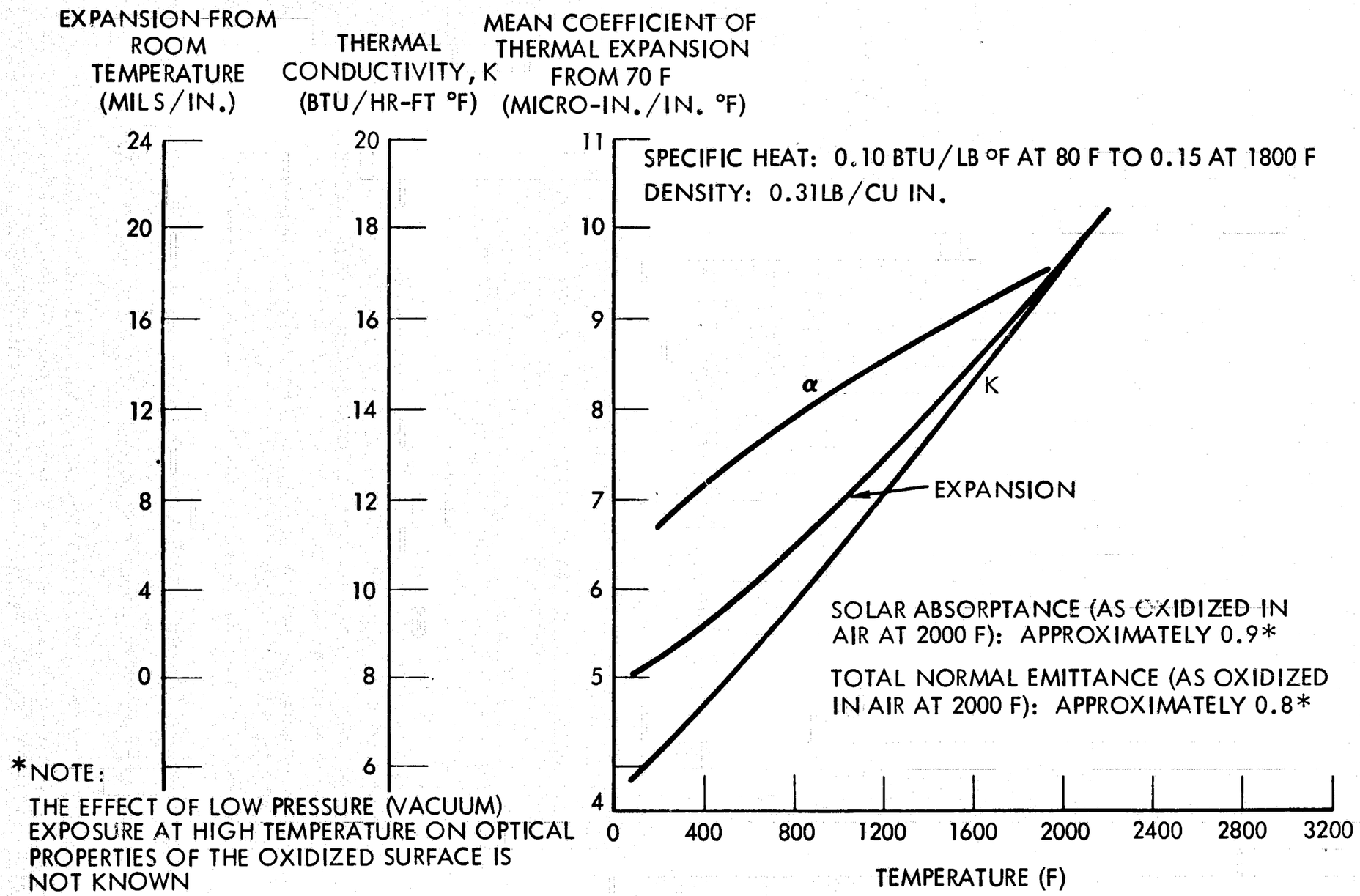

Figure 8.4-4. Effect of Temperature on TD NiCr Physical Properties

TD NiCr should be used only in areas requiring its high-temperature capability, which means that creep must be considered in each application. One of the limitations of the material is that the creep ductility at 2000 F is low (approximately 0.5 percent to rupture in the transverse direction). Creep deformation also reduces subsequent ductility and strength in the lower temperature range. Thus, creep deformation must be held to a maximum of 0.1 percent in the transverse direction. Test data indicate that the creep properties of the material differ in the longitudinal and transverse directions.

In common with most other nickel base alloys, TD NiCr should not be exposed to sulfur-bearing materials while at elevated temperatures.

From the fabricability standpoint, TD NiCr sheet in the 0.015 to 0.030 inch thickness range can be cold formed 90 degrees to less than a 5T radius. The question of recrystallization following such forming remains to be investigated. Approximately a 20-degree springback will occur. Dimpling can be done if the proper size hole is predrilled and deburred.

Fusion welding causes agglomeration of the thoria in the molten zone with resulting loss in dispersion strengthening. Therefore, fusion welding should not be used except possibly for sealing in areas where strength is not a major consideration, especially at high temperatures. Because of the narrower weld zone, EB welding is less detrimental than TIG, but tensile strength reduction of 35 percent at room temperature and 75 percent at 2000 F is to be expected.

Resistance (spot) welding is feasible, subject to the limitations of spot welded joints, and is a preferred method for joining TD NiCr.

Brazing of TD NiCr is possible but not practical for general application in the temperature range where the alloy would normally be used. An exception would be low stress applications such as honeycomb sandwich core-to-face brazing.

Joining with mechanical fasteners is feasible if the fasteners are made of TD NiCr, but the fastener manufacturer must be aware of the precautions necessary to achieve the required microstructure for creep resistance. The heads formed on rivets in making a joint are subject to the recrystallization degradation that follows severe forming without subsequent annealing. Edge distances of 2.5D should be used.

Haynes 188. Haynes 188 is a recently developed cobalt base high-temperature alloy now in commercial production. It is basically a modification of L605 alloy designed to have improved oxidation resistance to 2000 F and less susceptibility to loss of ductility in the 1200 to 1600 range. The alloy is used in the solution-treated (annealed) condition. Normal maximum operating temperature is about 1800 F but it can be used for short periods at 2000 F, depending on stress level and the amount of creep deformation acceptable. At elevated temperatures creep is the primary consideration as a life-limiting characteristic (see Figures 8.4-5 and 8.4-6).

Haynes 188 has fabricability characteristics similar to L605. It can be cold formed by most common processes. In severe forming operations, intermediate solution annealing treatment may be necessary because of the work-hardening tendency of the alloy. Haynes 188 can be fusion welded by TIG or EB using similar techniques to those used for L605. Resistance (spot) welding is also practical. On the basis of experience with L605, diffusion bonding of Haynes 188 can be performed at about 2150 F.

Rene' 41. Rene'41 is a precipitation-hardening nickel base alloy capable of being heat-treated to moderately high strengths. Two standard aging treatments are used: 1400 F for 16 hours for good short-time moderate temperature properties and 1650 F for 4 hours for good creep strength and stability above 1400 F. Properties of Rene'41 with the 1400 F aging treatment are given in MIL-HDBK 5A. Table 8.4-6 and Figures 8.4-7 and 8.4-8 present preliminary data on Rene 41 in the 1650 F aged condition.

Rene' 41 has good short-time yield strength to 1800 F, but for extended use above 1600 F, it is subject to intergranular oxidation. The high aging temperature also results in aging distortion problems in light gauge parts.

Because of the difficulties involved in heat treatment and fabrication Rene'41 should not be used unless its strength in the 1300 to 1700 F range is required.

Rene'41 alloy is oxidation resistant in air to 1600 F and does not oxidize excessively in a general (overall) manner to 1800 F. However, above 1600 F the alloy is subject to intergranular oxidation. This may not seriously affect the properties of moderately heavy sections but can cause a marked reduction of ductility together with the associated effects on other properties in light gauges.

Creep must be considered as a life limiting characteristic in the elevated temperature range above about 1100 F.

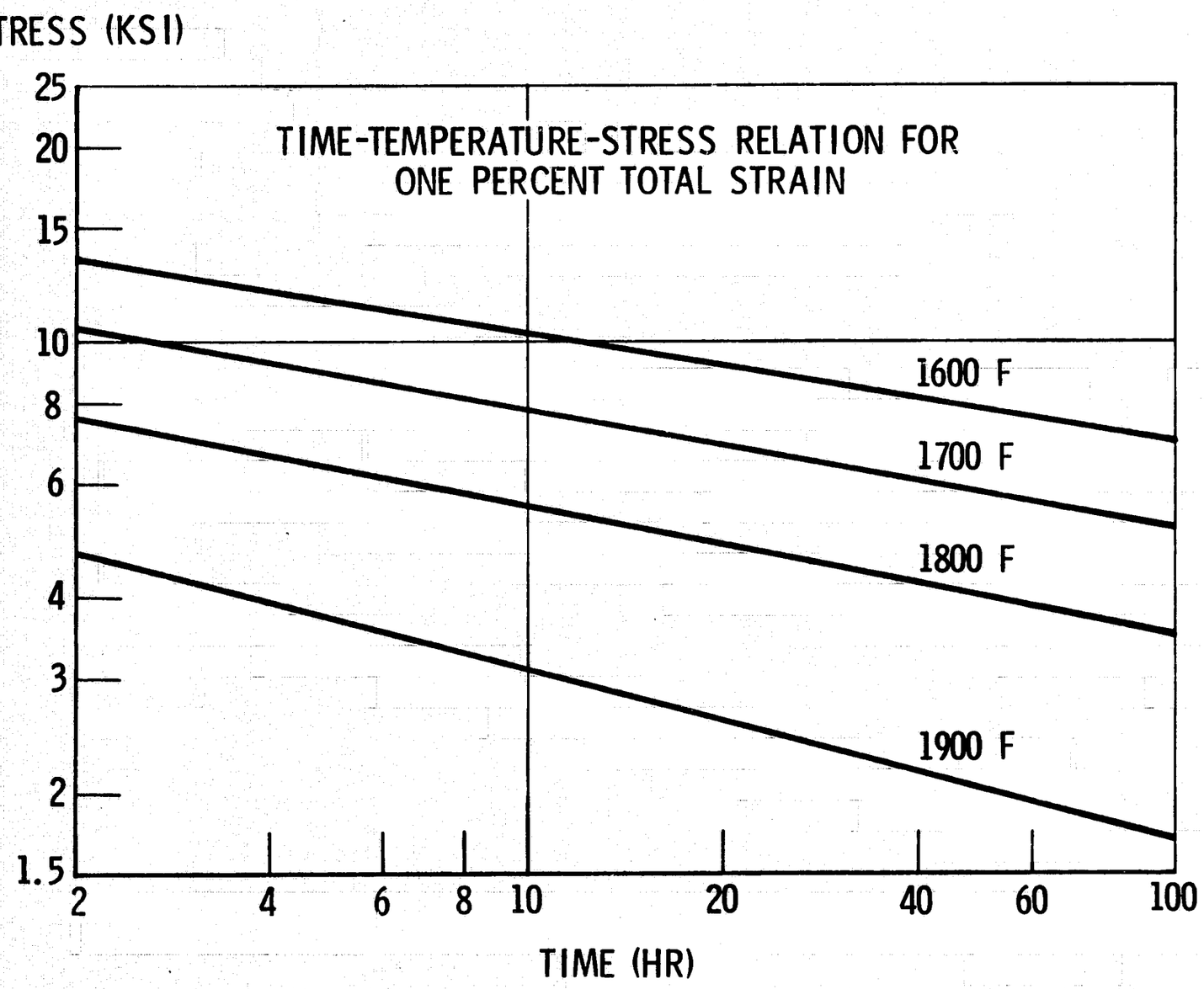

Figure 8.4-5. Effect of Temperature on Properties of Haynes 188 Cobalt Alloy Sheet and Bar

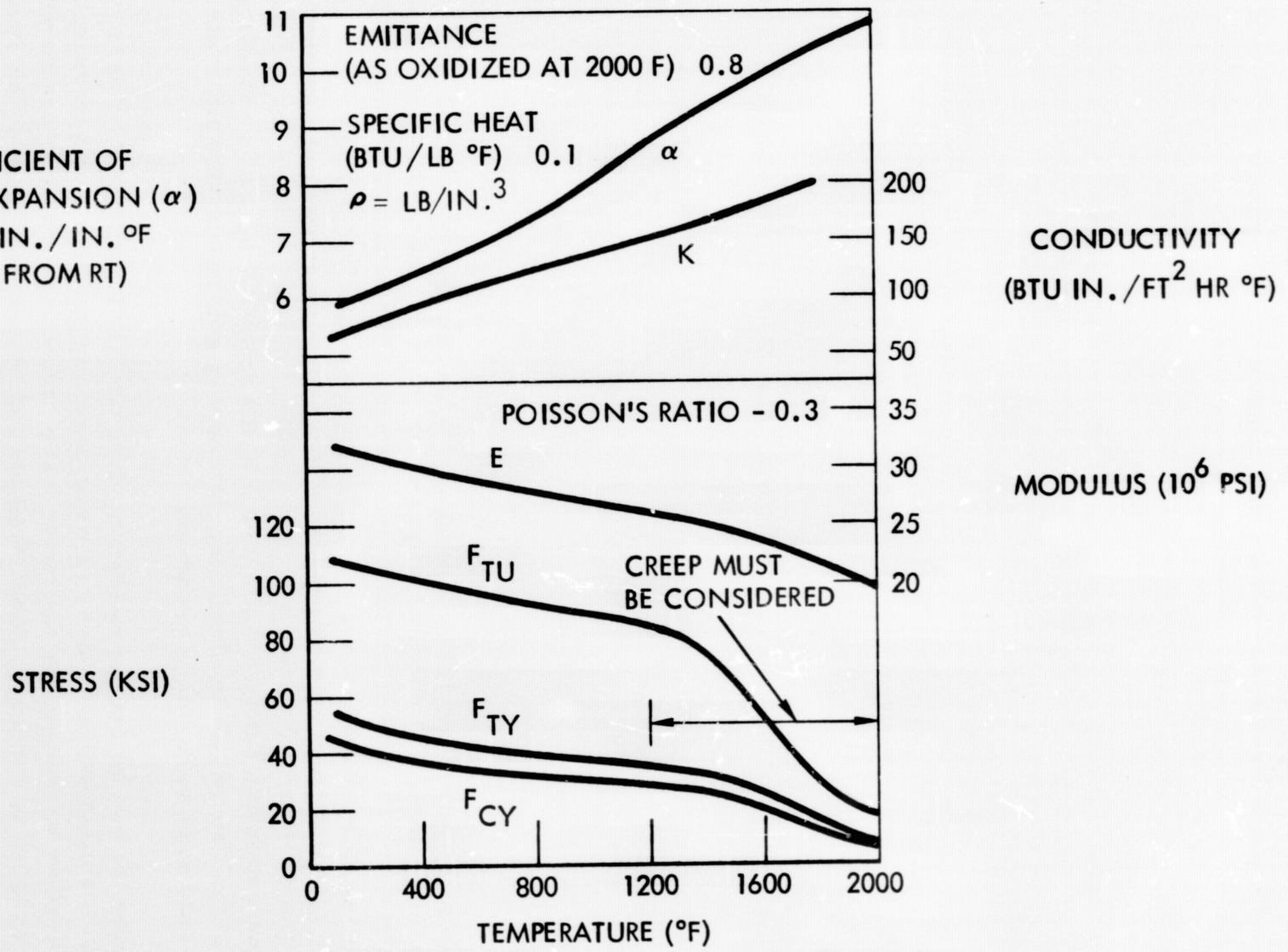

Figure 8.4-6. Effect of Temperature on Properties of Haynes 188 Cobalt Alloy Sheet (0.020- to 0.080-Inch)

Table 8.4-6. Rene 41 (1650 F Age)
Summary of Room Temperature Properties

Mechanical Properties (Preliminary Minimum Values)		Physical Properties (Average)	
F_{tu} (ksi)	140	E&E_c (10^6 psi)	31.6
F_{ty}, F_{cy} (ksi)	100	G (10^6 psi)	12.1
F_{bry} (e = 2D) (ksi)	180	ρ (lb/cu in.)	0.298
F_{su} (ksi)	90	α (micro in./in. F)	(See Figure 8.4-7)
		k (Btu/hr ft F)	(See Figure 8.4-7)
		Specific heat (Btu/lb F) (70-1500 F)	0.11

Rene' 41 should be formed in the solution-treated condition. It is considerably more difficult to form than the type 304 or 321 stainless steels, requiring more force and permitting a smaller amount of deformation before reannealing is required, i.e., it work hardens rapidly. The hardness and strength of solution-treated Rene' 41 is extremely dependent on the quenching rate in the 1850 to 1500 F range. Air cooling of sheet gauges (or a delay of 15 seconds between furnace and quench bath) from the solution annealing temperature can result in yield strength nearly equivalent to aged material, which could lead to forming problems.

Rene' 41 can be fusion welded by TIG or EB techniques. There has been a considerable history of weld cracking problems in restrained welds; studies to determine the cause have produced contradictory results. Fusion welding is normally performed on solution-treated material; however, one study indicates more cracking problems when the material has been water quenched from the solution temperature than when it has been cooled at 75 F per minute to below 1200 F, i.e,, a slack-anneal or an isothermal aging treatment. Following welding, parts are given a re-solution treatment (which provides stress relief) and then the required aging treatment. The solution treatment can cause severe distortion of sheet weldments.

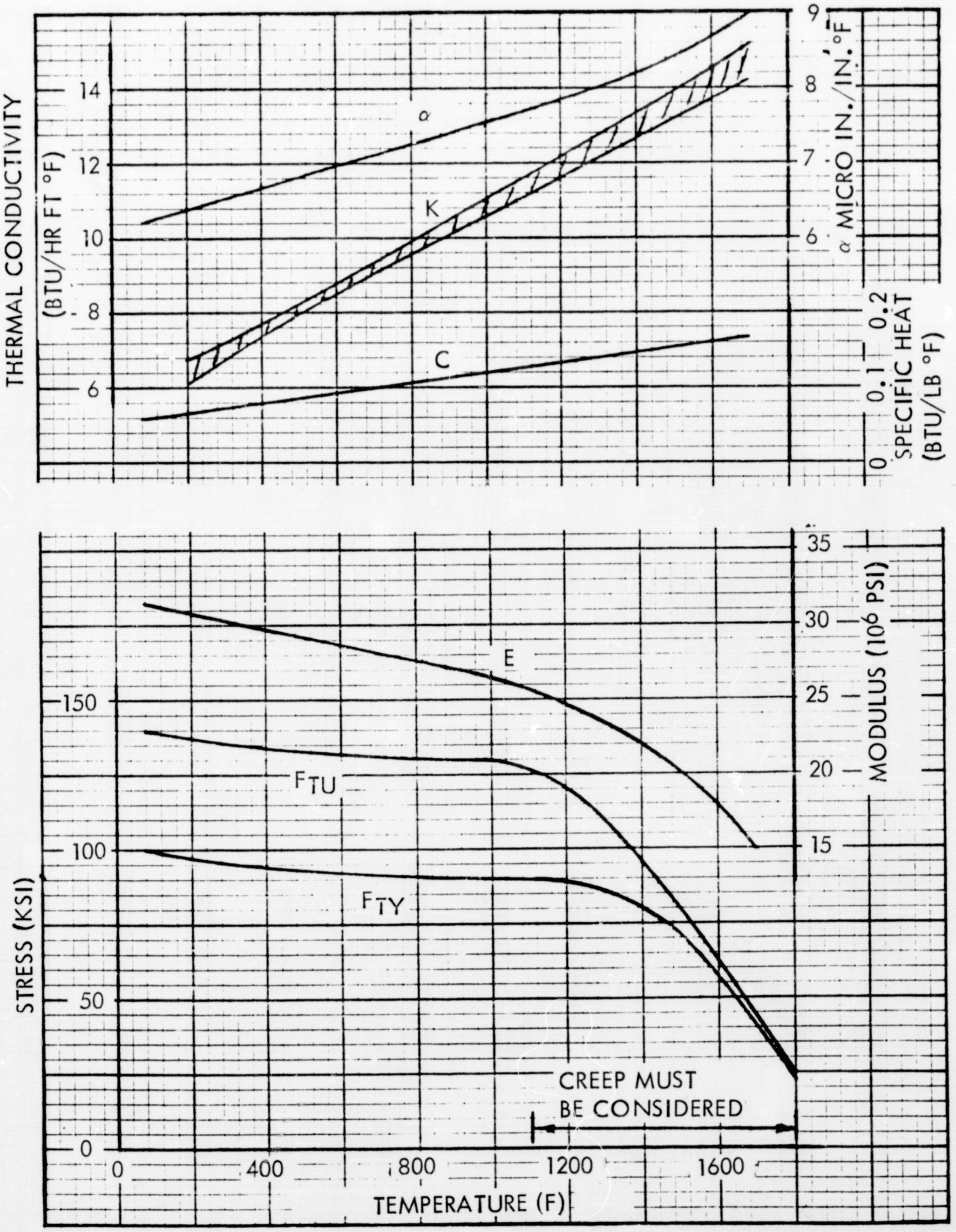

Figure 8.4-7. Effect of Temperature on Properties of Rene´41

NOTE: CREEP DESIGN PROPERTIES FOR RENE 41 SHEE, PLATE, AND BAR IN SIZES AND HEAT TREATMENT ARE GIVEN IN THE FOLLOWING FIGURE. BECAUSE OF THE SUSCEPTIBILITY OF THE ALLOY TO INTERGRANULAR OXIDATION AT HIGH TEMPERATURES, LIGHT GAGES (I.E., BELOW 0.030 INCH) ARE NOT RECOMMENDED FOR REPEATED OR EXTENDED USE ABOVE 1600 F.

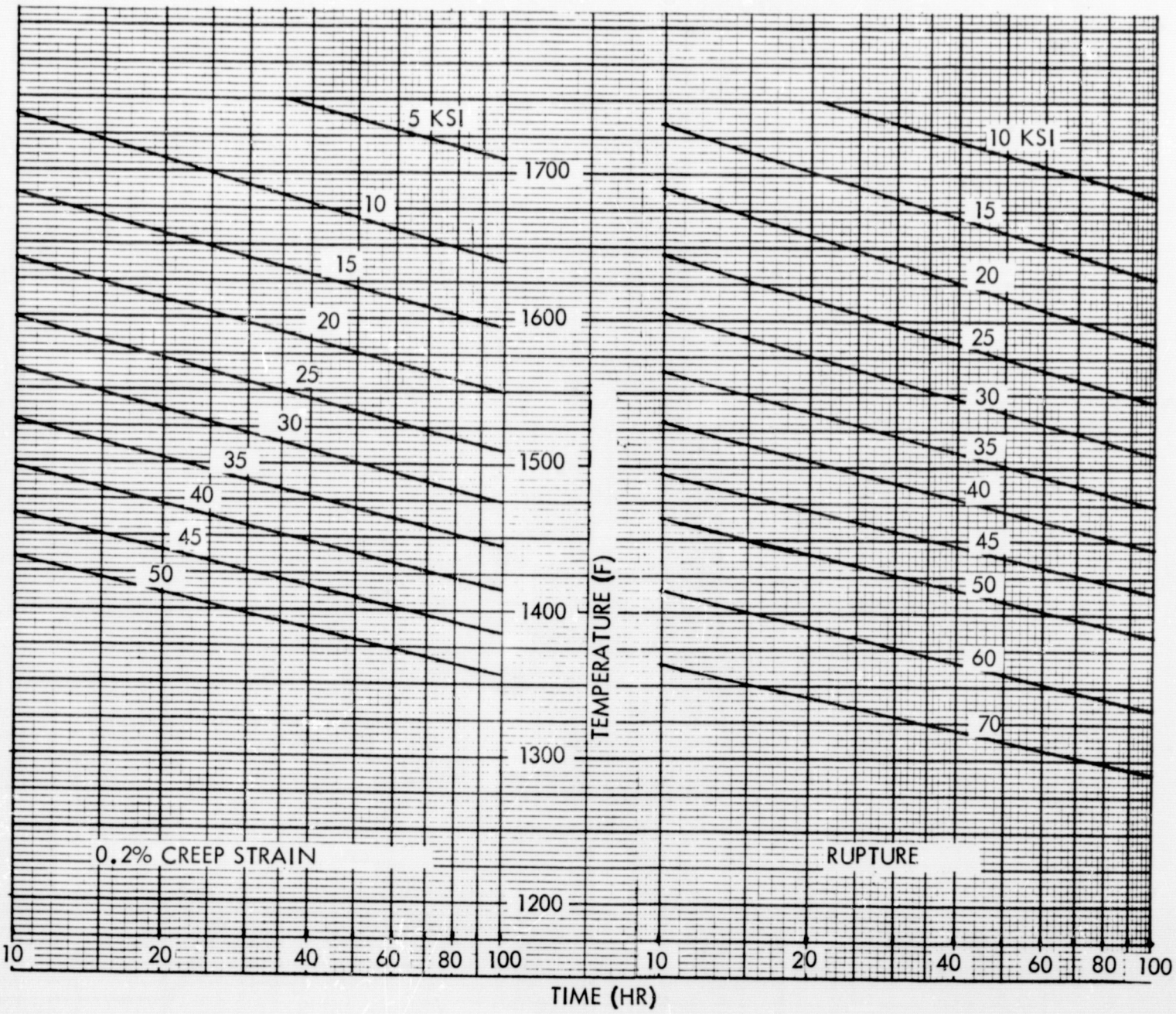

Figure 8.4-8. Creep Properties of René 41

Resistance (spot) welding can be done in the solution treated or the aged condition, but in either case it is followed by aging.

Rene'41 machines in a manner typical of the precipitation-hardening nickel base alloys. It is tough and gummy in the solution-treated condition and harder but less gummy as aged; therefore, it is usually machined in the aged condition. It work hardens rapidly, requiring positive feed and sharp tools, carbide for finishing, and cobalt high-speed steel for rough cuts.

Inconel 718. Inconel 718 is a precipitation-hardening alloy with good ductility and strength to 1300 F. It can be welded easily and has good resistance to post-weld (strain-age) cracking. Because of its good ductility, the alloy can be fabricated more economically than other precipitation-hardening nickel-base alloy. Mechanical and physical properties are outlined in Table 8.4-7.

Titanium 6 Aluminum 4 Vanadium (Ti6Al-4V). The trade-off studies described elsewhere in this report indicated that Ti 6Al-4V, because of its high strength-to-density ratio, is the most weight effective material currently available and has been selected as the primary structural candidate for the orbiter. It maintains excellent mechanical properties to 650 F with over-temperature capability to 1000 F; however, it is not expected to exceed 600 F on the shuttle application. Sheet and extrusion properties as extracted from Mil Handbook 5A and NR Material Specification LB0170-147, respectively, are listed in Tables 8.4-8 and 8.4-9.

Insulation - Internal

Insulative materials covering the temperature range from -423 F to 300 F are characterized in this section and properties are summarized in Figure 8.4-9. The majority of the materials considered are available now as production items but several, such as the phase change material and zirconia fibrous materials require further development.

Zirconia Fibers

Leading edge areas will reach temperatures in the 3000 F regime. Insulation materials to back up the diborides that will function efficiently and have reasonable life above 2700 F in an oxidizing environment have been difficult to locate. The material with the greatest potential of meeting most insulation ground rule requirements is Zircar, a zirconia fiber base family of high temperature insulation produced by Union Carbide Corporation. These yttria-stabilized zirconia materials are available in three woven or knitted cloth types and two mechanical-interlock felt types. Table 8.4-10 lists the properties of each type.

Table 8.4-7. Summary of Material Properties of Inconel 718

Material Properties	Minimum Guaranteed Values at Temperatures (F) and Exposure Times (hours) Specified													
	-420 NA*	-320 NA*	-200 NA*	-100 NA*	R. T. NA*	200 NA*	400 NA*	600 NA*	800 NA*	1000 NA*	1100 NA*	1200 NA*	1300 NA*	1400 NA*
Mechanical Properties														
F_{tu}(ksi)	219	210	200	192	180	175	170	167	164	158	153	145	128	88
F_{ty}(ksi)	188	177	165	158	150	146	142	139	137	134	130	125	108	84
F_{cy}(ksi)	188	177	165	158	150	146	142	139	137	134	130	125	108	84
F_{su}(ksi)**	134	128	122	117	113	107	104	102	100	97	93	89	78	54
F_{bru}(ksi) e/D = 1.5														
e/D = 2.0**	400	385	365	350	330	320	310	305	300	290	280	260	225	150
F_{bry}(ksi) e/D = 1.5														
e/D = 2.0**	310	290	270	260	250	240	232	228	225	220	212	200	174	130
Elongation (percent)	14	14	14	16	16	16	17	19	19	19	21	21	22	26
Physical Properties														
E (10^6 psi)	30.2	30.1	30.0	29.8	29.5	29.2	28.5	27.5	26.5	25.4	24.8	24.2	23.6	23.0
E_c (10^6 psi)	30.2	30.1	30.0	29.8	29.5	29.2	28.5	27.5	26.5	25.4	24.8	24.2	23.6	23.0
μ					0.29									
α (10^{-6} in./in./F)	4.5	4.9	5.4	5.8		7.2	7.5	7.7	7.8	8.0	8.2	8.3	8.6	8.9
k (Btu in./hr. sq. in. F)	0.33	0.37	0.42	0.46	0.51	0.59	0.67	0.76	0.86	0.94	0.98	1.01	1.06	1.11
c (Btu/lb F)					0.104									
ρ(lb/cu in.)					0.296									

*Exposure time does not apply to this material.
**Shear and bearing properties are based on ratios to tensile properties obtained on similar alloys.

Table 8.4-8. Design Mechanical Properties of Ti-6Al-4V (Sheet, Strip, and Plate) (From MIL HDBK 5A)

Alloy	MIL-T-9046 Type III, Comp C		
Form	Sheet, strip and plate		
Condition	Solution treated and aged		
Thickness or diameter, in. ≤ 0.1875			
Temperature (F)	RT	400	600
Mechanical properties:			
F_{tu} ksi	160	129.5	121.0
F_{ty} ksi	145	110.0	78.6
F_{cy} ksi			
L	154	115.5	100
F_{su} ksi	100	81.0	75.0
E, 10^6 psi	16.0	14.4	13.8
E_c, 10^6 psi	16.4	14.7	14.1
G, 10^6 psi	6.2	—	—
ρ lb/in.^{3}	0.160	—	—

Table 8.4-9. Ti-6 Al-4V Extrusions (Mechanical Properties - Conditions A, ST, and STA)

Extruded Thickness and Condition	Temperature	Tensile Strength (psi)	Yield Strength (psi)	Elongation (in.)		Reduction of Area (in.)	
				Long.	Trans	Long.	Trans
Condition A:							
(through 2 inches)	RT	130,000	120,000	10	4	20	15
	700	85,000	73,000	-	-	-	-
Condition ST:							
(through 2 inches)	RT		155,000	6	4	12	12
Condition STA:							
(through 1 inch)	RT	160,000	150,000	6	4	12	12
	700 F	110,000	90,000	-	-	-	-
(1.01 through 2 inches)	RT	150,000	140,000	6	4	12	12
	700 F	105,000	85,000	-	-	-	-

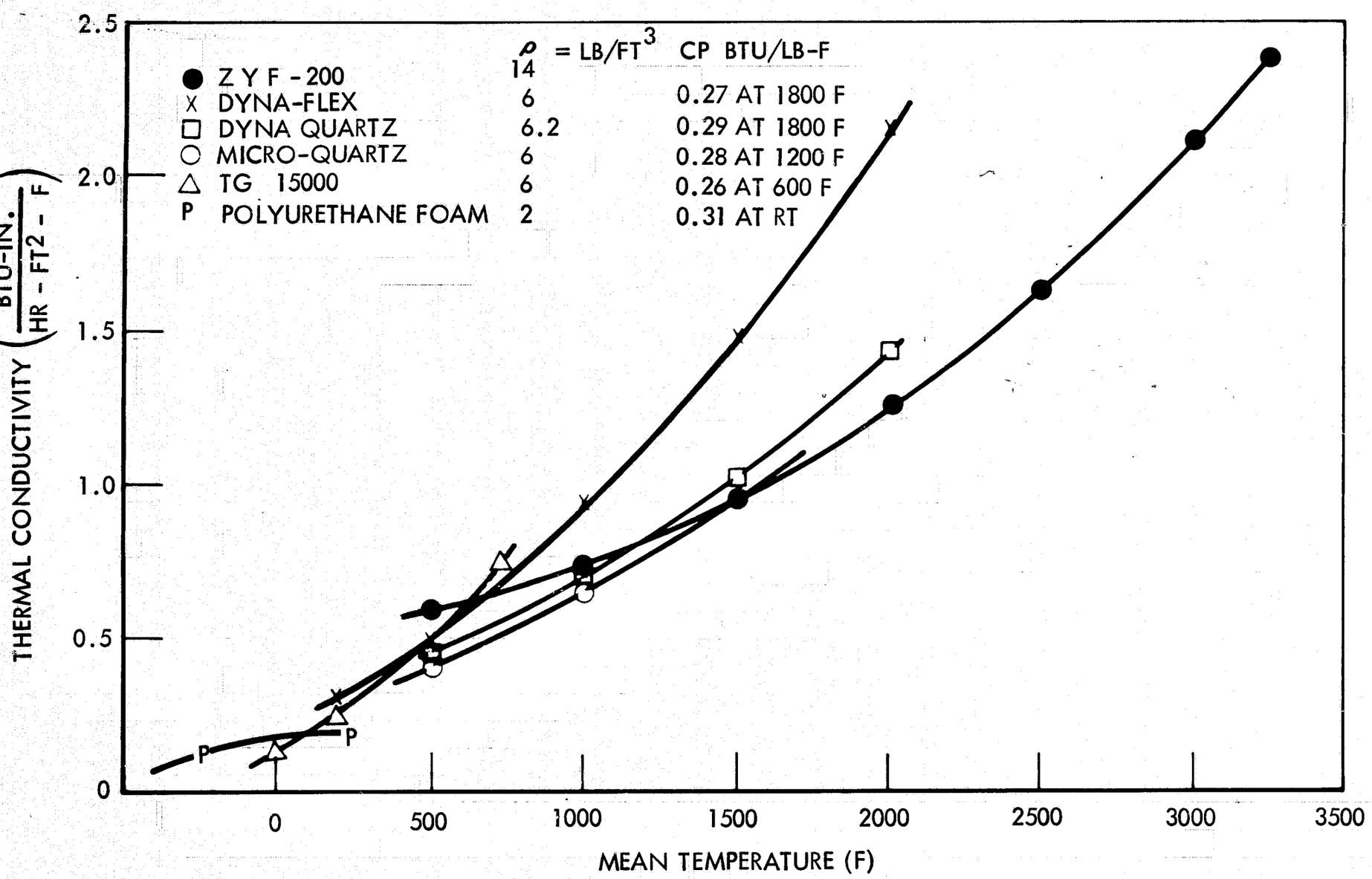

Figure 8.4-9. Typical Thermal Conductivity Properties of Insulation Materials

Space Division
North American Rockwell

Table 8.4-10. Zircar Product Forms and Properties

	ZYK-15	ZYW-15	ZYW-30	ZYF-100	ZYF-200
Thickness (mils)	14-17	13-15	28-31	80-100	180-200
Fabrication form	Knit	Weave	Weave	Felt	Felt
Fabrication type	Tricot	Plain	5-H satin	Needled	Needled
Weight (oz/yd)	10	8	22	15	30
Bulk density (lb/ft^3)	56	48	63	14	14
Breaking strength (lb/in. width)	1.0	2.5	6.0	1.5	3.0
Elongation at break (percent)	7.3	4.4	8.0	4.8	4.0

In addition to the product forms listed in Table 8.4-10, zirconia fibers are woven into a 15 mil thick, 3/8 inch wide braided tape in lengths up to 100 feet.

Zirconia offers the lowest thermal conductivity of any of the commercially available refractory materials. In the felted form, the thermal conductivity (Figure 8.4-9) is even further reduced. This low thermal conductivity is reportedly maintained even though the material stiffens on use at temperatures above 3000 F.

Zirconia, being a ceramic material, is inherently brittle. While the small 4- to 6-micron fiber diameter imparts a wide degree of flexibility to the textile forms, care still must be taken not to subject zirconia to shear loads which might be generated by tearing or grinding forces. This precaution is of greater concern once the material has been exposed to 3000 F or higher where material sintering and embrittlement takes place.

In addition, zirconia's service life is limited when placed in direct contact with carbon or carbon-silica leading edge materials, as well as insulation materials containing silica such as Dyna-Flex, Dyna-Quartz, or Micro-Quartz. Contact with these materials at elevated temperatures could cause zirconia to lose oxygen in a vacuum or form low melting compounds which could seriously impair insulation performance.

Since Zircar products are relatively new, long-term performance data are not available and, therefore, will have to be developed in the laboratory using ILRV performance criteria.

Dyna-Flex and Dyna-Quartz

In the temperature regime from 2000 to 2700 F, Johns-Manville alumina-silica-chromia base Dyna-Flex and high purity silica base Dyna-Quartz are the main candidate materials. Dyna-Quartz, available in densities from 4.5 to 12 lb/ft^3, is a semi-rigid material that can be molded into simple contours. Thermally efficient Dyna-Quartz is structurally poor and consequently must be supported and contained to permit attachment to the surrounding structure and prevent breakup due to vibrational loads. During installation, the insulation package must be carefully handled to prevent insulation damage that could be aggravated by flight loads. The package should be vented to permit depressurization and pressurization, and be structurally adequate to prevent insulation flexure. Foils and wire and screen containers from Hastelloy X and L605 are candidate package materials for temperatures up to 2000 F.

In contrast to Dyna-Quartz, Dyna-Flex is flexible and able to withstand substantial working of the material without failure. It can only be conjectured, since test data are not available, that the flexibility of Dyna-Flex does not degrade with exposure to flight thermal and mechanical loads. The more durable Dyna-Flex is less expensive by almost a factor of 10. The flexible nature of Dyna-Flex could also greatly ease installation and maintenance effort and consequently lower associated costs. The combination of flexibility, potential durability, and lower cost of material, manufacturing, and maintenance more than compensates for the higher thermal conductivity of Dyna-Flex and makes it the preferred insulation material over the temperature range from room temperature to 2700 F.

TG 15000

The TG 15000 material was selected as the intermediate insulation on the basis of weight, thermal efficiency, handleability, and cost. The properties of this material are listed in Table 8.4-11. The method by which the TG 15000 will be mounted, packaged, or contained has not been defined. TG 15000 is used successfully on the Apollo.

Superinsulation

Polyurethane foam will adequately fulfill the insulation requirements for the main tanks but is not sufficient to meet the more stringent requirements of space storage. Superinsulation is composed of multiple layers of metallized plastic film. The apparent conductivity is typically 4.8×10^{-4} Btu-in./hr-ft^2-F with advanced systems promising 4.8×10^{-5} Btu-in./hr-ft^2-F. The structural properties of superinsulation are basically those of Mylar or Kapton film. Maintenance of reflective

Table 8.4-11. TG 15000 Properties

Source	Hitco
Density	3 lb/ft ^{3}
Melting point	1200 F
Temp limit for multiple reuse	600 F
Shrinkage	0.5% at 700 F
Weight loss	12% max at 700 F
C_p (specific heat)	0.24 Btu/lb F at 200 F 0.27 Btu/lb F at 600 F
K (thermal conductivity)	0.6 Btu-in. /hr-ft^2-F at 600° F
K ρ	1.8 Btu-in. /hr-ft^2 -F x lb/ft^3

layer separation to reduce interlayer conduction and facilitate evacuation of trapped gases, attachment of the various multilayer blankets to surrounding tank structure, and the development of a reliable purge or vacuum bag cover for ground-hold conditions are problem areas which have not been fully resolved. Fabrication of a superinsulation system with the required purge bag and its associated plumbing would be more expensive than the polyurethane spray foam concepts to be discussed unless the purge system is a safety requirement to reduce hazards from possible hydrogen leakage.

Phase-Change Materials

Phase change materials have been studied to reduce overall insulation thickness and weight. Both solid-to-solid and solid-to-liquid systems have promise although the latter has packaging and attachment problems that detract from its overall effectivenss. Table 8.4-12 lists the potential materials and some of the available data. Additional materials are being sought.

Cryogenic Insulation

Polyurethane foam, two lb/ft^3 density, has proven to be an effective insulation material on the S-II stage of the Saturn launch vehicle. The technical and manufacturing data developed during the spray foaming of the S-II hardware are directly applicable to insulating ILRV integral or nonintegral cryogenic tanks. Development of a primer system that is compatible with mission parameters will be required. Maintenance/repairability of foam insulation on the S-II has been no great difficulty. In fact, the low maintenance required is one of the assets of this material. Typical thermal conductivity values for foam are shown in Figure 8.4-8. Other typical foam properties are listed in Table 8.4-13.

Table 8.4-12. Potential Phase Change Materials

Material	Heat of Fusion (ΔH_f) (Btu/lb)	Temperature (F)	ρ_s (lb/ft^3)	ρ_L (lb/ft^3)	ΔV (%)	$\rho \times \Delta H_f$ (Btu/ft^3)	T_B (F)	C_P S	C_P L	K (Btu/hr-ft-F) S	K (Btu/hr-ft-F) L	Remarks
1. Polyisoprene - trans	81	150 180	--	--			--	--	--	--	--	
2. Acetamide, C_2H_5ON	104	160	72	62	8	7500(L)	432	--	--	--	--	Melting temperature changes with time due to polymerization.
3. m-Stearic acid, $C_{18}H_{36}O_2$	85.5	157	52.8	47.5	10	4520 4070 (L)	455	0.399	0.550	0.093		Fatty acid, Baker USP grade, wax like. Slight H_2O solubility.
4. Bromocamphor, $C_{10}H_{15}OBr$	75	171	90.5	80	12	6800 (S)	526	--	--	--	--	Crystals or powder, H_2O insoluble, store in dark place.
5. Durene, $C_{10}H_{14}$	67	175	56	52	7.3	3750 (S)	380	--	--	--	--	Crystals, water insoluble. No shipping regulations.
6. P-Chloroaniline, C_6H_6CIN	67	160	89	--	--	5960 (S)	447	--	--	--	--	Yellow oil when produced.
7. Dotriacontane, $C_{32}H_{66}$	65	158	48	--	--	3140 (S)	591	--	--	--	--	Straight chain paraffin. Crystal possible availability problem.
8. Octacosane, $C_{28}H_{58}$	97-109	141	--	48.6	--	4700 4260 (L)	--	--	--	--	--	Straight chain paraffin. Possible availability problem.
9. Hydrogenated cottonseed oil	80	144	--	--	--		--	--	--	--	--	Low thermal conductivity.

Nomenclature:

Tm	Phase change temperature	$C_P(s)$	Specific heat of solid phase
$\rho(S)$	Density of solid phase	$C_P(L)$	Specific heat of liquid phase
$\rho(L)$	Density of liquid phase	K(S)	Thermal conductivity of solid phase
ΔV	Change in volume	K(L)	Thermal conductivity of liquid phase
T_B	Boiling temperature		

The only practical limitation with using the well-developed S-II spray foam insulation for main ILRV cryogenic tankage is the maximum upper temperature allowable if the zero refurbishment criterion is to be observed. Thermal gravimetric analysis data indicate that the foam starts to degrade significantly at temperatures above 175 F. Higher operating temperature (300 F) polyurethane foams are becoming available; however, time has not been sufficient to fully characterize their thermal, mechanical, and processing properties for this ILRV study.

Standoff Materials

Supports or standoffs for the thermal protection system for metallic heat shield panels require an insulating capability to minimize heat conduction to the internal supporting structure. The metallic portion of the standoff may be made of materials identical to the support structure, and will not be discussed further. The insulating capability must derive from nonmetallic materials inserted between the metallic portions.

The alumina ceramics are made in different grades containing varying Al_2O_3 contents from about 85 to 99.9 percent. The high purity

Table 8.4-13. Typical Properties of Polyurethane Foam

	Temperature, F			
Density (lb/ft^3) 1.8 ± 0.2	-423	-300	RT	+150
Tensile strength				
Parallel to rise (psi)		45	62	44
Normal to rise (psi)		32	41	34
Compression strength				
Parallel to rise (psi)		42	22	22
Normal to rise (psi)		43	22	22
Shear strength				
Parallel to rise (psi)	35		37	32
Normal to rise (psi)	25		24	23
Coefficient of expansion (in./in. F)	(50 to -300 F) 5.8×10^{-5}			
Percent closed cells	90.4			

grades generally have higher strengths (especially at elevated temperature) and higher elastic moduli. For high-temperature applications requiring structural capability, the 96 to 99.5 percent alumina grades have the best combination of mechanical properties. The 99 to 99.5 percent grades have higher thermal conductivity, making them potentially slightly more resistant to thermal shock, while the 96 percent grade would be better as a thermal isolator. There is considerable variation in properties, depending on the manufacturer. Figure 8.4-10 presents properties of some of the alumina ceramics. The high alumina ceramics melt at approximately 3500 F and are quite stable in air. They have good but not outstanding thermal shock resistance (relative to other ceramics). Because of their brittleness, the high alumina ceramics are susceptible to fracture if local strains exceed the capability of the material, i.e., local yielding does not occur. Tensile stresses and stress concentrations must be minimized and attachments must be designed to minimize the possibility of thermally induced stresses. Because dense alumina ceramics are very hard and cannot be machined except with diamond tools, they are normally procured in the shape in which they are to be used. Joining is normally by mechanical fastener with precautions to avoid stress concentration.

Pyroceram* is a name applied to a group of ceramics formed by crystallization from a glassy state. Corning grade 9608 has properties that are attractive for the thermal insulation function in a standoff with an operating temperature up to approximately 2000 F. These properties are a combination of good strength (10 ksi modulus of rupture at 1800 F), low thermal conductivity (1.25 Btu/hr ft F at 1650 F), and very good thermal shock resistance. In common with other ceramics, Pyroceram is brittle and design must take this into consideration.

For areas involving a maximum temperature of 1200 F or less, asbestos-silica board (Marinite**) may be used as thermal insulation structurally. Typical modulus of rupture is low (1500 psi for 65 pounds per cubic foot material), but the material is not as sensitive to stress concentration as the ceramics (normal fastener techniques can be used) and, therefore, may be preferred in the applicable temperature range. Thermal conductivity is low, approximately 0.15 Btu/hr ft F in the temperature range up to 1200 F. Lower densities (23 and 36 pounds per cubic foot) are available but are not as suitable for structural application as the higher density material.

---

* TM, Corning Glass Works
** TM, Johns-Mansville

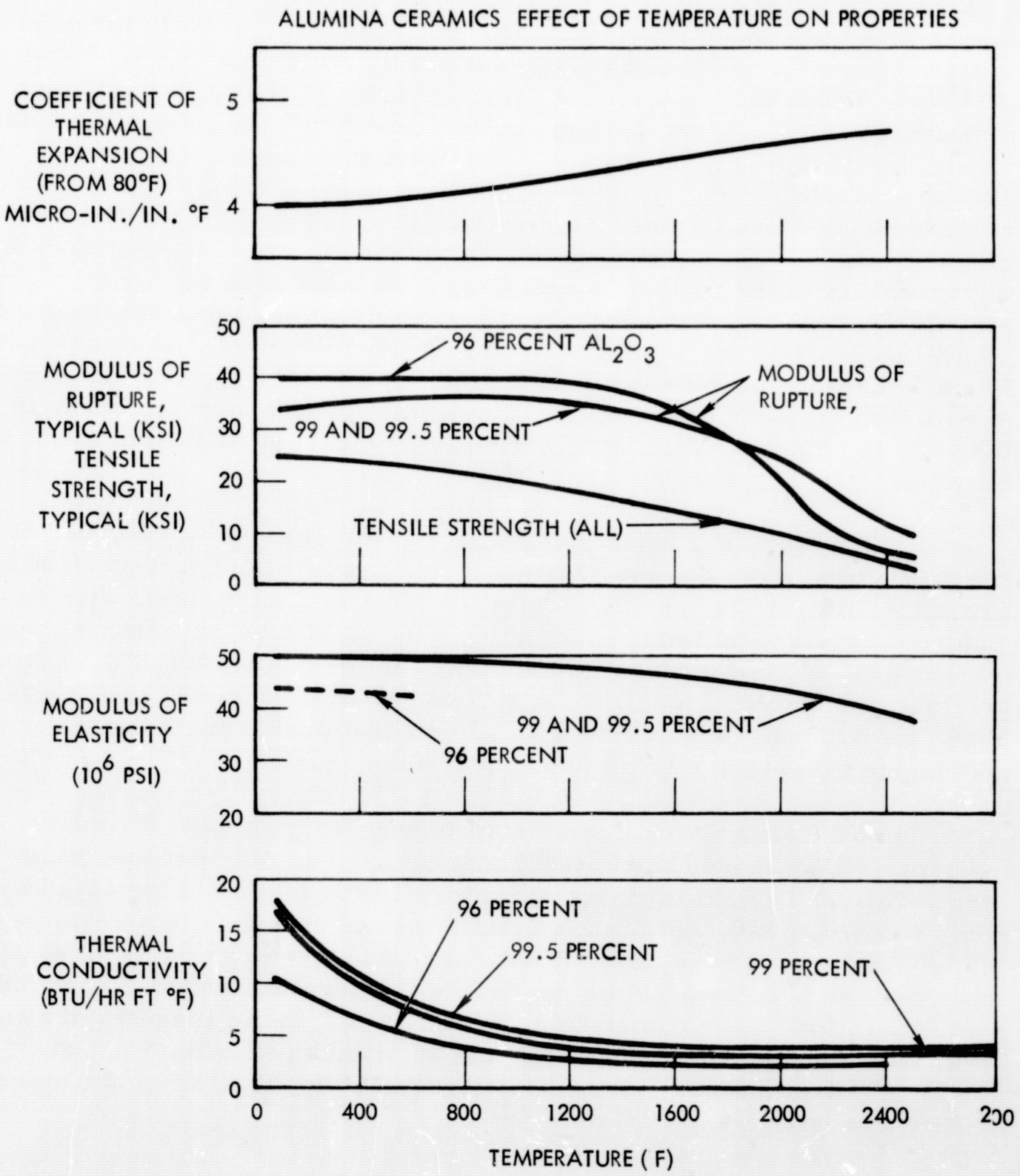

Figure 8.4-10. Typical Properties of Alumina Ceramics

8.4.4 Structure

Structural metallic materials have been previously characterized for heat shield application. Hot structure use of these materials as well as nonmetallic laminates and cryogenic tankage are also to be considered.

Hot Structure

Material properties for Haynes 188, René 41, Inconel 718, and Ti-6Al-4V are listed in previous paragraphs. When the metals are used in "hot structure," the maximum temperature must be reduced to levels commensurate with the structural requirements. Table 8.4-14 gives approximate maximum temperatures for such structural use.

Cool Structure

The configurations depicted in the TPS and the Structures sections of this document utilize a plastic sandwich as the outer member of the booster structure. Two materials have been selected for this application based on the location and maximum temperatures anticipated.

A phenolic sandwich, consisting of two-ply facing sheets and HRP honeycomb core of 3- or 4-pound density, will be used as a support structure under the external insulation. Significant areas of the outer shell of the upper side of the vehicle will not have external insulation and the sandwich will be the outer vehicle surface. A polyimide sandwich, consisting of two-ply facing sheets and HRH honeycomb core of 3- or 4-pound density, will be used for the outer shell structural laminate. Preliminary values for the two-ply laminate sandwiches are presented in Table 8.4-15.

Ti-6Al-4V, Al-2219, and Al-7075 will also be utilized as required for cool structure (<300 F). Al-7075, in the T73 temper for use where a stress corrosion potential exists and the T6 temper for other areas is described in Table 8.4-16. The T76 temper is also available.

Table 8.4-14. Approximate Maximum Temperatures for Hot Structure Applications

Material	Temperature (F)
Haynes 188	1800
René 41	1600
Inconel 718	1200
Ti 6Al 4V	650

Table 8.4-15. Preliminary Numbers for Design Tradeoffs

1. Phenolic sandwich, two-ply facing sheets, 1 inch HRP core 4-pound density, 100 hours exposure

	70 F	400 F
Tensile ultimate stress	36,000 psi	27,000 psi
Tensile modulus	3.2×10^6 psi	3.0×10^6 psi
Edgewise compressive ultimate stress	34,000 psi	27,000 psi
Edgewise compressive modulus	3.2×10^6 psi	2.9×10^6 psi
Flexure ultimate stress	49,000 psi	40,000 psi
Flexure modulus	3.1×10^6 psi	2.6×10^6 psi

2. Polyimide sandwich, four-ply facing sheets, 1 inch HRH core 4-pound density, 100 hours exposure

	70 F	600 F
Edgewise compressive ultimate stress	39,000 psi	16,000 psi
Flatwise compressive stress	700 psi	320 psi
Core shear	170 psi	80 psi

3. Polyimide laminate, 1/8 inch, 100 hours exposure

	70 F	400 F	600 F
Tensile ultimate stress	40,000 psi	33,000 psi	29,000 psi
Tensile modulus	2.7×10^6 psi	2.3×10^6 psi	2.1×10^6 psi
Compressive ultimate stress	32,000 psi	19,000 psi	13,000 psi
Compressive modulus	2.8×10^6 psi	2.5×10^6 psi	2.3×10^6 psi

Table 8.4-16. Design Mechanical and Physical Properties of Clad 7075 Aluminum Alloy (MIL HDBK 5)

Alloy	QQ-A-250/13 (Clad 7075)							
Form	Sheet							
Condition	-T6							
Thickness, in	0.012-0.039		0.040-0.062		0.063-0.187		0.188-0.249	
Basis	A	B	A	B	A	B	A	B
Mechanical properties:								
F_{tu} ksi								
L	70	73	72	74	73	75	75	77
LT	70	73	72	74	73	75	75	77
ST	....	....	....	....	....	....	....	....
F_{ty} ksi								
L	61	64	63	65	64	66	65	67
LT	60	63	62	64	63	65	64	66
ST	....	....	....	....	....	....	....	....
F_{cy} ksi								
L	62	65	64	66	65	67	66	68
LT	64	67	66	68	67	69	68	70
ST	....	....	....	....	....	....	....	....
F_{su} ksi	42	44	43	44	44	45	45	46
F_{bru} ksi [a]								
(e/D = 1.5)	105	110	108	111	110	112	112	116
(e/D = 2.0)	133	139	137	141	139	142	142	146
F_{bry} ksi [a]								
(e/D = 1.5)	85	90	88	91	90	92	91	94
(e/D = 2.0)	98	102	101	104	102	106	104	107
e, percent								
L	7	....	8	....	8	....	8	....
LT	7	....	8	....	8	....	8	....
ST	....	....	....	....	....	....	....	....
E, 10^6 psi								
Primary	10.3				10.3		10.3	
Secondary	9.5				9.8		10.0	
Ee, 10^6 psi								
Primary	10.5				10.5		10.5	
Secondary	9.7				10.0		10.2	
G, 10^6 psi	....				....		....	
μ	0.33							
α, lb/in.^{3}	0.101							

Cryogenic Tankage

The aluminum alloy, 2219, in the T87 temper, has been selected as the primary candidate material for the LO_2 and LH_2 fuel tanks because of its resistance to stress corrosion, weldability-fabricability qualities, cryogenic properties, and strength in the short transverse direction. Material properties are listed in Table 8.4-17.

8.4.5 Advanced Composites

The potential weight savings of advanced composites, as indicated in the Structures section, appears extremely attractive compared with conventional constructions, even with raw materials costing significantly more.

Highly loaded areas of the shuttle vehicles were considered for potential composite use since advanced composite materials are highly efficient on a strength-to-density and a stiffness-to-density basis. Because of geometric configurations, however, not all of these areas are suitable to composites

Table 8.4-17. Aluminum 2219 T87 Properties
(0.040- to 0.249-Inch)

Property		Temperature, F			
		175	70	-150	-323
F_{tu} ksi	L	58.5	63	68	78.5
	T	59.5	64	69	79.7
F_{ty} ksi		48.3	52	55.8	62
F_{cy} ksi	L	48*	52	56*	62*
	T	51*	55	58*	65*
F_{pl} ksi		36	40	43	46
F_{su} ksi		33*	37	40*	43*
E x 10^6 psi		10.4	10.5	11.2	11.8
G x 10^6 psi			4.0		
ρ lb/in.^{3}			0.102		
α 10^{-6} in./in./F			12.7 (RT to 300 F)		

*Preliminary values

(composites are most efficient when fibers can be placed in a uniaxial direction). Typical mechanical properties are outlined in Table 8.4-18.

Major weight savings may be achieved through the use of the composites described in areas which have the common factors of high loads applied in substantially invariant directions, relatively low operating temperatures (less than 350 F), and applicability to general classes of aerospace parts. Possible applications include corrugation stiffened fuselage panels, landing gear frame, and honeycomb sandwich thrust cone. Weight savings of about 50 percent over the most efficient conventional structure may be shown for the application described.

The reduction in properties at 350 F indicates that a matrix material with higher temperature capabilities may be required to effectively utilize the properties of the fibers.

Since glass fabric laminates utilizing polyimide resin show excellent retention of mechanical properties for long times at temperatures up to 600 F, this resin system is an obvious candidate matrix. Preliminary work on advanced composites utilizing this matrix is now underway.

8.4.6 Fracture Mechanics

Fracture mechanics techniques are applicable to a number of areas during the design phases of a program. Initially, fracture toughness as a material property is used as one of the material selection criteria as in the case of ILRV pressure vessels where 2219 aluminum was selected. Other areas where fracture mechanics will be applied as design and fabrication proceed include process selection, design criteria definition including margin of safety, inspection philosophy, and pressure vessel proof-testing plan for acceptance, and as a measure of remaining life during operation.

Table 8.4-18. Design Mechanical Properties

Fiber/Resin	Temperature (F)	Uniaxial Tension			Edgewise Compression
		Ultimate		Modulus	Ultimate
		0° (ksi)	90° (ksi)	0° (psi)	0° (ksi)
Graphite-epoxy	75	150	10	25×10^6	180
	350	105	7	18×10^6	120
Boron-epoxy	75	180	10	30	250
	350	137	7	(20)	(150)

Values ( ) are estimated. Other values represent design data developed at NR Space Division.

PRECEDING PAGE BLANK NOT FILMED.

8.5 STRUCTURES ANALYSIS

The structure analysis was directed toward evaluation of candidate structure/thermal protection concepts and configurations, and definition of the structural elements of selected orbiter and booster vehicles. Emphasis was placed upon development of a structure definition that would facilitate generation of accurate weight estimates.

This section of the report contains design criteria, material mechanical properties, and the design temperatures and loads of the ILRV; a review of the baseline vehicle structure definition developed by NASA MSC; several trade studies used to select the structural concept where it was not obvious which structural concept would be lighter; and structural analysis in support of the preliminary design of the orbiter and booster vehicles. Some potential weight saving concepts came to light after most of the analyses were completed. These studies, which were not made, are identified at the end of this section.

This analysis identifies the structural concepts, materials, and material sizes required for the components of the orbiter and booster. In addition to establishment of the structural integrity of the vehicles and the structure sizes, calculation of the weight of the structure for both vehicles was achieved through the analysis.

Wherever detailed information was not available for structural analysis, statistical data were recommended for the structural weights. Examples where statistical data were used are the leading edges and control surfaces of the wings, and the horizontal and vertical tails. Other examples are the nose gear and main gear for both vehicles.

8.5.1 Design Criteria

Structural Design

The design philosophy and criteria governing preliminary structural design of the flight vehicles for the ILRV system are defined as follows:

1. Design Philosophy

   The structure shall possess sufficient strength and rigidity to service the critical loading conditions and associated environments that exist within the envelope of mission requirements.

The structure shall be designed to survive the specified number of missions with a minimum of structural refurbishment, and in a manner that does not reduce the probability of the successful completion of any mission. Consideration shall be given to the cumulative deteriorating effect of repeated exposure to the critical environment conditions, such as temperature, creep, and fatigue.

The structure shall be designed by flight conditions wherever possible. The nonflight conditions and environment shall influence the design to the minimum extent.

2. Design Conditions and Environments

All factors that can influence the structural design shall be considered. These factors will include heating, vibration, shock, acoustics, and aerodynamic buffeting.

a. External and Internal Load Distribution

External loads shall be determined by conservative analyses of the design environment. The aerodynamic loads may be determined from appropriate wind tunnel tests or calculated by sound engineering methods.

b. Combined Loads and Internal Pressure

When internal pressure, such as that experienced in the propellant tanks, results in a stabilizing effect or otherwise benefits the structural load-carrying capability, the minimum limit internal operating pressure shall be used instead of using the ultimate design internal pressure.

c. Malfunctions

The vehicle structure shall be designed to provide for safe mission termination in the event that two subsystem failures occur.

d. Load and Thermal Fatigue

The effects of repeated loads and elevated temperature shall be considered in the structural design. The structural adequacy of the vehicle in flight shall not be impaired by fatigue damage resulting from exposure to nonflight and launch environments.

e. Vibrational and Acoustical Loadings

The effects of the vibrational and acoustical environments shall be considered a part of the overall loading.

f. Creep Deformation

The effects of permanent creep deformation shall be considered.

g. Thermal Stresses

The effects of thermal stresses shall be combined with the appropriate load stresses when calculating required strength. Thermal stresses shall be based on the applied temperatures, heating rates, etc., and shall not be multiplied by a factor of safety.

3. Material Properties and Allowables

a. Sources

Conventional material strengths and other mechanical and physical properties shall be selected from authorized sources such as MIL-HDBK-5A and from contractor test values when appropriate. Allowable strengths and other mechanical properties used shall be appropriate to the loading conditions, design requirements, and stress states for each structural member.

b. Values

Allowable material strengths used in design shall reflect the effects of load, temperature, and time associated with the design environment. Allowable yield and ultimate properties will be as follows:

(1) Minimum guaranteed values for single-load-path structures.

(2) 90-percent probability values for multiple-load-path structures.

4. Design Strength Requirements

   a. At Limit or Applied Load

      The structure will be designed to have sufficient strength to withstand simultaneously the limit loads, applied temperature, and other accompanying environmental phenomena for each design condition without experiencing any permanent deformation.

   b. At Ultimate Load

      The structure will be designed to withstand simultaneously the ultimate loads and applied temperature without failure. No factor of safety is applied to the temperature.

5. Stiffness Requirements

   a. Under Limit Loads

      Up to limit loads, the structure will not experience deformation that would significantly reduce the probability of the successful completion of any mission.

   b. Under Ultimate Loads

      Structural deformations will not precipitate structural failure during any design conditions and environment at loads less than ultimate loads.

   c. Aerolastic Requirements

      Destructive flutter, other related dynamic instability, or divergence phenomena will not occur on the vehicles or their components at any condition along the design trajectories.

6. Thermal Requirements

   Aerodynamic heating will be based on the design trajectories.

   Thermal effects on the structure, including heating rates, temperatures, thermal stresses, and deformations, and mechanical and physical property changes, will be based on the critical design heating environment.

7. Limit Load Factors

The limit load is the maximum anticipated combination of loads. The limit load factors will be determined for preliminary design based on the following constraints.

a. Ascent - Nominal maximum longitudinal load factor will be n = 3.0 g.

b. Reentry - Minimize the maximum surface temperature of the vehicle.

c. Low-Speed Flight - Maximum normal load factor will be limited to n = 2.5 g.

d. Landing - Landing load factor will be 2.68 g.

8. Dynamic Amplification Factors

The following dynamic amplification factors will be applied to the results of the rigid-body limit loads analysis:

a. Landing, nose gear, 1.60

b. Landing, main gear, 1.20

c. Maximum $q\alpha$ during boost, 1.10

9. Ultimate Factors of Safety (Factor used in multiplying limit load)

a. Aerodynamic, landing, thrust, and associated inertia-loads, 1.50

b. Propellant tank pressures, 1.50

c. Personnel compartment pressures, 2.00

10. Lifetime

The proposed lifetime will be based on 100 orbiting missions with the associated flight testing and ferrying.

8.5.2 Material Properties

Tables 8.5-1a, -1b, -1c, and -1d indicate the materials and their mechanical properties used in the structural analyses.

Table 8.5-1a. Materials Properties

	Aluminum 2219-T87				Titanium 6AL-4V STA		
Property	175 F	70 F	-150 F	-297 F	70 F	400 F	600 F
F_{tu} (ksi)	58.5 59.5	L 63 T 64	68 69	75.6 76.8	160	129.5	121.0
F_{ty} (ksi)	48.3	52	55.8	61	145	110.0	98.6
F_{cy} (ksi)	48* 51*	L 52 T 55	56* 59*	61* 64*	L 154 T 162	115.5 121.5	100.0 105.3
F_{pl} (ksi)	36	40	43	46	130	95	85
F_{su} (ksi)	33*	37	40*	43*	100	81.0	75.0
E (10^6 psi)	10.4	10.5	11.2	11.7	16.0	14.4	13.6

GLASS-REINFORCED-PLASTIC, TWO-PLY LAMINATE FACINGS FOR HONEYCOMB SANDWICH, SINGLE-STAGE MOLDED PARTS

	Phenolic		Polyimide		
	70 F	400 F	70 F	400 F	500 F
F_{tu} (ksi)	36	27	40	33	29
$F_{c_{local}}$ (ksi)	34	27	32	19	13
E_c (10^6 psi)	3.2	2.9	2.8	2.5	2.3
E_t (10^6 psi)	3.2	3.0	2.7	2.3	2.1

*Preliminary Data

Table 8.5-1b. Materials Properties, Rene' 41 1650 F Age
(Preliminary Values)

Property	Temperature		
	70 F	1000 F	1700 F
F_{tu} (ksi)	140	130	25
F_{ty} (ksi)	97	90	23
F_{cy} (ksi)	99	93	22
F_{pl} (ksi)	73	65	16.5
F_{su} (ksi)	84	—	—
E (10^6 psi)	31.6	26.5	12.0

Table 8.5-1c. Materials Properties, Inconel 718

Property	Temperature		
	70 F	1000 F	1400 F
F_{tu} (ksi)	180	158	88
F_{ty} (ksi)	150	134	84
F_{cy} (ksi)	150	134	84
F_{pl} (ksi)	120	115	75
F_{su} (ksi)	113	97	54
E (10^6 psi)	29.5	25.4	23

Table 8.5-1d. Materials Properties,
Aluminum 2014-T6

Property	Temperature			
	175 F	70 F	-150 F	-297 F
F_{tu} (ksi)				
L	61	65	69	73.5
T	60	64	68	72.3
F_{ty} (ksi)				
L	56	58	61	66
T	55	57	60	65
F_{cy} (ksi)				
L	54	58	61*	66*
T	54	58	61*	66*
F_{pl} (ksi)	46	53	56*	61*
F_{su} (ksi)	37	39	41*	42*
E (10^6 psi)	10.3	10.5	11.1	11.7

*Preliminary values.

8.5.3 Baseline Vehicle Structure Review

To facilitate definition of sizes of vehicles to deliver payloads up to 50,000 pounds, the baseline vehicle configured by NASA/MSC to deliver a 12,500-pound payload was reviewed and structure weight factors were established.

Computation of the loading environment for the baseline vehicle was based upon projected aerodynamic characteristics and the prelaunch and flight conditions. The design limit loads for the baseline vehicle body and wing are presented in Tables 8.5-2 and 8.5-3 respectively.

The baseline vehicle structure and thermal protection system (Figure 8.5-1) were reviewed; and it was concluded that the basic concept provides a low-weight, reliable design. Vehicle size and feasibility are influenced significantly by structure weight; therefore, the baseline vehicle structure was analyzed to establish weights.

Table 8.5-4 shows the structure items considered, their estimated weight, and source of the weight estimate. The propellant tankage, thrust structure, and skirts, represent 70 percent of the total calculated weight. Confidence in the tankage weight estimate is high, because the analytical model used predicts the actual S-II stage tankage weight very closely. The calculated weight for the baseline vehicle (12,500-pound payload) is increased by 5,391 pounds to account for unknowns and contingencies, which represent a 10-percent increase in tankage weight and a 100-percent increase in other structural elements that were not subjected to detailed analysis at this stage of the study. The total weight represents a body structural weight factor of 3.35 pounds per square foot at 6,000 square feet of body wetted area.

Orbiter configurations with the large cargo bay located at the stage c.g. may require more complex tankage and noncontinuous tankage; therefore, tankage may not provide the best primary load-carrying structure. The relative merits of integral and suspended tankage were analyzed in trade studies that are documented later in this section.

Comprehensive structural analyses were later performed on a selected vehicle (50,000-pound payload), and the structure weights established for the baseline system were used to generate weight scaling factors for the initial sizing of the selected vehicle.

Table 8.5-2. Body Structure Design Loads

Loads Stations	Condition	Limit Loads		
		Shear x 10^{-3} (lb)	Axial x 10^{-3} (lb)	Moment x 10^{-6} (in.-lb)
Booster				
Holddown station	Prelaunch	-68	-1351	132
Main landing gear	Max q α	-446	-1489	-156
	Landing	-150	-85	-95
Aft attachment	Max q α	340	-1561	-66
	Landing	95	-30	-60
Fwd attachment	Landing	46	-15	-9
	Max q α	-31	-113	5
Orbiter				
Aft attachment	Max accel	3	-960	-
	Max q α	-24	-622	-18
Main landing gear	Max q α	86	-477	-37
	Landing	-60	-35	-28
Fwd attachment	Landing	62	-21	-18

Table 8.5-3. ILRV MSC Configuration Wing Limit Load

	Orbiter at 103-in. From $\mathbb{C}_L$		Booster at 156 in. From $\mathbb{C}_L$	
Condition	Shear x 10^{-3} (lb)	Moment x 10^{-6} (in.-lb)	Shear x 10^{-3} (lb)	Moment x 10^{-6} (in.-lb)
Max q α	-162.0	14.8	-487.0	86.2
2.5-g maneuver	-90.0	8.0	-120.0	19.1

NOTE: Loads include dynamic factor
1.1 for max q α
1.25 for 2.5-g maneuver

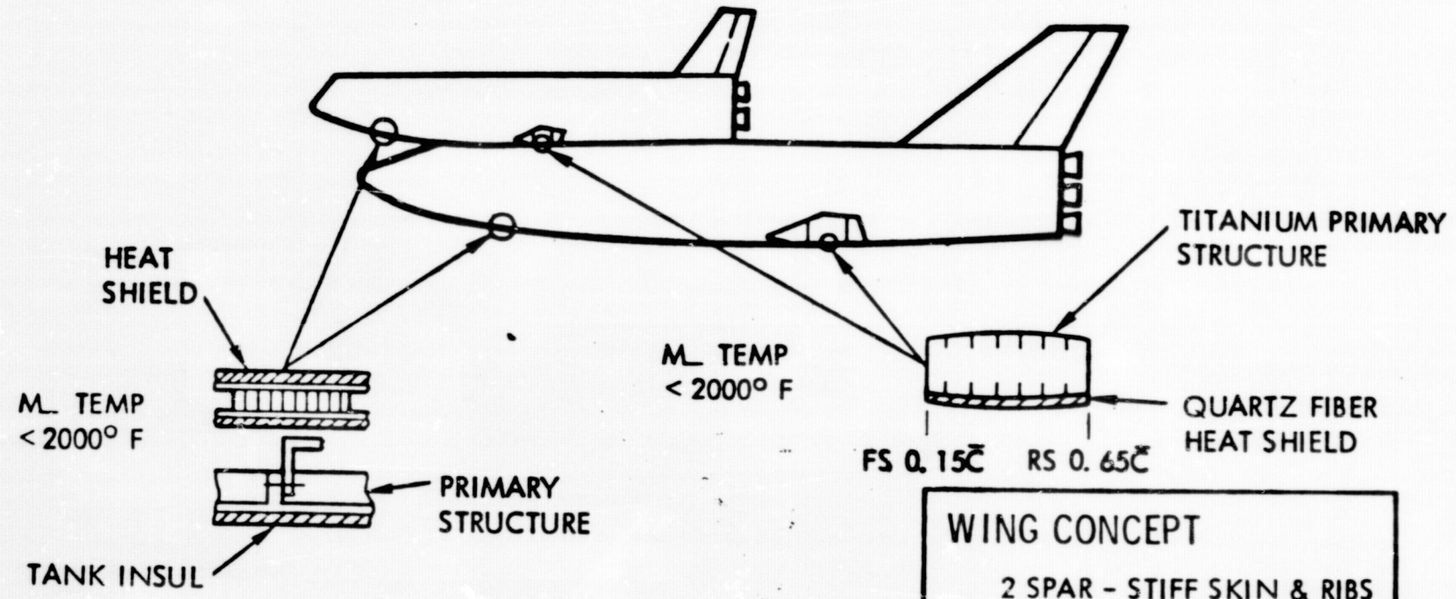

WING CONCEPT
2 SPAR - STIFF SKIN & RIBS

- TITANIUM GOOD F_{TU}/ρ (RT - 800°F)
- MAINTAIN SAME TEMP UPPER & LOWER M_ - GOOD STRUCTURING
- STIFFENED SKIN - OK FOR LOW LOADING INDEX
- HIGH ASPECT RATIO MAY PRESENT FLUTTER PENALTY
- WING TO FUSELAGE ATTACHMENT GOOD-MINIMIZES THERMAL STRESS & DEFORMATION

FUSELAGE CONCEPT
INTEGRAL TANK FRAMES & STIFF SKIN

- EFFICIENT STRUCTURAL CONCEPT
- ALUMINUM GOOD F_{TU}/ρ AT CRYOGENIC TEMP (2219AL)
- DEEPER STABILITY FRAMES-INCREASE EFFICIENCY
- FIBERGLASS FRAMES - DECREASE HEAT SHORT
- STRUCTURAL TEMP 175°F MAX - LIMITED BY POLYURETHANE FOAM REUSE

Figure 8.5-1. Baseline Structures Review

Table 8.5-4. Structural Weight Estimates for Baseline/Orbiter Body and Tankage (12,500-Pound Payload)

Item	Weight (lb)	Source
Cockpit	600	From Sabreliner
Passenger Cabin	1,122	Ratioed from DC-10
Transition Structure, Tank to Cabin and to Nose Gear	400	Estimated
LO_2 Tanks	1,760	Analysis based on S-II data
Common Bulkhead	1,110	Analysis plus ratio of S-II data for waffle as percent of bulkhead
LH_2 Tank	5,275	Analysis based on S-II data
LH_2 Aft Tank Bulkhead	195	Analysis
Aft Skirts	517	Estimated
Thrust Structure	1,400	Scaled from S-II
Special Tank Rings		
Wing to body	541	Analysis
Vertical and horizontal tail	860	Analysis
Fwd attach to booster	400	Ratioed from wing to body ring
Drag Structure for Aft Attach to Booster	524	Analysis
Calculated Weight Subtotal	14,704	
Unknowns and Contingency	5,391	10 Percent of tankage, thrust structure, and skirts 100 percent other structural elements
Total	20,095	

8.5.4 Loading Conditions and Temperatures

The vehicle configuration used as a basis for trade studies was configured to deliver a 50,000-pound payload. This vehicle, for which loading conditions were computed, is illustrated in Figures 8.2-13 and 8.2-14 (References 2234-68 and 69). Detailed loads information is shown in Section 7.6. The configuration illustrated was updated during the final phase of the study to reflect the results of detailed subsystem analyses and revised subsystem weights and vehicle sizes. This final configuration is shown in Figures 8.2-26 and 8.2-23 (Reference 2234-76 and 79). In general, the final vehicle configuration is similar to the baseline for a 50,000-pound payload, and most of the loads are applicable to the final configuration. Wherever a significant difference occurred, the loads were adjusted. One example is the shortening of the span between the forward and aft booster/orbiter attachment. This increases the coupling loads and the loads were ratioed upward by the ratio of the old span over the new span.

Critical design conditions are identified in this report in the analysis section for each component.

Critical load conditions for the orbiter and the booster are shown in Figures 8.5-2 and 8.5-3. The design load intensity for body bending and axial loads is shown in Figure 8.5-4 for both vehicles. It is noted that the maximum booster body load intensities are twice the maximum orbiter body load intensities and also that most of the body will be designed by compression loads.

Structural temperatures can be divided into two classes. The first class comprises all structure that is protected by the LI-15 external insulation. Here, insulation thickness is based on limiting the adhesive-bonded interface to a maximum temperature of 400 F. The other class of structural temperatures is for the components that are not protected. Booster and orbiter temperatures are shown in Figure 8.5-5.

8.5.5 Structure and Thermal Protection Trades

In several areas, the structural concepts, materials and thermal protection systems that are best for these vehicles are not obvious. Trade studies were performed to establish the concepts that would result in the lowest weights without consideration for cost. In future studies, these and other weight saving concepts can be related to the costs per pound of weight saved. In the final decision, these data can be related to some allowable cost per pound of weight saved for each of the two vehicles.

Trade studies of potential weight savings, which were discerned in the latter phases of this contract, but which have not been performed, are indicated in Section 8.5.9.

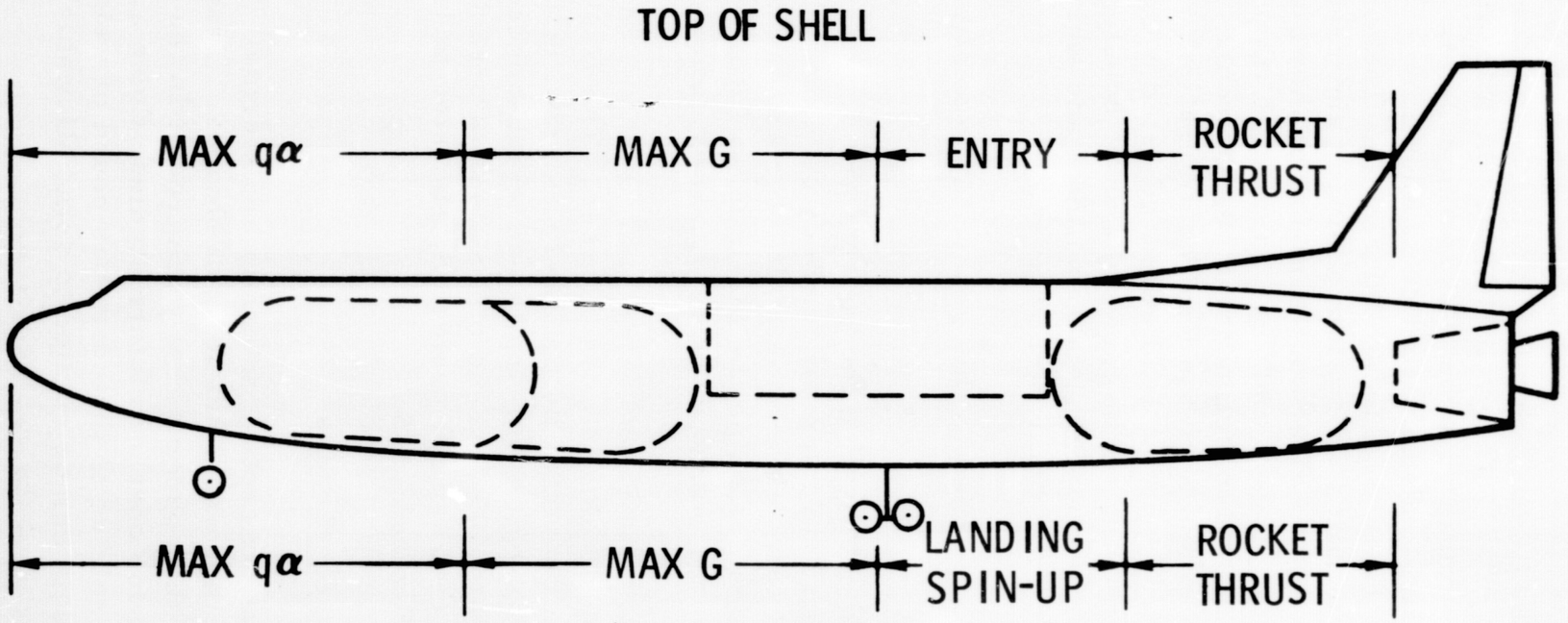

- ALL LIFTING & CONTROL SURFACES DESIGNED BY MAX qα
- ALL TANKS DESIGNED BY MAXIMUM G
- PAYLOAD LONGITUDINAL BENDING CRITICAL FOR LANDING
- PAYLOAD LONGITUDINAL LOADS CRITICAL FOR MAXIMUM ACCELERATION

Figure 8.5-2. Orbiter Critical Load Conditions

Figure 8.5-3. Booster Critical Load Conditions

Space Division
North American Rockwell

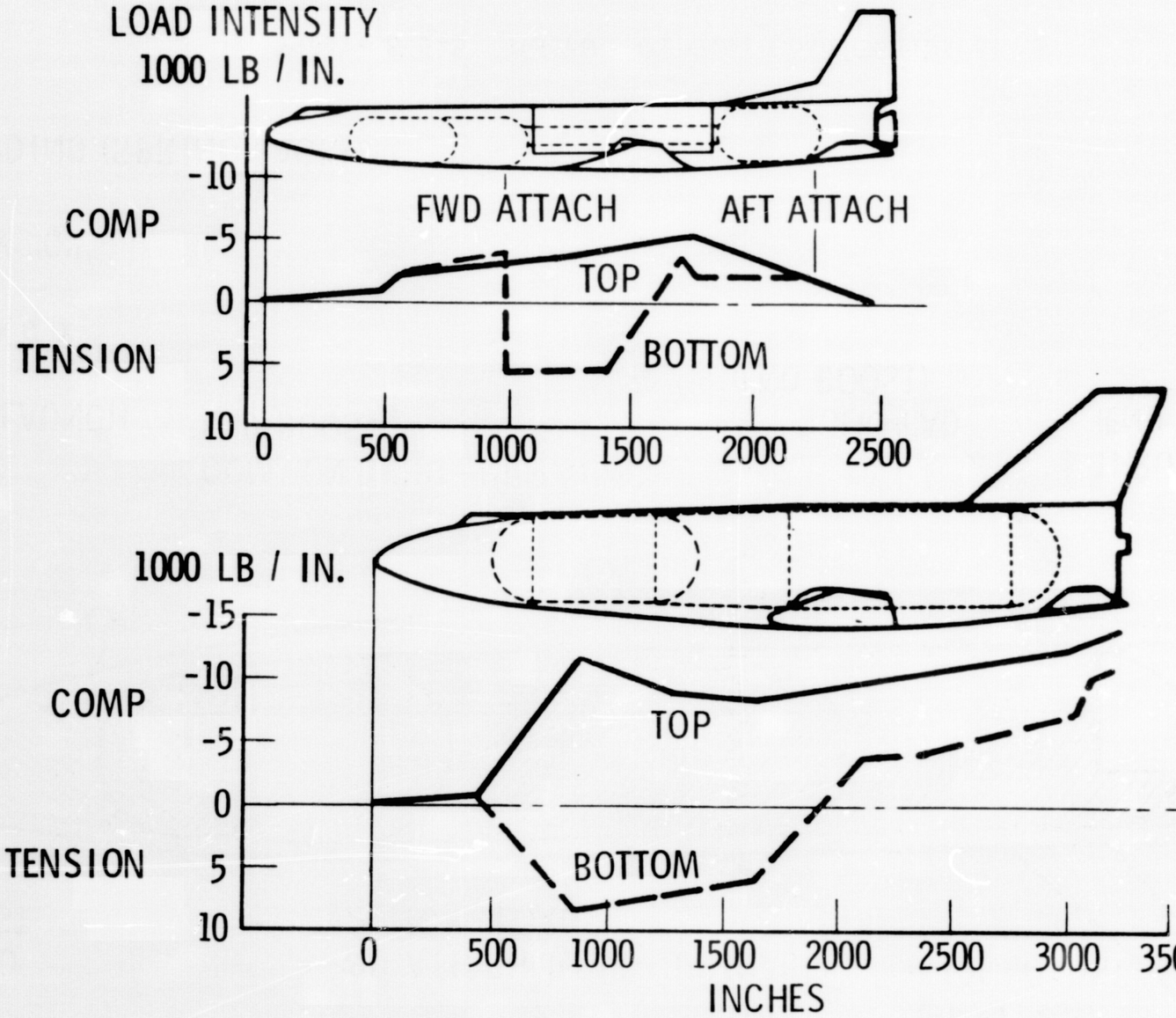

Figure 8.5-4. Design Load Intensity

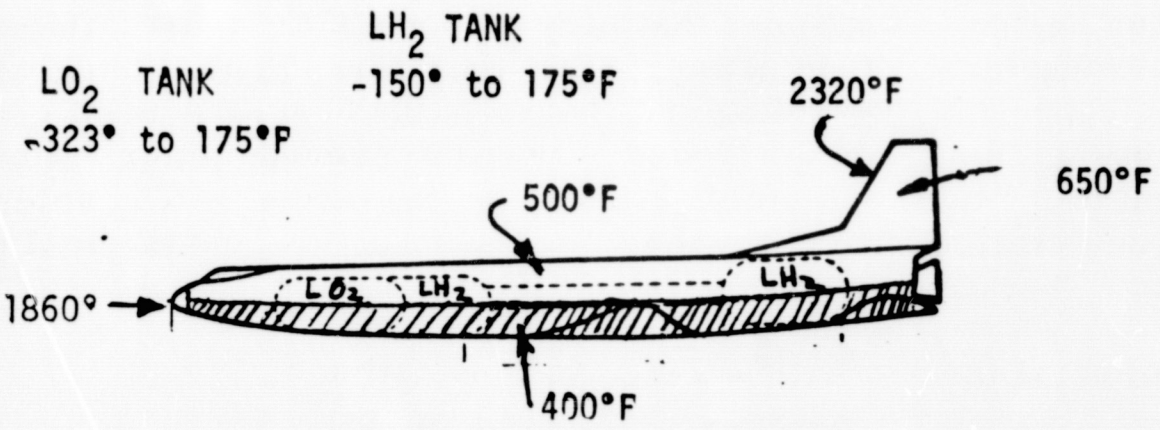

WING L.E. 3000° - 3600°F

ORBITER

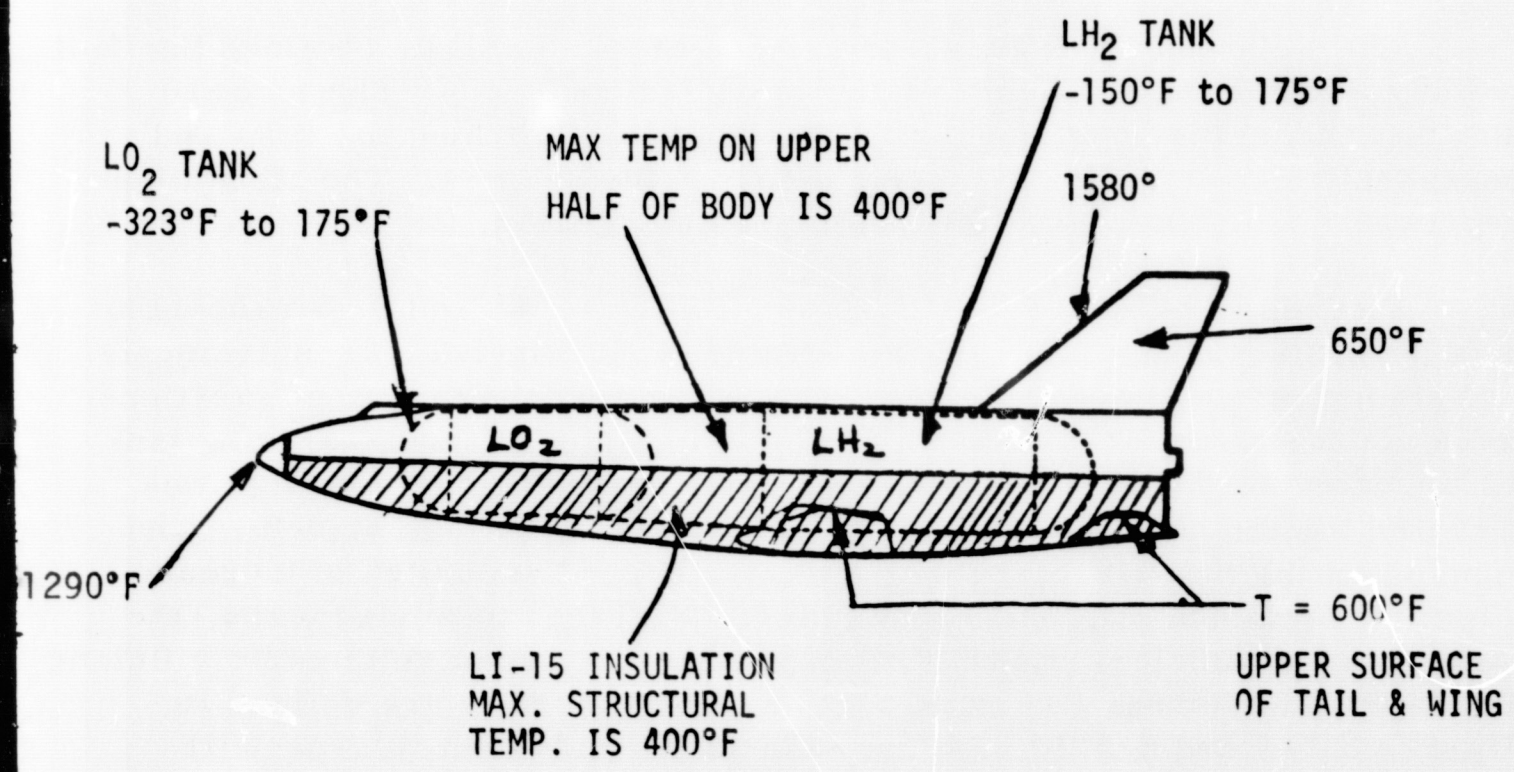

BOOSTER

Figure 8.5-5. Maximum Structural Temperatures

Trade of Outer Shell Versus Integral Tank Structure on Orbiter

The requirement for provision of a 15-foot-diameter, 60-foot-long cargo bay necessitates either interruption of propellant tank structure or compromises design in a manner that prevents use of the most efficient tank structure arrangement. It is not apparent, therefore, that an integral tank structure to support body bending and shears is the best structural concept for the orbiter. This trade study was initiated to provide better visibility for selection of the body structural concept for the orbiter. The study includes consideration of four concepts for the structure and thermal protection system. They are:

1. Integral tank structure and LI-15 insulation
2. Integral tank structure and René 41 heat shields
3. Pressure-designed tankage and René 41 outer shell structure
4. Pressure-designed tankage and 6Al-4V STA titanium outer shell structure with LI-15 insulation

The weight of the body structure and the TPS will be obtained per foot of body length at two stations as shown on Figure 8.5-6. The forward station analyzed is at 20 percent of the body length behind the nose and represents a typical high-temperature, low-load region. The aft station represents a high-load and lower temperature region.

Figures 8.5-7 through 8.5-10 and Tables 8.5-5 and 8.5-6 show the data generated in this study on temperatures, loading, TPS requirements, and structural section properties. It is noted that the tank configurations were not the same for the suspended tank and integral load-carrying tank arrangements. For the integral load-carrying tankage, the design was directed toward providing continuity of load-carrying tank structure and supplementing this structure with a skin-stiffened structure to increase effective depth and efficiency in bending. With the suspended tanks, the largest tank diameters possible were used to maximize volumetric efficiency. The tank and external structure sections and materials are defined in Figures 8.5-9 and 8.5-10 with the associated equivalent thickness (t) requirement to withstand critical loading conditions. Figure 8.5-6 shows the resulting weights per foot of body length for the four concepts. For both the forward and aft station, the concept with the external load carrying structure and LI-15 shows the lowest weights. It is also noted that this structure/thermal protection concept allows design flexibility, and the

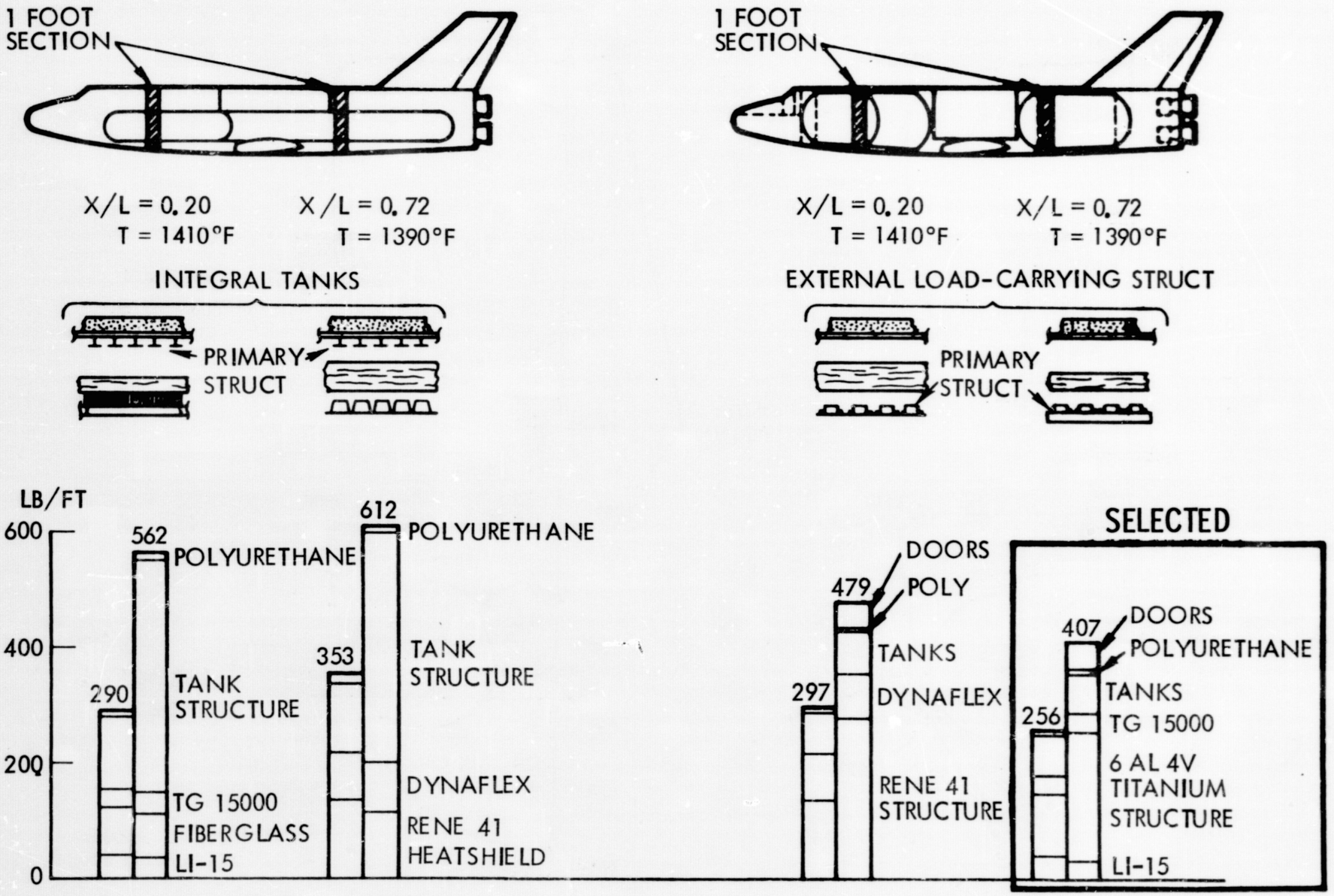

Figure 8.5-6. Orbiter Structure and Thermal Protection Trade

Space Division
North American Rockwell

Figure 8.5-7. Orbiter Temperatures

Space Division
North American Rockwell

LI-15 INSULATION
ON OUTER SURFACE
(TG 15000 INSIDE)

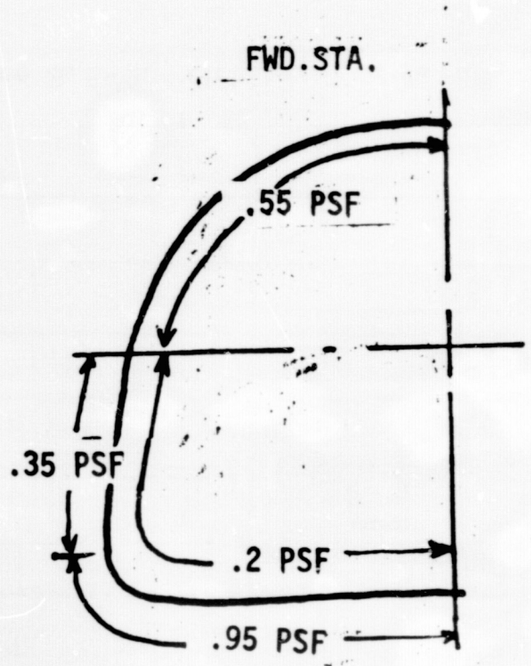

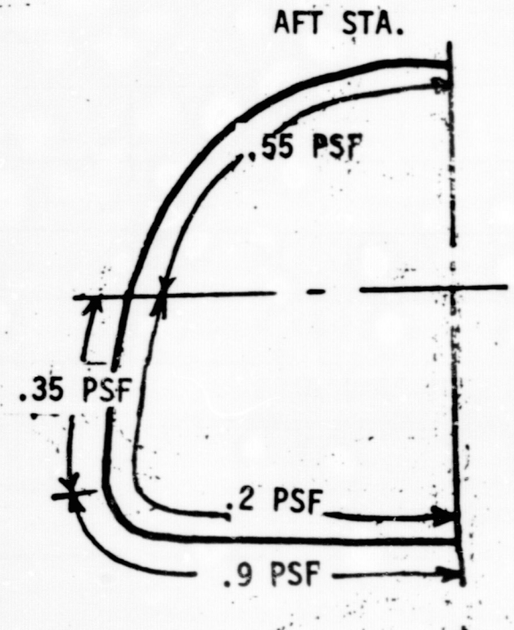

DYNAFLEX
INSULATION
INTERNALLY

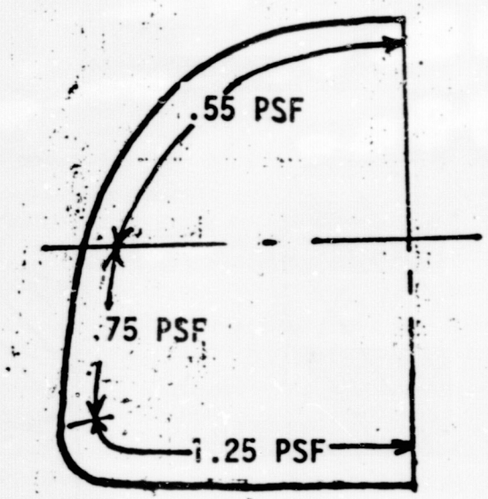

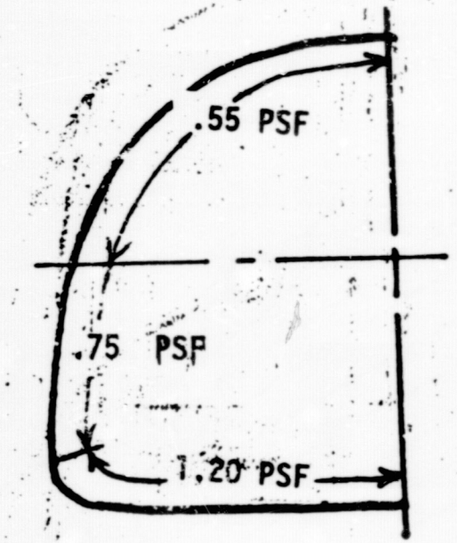

ABOUT SAME WEIGHTS
FOR EITHER TPS

Figure 8.5-8. Orbiter Thermal Protection Systems

CONDITION
MAX $q\alpha$
A = -3.3×10^5 lbs
S = 3.8×10^5 lbs
M = 4.95×10^7 in lbs
(Ultimate Loads)

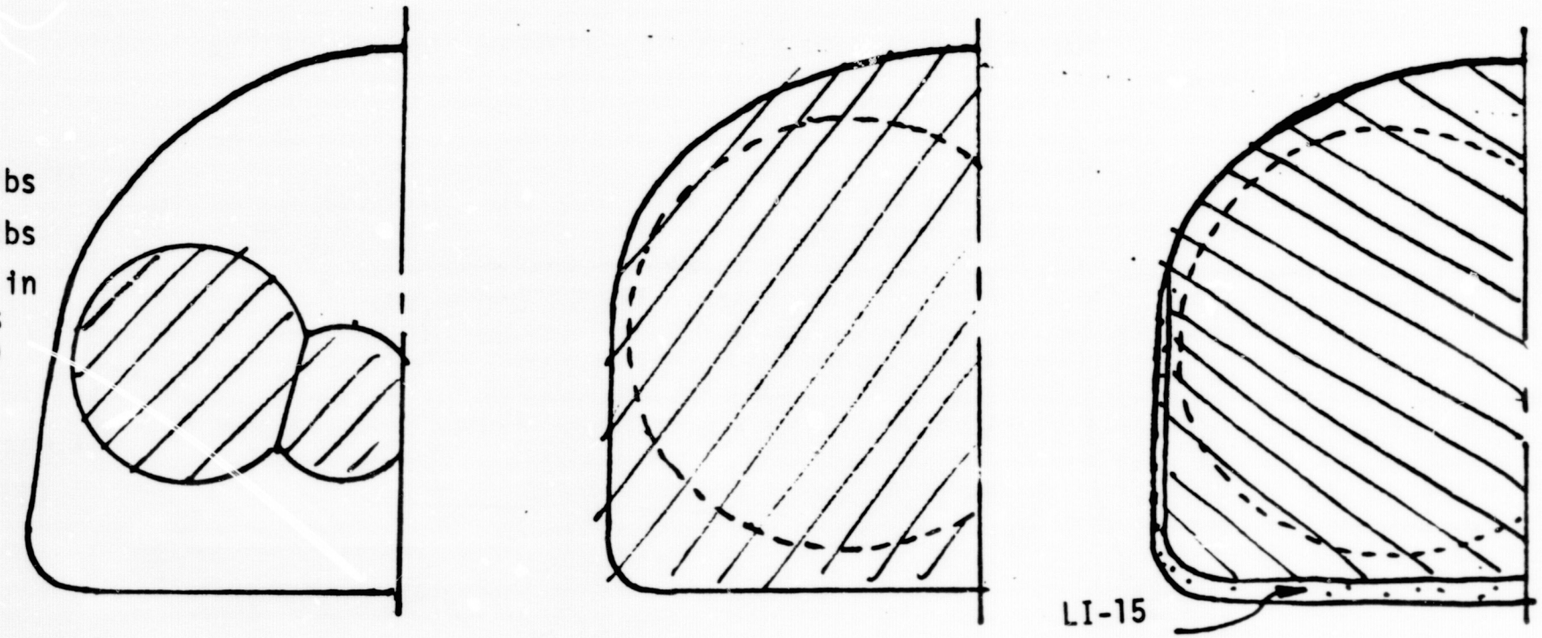

STRUCTURE →	INTEGRAL TANK	OUTER SHELL	OUTER SHELL WITH LI-15 INSULATION
MATERIAL	2014-T6 ALUM.	RENE' 41	6A1-4V STA. TI.
SECTION	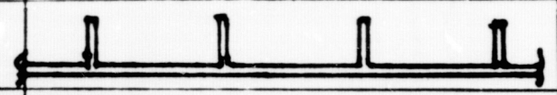	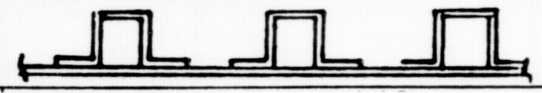	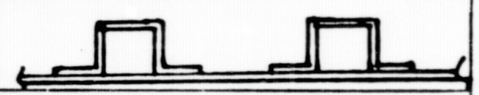
AREA	99.3 (sq. in.)	38.5 (sq.in.)	55.0 (sq. in.)
INERTIA	1.59×10^5 (in^4)	4.65×10^5 (in^4)	6.63×10^5 (in^4)
$N_{X_{MAX}}$	1565 (lbs/in)	715 (lbs/in)	715 (lbs/in)
FRAME SPACING	10 (in)	40 (in)	40 (in)
$\bar{t}$	.077 (in)	.033 (in)	.047 (in)

Figure 8.5-9. Orbiter Forward Station Structure

LOADING
CONDITION
MAX "G" BOOST
A = -3.38×10^6 lbs
S = 2.85×10^5 lbs
M = 3.9×10^8 in/lbs
(Ultimate Loads)

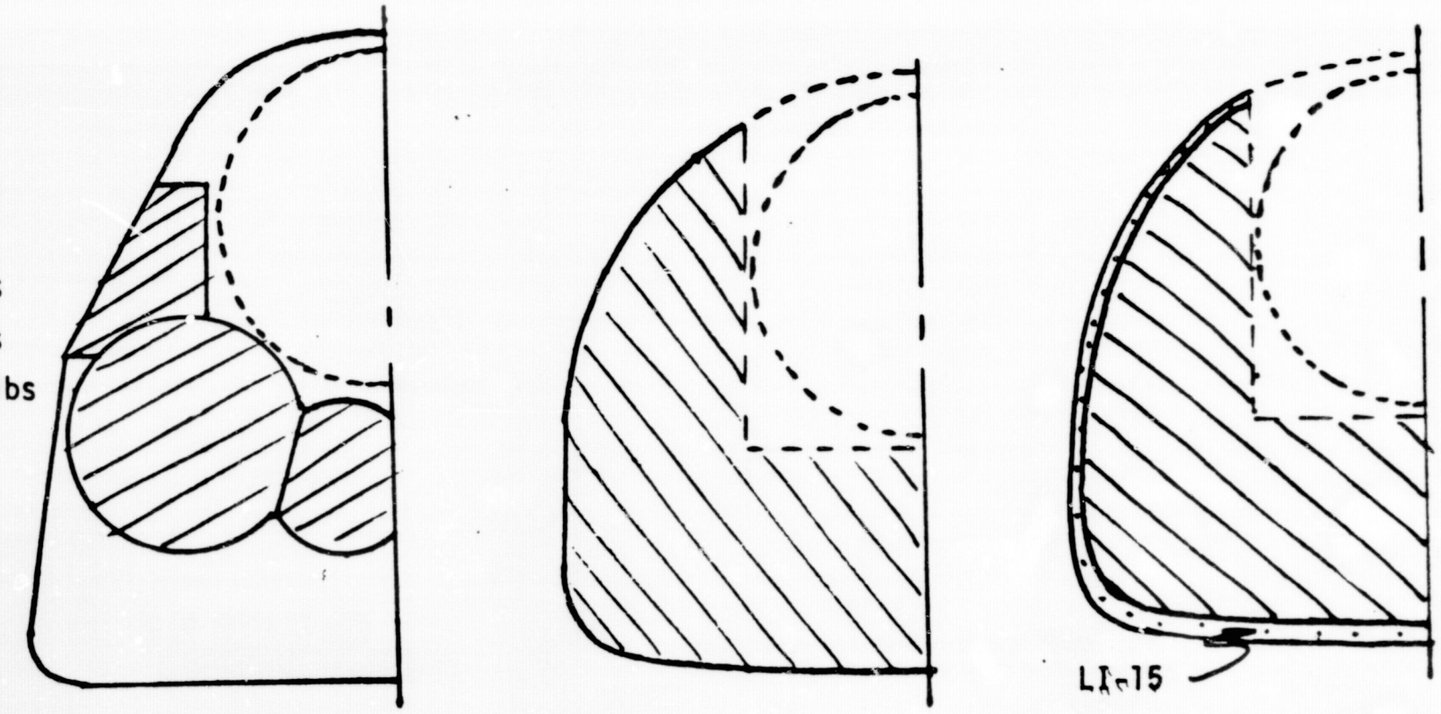

STRUCTURE ⟶	INTEGRAL TANK	OUTER SHELL	OUTER SHELL WITH LI-15 INSULATION
MATERIAL	2014-T6 ALUM	RENE' 41	6Al-4V STA. TI.
AREA	331 (sq in)	77.3 (sq in)	111 (sq in)
INERTIA	1.12×10^6 (in^4)	8.42×10^5 (in^4)	1.21×10^6 (in^4)
N_X MAX	7380 (lbs/in)	9480 (lbs/in)	9480 (lbs/in)
FRAME SPACING	14 (in)	21 (in)	21 (in)
$\bar{t}$	.197 (in)	.0864 (in)	.124 (in)

Figure 8.5-10. Orbiter Aft Station Structure

Table 8.5-5. Orbiter Loading Conditions

Condition	Applied Loads (Limit)					
	Max G	Max qα*	Landing Spinup	Landing Springback	Reentry	2.5-G Maneuver
Forward Station						
Axial load (lb)	-0.7×10^5**	-2.2×10^5	0.3×10^5	0.24×10^5	—	—
Shear (lb)	5.0×10^4	25.3×10^4	-3.0×10^4	2.6×10^4	-1×10^4	-5×10^4
Moment (in-lb)	0.1×10^8	0.33×10^8	0.015×10^8	0.15×10^8	-0.02×10^8	0.15×10^8
Aft Station						
Axial load (lb)	-22.5×10^5	-14.3×10^5	-0.7×10^5	-6×10^5	—	—
Shear (lb)	19.0×10^4	13.2×10^4	-8.0×10^4	2.0×10^4	4×10^4	8.4×10^4
Moment (in-lb)	-2.6×10^8	-2.3×10^8	-0.24×10^8	0.14×10^8	0.15×10^8	0.47×10^8

* Includes 1.1 dynamic factor.
** (-) represents compression.

Table 8.5-6. Orbiter Critical Design Conditions

	Forward Station	Aft Station
Structural Shell	Max q α	Max G
Heat Shields	Reentry Max q α	Reentry Max q α
Insulation	Reentry	Reentry
Membrane Designed Tanks	Max G	Max G

selected TPS provides design margin for the predicted thermal environment. It also provides inherent safety in more severe temperature conditions than those predicted for the mission, as temperatures in excess of 2,500 F will cause TPS ablation as opposed to a catastrophic failure.

The loading for this study is based on location of the drag attachment between the orbiter and the booster at the aft attach point. In a later trade study, it was decided to locate the drag attachment at the forward location. Although the body loads are different with attachment location, it is considered that this variable would not change the structure/TPS concept selection. This conclusion is based on the fact that the selected concept was the lightest in both a high-load and a low-load region.

Separation Tanks Versus Tank With Common Bulkhead on Booster

This trade study was performed to determine whether separate propellant tanks or tanks with a common bulkhead offered the greatest merit for the booster. The study involves two concepts. Concept 1 is shown in Figure 8.5-11A with separate tanks. Concept 2 is shown in Figure 8.5-11B with a common bulkhead. Shortening of the LH_2 tank for Concept 2 while retaining the same volume as Concept 1 is shown in Figure 8.5-11C.

For same volume of LH_2 tank, $V_1 + V_2$ = volume of hemisphere.

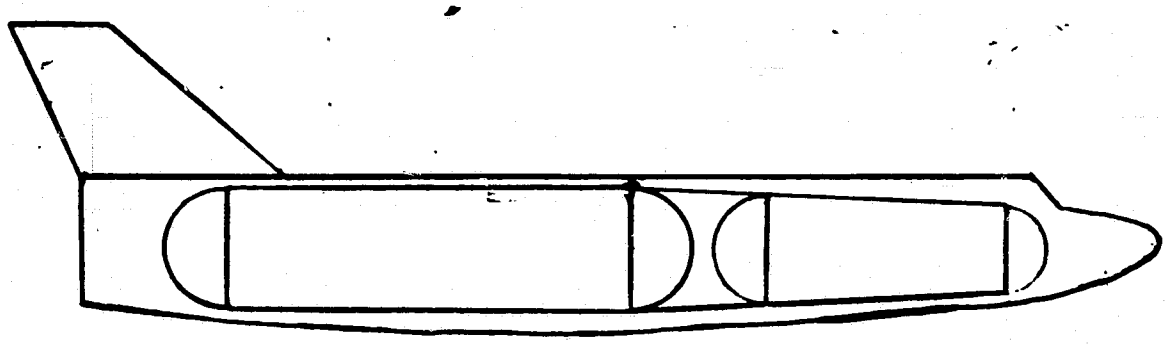

A. CONCEPT 1

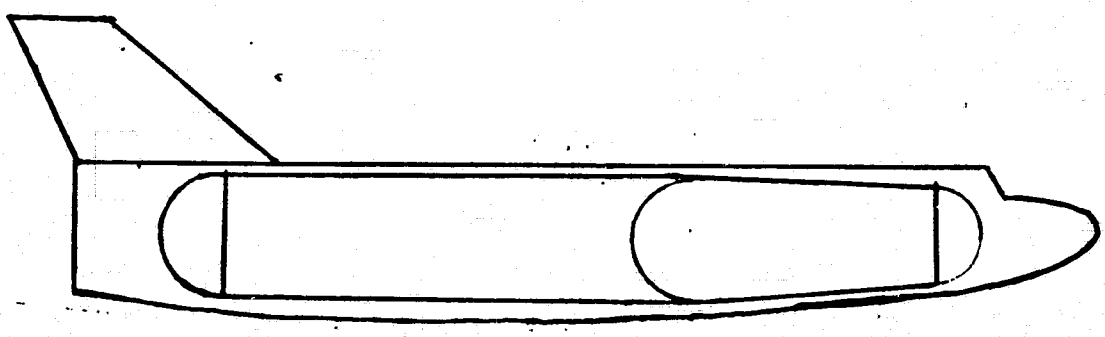

B. CONCEPT 2

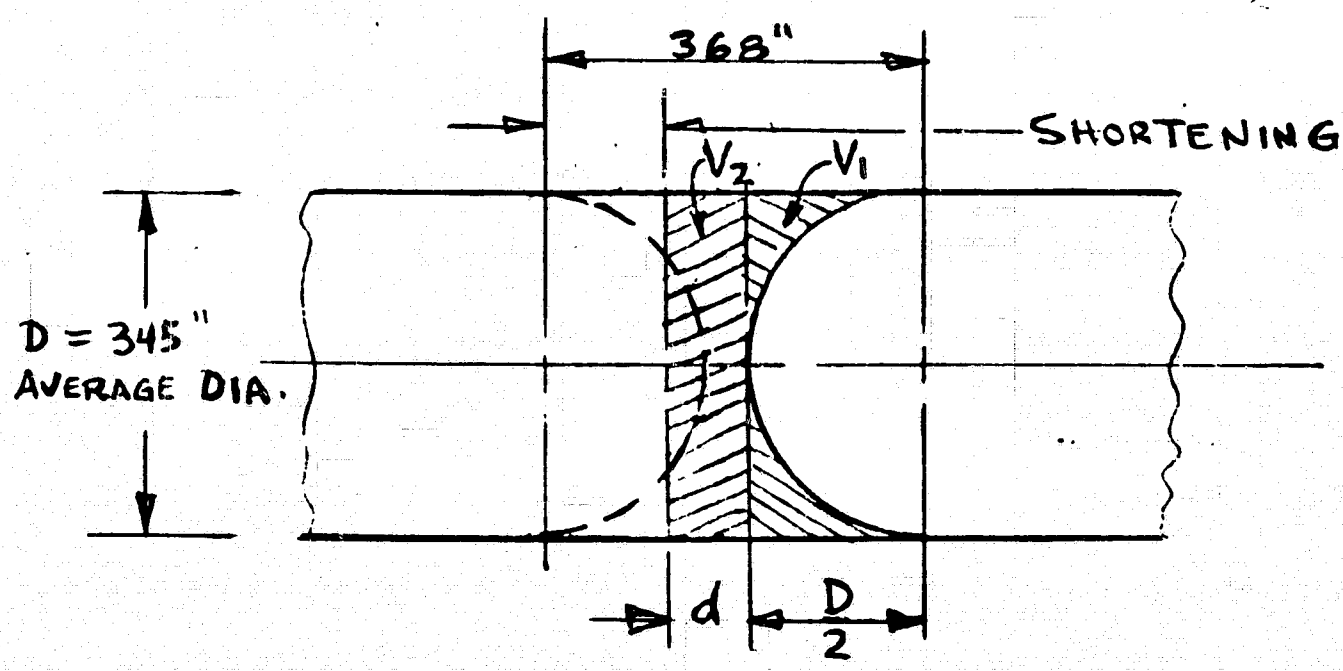

C.

Figure 8.5-11. Concepts 1 and 2 and Shortened LH_2 Tank Possibility

$$\frac{\pi D^3}{24} + \frac{\pi D^2 d}{4} = \frac{\pi D^3}{12}$$

$$d = \frac{D}{6} = 57.5 \text{ in.}$$

therefore,

$$\text{shortening} = 368 - (172.5 + 57.5) = 138 \text{ in.}$$

Weight savings for Concept 2 over Concept 1 are (1) elimination of one LH_2 head, (2) shortening of intertank structure (equivalent thickness $\bar{t}$, for tankage and unpressurized structure of each concept here are nearly equal), and (3) elimination of some TPS and support structure. These statements assume that the external body length will be shortened. No insulation is considered for the LO_2 bulkhead, because the LH_2 will not be in contact with the bulkhead.

1. Weight of LH_2 head

$$W_1 = 1.10^* \rho t S = 1.10 \rho \left(\frac{PR}{2 F_{TU}} \right) \frac{\pi}{2} D^2$$

$$W_1 = 1.10 \ (0.10) \left(\frac{52.5 \times 182.5}{2 \times 72000} \right) 1.57 \ (365)^2$$

$$W_1 = 1540 \text{ lb}$$

2. Weight of shortened intertank structure

$N_X = 9020$ lb/in. (fully fueled on pad)

$\bar{t} = 0.322$ (from computer run)

$W_2 = \rho \bar{t} \ (\pi D)$ shortening

$W_2 = 0.10 \ (0.322) \ (3.14 \times 345) \ 138$

$W_2 = 4800$ lb

*Accounts for lands and mismatch at weld joints.

3. TPS and support weight saving for shortening of body length. Assume TPS and support structure will average 1.25 lbs/sq ft.

Perimeter = 113 ft (outer mold line)

Shortening = 138" or 11.5 ft

$$W_3 = 113 \times 11.5 \times 1.25$$

$$W_3 = 1629 \text{ lbs}$$

Total weight saving of Concept 2 over Concept 1 is

$$W_T = W_1 + W_2 + W_3$$

$$W_T = 1,540 + 4,800 + 1,620$$

$$W_T = 7,960 \text{ lbs}$$

Forward Versus Aft Drag Attachment

The orbiter and the booster are held together by four attachments, two at Forward Station 2870 and two at Aft Station 1430. The attachment configuration and loads are shown in Figure 8.5-12 for both the forward and aft drag attach concepts. This study was performed to obtain estimates of the weight difference on the vehicles when the drag loads are transferred at the forward versus the aft attach. The maximum drag load occurs during boost and when the booster is near burnout. At this time, the acceleration applied to the fully fueled orbiter is at a maximum of 3 g's. Sixty percent of the weight of the orbiter is made up of the liquid oxygen on board. This oxygen tank is well forward on the body, being just aft of the crew cabin and passenger compartment. It becomes obvious that a forward drag attachment would save some weight on the orbiter, whereas some weight will have to be added to the booster. The selection for the drag attachment is based on the fact that one pound saved on the orbiter will offset up to 7 pounds added to the booster; therefore, the relative weight changes are important, not just the absolute weight change.

The critical design loads for the booster between the two attach stations are shown in Table 8.5-7. The critical loading with the forward attachment is for the maximum g condition, whereas the aft attach critical loading condition is at maximum $q\alpha$. With the forward drag attachment, the booster is 10,000 pounds heavier than when an aft drag attachment is used.

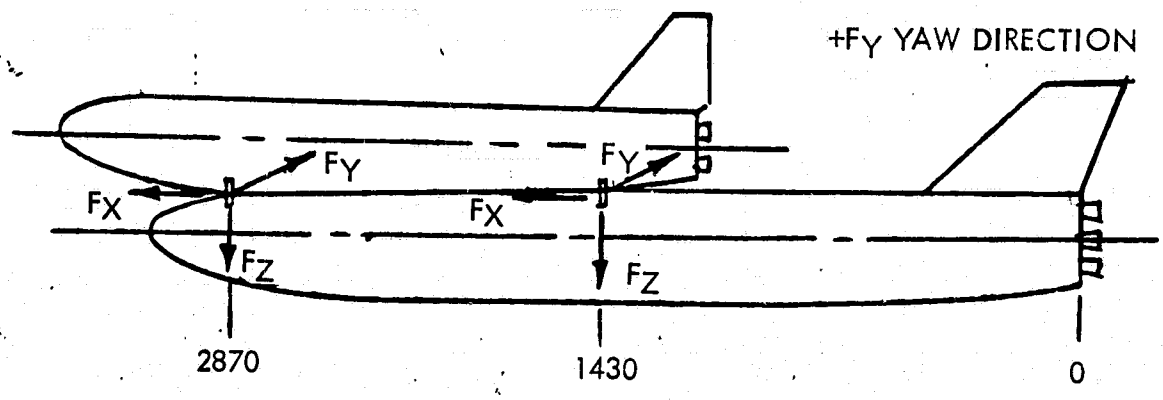

LOAD DIRECTIONS SHOWN ARE ORBITER REACTIONS

AFT DRAG ATTACH

LIMIT LOADS (1000 LB)						
LOAD CONDITION	FWD ATTACH STA 2870			AFT ATTACH STA 1430		
	F_X	F_Y	F_Z	F_X	F_Y	F_Z
MAX Q α	—	±132.	-456.	1608.	±127.	-222.
MAX. AXIAL ACCELERATION	—	—	13.	2630.	—	-223.

FWD DRAG ATTACH

LOAD CONDITION	FWD ATTACH STA 2870			AFT ATTACH STA 1430		
	F_X	F_Y	F_Z	F_X	F_Y	F_Z
MAX. Q α	1608.	±132.	-383.	—	±127.	-245.
MAX. AXIAL ACCELERATION	2630.	—	130.	—	—	-340.

Figure 8.5-12. Limit Attachment Loads

Table 8.5-7. Booster Comparative Loadings for Forward Versus Aft Drag Attach

Station	Forward Attach				Aft Attach			
	Critical Moment (10^{-6} lb-in.) (Limit)	Critical Axial (10^{-6} lb) (Limit)	Critical Comparison N_x (ULT.) (lb/in.)		Critical Moment (10^{-6} lb-in.) (Limit)	Critical Axial (10^{-6} lb) (Limit)	Critical Comparison N_x (ULT.) (lb/in.)	
			Top Fiber	Bottom Fiber			Top Fiber	Bottom Fiber
2850 (Top of LO_2 tank)	550	2.6	18,600		30	0.35	900	1,400
2100 (Base of LO_2 tank)	500	2.75	9,900	3,900	485	0.45	1,500	6,900
2100 (Top of LH_2 tank)	500	3.80	11,200	7,000	485	2.70	4,300	9,900
1650 (LH_2 tank)	425	3.90	10,300	6,300	440	3.0	5,400	9,400

Space Division
North American Rockwell

The critical orbiter design loads for the forward and aft drag attach concepts are shown in Figure 8.5-13. In the area of the drag attachment, it is assumed that the local distribution of the concentrated load will require about the same weight, whether the drag attachment is forward or aft; therefore, the three stations used for the weight comparison are at stations where the bending moment has been developed from the transfer of the axial load to the neutral axis of the shell station. Figure 8.5-13 shows the weight per foot of body shell at these three stations. In Figure 8.5-14, the same data are plotted versus body length. The difference in the body shell weight is calculated from this graph to be 2,100 pounds. This figure represents the weight saving on the orbiter when using a forward drag attach.

In summary, the forward drag attachment was selected for these vehicles because of a slight overall system weight benefit and because of vehicle weight sensitivity to orbiter subsystem weight growth. A weight saving of 2,100 pounds on the orbiter more than offsets the 10,000 pounds of weight added to the booster.

Orbiter Tank Trade

A parametric investigation of orbiter propellant tank configurations was conducted for vehicles using external load-carrying structure that would not transfer loads to the tankage. The three orbiter tankage configurations investigated are shown in Figure 8.5-15. The tank weights of the concepts illustrated are Concept 1, 7,629 pounds; Concept 2, 6,316 pounds; and Concept 3, 8,004 pounds.

Concept 2 has the lightest tankage weight because the tanks are spherical (except for a relatively short cylindrical section) in contrast to the long cylinders of Concept 1. The Concept 3 tankage itself is heavier than the separate tanks of Concept 2 because of the use of a common bulkhead and the longer cylindrical section. Concept 3, however, provides the best volumetric efficiency in the vehicle and minimizes body length and surface area. This concept was selected for the final vehicle design.

8.5.6 Structure and Thermal Protection System Definition

The previously described trade studies were used to select the booster and orbiter structure and thermal protection concepts used in the analysis of the selected system to establish a definition of structural sizes.

Structure Concept Selection

The booster body with the large diameter and continuous tankage appears well suited to an integral tank structure. Based on initial trade studies, the selected booster concept uses integral tanks. A secondary

FORWARD ATTACH

LOADS (ULTIMATE)

A	-3.3×10^5	1.05×10^6	-1.73×10^6
S	3.8×10^5	2.85×10^5	—
M	4.95×10^7	3.3×10^8	$-.945 \times 10^8$
WTS./FOOT			
OUTER SHELL	106	115	108
BODY STA.	490	1350	1767

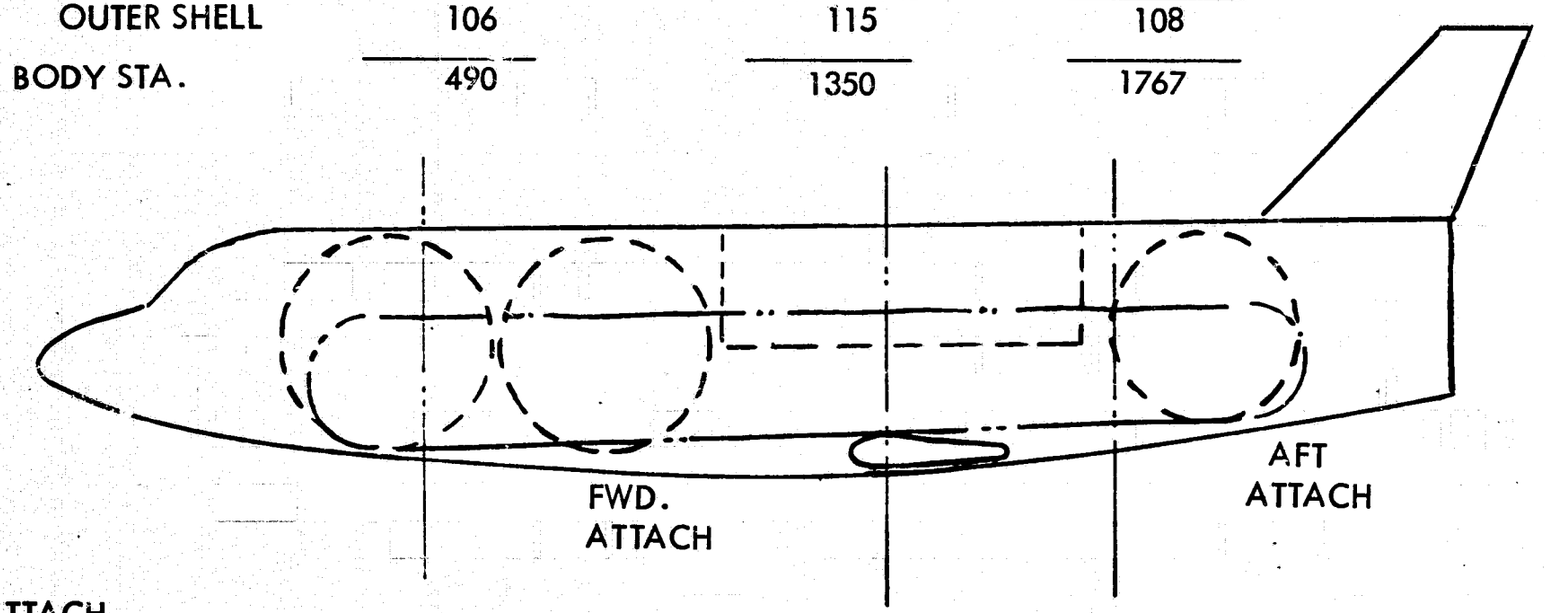

AFT ATTACH

LOADS

A	-3.3×10^5	-3×10^6	-3.38×10^6
S	3.8×10^5	2.55×10^5	2.85×10^5
M	4.95×10^7	-2.4×10^8	-3.9×10^8
WTS./FOOT			
OUTER SHELL	106	119	162

Figure 8.5-13. Orbiter Loads for Forward and Aft Attachments

Space Division
North American Rockwell

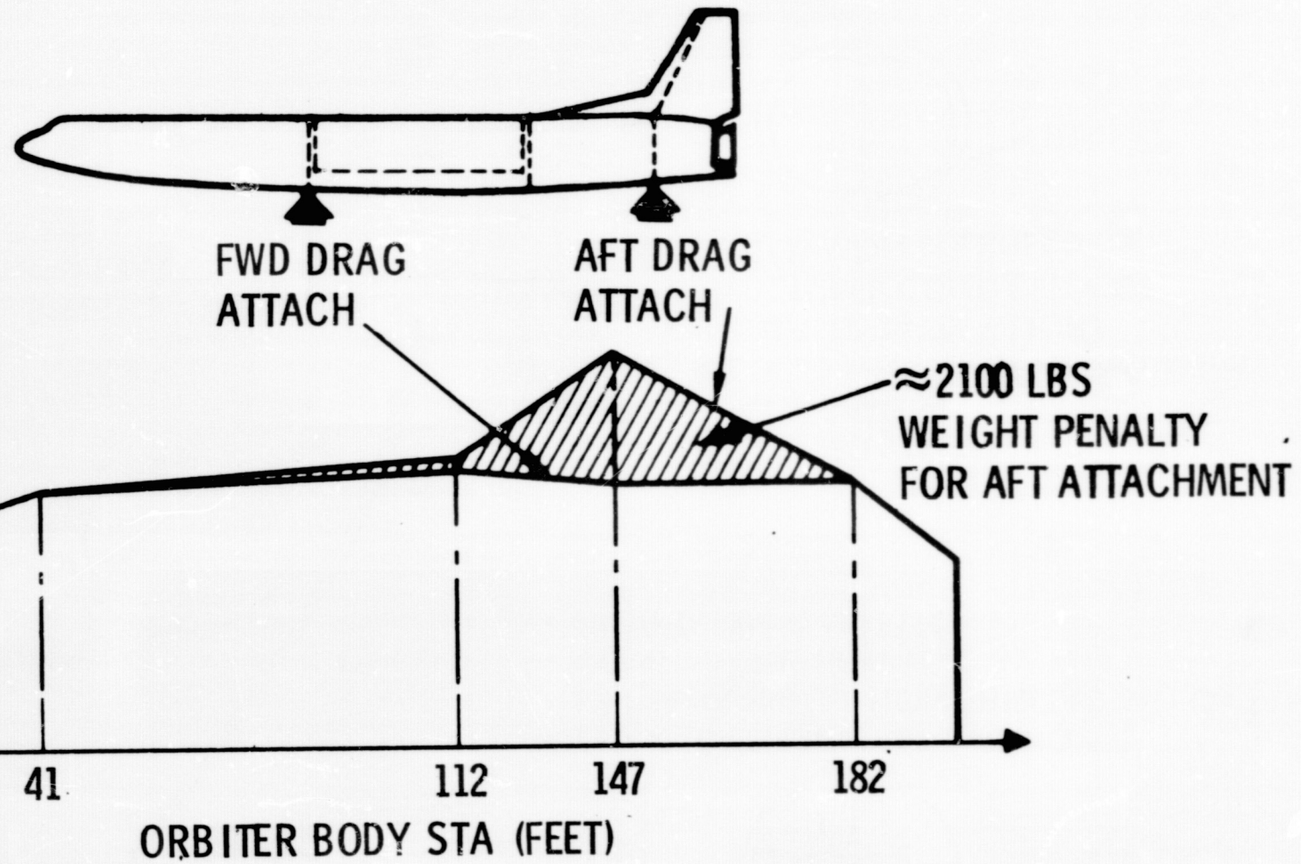

- FORWARD DRAG ATTACHMENT RESULTS IN
  - LOWER ORBITER WEIGHT (≈ 2100 LBS)
  - HIGHER BOOSTER WEIGHT (≈10, 000 LBS)

- SELECTED FORWARD DRAG ATTACHMENT FOR DESIGN
  - OVERALL SYSTEM WEIGHT BENEFIT ≈ 900 LB PAYLOAD
  - ORBITER MORE WEIGHT-SENSITIVE

Figure 8.5-14. Drag Attachment Location

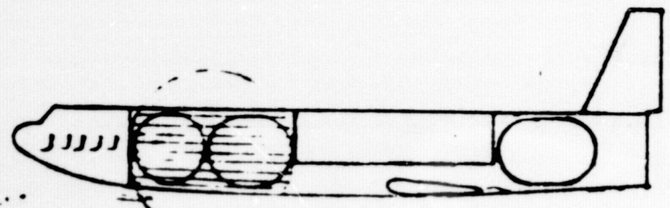

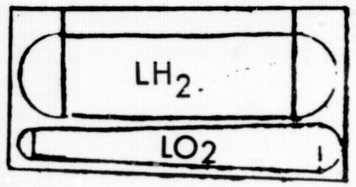

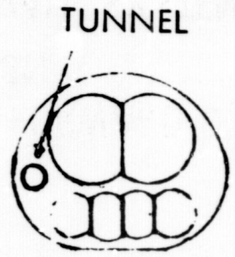

CONCEPT 1
- REDUCED BENDING AT MAX "G"
- LH_2 TANK INSULATION SHIELDED BY LO_2 TANK
- CONTINUOUS HEAT LEAK
- HIGH THERMAL STRESSES

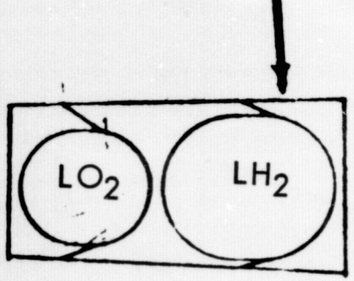

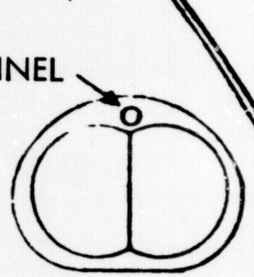

CONCEPT 2
- SIMPLICITY OF SUPPORTS
- REDUCED HEAT LEAK
- MINIMAL THERMAL STRESSES
- INCREASED BENDING AT MAX "G"
- UNIFORM LOAD TO SHELL

CONCEPT 3
- INCREASED SPACE FOR TUNNEL & ATTACHMENTS
- REDUCED WEIGHT OF ATTACHMENTS
- INCREASED TANK WEIGHT
- STRUCTURAL COMPLEXITY OF COMMON BULKHEAD

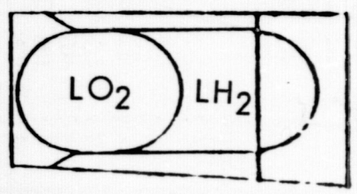

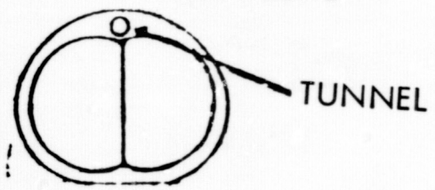

Figure 8.5-15. Orbiter Forward Tankage Concepts

Space Division
North American Rockwell

structure carrying loads to the tanks is used to support the fiberglass honeycomb sandwich panels to which the LI-15 insulation will be bonded. The insulation is on the lower half of the body. The upper half has exposed polyimide-glass-reinforced honeycomb-sandwich panels. The tanks are made of 2219 T-87 aluminum plate. The polyurethane foam insulation is on the inside of the LH_2 tank. The LO_2 tank has no insulation.

All the aerodynamic surfaces will have 6Al-4V STA titanium structures. The lower surface of the wing and the horizontal tail are protected by LI-15 insulation. The upper surfaces are bare titanium structure. Both sides of the vertical tail have exposed titanium structure.

A diagram of the structural concepts and thermal protection systems for the booster is shown in Figure 8.5-16.

The structure and thermal protection system for the body of the orbiter was studied in the trades previously described. These studies showed that an outer shell structure made of 6Al-4V STA titanium and protected by LI-15 insulation would have the lightest weight and an adequate temperature safety margin. In this concept, the tankage does not support overall body bending and shear loads. The tankage resists the internal pressure plus hydrostatic pressures from vehicle accelerations. In addition, the tankage must distribute these inertia loads to the outer shell through an intermediary bulkhead.

The aerodynamic surfaces are similar in construction, material, and thermal protection systems to those on the booster, except for the upper surfaces of the wing and the horizontal tail, which on the orbiter are covered with a minimum 1/4-inch thickness of LI-15 insulation. A diagram showing the structural concepts selected is shown in Figure 8.5-17. LI-15 insulation was used extensively. However, mechanical property data were not available for this material; therefore, no structural integrity evoluation was made.

8.4.7 Booster Structure

The structural analysis and definition of the booster structure elements is presented in the following paragraphs.

Booster Body Structure. The booster body structure is the primary load-carrying structure upon which all the aerodynamic surfaces, the heat shield, landing gear, and thrust structure are mounted. This body structure is also the LH_2 and LO_2 propellant container, thus the propellant tankage structure and the aerodynamic and inertial load-carrying structure are integral. This structure must be reusable for 100 missions and, therefore, must sustain without permanent deformation the total spectrum of loadings imposed during prelaunch, engine ignition, liftoff, boost, engine shutdown, orbiter separation, reentry, flyback, and landing.

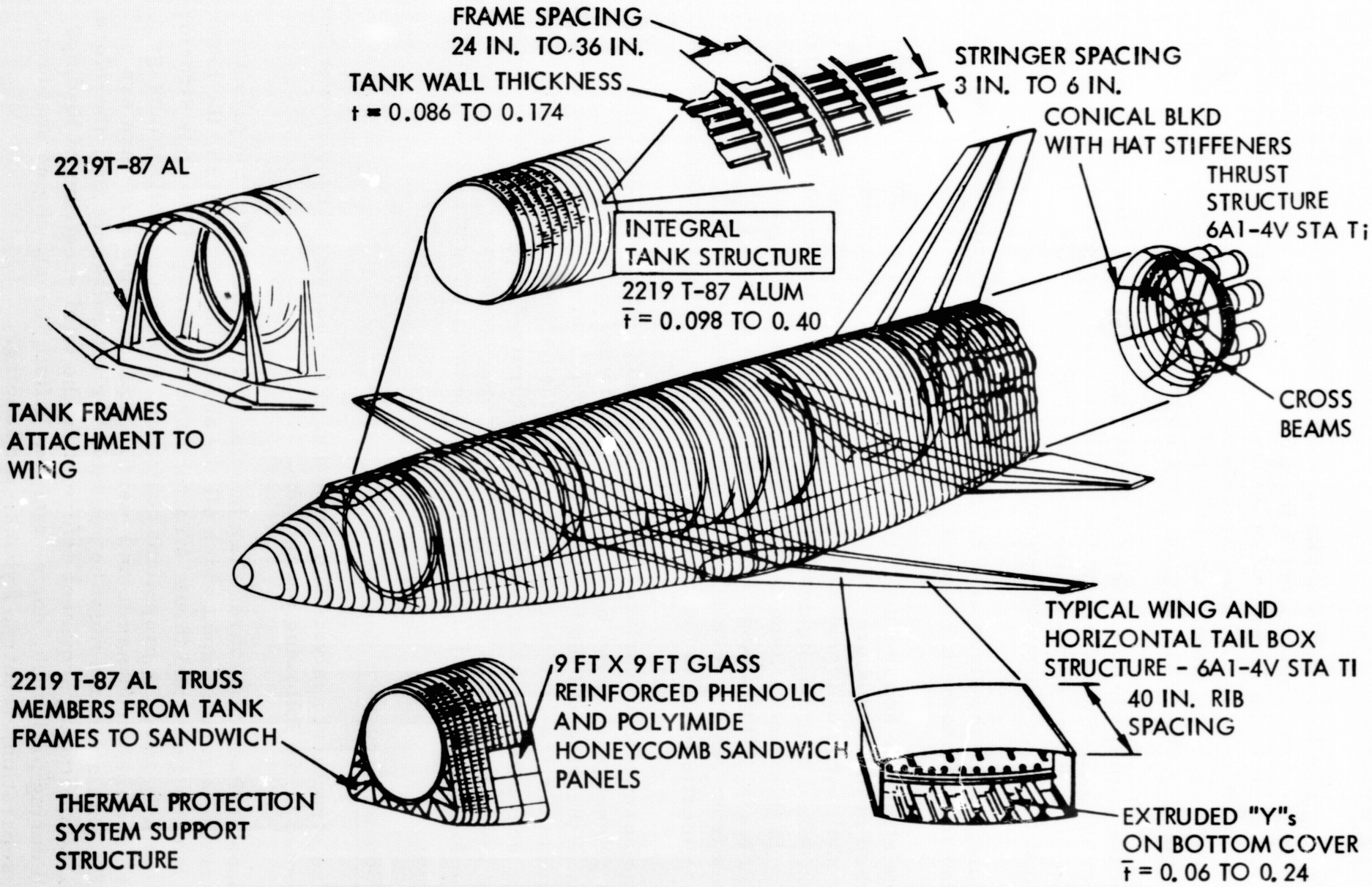

Figure 8.5-16. Booster Structure Definition

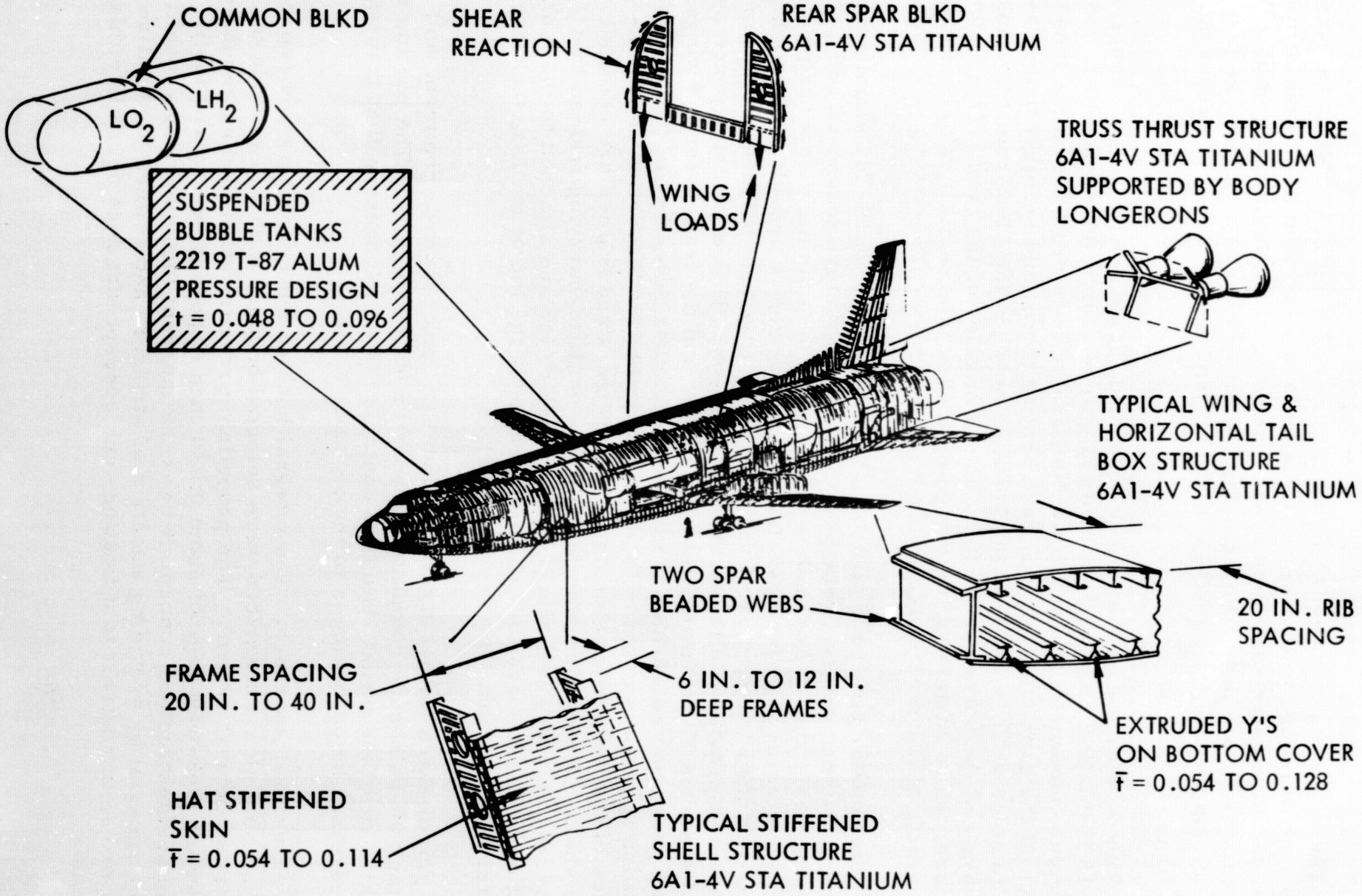

Figure 8.5-17. Orbiter Structure Definition

These loading conditions in general are combinations of axial and shear loads, body bending, torsional moments, and tank-pressure-induced longitudinal and circumferential membrane stresses. The structural components must survive these loads. Sufficient structural stiffness also must be provided to comply with the vehicle control system and to preclude a resonance failure.

The booster body structure is contained inside a heat shield composed of LI-15 insulation attached to a layer of glass-reinforced-composite honeycomb-sandwich panels. TG-15000 insulation is provided on the inner surface of the panels to limit the peak heating (boost and reentry) temperatures to no more than 175 F at the bondline between the aluminum LH_2 tank structure and the polyurethane foam on the interior of the tank. This body structure, while sustaining the foregoing loads, is essentially shielded from the severity of the reentry thermal environment.

The booster tank body structure is fabricated of 2219-T87 aluminum in view of its formability, weldability, and high fracture toughness and corrosion resistance. For leak protection and longitudinal compression stability, integral skin-stringer-frame construction is provided. In the high load areas, the stringers are I sections. The LH_2 tank polyurethane foam insulation is provided on the interior of the tank. This eliminates penetration of the foam by the heat shield attachment and the frames for the wings, landing gear, and aerodynamic surfaces. Another advantage of the interior insulation is that the interior is more accessible for inspection and maintenance of the insulation; therefore the stringers and frames are external to the shell. The column stability frames and load-carrying frames that support the landing gear, wings, tails, and orbiter are attached to the tank structure. The two orbiter attach longerons at the top of the LO_2 tank are integral with the tank.

An aft skirt, thrust structure, and LO_2 tank forward, common, and LH_2 tank aft bulkheads complete the booster body structure. The portion of the skirt aft of the thrust structure contains the four longerons that transmit the prelaunch holddown loads to the aft skirt shell.

Structural Approach. The integral booster body structure and separate external heat shield described were selected because they will provide the lightest structural system. The propellant pressurization loading requires an average tank-wall gage of about 0.140 inch (2 pounds per square foot). The integral-structure concept utilizes the inherent load-carrying capability of this material by providing a matrix of stringers and frames to stabilize these skins, in contrast to a floating-tank concept that does not utilize this material.

As stated previously, the orbiter attachment longerons are provided at the forward portion of the LO_2 tank. The drag and longitudinal inertial loads from the orbiter, therefore, are supported at the most forward portion of the booster. If the drag loads were supported at the aft attach on the booster, the booster structural weight would be reduced; however, the orbiter weight is increased. The total vehicle system weight is lower with the forward drag attachment design.

Structural Criteria. The overall structural criteria used in this study to determine the structural design of the booster vehicle is described in Section 8.5.1. Specific criteria directly applicable to the booster tankage structure are as follows: The booster must have free standing capability on the launch pad under any or all of the following conditions:

1. All tanks empty and unpressurized
2. Any combination of tanks fueled and unpressurized
3. Any combination of some tanks fueled and pressurized with the remaining tanks empty or fueled but unpressurized
4. All tanks fueled and pressurized

Vehicle body loads are described in Volume III of this report. LH_2 and LO_2 tank pressures used in the analysis were as follows:

1. Maximum relief valve pressure LH_2 tank, 35 psia
2. Minimum regulator valve pressure LH_2 tank, 30 psia
3. Maximum relief valve pressure LO_2 tank, 22 psia
4. Minimum regulator valve pressure LO_2 tank, 15 psia

It is pertinent that compression-load intensity relief was considered for the maximum g and maximum $q\alpha$ loadings. The relief is based on the limit load resulting from the minimum regulator pressure.

The equation used to determine the load intensities in the tanks is therefore

$$N_X = \frac{(S.F.)}{\pi R}\left[\frac{A}{2} + \frac{M}{R}\right] - \frac{P_{min} R}{2}$$

where

N_X = ultimate compression longitudinal load intensity in pounds per inch

A = the limit axial compression load in pounds

M = the limit bending moment in pound-inches

R = the body radius in inches

P_{min} = the minimum regulator valve pressure less the ambient pressure in psia

The structural temperatures anticipated in the tank and skirt designs are as shown in Table 8.5-8.

Analysis. The structural analysis performed to establish the size of the LO_2 and LH_2 tanks and the skirt cylindrical shells is as follows:

The body axial load and bending moments at the designated discrete stations are tabulated in Table 8.5-9. The prelaunch loads for wind from the orbiter side are based on the orbiter unfueled, while the prelaunch moments for wind from the other side are based on the orbiter fully fueled.

Table 8.5-10 illustrates the computed longitudinal load intensities for the expected critical conditions defined in Table 8.5-9. The final critical load intensities that designed the body structure for the top, bottom, and side fibers are shown in Table 8.5-11 along with the required equivalent thickness ($\bar{t}$) The $\bar{t}$ values include the minimum required tank skin thickness for pressure and the additional material for the stringers and stability frames.

Table 8.5-8. Structure Temperatures (F)

	Prelaunch (No Fuel)	Liftoff	Max g	Entry
LO_2 tank (top)	70	-297	150	175
LO_2 tank (base)	70	-297	70	175
LH_2 tank (top)	70	-150	70	175
LH_2 tank (base)	70	-150	-50	175
Skirt	70	70	175	175

Table 8.5-9. Booster Body Structure Moments and Axial Loads

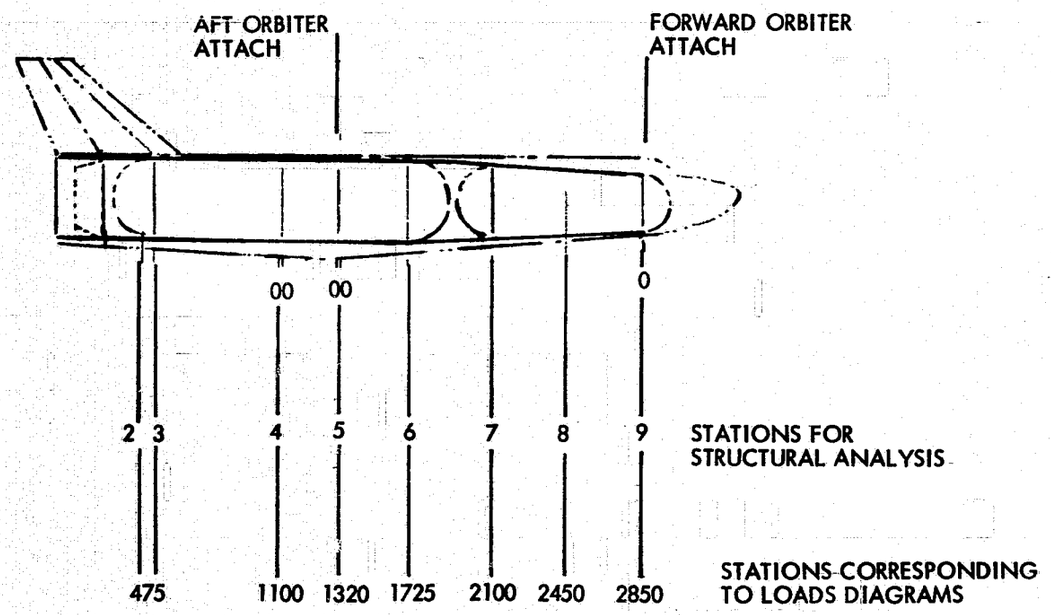

Moments are in lb-in. x 10^{-6}
Axial loads are in lb x 10^{-6}
+ Moment is tension on bottom fiber
+ Axial load is tension

Station	Prelaunch Wind From Orbiter Side		Prelaunch Wind From Booster Side		Max q α		Max q		Reentry	Flyback	(Spinup)		(Springback)	
	Mom.	Axial	Mom.	Axial	Mom.	Axial	Mom.	Axial	Mom.	Mom.	Mom.	Axial	Mom.	Axial
9	-30.0	-0.05	30.0	-0.05	-22.0	-0.30	-10.0	-0.10	-15.0	10.0	-20.0	0.05	-30.0	-0.04
8	8.1	-0.33	240.0	-0.90	110.0	-2.0	575.0	-2.75	-43.0	27.5	-10.0	0.09	-70.0	-0.08
7	-6.2	-0.38	290.0	-0.95	-110.0	-2.0	550.0	-2.80	-65.0	34.0	-30.0	0.12	-150.0	-0.11
6	-55.0	-2.58	360.0	-3.15	-55.0	-4.6	450.0	-3.90	-72.0	32.0	-75.0	0.16	-280.0	-0.15
5	-94.0	-2.68	440.0	-3.25	0	-4.8	320.0	-4.10	-55.0	-5.0	-290.0	-0.15	-310.0	-0.14
4	-154.0	-2.78	480.0	-3.35	-12.0	-5.2	175.0	-4.50	-60.0	12.0	-240.0	0	-310.0	0
3	-314.0	-2.93	620.0	-3.50	-192.0	-5.9	-120.0	-5.0	-30.0	-27.0	-120.0	-0.18	-60.0	0.16
2	-314.0	-3.28	620.0	-3.85	-192.0	-6.0	-120.0	-5.0	-30.0	-27.0	-120.0	-0.18	-60.0	0.16

Table 8.5-10. Critical Booster Body Structure Loading Intensities

Station	Top or Bottom Fiber	Prelaunch (Wind From Booster Side)			Prelaunch (Wind From Orbiter Side)			Max qα				Max g				Landing Springback			N_t Due to Pressure
		N_M	N_A	N_C	N_M	N_A	N_C	N_M	N_A	N_{PR}	N_C	N_M	N_A	N_{PR}	N_C	N_M	N_A	N_C	
9	B	0.560	-0.08	0.48	-0.560	-0.08	-0.64	-0.410	-0.48	2.0	0.11					-0.56	-0.06	-0.62	5.3 (RT)
	T	-0.560		- 0.64	0.560		0.48	0.410		2.34	2.27					0.56		0.50	
8	B	3.88	-1.25	2.63				-1.79	-2.77	2.60	1.62	9.3	-3.80	2.82	8.32	-1.13	-0.11	-1.24	6.8 (-323)
	T	-3.88		- 5.13				-1.79		0.96	-3.60	-9.3		1.29	-11.81	1.13		1.02	
7	B	3.78	-1.18	2.60				-1.43	-2.48	1.20	-2.71	7.2	-3.48	3.15	6.87	-1.97	-0.14	-2.11	10.8 (-323)
	T	-3.78		- 4.96				1.43		2.79	1.74	-7.2		1.44	- 9.24	1.97		1.83	
6	B	4.70	-3.92	0.78								5.85	-4.90	4.50	5.45	-3.65	-0.19	-3.84	10.1 (RT)
	T	-4.70		- 8.62								-5.85		2.88	- 7.87	3.65		3.46	
5	B	5.75	-4.05	1.70								4.15	-5.10	4.50	3.55	-4.01	-0.18	-3.83	10.1 (RT)
	T	-5.75		- 9.80								-4.15		2.88	- 6.37	4.01		4.19	
4	B	6.30	-4.18	2.12								2.30	-5.6	4.50	1.20	-4.01	0	-4.01	10.7 (0)
	T	-6.30		-10.48								-2.30		2.88	- 5.02	4.01		4.01	
3	B	8.15	-4.38	3.77	-4.15	-33	-7.45	-2.54	-7.40	2.64	-7.30								11.5 (-50)
	T	-8.15		-12.53	4.15		0.85	2.54		4.16	-0.7								
2	B	8.15	-4.82	3.33	-4.15	-3.74	-7.89	-2.54	-7.50		-10.04								(0)
	T	-8.15		-12.97	4.15		0.41	2.54			-4.96								

By inspection of Table 8.5-9 the conditions not shown are not expected to be critical.

N_M is ultimate longitudinal load intensity due to bending moment.

N_A is ultimate longitudinal load intensity due to axial load.

N_{PR} is limit longitudinal load intensity relief for compression load intensity, or ultimate longitudinal load intensity additional to tensile load.

N_C is resultant critical load intensity in pounds per inch x 10^{-3} (positive N_C denotes tension).

N_t is ultimate hoop tensile load intensity due to internal pressure

[ ] is critical design load

Table 8.5-11. Booster Tank Sizing

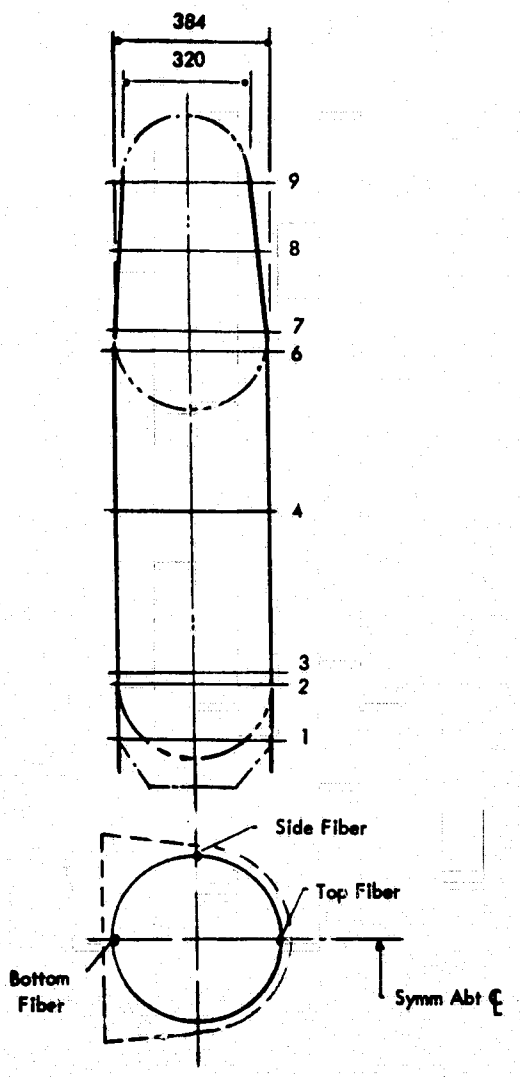

	Sta	Skin	Top		Bottom		Side	
			N_x	$\bar{t}$	N_x	$\bar{t}$	N_x	$\bar{t}$
LO_2 Tank	9	0.088	640	0.109	640	0.109	160	0.098
	8	0.086	11,810	0.340	1,240	0.140	2,510	0.210
	7	0.138	9,240	0.330	2,710	0.213	2,040	0.210
LH_2 Tank	6	0.168	8,620	0.320	3,840	0.232	3,920	0.244
	4	0.168	10,480	0.350	4,010	0.248	5,740	0.275
	3	0.174	12,530	0.400	7,450	0.302	5,320	0.275
Skirt	2	-	12,970	0.360	10,040	0.300	8,200	0.280

The data shown in Table 8.5-11 were calculated with the skin-stringer-frame computer program subroutine of one of the NR computer programs. In view of the reusability requirements, the skins are not permitted to buckle at stresses below the ultimate stresses. Table 8.5-12 illustrates the basic analytical relations used for the area requirements of the hat sections and the integral T stringer designs. The equations for the I section designs are similar.

The $\bar{t}$ data shown in Table 8.5-11 reflect stringer depths varying from 1.5 to 2.5 inches from the low to high load intensity regions and stringer pitches varying from 3 to 6 inches and frame spacings from 24 to 36 inches. Within the scope of this study, the load intensity values shown in Table 8.5-10

were not reiterated to account for the change in moment of inertia and section modulus resulting from the tapering of the $\bar{t}$ across the tank cross section. Also, Table 8.5-11 illustrates the optimum $\bar{t}$ for each different but individual N_X at any one station. These individual optimum $\bar{t}$'s for the top, bottom, and side fibers at each station were based upon different frame spacings. The frame spacings must be the same around the tank, and a realistic design will result in a slight weight increase above that shown in Table 8.5-11; however, the body loadings used are higher than those expected for the final configuration since they were based on the vehicle with separate bulkheads. That vehicle is approximately 22 feet longer than the final configuration; hence, the prelaunch, maximum $q\alpha$ and maximum g bending moments are higher. It is expected that the foregoing weight increases and decreases are generally of the same magnitude; therefore, the $\bar{t}$ values shown are sufficiently accurate for the weights estimate.

Booster Tank Bulkheads. Forward and aft bulkheads are provided for closure of the LO_2 and LH_2 tank conical and cylindrical body sections. A common bulkhead is provided for separation of LO_2 and LH_2 propellant. These bulkheads are designed to different loading conditions, but in general they are designed to withstand a combination of gas pressures and propellant hydrostatic head.

The selected vehicle configuration employs hemispherical bulkheads, since that shape provides the lightest bulkhead weight/volume characteristics and, most important, does not influence the vehicle length.

Booster Forward LO_2 Bulkhead. The forward bulkhead critical design condition occurs at booster burnout, at which time, the bulkhead experiences the highest temperature. Differential pressure across the bulkhead is the maximum relief valve pressure. The required gage at the bulkhead is 0.045 inches, which would be increased in the discontinuity stress area.

Booster Common Bulkhead. The common bulkhead is an aluminum-faced, phenolic-core honeycomb sandwich similar in structural concept to the common bulkhead design of the S-II stage in the Saturn V launch vehicle. Critical design conditions occur during prelaunch and at booster burnout. The critical prelaunch condition sizes the thickness of the face sheet in tension and occurs when the LO_2 tank is both fueled and pressurized and the LH_2 tank is unpressurized. The burnout condition results in a compressive differential pressure across the common bulkhead due to the difference in the LH_2 tank maximum relief pressure and the LO_2 minimum regulator pressure. When combined, these conditions require a sandwich bulkhead with each face sheet thickness equal to 0.038 inch and a sandwich depth of 2.75 inches.

Table 8.5-12. Study Analytical Relations

Item of Interest	Construction Geometry		Comments
Euler Buckling Stress Allowable	$\frac{\sigma_e}{\eta} = \frac{C\pi^2 E}{(\ell/\rho)^2}$		Critical stress for $\frac{\sigma_e}{\eta\sigma} \leq 0.50$
Local Crippling Stress Allowable	$\frac{\sigma_1}{\eta} = 3.62\,E\left[\frac{t_1}{1.4a}\right]^2$ $\frac{\sigma_2}{\eta} = 3.62\,E\left[\frac{t_1}{p-1.4a}\right]^2$ $\frac{\sigma_3}{\eta} = 3.62\,E\left[\frac{t_2}{a}\right]^2$ $\sigma_1 = \sigma_2 = \sigma_3$	$\frac{\sigma_1}{\eta} = 3.62\,E\left[\frac{t_1}{p}\right]^2$ $\frac{\sigma_2}{\eta} = 0.58\,E\left[\frac{t_2}{a}\right]^2$ $\sigma_1 = \sigma_2$	
Combined Inelastic Bending and Local Crippling Allowable	$\sigma_c = \sigma\left[1 - \frac{\sigma\eta}{4\sigma_e}\right]$ where $\sigma = \sigma_1, \sigma_2, \sigma_3$		Critical stress for $\frac{\sigma_e}{\eta\sigma} \geq 0.50$
Frame Equivalent t	$t_f = \left[\frac{0.0000684\ \pi N_x}{10.5\,L^3 E}\right]^{1/2} \times 2R^2$		t_f derived from Shanley Requirement $EI_f = M_e D^2/16,000\,L$

The following shell stability formula was used:

$$P_{cr} = \frac{1.09h}{r^2} Et_f$$

where

h = sandwich height in inches

r = sphere radius in inches

E = compressive modulus of elasticity

t_f = single face sheet thickness

Booster Aft LH_2 Tank Bulkhead. The aft bulkhead critical design condition occurs at booster burn out. The differential pressure across the bulkhead at this point is the LH_2 maximum relief valve pressure of 35 psia. The required gage of the dome is 0.078 inch.

Booster Thrust Structure. A preliminary design and stress analysis of the booster thrust structure shown in Figure 8.5-18 has been performed. This particular geometric configuration was selected since it resulted in the minimum engine pitch circle diameter (minimization of base heating) and permitted a practical lightweight structural configuration.

The thrust structure must transmit the load from ten 550,000-pound vacuum-thrust engines to the booster body structure perimeter, and it must sustain the load conditions that occur with all engines gimbaled concurrently with the applied engine gimbal actuator loads or with one engine out. The thrust structure must also provide structural rigidity compatible with the actuator engine control system.

To transmit these loads to the perimeter of the booster body structure, a skin-stringer-frame conical shell is provided. The eight outboard engine thrust loads are applied directly through the individual gimbal blocks attached to eight longerons. The two inboard engine thrust loads are applied to four crossbeams through compatible deflection of a rigid octagonal structure as shown in Figure 8.5-19. The four crossbeams transfer the total thrust of these two engines to the eight longerons. In addition, the crossbeams react the horizontal force component of the engine thrust load at the longerons. Total thrust loads are, in turn, sheared into the skin stringer shell. Six frames are provided on the shell at equal intervals to

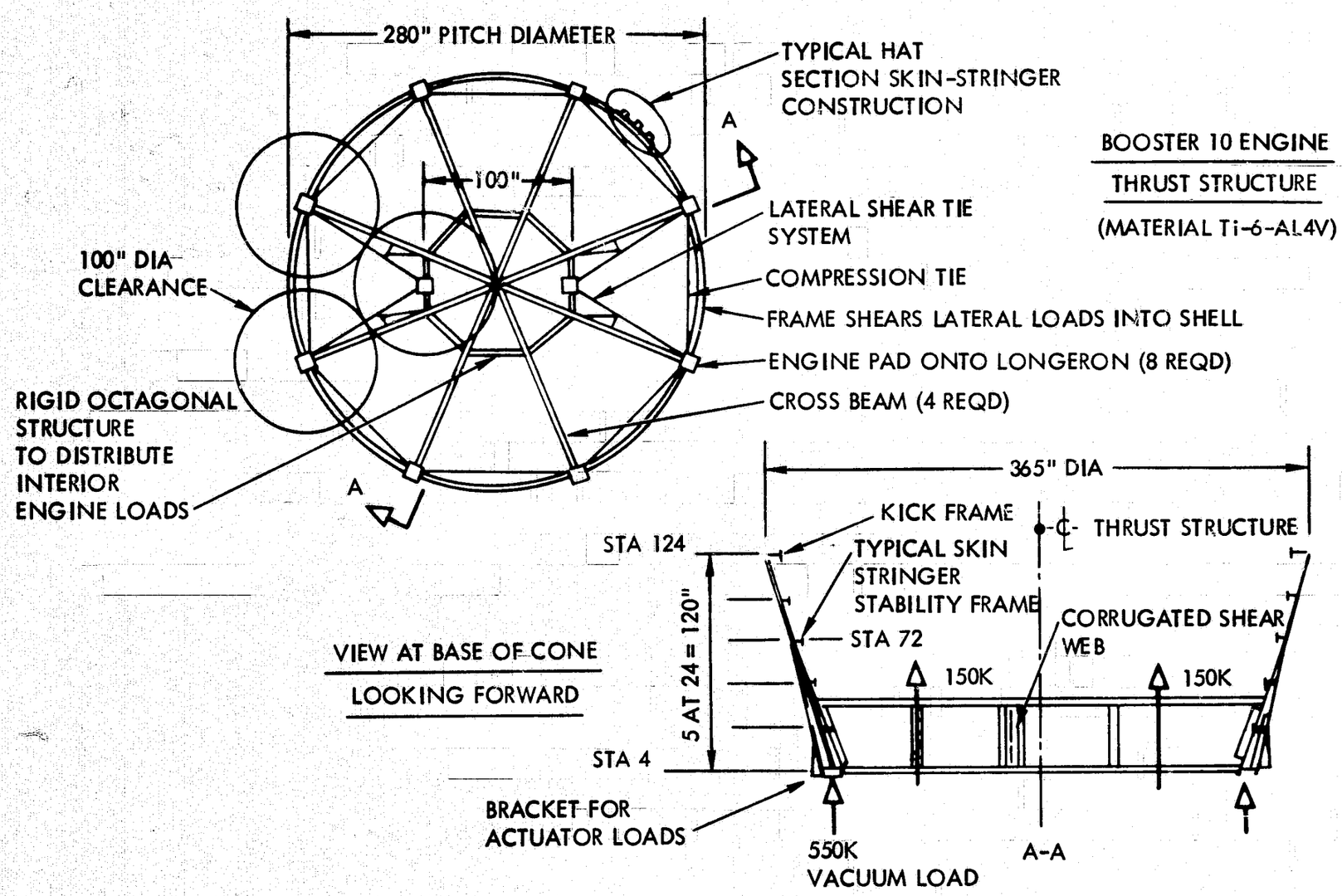

Figure 8.5-18. Booster Thrust Structure

Space Division
North American Rockwell

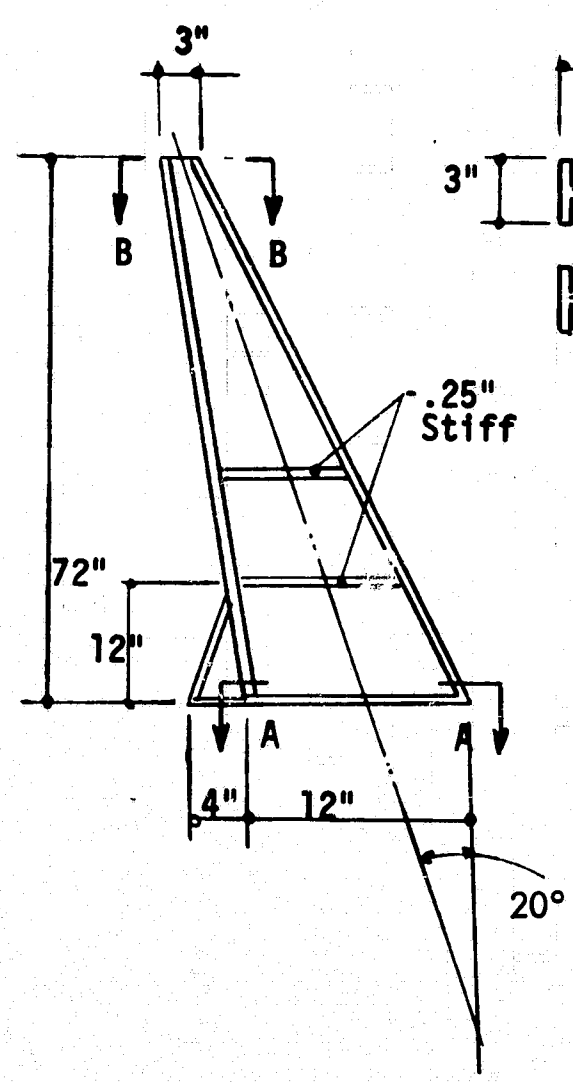

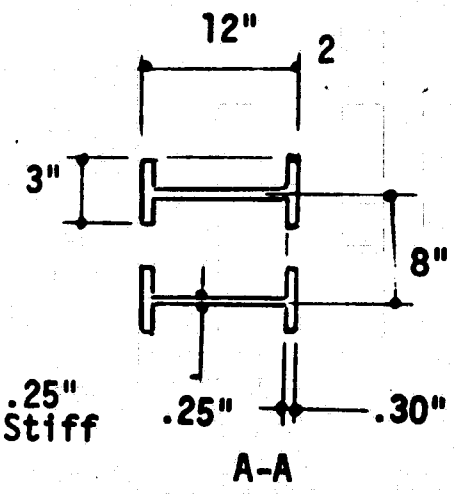

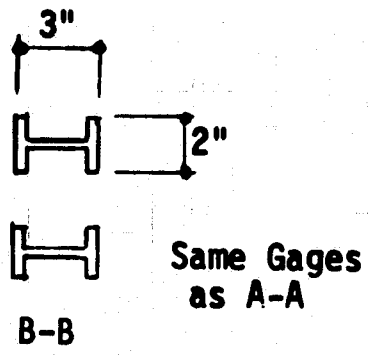

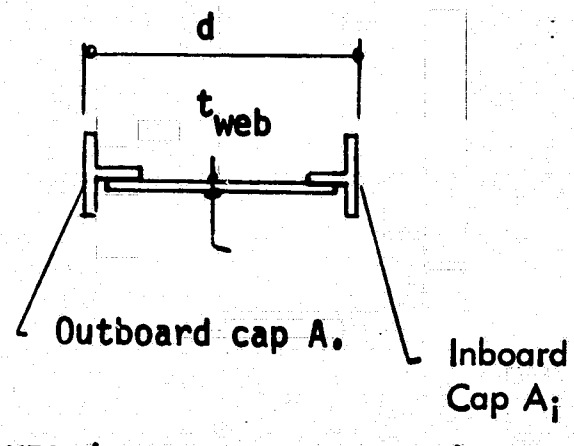

FRAMES (STABILITY AND LOAD)

STATION	R	d	A_i	A_o	t_{web}
4	140	10	1.15	1.15	.060
28	148	10	.37	.37	.062
52	156	10	.45	.45	.062
76	164	10	.93	.47	.040
100	173	10	.64	.64	.062
128	182	14	1.3	1.3	.075"

Figure 8.5-19. Thrust Structure Longerons

stabilize the skin stringer column designs, to react longeron kick loads, and to shear lateral forces into the shell. A system of compression ties and lateral supports are provided for efficient transfer of side forces into the aftmost frame and for stabilization of the crossbeam compression cap.

The preliminary-design-type stress analysis of this configuration was based upon the foregoing strength requirements and the use of titanium 6AL-4V throughout the design. A titanium 6A1-4V design is expected to have less weight than an aluminum design in view of the high loading intensities.

The thrust structure shown in Figure 8.5-18 has a maximum shell diameter of 365 inches. Further vehicle iteration resulted in a maximum diameter of 392 inches. Although this specific analysis was not updated, the thrust structure weight corresponding to the 365-inch-diameter shell was extrapolated to account for the increased diameter.

The following section contains the main features of the analysis performed.

Skin Stringer Design. The skin stringer analysis was based on experience with the S-II stage thrust structure design. Early designs of that structure have a near sinusoidal variation of longitudinal compression load intensity along the perimeter of the maximum diameter. Peak longitudinal load intensity near the longeron is three times greater than the loading midway between longerons. This condition is primarily due to the fact that four longerons are used; therefore, each longeron loading must be distributed out to 45 degrees away from the longeron. In this design, the eight longerons used reduce this requirement to 22.5 degrees. On the basis of the foregoing and since a shear-lag analysis was not within the scope of this study, it was assumed that the ratio between the peak loadings was approximately 1.5 times the loading midway between longerons, rather than the factor of 3 used for the S-II.

The critical skin-stringer design occurs with all the engines at full vacuum thrust and at a maximum gimbal angle of 7 degrees. The total ultimate axial load P is, therefore,

$$P = 1.5 \times 10 \times 550,000 \times \sin(83^\circ) = 8,120,000 \text{ lb} .$$

Total lateral shear V is

$$V = 1.5 \times 10 \times 550,000 \times \sin(7^\circ) = 1,000,000 \text{ lb} .$$

Maximum N_x (for a uniform distribution of load) at the base of the cone is therefore,

$$N_x = \left[\frac{8,120,000}{2\pi(182.5)} + \frac{1,000,000 \times 128}{\pi(182.5)^2}\right] \frac{1}{\cos(20°)} ; \; N_x = 8,900 \text{ lb/in} \quad .$$

Peak N_x (at the longeron) = 1.20 x 8,900 = 10,680 lb/in.

Minimum N_x between longerons = 7,120 lb/in.

A skin-stringer combined local crippling and inelastic bending analysis for these two load intensities for Ti-6Al-4V resulted in the designs shown in Figure 8.5-20.

On the basis of the foregoing designs and extrapolation from the S-II thrust structure analysis, the skin and stringer sizes shown in Figure 8.5-19 were determined.

Crossbeam Designs. The crossbeam design was based on the ultimate loading shown in Figure 8.5-21 (all loads are in thousands of pounds). These loads include a 10-percent increase to allow for non-uniformity of applied loads on the four crossbeams due to differential deflection.

The most efficient design for the crossbeam is a deep corrugated shear web to provide the shear continuity between the two caps. Resulting cap and web designs are shown in Figure 8.5-22. The I section is provided on the aft cap for column stability in the lateral direction.

Longerons. Longeron designs are based on the ultimate design loads shown in Figure 8.5-23 (all loads are in thousands of pounds). The 100,000-pound forces comprising a couple are the estimated engine actuator loads. Structural sizes are shown in Figure 8.5-19. Use of the two I sections minimizes total longeron section depth and precludes local bending about the minor axis of the longeron.

Frames. Frames at Stations 28, 52 and 100 are designed to stabilize the shell skin stringer column designs.

Frames at Station 4, 76, and 128 were designed as follows: The frame at Station 128 was designed by the kick load resulting from the 20 degree angle between the thrust structure conical shell and body structure shell. The frame at Station 4 was designed for the kick loads shown in the foregoing

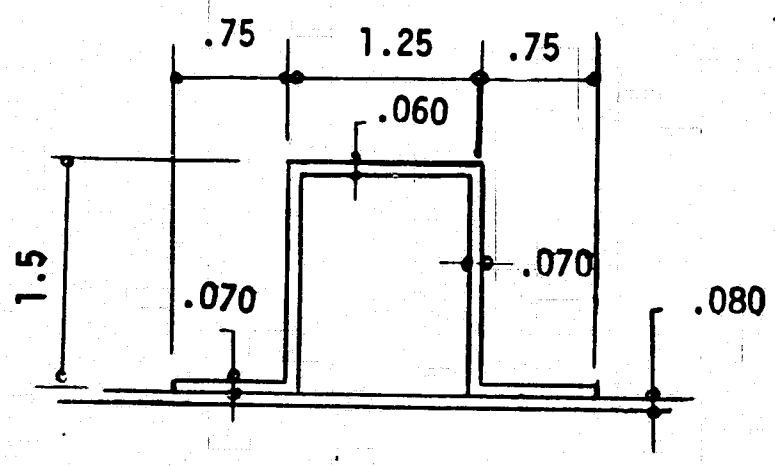

PITCH = 4.2 in @ Max Dia

N_X = 10680 lb/in
(Temp=70°F)

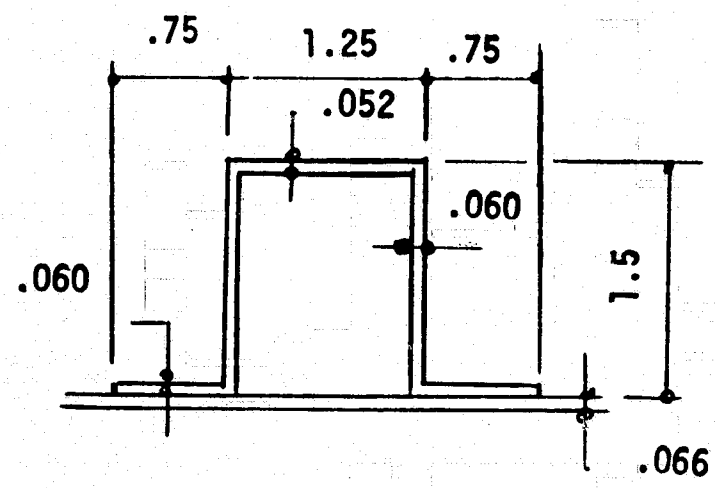

PITCH = 4.2 in @ Max Dia

N_X = 7120 lb/in
(Temp=300°F)

Figure 8.5-20. Skin-Stringer Designs

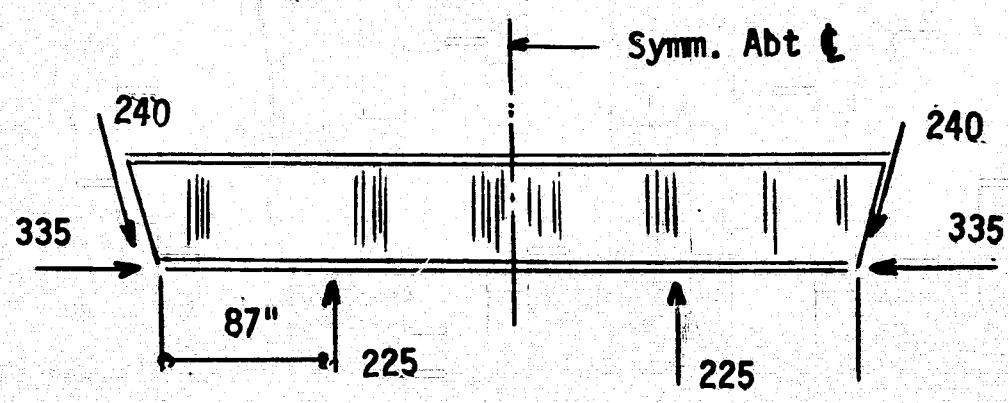

Figure 8.5-21. Crossbeam Design Loads

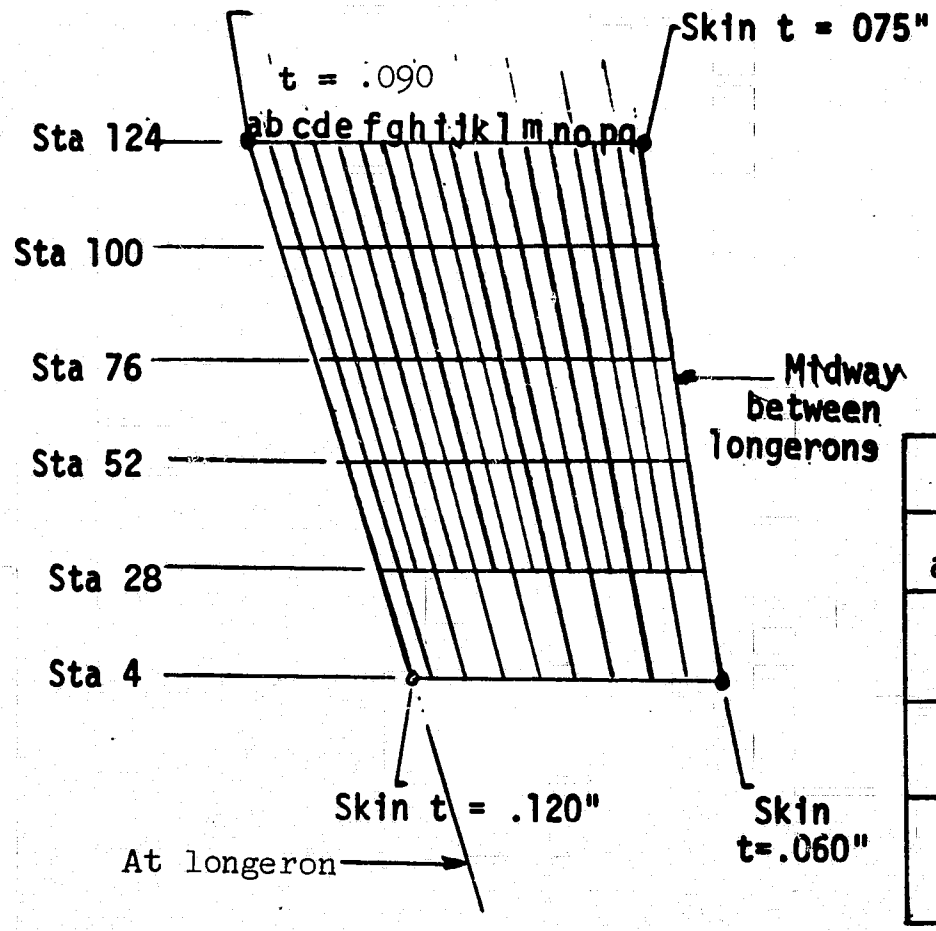

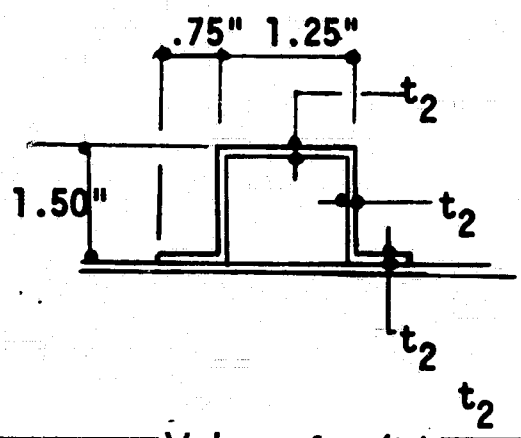

Values of t_2 (in) STA 4 to 100			
a to d	e to i	j to m	n to g
.070	.065	.060	.056
STA 100 to 124			
.100	.090	.080	.070

CROSS BEAM DESIGN

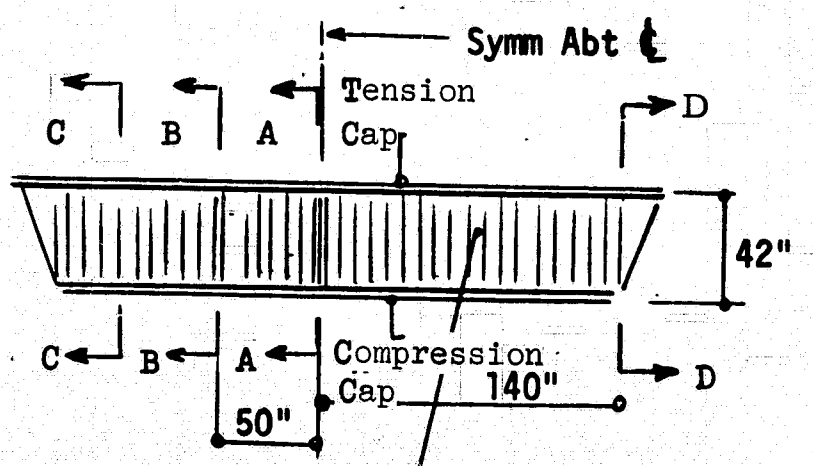

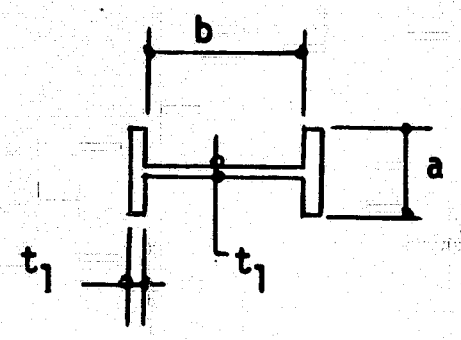

Typical Cap

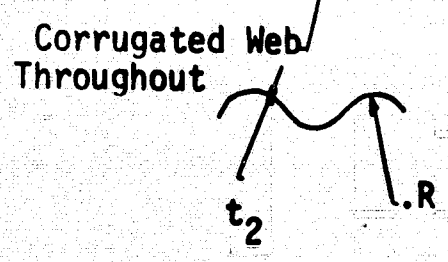

C = Compression Cap
T = Tension Cap

SECT		a	b	t_1	t_2	R
A-A	C	2.0	4.0	.83	.056	2.3
	T	--	4.0	.84		
B-B	C	2.0	4.0	.83	.100	2.75
	T	--	4.0	.84		
C-d	C	2.0	4.0	.59	.100	2.75
	T	--	3.0	.54		
D-D	C	--	4.0	.35	.100	2.75
	T	--	2.0	.35		

Figure 8.5-22. Thrust Structure

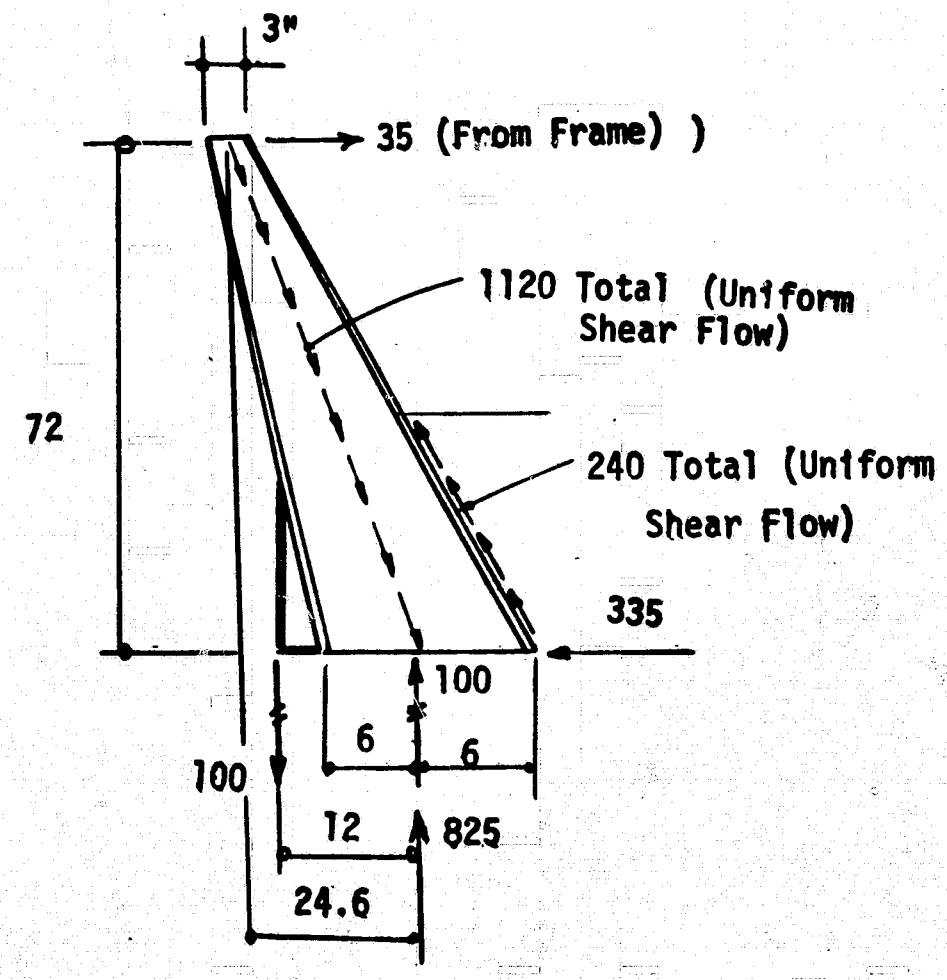

Figure 8.5-23. Longeron Design Loads

longeron free-body diagram. The one-engine-out condition was critical. The frame at Station 76 was also designed by the one-engine-out condition.

Booster Main Frames for Large Concentrated Loads, Wing Frame. A wing frame assembly, consisting of a pair of struts and a ring frame, is provided at each wing spar to transfer the spar shear into the body structure. Figure 8.5-24 illustrates this ring-frame assembly and includes the free-body diagram used in this gross review for structural sizing.

The struts are designed as a pin-ended column to preclude local crippling or Euler column failure. For lateral stability, a floating shear lug is provided between the frame and wing upper cap. The following analyses were used to determine the Ti-6Al-4V 13-inch-diameter by 0.137-inch-thick wall tube.

$$\sigma_{Euler} = \frac{\pi^2 E r^2}{2\ell^2} = \frac{9.9 \times 16 \times 10^6 \times (6.5)^2}{2 \times (200^2)} = 84,000 \text{ psi}$$

$$\sigma_{crippling} = \frac{0.25 E t}{r} = 0.25 \times 16 \times 10^6 \times \frac{0.137}{6.5} = 84,000 \text{ psi}$$

The actual stress is

$$f = \frac{480,000}{2\pi(6.5)(0.137)} = 84,000 \text{ psi}$$

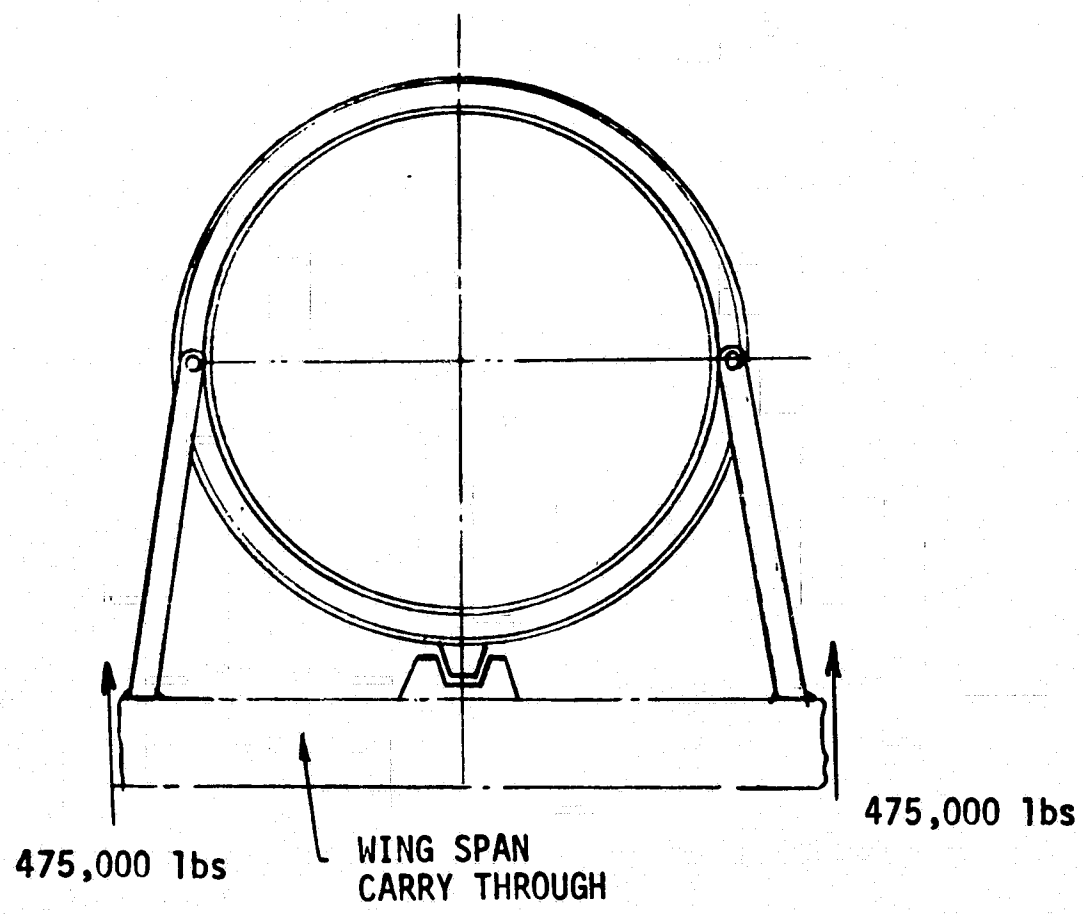

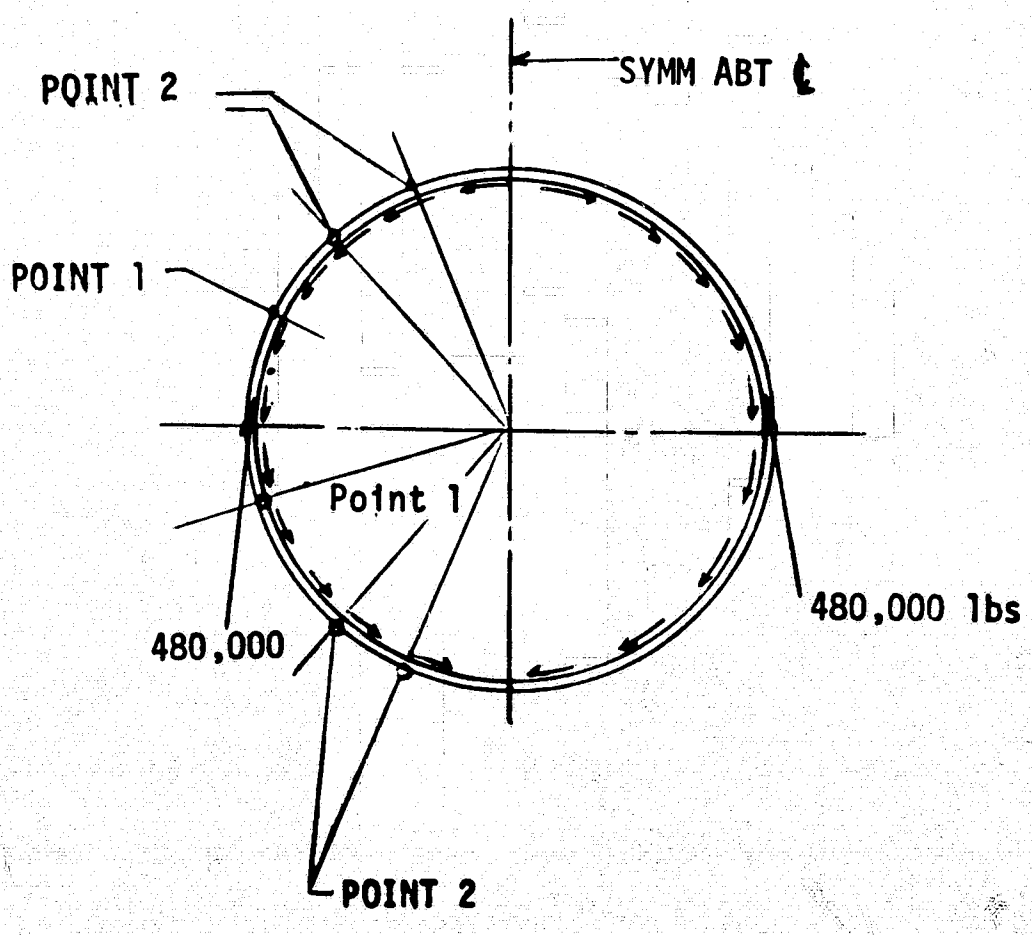

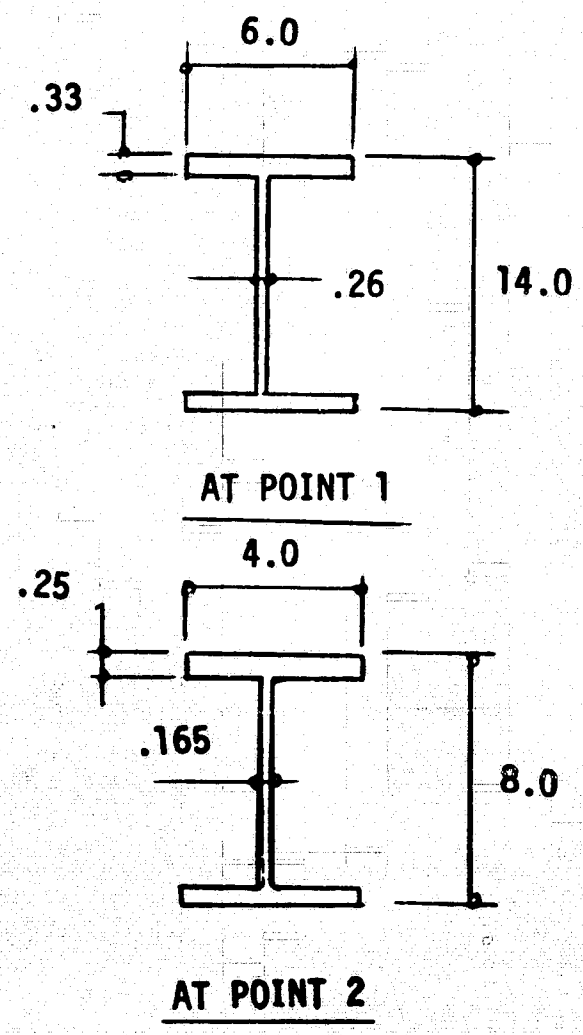

Figure 8.5-24. Wing-Frame Loads and Sections

The circular frame was designed to satisfy the internal moments and forces resulting from the loading shown in Figure 8.5-24. Maximum moment and associated compressive axial force at Point 1 are as follows:

$$M_{max} = 0.029\ (480,000)\ (192) = 2,700,000\ \text{lb-in}$$

$$N = 0.285 \times 485,000 = 140,000\ \text{lb}$$

The Ti-6Al-4V section required is shown in Figure 8.5-24 and satisfies the load requirements in the following manner:

$$\sigma_{flange} = 0.59 \times 16 \times 10^6 \left(\frac{0.33}{3.0}\right)^2 = 114\ \text{ksi allowable}$$

$$\sigma_{web} = 16.0 \times 16 \times 10^6 \times \left(\frac{0.26}{13.3}\right)^2 = 97\ \text{ksi allowable}$$

$$\sigma_{\text{applied to flange}} = \frac{140}{7.3} + \frac{2,700 \times 7}{237} = 99\ \text{ksi}$$

$$\sigma_{\text{applied to web}} = 95\ \text{ksi}$$

Point 2, illustrated in Figure 8.5-21, is representative of the minimum load requirement of this frame for weight-averaging purposes. The moment and axial loads are as follows:

$$M_{min} = 0.011 \times 480,000 \times 192 = 1,000,000 \text{ lb-in}$$

$$N = 48,000 \text{ lb}$$

$$\sigma_{flange} = 0.59 \times 16 \times 10^6 \times \left(\frac{0.25}{2}\right)^2 = 135 \text{ ksi allowable}$$

$$\sigma_{web} = 16 \times 16 \times 10^6 \times \left(\frac{0.165}{7.5}\right)^2 = 117 \text{ ksi allowable}$$

$$\sigma_{\text{applied to flange}} = \frac{48}{3.25} + \frac{1,000 \times 4}{35.8} = 128 \text{ ksi}$$

$$\sigma_{\text{applied to web}} = 117 \text{ ksi}$$

The average cross-sectional area of these frames was used for the weights analysis.

Support Structure for Booster Thermal Protection System. The heat shield support structure is the mounting platform to which the LI-15 and TG 15000 insulation are secured. This heat shield structure must survive the entire spectrum of aerodynamic and acoustically induced differential pressures, inertial loads, and thermally induced stresses for up to 100 missions.

The heat shield structural concept is shown in Figure 8.5-25. The LI-15 exterior insulation is bonded to the 1.10-inch phenolic glass-reinforced laminate honeycomb sandwich with a silicone adhesive. On the top of the vehicle, where LI-15 is not required, a polyimide glass-reinforced honeycomb sandwich is used. The face sheets are two-ply laminates for a total thickness of 0.020 inch. These panels are mounted onto the outer cap of the booster body structure frames; therefore, they must span the distance between the frames. TG 15000 insulation is expected to be placed between the inner face of the sandwich and a light mesh membrane attached to the panel. It is pertinent to note that, for the lower portion of the booster,

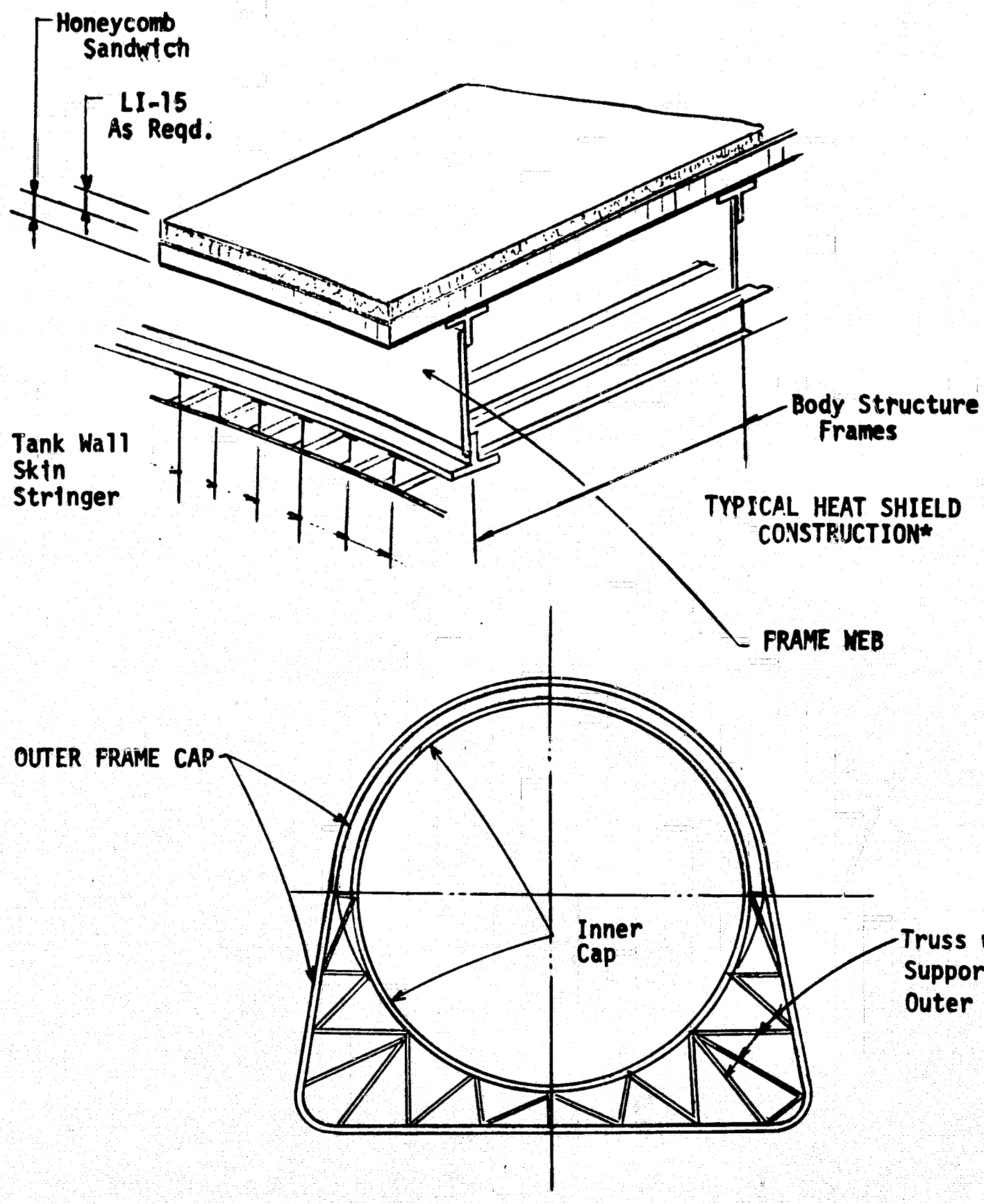

* FOR LOWER SURFACE TRUSS WORK
REPLACES FRAME WEB

Figure 8.5-25. Typical Heat Shield Construction

the body structure frame is extended to the mold line by a truss configuration as shown in Figure 8.5-25.

Environmental Requirements. On the basis of the combined static and dynamic pressures shown in Figure 8.5-26 and for the purposes of this study, it was assumed that the most severe dfferential pressure across the sandwich can be limited to 2 psi throughout the mission by proper control of the pressure between the heat shield support structure and the tank.

In the absence of data describing the aerodynamic and acoustical environmental criteria and to provide a smooth surface for the booster airplane flight performance, the peak panel deflection is limited to one percent of the panel span length.

Thermal environment criteria used in this analysis of the heat shield support structure consist of a peak temperature on the outer face of 400 F at the bond line and a maximum gradient of 100 F across the section.

Structural Approach. The phenolic glass-reinforced laminate honeycomb sandwich panels were selected on the basis of their suitability for the 400 F bondline temperature and their high strength-to-weight ratio. A square grid framework consisting of beams to support the panels was considered along with the selected design. With this framework, the minimum sandwich feasible was assumed to be 3/4 inches deep. This design represents the minimum sandwich weight and maximum support structure weight. The other end of the design spectrum was an increased sandwich depth without the grid work; i.e., maximum sandwich weight with no support structure other than the body structure existing frames (designed by other conditions).

Structural Analysis. Structural analysis indicated the latter design was lighter by 0.19 pound per square foot as shown by the following unit weights:

	Concept	
Unit	Minimum Panel Design With Framework (lb/ft^2)	Panel Design Without Framework (lb/ft^2)
Face Sheet	0.40	0.40
Core	0.19	0.28
Bond	0.30	0.30
Framework	0.28	--
Total (Weight)	1.17	0.98

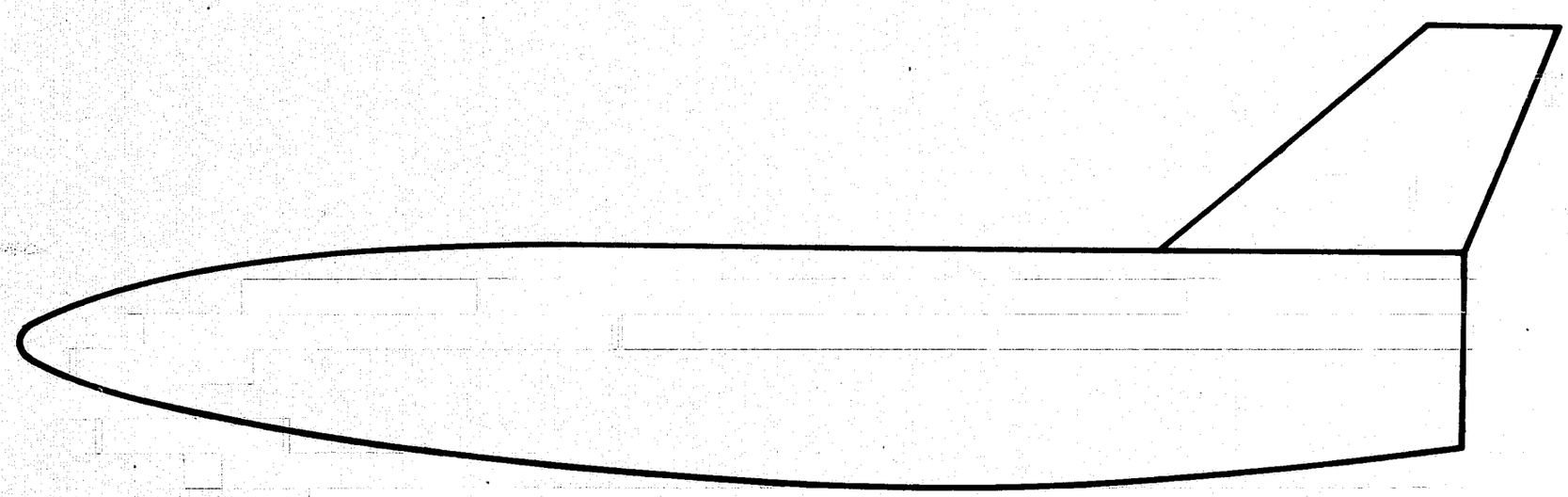

X/L	0	.2	.4	.6	.8	1.0
ASCENT PRESSURE AT MAX Q (LBS/FT^2) (TIME = 76 SEC) BOTTOM AND SIDES	1510	800	789	788*	788	788
ENTRY PRESSURE AT MAX RADIATION EQUILIBRIUM TEMPERATURE (LB/FT^2)	221	145	130	112	90	76
MAXIMUM ENTRY PRESSURE (LB/FT^2)	335	159	149	123	110	100

* Side Pressure May Be Somewhat Higher Due to Wing Interference

Figure 8.5-26. Pressure Distribution on Sides and Bottom of ILRV Booster Fuselage

These data were obtained on the basis of the following structural analysis equations.

The selected design is visualized as a continuous one-way plate spanning across the frames. The maximum deflection y and bending moment M in the exterior span are expressed by

$$y = 0.0054 \frac{W \ell^4}{EI}$$

and

$$M = \frac{1}{10} w \ell^2$$

For $y = 0.01 \ell$, the maximum span compatible with the deflection requirement is defined by

$$\ell = 1.22 \left[\frac{EI}{w}\right]^{1/3},$$

where

$$I = \frac{t_f h^2}{2}$$

For $E = 3.2 \times 10^6$ psi, $t_f = 0.020$ inch, $h = 1.10$ inches, and $w = 2$ lb-in./in. (limit), the permissible span length is 34 inches. (The same length was used in the alternate design utilizing a 3/4-inch-thick panel supported in a square grid framing configuration.) This spacing is expected to be compatible with the frame spacing required to stabilize the body structure skin-stringer column designs.

The maximum moment for w = 3 lb/in/in (ultimate) is 350 lb-in./in. and imposes a face sheet stress of 16,000 psi. The stresses due to a 100 F gradient across the sandwich for the worst case is 1,500 psi. No significant thermal stresses are permitted to occur in the longitudinal direction; i.e., the attachment of the panel to the frame accommodates the relative longitudinal dimensional changes.

Frame Extension Structure. Extension of the frames provided to stabilize the booster-body-structure skin-stringer column designs is required to support the honeycomb sandwich panels located on the lower half of the booster fuselage (Figure 8.5-25). The primary function of this structure is to transfer the panel air loads into the basic body frame. The truss configuration shown is expected to be the lightest design for this application. It should be lighter than a stiffened shear web with lightening holes. Furthermore, the thin gage of a near competitive shear web with lightening holes could present a potential flutter problem.

Loading distribution for the trusswork is shown in Figure 8.5-27. It is assumed that the structural temperatures on the outer chord do not exceed 250 F. The inner chord is designed with 100 F properties. The properties of aluminum 2219-T87 were used for this analysis.

The outer cap is designed as a continuous-beam column spanning between the trusswork members shown. Beam loading requirements were most significant in sizing the cap members. The maximum bending moment of the beam at the support was determined by $M = 1/12\ wl^2$; and for $w = 102$ lb/in. and $\ell = 34$ inches, $M = 39,200$ lb-in. An average axial load (for weight sizing purposes) of 4000 pounds was used. The typical section shown in Figure 8.5-28 was determined. Additional moment due to beam deflection and axial load was considered and determined to be negligible. Allowable crippling stresses were determined as follows:

For the flange,

$$\frac{\sigma_f}{\eta} = 0.59\ E \left[\frac{t_f}{b_f}\right]^2$$

$$\sigma_f = 52 \text{ ksi}$$

For the web,

$$\frac{\sigma_w}{\eta} = 16.0\ E \left[\frac{t_w}{d}\right]^2$$

$$\sigma_w = 50 \text{ ksi}$$

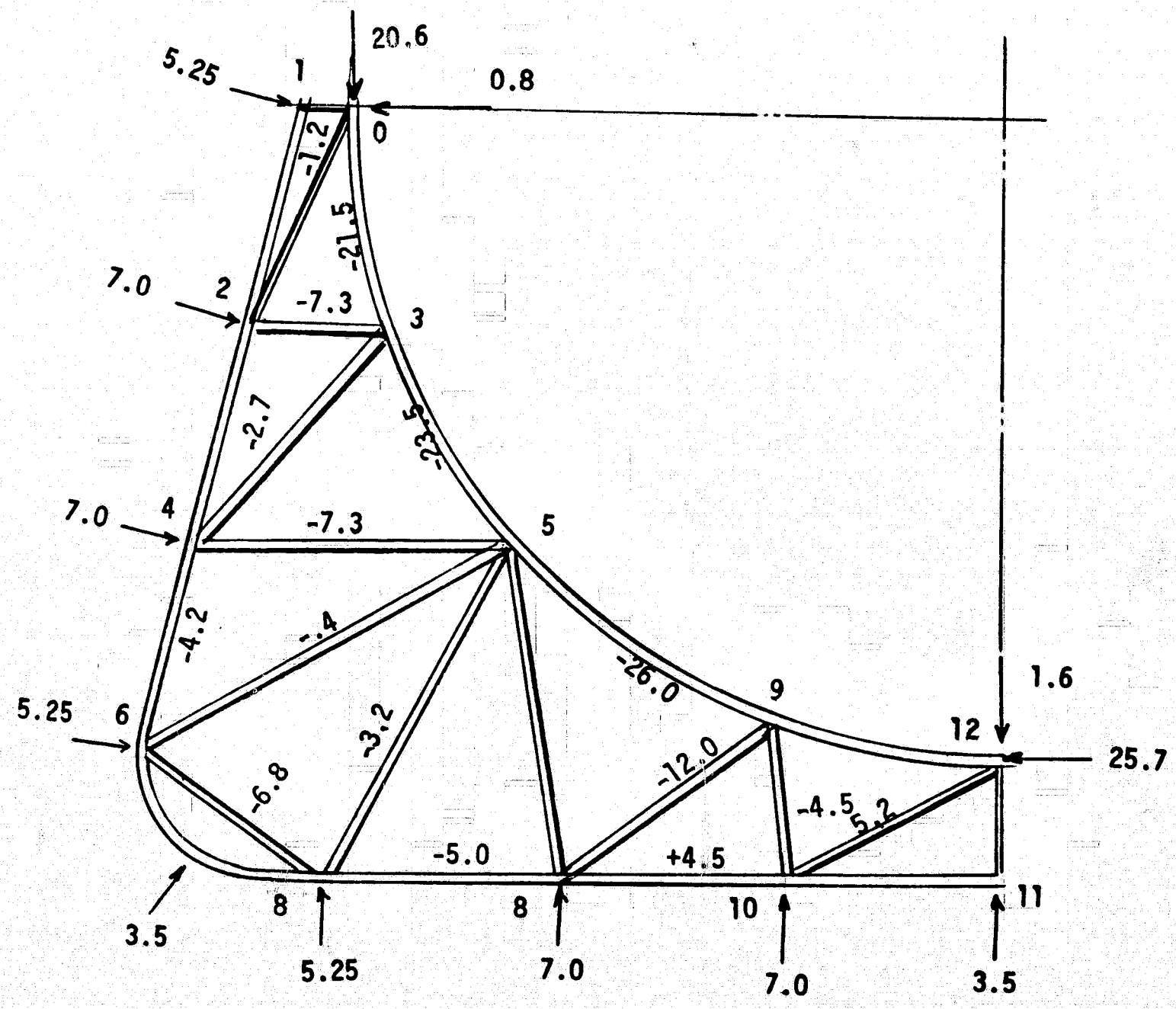

Figure 8.5-27. Truss Support Structure for Fiberglass-Reinforced Sandwich Panels

The peak compression stress at the support and at the center of the cap is

$$f = \frac{4,000}{0.69} + \frac{3,920 \times 1.75}{1.50} = 5.8 + 46 = 51.8 \text{ ksi}$$

and at the top of the web is 50 ksi.

The diagonals of the truss are designed to satisfy the compressive stresses for the given loads diagram. A local buckling requirement is not critical for the circular columns used in this analysis; therefore, a minimum gage of 0.040 inch is used for the aluminum members. All members are designed as pin-ended columns to the Euler column buckling criteria, with a minimum L/ρ of 120 maintained where the load is not critical. The resulting design is shown in Table 8.5-13.

The truss inner cap is provided by the stability or load frames on the basic load-carrying shell. Rigorous analysis to determine the specific structural requirements to satisfy the combination of the frame requirements to stabilize the body structure skin-stringer columns and the compression loads (Figure 8.5-27) was not performed in this study. The approach used was to determine the weight required for the compressive loading alone and to add only that portion of the weight in excess of that provided by the shell stability criteria of the frames. An average compressive force of 26,000 pounds was used to estimate the inner cap weight requirement. Since the member was analyzed as a pin-ended curved column, the axial load and bending-induced stresses were determined. Here also, the additional moment due to the product of the axial load and load induced deflection of the member was negligible.

The computed moment = 26,000 x 2.75 inches = 72,000 inch-pounds. The section shown in Figure 8.5-29 is based on a 100 F temperature and was used with the critical compression stress determined as follows:

$$\sigma_f = \frac{26,000}{1.31} + \frac{72,000 \times 2.5}{6.15}$$

$$f_{\text{flange}} = 49,000 \text{ psi}$$

$$f_{\text{web}} = 48,000 \text{ psi}$$

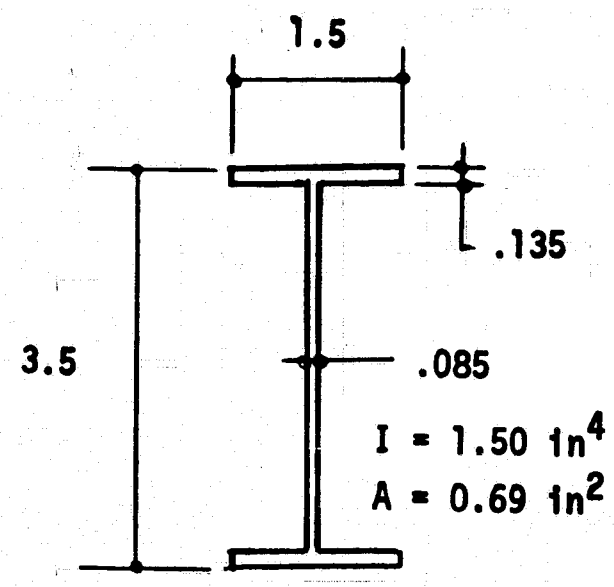

Figure 8.5-28. Frame-Extension Beam Section

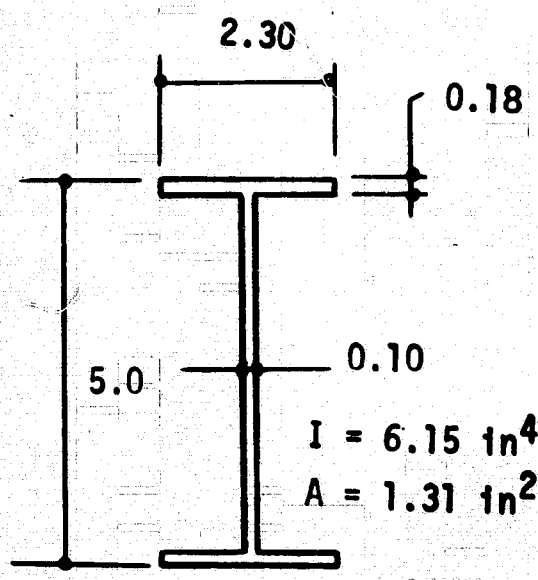

Figure 8.5-29. Frame Beam Section

$$\sigma_{(flange)} = 0.59 \times E \left[\frac{t_f}{b_f}\right]^2$$

$$\sigma_{flange} = 54,000 \text{ psi}$$

$$\sigma_{(web)} = 16.0\ E \left[\frac{t_w}{b_w}\right]^2$$

$$\sigma_{web} = 48 \text{ ksi}$$

The frame area of 1.31 square inches was then compared with the stability frame areas provided on the body structure. Additional frame material was added to the body structure frames where required.

Table 8.5-13. Heat Shield Truss Web Members*

Member	Column Load (lb)	Length (in.)	Tube Radius (in.)
0-1	5550	15	0.54
0-2	Negligible	75	0.89
2-3	7300	45	1.05
3-4	Negligible	90	1.34
4-5	7300	100	1.82
5-6	400	125	1.47
5-7	3200	120	1.55
5-8	Negligible	100	1.18
8-9	12000	80	1.84
9-10	4500	50	0.96
10-12 *	5200	75	1.20
12-11	7000	35	0.88

*These designs are of constant cross-section, t = 0.040 inches. Future study should investigate use of tapered sections of non-circular section to minimize connections and basic measured weight.

Booster Wing Structure. The wing loads are computed for the configuration shown in Figure 8.2- (Drawing 2234-69). These loads are also applicable to the latest configuration shown in Figure 8.2- (Drawing 2234-76). Wing geometry and areas are the same.

The structural box of the wing extends from 0.15 chord to 0.65 chord and the center section carries through the body. At the side of the body, the symmetrical airfoil has a 14-percent thickness, which tapers to a 12-percent thickness at the tip.

The ultimate bending moments for the booster are:

$$M_{\text{side of body}} = 1.5(-2.98 \times 10^8) = -4.47 \times 10^8 \text{ in.-lb}$$

$$M_{1/3 \text{ exp span}} = 1.5(-1.09 \times 10^8) = -1.635 \times 10^8 \text{ in.-lb}$$

These moments are down-bending (compression on lower cover) and occur during boost for the maximum $q\alpha$ condition.

The method of analysis for the booster wing follows that shown for the orbiter wing analysis.

The lower compression cover of the booster will be sized for the loads in Table 8.5-14 using Y-tee stiffeners of 6Al-4V STA titanium alloy. Sizes for the lower cover of the booster wings are presented in Table 8.5-15.

The upper cover of the booster wing is sized to F_{tu} for the same N_x loading used on the lower cover. The upper cover is also checked for 50 percent of this loading in compression. This represents the positive bending maximum $q\alpha$ condition during boost. The sizes for the booster wing upper cover are presented in Table 8.5-16.

At the time the weight calculations were made, it was assumed that the upper cover weight was equal to the lower cover. The weight saving indicated above for the upper cover is not reflected in the weight statement. This weight saving is about 6,300 pounds for the booster wing. As shown in the flutter checks, this weight saving may not be realized.

Based on statistical data developed for aircraft in the Los Angeles Division of NR, 3.5 pounds per square foot is used for the weight of leading edges and 5 pounds per square foot for the flap, aileron, and trailing-edge structures of this wing. A factor of 127 percent is applied to the calculated weight of the wing box to obtain actual wing hardware weight.

Table 8.5-14. Booster Wing Analysis Data

Wing Station	Chord (in.)	Maximum Thickness (in.)	Structural Average Thickness (in.)	Box Width (in.)	Moment (in. - lb x 10^6)	Axial Load N_x (lb/in.)
Side of Body	514	72	65.5	257	-447	26,600
1/3 of Outer Span	400	53.2	48.4	200	-163.5	16,900
2/3 of Outer Span	290	36.8	33.5	145	- 49.3*	10,130
Tip	190	22.8	20.8	95	0	0

*Ratioed from corresponding moments on orbiter wing
$BM_{2/3} = BM_{root} (OM_{2/3}/OM_{root})$.

Table 8.5-15. Booster Wing Lower Cover Sizes

Wing Station	N_x (lb/in.)	L (in.)	E (psi)	$\bar{t}$* (in.)	Stress (psi)
0	26,600	40	16 x 10^6	0.233	-114,000
1/3	16,900	40	16 x 10^6	0.185	- 91,300
2/3	10,130	40	16 x 10^6	0.143	- 71,000
1	0	40	16 x 10^6	0.054 (minimum)	-

* $\bar{t} = (N_x L/\epsilon E)^{1/2}$

Table 8.5-16. Booster Wing Upper Cover Sizes

Wing Station	N_{xc} (lb/in.)	$\bar{t}_{comp}$ (in.)	N_{xt} (lb/in.)	$\bar{t}_{tens.}$ (in.)	$\bar{t}_{Design}$ (in.)
0	13,300	0.163	26,600	0.166	0.166
1/3	8,450	0.131	16,900	0.106	0.131
2/3	5,065	0.101	10,130	0.063	0.101
1	0	0	0	0	0.054 (Min.)

Based on flutter requirements, a preliminary wing torsional stiffness requirement was calculated for the booster wing and is shown in Figure 8.5-30. The available torsional stiffness from the Structures-Group-designed box is calculated below.

These calculations are based on the wing shins having the same thicknesses at the root section or the side of the body. Skin thickness is:

$$t_s = \frac{\bar{t}\,(1 + r_{bz})}{\alpha}$$

$$t_s = \frac{0.233\,(1 + 0.94)}{6.12} = 0.074$$

The spar web effective thickness is obtained from the optimum chart shown in Figure 8.5-26. For preliminary design, this 8Al-1Mo-1V titanium chart is adequate for the 6Al-4V titanium. Here the ultimate shear load is:

$$P_{su} = 1.5 \times 6.37 \times 10^5 = 9.56 \times 10^5 \text{ lb}$$

Note: This curve does not include the effect of the adverse engine c. g. location

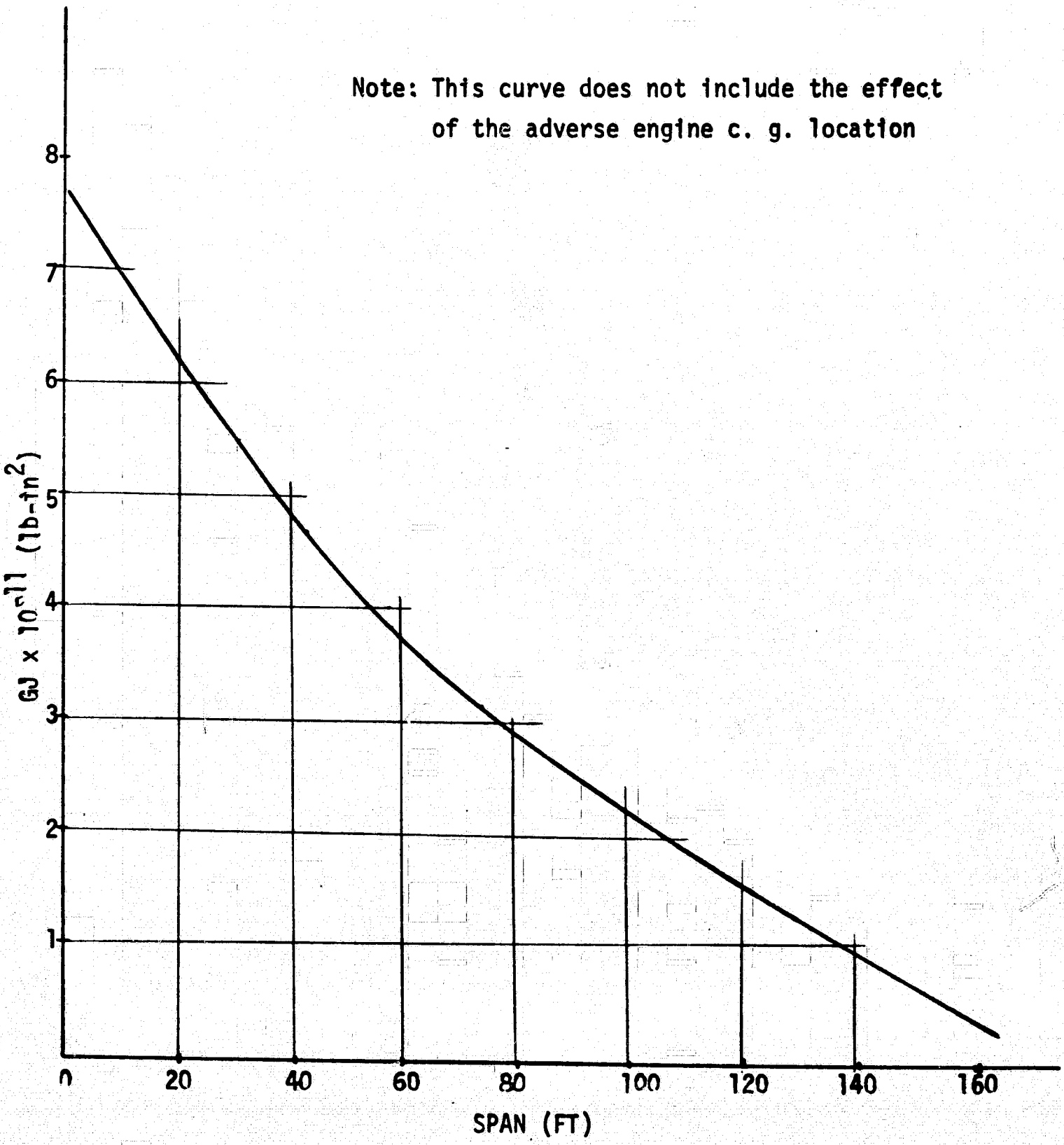

Figure 8.5-30. Preliminary Wing Torsional Stiffness Based on Flutter Requirements

$$q = \frac{9.56 \times 10^5}{2 \times 65.5} = 7300 \text{ lb/in.}$$

$$q/b = \frac{7300}{65.5} = 111.3$$

$$\frac{\bar{t}}{b} = 0.0018$$

$$\bar{t} = 0.118$$

From Figure 8.5-31 for diagonal tension stiffened sheet, the web thickness for this is 0.092 inch.

The resulting box section at the side of the body is shown below:

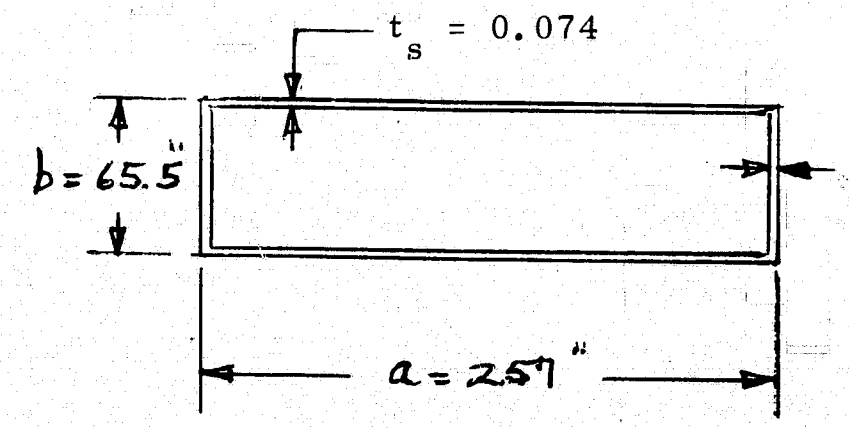

$t_w = 0.092$ (same for front spar)

0.074 (same for bottom cover)

It is assumed for these calculations that the critical flutter stiffness requirement occurs during the maximum q α condition in the boost configuration. During this condition, the lower cover is protected by LI-15 insulation, and the titanium will be at ambient or room temperature. The top of the wing is unprotected and will be at 400 F. The modulus of rigidity of 6Al-4V STA titanium is 6.2×10^6 at room temperature and 5.6×10^6 at 400 F. An average value of 5.9×10^6 will be used

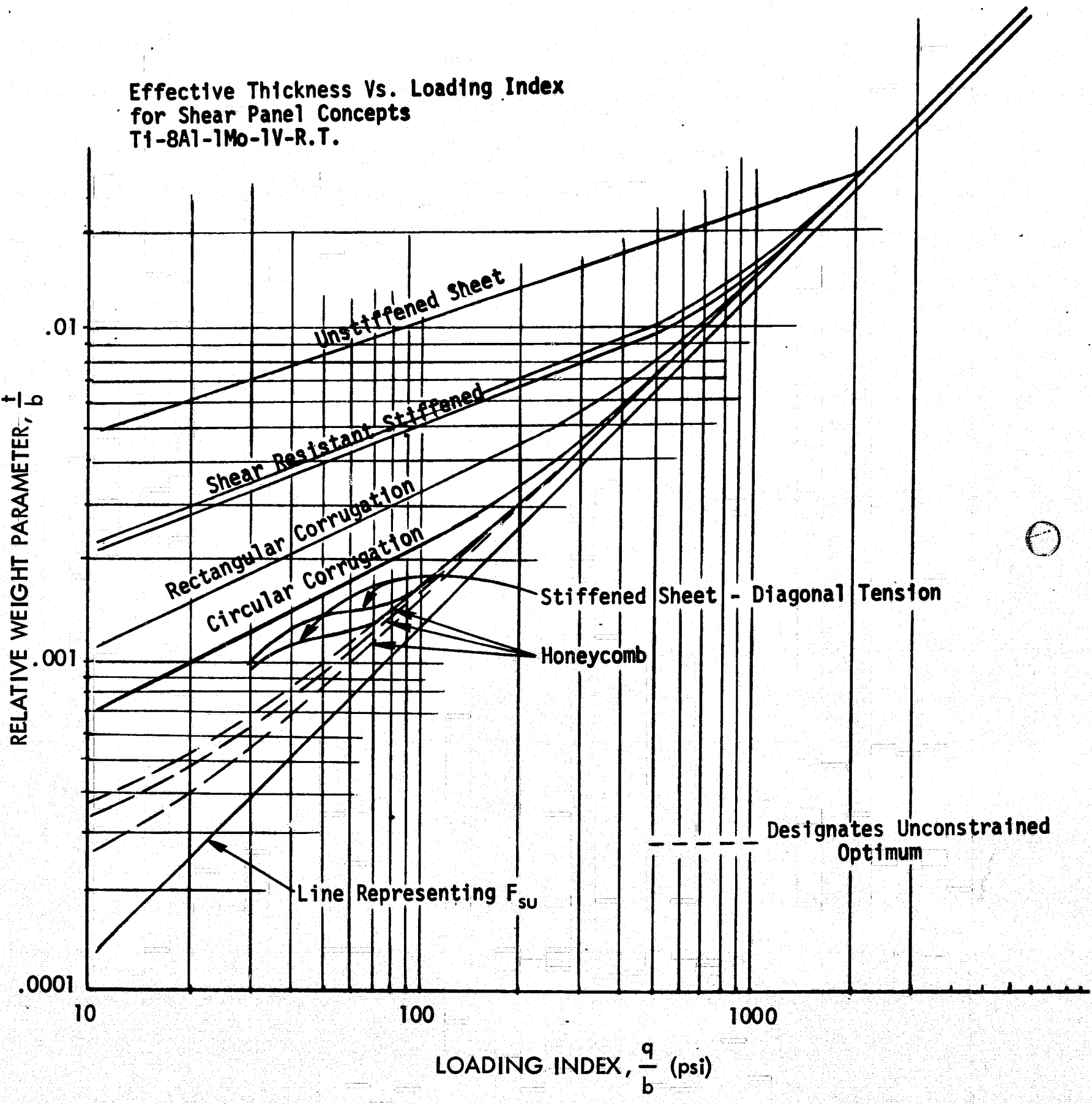

Figure 8.5-31. Optimum Shear Webs

$$J = \frac{2t_w t_s (a^2 b^2)}{at_w + bt_s}$$

$$= \frac{2 \times 0.92 \times 10^{-1} \times 0.74 \times 10^{-1} \overline{\quad}^2 \quad \overline{\quad}^2 (2.57 \times 0.655)\, 10^8}{2.57 \times 10^2 \times 0.92 \times 10^{-1} + 0.655 \times 10^2 \times 0.74 \times 10^{-1}}$$

$$= 1.36 \times 10^5$$

$$GJ = 5.9 \times 10^6 (1.36 \times 10^5)$$

$$GJ = 8.03 \times 10^{11}$$

This value is 5-percent higher than the maximum GJ requirement of 7.65×10^{11} shown in Figure 8.5-25 and the wing box is acceptable for this flutter requirement.

In summary, all the weight savings shown for the upper wing cover will not be realized if the preliminary flutter requirements shown in Figure 8.5-30 are substantiated.

Booster Horizontal and Vertical Tail Structures. Horizontal tail structure was sized by methods very similar to those used on the wing. The box structure of the tail also has a carry-through section in the body region. The tail is sized for 6Al-4V STA titanium alloy to the loading from the maximum q α condition during boost.

The vertical tail was sized to the maximum q α boost condition. For a 5-degree sideslip, the side load equals 711,000 pounds ultimate at the tail centroid. The root ultimate moment equals 142.5×10^6 inch-pounds. 6Al-4V STA titanium alloy will also be used for sizing the vertical tail. The vertical tail has no LI-15 insulation. Metal structure is exposed to the heating environment. The maximum temperature is 400 F on the box structure during the critical design condition maximum q α. Maximum temperature on the side of the vertical tail is expected to be 650 F.

Structural sizing is based on a 12-percent-thick tail.

The box structure extends from 29 percent to 65 percent of the chord; and at the root section, all the bending and shear loads are concentrated in

the two spars. The total box structure is fully effective from about 40 percent to 100 percent of the span.

Cap loads at the root section are:

$$N_x = \frac{1.425 \times 10^8}{61.4 \times 2} = 1.16 \times 10^6 \text{ lb}$$

$$\text{Cap area} = \frac{1.16 \times 10^6}{0.95 \times 10^5} = 12.2 \text{ sq in.}$$

Box structure is sized by the same methods used for the wing structure.

Statistical values of 3.5 and 5 pounds per square foot were selected for weight estimation of the leading edge and the rudder.

8.5.8 Orbiter Structure

The structural analysis and definition of the orbiter structure elements are presented in the following paragraphs.

Orbiter Tankage. Orbiter tankage contains the LH_2 and LO_2 propellants. The tankage must sustain the associated spectrum of loads and be reusable for 100 missions. Primary loadings are the pressurization system gas pressures combined with the pressures resulting from acceleration of the propellant mass.

The orbiter tankage is contained within, and supported from, the outer primary load-carrying structure. The configuration is essentially two nested cylinders with closure provided by nested hemispherical bulkheads. The additional manufacturing complexity of the nested design is recognized, but its weight advantages and higher volumetric efficiency could not be ignored.

Since a membrane tensile stress environment is anticipated (excepting local discontinuity areas), the entire orbiter tankage is of monocoque construction except at the bulkhead area common to the LO_2 and LH_2 propellants. Sandwich construction similar to that of the common bulkhead in the Saturn S-II stage will be used. Aluminum 2219-T87 is utilized throughout the tankage because of its formability, weldability, good resistance to stress corrosion, and high fracture toughness. A polyurethane

foam insulation is applied to the inner surface of the LH_2 tankage to limit the LH_2 boiloff during prelaunch and boost.

The tankage support system consists of a conical shell structure attached to the LO_2 tank aft bulkhead. This structure transmits the longitudinal component of the inertial loads to the outer structure. In addition, frames are provided to laterally support the tankage. The design of these supports must comply with the differential deformation between the tankage and the outer shell caused by tank shrinkage during fueling, tank growth during pressurization, and growth of the outer shell during reentry.

Figure 8.5-32 illustrates the estimated structural gages for the orbiter tankage configuration shown in Drawing 2234-79. These gages were determined by standard pressure vessel equations applicable to the particular geometric shapes. Pressurization system gas pressures*, structural temperatures, and material allowables, delineated for the booster were used in this analysis. The critical conditions are shown in Table 8.5-17, and tank geometry and wall thicknesses are shown in Figure 8.5-27.

Outer Body Orbiter Shell Structure. As noted in the trade studies, an outer shell structure protected by LI-15 insulation was selected for the body of the orbiter. The structural material is 6Al-4V STA titanium alloy. This shell is made up of optimized hat stiffened panels supported at frames that are spaced from 20 to 40 inches apart. The equivalent thickness ($\bar{t}$) of the stiffened panels varies from a minimum of 0.054 to 0.114 inches. The tankage is made of 2219 T-87 aluminum sheet or plate. Tank walls are designed by internal pressure and hydrostatic pressure and, locally, by the attachment to the conical bulkheads, which transmit their inertia loads to the outer shell. Tank wall thicknesses vary from 0.048 to 0.096 inches.

*Except for a maximum relief valve pressure of 32 psia in LO_2 tank from prelaunch to orbiter ignition.

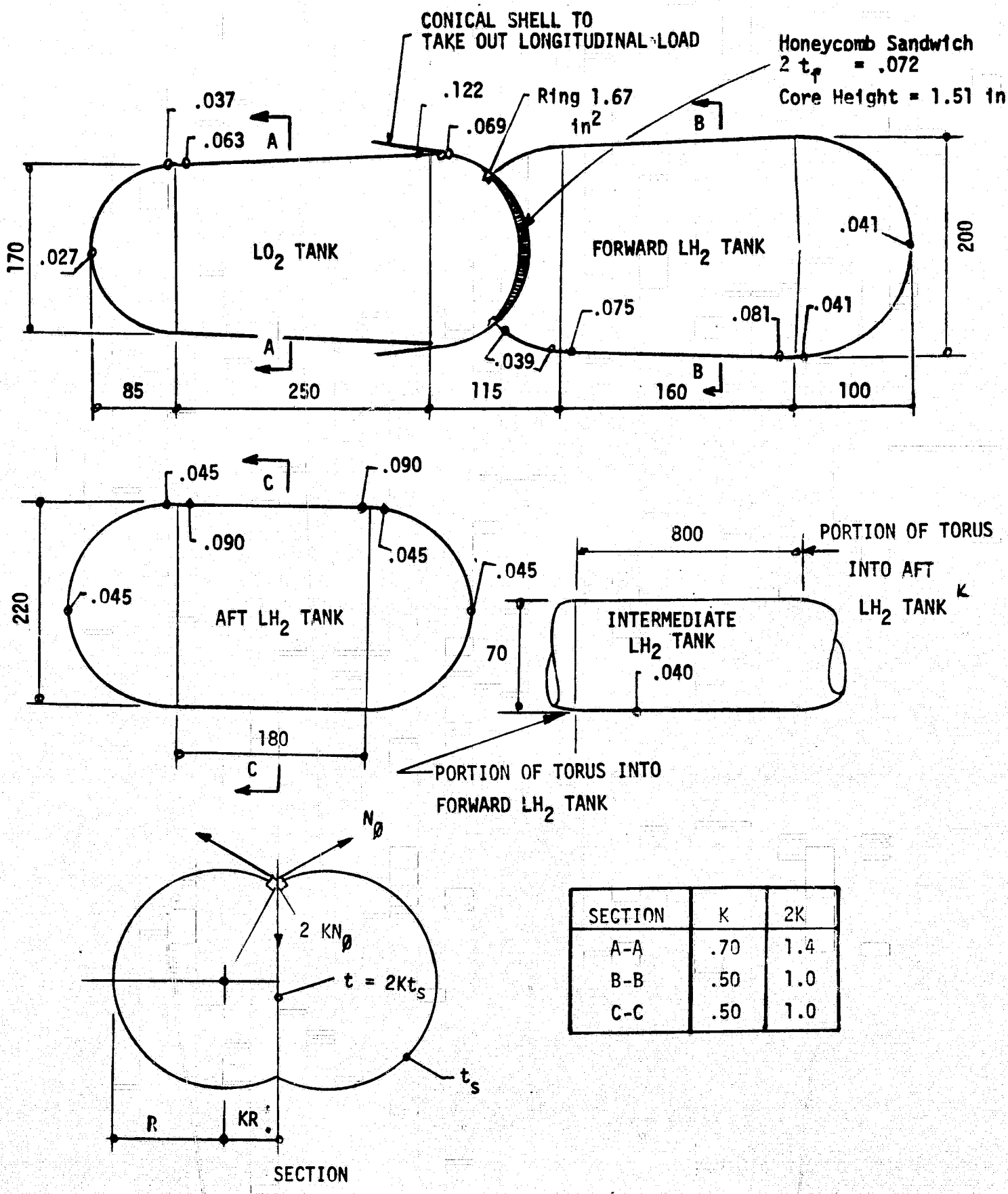

SECTION	K	2K
A-A	.70	1.4
B-B	.50	1.0
C-C	.50	1.0

Figure 8.5-32. Orbiter Tank Gages

Table 8.5-17. Critical Orbiter Tank Design Conditions

Tank	Component	Radius (in.)	Critical Condition	Limit Critical Pressure (psia)	Critical Temperature (deg F)
LO_2	Dome, Forward Bulkhead	85	Minimum Gauge	-	
	Equator, Forward Bulkhead	85	Maximum g	39.4	-297
	Forward cylinder	85	Maximum g	39.4	-297
	Aft cylinder	92	Maximum g	70.7	-297
	Equator, Common Bulkhead	92	Maximum g	70.7	-297
	Dome, Common Bulkhead	92	Maximum g and orbiter burnout	82.0	-297 70
Forward LH_2	Forward bulkhead	92	Orbiter burnout	35.0	70
	Forward cylinder	92	Orbiter burnout	35.0	70
	Aft cylinder	100	Orbiter burnout	35.0	70
	Aft bulkhead	100	Orbiter burnout	35.0	70
Internal LH_2 tank	Both bulkheads	35	Minimum gauge	-	-
	Cylinder	35	Minimum gauge	-	-
Aft LH_2	Both bulkheads	110	Orbiter burnout	35.0	-50
	Cylinder	110	Orbiter burnout	35.0	-50

The outer body shell structure is sized at the five stations shown below.

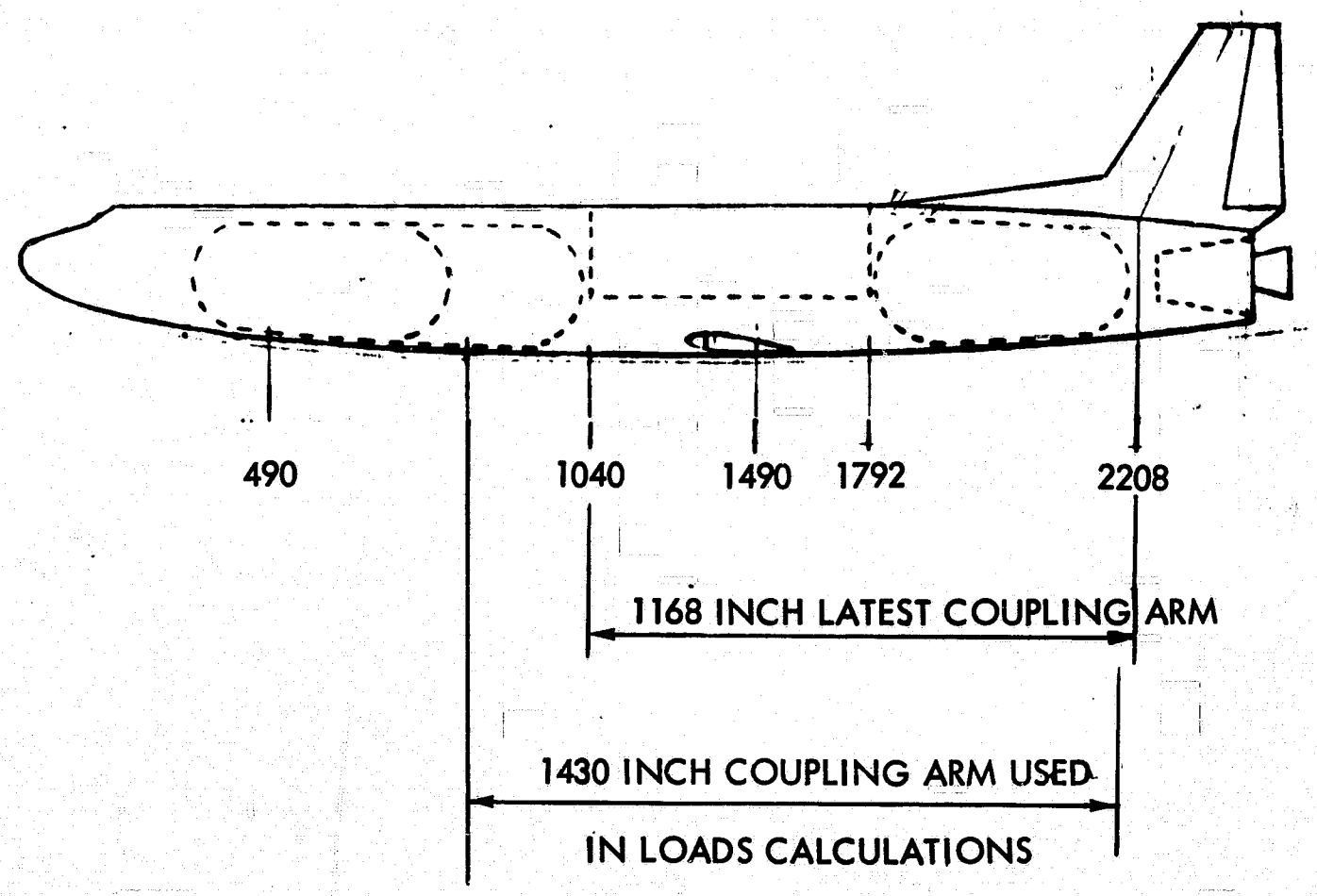

Body cross sections are based on the latest drawing of the orbiter (Drawing 2234-79), and at the stations noted in the above diagram. The body loads were calculated for the orbiter illustrated in Figure 8.2-13 (Drawing 2234-68). The bodies of the two specified orbiter configurations are about the same length, and the large masses are distributed in about the same way. The major differences are:

1. The orbiter-to-booster attachment spacing is smaller on Figure 8.2-23 (Drawing 2234-79).

2. The wing is farther aft on Figure 8.2-23 (Drawing 2234-79).

Item 1 has a significant effect on the transverse loads between the orbiter and the booster. The aft attachment point is about the, same but the forward attachment point is about 300 inches aft of the body configuration used for loads analysis. This arrangement affects the local ring frames and shell shears. Transverse coupling loads are increased by ratioing the computed loads upwards, using the ratio of the old distance over the smaller new distance. The applied bending moment is the same, but it will be applied at Station 1040 rather than at Station 740.

Item 2 is accommodated by applying the calculated bending moment, shears, and axial loads for the wing reaction area at the latest wing position.

Figure 8.5-33 shows the critical loading conditions for the orbiter body. It is apparent that most of the body is designed by the maximum g condition. Because of the local distributions of the large concentrated loads, the structural model shown in Figure 8.5-34 is used for the bending and axial cap loads and shear flows.

Orbiter Vertical Tail Support Ring. The frame at Station 2208 is one of two rings that support the vertical tail. In addition the bottom section of this frame (Figure 8.5-35A) supports the aft attach loads between the orbiter and the booster

$$P = \frac{1.5(57,100)}{2} = 42,800 \text{ lb}$$

$$M = \frac{1.5(5.42 \times 10^6)}{2} = 4.065 \times 10^6 \text{ (in.-lb)}$$

$$q_1 = \frac{4.28 \times 10^4}{2 \times 3.55 \times 10^2} = 60.4 \text{ lb/in.}$$

$$q_2 = \frac{4.065 \times 10^6}{2(2.2 \times 3.55)10^4} = 26 \text{ lb/in.}$$

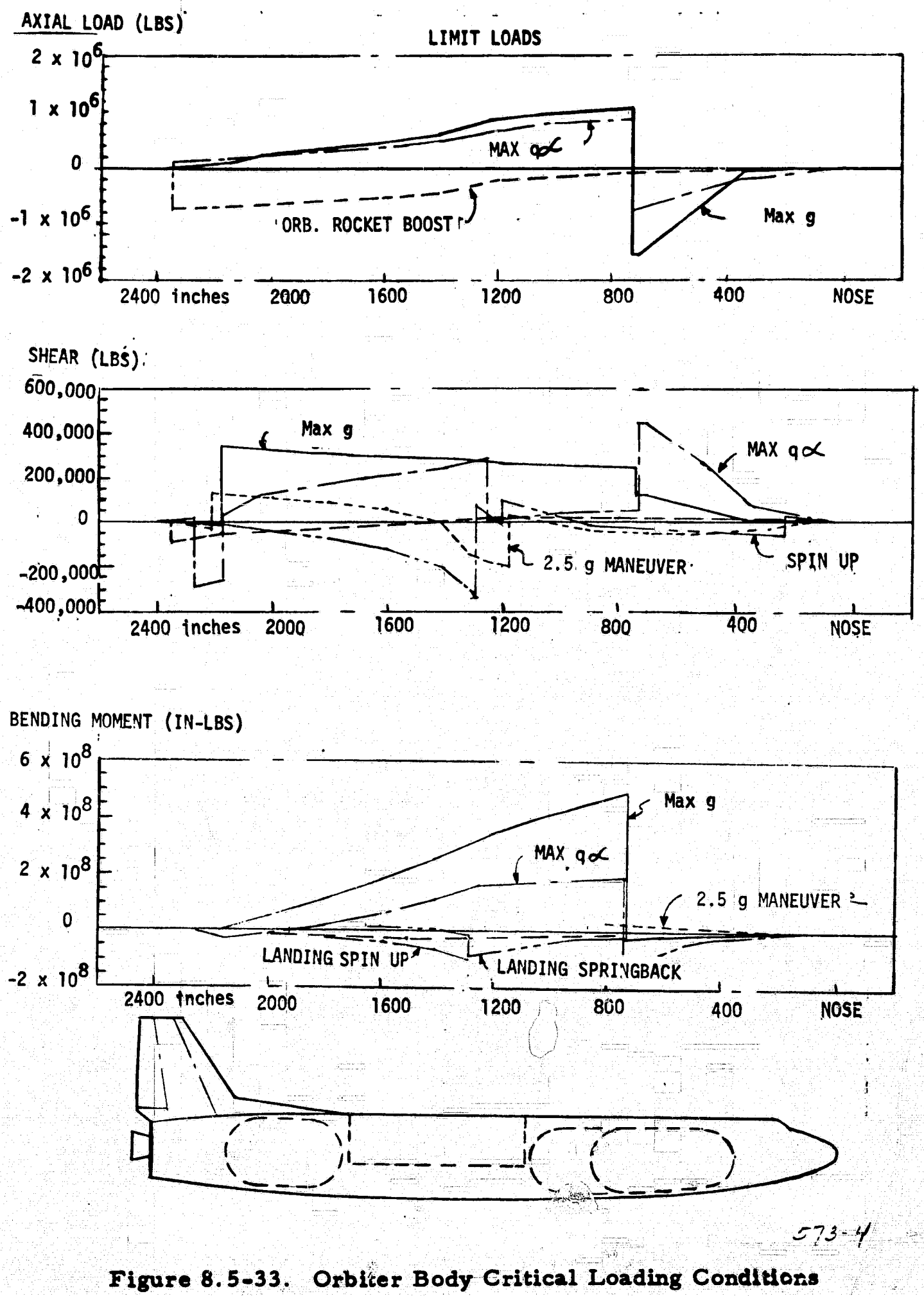

Figure 8.5-33. Orbiter Body Critical Loading Conditions

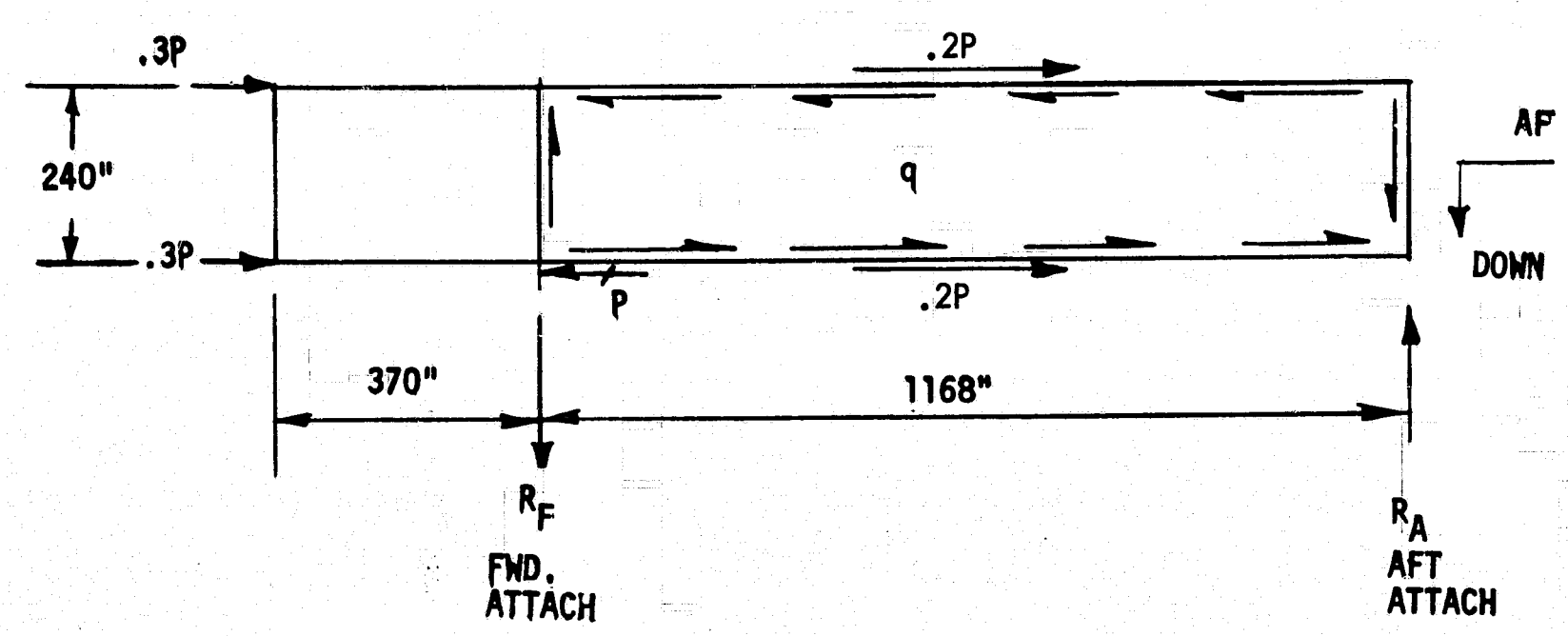

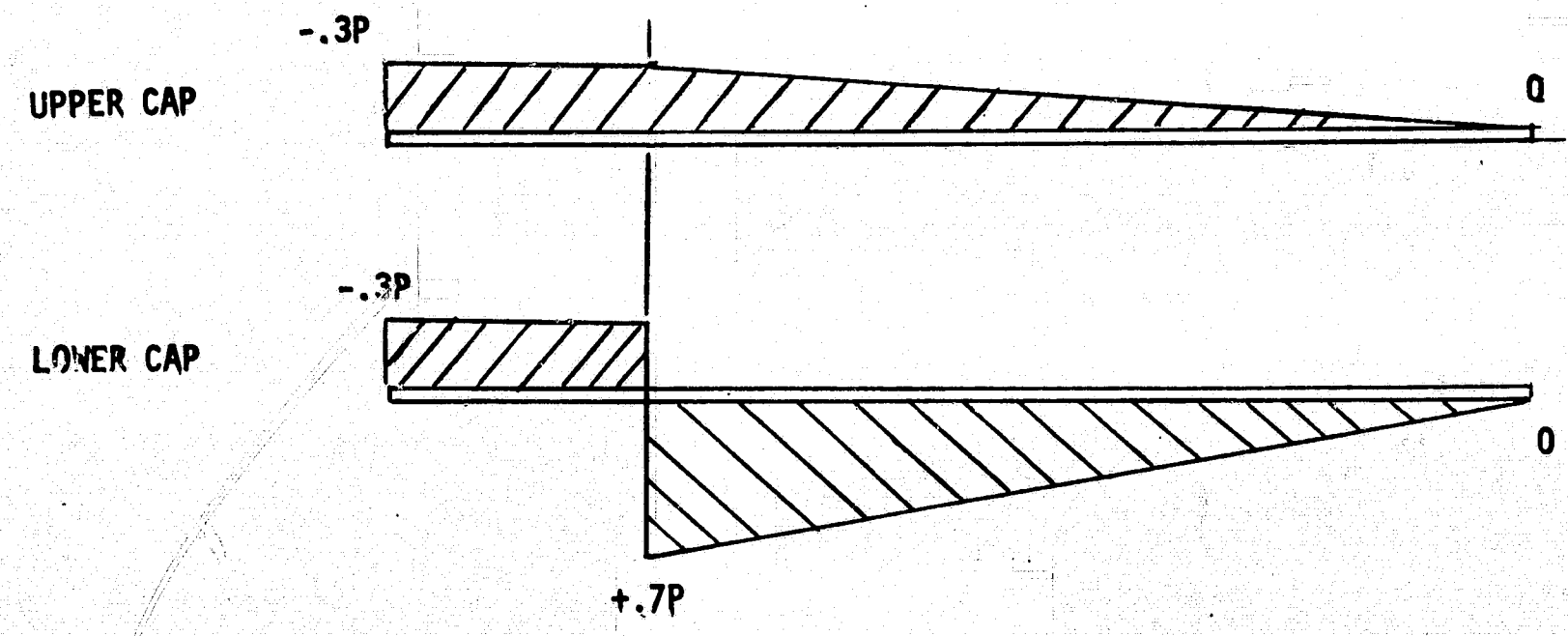

$$P = 3.95 \times 10^6 \text{ LB ULT}$$

$$R_F = R_A = \frac{3.95 \times 10^6}{2} \times \frac{240}{1168} = 4.07 \times 10^5 \text{ LB}$$

$$q = \frac{4.07 \times 10^5}{*2 \times 240} = 847 \text{ LB/IN.}$$

Figure 8.5-34. Structural Model for Maximum G Condition (Sheet 1 of 6)

*Two Sides

STA. 670

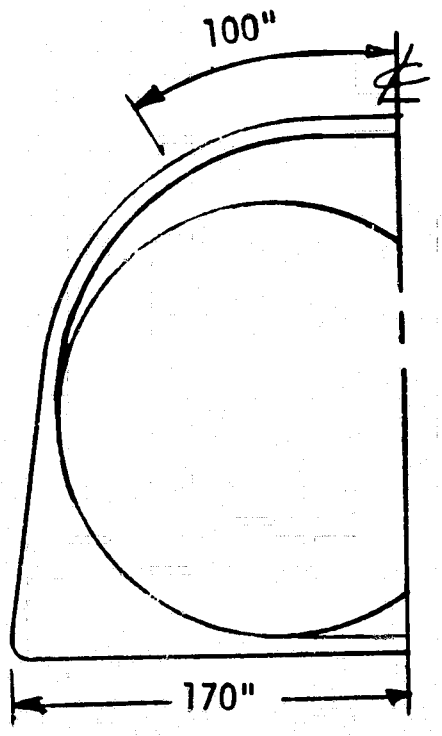

SCALE 1" = 100"

TITANIUM TEMP. ON TOP = 400 F

$$N_{C_{TOP}} = -\frac{0.30\ (3.95 \times 10^6)}{2 \times 10^2} = -5930\ \text{LB/IN.}$$

HAT STIFFENED SKIN PANELS OF 6A1-4V STA TITANIUM

$$\bar{t} = \left(\frac{N_C L}{\epsilon E}\right)^{1/2}$$

$$\bar{t} = \left(\frac{5.93 \times 10^3 \times 2.1 \times 10}{0.93 \times 1.44 \times 10^7}\right)^{1/2} = 0.096\ \text{IN.}$$

$$N_{C_{BOT}} = -\frac{0.30\ (3.95 \times 10^6)}{2 \times 1.7 \times 10^2} = -3490\ \text{LB/IN.}$$

TITANIUM TEMP ON BOTTOM = R.T.

PROTECTED BY LI-15 INSULATION

$$\bar{t} = \left[\frac{3.49 \times 10^3 \times 2.1 \times 10}{0.93 \times 1.6 \times 10^7}\right]^{1/2} = 0.070\ \text{IN.}$$

STA 1040 TOP

TAPER LONGERON (TWO PLACES)

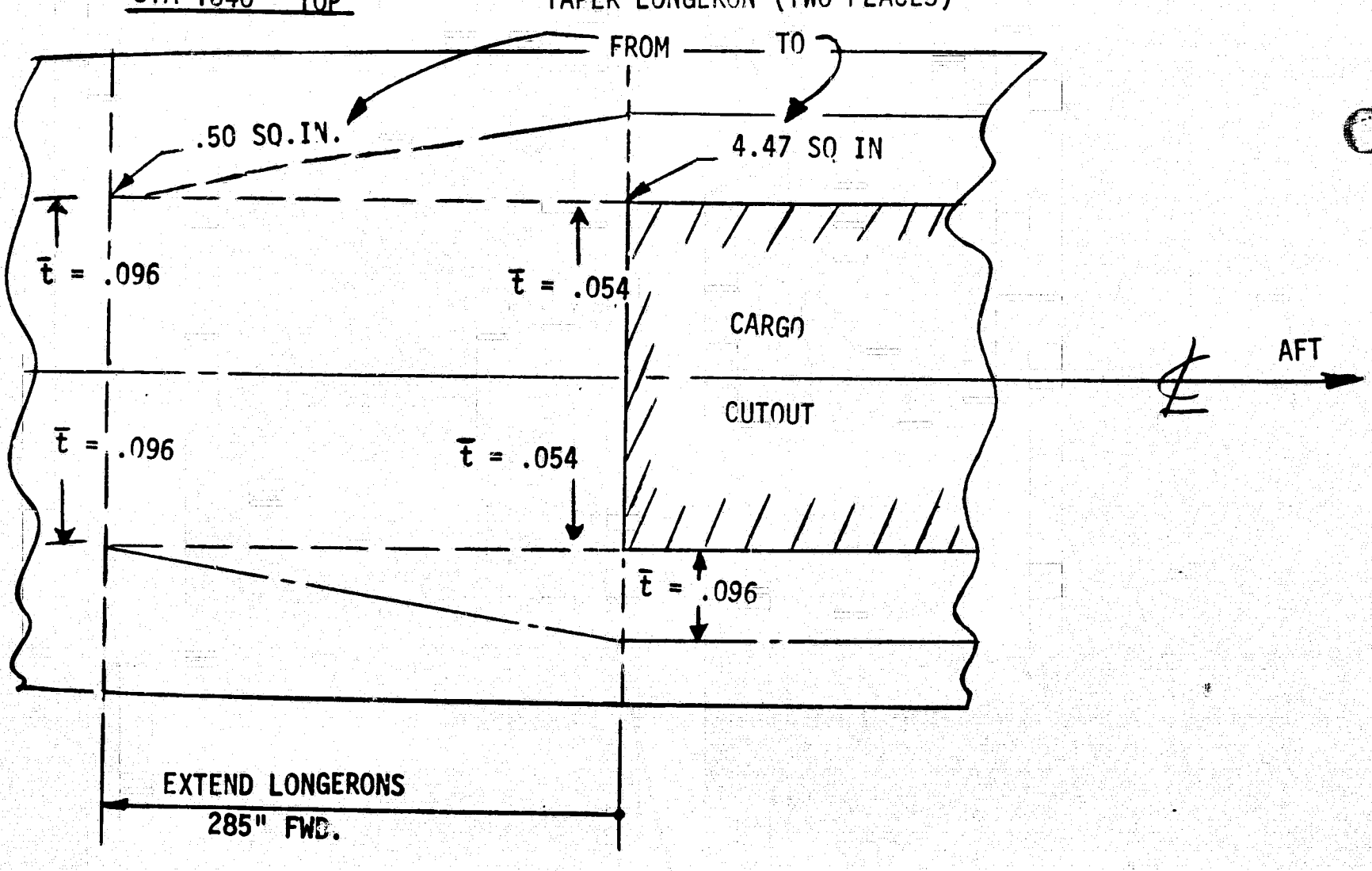

STA.755 STA.1040

Figure 8.5-34. Structural Model for Maximum G Condition (Sheet 2 of 6)

STA. 1040 TOP (CONT)

STRESS CHECK BY CUTOUT

$A = A_{LONG} + A_{STIF.\ SKIN}$

$A = 4.47 + 53.5\ (0.096) = 9.60$ SQ IN.

$$\sigma_C = -\frac{0.3\ (3.95 \times 10^6)}{2 \times 9.6} = -61,700 \text{ PSI}$$

STIFFENED SKIN OK BY COMPARISON WITH STA. 670 CHECK

STA. 1040 BOTTOM

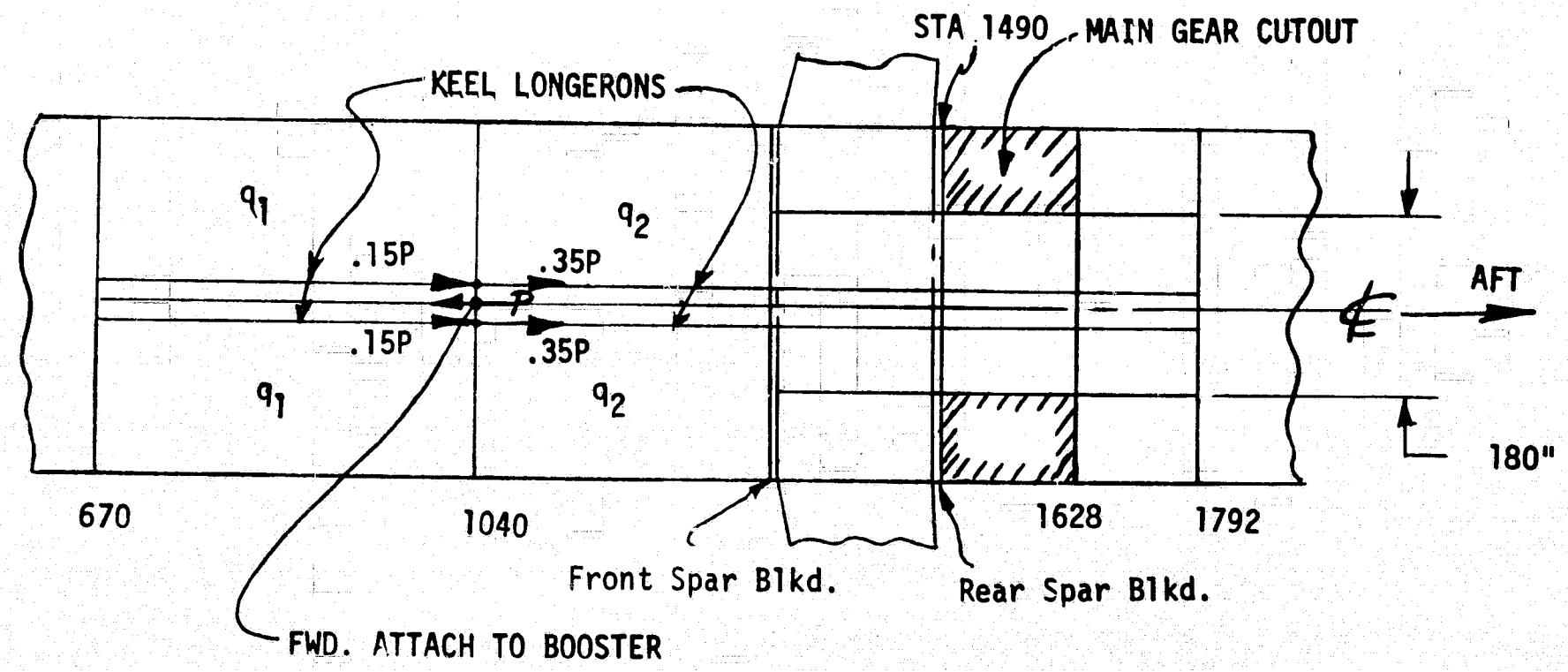

VIEW LOOKING UP AT BOTTOM (SCALE 1 IN. = 200 IN.)

$P = 3.95 \times 10^6$

$$q_1 = \frac{0.15\ (3.95 \times 10^6)}{3.7 \times 10^2} = 1600 \text{ LB/IN.}$$

$$q_2 = \frac{0.35\ (3.95 \times 10^6)}{7.52 \times 10^2} = 1840 \text{ LB/IN.} \quad (\text{ALSO} = 0.465 \times 10^{-3} P)$$

Figure 8.5-34. Structural Model for Maximum G Condition (Sheet 3 of 6)

STA. 1040 BOTTOM (CONT)

SHEAR PANELS
FOR A BUCKLING ALLOWABLE STRESS OF 80,000 PSI

$b/t = 34;\ t_1 = \frac{1600}{80,000} = 0.02;\ t_2 = \frac{1840}{80,000} = 0.023$

BOTH PANELS WILL BE MIN. GAGE $\bar{t} = 0.054$
HAT STIFFENERS WILL BE 5/8 TO 3/4 IN. APART ADJACENT TO LONGERONS

LONGERON AREAS

A_{670} = MIN. FOR FABRICATION

$A_{1040_{FWD}} = \frac{0.15\ (3.95 \times 10^6)}{*1.0 \times 10^5} = 5.91$ SQ IN. (EACH LONGERON)

*CRIPPLING ALLOWABLE BASED ON
$b/t = 8$ FOR ONE EDGE FREE
$b/t = 27$ FOR NO EDGE FREE

COLUMN $L/\rho = 40$

$A_{1040_{AFT}} = \frac{0.35\ (3.95 \times 10^6)}{1.6 \times 10^5} = 8.65$ SQ IN. (EACH LONGERON)

STA. 1490 (REAR SPAR BULKHEAD)

TOTAL LOAD ON BOTTOM AT STA. 1490

$= 0.7P\left(\frac{718}{1168}\right) = 0.43P$

LOAD IN LONGERONS

$= 0.7P - 2\ (0.465 \times 10^{-3}\ P)\ 0.45 \times 10^3 = 0.28\ P$

LOAD IN SHELL

$= 0.43P - 0.28P = 0.15P$

$\bar{t} = \frac{0.15\ (3.95 \times 10^6)}{1.6 \times 10^5 \times 1.8 \times 10^2} = 0.0206$ (BELOW MINIMUM)

USE
$\bar{t} = 0.054$

Figure 8.5-34. Structural Model for Maximum G Condition (Sheet 4 of 6)

BODY STA. 1490 AT WING REAR SPAR

CHECK OF UPPER SHELL FOR MAXIMUM G CONDITION

$$\text{LOAD} = \frac{718}{1168}(0.3 \times 3.95 \times 10^6) \text{ COMPRESSION}$$

$$P = 7.3 \times 10^5 \text{ LB}$$

$$A = A_{LONG} + A_{STIF.\ SKIN};\ A_{LONG} = 2 + \left(\frac{302}{752}\right) 247 = 3.0$$

$$A = 2\ [3.0 + 50 \times 0.075] = 13.50$$

$$\sigma = -\frac{7.3 \times 10^5}{13.5} = -54000;\ N_x = -0.065\ (58400) = -3500$$

THE STA. 670 ANALYSIS SHOWS THAT A 3490-LB/IN. LOAD CAN BE CARRIED BY $\bar{t} = 0.070$ STIFFENED SHEET WITH 21-IN. FRAME SPACING

COMPRESSION ON BOTTOM OCCURS FOR LANDING SPIN-UP CONDITION

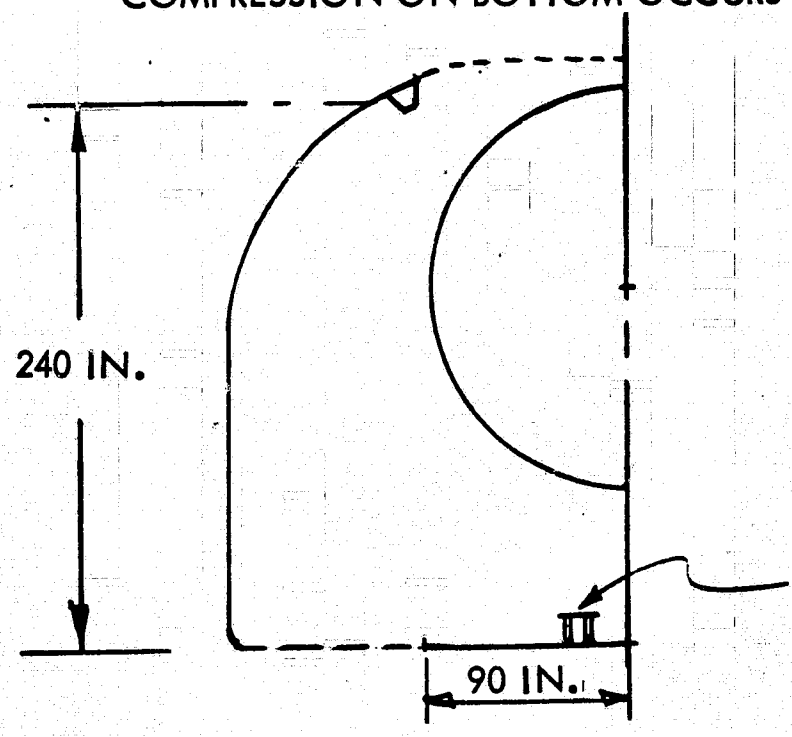

$$M = 1 \times 10^8 \text{ IN.-LBS}$$

COUPLE LOAD

$$P_C = \frac{1.5 \times 1 \times 10^8}{2 \times 240} = 6.24 \times 10^5$$

$$A_{STIF.\ SKIN} = 180\ (0.054) = 9.7 \text{ SQ IN.}$$

$$A_{LONG} = 6.93 \text{ (TOTAL)}$$

$$\sigma = -\frac{6.24 \times 10^5}{16.63} = -37{,}600 \text{ PSI}$$

HAT STIF. SKIN ALLOWABLE

$$N_C = \frac{\bar{t}^2 \epsilon E}{L} = \frac{0.54^{-2} \times 10^{-2} \times 0.93 \times 1.6 \times 10^7}{2 \times 10} = 2160 \text{ LB/IN.}$$

$$\sigma_A = -\frac{2160}{0.054} = -40{,}000 \text{ PSI} \quad \therefore \text{ ABOVE STRESS OK}$$

Figure 8.5-34. Structural Model for Maximum G Condition (Sheet 5 of 6)

COLUMN CHECK OF UPPER LONGERON

ALONG CARGO BAY DOOR CUTOUT

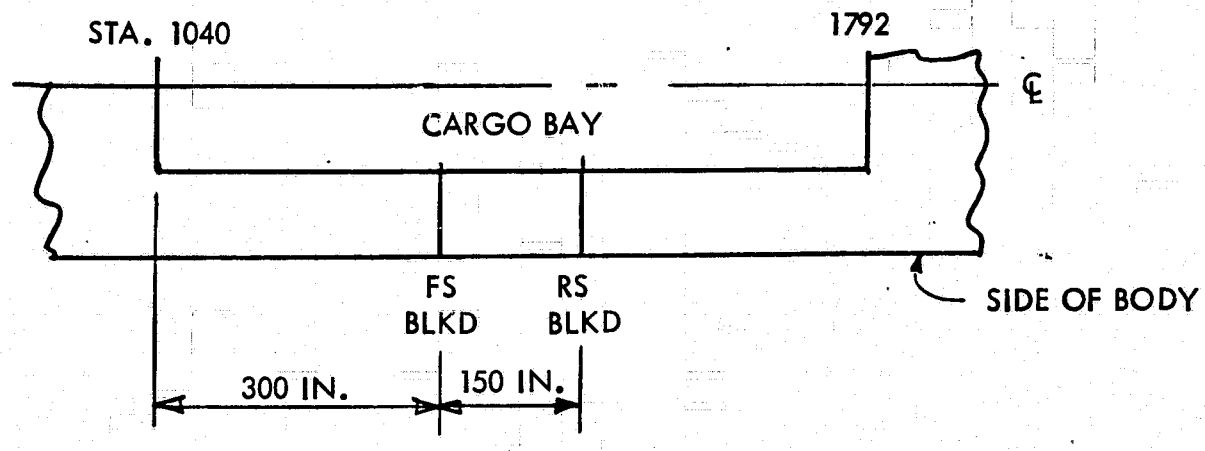

ASSUME COLUMN IS SUPPORTED AT SPAR BULKHEADS

MAXIMUM COLUMN LENGTH = 300 IN.

$$\text{AVERAGE STRESS} = \frac{54,000 + 61,700}{2} = 57,900 \text{ PSI}$$

$$\text{REQUIRED } \frac{L}{\rho} = 52 \text{ FOR 6Al - 4V STA Ti}$$

$$\rho = \frac{300}{52} = 5.77$$

$$\rho = \left(\frac{I}{A}\right)^{1/2}$$

$$(I)^{1/2} = \rho\,(A)^{1/2} = 5.77^{*}\ (3.73)^{1/2}$$

$$I = 124.2$$

ASSUME SQUARE BOX SECTION WITH .80 PERCENT OF AREA IN TWO SIDES PARALLEL TO MOLD LINE.

$$I = 124.2 = 2\,(bt)\left(\frac{b}{2}\right)^2$$

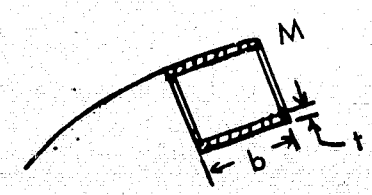

LET $A_{CAPS} = 3 = 2\,bt$; $bt = 1.5$

$$\therefore\ 124.2 = 3\frac{b^2}{4}\ ;\ b^2 = 165.6\ b \approx 13$$

$$t = \frac{3}{26} = .115 \text{ (WILL BE STIFFENED)}$$

*AVERAGE AREA

Figure 8.5-34. Structural Model for Maximum G Condition (Sheet 6 of 6)

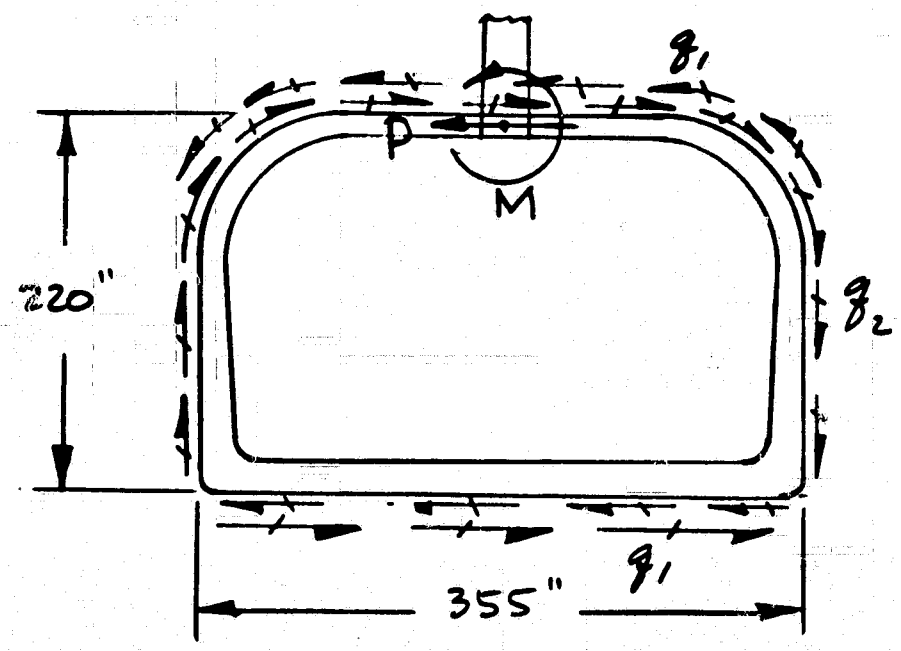

A

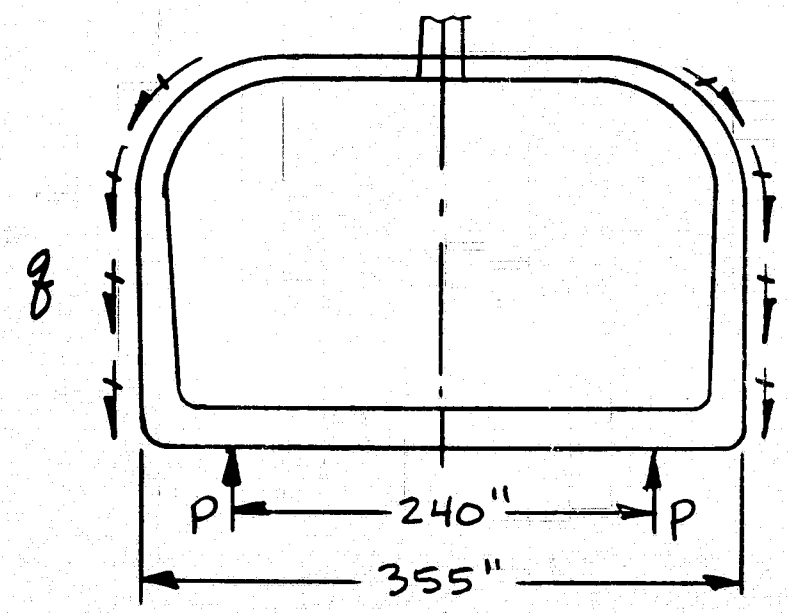

B

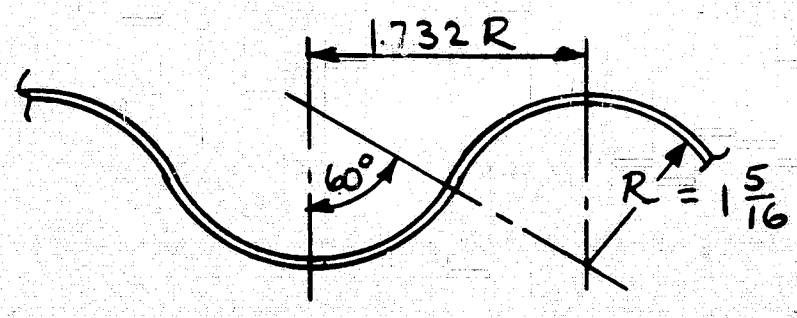

C

Figure 8.5-35. Vertical Tail Support Ring

Critical areas for frame design are adjacent to the concentrated loads at the top centerline. Concentrated moment and axial load at the top centerline divide half to the left side and half to right side. Design values are:

$$\frac{M}{2} = \pm 2.03 \times 10^6 \quad , \qquad \frac{P}{2} = \pm 2.14 \times 10^4$$

Assume an 8-by-10 inch rectangular box section for the frame and an average allowable of 90,000 psi for tension and compression. The cap area is:

$$A_C = \frac{2.03 \times 10^6}{1.0 \times 10 \times 0.9 \times 10^5} + \frac{2.14 \times 10^4}{2 \times 0.9 \times 10^5}$$

$$A_C = 2.26 + 0.12 = 2.38 \text{ sq in.}$$

Assume equivalent thickness of side webs of box section to be 0.10-inch. Webs will have lightening holes.

The lower section of this frame is critical for the orbiter-to-booster attach loads. The maximum loads perpendicular to the bottom of the frame and in the plane of the frame occur during both the maximum $q\alpha$ condition and maximum acceleration condition during boost. The calculated loads are adjusted (Figure 8.5-35B) to the smaller distance between the forward and the aft attachment as shown in Figure 8.2- and 8.2- (Drawing 2234-76 and 2234-79.)

$$P = \frac{1.5(2.23 \times 10^5)}{2} \frac{(1,440)}{(1,168)}$$

$$P = 206,000 \text{ lb}$$

$$q = \frac{206,000}{220} = 940 \text{ lb/in.}$$

Assume that the bottom frame section is the same size as the upper in the form of an 8-by-10-inch box section. Conservatively, assume pin joints at ends of bottom frame section.

$$M = 2.06 \times 10^5 \left(\frac{355 - 240}{2}\right) = 1.184 \times 10^7$$

For 90,000 psi allowables, cap area is:

$$A_C = \frac{1.184 \times 10^7}{10 \times 0.9 \times 10^5} = 13.2 \text{ sq in.}$$

Increasing depth from 10 to 18 inches,

$$A_C = 13.2 \left(\frac{10}{18}\right) = 7.33 \text{ sq in.}$$

$$\text{Max shearflow} = \frac{2.06 \times 10^5}{2 \times 1.8 \times 10} = 5220 \text{ lb/in. (in frame webs)}$$

The thickness of a corrugated sine wave used for this frame is as follows (Figure 8.5-35C):

$$q/b = \frac{5,220}{18} = 290$$

From optimum curves in Figure 8.5-36,

$$\frac{b}{t} = 230$$

$$\therefore \quad t = 0.078, \quad \bar{t}_\omega = 1.21\, t$$

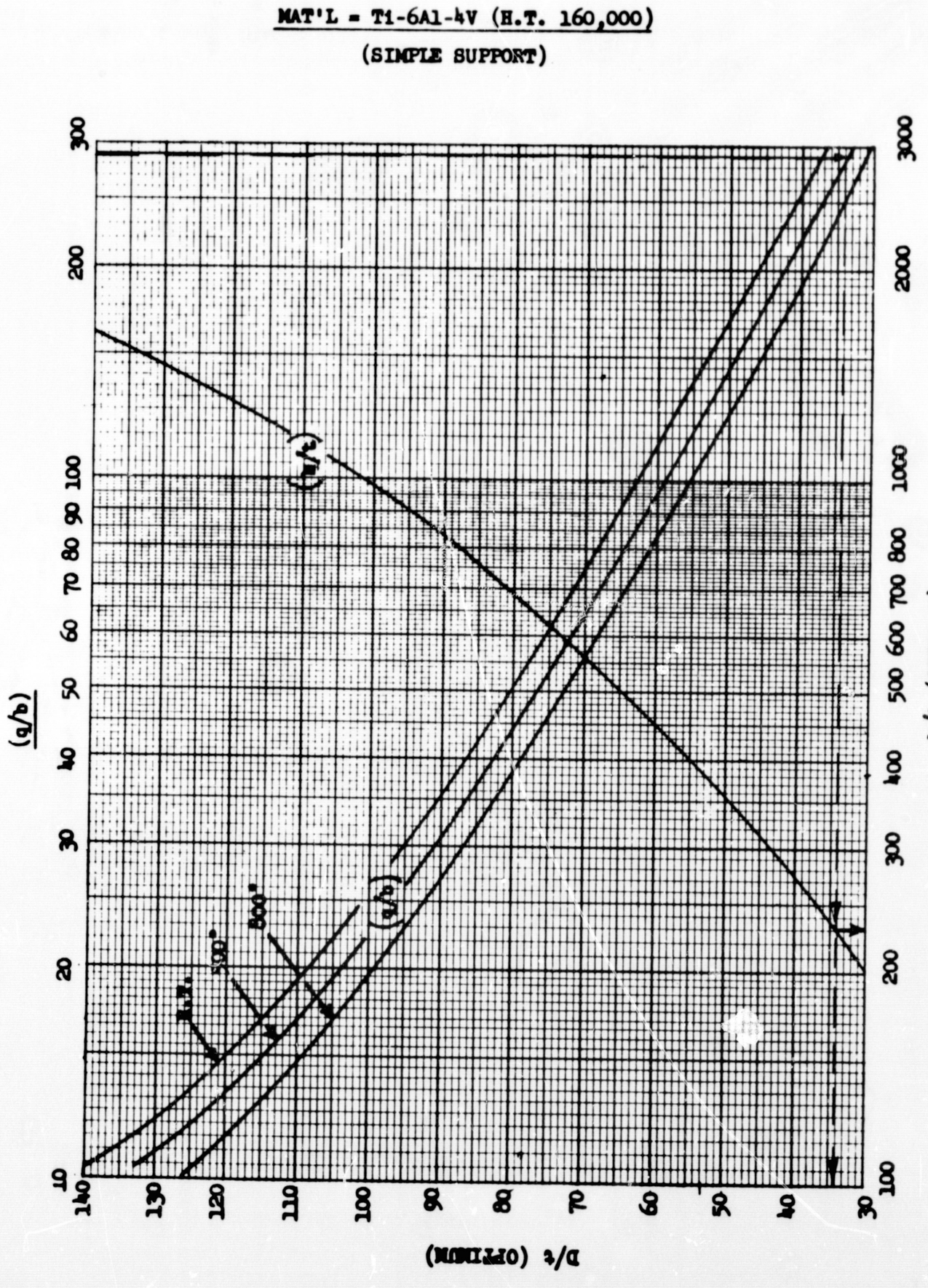

Figure 8.5-36. Optimum Design Curve for Corrugated Shear Webs

Side members of the frame between the top and bottom frame segments will be tapered from bottom requirements to top requirements.

This preliminary type of structural analysis was also used to size other concentrated load frames, such as the wing and horizontal tail attach frames and the forward frame for the booster attachment.

Orbiter Wing Structure. The wing loads were computed for the configuration shown in Figure 8.2- (Drawing 2234-68). This wing is very similar to that shown on Figure 8.2- (Drawing 2234-79), but it is slightly smaller in area. The structural sizing is based on the wing shown in Figure 8.2- (Drawing 2234-68) and the loads calculated for this wing.

This sizing exercise results in unit cover areas per inch of chord, which when applied to the larger wing, provide the required larger moment capacity. These unit areas are also be applied to the larger wing for weight calculation purposes.

The structural box of the wing extends from 0.15 chord to 0.65 chord. At the side of the body, the symmetrical airfoil has a 14 percent thickness with a taper to 12-percent thickness at the tip.

The ultimate bending moment is shown in Figure 8.5-37. This occurs at the maximum $q\alpha$ condition during boost. This is a negative moment resulting in compression on the bottom covers.

An average box height for the symmetrical airfoils 0012-64 and 0014-64 is about 91 percent of the maximum depth.

Orbiter wing geometry and loads are shown in Figure 8.5-38.

The compression cover areas are based on Report TFD-65-496, Optimization of Multirib and Multiweb Wing Box Structures Under Shear and Moment Loads. This report was prepared by the Los Angeles Division of North American Rockwell Corporation.

The most efficient stiffened panel for a wide-column concept is the straight Y-tee stiffened section as indicated in the sketch.

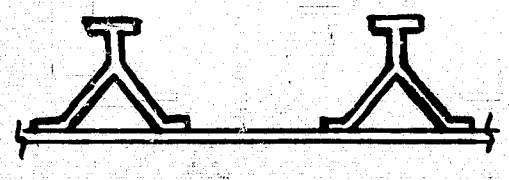

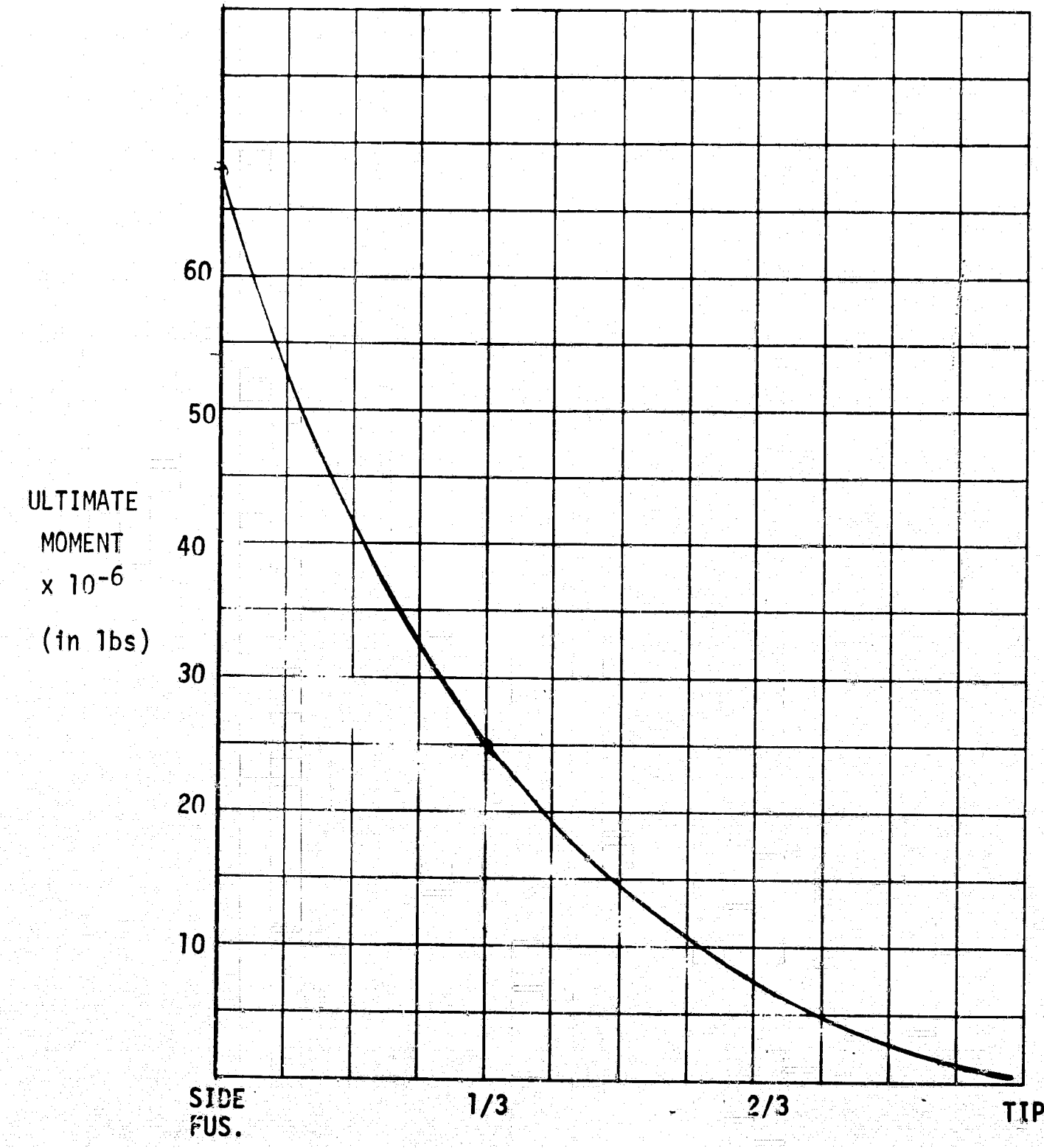

Figure 8.5-37. Orbiter Wing Bending Moment for Maximum q α Condition

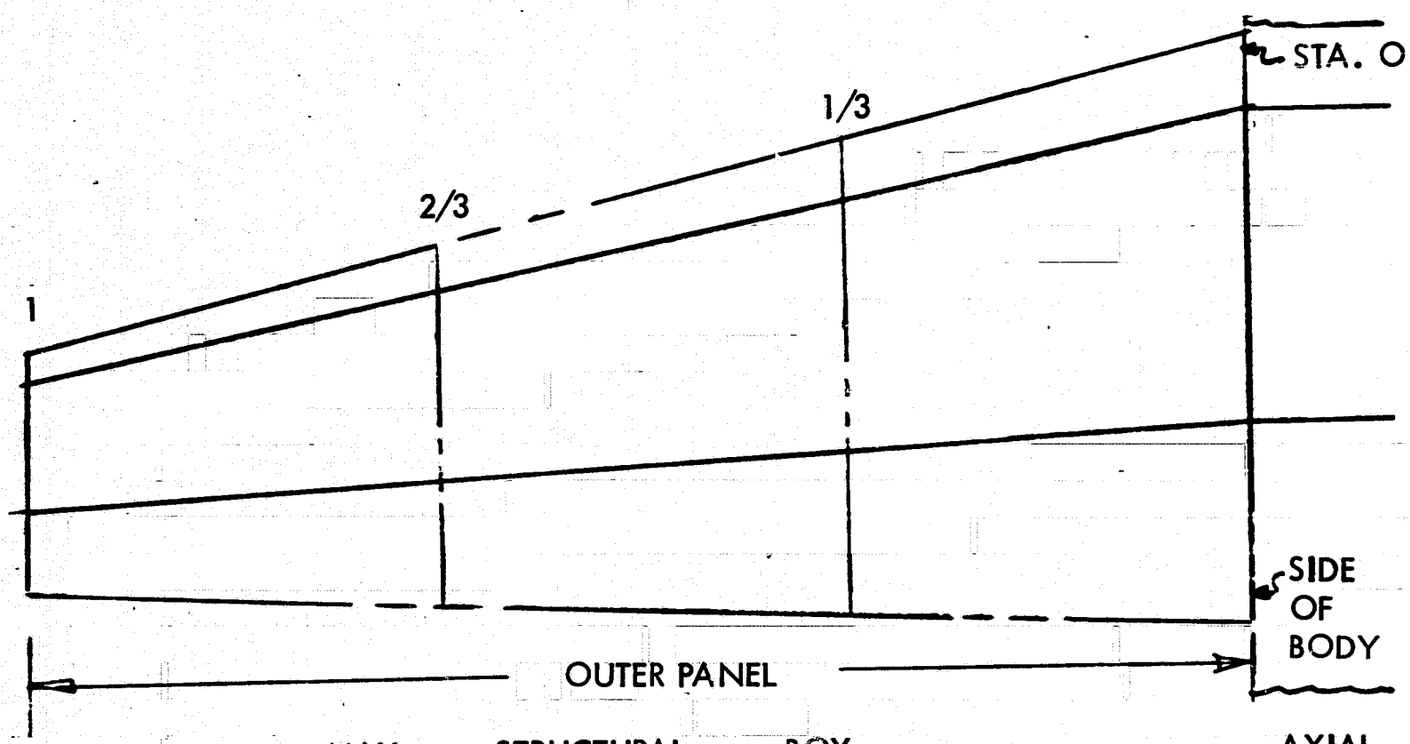

WING STA.	CHORD (IN.)	MAX. THICK. (IN.)	STRUCTURAL AVG. THICK. (IN.)	BOX WIDTH (IN.)	MOMENT (IN LBS X 10^6)	AXIAL LOAD N_X (LBS/IN.)
0	286	40	36.5	143	68	13,100
1/3	230	31.4	28.5	115	25	7,600
2/3	170	22.6	20.6	85	7.5	4,300
1	115	13.8	12.6	57.5	0	0

Figure 8.5-38. Orbiter Wing Geometry and Loading

The efficiency of this section is 1.23, which is well above most other wide-column concepts, and will be used for the compression cover sizing. For example, a Z stiffened panel has a maximum efficiency of 0.911.

For an optimum design where the column buckling occurs at the same stress as the local buckling, most optimum sections have stress levels that are in the elastic range of the material. For moderately high loads, the stresses are near the proportional limit; therefore, the following equation from the earlier mentioned reference will be used to size the cover area requirements with no plasticity corrections. The effective thickness of the stiffened skin cover ($\bar{t}$) is obtained from the following equation:

$$\bar{t} = \left(\frac{N_x L}{\epsilon E} \right)^{\frac{1}{2}}$$

where

L = rib spacing

ϵ = 1.23 (the maximum efficiency)

The material chosen for the wing box structure is 6Al-4V STA titanium alloy. The maximum temperature of the bottom wing cover during the maximum $q\alpha$ condition is the ambient temperatures at the launch site. Room temperature properties are used. The top and bottom of the wing are protected by LI-15 insulation. During this condition, the outer surface of the insulation reaches a peak of about 700 F on the lower surface. Table 8.5-18 presents orbiter wing box analysis data.

On a similar wing that was optimized in the referenced report, the ribs and spars totaled to 26 percent of the compression cover. This value will be used for weight estimation of the substructure.

The tension cover can be lighter than the compression cover. The static strength allowable is considerably higher for the limited life of 100 missions. No significant fatigue failures would be expected unless operating stresses approached the tensile yield strength of the titanium, and

Table 8.5-18. Orbiter Wing Box Analysis Data

Wing Station	N_x (lb/in.)	L (in.)	E (psi)	t (in.)	Stress** (psi)
0	13,100	20	16×10^6	0.115	114,000
1/3	7,600	20	16×10^6	0.088	86,300
2/3	4,300	20	16×10^6	0.066	65,200
1	0	20	16×10^6	0.054*	

*Minimum gage for fabrication and maintenance.
**Note that these stresses are in the elastic range, $F_{PL} = 130.000$.

this condition is not expected. If the structure were designed to F_{tu}, the operating stress level would not exceed 74 percent of F_{ty}. The positive bending during the maximum qα condition is only 50 percent of the negative bending. The positive bending from the aircraft maneuver condition is also expected to be approximately 50 percent of the maximum qα negative bending; therefore, it is recommended that the upper cover be designed to 50 percent of the lower cover load in compression or to F_{tu} for the lower cover loading, whichever is critical. Results of this structural approach are shown in Table 8.5-19 for the upper cover.

At the time the weight calculations were made, it was assumed that the upper cover weight was equal to the lower cover. The weight saving indicated above for the upper cover is not reflected in the weight statement. This weight saving is about 1,000 pounds for the orbiter wing.

A factor of 127 percent times the calculated weight of the wing box was used to obtain an actual hardware weight.

Table 8.5-19. Orbiter Wing Lower Cover Sizes

Wing Station	N_{xc} (lb/in.)	$\bar{t}_{comp}$ (in.)	N_{xt} (lb/in.)	$\bar{t}_{tens}$ (in.)	$\bar{t}_{design}$ (in.)
0	6,550	0.081	13,100	0.082	0.082
1/3	3,800	0.062	7,600	0.048	0.062
2/3	2,150	0.047	4,300	0.027	0.054 (minimum)
1	0	-	0	-	0.054 (minimum)

Based on statistical data, the following weight factors were used: 3 pounds per square foot for the leading edge structures and 5 pounds per square foot for the flap, aileron, and trailing edge structures of this wing.

Orbiter Horizontal and Vertical Tail Structures. The horizontal tail structure for the orbiter was sized by methods similar to those used on the wing. The box structure of the tail also has a carrythrough section in the body region. The tail is sized for 6Al-4V STA titanium alloy for the loading experienced at the maximum $q\alpha$ condition during boost.

The vertical tail is also sized to withstand load experienced during the maximum $q\alpha$ boost condition. The loading and the structural geometry are based on Figure 8.2- (Drawing 2234-68). The side load is 317,000 pounds and the moment at the root of the vertical tail is 48×10^6 inch-pounds. The structural analysis is similar to that used for the booster vertical tail. This tail structure was sized for 6Al-4V STA titanium alloy.

8.5.9 Potential Weight Savings

The sensitivity of this shuttle system to weight growth is well-recognized. The weight-saving ideas that follow have not been incorporated into the system.

1. Oblate spheroidal tank caps occupy much less space than hemispherical caps and may reduce weight.

2. A changed angle of incidence of wings and tails on orbiter and booster will reduce the bending moment during boost. These bending moments are considerably greater than experienced in a normal aircraft flight maneuver of 2.5 g. Wing bending moments computed on 8 August 1969 for the vehicle configured to deliver 12,500-pound payload (Section 8.4.4) show maximum $q\alpha$ to be 185 percent of aircraft maneuver for the orbiter and 450 percent of aircraft maneuver for the booster. From a flutter consideration, it is desirable to obtain about equal positive and negative bending moments during boost.

3. Use of the upper half of the booster integral tank as the outer mold line structure with increased thickness of insulation on the inner surface offers potential weight reduction.

4. Prelaunch loads design a large portion of the booster LH_2 tank structure. Possible relief for weight savings can be realized with a wind breaker structure or constraint for the vehicle on the launch pad.

5. Use of graphite and boron polyimide composites will save significant structural weight. The following components are candidates for use of filamentary resin composites up to 600°F.

   a. Wind and tail structures on both vehicles

   b. Rocket engine thrust structures

   c. Truss structure from booster tank frames to outer mold line fiberglass sandwich panels that support the LI-15 insulation

   d. Outer body stiffened shell and frames on orbiter

Table 8.5-20 shows comparative weights of filamentary composites and the titanium structure that was used in the booster vehicle thrust structure. These data indicate a weight saving of at least 25 percent for this thrust structure.

Table 8.5-20. ILRV Booster Thrust Structure Weight (Pounds)

Element	Titanium	Boron/Epoxy	Graphite/Epoxy
Center Engine Support Structure	3,690	2,039	2,049
Major beams	3,372	1,196	1,050
Minor beams	318	724	876
Center beam	-	59	63
Struts	-	60	60
Aft Shell (Station 0-72)	5,711	3,877	4,074
Skin	1,260	1,342	1,474
Stringer	1,115		
Longerons	1,434	940	1,000
Frames	1,472	1,595	1,600
Compression tie	430		
Forward Shell (Station 72-120)	3,023	1,957	2,070
Skin	819	1,054	1,160
Stringers	1,117		
Frames	1,087	903	910
Miscellaneous Fittings	996	996	996
	13,420	8,869	9,189
Growth (10 percent)	1,342	887	919
	14,762	9,756	10,108

8.6 THERMAL PROTECTION ANALYSIS

Studies of the thermal protection system for the ILRV included a review of a baseline vehicle thermal protection system, evaluation of candidate thermal protection system options, and definition of a selected system. The system includes insulation to prevent excessive propellant boiloff, and thermal protection to limit structure temperatures during ascent and reentry phases of the shuttle vehicle mission. The selected thermal protection system is designed to minimize weight and provide a reliable and reusable system requiring minimal refurbishment.

Vehicle flight modes and conditions that govern vehicle thermal environment are influenced by mission and vehicle performance requirements. Within mission constraints, however, the flight mode is selected to minimize temperatures and heat loads experienced during the mission. This approach complements the goal of providing a low-weight, reusable thermal protection system. The ascent trajectory for the vehicle is selected to limit temperatures during this phase of the mission without excessive degradation of vehicle performance. To decrease heating during reentry, lift loading is minimized by entering at a high angle of attack with a maximized lift coefficient. The total heat load with this reentry mode is also less than that which would be experienced with the vehicle entering at a lower angle of attack. A comparison of vehicle temperatures experienced at high and low angles of attack is illustrated in Figure 8.6-1. The lower temperatures permit more latitude in material selection. They also permit a greater margin between the operating temperatures of a thermal protection system/structure concept and the maximum allowable temperatures of that concept.

The high angle of attack on reentry also causes separation of the boundary layer from the top of the vehicle, producing a mild environment at that surface. This separation reduces temperatures and heat loads at both the top surface of the body and the vertical fin.

A review of the baseline vehicle indicates that the principal high-temperature problem areas are on the wings (Figure 8.6-2). The relatively sharp radius of the wing leading edges causes locally high heating rates. These high rates require additional thermal protection at the leading edges. Also, as the body shock wave impinges on the wing, the resulting flow interference effects on the underside and leading edge of the wings increases the local heating.

These comments regarding the ILRV entry concept are applicable regardless of the particular thermal protection system being considered. The concept is attractive from a thermal viewpoint, since the thermal protection system weight is low. Furthermore, a greater temperature margin can be designed into this concept than could be achieved with a more severe, low-angle-of-attack entry.

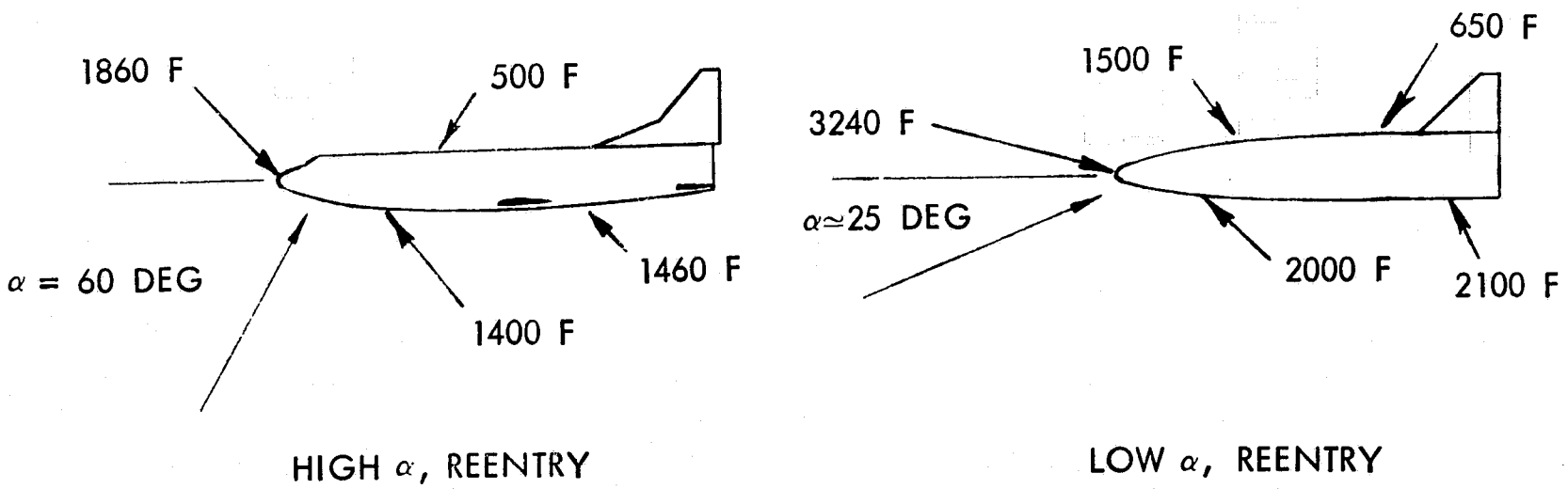

Figure 8.6-1. Typical Maximum Orbiter Temperatures for Reentry at High and Low Angles of Attack

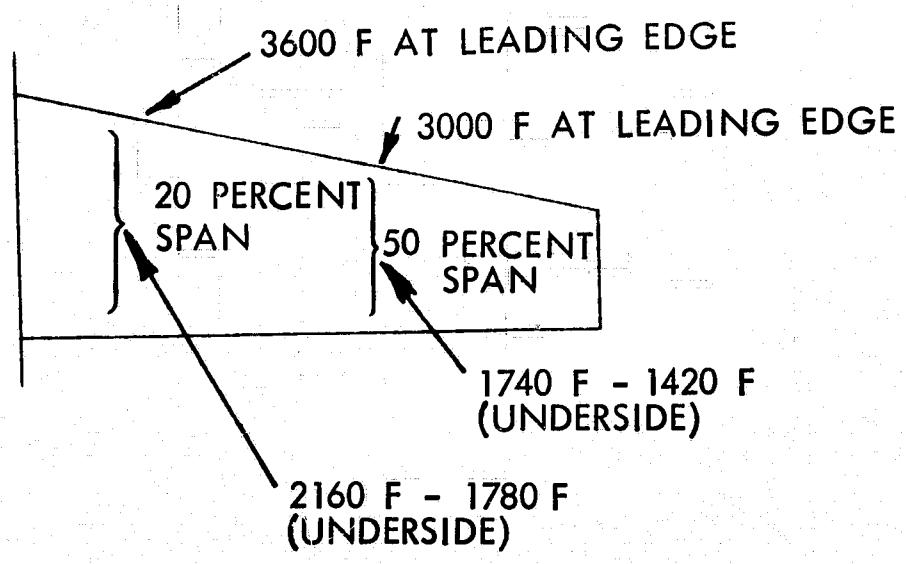

Figure 8.6-2. Typical ILRV Maximum Temperatures for Orbiter Wing

8.6.1 Baseline Thermal Protection System

The baseline ILRV, as previously discussed, uses a reentry mode that minimizes heating. Temperatures on the underside of the vehicle are generally less than 2000 F, but higher temperatures are experienced on leading edges and in flow interference areas. The most significant high-temperature problem area for the ILRV configuration is along the leading edges of the wings and horizontal fins. During entry, typical maximum temperatures in these areas are on the order of 3000 F for the orbiter. Shock interference can increase the severity of this problem. As the body shock wave impinges, flow interference occurs and increases temperature on the underside of the wing at approximately 20 percent of the distance from wing root to wing tip. Peak leading-edge temperatures in this area are about 3600 F. Along the underside of the orbiter wing, the interference heating causes peak temperatures of 1780 to 2160 F, compared with 1420 F to 1740 F for typical undisturbed locations. The presence of the wing causes locally higher heating on the sides of the body; however, the effect of this local heating can be accounted for by additional insulation in the affected areas. The baseline vehicle temperatures and thermal protection concept are illustrated in Figure 8.6-3.

The most notable feature of the baseline configuration is the use of external insulation. The material considered for this evaluation is LI-15 (being developed by Lockheed Missile and Space Division, Sunnyvale), which is a quartz fiber material with a silica binder. The external insulation concept has several features that make it attractive when compared with conventional metallic radiative panel/internal insulation concepts.

The multiple-use operational temperature limit for LI-15 is 2500 F (development target). Only a few metals are suitable as radiative heat shields at that temperature level. The metals most commonly considered for 2500 F operation are coated columbium and tantalum. The external insulation concept has the advantage of a greater temperature margin than these metals. If the design environment for the vehicle is exceeded, a metallic radiation heat shield may be subject to melting or burn-through; however, it is expected that a material such as LI-15 would degrade and tend to act as an ablator if its operational temperature were exceeded. Thus, the external insulation concept would be more likely to remain intact and permit a safe landing after an entry at unexpectedly high heating rates. The external insulation concept enjoys an even greater temperature margin over the metals that might be used for a lower temperature capability radiative heat shield (e.g., TD Ni Cr, Haynes 188, Renē 41, etc.).

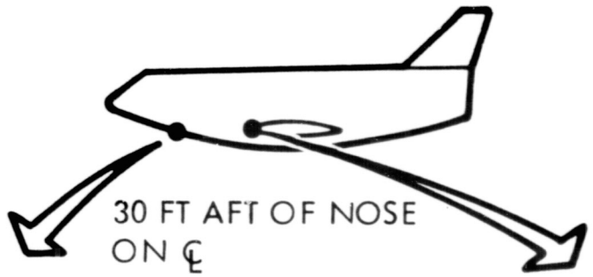

EQUIL TEMP 1550F

$\dot{q}$ = 6.2 Btu/FT^2-SEC

Q = 1500 Btu/FT^2

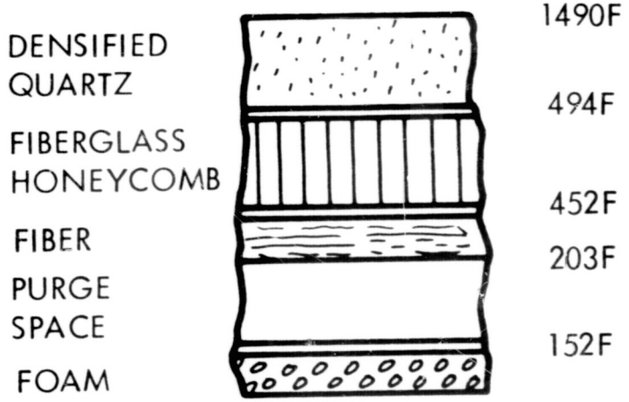

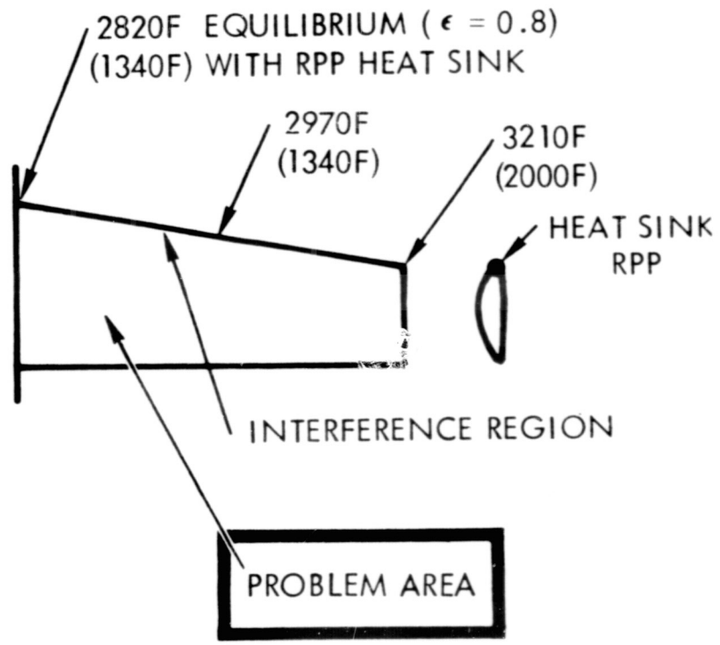

- TPS ON BODY ADEQUATE, WEIGHT FACTOR VALID
- DENSIFIED QUARTZ – FAIL SAFE CAPABILITY, LOW CONDUCTANCE ATTACH
  – WATER ABSORPTION, HANDLING DAMAGE, DEVELOPMENT REQUIRED
- HEAT SINK/CARBON MATERIAL REQUIRED ON LEADING EDGE
- OXIDATION COATING REQUIRED ON RPP

Figure 8.6-3. Baseline 12,500-Pound-Payload Vehicle Thermal Protection

Space Division
North American Rockwell

Use of low-conductance attachments is desirable for both space operations and aerodynamic heating. In space, it is expected that operational constraints may dictate the attitude of the orbiter. For example, a requirement may exist to hold a sensor in a particular attitude; or, the orbiter might be joined to a space station and constrained to accept the attitude requirements of the space station. Since a surface could reach relatively high or low steady-state temperatures under these conditions, a low-conductance attachment is preferable to protect temperature-sensitive subsystems and materials inside the orbiter. Similarly, low conductance attachments will better protect these areas from the high temperatures experienced during entry.

An additional advantage of the external insulation concept is the fact that it permits the use of low-conductance attachments between the outer vehicle surface and the structure. With a metallic radiative panel/fibrous insulation heat shield, higher conductance attachments must be used to attach the radiative panel to the structure. Low-conductance materials (such as fiberglass), which might be used in this application, are not capable of withstanding the high temperatures reached by a radiative panel during entry. Since the back surface of the external insulation reaches a much lower maximum temperature during entry, the use of low-conductance attachments is possible.

There are several problem areas associated with the external insulation concept which must be resolved before this approach can be used. The severity of these problems is increased by the reusability requirement. LI-15 external insulation may be prone to mechanical damage from handling and abrasion. Among the methods being investigated by the manufacturer to solve this problem is densification of the outer surface. Surface treatments have been considered for this purpose. Surface treatments also help in another problem area. LI-15 is subject to moisture absorption when exposed to rain or a high humidity environment. With an orbiter whose surface area (including fuselage, wings, and fins) is on the order of 23,000 square feet, this moisture could cause a substantial increase in weight. During boost, aerodynamic heating could vaporize the absorbed moisture, generating high pressures inside the external insulation, which could cause cracking and spalling of the external insulation. Hydrophobic coatings can be used to reduce moisture absorption; however, these coatings must be reapplied frequently. To minimize refurbishment time and cost, it would be desirable to use a coating that lasts at least several flights. The surface densification used for mechanical damage protection also tends to reduce moisture absorption. Regardless of the technique used to reduce moisture absorption, it would be undesirable to seal the surface completely against air. The conductivity of a porus material such as the external insulation is lower in a vacuum than in air. This is a favorable feature because it

increases the isolation of the interior of the vehicle from the temperature extremes experienced in space by the outer surface. It is desirable, therefore, to provide venting for the external insulation in space. Experience in the Apollo program has shown that coatings are available which control moisture absorption but permit air to be vented.

To minimize LH_2 boiloff, polyurethane foam is used on the inside of the propellant tank. Between the densified quart and propellant tanks, a fiberglass honeycomb and fiber insulation are used. These materials limit the temperature to 175 F at the bondline between the polyurethane insulation and tank wall.

In summary, the basic ILRV concept is attractive from a thermal protection standpoint. The high angle of attack, low lift-to-drag ratio entry produces a relatively mild aerodynamic heating environment, which in turn, reduces thermal protection system weights significantly from those required for a low-angle-of-attack, high lift-to-drag-ratio vehicle. The weight reduction is attainable regardless of the particular thermal protection technique to be used. In addition, the ILRV concept provides better temperature margins. Continued development and testing of the external insulation is necessary to overcome those problems noted and to prove its applicability to ILRV. Should the external insulation prove to be unsatisfactory for ILRV application, however, the vehicle concept is still feasible using alternate techniques, such as a metallic radiative heat shield. Another alternative is a nonmetallic radiative heat shield, using a material such as RPP (reinforced pyrolized plastic). A low density ablator on replaceable panels also might be used as an interim solution until a reusable heat shield is developed.

8.6.2 Thermal Protection Trades

The objective of the thermal protection trade analysis was to evaluate the ILRV baseline thermal protection system and alternatives to that system. The thermal protection system cannot be evaluated independently of the structure. Structure and thermal protection options and results of the system trades are presented in Section 8.5.

Among the factors considered in evaluating these concepts were weight, complexity, maintenance, and safety. For vehicles of the size being considered in this study, a relatively small change in insulation thickness can produce a substantial weight change. For example, a 50,000-pound-payload orbiter has a surface area on the order of 23,000 square feet. A change in insulation unit weight of only 0.1 pound per square feet can cause a total weight change of over a ton.

Thermal protection system complexity, maintenance, and safety margin are particularly important because of the number of reuses intended for an ILRV system. The thermal protection system must be able to withstand the mission environment cycle, including exposure to vibration, pressure changes, high and low temperature extremes, and moisture, without serious degradation. The system must be designed to minimize the need for inspection and repair, since these recurring functions could have a substantial effect on total operational costs.

The minimum required insulation thicknesses and weights were determined analytically by applying the launch or entry aerodynamic heat flux to a representative insulation/structure cross section. The insulation requirements were determined for both high-heating and low-heating locations on the vehicle. The insulation requirements for intermediate locations were determined by interpolating between these extremes. For the assumed initial temperatures and heating period, the insulation thickness was determined to be (primarily) a function of heat load, heating time and maximum allowable temperature. For the fibrous insulations considered, the relevant material properties were allowed to vary as a function of temperature and, in the case of conductivity, as a function of pressure. The outer surface of the cross section was permitted to reradiate to space, with an emissivity of 0.8. The innermost surface was assumed to be adiabatic. Of the parameters noted, the maximum backface temperature has a particularly strong impact on insulation weight. For example, raising this limit from 175 F to 200 F can decrease insulation weight by 20 percent.

The initial outer surface temperature of the orbiter insulation was assumed to be 200 F. In the 270-nautical-mile, 55-degree inclination orbit considered in this analysis, it is possible for a surface to be exposed to the sun throughout the orbit. A surface continuously exposed to the sun in this orbit will reach 200 F with a solar absorptivity/infrared emissivity ratio of 0.8. Although it is possible to achieve a lower maximum surface temperature through the use of proper coatings, it was assumed that orbital, entry, and atmospheric operations would tend to degrade the surface characteristics so that 200 F is a reasonable assumption. The initial inner surface temperature was assumed to be 100 F. Past experience on the Apollo program has shown that the conditions and assumptions used in this analysis are reasonable for a vehicle in earth orbit.

To assure that the predicted insulation requirements were not optimistic, the analytical models used to determine insulation thicknesses were evaluated for periods sufficient to allow all in-depth temperatures to reach maximum. With the low heat load and short heating period for the ILRV, heat soak-back is not so critical a design requirement for TPS as it would be under a low-angle-of-attack concept. Soak-back does exist, nevertheless, and must be considered.

Materials selection involved several considerations, among which were thermophysical properties, cost, manufacturing complexity, maintenance, and safety. Both maintenance and safety are affected by the cumulative time that materials are subjected to elevated temperatures during 100 missions. The thermal properties of many materials, including foam and fibrous insulations, tend to degrade as the time spent at high temperatures increases. If this factor were not considered in material selection, periodic refurbishment costs would increase substantially, particularly, where insulation is located between the outer shell and the main fuel tanks. Numerous access panels would be required for regular inspection, repair, and replacement of insulation at these locations.

Booster Thermal Protection Options

The booster oxygen tank was considered separately from the hydrogen tank. Because of the highly reactive nature of oxygen with the conventional cryogenic foam insulations, it does not appear practical to use insulation inside the tank. The primary choice, therefore, was between insulation outside the tank and no insulation. It is expected that safety considerations will require a gaseous purge between the tank wall and the outer shell to prevent the collection of gaseous oxygen. This purge will also serve to prevent the formation of frost.

For the hydrogen tank, elimination of the cryogenic insulation was not considered. In addition to causing excessive boiloff rates, a hydrogen tank without insulation would require an expensive helium purge to prevent nitrogen or air liquefaction. Use of external cryogenic insulation on the hydrogen tank offers an advantage in application cost. If insulation machining is required, it can be accomplished at lower cost with outside insulation. Inside insulation offers easier access for inspection and repair. With the outside insulation, either the heat shield would have to be dismantled to repair the insulation or access panels would have to be provided. It is expected that some cryogenic insulation repair will be necessary during the life of the vehicle. Inside insulation eliminates heat shorts at the tank supports. Since the tank wall has a specific diameter for a given fuel capacity, the tank weight will be higher if the tank is enlarged to accommodate inside insulation. Also, the higher wall temperature during launch with inside insulation requires a thicker wall. For an inside foam insulation, a surface film will be required to minimize hydrogen seepage into the foam.

The critical factor in selecting the location of the LH_2 tank insulation is the requirement for inspection and repair between flights. For the ILRV, therefore, polyurethane located inside the tank is the selected design approach.

The upper surface of the booster fuselage experiences a relatively mild environment during launch and flyback. Therefore, the use of external insulation or a high-temperature radiative panel is not required. Insulation will be required inside the outer shell, particularly in the area of the hydrogen tanks. The principal insulation candidates were Dynaflex and TG-15000. While not the most thermally efficient material available, Dynaflex is more flexible and structurally durable than most other candidate insulations. Installation and maintenance costs should be relatively low with Dynaflex. In addition, it has good high-temperature capabilities, with a reported (vendor's data) temperature limit for multiple reuse of about 2600 F. TG-15000 also exhibits good handling and manufacturing characteristics; however, its temperature limit for multiple reuse is about 600 F. Both TG-15000 and Dynaflex are quite inexpensive compared with other candidate insulations.

Among the other insulations considered were Dynaquartz, Microquartz, and Min-K. Dynaquartz is a semirigid, structurally weak material that would probably require additional support to be held in place. Microquartz is a felted, rather fluffy material with a temperature limit of about 1800 F. Since its structural properties are low, it must be supported and contained for the application being considered here. High-temperature shrinkage appears to be a problem with both Microquartz and Min-K. The Min-K insulations are relatively heavy and expensive. For the ILRV, the TG-15000 insulation was selected over the Dynaflex material because of superior insulation properties and, therefore, a lower weight system.

The lower fuselage experiences higher temperatures and heat loads than the upper fuselage. Materials with higher temperature capabilities and more insulation are required in these areas. One of the thermal protection concepts considered in this area was the baseline configuration, consisting of an external insulation, such as LI-15, installed on a structural substrate in series with a fibrous internal insulation. The alternative to this configuration was a radiative, non-insulating panel, backed by a layer of fibrous insulation. These external insulation concepts are illustrated in Figure 8.5-4. For the moderate environment experienced by the booster, a number of superalloys are available as radiative panel materials. Selection of material depends primarily on structural considerations and has a negligible effect on insulation requirements. A composite insulation system consisting of a fibrous insulation backed by a chemical heat-sink phase-change material (solid-liquid or solid-solid) was not considered in this investigation. In vehicles with high heat loads, a composite insulation system is useful, reducing insulation thickness by about 50 percent and insulation weight by about 15 percent. With the relatively low insulation weights required for the ILRV concept, however, it is uncertain that the theoretical weight saving can be attainable in practice.

The wing thermal protection options are similar to the fuselage options. The choice is basically between external insulation and a radiative panel with fibrous internal insulation. There is an additional consideration involving the use of external insulation on the wing. It is expected that the wings will flex during entry and landing operations; consequently, the external insulation design must accommodate this bending without degradation. Thermal expansion compatibility also must be considered in the detailed design of the attachment of the external insulation.

Since the booster begins flyback immediately after launch and separation, the candidate thermal protection systems were sized for the combined launch and flyback heat loads. Of the maximum temperatures reached during the launch and the flyback phases, the higher was used for determining material applicability. The selected external thermal protection system is LI-15.

Orbiter Thermal Protection Options

The orbiter thermal protection options are generally similar to those for the equivalent locations on the booster. The principal differences are that the orbiter experiences greater heat loads and requires more insulation, and the leading edges of the orbiter wings and horizontal fins reach much higher temperatures than those of the booster.

The choice for the main oxygen tank is between insulation on the outer surface of the tank and no insulation. For the main hydrogen tank, the option is between insulation on the outer tank surface and insulation on the inner tank surface. The considerations involved in selecting the tankage insulation have been discussed above for the booster tankage.

The orbiter also requires separate tanks for oxygen and hydrogen for orbital maneuvers and the initiation of entry. For these tanks, long-term storage (up to 30 days) must be considered. In addition to the foam insulation considered for the main tanks, multilayer insulation is a candidate for use with the orbiter maneuver tanks. Multilayer insulations require a purge or evacuation while insulating cryogenic fuels in the atmosphere. In the vacuum of space, multilayer insulations have a low effective conductivity, which makes them attractive for long-term storage.

During entry, the upper surface of the orbiter fuselage will approach a maximum temperature of 500 F, which is no greater than the maximum temperatures experienced by the upper surface of the booster fuselage; consequently, the material choices remain the same. Orbiter insulation will be thicker because of higher heat loads and longer heating periods.

The lower orbiter fuselage experiences moderately higher temperatures and higher heat loads during entry than the booster. The materials most affected by the higher temperatures are the metals considered for the outer skin for the radiative panel/fibrous insulation concept. The temperature increase is not sufficient to have a significant effect on the choice of internal insulation material. The higher heat loads will require greater insulation thicknesses on the orbiter than on the booster.

An example of the trades involved in selecting a thermal protection system is shown in Figures 8.6-4 and 8.6-5. The configurations considered for the lower orbiter fuselage are (a) the baseline concept consisting of external insulation with fibrous internal insulation and (b) a metallic radiative panel with fibrous internal insulation. These configurations were evaluated analytically to determine the thicknesses required for a given maximum tank wall temperature. In this example, a maximum tank temperature of 175 F was used (consistent with a 175 F reuse temperature for the foam). Figure 8.6-5 indicates that the external insulation concept exhibits a weight advantage over the alternative concept. It should be noted that the temperature limits used for the insulation materials in this investigation (such as 2600 F for Dynaflex, 600 F for TG-15000, and 175 F for polyurethane foam) are projected limits for multiple reuse. It is expected that a test program will be required to better determine the temperature limits of these materials under operational conditions.

The leading edges of the orbiter wings and horizontal fins reach much higher temperatures than those of the booster. These higher temperatures have a strong effect on the thermal protection options. The maximum orbiter leading-edge temperatures are typically about 3000 F. In the area of shock impingement, they approach 3600 F. A leading edge-material option for the baseline thermal protection system is RPP, a pyrolyzed carbon laminate. This carbonaceous material, which requires a coating to prevent oxidation, has a maximum multi-use temperature limit of about 3000 F. It is expected that the coating would require periodic reapplication to prevent oxidation. An alternative approach to protecting the leading edge is to use a heat sink, relying on a mass of material to depress the temperatures. Beryllium was considered for this application because of its high specific heat. The principal disadvantage of this approach is the high weight of material required. Another alternative is the use of a ceramic material for the leading edge. Ceramics can experience extremely high temperatures without oxidation or degradation; however, they are brittle and usually sensitive to thermal shock. Ceramic components and their attachments must be designed to minimize tensile stresses and stress concentrations. A ceramic material was selected for wing leading edges.

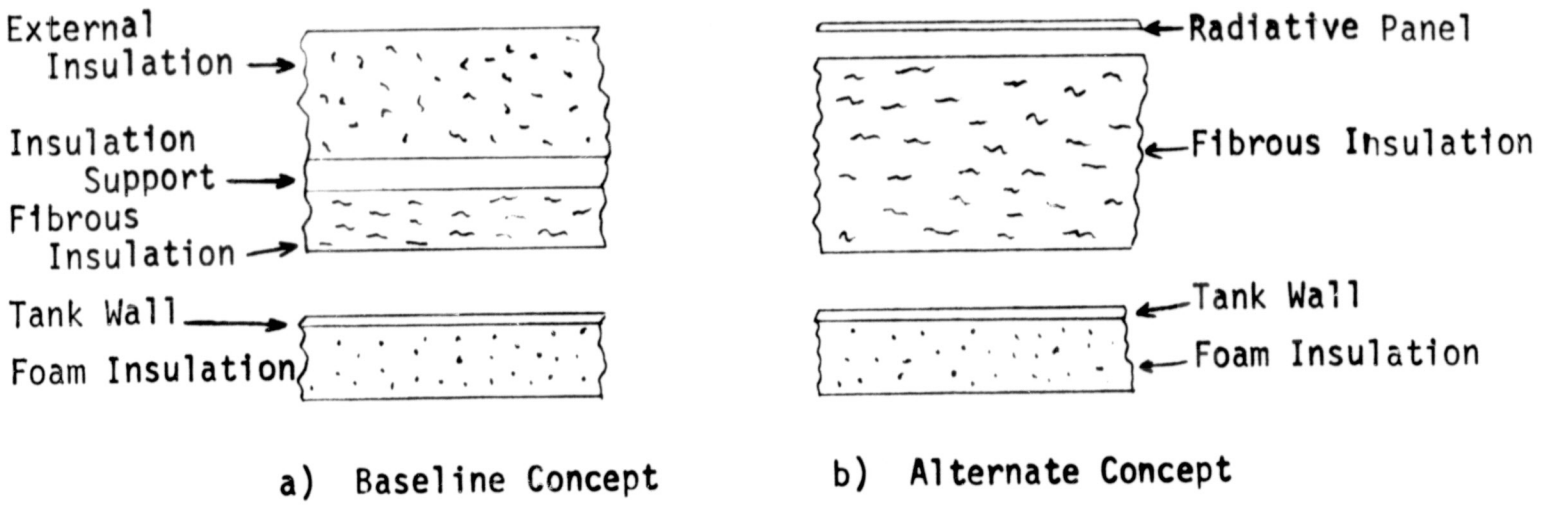

Figure 8.6-4. Typical Thermal Protection System Cross Sections

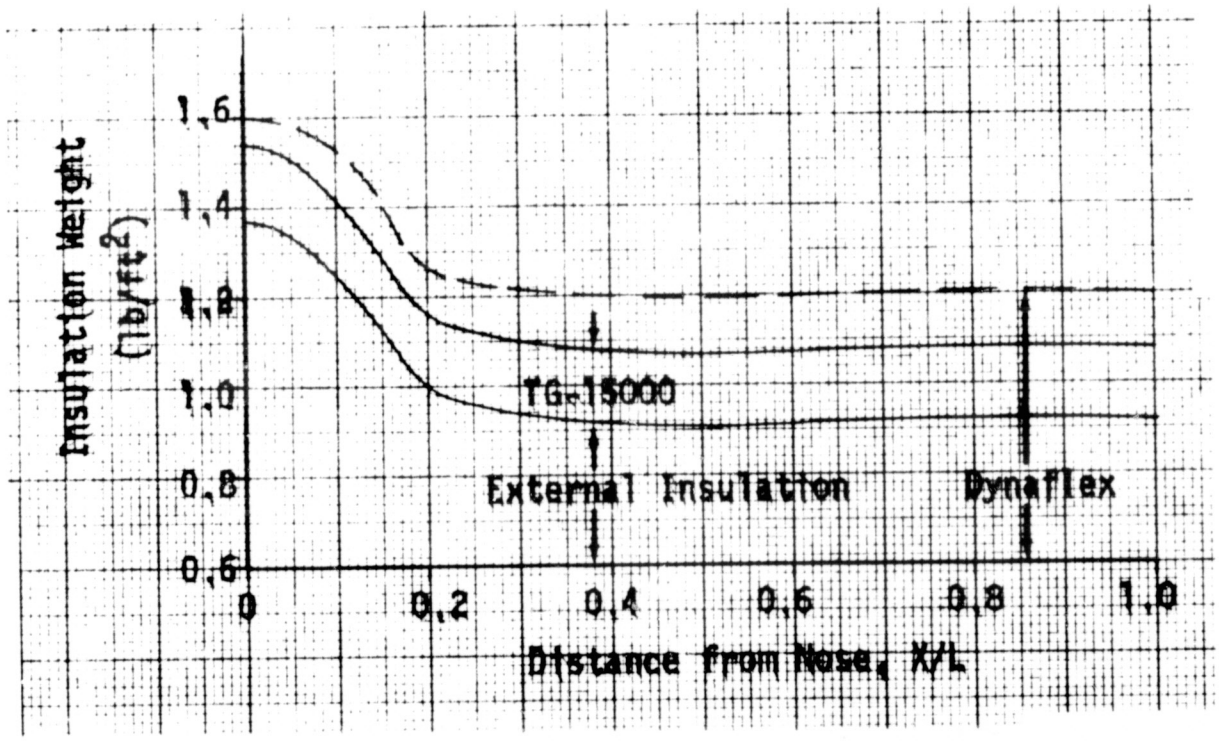

Figure 8.6-5. Insulation Weight Comparison for Orbiter Underbody Centerline

Insulation will be required behind the leading edge to prevent overheating of the wing structure. For leading edge concepts such as the ceramics, which do not lower the temperatures appreciably, a very high temperature insulation such as zirconia felt must be used. The layer of zirconia felt can be backed up by a layer of more efficient insulation, such as Dynaflex.

8.6.3 Thermal Protection System Definition

A thermal protection system has been defined for the 50,000-pound payload orbiter and booster (Figure 8.6-6). Thermal protection systems for vehicles in the 10,000-pound or 25,000-pound payload class will be similar, with minor differences in insulation thickness requirements. The booster oxygen tank has no cryogenic insulation, which provides a significant reduction in system weight at the cost of an increased boiloff rate. Eliminating the oxygen tank insulation removes the maintenance problems associated with periodic inspection and repair of the insulation. For the hydrogen tank, one inch of internal foam was selected. Ease of inspection and repair was the overriding consideration in choosing the internal insulation. The insulation will require a surface film to minimize penetration of the hydrogen into the foam. The insulation selected was a 2-pound-per-cubic-foot polyurethane foam (NOPCO BX-250A). This foam was chosen for its light weight and low maintenance requirements. The principal drawback of this foam for multiple reuse is its maximum temperature limit (175 F). The one-inch thickness was chosen to raise the tank wall temperature so that dry nitrogen can be used as a purge. The nitrogen purge eliminates the dangers associated with hydrogen and/or oxygen leakage. The purge also eliminates the formation of frost on the tank surface and the vehicle weight increase caused by that frost.

The maximum temperature distribution on the upper surface of the booster during flyback is shown in Figure 8.6-7. The peak temperatures during launch will be lower than these values. TG-15000 insulation was selected for the top of the fuselage because of its light weight and relatively good handling characteristics. The amount of insulation required to keep the backface temperatures below 175 F and 200 F are shown in Figure 8.6-8. The 175 F limit is required by the foam insulation on the hydrogen tank. As indicated by the 200 F curve, insulation weight requirements drop significantly when the temperature restrictions are eased.

Along the booster sides, the external insulation (LI-15) with TG-15000 internal insulation concept was selected. It was assured that the minimum thickness practical to fabricate LI-15 was 0.25 inch, which is greater than the thickness required by thermal considerations. The LI-15/TG-15000 concept, nevertheless, has a weight advantage over a metallic heat shield/Dynaflex configuration. The thermal protection system weights along the

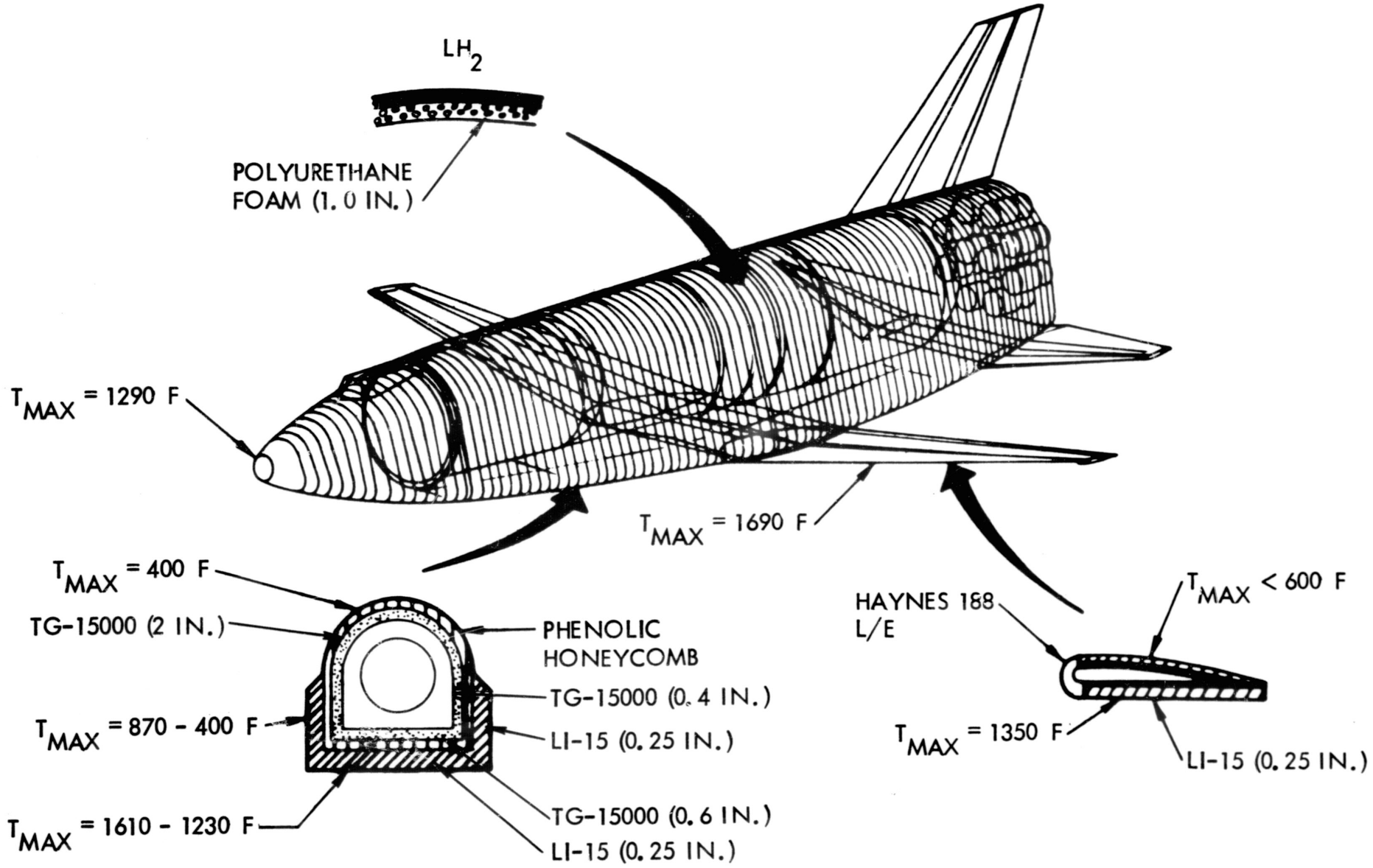

Figure 8.6-6. Booster Thermal Protection System Definition

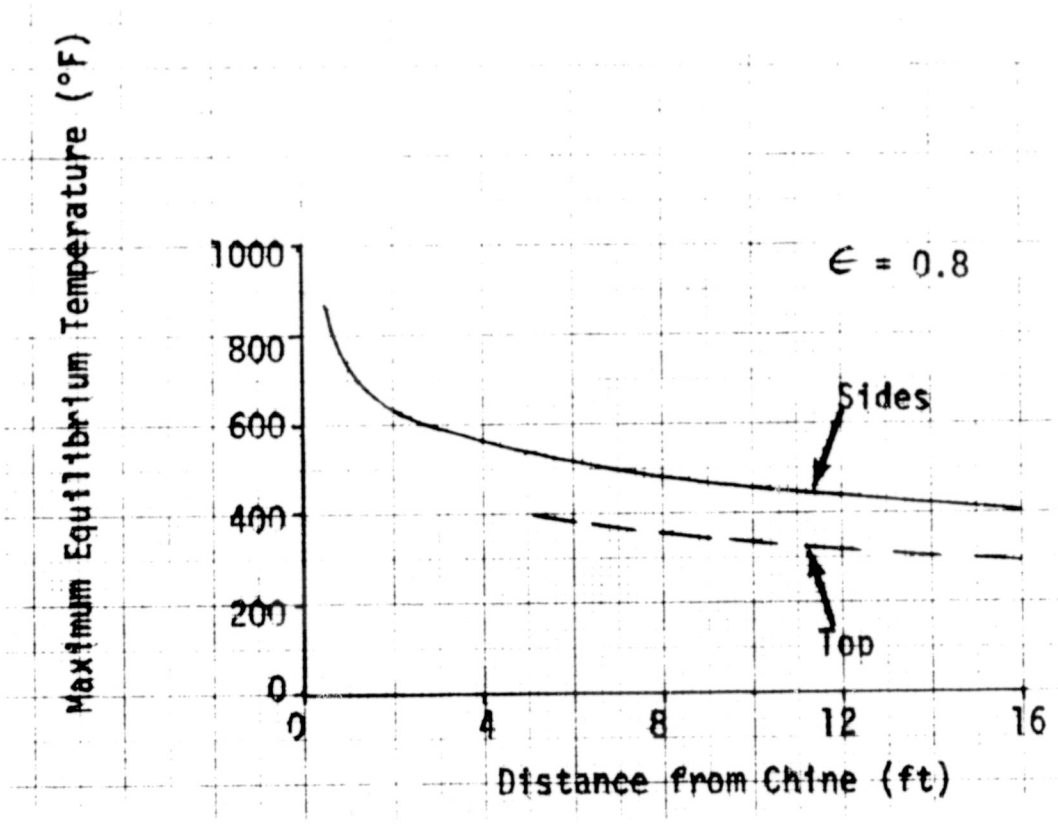

Figure 8.6-7. Maximum Temperature Distribution for Booster Sides and Top

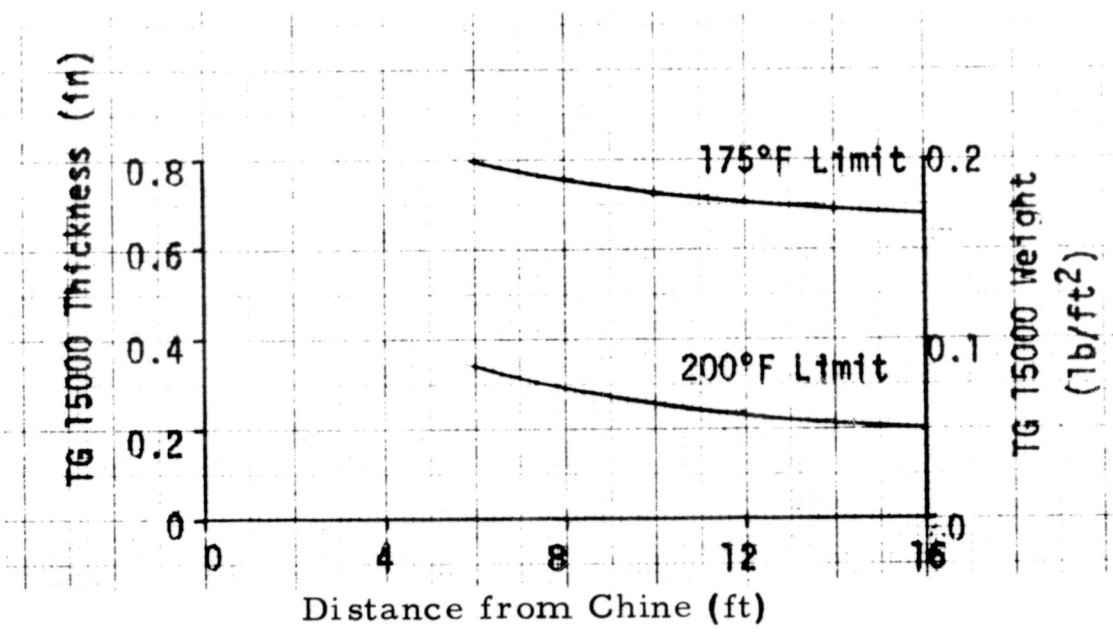

Figure 8.6-8. Insulation Requirements for Booster Top

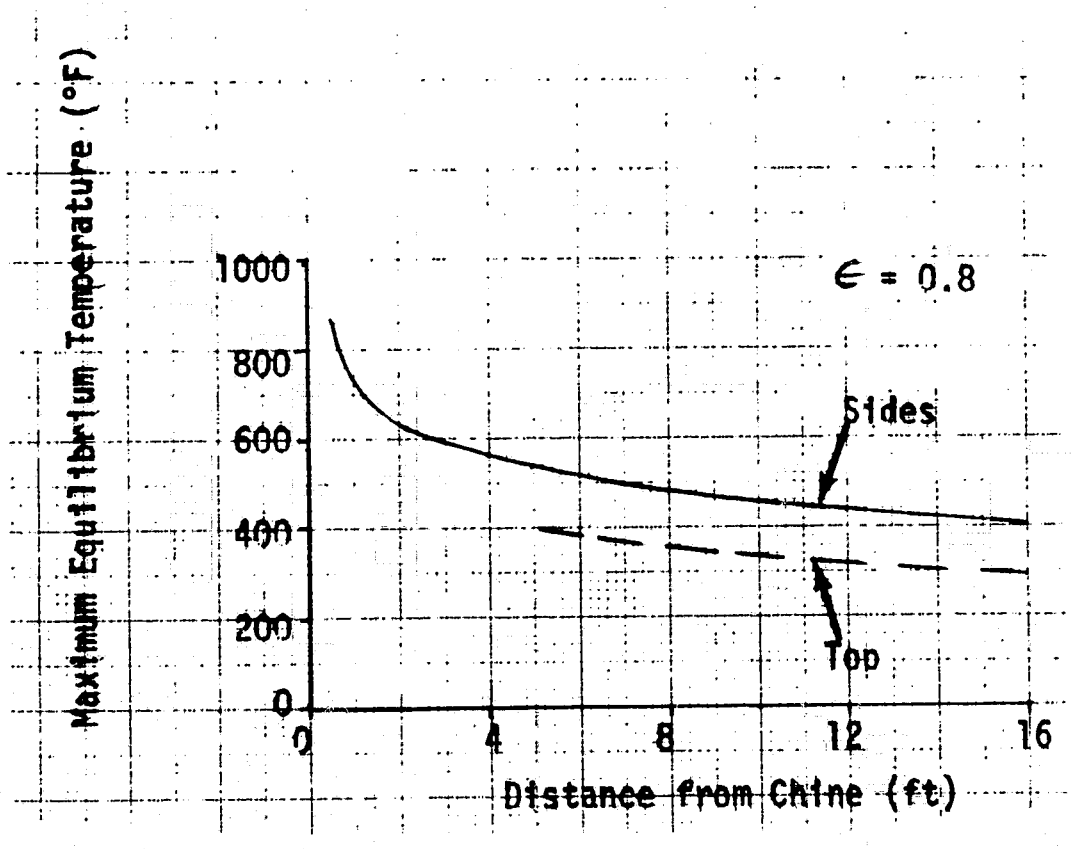

Figure 8.6-7. Maximum Temperature Distribution for Booster Sides and Top

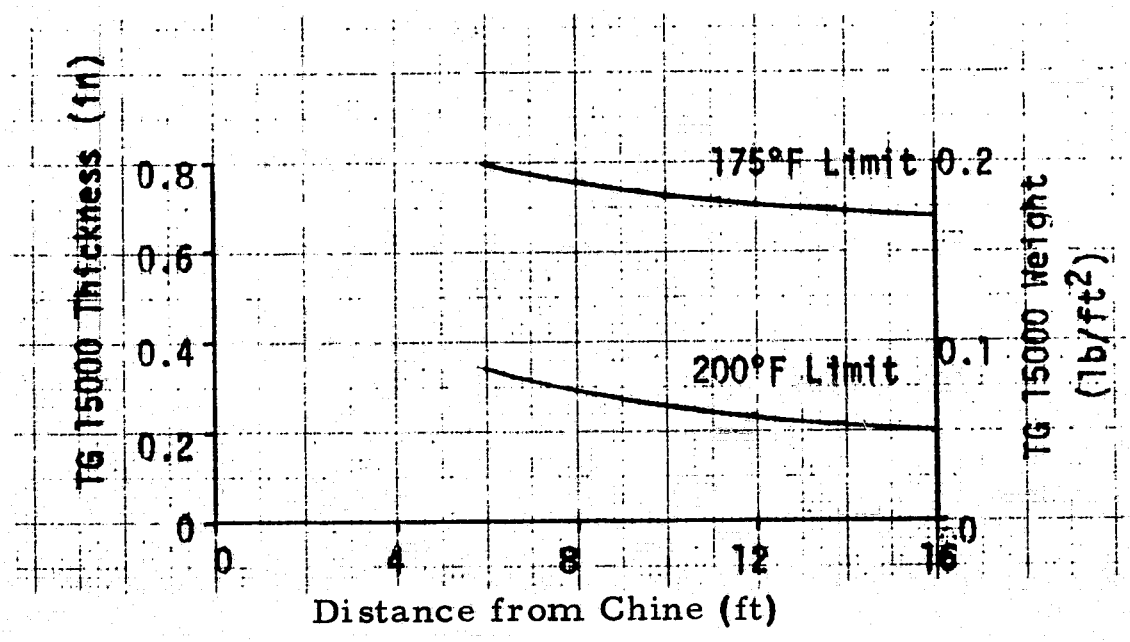

Figure 8.6-8. Insulation Requirements for Booster Top

booster sides can be reduced if it proves practical to fabricate the external insulation in thinner gauges. Approximately 0.1 pound per square foot of TG-15000 insulation (3 pounds per cubic foot) will be required behind the external insulation.

The maximum surface temperature distribution along the lower fuselage of the booster is presented in Figure 8.6-9. The abrupt temperature increase near the nose is caused by transition to turbulent flow. The LI-15/TG-15000 concept was selected for this area because it had the advantage both in weight and safety margin. The external insulation requirements are shown in Figure 8.6-10. The maximum LI-15 backface temperature of 400 F was limited by the adhesive used to bond the LI-15 to its support panel. Along much of the under surface, the thermally required thickness is less than the assumed minimum gauge of 0.25 inch. The TG-15000 weight along the under surface is about 0.15 pound per square foot.

The under surface of the booster wing experiences relatively mild peak temperatures (Figure 8.6-11). Transition to turbulent flow causes the temperature rise between X/C of 0.1 and 0.2. For the wing under surface, the external insulation was selected (Figure 8.6-12) with the insulation bonded directly to the wing structure. For the booster wing, the temperature of the upper surface does not exceed 600 F; therefore, no insulation is required in this area. The leading edges of the booster experience moderate temperatures (less than 1700 F) during launch and flyback. A superalloy such as Haynes 188 can be used in these areas.

The selected orbiter thermal protection system is illustrated in Figure 8.6-13. The main orbiter fuel tanks have thermal protection requirements similar to those of the booster tanks; no insulation on the oxygen tank and one inch of polyurethane foam inside the hydrogen tank. A nitrogen gas purge will also be required for the orbiter. For the orbital maneuver tanks, multilayer insulation will be used for the oxygen tank. Multilayer insulation over polyurethane foam will be used for the hydrogen tank. These insulation combinations were selected to reduce boiloff in orbit and permit the use of the same nitrogen purge used for the main tanks on the ground.

The upper fuselage of the orbiter also has thermal protection requirements similar to those of the booster. TG-15000 insulation was used inside the outer shell. The maximum surface temperatures experienced by the orbiter top during entry are shown in Figure 8.6-14. Insulation requirements are presented in Figure 8.6-15. On the orbiter fuselage sides, the LI-15/TG-15000 concept was selected because of its lighter weight and safety margin. Maximum temperatures on the orbiter sides are shown in Figure 8.6-16. The external insulation requirements are presented in Figure 8.6-17. These thicknesses are based on a maximum backface

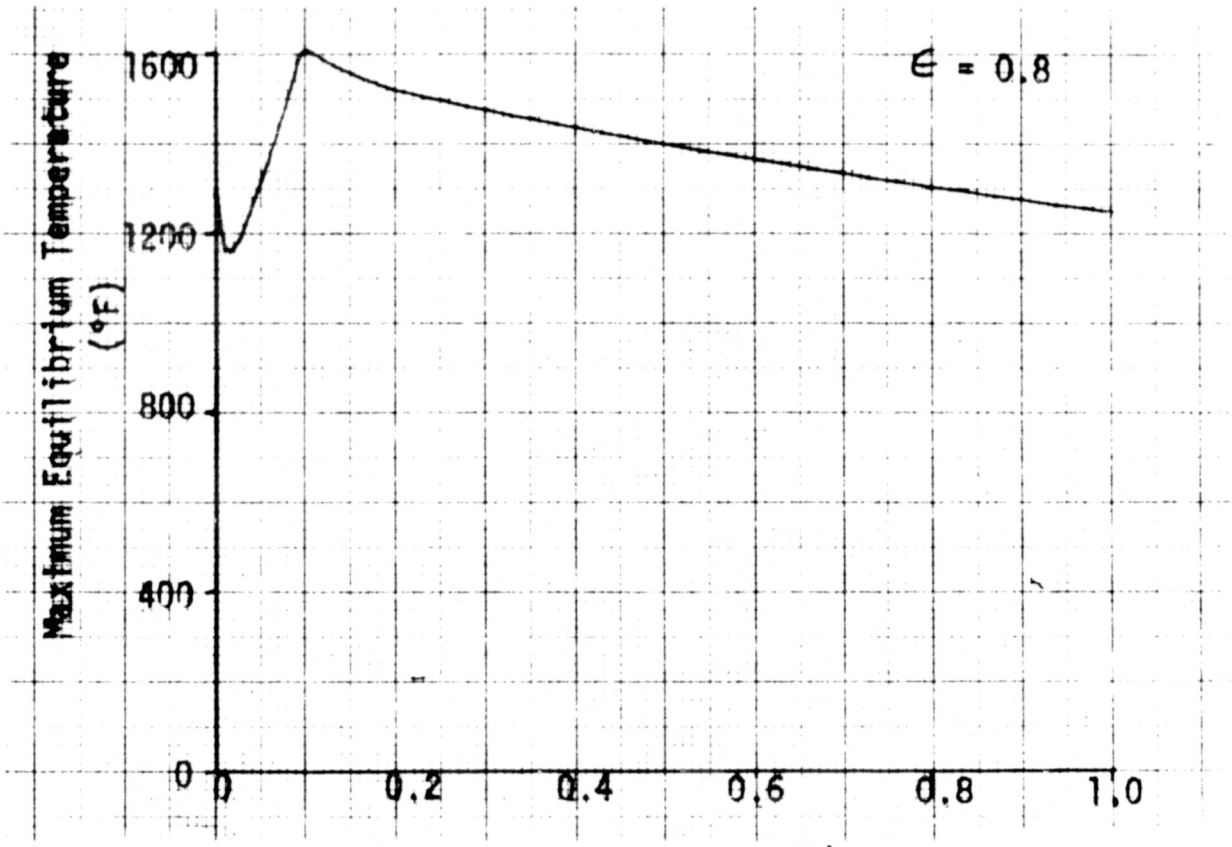

Figure 8.6-9. Maximum Temperature Distribution for Booster Underbody Centerline

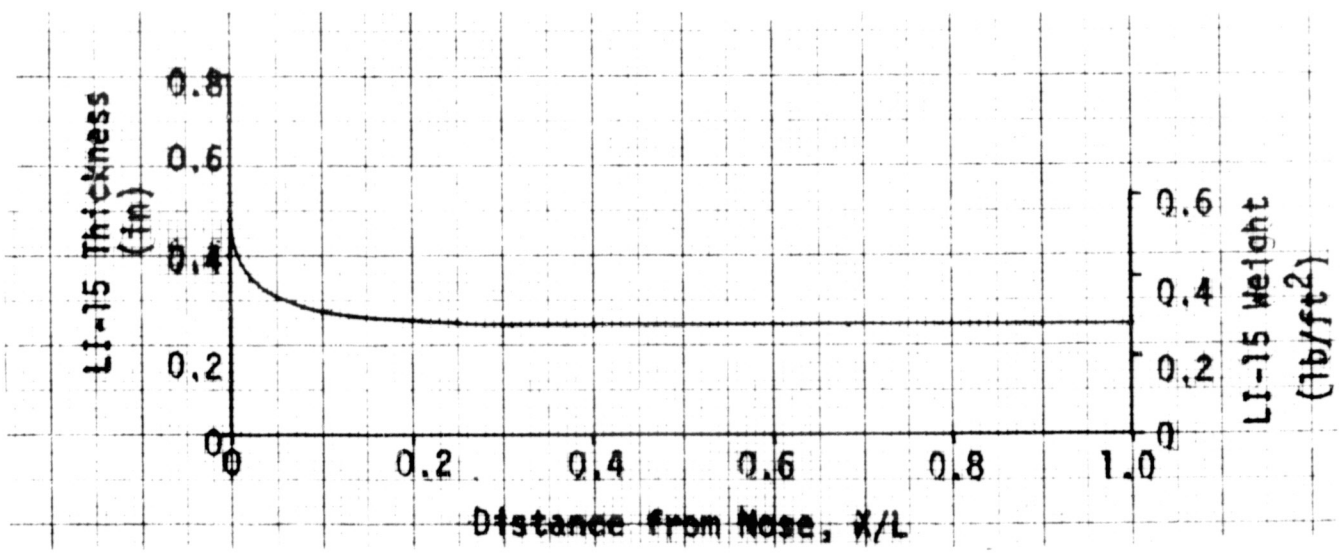

Figure 8.6-10. External Insulation Requirements for Booster Underbody Centerline

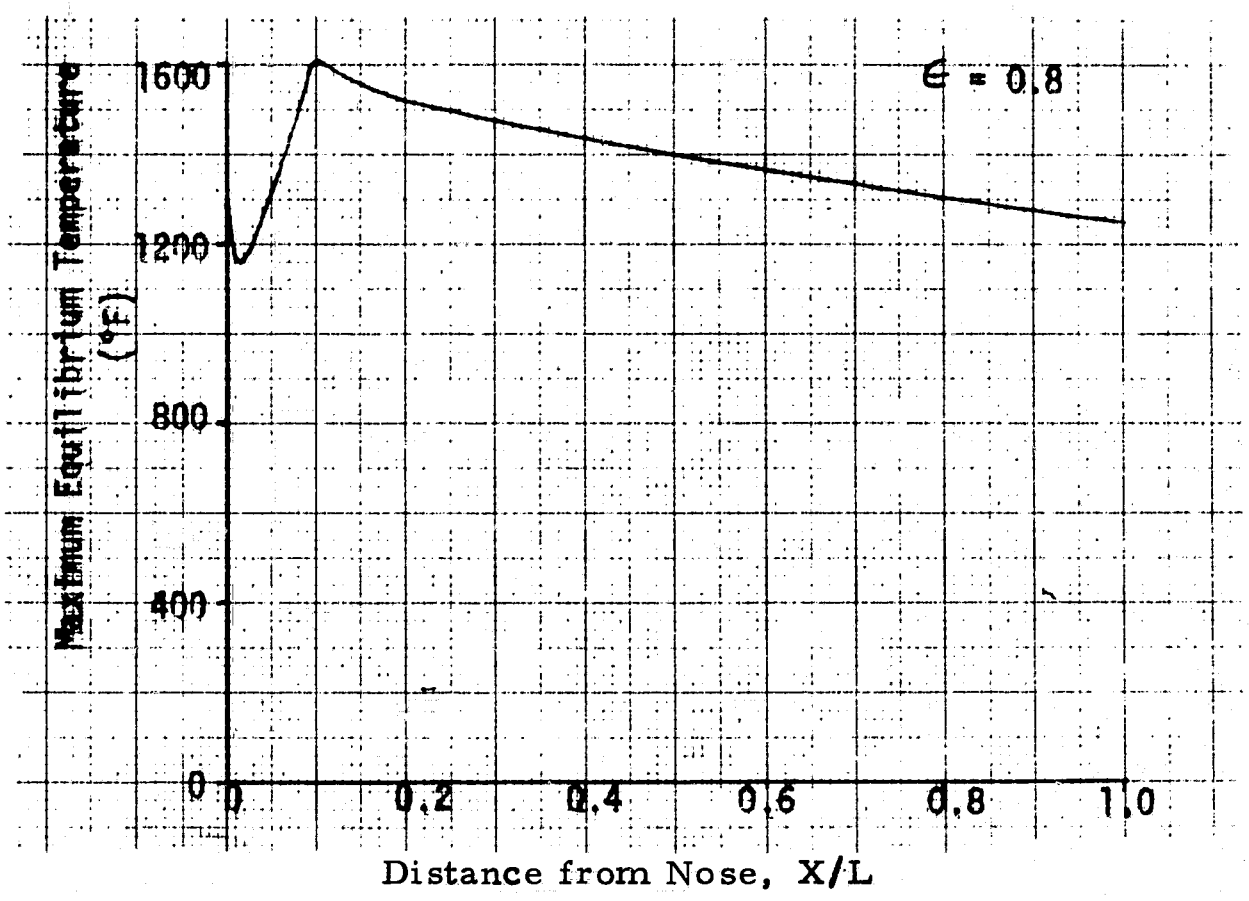

Figure 8.6-9. Maximum Temperature Distribution for Booster Underbody Centerline

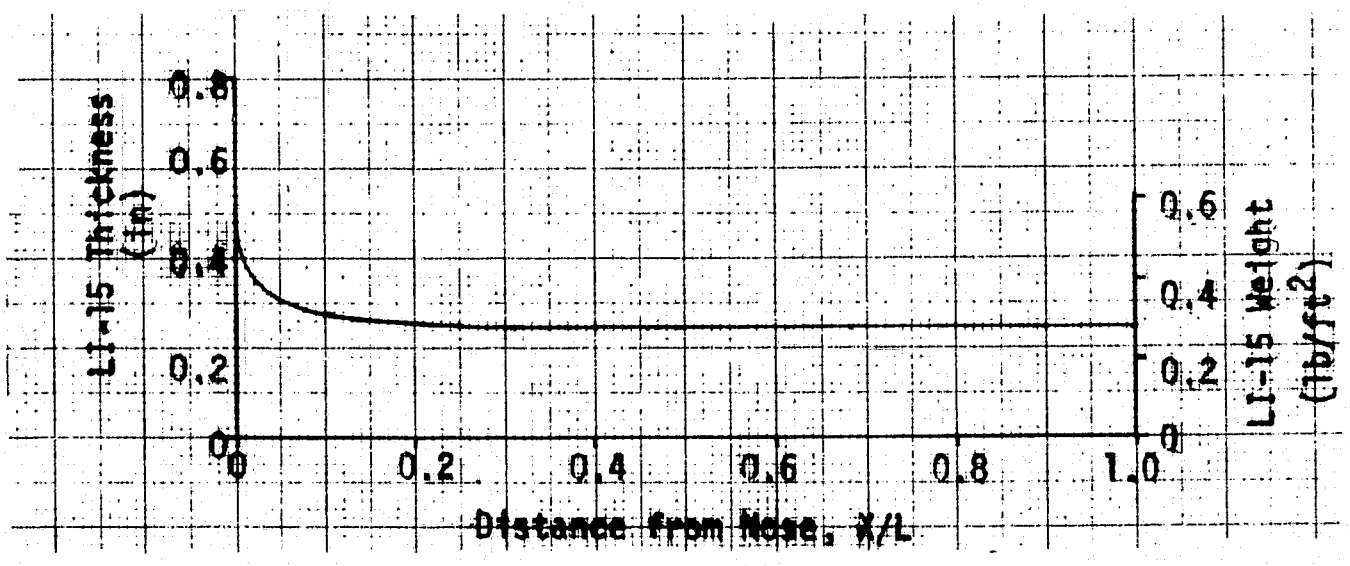

Figure 8.6-10. External Insulation Requirements for Booster Underbody Centerline

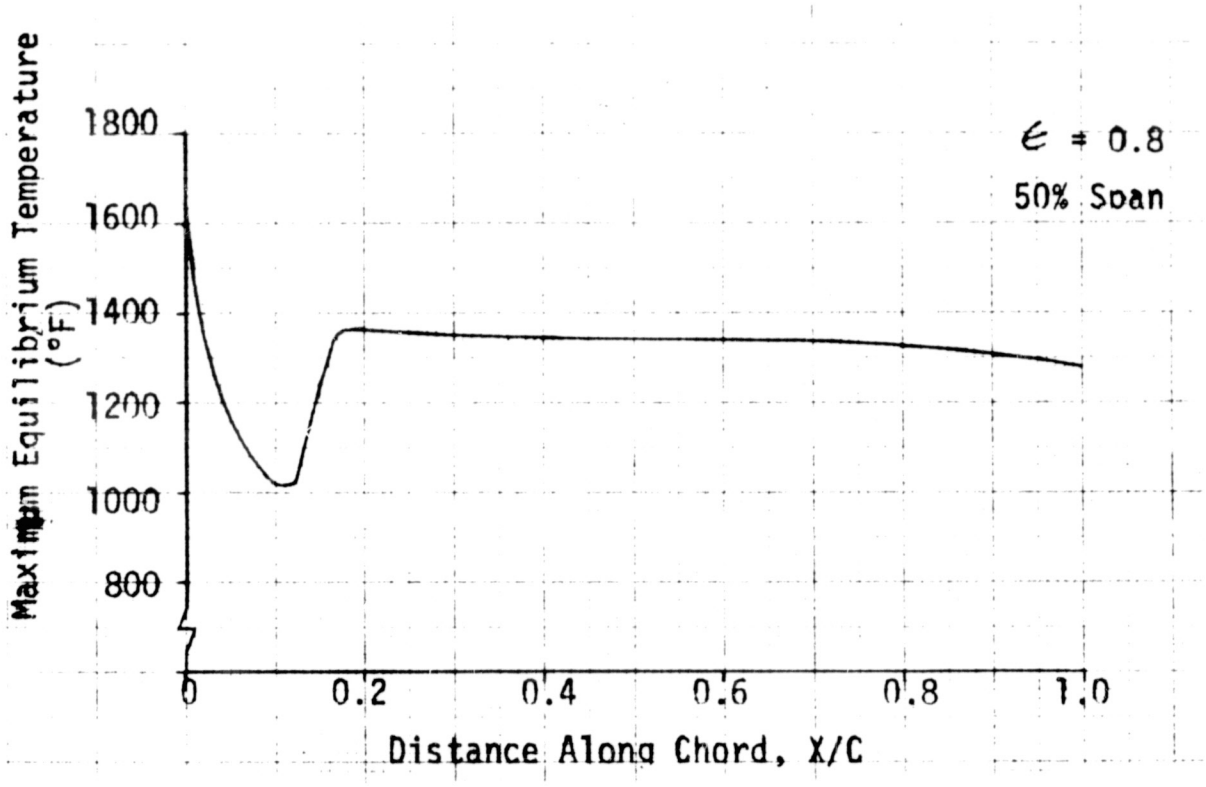

Figure 8.6-11. Maximum Temperature Distribution for Booster Wing Undersurface

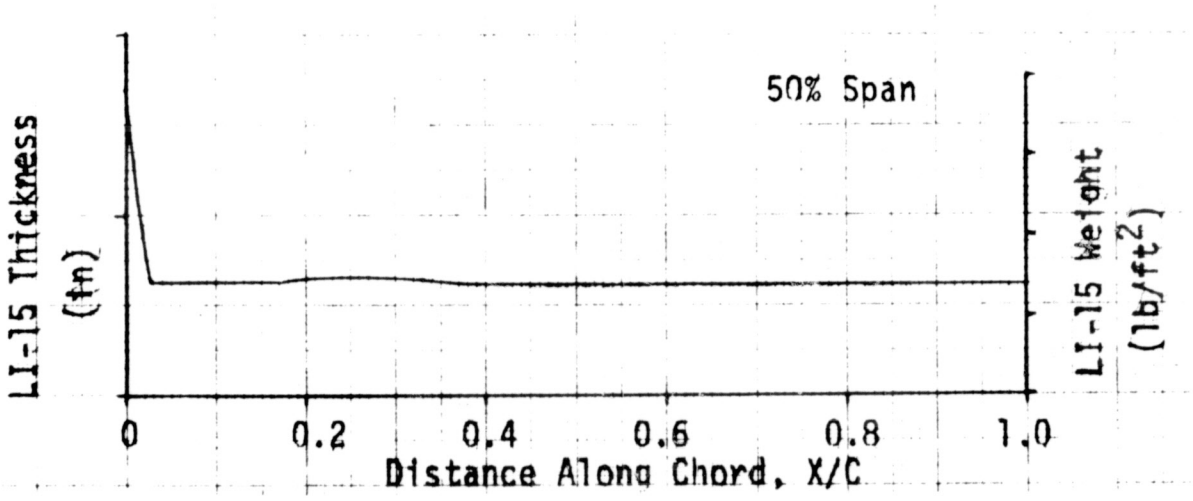

Figure 8.6-12. External Insulation Requirements for Booster Wing Undersurface

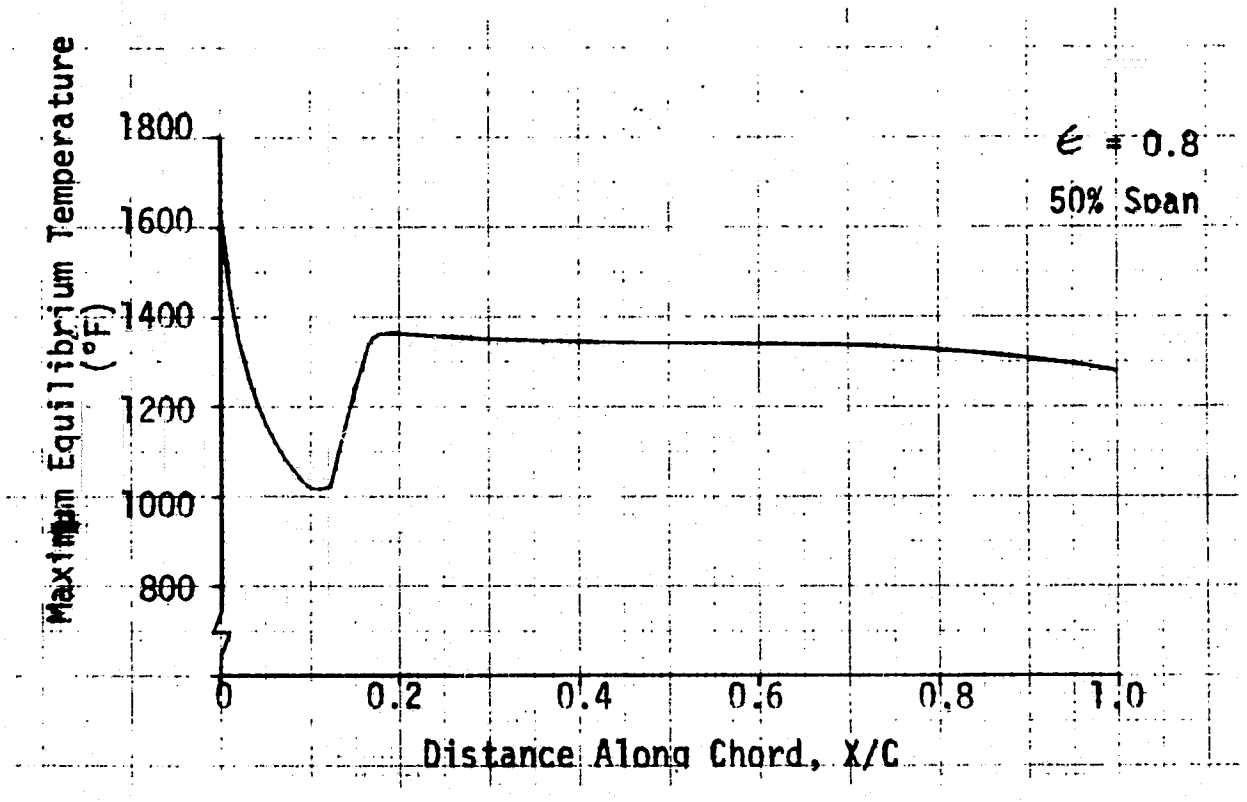

Figure 8.6-11. Maximum Temperature Distribution for Booster Wing Undersurface

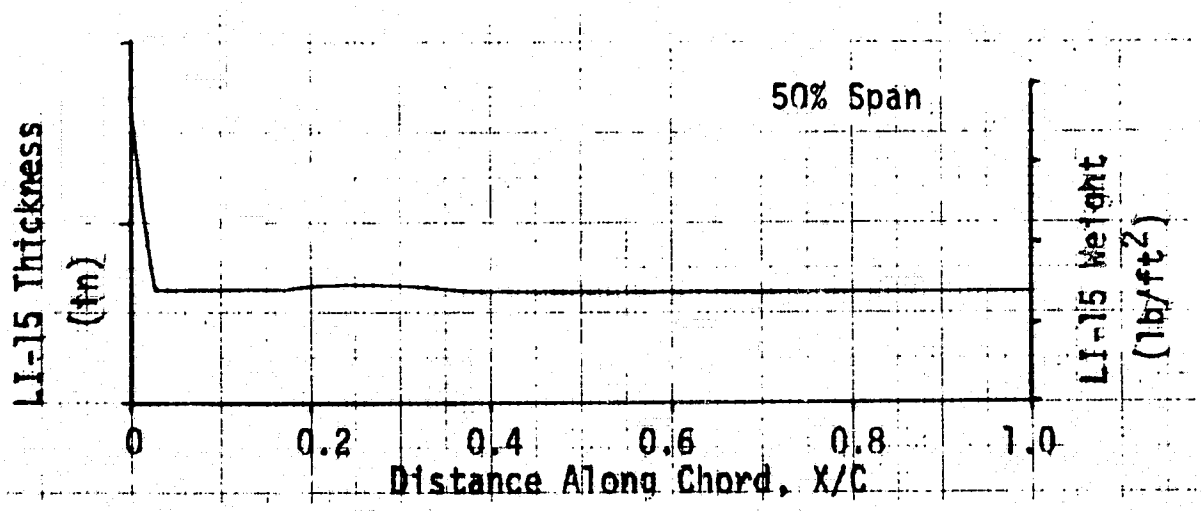

Figure 8.6-12. External Insulation Requirements for Booster Wing Undersurface

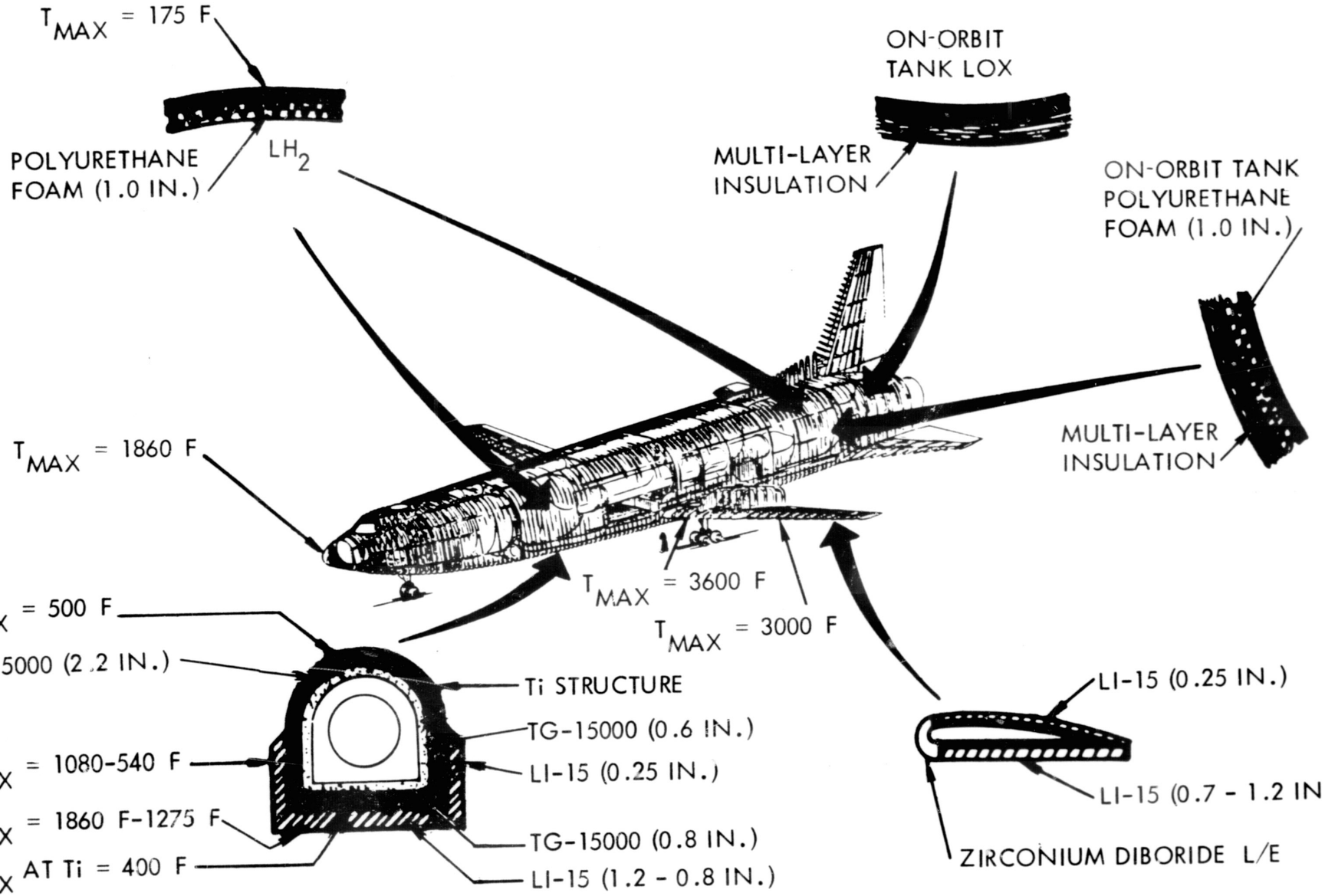

Figure 8.6-13. Orbiter Thermal Protection System Definition

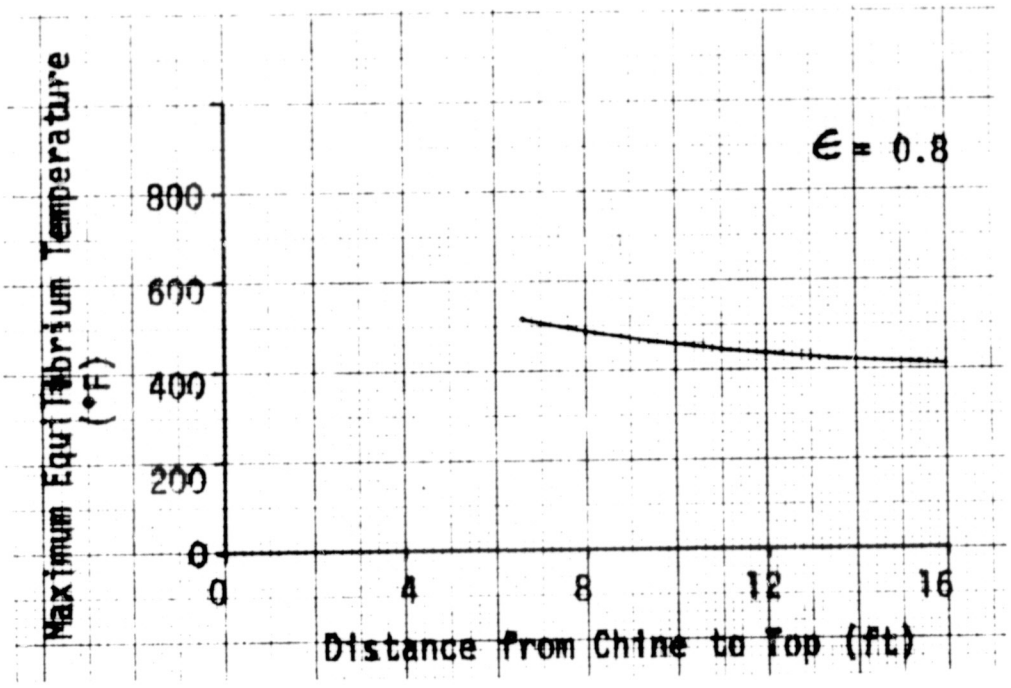

Figure 8.6-14. Maximum Temperature Distribution for Orbiter Top

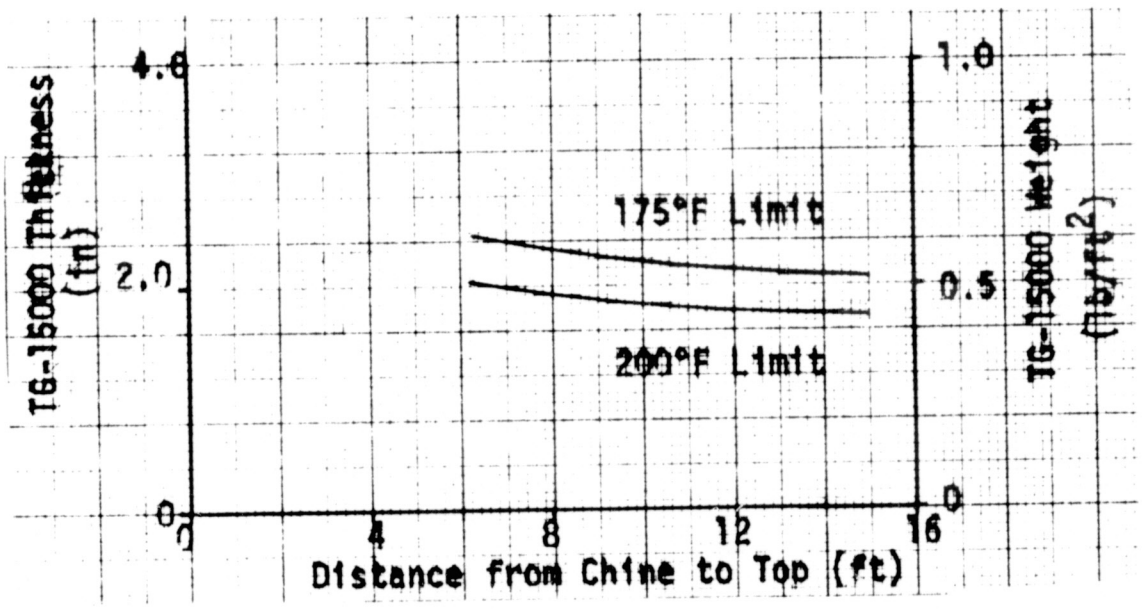

Figure 8.6-15. Insulation Requirements for Orbiter Top

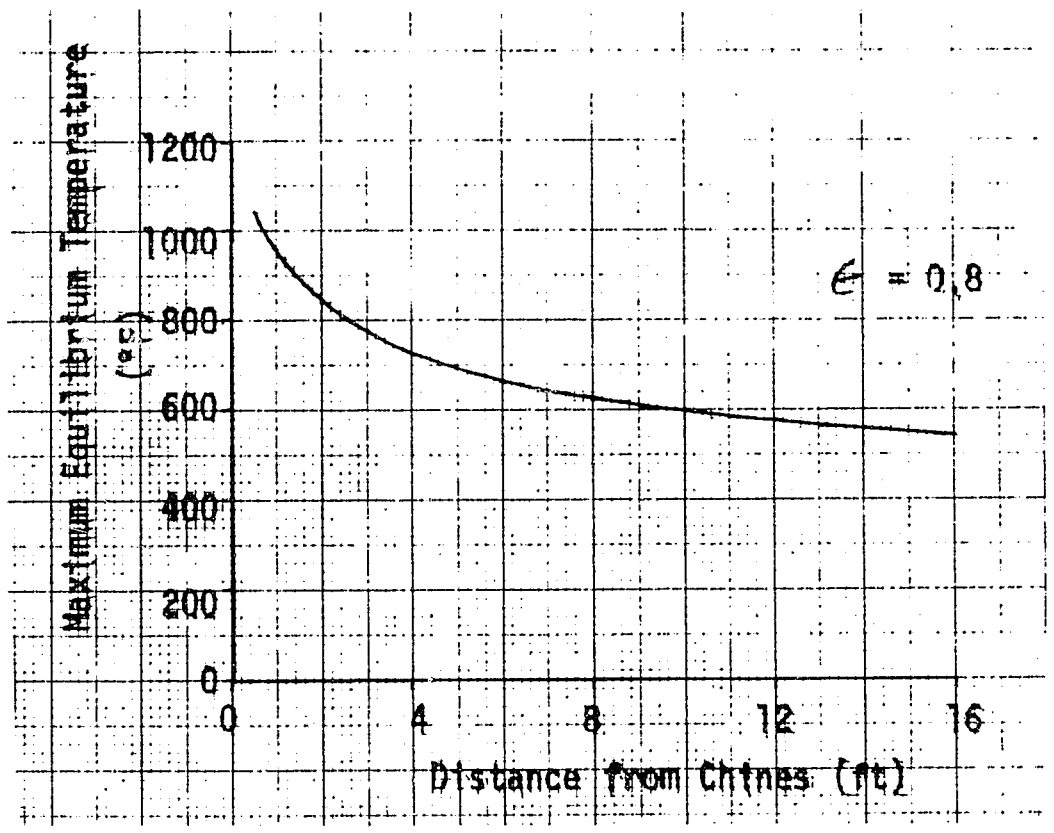

Figure 8.6-16. Maximum Temperature Distribution for Orbiter Top

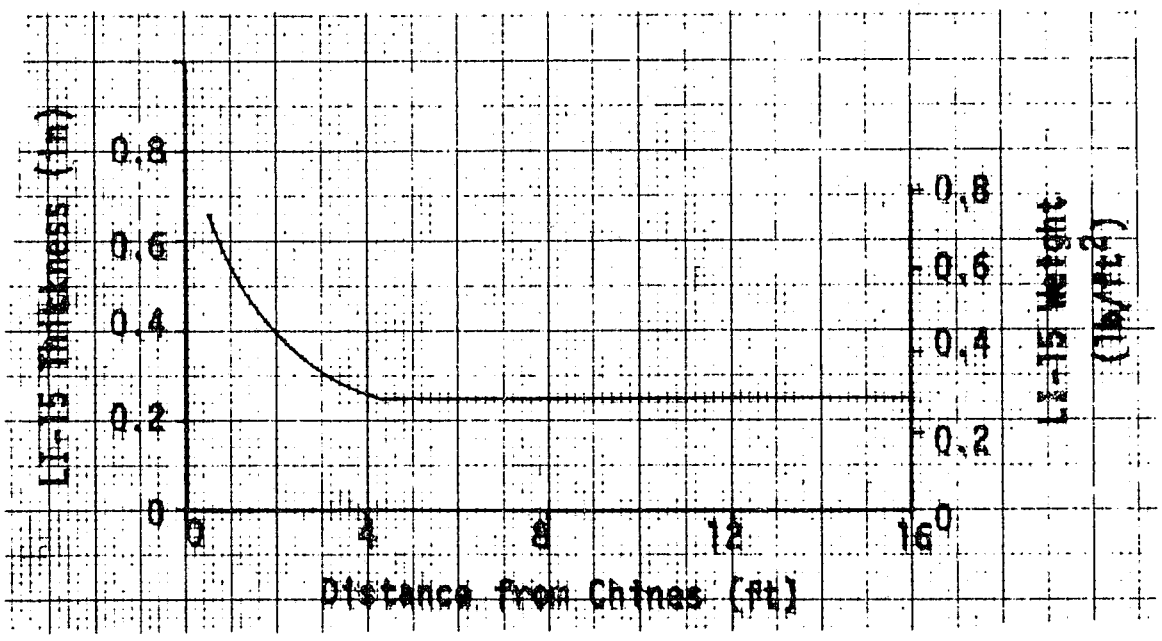

Figure 8.6-17. External Insulation Requirements for Orbiter Sides

temperature of 400 F and a minimum gauge of 0.25 inch. The internal insulation weight (TG-15000) is about 0.15 pound per square foot.

The external insulation concept was also used for the lower orbiter fuselage. This selection was based on the lower weight, greater safety margin, and better space heat transfer characteristics offered by this concept. Maximum surface temperatures along the under surface are shown in Figure 8.6-18. External insulation thickness requirements are shown in Figure 8.6-19. Internal insulation requirements are presented in Figure 8.6-20.

Peak surface temperatures along the under surface of the orbiter wing (Figure 8.6-21) are somewhat higher than on the under surface of the fuselage. The higher temperatures at 20-percent span are caused by flow interference effects. The external insulation concept was chosen for this area for the reasons noted previously. Thickness requirements are presented in Figure 8.6-22.

Peak temperatures on the upper surface of the orbiter wing are sufficiently high (Figure 8.6-23) during entry to require thermal protection; however, the minimum gauge (0.25 inch) of external insulation will be sufficient to keep the structure below 600 F.

For the leading edges of the orbiter wings and horizontal fins, a ceramic, zirconium diboride was selected. RPP was eliminated because its temperature limit for multiple reuse is marginal in undisturbed regions and inadequate in the shock-impingement regions. The beryllium heat sink was eliminated because of excessive weight (3500 pounds to protect the wings and fins from the leading edge to X/C of 0.07). Zirconium diboride was selected because of its high temperature limit and good thermal shock characteristics. A layer of zirconia felt, backed by a layer of Dynaflex, is used to insulate the wing structure from the leading edge.

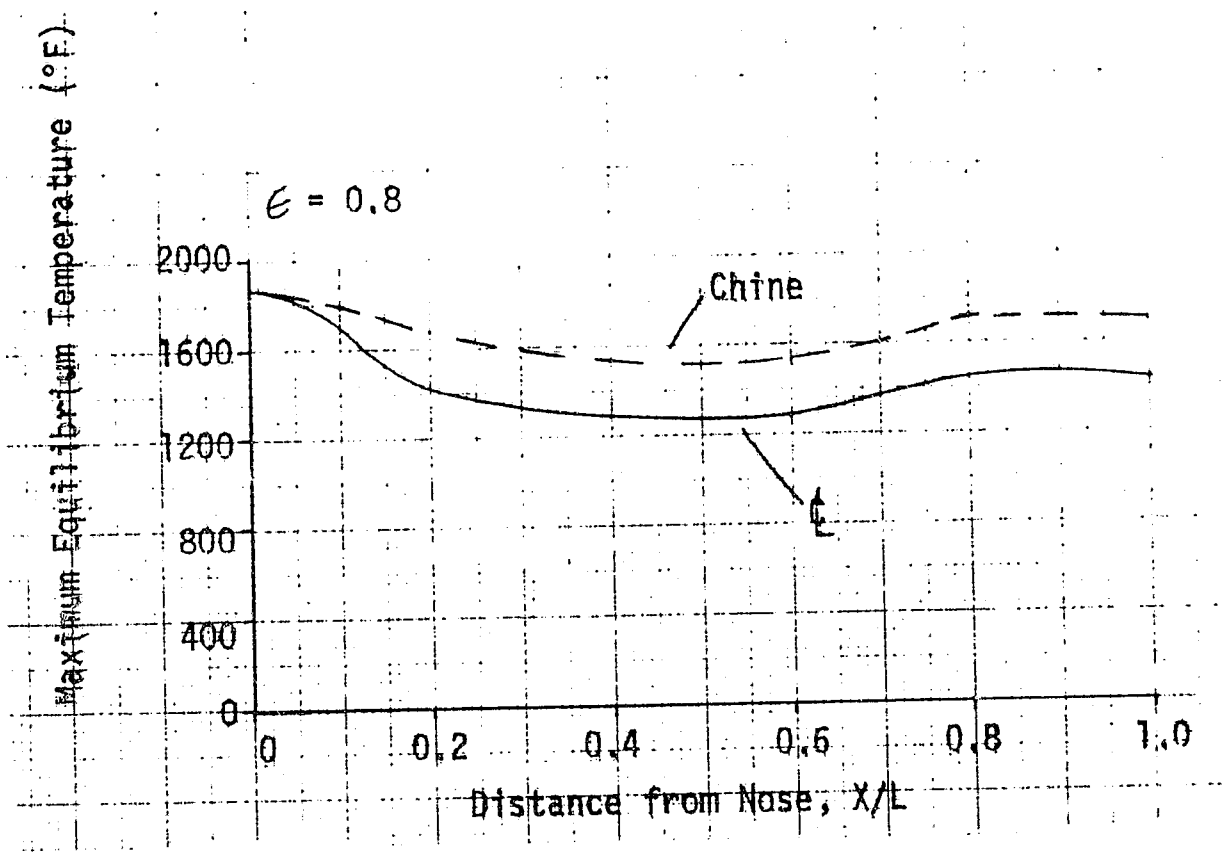

Figure 8.6-18. Maximum Temperature Distribution for Orbiter Top (Chine and Centerline)

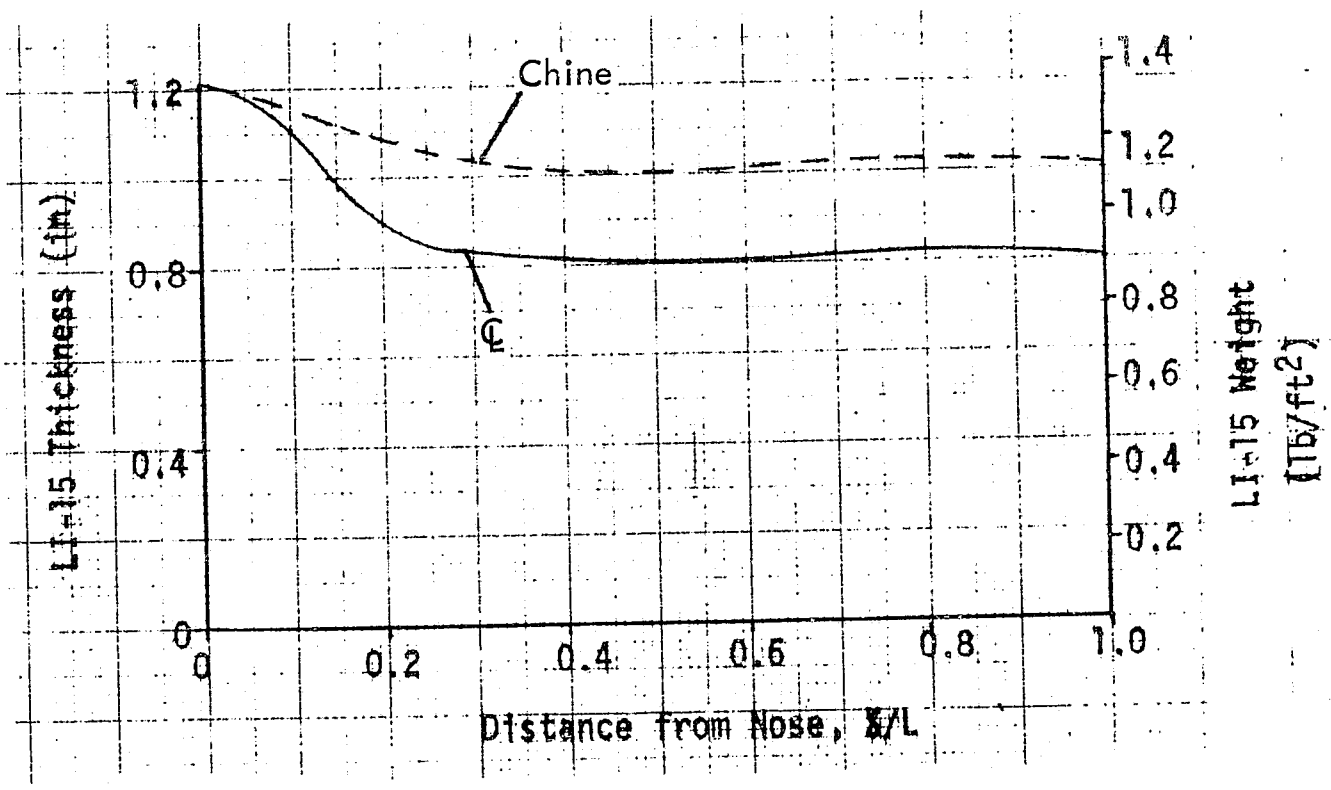

Figure 8.6-19. External Insulation Requirements for Orbiter Underbody

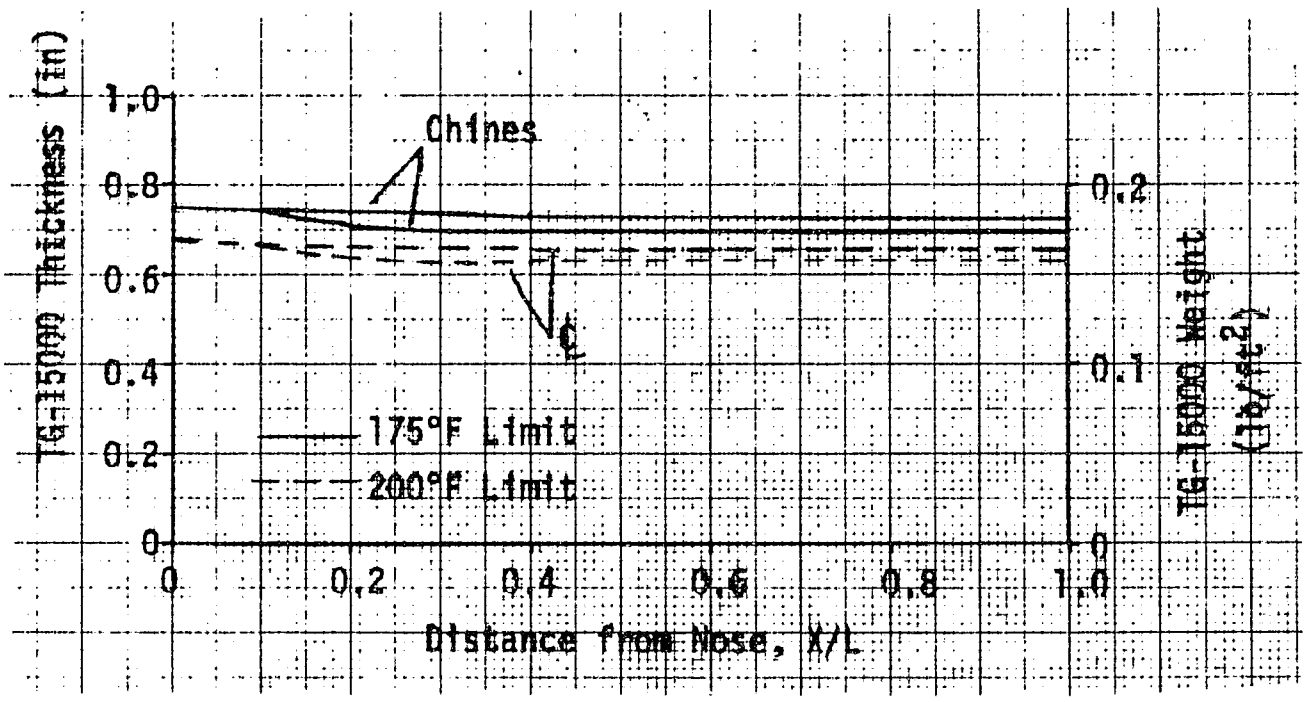

Figure 8.6-20. Internal Insulation Requirements for Orbiter Underbody

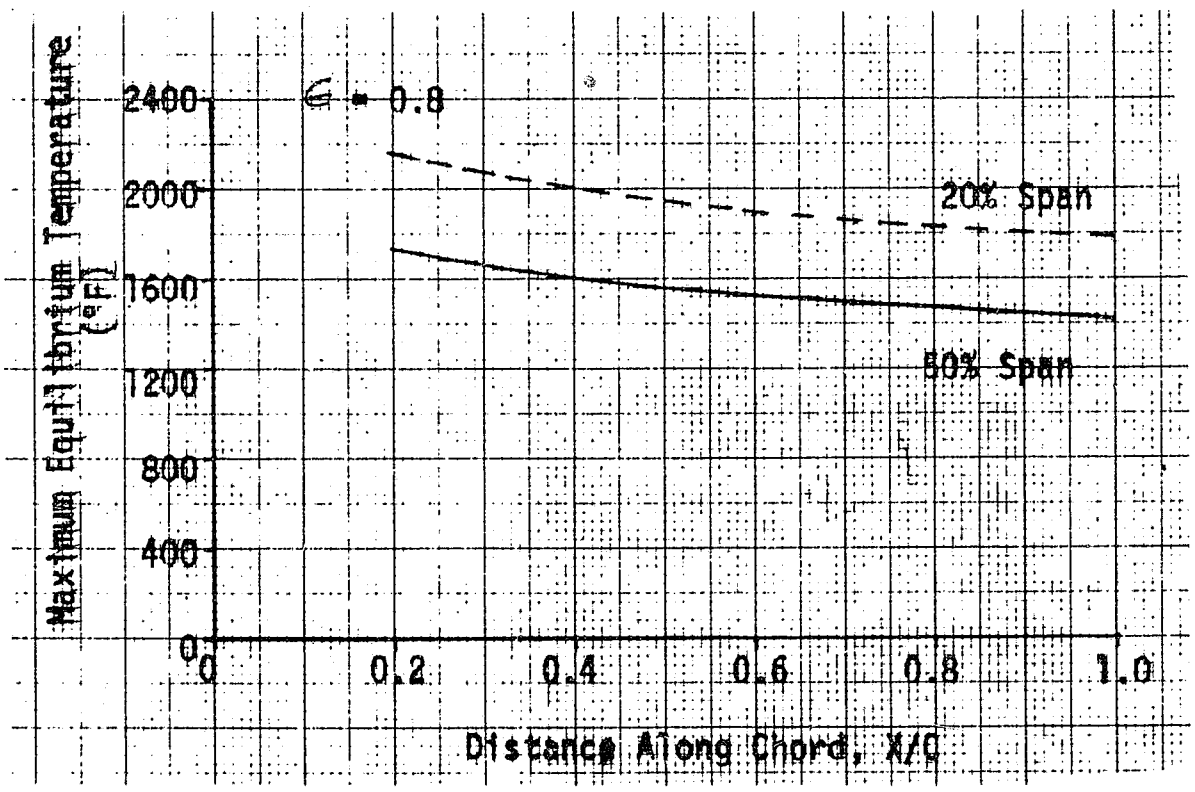

Figure 8.6-21. Maximum Temperature Distribution for Orbiter Top

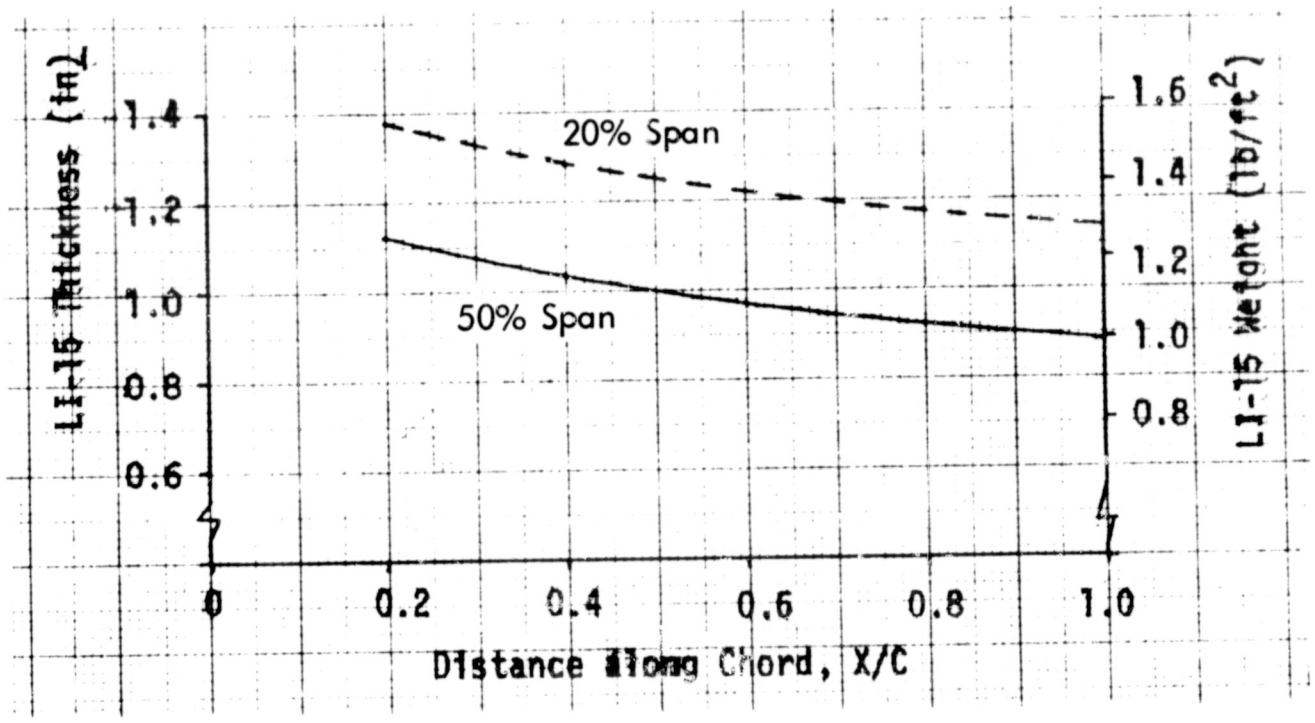

Figure 8.6-22. External Insulation Requirements for Orbiter Wing Undersurface

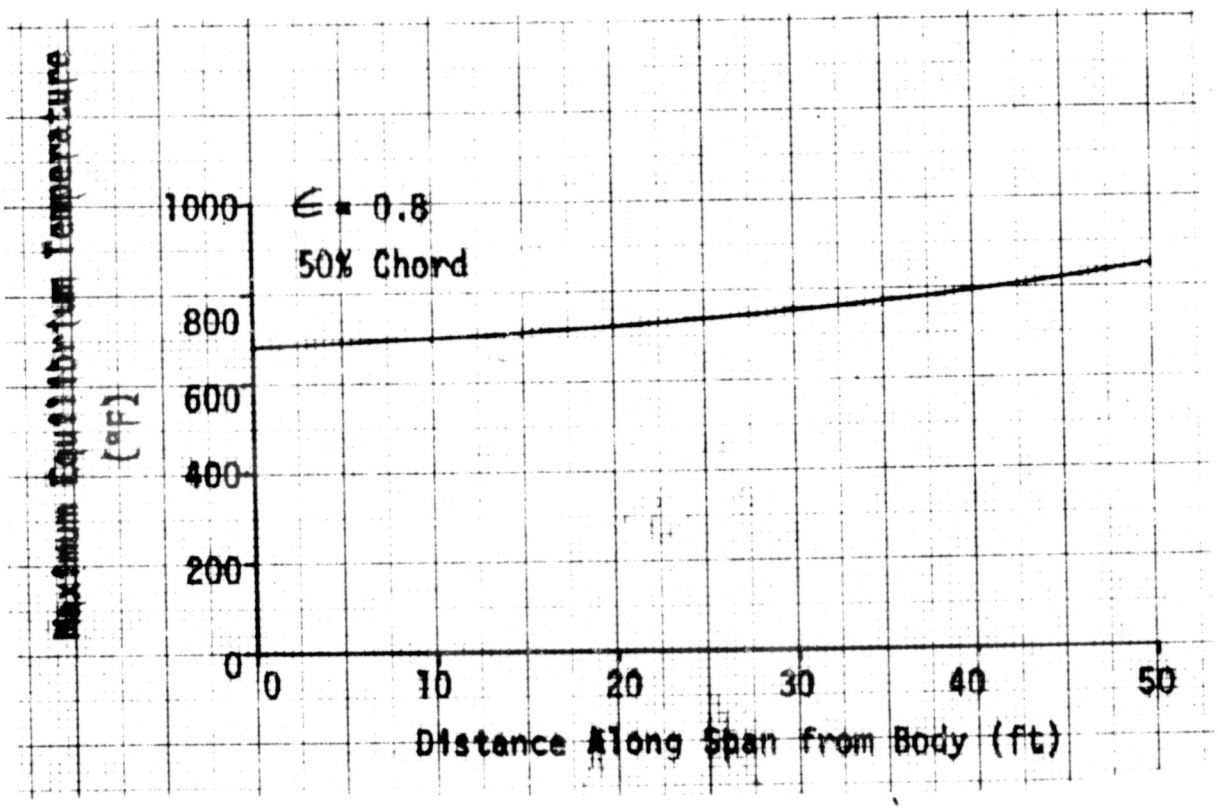

Figure 8.6-23. Maximum Temperature Distribution for Orbiter Wing Undersurface

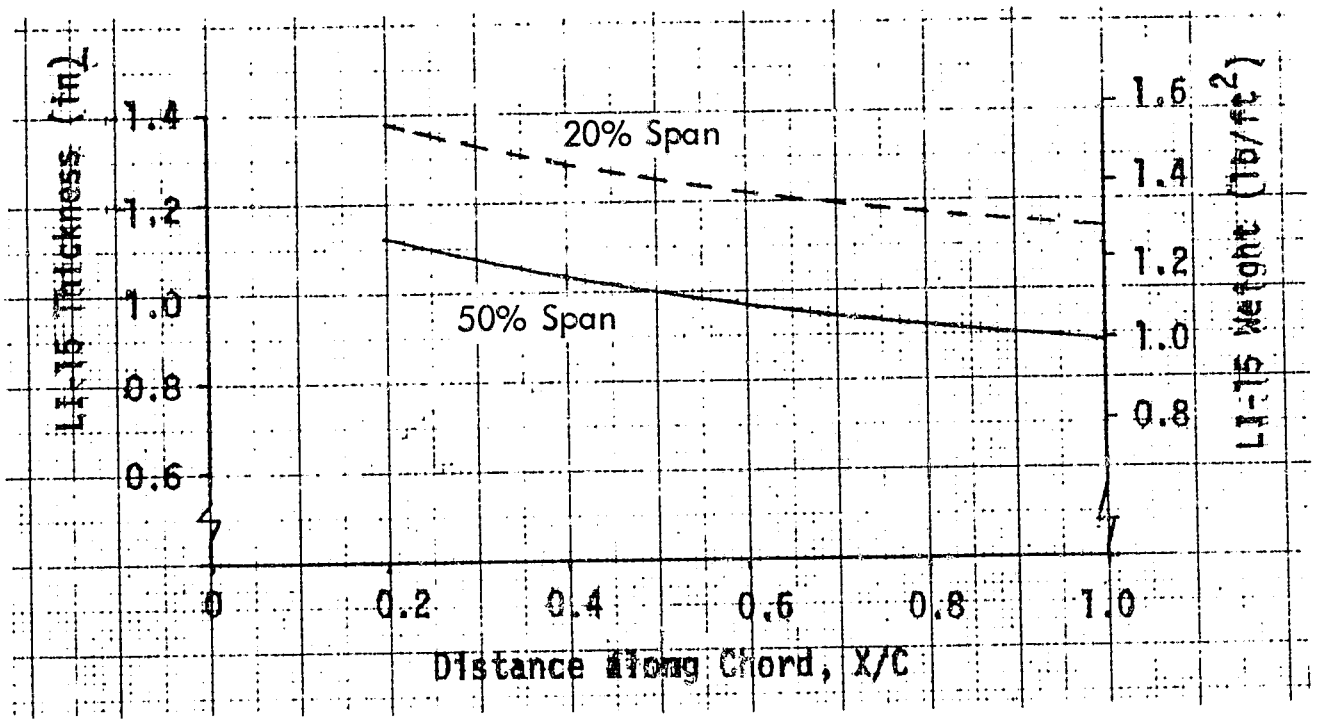

Figure 8.6-22. External Insulation Requirements for Orbiter Wing Undersurface

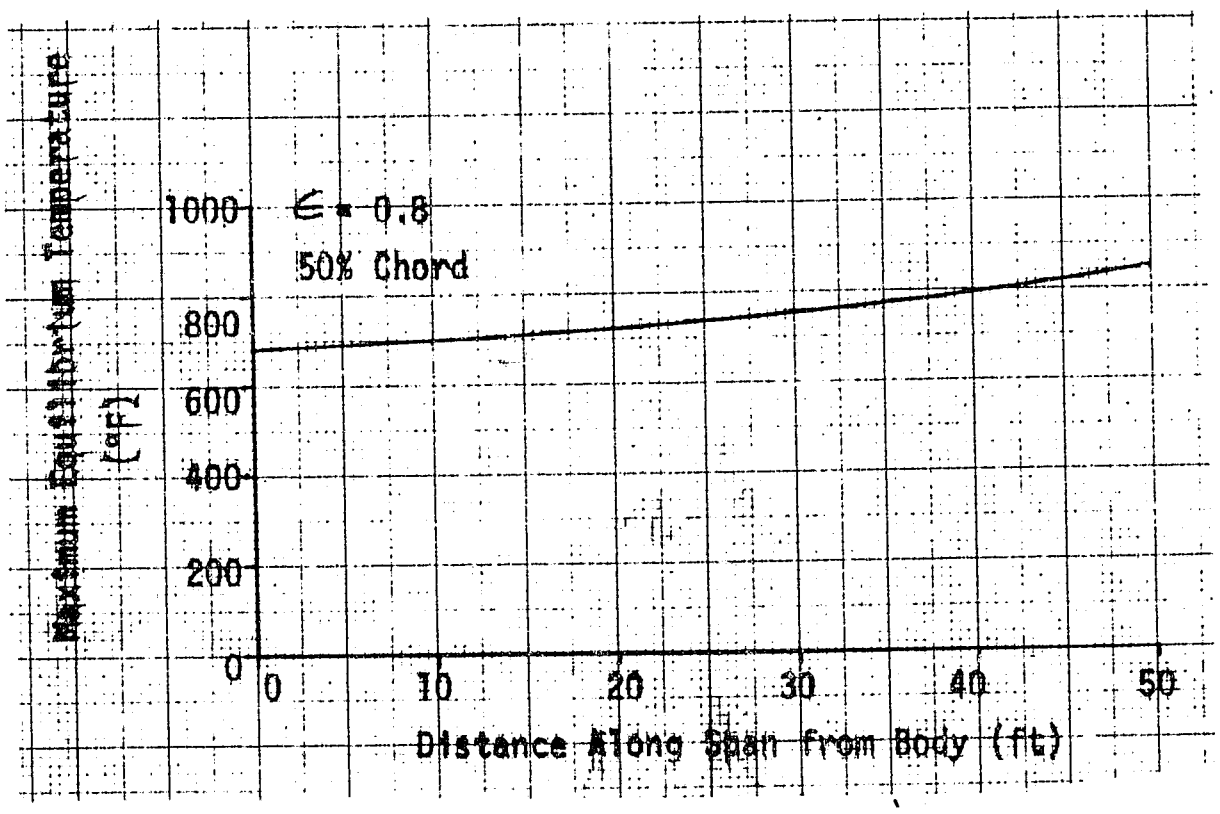

Figure 8.6-23. Maximum Temperature Distribution for Orbiter Wing Undersurface

8.7 PROPULSION SYSTEM

Rocket propulsion and airbreathing propulsion systems are used by both the booster and orbiter vehicles. Rocket propulsion is used for boost to orbit, on-orbit maneuvers (orbiter only) and vehicle control. An important requirement for the shuttle vehicle is reusable rocket propulsion to minimize shuttle system operational costs. Airbreathing propulsion is used in the primary mission for cruise back to the landing site (booster only), landing, and go-around. In addition, the airbreathing propulsion will provide the primary propulsion function during ferry flight from the manufacturing site and alternate landing sites. The objective of the propulsion studies was to provide parametric propulsion system data for vehicle concept sizing of various payloads, develop conceptual system definition of a selected shuttle system for system weight and cost analyses, identify propulsion system requirements, and identify technology requirements.

8.7.1 Vehicle Concept Sizing

In the early phase of the study, the size of the shuttle vehicle to deliver 10,000, 25,000, and 50,000 pounds of payload to orbit with various cargo bay sizes was being determined. In support of this activity, parametric rocket engine data were prepared. The rocket engine being considered at this phase of the study was a high-chamber-pressure, bell-nozzle engine. The parametric engine data are classified and presented in an appendix to this report volume. The data provide engine specific impulse, weight, and geometry as a function of thrust expansion ratio and mixture ratio. These data were obtained from AFRPL-TR-69-19, Air Force Reusable Rocket Engine Program, XLR 129-P-1 Engine Performance, dated April 1969, prepared by Pratt & Whitney Aircraft.

A study ground rule is that the same basic engine will be used in both the booster and orbiter; however, since the booster and orbiter require considerably different nozzle expansion ratios, two different nozzles are used. As illustrated in Figure 8.7-1, a common power pack (turbo pumps, controls, combustion chamber, and nozzle to an expansion ratio of approximately 5:1) is used with a low expansion ratio fixed nozzle added for the booster and a high expansion ratio two-position nozzle added for the orbiter. An alternative is to attach the orbiter nozzle extension at the booster nozzle exit plane and thereby have more common hardware. However, this would degrade engine specific impulse because of the nonoptimum nozzle contour for one of the stages. The former concept was adopted for this study.

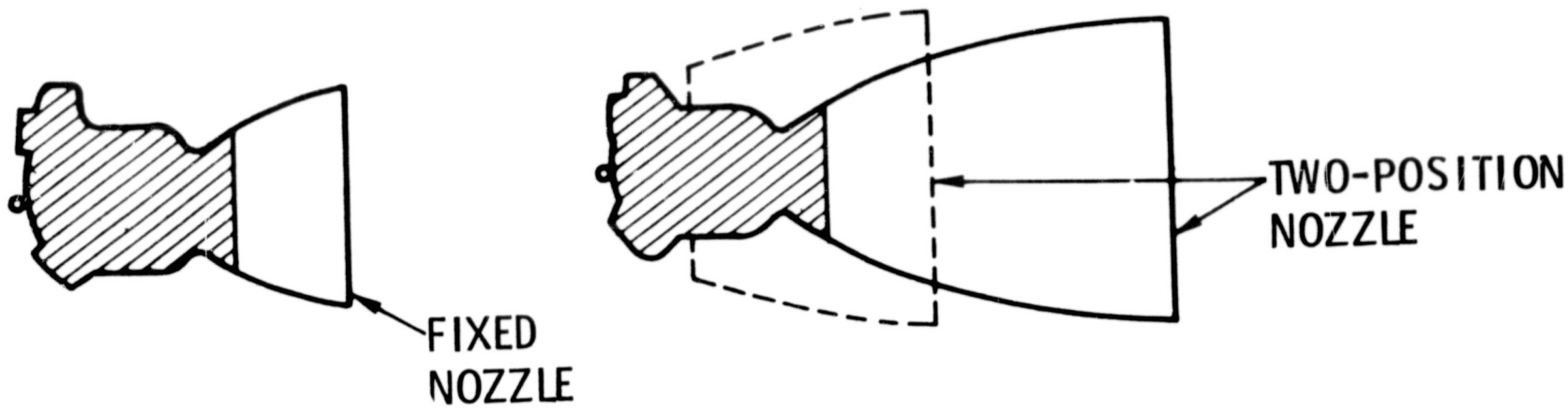

Figure 8.7-1. Booster and Orbiter Rocket Engine Commonality

Based on the vehicle sizing analysis (reported under "Performance" in Volume III), the engine requirements for the range of payloads were established. A summary of the number of engines used per stage and the required thrust level is presented in Table 8.7-1. A study ground rule for the 10,000-pound class vehicle was that the payload load capability would be

Table 8.7-1. Main Rocket Engine Thrust Requirements for Payload Range

Payload (1000 lb)	Cargo Size	No. Eng/Thrust (1000 lb)	
		Booster (SL)	Orbiter (vac)
7.7	2000 ft^3	8 x 260	2 x 300
25	15 ft dia x 30 ft long	10 x 326	2 x 375
25	15 ft dia x 60 ft long	10 x 375	2 x 430
50	15 ft dia x 60 ft long	9 x 482	2 x 555
50	22 ft dia x 60 ft long	10 x 500	2 x 575

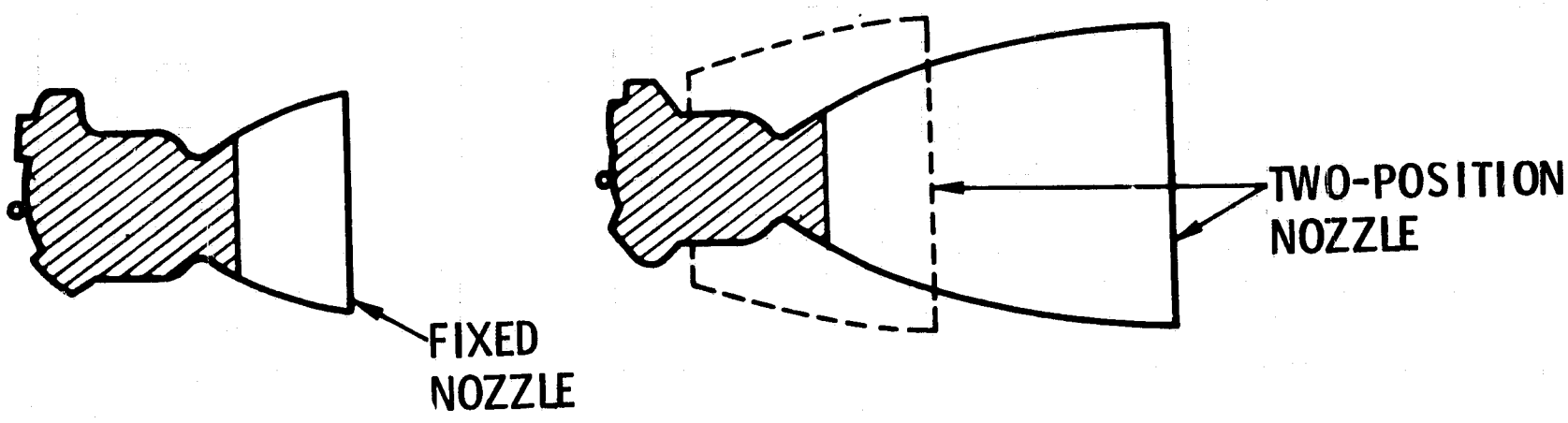

Figure 8.7-1. Booster and Orbiter Rocket Engine Commonality

Based on the vehicle sizing analysis (reported under "Performance" in Volume III), the engine requirements for the range of payloads were established. A summary of the number of engines used per stage and the required thrust level is presented in Table 8.7-1. A study ground rule for the 10,000-pound class vehicle was that the payload load capability would be

Table 8.7-1. Main Rocket Engine Thrust Requirements for Payload Range

Payload (1000 lb)	Cargo Size	No. Eng/Thrust (1000 lb)	
		Booster (SL)	Orbiter (vac)
7.7	2000 ft^3	8 x 260	2 x 300
25	15 ft dia x 30 ft long	10 x 326	2 x 375
25	15 ft dia x 60 ft long	10 x 375	2 x 430
50	15 ft dia x 60 ft long	9 x 482	2 x 555
50	22 ft dia x 60 ft long	10 x 500	2 x 575

determined for a system using eight-bell engines in the nominal class of the P&W high-chamber pressure bell demonstration engine being designed in the current Air Force Advanced Development Program. Following discussion with P&W and NASA/MSC, a 300,000-pound vacuum thrust engine was selected to satisfy this requirement. The vehicle sized provided 7,700 pounds of payload. The number of engines and engine thrust level for the 25,000- and 50,000-pound payload vehicles were optimized within the constraints of a common engine in booster and orbiter, a minimum of two engines in the orbiter for engine out capability, orbiter T/W at sea level greater than 1.25:1 for abort capability, and booster T/W greater than 1.25:1 at liftoff. The characteristics of the engines are identified in Table 8.7-1 and presented in Table 8.7-2. In addition, the engine mixture ratio is selected as 6:1 for both the booster and orbiter based on performance optimization studies. However, selection of a mixture ratio between 5.5:1 and 6.5:1 has a neglegible effect on vehicle gross weight required for a given payload. Engine throttle requirements for limiting the maximum acceleration to 3 g is approximately 75 to 80 percent of maximum thrust for the booster, and approximately 55 to 60 percent of maximum thrust for the orbiter. In addition, it was assumed that the orbiter engines will be throttled to approximately 10 percent for orbiter on-orbit maneuvers.

8.7.2 Propulsion System Trades and Special Studies

Following the concept sizing study phase, a shuttle vehicle with 50,000 pounds of payload capability and 15-foot diameter by 60-feet-long cargo bay was selected for conceptual design analysis. This section documents the propulsion system trades leading to the conceptual design definitions.

In addition, during the course of the study, NASA requested technical data on shuttle vehicles having 3,000,000 and 3,500,000 pounds of gross weight and using 400,000-pound-sea-level-thrust rocket engines. Some of the propulsion system trades were, therefore, conducted on shuttle vehicles with these characteristics. The results of these studies are also reported in this section.

Use of 300,000-Pound Rocket Engine

Shortly after selecting the 50,000-pound payload vehicle for design stufies, MSC asked NR to assess the impact of using a multiple engine configuration in which the thrust level of each engine is limited to 300,000 pounds of vacuum thrust. An evaluation of the baseline 50,000-pound payload shuttle system with 15-foot diameter by 60-foot-long cargo bay was made to show the effect of limiting the rocket engine thrust level to

Table 8.7-2. Rocket Engine Characteristic, Concept Sizing Phase

Characteristic	Payload Class									
	7700 lb		25,000 lb		25,000 lb		50,000 lb		50,000 lb	
			15 x 30 ft		15 x 60 ft		15 x 60 ft		22 x 60 ft	
	Booster	Orbiter	Booster	Orbiter	Booster	Orbiter	Booster	Orbiter	Booster	Orbiter
Thrust, SL (1000 lb)	260	--	326	--	375	--	482	--	500	--
VAC (1000 lb)	286	300	358	375	413	430	530	555	550	575
Expansion ratio, extended	35:1	120:1	35:1	120:1	35:1	120:1	35:1	120:1	35:1	120:1
retracted	--	60:1	--	60:1	--	60:1	--	60:1	--	60:1
Length, extended (in.)	91	165	100	180	108	190	122	220	124	222
retracted (in.)	--	92	--	102	--	108	--	124	--	127
Nozzle exit diameter (in.)	48	87	54	97	58	105	65	123	67	125
Weight (lb)	2810	3100	3410	3650	3880	4200	4850	5250	5000	5400

Table 8.7-2. Rocket Engine Characteristic, Concept Sizing Phase

Characteristic	Payload Class									
	7700 lb		25,000 lb		25,000 lb		50,000 lb		50,000 lb	
			15 x 30 ft		15 x 60 ft		15 x 60 ft		22 x 60 ft	
	Booster	Orbiter	Booster	Orbiter	Booster	Orbiter	Booster	Orbiter	Booster	Orbiter
Thrust, SL (1000 lb)	260	--	326	--	375	--	482	--	500	--
VAC (1000 lb)	286	300	358	375	413	430	530	555	550	575
Expansion ratio, extended	35:1	120:1	35:1	120:1	35:1	120:1	35:1	120:1	35:1	120:1
retracted	--	60:1	--	60:1	--	60:1	--	60:1	--	60:1
Length, extended (in.)	91	165	100	180	108	190	122	220	124	222
retracted (in.)	--	92	--	102	--	108	--	124	--	127
Nozzle exit diameter (in.)	48	87	54	97	58	105	65	123	67	125
Weight (lb)	2810	3100	3410	3650	3880	4200	4850	5250	5000	5400

300,000 pounds of vacuum thrust. At that time, the baseline vehicle gross weight at liftoff was 3,985,000 pounds and was configured with two 640,000-pound vacuum thrust engines (ϵ = 120:1) in the orbiter. Nine of the same basic engines were provided in the booster and delivered 555,000 pounds of sea level thrust with a 35:1 expansion ratio nozzle. The characteristics of the 640,000- and 300,000-pound-vacuum-thrust engines are shown in Table 8.7-3, based on high chamber pressure P&W data.

The booster and orbiter characteristics with the 300,000-pound engine are:

Booster

Vehicle weight at liftoff	3,985,000 lb
Number of engines	19
Sea level thrust	4,940,000 lb
T/W at liftoff	1.24
T/W with one engine out	1.18

Orbiter

Orbiter weight at ignition	835,000 lb
Number of engines	4
Vacuum thrust	1,200,000 lb
Sea level thrust	992,000
T/W at ignition	1.44
T/W with one engine out	0.72
T/W at sea level (abort)	1.19

Table 8.7-3. Characteristics of 640,000- and 300,000-Pound-Thrust Engines

Parameter	640 K lb Vacuum Thrust		300 K lb Vacuum Thrust	
	Booster	Orbiter	Booster	Orbiter
Thrust, vac (1,000 lb)	610	640	286	300
SL	555	530	260	248
Expansion ratio Extended	35 (fixed)	120	35 (fixed)	120
Retracted		60		60
Length* Extended (in.)	132	235	88	145
Retracted (in.)	—	133	—	92
Nozzle diameter (in.)	71	128	48	88
Weight (1,000 lb)	5500	5950	2800	3070

*Base nozzle contour.

Nineteen engines are required in the booster to provide approximately the same initial T/W as the baseline configuration. A possible installation of the 19 engines is shown in Figure 8.7-2. Twelve engines are mounted on an outer ring and conical thrust structure. Six engines are mounted on an inner ring and conical thrust structure. The center engine is mounted on a cross-beam or truss thrust structure. The engine spacing allows ±7 degrees gimbal without engine interference. The 19 engines can be installed in the same vehicle base area. The engine feed line diameters are 12 and 13 inches for LO_2 and LH_2, respectively. Nineteen individual LH_2 lines are routed from a central LH_2 Sump. Three to four LO_2 lines would bring the LO_2 from the forward located LO_2 tank to an engine compartment manifold. Nineteen individual LO_2 feed lines are routed from the manifold. The incremental system weight for engines and systems is estimated to be +3600 and +6000 pounds, respectively, which is two percent of the baseline booster dry weight.

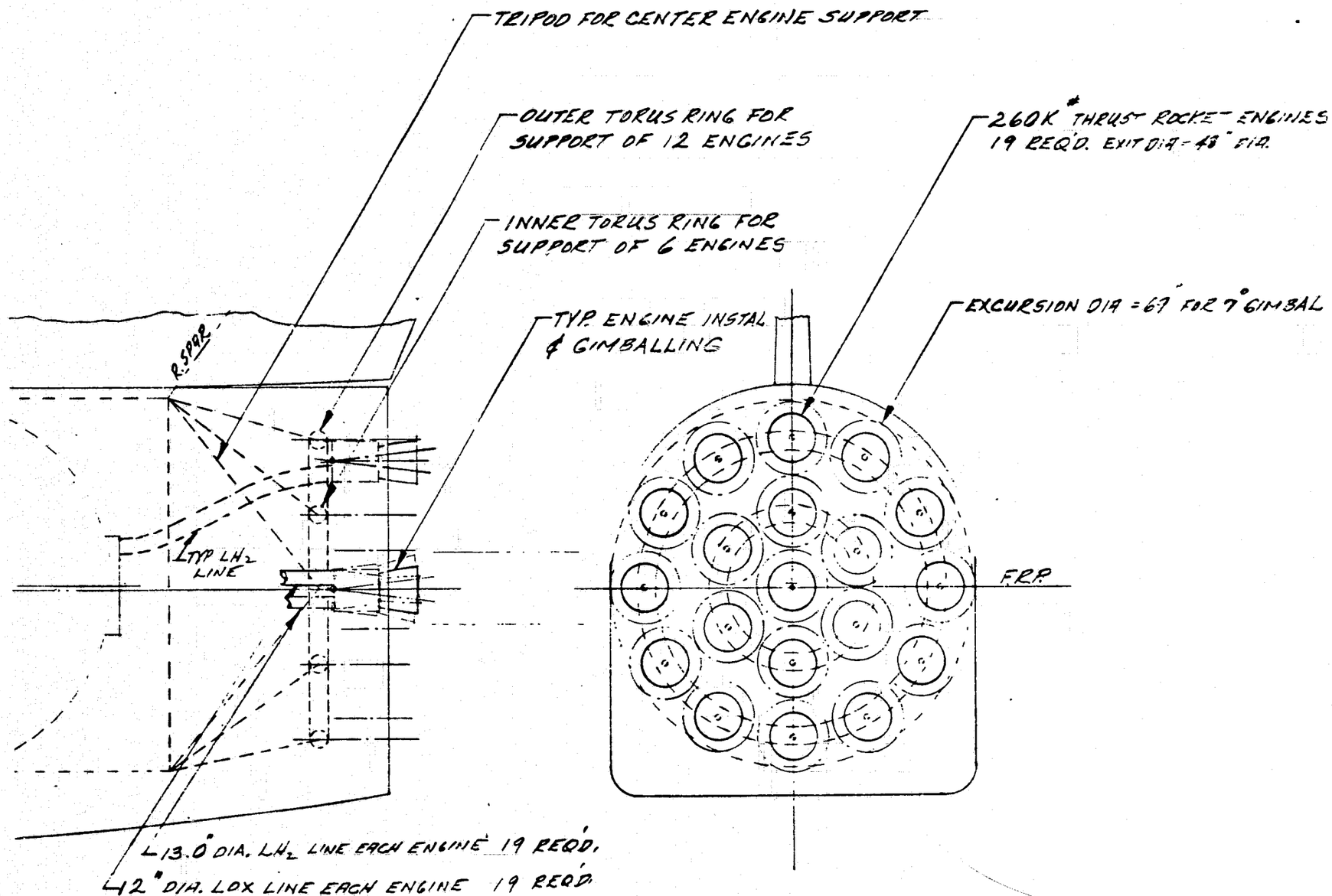

Figure 8.7-2. Booster Configuration With 300,000-Pound Vacuum-Thrust Engines

Space Division
North American Rockwell

Four engines in the orbiter provide a lower T/W than the baseline orbiter, but provides sufficient T/W for sea-level abort and for flight with one engine out at altitude. The installation is shown in Figure 8.7-3. The four engines are mounted on a conical thrust structure. The engine spacing allows ±7 degrees gimbal angle. The four engines can be installed in approximately the same base area. Minor modification to the mold line is required to maintain the 120:1 nozzle expansion ratio. Alternatives which do not require modification of the base are to reduce gimbal angle to 5.5 degrees or reduce nozzle expansion ratio to 102 (0.54-percent reduction in I_{sp}). Engine feed line sizes are the same as the booster. The incremental system weight for engines and system is estimated to be +380 and +1000 pounds, respectively which is 0.8 percent of the baseline orbiter dry weight. To provide the same engine thrust as that for the baseline orbiter, the incremental engine weight is 1180 pounds, which combined with 1000 pounds of system weight increase, represents 1.2 percent of the baseline orbiter dry weight.

A comparison of the 300,000-pound-thrust engine system and the baseline system is summarized in Table 8.7-4.

Table 8.7-4. Comparison of 300,000-Pound-Thrust Engine System to Baseline System

Factor	Booster		Orbiter	
	Baseline*	300,000-lb Vac.	Baseline*	300,000-lb Vac.
Number of engines	9	19	2	4
Base area	Same	Same	Same	Minor Modification
Weight increment (lb)	0	+9600	0	+1380
Installation complexity	Base	Significant increase	Base	Minor increase

*640,000-pound vacuum thrust engine

Figure 8.7-3. Orbiter Configuration With 300,000-Pound Vacuum-Thrust Engines

Space Division
North American Rockwell

Bell Engine and Aerospike Engine Comparison

The primary rocket engine type used in the shuttle vehicle studies was the high-chamber-pressure bell engine as directed in the study guidelines. The aerospike engine type was considered as an alternative. Performance and installation impact were grossly assessed and the results are discussed in this section. These studies were conducted with a 3,500,000-pound, gross weight, vehicle and a 400,000-pound-thrust engine.

Before presenting the study, a summary of the two engine concepts will be presented. The LO_2/LH_2 bell engine is currently in an Air Force Advanced Program Development (APD) Phase being conducted by Pratt and Whitney. Component development is currently being conducted. The APD program plans call for ground testing of a demonstrator engine based upon lightweight component designs with additional margins required for a low risk demonstrator engine program, and design definition of a flight-weight engine. This APD is currently scheduled for completion in the third quarter of 1970.

NR's Rocketdyne Division has been developing the LO_2/LH_2 aerospike engine concept for many years. The LO_2/LH_2 aerospike engine has been the subject of many NASA and Air Force studies and component test programs have been conducted under NASA and Air Force contracts.

Bell Engine Description. The bell engine is a high-chamber-pressure LO_2/LH_2 engine using interchangeable nozzle extensions for the booster and orbiter with a basic turbopump and combustion chamber module. A two-position nozzle can be provided to minimize stowed engine length and improve engine performance variation with altitude. Part of the nozzle is retracted over the forward portion of the thrust chamber during low-altitude operations and extended to the high area ratio position for high-altitude operations.

A simplified propellant flow schematic illustrating the propellant flow paths and functional component arrangement of the engine is shown in Figure 8.7-4. The high-pressure rocket engine uses a staged combustion cycle in which most of the fuel is burned with a portion of the oxidizer in the preburner to provide turbopump power before combustion with the remainder of the oxidizer in the main burner chamber. Fuel and oxidizer enter the engine through the engine-driven, low-speed inducers. The low-speed inducers are used to minimize the fuel tank pressure requirements, while allowing high-speed main propellant pumps for high turbopump efficiencies. The fuel low-speed inducer is a single shaft unit with an axial flow inducer driven by a two-stage, axial-flow, partial-admission impulse turbine. The oxidizer low-speed inducer is also a single-shaft unit with an axial flow inducer driven by a single-stage radial inflow turbine.

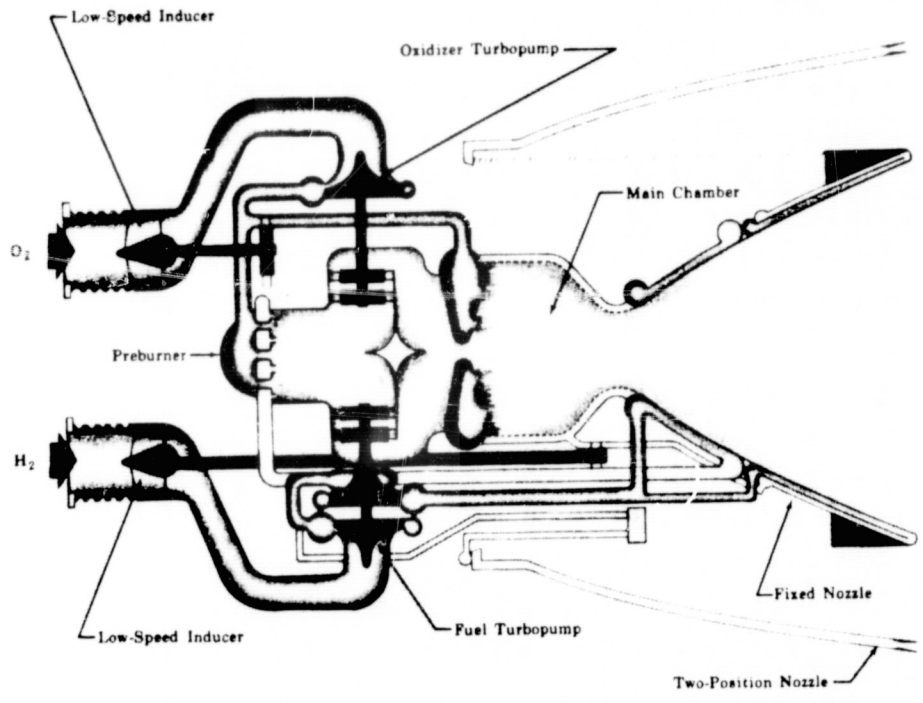

Figure 8.7-4. Bell Engine Propellant Flow Schematic

The main fuel turbopump is a single-shaft unit with two back-to-back centrifugal pump stages driven by a two-stage, pressure-compounded turbine. The fuel flow is pumped to the system operating pressure levels by the main fuel pump. The hydrogen is then ducted to cool the regenerative sections of the nozzles. The principal fuel flow path from the pump is through the upstream portion of the primary nozzle, and then into the preburner chamber through the preburner injector. The remainder of the fuel flows through the downstream portion of the primary nozzle and then through the fuel low-speed inducer drive turbine before being passed into the main chamber as transpiration coolant. A small amount of fuel is bled off between the main fuel pump stages to provide coolant for the two-position nozzle. This coolant flows to the nozzle through a regulating orifice and a shutoff valve that is provided to stop the flow when the two-position nozzle is in the retracted position. The area ratio, at which the fixed primary nozzle ends and the two-position, translating nozzle starts, is varied to optimize the performance for the specific application.

The oxidizer turbopump is a single-shaft unit with a single, centrifugal pump stage driven by a two-stage, pressure-compounded turbine. After being pumped to the system operating pressure levels by the main oxidizer pump, the oxidizer is divided between the preburner and the main burner chamber. The principal oxidizer flow passes through and is the working fluid for the oxidizer low-speed inducer turbine before being injected into the main chamber. The remainder, a smaller scheduled portion of the oxidizer, is ducted to the preburner where it is burned with the fuel. The

resulting combustion products flow through ducts to the two main turbines, which are arranged in parallel. The energy required to drive the main pumps is extracted from these combustion products, which then exhaust from the turbines and mix in a common passage of the transition case. These gases then pass through the main burner injector and into the main burner combustion chamber where they mix and burn with the principal oxidizer flow. These combustion gases are then expanded through the bell nozzle to provide thrust.

The preburner injector consists of dual-orifice, tangential-swirler oxidizer injector elements and fixed area fuel injector elements. A preburner oxidizer valve is incorporated at the inlet to the injector assembly to vary the total oxidizer flow rate for turbine inlet temperature control and to adjust the relative flow of the primary and secondary oxidizer elements. The preburner combustion chamber is contained within the transition case, which also contains the turbine drive gas ducts. The main turbopumps are attached to the transition case with a single flange and bolt circle arrangement to provide ease of access for turbopump maintenance.

The nozzle, which attaches downstream of the throat, is composed of two regeneratively cooled primary sections and a low-pressure, dump-cooled, two-position nozzle. The regeneratively cooled sections are conventional tubular heat exchangers; the two-position nozzle employs lightweight sheet metal construction.

Engine controls are provided to select and maintain any propellant mixture ratio between 5:1 and 7:1. Engine thrust is maintained constant over the mixture ratio range. In addition, thrust can be throttled down to 10 percent of maximum thrust.

The engine is capable of ±7 degrees gimbal. The engine can supply GH_2 and GO_2 pressurant and provide a heat source for helium pressurant. The engine is reusable and is designed for 10 hours time between overhauls, 100 reuses, and 300 starts.

Aerospike Engine Description. The LO_2/LH_2 aerospike engine is pump-fed with a regeneratively cooled chamber which employs channel construction in the combustor and a tube-wall nozzle. The engine operates on an open-flow power cycle, shown schematically in Figure 8.7-5, with the pumps driven by individual turbines powered by low mixture ratio combustion gases provided by the turbine drive combustor (TDC).

During start and idle mode operation, the TDC operates on gaseous, liquid, or two-phase propellants under tank pressure and provides feed system conditioning while accelerating the turbopumps for mainstage operation.

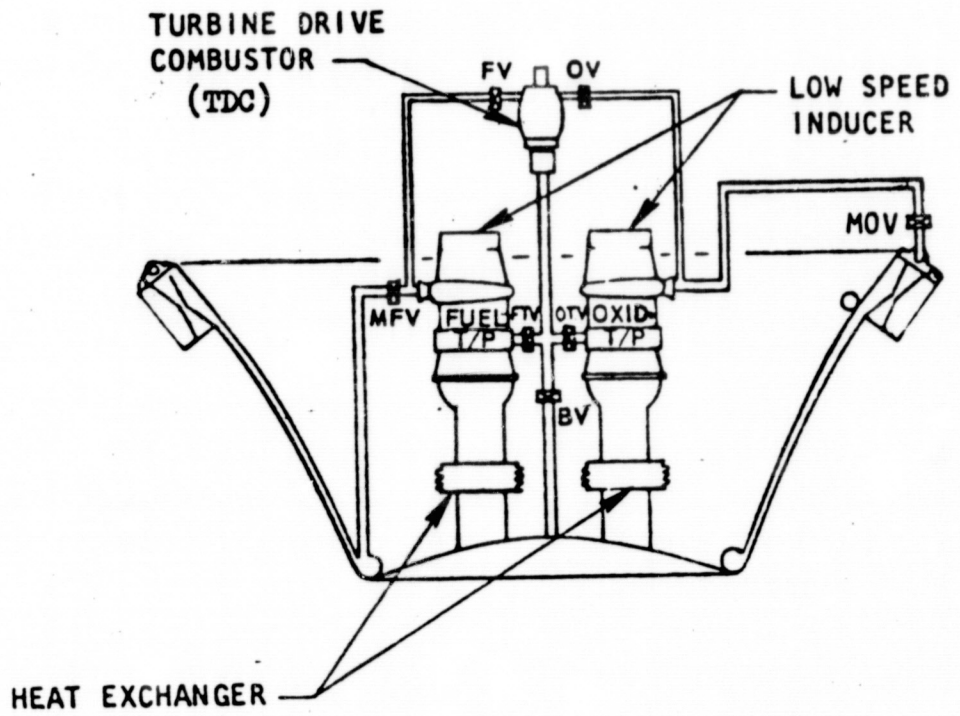

Figure 8.7-5. 400,000-Pound-Thrust
Aerospike-Engine Schematic

In addition, the thrust provided by ducting the gases into the base region may be used for propellant settling. Idle mode operation results in a thrust level of approximately 0.2 percent of full thrust.

In addition to idle mode operation the engine system is capable of mainstage throttling. The throttling range is continuous from 100 to 10 percent of full thrust. Thrust and mixture ratio control capability is provided.

The engine will not require insulation for protection from exhaust plume recirculation since the engine components on the aerospike engine configuration are buried within the engine compartment. The engine system is also equipped with heat exchangers capable of heating either liquid propellants tapped from the engine, or vehicle-supplied helium, for use in pressurizing the vehicle propellant tanks during mainstage operation.

The engine is designed for a minimum of 10 hours of operating time between overhauls (TBO). Within this limit, it is capable of up to 500 starts, 500 thermal cycles, 10,000 valve cycles, and unlimited continuous run duration (to oxidizer depletion).

Thrust vector control is provided by a gimbal bearing and two actuators mounted to the engine thrust structure 90 degrees apart. The thrust vector can be deflected up to 7 degrees in each plane. The gimbal axis is located in the plane of maximum diameter, resulting in a dynamic envelope equal to the static envelope.

The thrust chamber design uses the segmented combustor approach in conjunction with a combination of casting and electroforming fabrication technique resulting in low development program costs. The nozzle is attached to the combustor section at an expansion ratio of 6 and uses tube wall construction. Concentric injector elements are used because of the excellent combustion characteristics demonstrated in a number of oxygen/hydrogen engines.

The fuel and oxidizer turbopumps are designed to provide low NPSH operating capability, high efficiency, reliability, and maintainability. Bearings, seals, and tip speeds were selected based on previous experience and long life considerations. The fuel pump consists of a two-stage centrifugal pump with a low-speed preinducer. The main pump is driven by a multi-stage turbine and the preinducer by a separate turbine. These turbines are connected in series. The oxidizer pump consists of one centrifugal stage and a low-speed preinducer. The main pump is driven by a multi-stage turbine and the preinducer by a separate turbine. Again, both turbines are in

series. The preinducer and main turbopumps are all located within the aerospike engine envelope. An accessory drive is provided on the oxidizer preinducer turbine to power the gimbal system hydraulic pump.

Each engine system is equipped with a pogo suppression device at the oxidizer pump inlet to prevent the oscillations experienced in previous launch vehicles. These oscillations are due to the inherent resonance in the vehicle structure and propellant feed system. On command from the control system, which senses vehicle acceleration, a quantity of fluid is displaced in such a way that the oscillations are cancelled. The fuel feed system does not require such a device due to the lower flowrate and the compressibility of the fuel, which tends to damp the oscillations.

The base closure provides maximum nozzle efficiency over the entire thrust range, from maximum mainstage to idle-stage operation. The concave shape and porous injection section provide a uniform distribution of the secondary flow and yields a lightweight structure. The base closure consists of a thin Hastelloy C membrane and a Hastelloy C manifold joined by welding. The manifold is used to distribute gas to injection ports located in the membrane. Valve and seal vent lines are routed through the base closure. A removable panel in the central region of the membrane provides access to interior engine components.

The turbine drive combustor (TDC) produces low mixture ratio combustion gases to power the turbines and, during idle mode operation, to provide idle mode thrust. During start and idle mode, the TDC will operate on gaseous, liquid, or two-phase propellants. Throttle valves located in the TDC feed lines control propellant flowrates and mixture ratio during engine operation.

Rigid high-pressure propellant and hot gas lines are used to achieve a lightweight engine with simplicity of design and ease of component packaging. The main propellant valves and TDC propellant valves are variable position valves which function as control valves as well as on-off valves. The hot gas valves also function both as on-off valves and control valves.

The base closure provides maximum nozzle efficiency over the entire thrust range, from maximum mainstage to idle-stage operation. The concave shape and porous injection section provide a uniform distribution of the secondary flow and yields a lightweight structur.

System Comparison. The comparison of a bell engine and aerospike engine cannot be adequately done by comparing engines alone. The comparison must be on an installed performance basis. The first task was to establish the relative engine sizes which could be installed within the vehicle.

The vehicle configuration under study (3,500,000 pounds of gross weight) requires eleven 400,000-pound sea level thrust engines in the booster and two engines in the orbiter. The bell engine and aerospike engine diameter which could be installed into the same vehicle base area, are illustrated in Figure 8.7-6. As can be seen in the figure, providing ±7 degree gimbal capability for the bell engine caus the dynamic envelope (dashed line) to be considerably larger than the static envelope (solid line). Clearance is provided for the condition where engines are gimbaled toward one another.

The aerospike engine configuration has the maximum engine diameter (combustion chamber) in the plane of the gimbal axes. Therefore, the static and dynamic envelope of the aerospike engine is the same. Another feature of the aerospike engine which must be considered is that a dual combustor configuration can be employed. The dual combustor concept has an inner and outer combustor installed in the same horizontal plane. This allows the thrust to be doubled within approximately the same engine diameter. The use of six dual-combustor engines on the booster allows an increase in engine diameter and performance for the same stage thrust level. The engine sizes which can be installed within the vehicle base are shown in Table 8.7-5.

Table 8.7-5. Bell and Aerospike Engine Installed Sizes

Engine	BOOSTER		ORBITER	
	No. of engines	Diameter (in.)	No. of engines	Diameter (in.)
Bell engine	11	60	2	110
Aerospike engine				
Single combustor	11	88	2	156
Dual combustor	6	123		

Based on the allowable engine sizes, the engine characteristics and installed performance can be established. The bell and aerospike engine performance and geometry data are from (1) AFRPL-TR-69-19, Air Force Reusable Rocket Engine Program, XLR 129-P-1 Engine Performance, dated April 1969, and (2) Rocketdyne Report R-8003, Design and Operational Data for the Reusable O_2/H_2 Aerospike Engine, dated September 1969. A number of optional engine development and vehicle design approaches exist. Table 8.7-6 presents bell and aerospike engine characteristics for several options. The data shows that if a single engine is developed for both booster and orbiter, the expansion ratio is considerably less than that desired for the orbiter vehicle and this would result in major payload degradation.

- STUDY FOR 3.5 $\bar{M}$ LB GROSS WT SYSTEM, 400 K LB SL THRUST ENG
- INSTALLED ENGINE CHARACTERISTICS ESTABLISHED FOR REPRESENTATIVE VEHICLE BASE

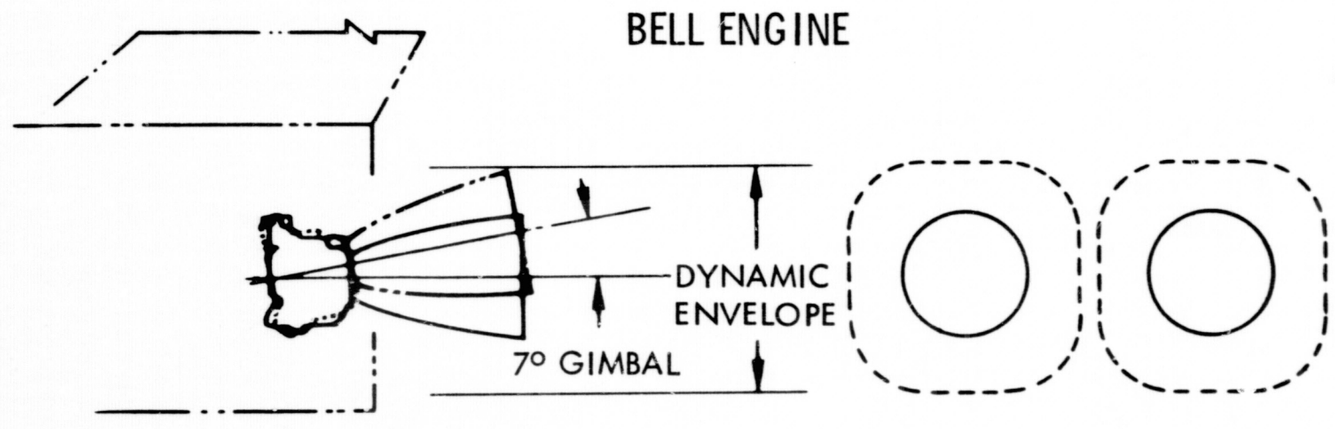

- BOOSTER
  11 ENGINES, 80 IN. DIA
- ORBITER
  2 ENGINES, 110 IN. DIA

- BOOSTER
  SINGLE COMBUSTOR
  11 ENG, 88 IN. DIA
  DUAL COMBUSTOR
  6 ENG, 123 IN. DIA
- ORBITER
  2 ENG, 156 IN. DIA

- DYNAMIC & STATIC ENVELOPE EQUAL

Figure 8.7-6. Bell and Aerospike Engines Installed Sizes

- STUDY FOR 3.5 $\bar{M}$ LB GROSS WT SYSTEM, 400 K LB SL THRUST ENG
- INSTALLED ENGINE CHARACTERISTICS ESTABLISHED FOR REPRESENTATIVE VEHICLE BASE

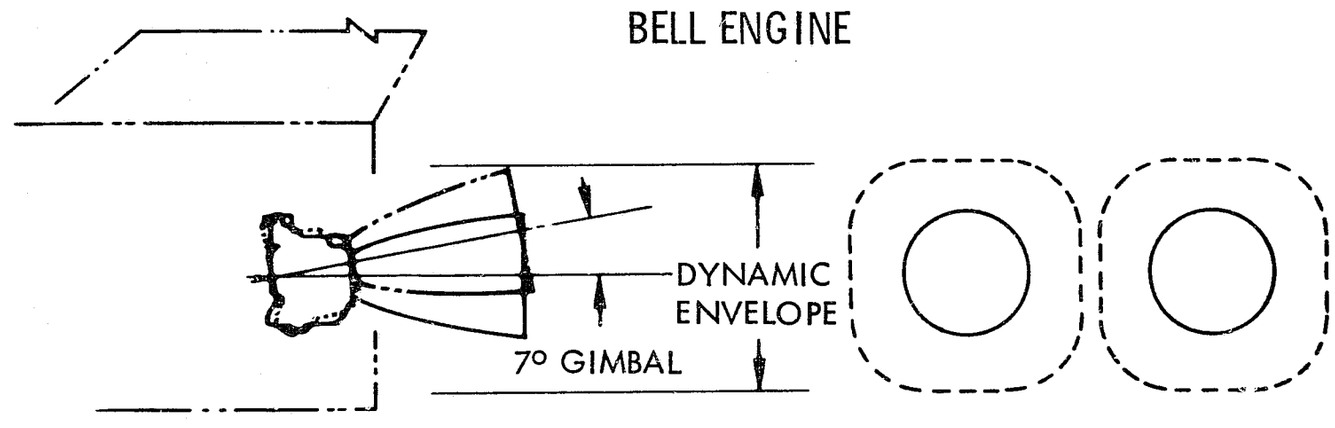

Figure 8.7-6. Bell and Aerospike Engines Installed Sizes

Where a common power head is developed for the bell engine and different nozzles are used on booster and orbiter, the expansion ratio of orbiter engine can be significantly increased. Expansion ratios for booster and orbiter engines are 35 and 120, respectively. These expansion ratios are constrained to diameters of 60 and 110, respectively, for the booster and orbiter due to limits imposed by the vehicle base size. This approach is selected for comparison and is compared to two aerospike engine options in Figure 8.7-7.

Where an aerospike engine is used, the maximum diameter is 156 inches for the orbiter and 88 inches for the booster. This results in expansion ratios of 50 and 161, respectively, for a chamber pressure of 2500 psia. This option approaches the development of two different engines for booster and orbiter, however, and would necessitate the following:

1. Development of combustors with two different diameters.

2. Development of segments with two throat areas.

3. Development of two plugs.

4. Development of two engine thrust structures.

Another option which exists with the aerospike engine, as previously stated, is to produce a dual combustor for the booster engine. The dual combustor engine uses a dual pump set with one pump set feeding each combustor and, therefore, operating as two engines. This facilitates an increase in thrust per engine, and reduction in number of engines necessary on the booster compared to an installation with single combustor engines. The reduction in number of booster engines allowed the increase in engine diameter and increased performance compared to that for a single engine development. Engine characteristics for this approach which was selected for comparison are defined in Table 8.7-6. Note that the orbiter engine diameter is only 120 inches (limited by the booster) even though the vehicle base will accept an engine of 156 inches in diameter.

The performance capability of the bell engine system and aerospike engine system with common hardware is essentially the same. The bell

Figure 8.7-7. Bell and Aerospike Engines Options

Table 8.7-6. Bell Engine and Aerospike Engine Characteristics Comparison

Engine Characteristic	Single Engine Development	Single Engine "Plus" Development		Dual Combustor Development	
		Booster	Orbiter	Booster	Orbiter
Bell Engine					
Thrust, SL (1000 lb)	400	400	388/		
Thrust, VAC (1000 lb)	442	442	430/464		
Expansion ratio	35:1	35:1	35/120		
Diameter (in.)	60	60	110		
Length (in.)	112	112	135/205		
Weight (lb)	4150	4150	4350		
Aerospike Engine					
Thrust, SL (1000 lb)	400	400	400	800	385
Thrust, VAC (1000 lb)	453	453	486	903	453
Expansion ratio	50	50	161	50	95
Diameter (in.)	88	88	156	123	120
Length (in.)	35	35	59	45	45
Weight (lb)	3400	3400	5000	7050	3950

Space Division
North American Rockwell

system provides 31,800 pounds of payload and the aerospike system provides 30,600 pounds of payload.

The performance of the aerospike system with the 156-inch diameter engine was determined to be 37,300 pounds. These lead one to conclude that a dual engine development may be worth while. The performance aspects of dual engine development versus single engine development will be discussed in a later section.

Figure 8.7-8 illustrates booster and orbiter propulsion system installation configured for the bell engine and adapted for the aerospike. The booster has eleven 400,000-pound-thrust bell engines with exit diameter of 60 inches which results in expansion ratio of 35:1. Where six 800,000-pound-thrust dual combustor aerospike engines are used on the booster, the diameter is limited to 123 inches; this results in an expansion ratio of 50:1. To adapt the booster for an aerospike engine, the vehicle thrust structure and system attachments must be revised.

If the aerospike engine chamber is located at the same station as the bell engine exit plane, the aerospike gimbal point must be 67 inches aft of that for the bell engine. This causes an aft movement of 6 to 10 inches in the vehicle center of gravity for the aerospike engine installation. This would require minor revisions to aerodynamic surfaces.

The orbiter vehicle has two bell engines with expansion ratio of 120:1 and exit diameter of 110 inches. Where this orbiter is adapted to use the same basic aerospike engine to that used on the booster, the engine diameter is 120 inches with a single combustor. This results in an aerospike engine expansion ratio of 95:1 compared to 120:1 for the bell engines. Note that the engine diameter was limited by the booster installation and not the orbiter. To adapt the orbiter vehicle for the aerospike engine, the thrust structure and system attachments must be moved aft 112 inches compared to the bell engine installation. The 5 to 7 inches aft movement of C. G. would not result in major vehicle weight penalties.

A second approach which has not been considered in detail is to install the aerospike engine at the same booster and orbiter body station

BELL ENGINE

AEROSPIKE ENGINE

ORBITER

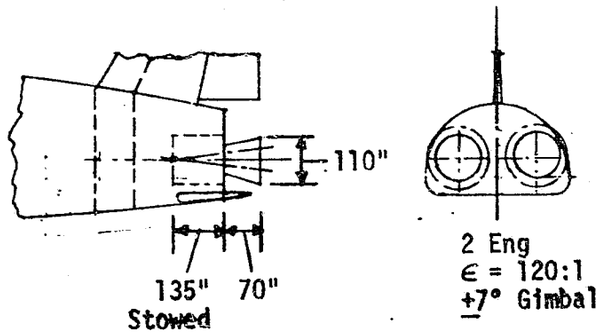

ORBITER

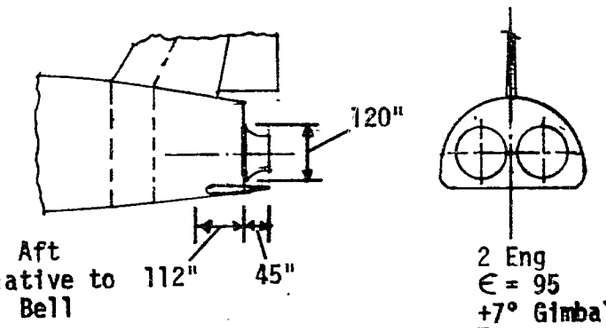

- Lower ∈ Nozzle, Limited by Booster Base to Use Same Engine
- Engine, T/S & Systems Moved Aft 112
- CG Aft 5-7 In. (OK)
- TPS for Plume Impingement

BOOSTER

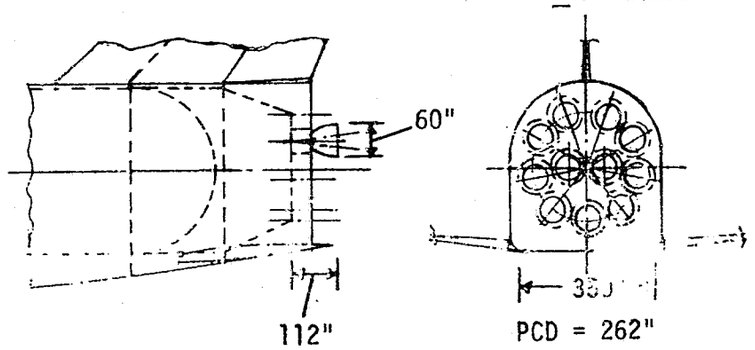

BOOSTER

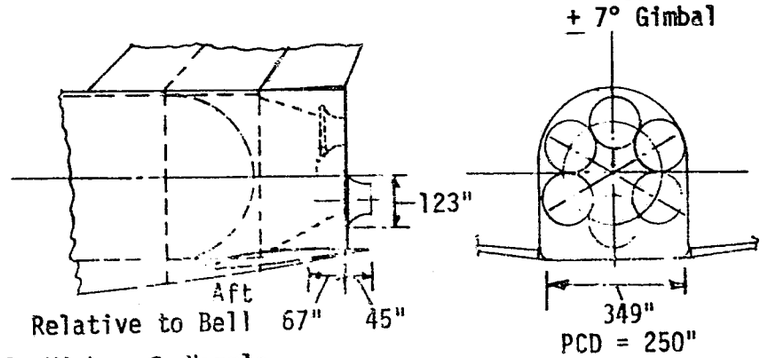

- Higher ∈ Nozzle
- Engine, T/S & Systems Moved Aft 67"
- New Thrust Structure
- Thrust Increased 12%
- CG Aft 6-10 in (OK)

Figure 8.7-8. Bell-Engine Configuration Adapted for Aerospike Engine

and allow aerospike engine plume impingement within the body. The body internal thermal protection system requirements may not be major.

Figure 8.7-9 illustrates booster and orbiter propulsion system installations configured for the aerospike engine and adapted to the bell engine. The booster has six 800,000-pound-thrust dual combustor aerospike engines mounted near the most aft body station. The engine diameter is limited to 123 inches by the available booster base area. The aerospike expansion ratio is 50:1. Where eleven, 400,000-pound-thrust bell engines are adapted to this design, the engine exit diameter is limited to 60 inches, which results in a nozzle expansion ratio of 35:1. A new thrust structure is required because of the change in number of engines. Since the vehicle/engine interfaces are different, propellant feed, engine actuation, and pressurization systems are modified. The bell engine gimbal axis is located at the same body station, and 67 inches of thermal protection system fairings is required to protect the exposed engines. The aft bell engine installation required modification to the horizontal tail. The aft c.g. movement is insignificant.

The orbiter vehicle has two 120-inch-diameter, single-combustor aerospike engines. This diameter provides an expansion ratio of 95:1. The inner combustor and a single pump set are used from the booster engine. The booster base area is somewhat larger than required for the two-engine installation, but more detail study is required to determine if the base area should be reduced. Where this orbiter is adapted to use bell engines, a 110-inch exit engine can be installed, providing an expansion ratio of 120:1.

The bell engines are installed at the same fuselage station, which requires a 112-inch thermal protection system fairing to protect the bell engines in the stowed position. The horizontal tail must be modified to prevent interference. The thrust structure may be acceptable for the bell-engine installation; however, vehicle/engine interfaces are different and will require modified propulsion systems.

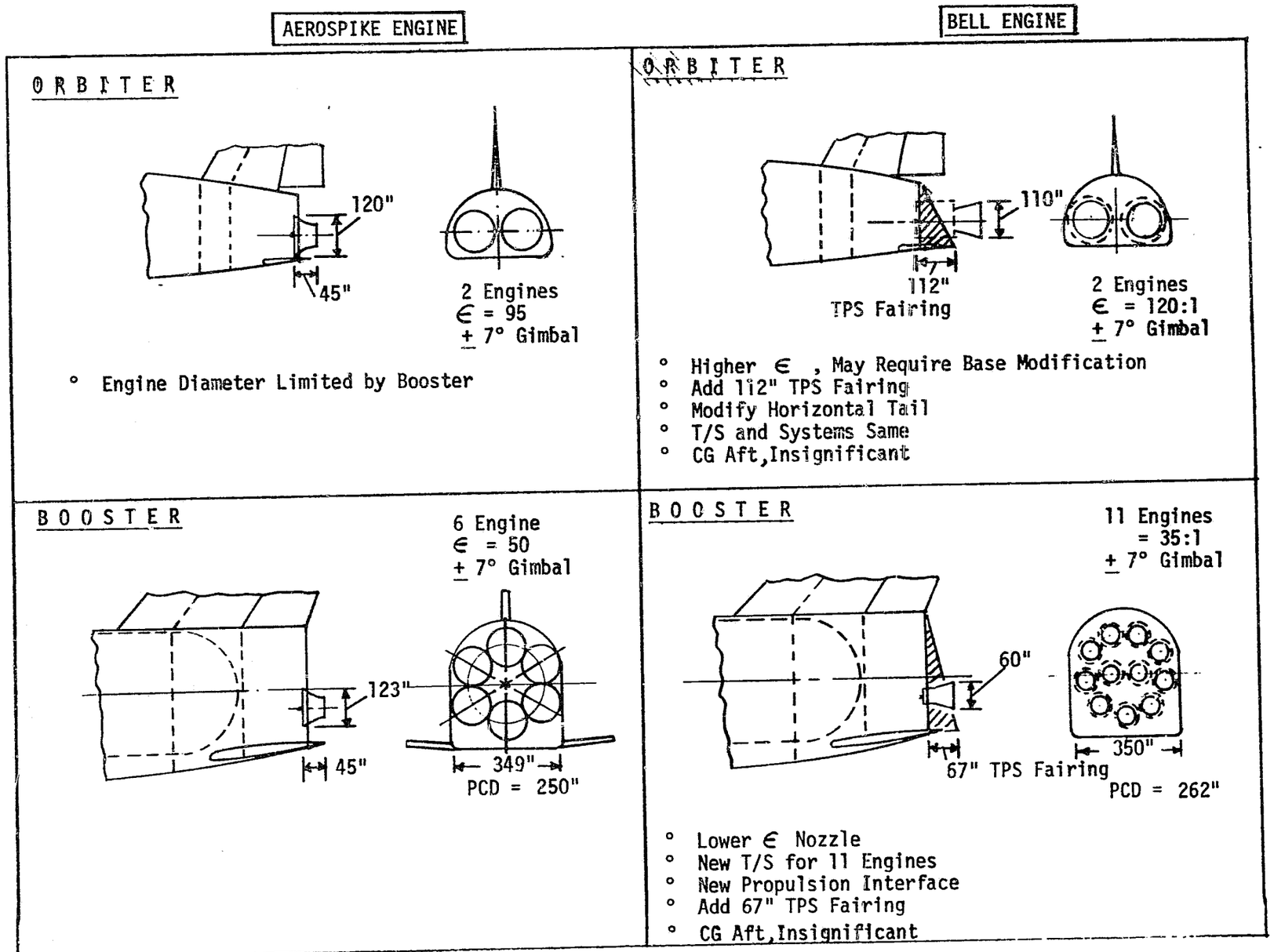

Figure 8.7-9. Aerospike-Engine Configuration Adapted for Bell Engine

Performance Impact of Single Engine Development

A study ground rule was to use a common engine in the booster and orbiter, presumably, to minimize the rocket engine development cost. A study was conducted to assess the vehicle performance penalty associated with this ground rule. This study was also conducted on the 3,500,000-pound-gross-weight vehicle so that both the bell and aerospike engines could be analyzed and compared with results in the previous section.

Based on previous launch vehicle studies, the use of seven engines was selected for the booster. This number of engines results in an engine configuration that makes efficient use of the vehicle base area, provides one-engine-out capability, and has a reasonable thrust level. The sea-level thrust required per engine is 625,000 pounds.

It was assumed that the orbiter stage would have two engines to provide sea-level abort capability (T/W >1.125 at sea level) with two engines and to provide engine-out capability at altitude. Engine thrust levels of 350,000, 450,000, and 550,000 pounds of vacuum thrust were considered. Both the bell engine and aerospike engine thrust levels are optimum at 450,000 pounds. The characteristics of the engines that will fit the vehicle base and vehicle performance comparison are summarized in Figure 8.7-10.

A dual-engine development for the bell engine system would increase vehicle payload capability by 4000 pounds, or 12.5 percent. A dual engine development for the aerospike engine system would increase payload capability by 7,800 pounds, or 25 percent. With a dual-engine development, the aerospike system payload capability is predicted to be 7 percent greater than the bell engine system.

Propulsion System Functional Trade

Following injection into a 50- by 100-nautical-mile orbit, the orbiter has propulsion function requirements for transfer to the space station orbit, rendezvous and docking with the space station, and deorbit for return to earth. Several propulsion system options and operating modes can be used to perform these functions. The systems to be considered are the main propulsion system, reaction control system, and auxiliary propulsion system. The first two are already available because of other propulsion requirements; the auxiliary propulsion system would be an added system.

The orbiter maneuvering profile is shown on Table 8.7-7 including mission phase, tine, and ΔV for a minimum and maximum duration mission. Based upon the maximum-duration mission and using the main engine in a

BOOSTER

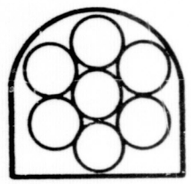

7 ENG

ORBITER

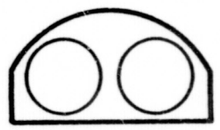

2 ENG

- CONSIDERED 350K - 550K LB VAC THRUST PER ORBITER ENGINE
- 450K LB VAC THRUST OPTIMUM

CHARACTERISTIC	BELL ENGINE				AEROSPIKE ENGINE			
	SINGLE ENG DEVEL		DUAL ENG DEVEL		SINGLE ENG DEVEL		DUAL ENG DEVEL	
	BOOSTER	ORBITER	BOOSTER	ORBITER	BOOSTER	ORBITER	BOOSTER	ORBITER
NO. OF ENGINES	11	2	7	2	6	2	7	2
THRUST, SL (1000 LB)	400		625		800		625	
VAC (1000 LB)		464		450		453		450
DIAMETER (IN.)	60	110	85	107	123	120	123	156
EXPANSION RATIO	35	35/120	45	35/120	45	95	66	173
PAYLOAD * (LB)	31,800		35,800		30,600		38,400	

* 3.5M LB GROSS WEIGHT SYSTEM

Figure 8.7-10. Performance Impact of Single-Engine Development

Space Division
North American Rockwell

Table 8.7-7. Orbit Maneuvering Profile

Number of Firings	Mission Phase	Minimum-Duration Mission		Maximum-Duration Mission	
		Time	ΔV fps	Time	ΔV fps
	Liftoff to burnout at 50 - nautical-miles injection	7.07 min	-	7.07 min	-
	Ascent				
	Coast to 100 nm	43.8 min	-	43.8 min	-
1	Circularize at 100 nm		90		90
	Coast	44.4 min	-	20.77 hr	-
2	First transfer		142		142
	Coast	45.0 min		45.0 min	
3	Second transfer (max has plane change and continue)		279		479
	Coast	46.2 min		46.2 min	
4	Braking to 260 nm		137		137
	Coast	0		27 min	
5	Terminate rendezvous first burn		21		21
	Coast	47 min		47 min	
6	Terminate rendezvous second burn at 270 nm		21		21
7 +	Docking Multiple burns and dock latch	30 min	100	30 min	100
	Total ascent	4.3 hr	790	24.8 hr	990
	Docked space station	30 days	-	30 days	-
	Descent (Separate from Space Station)				
1	Transfer burn to elliptical orbit 270 x 100 nm		0		370
	Coast	0		13.7 hr	
2	Retro-fire		425		130
	Coast to 400,000 ft	24 min		24 min	
	Coast to 128,000 ft	18 min		18 min	
	Coast to 40,000 ft	1.8 min		1.8 min	
	Pitch-down start Turbojets Landing approach to touchdown Go-around	 3 min 12 min		 3 min 12 min	
	Total descent	1.0 hr	425	14.7 hr	500
	Summary: Ascent Descent	4.3 hr 1.0 hr	790 425	24.8 hr 14.7 hr	990 500
	Total	5.3 hr +30-day dock	1,215	39.5 hr +30-day dock	1,490

throttled mode, a propellant utilization versus mission time was prepared as shown on Figure 8.7-11. Selection or apportioning of the orbiter maneuvering requirements to the various propulsion systems requires a trade of propellant and system weight versus operational requirements.

The engine thrust level and specific impulse for the various options are shown in Figure 8.7-12. The main engine is shown for the minimum throttle position (pump idle) and idle mode (tank-pressure-fed) operation. Note the wide variation or unpredictable performance depending on inlet conditions. A single RL10A3-3 at full thrust is shown. Two RCS points are shown: (1) two orbiter-size RCS motors and (2) two booster-size RCS motors. Of course, if higher thrust were required, additional RCS motors can be added at minimal penalty.

The orbiter propellant and burn-time requirements to accomplish the propulsion functions by various prospective systems are shown in Table 8.7-8. The use of the main rocket engine throttled to 10 percent of rated thrust was selected as the reference; and 24,699 pounds of propellant is required to accomplish a total ΔV of 1,390 feet per second, which excludes the 100 feet per second for docking. A major unknown at this time is the propellant losses to condition the engine for pump-fed operation. A propellant allocation of 3,420 pounds is provided for shutdown loss and engine chilling requirements based on preliminary data provided by P&W and assumed engine temperatures. The short burn time of 3 seconds for the 21-foot-per-second maneuvers (Number 5 and 6, Table 8.7-8) is obviously unrealistic for main-engine operation. A velocity increment of 50 feet per second is probably a minimum for main engine pump-fed operation.

If all of the orbit maneuvers were accomplished by the main engines operating on tank head pressure or idle mode, a saving of 1,151 pounds of propellant could be realized; however, it should be noted that engine performance will be a function of delivered propellant condition and may vary appreciably as shown on Figure 8.7-12; therefore, this propellant saving could vanish rapidly.

Similarly, if an auxiliary propulsion system (the Pratt & Whitney RL10A3-3 was assumed) were installed, a net orbiter weight saving equivalent to 1,970 pounds propellant can be realized. From the operational standpoint, the engine burn times would range from 8 to 221 seconds, which is compatible with this engine design.

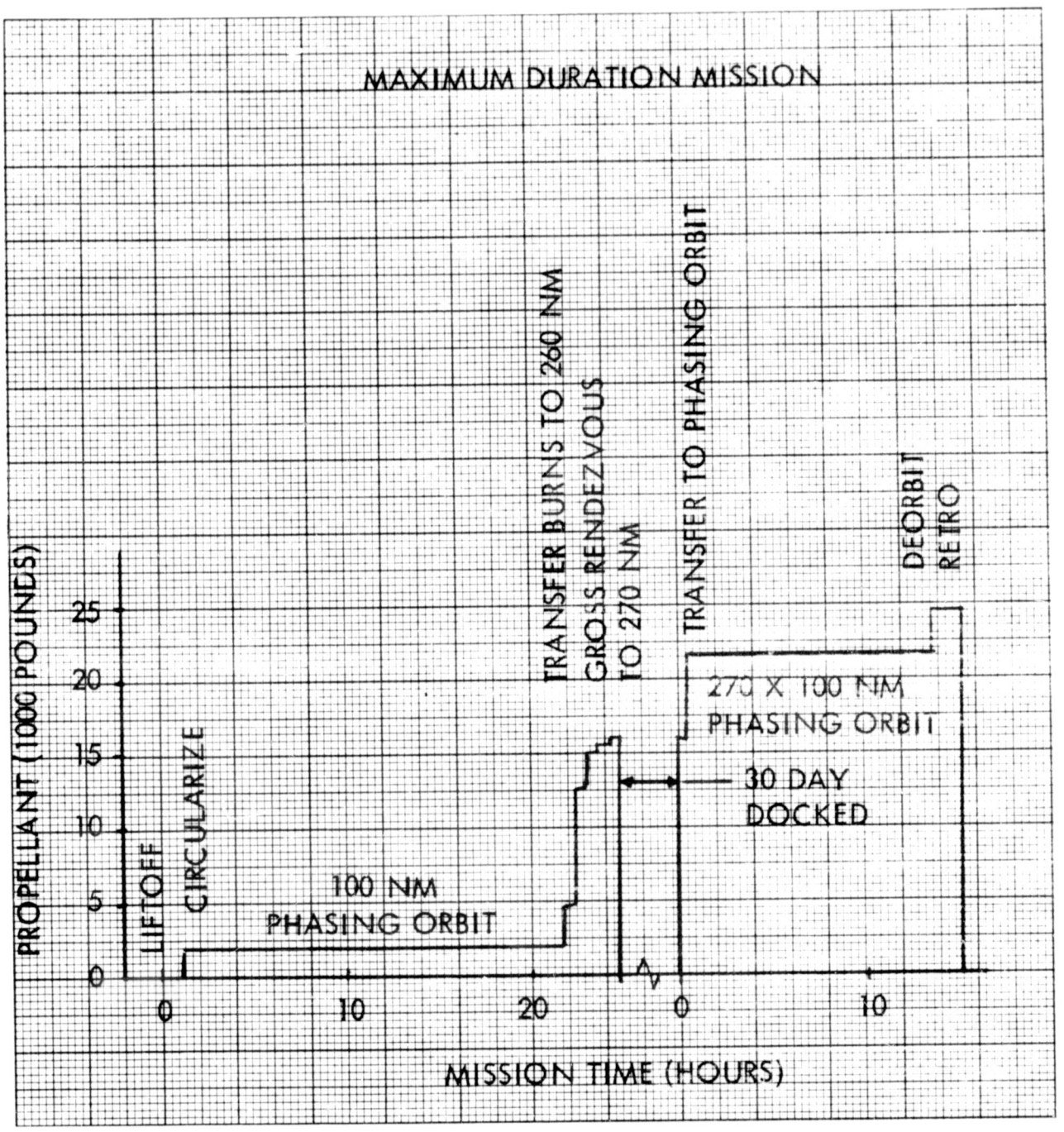

Figure 8.7-11. Orbit Maneuvering Propellant Schedule

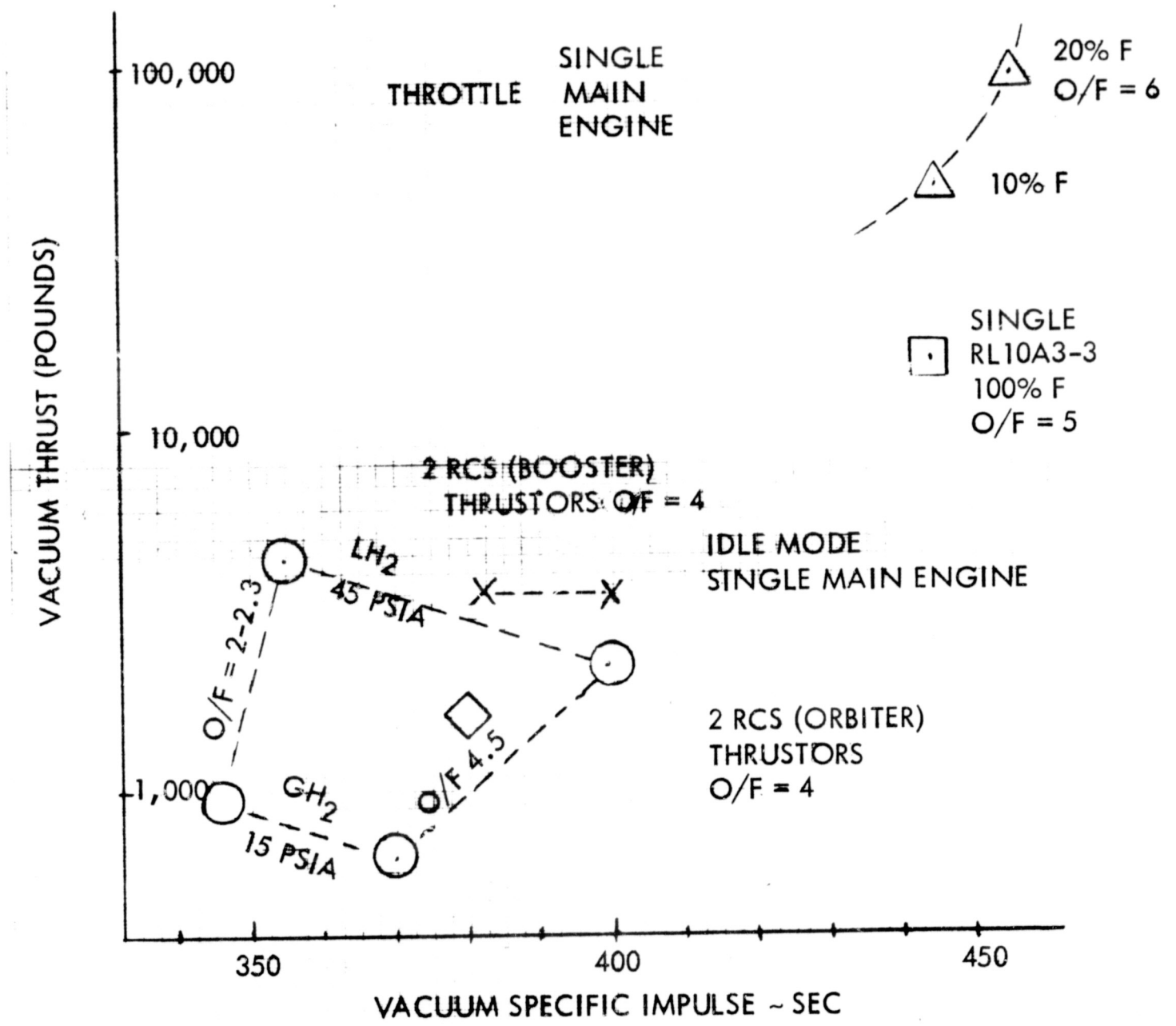

Figure 8.7-12. Orbit Maneuvering Propulsion Performance Spectrum

Table 8.7-8. Orbital Propulsion Requirements and Alternative

Maneuver	Δ V (fps)	Main Engine 10 percent Throttled		Main Engine Idle Mode		Secondary Engine RL10A3-3		RCS	
		W_p(lb)	t_b(sec)	W_p(lb)	t_b(sec)	W_p(lb)	t_b(sec)	W_p(lb)	t_b(sec)
1. Circularize	90	1,441	14	1,603	292	1,444	43	1,687	402
2. Transfer up	142	2,256	22	2,506	456	2,261	67	2,636	628
3. Transfer	479	7,446	72	8,253	1,501	7,462	221	8,671	2,065
4. Transfer	137	2,084	20	2,305	419	2,089	62	2,418	576
5. Terminal rendezvous	21	318	3	351	64	318	9	368	88
6. Terminal rendezvous	21	317	3	351	64	318	9	368	88
Dock / Undock									
7. Transfer Down	370	5,514	53	6,083	1,106	5,526	164	6,375	1,518
8. Deorbit	130	1,903	18	2,096	381	1,908	56	2,194	522
Subtotal	1,390	21,279	205	23,548	4,283	21,326	631	24,717	5,887
Propellant losses		3,420				1,000			
Total	1,390	24,699	205	23,548	4,283	22,326	631	24,717	5,887
Delta propellant weight		0		-1,151		-2,373		+18	
Delta system weight		0		0		+403		0	
Delta loaded weight		0		-1,151		-1,970		+18	

Constant vehicle burnout weight is 230,000 pounds at 50 nm.

If the orbiter maneuvers were accomplished by two orbiter RCS engines, 18 pounds of additional propellant would be required. Unfortunately, the RCS thrust level is so low that excessive burn times are required to accomplish certain maneuvers, 1,518 and 2,065 seconds. From the engine design standpoint, the extended burn time will present a major problem (cooling); however, if two or four of the booster RCS engines were substituted for the orbiter translation motors, this problem would be alleviated, burn times shortened, and a net fuel saving since the larger engine could potentially operate at a better SFC.

It was concluded that, for this study, the orbiter maneuvering propulsion function should be divided between the main engine and RCS engines for minimum system weight, complexity, and cost effectiveness. The main engine will perform velocity increments greater than 50 feet per second.

It is recommended that these options be subjected to comprehensive trades in future studies.

Ascent Propulsion, Pressurization System Trade

The ascent propulsion for both the booster and orbiter is a single-burn operation; therefore, the pressurization systems can be relatively simple. In addition, the LO_2 tanks are located forward and provide sufficient hydrostatic head to meet the engine LO_2 NPSH requirements without any ullage pressure. Three LO_2 tank pressurization systems were considered: self pressurizing by vaporization of bulk LO_2 with vapor pressure as the driving potential, heated GO_2 from the main engine, and heated helium stored at LH_2 temperature.

Results of the weight trade are shown in Tables 8.7-9 and 8.7-10 for the booster and orbiter. The self pressurization system concept assumes that the final GO_2 pressure is 15 psia at 163 R. The heated GO_2 and heated helium system assumed that the tank pressure is regulated to 20 psia maximum and that the average pressurant temperature is 350 R. The 350 R temperature selection is based on experience with the S-II stage pressurization system.

Although the self-pressurization system is the simplest, it was discarded because of the high pressurant weight. The heated GO_2 system was selected in preference to the somewhat lighter heated helium system to avoid the structural complications associated with mounting large helium receivers inside the LH_2 tank. Also the heated helium system has more of its system weight in hardware, which is the costly portion of the system.

Table 8.7-9. Booster LO_2 Pressurization System Weight Trade

Component \ Concept	Weight (lb)		
	Self-Pressurization (GO_2 (15 psia, 163 R)	Heated GO_2 (20 psia, 350 R)	Heated Helium (20 psia, 350 R)
Pressurant	10,100	6,030	695 (He) 485 (GO_2)
Pressure bottles	--	--	2600
Bottle mount	--	--	600
Regulator	--	30	30
Heat exchanger	--	400	200
Lines, fittings, brackets, etc.	--	500	500
Total	10,100	6,960	5110

Table 8.7-10. Orbiter LO_2 Pressurization System Weight Trade

Component \ Concept	Weight (lb)		
	Self-Pressurization GO_2 (15 psia, 163 R)	Heated GO (20 psia, 350 R)	Heated Helium (20 psia, 350 R)
Pressurant	2,120	1,275	150 (He) 103 (GO_2)
Pressure bottles	--	--	570
Bottle mounts	--	--	115
Regulator	--	30	30
Heat exchangers	--	80	70
Lines, and fittings	--	100	100
Total	2,120	1,485	1,138

Space Division
North American Rockwell

A gaseous hydrogen pressurization system was selected for the LH_2 tank without a trade. Hydrogen is the lightest pressurant available. Also, by tapping the GH_2 supply from the main engine, a simple system with minimum hardware is possible. This has been demonstrated in the S-II stage.

Airbreathing Engine Options

Subsequent to the selection of a 50,000-pound-payload shuttle system for detail analysis, studies were conducted to tradeoff the airbreathing propulsion system options. These options included the selection of engine type and fuel. As a goal, the selection of a currently operating turbojet was desired to limit air-breathing propulsion development to qualification for the space environment; however, use of advanced lightweight engines and hydrogen fuel was considered. A summary of potential turbojets for the shuttle vehicle is presented in Table 8.7-11.

Prior to embarking on analysis of the turbojet propulsion systems, certain aspects were investigated with the engine manufacturers. A preliminary air-breathing engine data request was submitted to the major air-breathing engine contractors. Their answers to the questionnaire are summarized in the following paragraphs.

1. What major engine and operational changes are required for use of hydrogen rather than JP-4 as the air-breathing engine fuel?

   All three engine contractors stated that there are no major problems. Both P&W and G. E. have had experience in converting existing JP fuel turbojet to operate on hydrogen fuel. The engine fuel control and fuel injector are the primary areas of concern in the conversion to hydrogen. All of the contractors expressed the opinion that hydrogen fuel would permit an increase in the operational and engine-starting envelope, which would be a desirable feature, as both orbiter and booster require high-altitude start of the turbojets?

2. For the space shuttle mission, what are critical engine environmental requirements?

   Assuming adequate thermal protection can be provided, the conditions of concern are those induced by an acoustic environment (sound level and vibration) during launch. The contractors did not feel that the launch environment would be critical in view of its similarity to that generally accepted for afterburning turbojet engines; however, it may be necessary to provide for engine rotation during launch to prevent brinelling of engine bearings.

Table 8.7-11. Jet Engine Summary

Manufacturer	Model Number	Application	Type	Status	Engine Performance: Sea Level Thrust (1000 lb)	Engine Performance: Sea Level SFC (lb/hr/lb)	Engine Performance: Static Cruise① Thrust (1000 lb)	Engine Performance: Static Cruise① SEC (lb/hr/lb)	Airflow/BPR③ (lbs/sec)	$F_{SLS/W}$	Diameter (in.)	Length (in.)	Weight (lb)	Remarks
Pratt & Whitney	TF33-P-7	C141	TF	Prod	21.0	0.56	9.1	0.70		4.5	52	142	4,675	Current production for military transport (C141)
	JT9D-15	747	TF	Prod	45.5	0.364	16.8	0.481	1517/4.9	5.43	95.6	128	8,370	Growth version for booster
	JT3D-7	707, 720, DC-8	TF	Prod	19.0	0.55	7.6	0.68		4.45	52	134	4,265	12,000-hr TBO 3964 eng sold
	TF30-P-8	A-7B	TF	Prod	12.2	0.63	5.0	0.73		4.8	42	128	2,526	Military fighter
	J60-P-6	T-2B	TJ	Prod	3.0	0.96	1.3	1.07		6.1	20	71	495	Military trainer
	STF320A-4	Study	TF	Paper	38.17	0.324	10.47	0.521	1800/12	10.0	114.7	60	3,820	Lift/cruise concept study
	STF250C-36	Study	TF	Paper	33.4	2.05	-	-	393/2.1	7.6	56.9	165	4,400	Duct heating turbofan
	STF 292	Study	TF	Paper	25.0	0.385	10.0	0.5	715/4.7	7.1	66	96	3,500	Unaugmented turbofan
	STF325A-1	Study	TF	Paper	55.0	0.329	21.7	0.6	1822/5.2	6.1	100	146	9,000	Advanced commercial engine scale 75 to 125 percent
	STF326A-1	Study	TF	Paper	30.0	0.329	11.8	0.6	994/5.2	6.5	74.5	115	4,600	Advanced commercial engine scale 75 to 125 per
	QE-3	Study	TF	Paper	21.9	0.347	-	-	768/5.2	4.5	70.9	116	4,900	NASA quiet engine
General Electric	J79-15	F-4C	TJ	Prod	17.0	1.945	-	-	169/0	4.62	38.2	208	3,685	USN/USAF fighter
	TF39	C5A	TF	Prod	41.1	0.313	16.5	0.45	1549/8.1	5.5	100	189	7,500+	Large transport engine
	CJ805-3	880	TJ	Prod	11.6	0.81	-	-	170/0	4.1	48.8	110	2,817	
	CJ805-23	990	TF	Prod	16.1	0.56	-	-	170	4.3	56	130	3,766	
	CF6-50	DC-10-30	TF	Study	47.3	0.38	-	-	1465/-	5.85	92	172	8,100	Advanced version of CF6
	GE4②	SST	TJ	Study	67.0	1.86	-	-	633/0	5.9	90	300	11,303	Derate and use dry version
Allison	XJ99	Lift/Fan	TF	Dev./ Test	8.9	1.19	-	-	100/	19.1	31	45	465	Advanced high T/W engine in development at Allison and Rolls in England

①Cruise at military or maximum control. Power at Mo = 0.4 and 20,000 feet
②Cruise at military or maximum control. Power at Mo = 0.4 and 25,000 feet
③Bypass ratio

Space Division
North American Rockwell

Engine contractor experience in space simulation testing has indicated that existing technology can provide solutions to most problems encountered; however, specific problem areas are difficult to identify in detail.

Possible engine changes include (1) removal or replacement of any material that would obviously be affected by the vacuum environment; (2) modification of the lubrication system to permit isolation of the supply during the storage period (this would require installation of valves in the supply, scavenge, and vent lines); (3) use of P&W 524 polyphenyl either oil, which would not leave residue upon evaporation; (4) possible use of a fluorocarbon additive to the oil to provide solid film coating for preventing of cold welding; and (5) possible changes to fuel system components to provide vacuum storage compatibility.

3. What air-breathing engine starting system should be considered for both booster and orbiter vehicles?

   All three engine contractors indicated that windmill, cartridge or stored gas starting systems would be acceptable. Two of the contractors specifically thought the windmill start mode would be acceptable and could be accomplished without endangering the vehicle. Typical windmill start times on the order of 10-to-30 seconds were offered as best guesses of the start time.

4. Can engine auxiliary power be supplied?

   All of the engine contractors agreed that auxiliary-powered take-offs could be supplied to meet vehicle auxiluary power levels and torque requirements; however, at this point in time no specific power levels could be assigned for this particular study effort. During the performance analysis, it was assumed that each engine would supply a minimum of 200 continuous horsepower for control surface and auxiliary power applications. This performance penalty was assumed to ensure that such a penalty was included in the analysis and should be confirmed in later studies.

It can be concluded from the preceding answers that air-breathing propulsion for use in both booster and orbiter is technically feasible and merely requires a definition of propulsion system size and investigation of space storage capability.

Booster thrust required versus altitude characteristics for constant-Mach-number flight was prepared by the Aerodynamics Group as shown on Figure 8.7-13. Based upon data presented in Table 8.7-10, the Pratt & Whitney JT9D-15 and TF33-P-7 engines were selected as being representative of available current off-the-shelf powerplants. Based upon typical subsonic inlet performance, pressure recovery was estimated to be 98 percent of free-stream total pressure. This pressure recovery level is consistent with data obtained on DC9, 707 and F86-type aircraft and will be readily obtainable on the ILRV vehicles. During subsonic flight, preliminary estimates of engine horsepower extraction range from 100 to 250 horsepower per engine to supply vehicle power (flight controls, landing gear, etc.). Based on this preliminary power estimate and a survey of typical engine performance penalties associated with power extraction, all installed performance includes an increase of SFC = 0.03 (equivalent to 200 horsepower) to account for power extraction. The power extraction loss was taken at all flight conditions without regard to engine power setting in lieu of a specific power required duty cycle.

Using the aforementioned engine performance penalties, installed engine performance for the Pratt & Whitney JT9D-15 and TF33-P-7 engines is shown in Figures 8.7-14 and 8.7-15, respectively. Based upon the one-engine-out go-around power required criteria, four JT9D-15 or six TF33-P-7 engines will be required. In contrast, four JT9D-15 or eight TF33-P-7 engines will be required to meet Mach 0.4 cruise at an altitude above 20,000 feet. Table 8.7-11 summarizes the booster turbojet engine selection data showing sea-level static engine performance and vehicle performance at cruise conditions (Mach 0.4 and approximately 20,000 feet). The JT9D-15 engine offers the lowest net propulsion system weight (excluding installation and propellant tankage). Furthermore, a net saving of 21,800 pounds of propellant can be realized by changing from JP to H_2 as the booster flyback fuel. Based upon the preliminary performance presentation the JT9D-15 engine was selected as the best booster turbojet engine candidate. JP fuel will be used in the baseline system; however, the use of hydrogen fuel offers a significant growth potential. The significance of hydrogen fuel is increased if the cruise fuel requirements are increased.

In a fashion similar to the booster turbojet engine selection, orbiter turbojet engine screening data were prepared. Orbiter go-around and cruise thrust requirements are shown in Figure 8.7-16. Installed engine performance for the Pratt & Whitney TF33-P-7 and JT3D-7 engines, including pressure recovery and power extraction losses, are shown in Figures 8.7-17 and 8.7-18, respectively. The TF33-P-7 engine will meet the one-engine-out go-around criteria and cruise with three engines; however, this will be an asymmetric engine installation and would be difficult to integrate in the ILRV vehicle. The JT3D-7 engine will require four engines to meet the

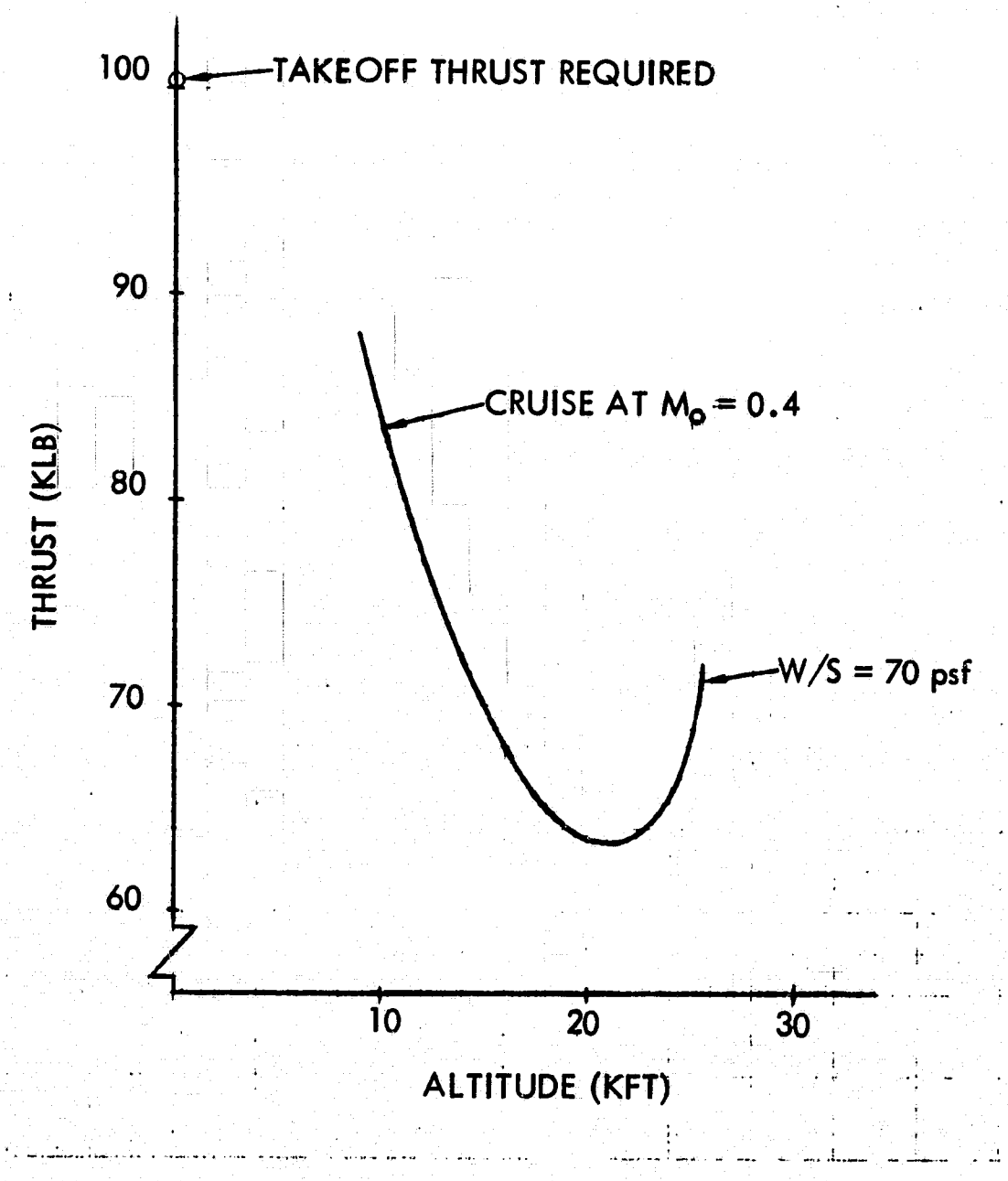

Figure 8.7-13. Booster Thrust Required

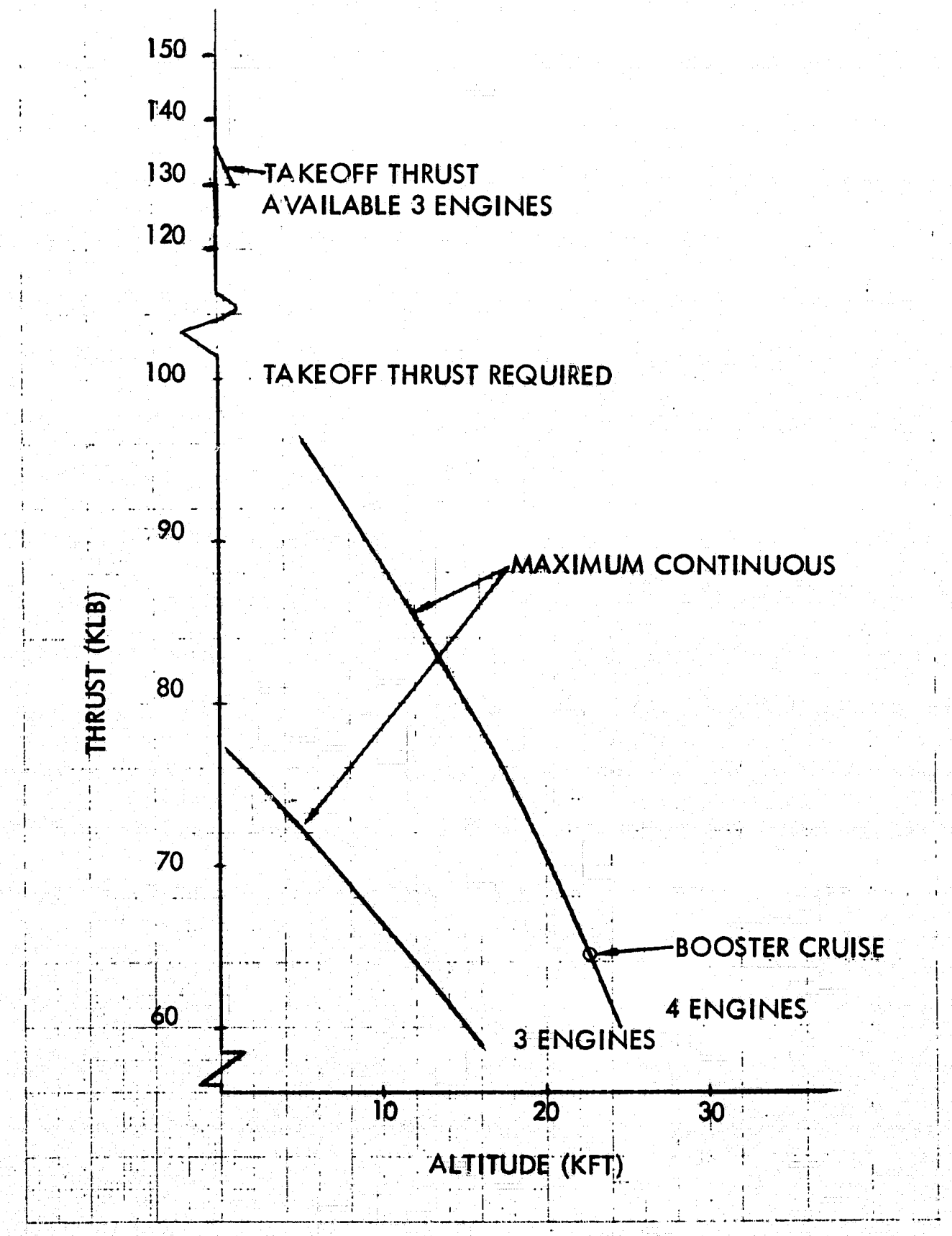

Figure 8.7-14. Pratt & Whitney JT9D-15 Engine Performance, Maximum Continuous and Takeoff Power

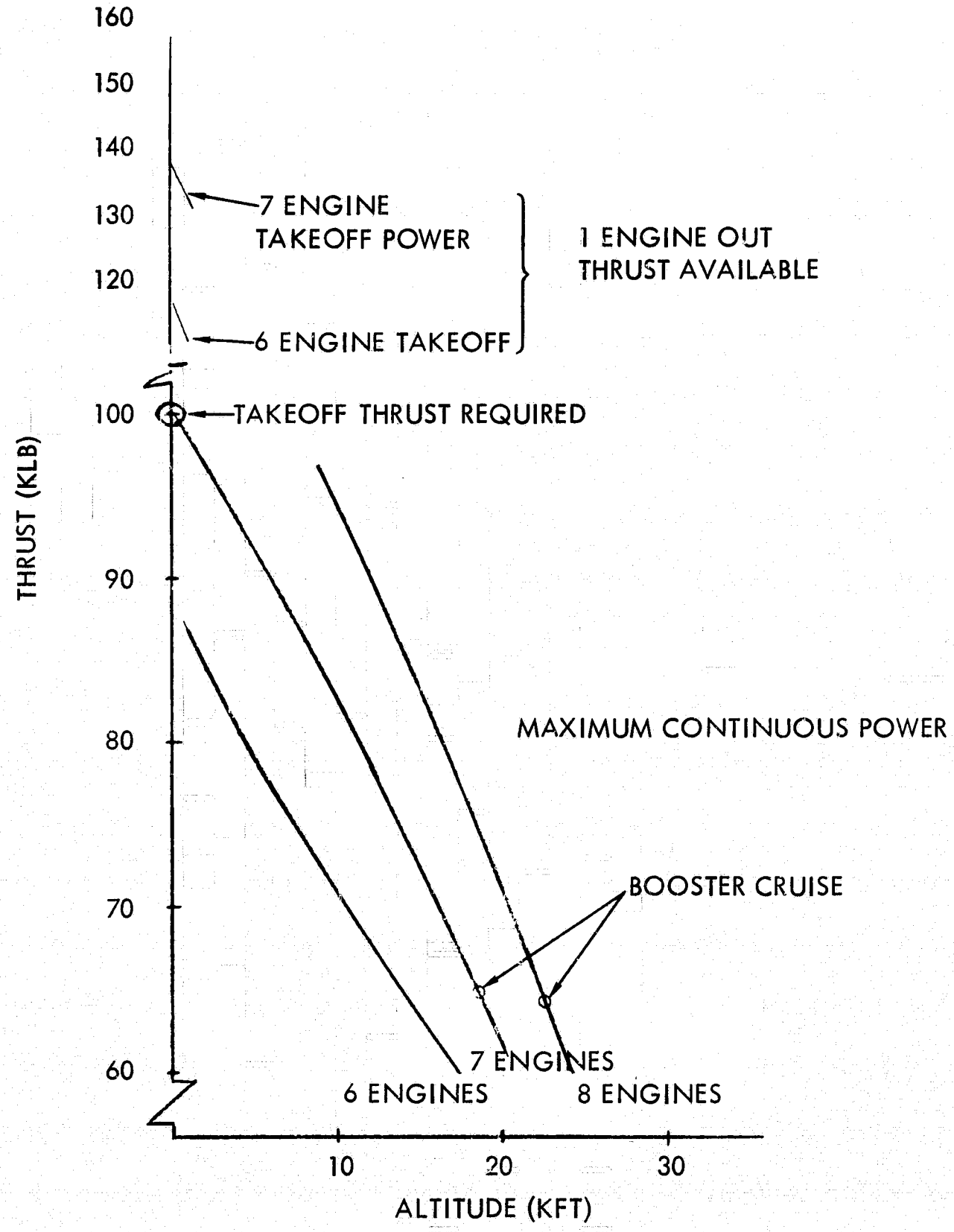

Figure 8.7-15. Pratt & Whitney TF33-P-7 Engine Performance, Maximum Continuous and Takeoff Power

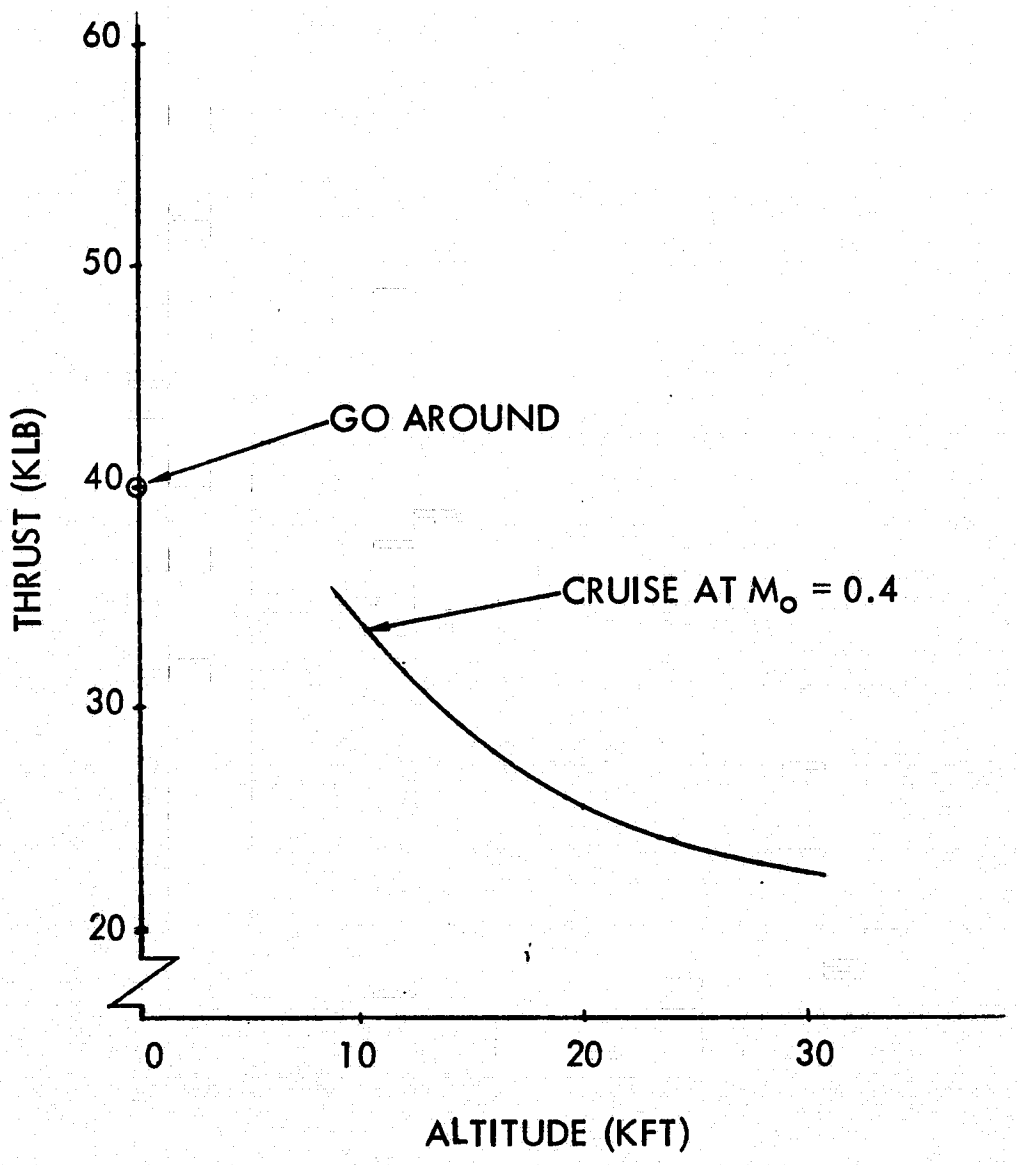

Figure 8.7-16. Thrust Versus Altitude for Orbiter

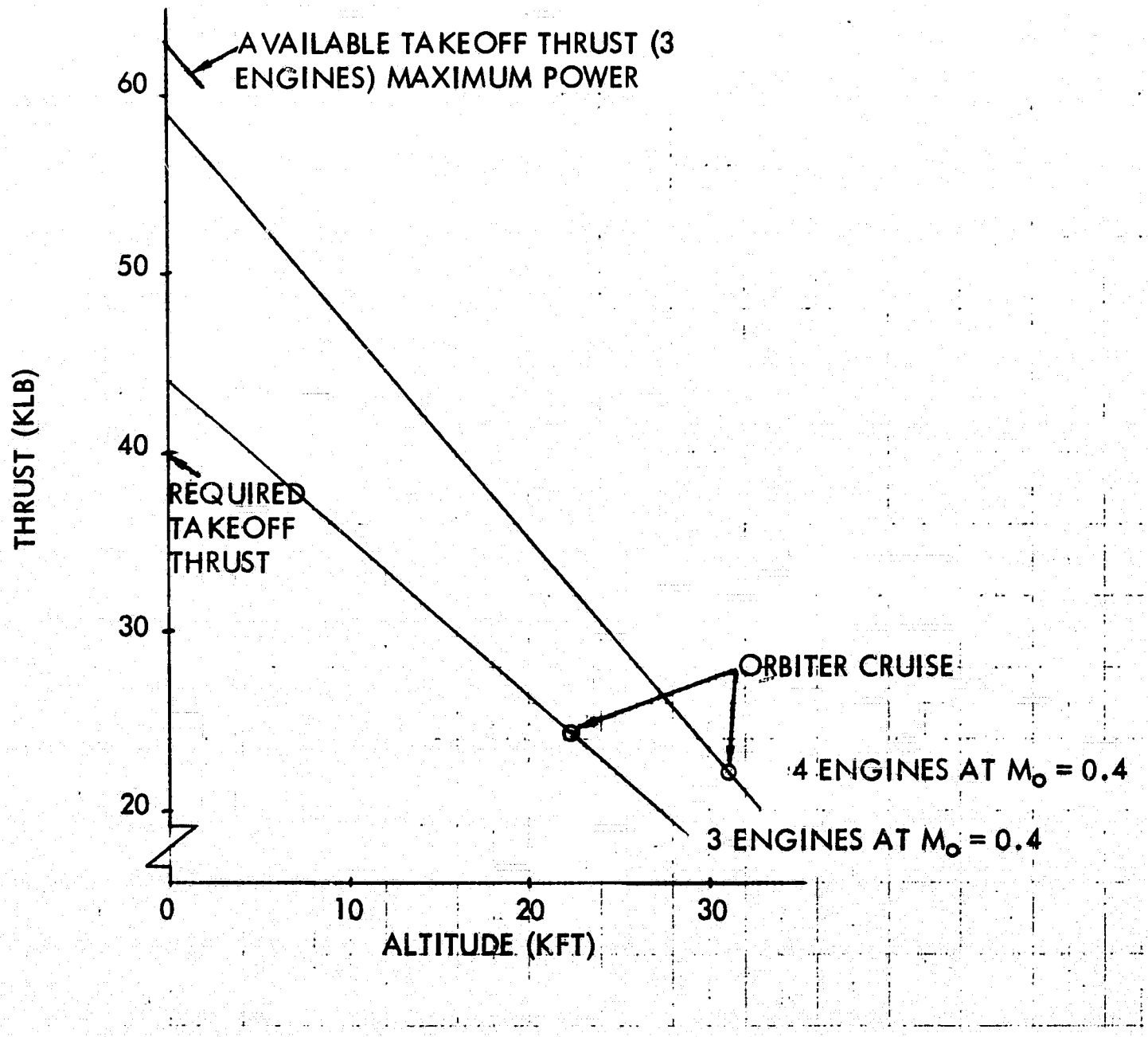

Figure 8.7-17. Pratt & Whitney TF33-P-7 Engine Data

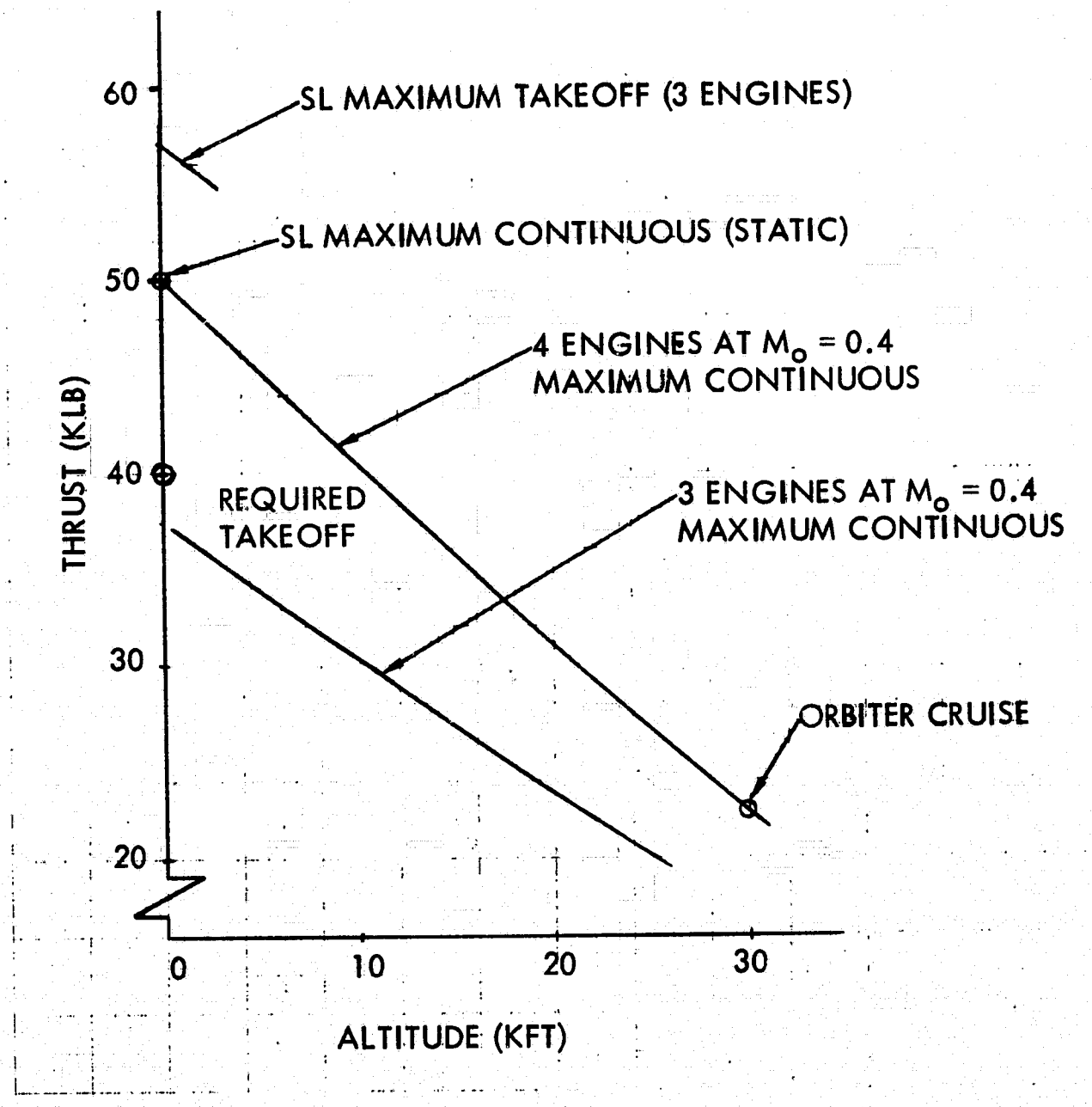

Figure 8.7-18. Pratt & Whitney JT3D-7 Engine Data

go-around and cruise requirements. Based on lowest gross weight to orbit for a symmetric configuration, the JT3D-7 engine was selected for additional design analysis. Table 8.7-12 shows a comparison of orbiter turbojet options. The relatively short orbiter cruise requirement (15 minutes) tends to reduce the overall effect of fuel requirements when considering JP and H_2 fuels. The orbiter turbojet fuel weight can be reduced by approximately 2,000 pounds when H_2 is used instead of JP fuel. An increase in fuel tank weight, however, would be necessary for H_2.

The most significant orbital weight saving can be accomplished by the selection of an advanced high-thrust-to-weight-ratio lift-type engine; i.e., Allison XJ99. As summarized on Table 8.7-13, a significant orbiter weight saving of approximately 12,000 pounds can be obtained by use of this type of engine currently in development and under demonstration test by Rolls-Royce Limited, Derby, England, and at Allison Division, General Motors, Indianapolis. The current XJ99 engine has a demonstrated T/W = 19:1, which is a significant improvement over typical off-the-shelf engines (T/W $\approx$ 5:1). For the subject analysis, T/W was reduced to 15:1 to reflect the installation of power takeoff pads and a cartridge starter. The following paragraphs will offer a brief description and design considerations for the high T/W engine.

Air-breathing power plants specifically designed for spacecraft atmospheric maneuvering and landing have not been designed as yet; however, certain short-takeoff-and-landing propulsion systems could readily be adapted to this application. Current propulsive-lift engine technology has been under development for the past decade by Continental Aircraft and Engine Company and the Allison Division of General Motors in conjunction with Rolls-Royce Limited (England). Presently, a direct-lift jet engine designated US/UK XJ 99 is undergoing demonstration tests. The test engine develops 8,916 pounds of thrust and is designed for a thrust-to-weight ratio of 19:1. The engine has an overall design pressure ratio of 8:1 which results in a relatively high thrust per unit airflow (89 pounds per pound) and thus reduces engine volume for a given thrust level. Typical engine scaling data and geometry variation with thrust is shown on Figures 8.7-19 and 8.7-20.

To achieve the high T/W levels, certain conventional engine features have been eliminated as discussed below.

Engine Starting System. Current high T/W engines use air bleed from the vehicle main engine compressor. Orbiter turbojet engines would have to be adapted to cartridge starters, air bottle start, windmill start or a combination of the above.

Table 8.7-12. Booster Turbojet Engine Summary

Manufacturing Model	Application	Type	Engine Data: Engine Performance: $F_{N_{SLS}}$ (1,000 lb)	Engine Performance: Fuel Type	Engine Performance: SFC (lb/hr/lb)	Size: D (in.)	Size: L (in.)	Weight (lb)	Cruise Condition: Time (hr)	Cruise Condition: Alt (1,000 ft)	Cruise Condition: M_N	Vehicle Data: Number of Engines	Vehicle Data: F_N (1,000 lb)	Vehicle Data: SFC (lb/hr/lb)	Vehicle Data: Weight: Engine (1,000 lb)	Vehicle Data: Weight: Fuel (1,000 lb)	Vehicle Data: Weight: Total (1,000 lb)
P&W TF33-P-7	Military transport (C-141), in production	TF	21	JP	0.56	52	142	4,675	1	23	0.4	8	64	0.72	37.4	46	83.4
P&W JT9D-15	Commercial transport (747)	TF	45.5	JP	0.364	95.6	128	8,370	1	23	0.4	4	64	0.52	33.5	33.2	66.7
P&W JT9D-15		TF		H_2	0.103	95.6	128	8,370	1	23	0.4	4	64	0.185	33.5	11.4	44.9

Table 8.7-13. Orbiter Turbojet Engine Summary

Manufacturing Model	Application	Type	Engine Data: Engine Performance: $F_{N_{SLS}}$ (1,000 lb)	Fuel Type	SFC (lb/hr/lb)	Size: D (in.)	L (in.)	Weight (lb)	Vehicle Data: Cruise Condition: Time Min	Alt (1,000 lb)	M_N	Number of Engines	F_N (1,000 lb)	SFC lb/hr/lb	Weight: Engine (1,000 lb)	Fuel (1,000 lb)	Total (1,000 lb)
P&W TF33-P-7	Military transport (C-141) in production	TF	21	JP	0.56	52	142	4,675	15	31	0.4	4	22.2	0.72	18.7	4.05	22.75
P&W TF33-P-7		TF	21	H_2	0.157	52	142	4,675	15	31	0.4	4	22.2	0.255	18.7	1.43	20.13
P&W JT3D-7	Commercial transport (707, 720B, DC-8) 12,000-hr TBD	TF	19	JP	0.55	52	134	4,260	15	30	0.4	4	22.5	0.735	17.05	4.13	21.18
P&W JT3D-7		TF	19	H_2	0.154	52	134	4,260	15	30	0.4	4	22.5	0.26	17.05	1.46	18.51
Allison ① XJ99	Military lift-fan in development reqs. scale up	TJ	8.9	JP	0.9	33	47	470	15	30	0.4	4 ②	22.5	1.0	3.6	5.6	9.2
Allison XJ99		TJ	8.9	H_2	0.252	33	47	470	15	30	0.4	4 ②	22.5	0.354	3.6	1.98	5.58

① Allison Engine T/W ≈ 15:1 to account for power takeoff and starting system.
Present T/W = 19:1 on development engine running in England.

② Scaled up version.

Space Division
North American Rockwell

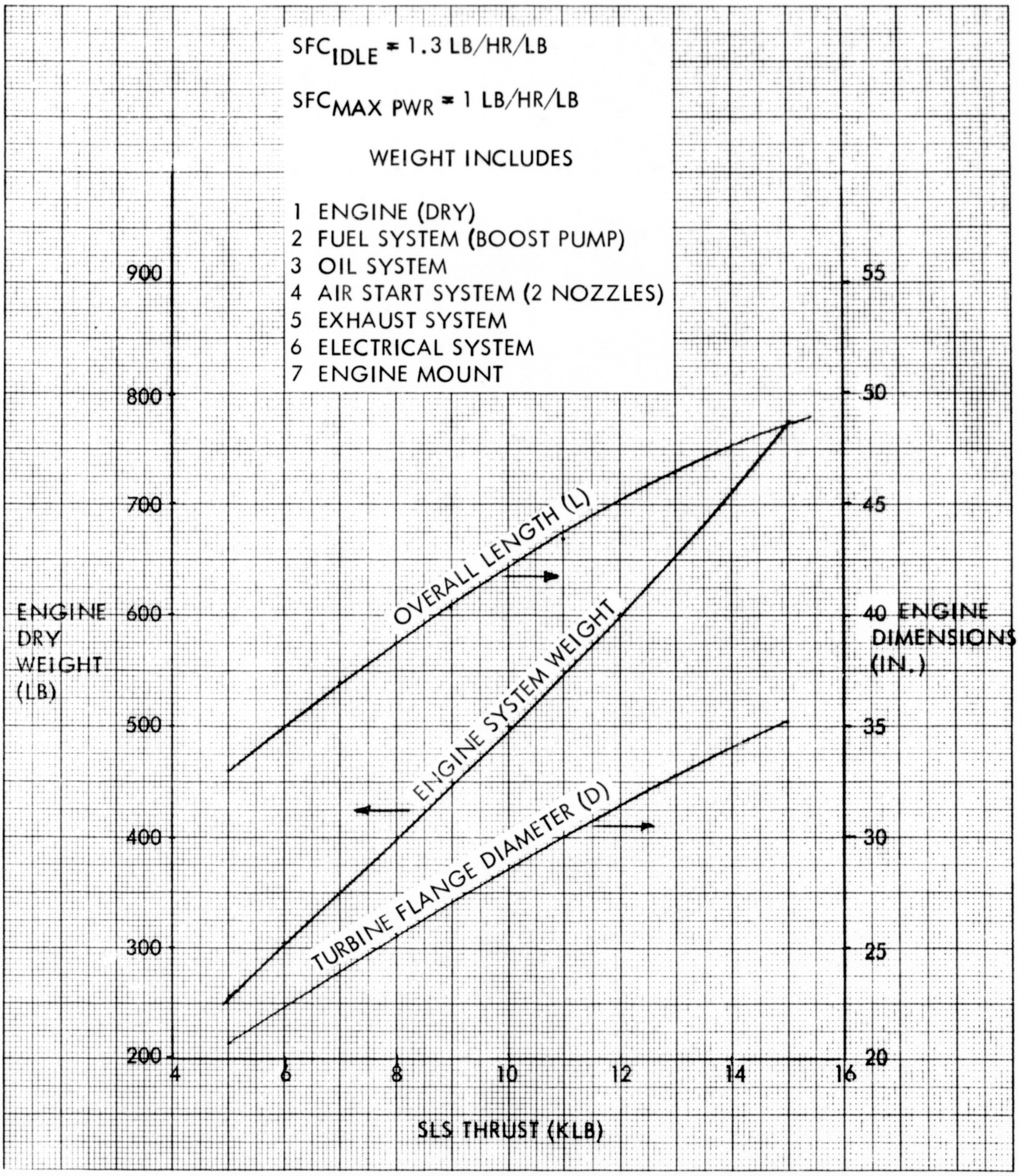

Figure 8.7-19. Lightweight Turbojet Engine Data

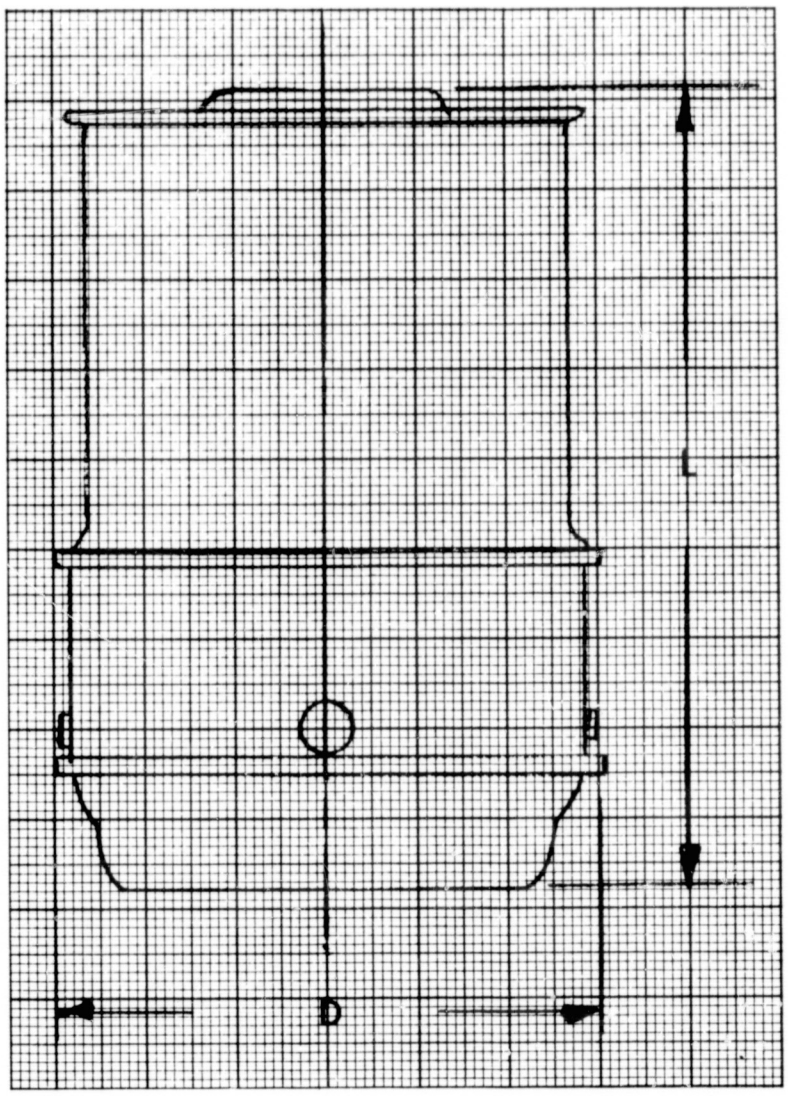

Figure 8.7-20. Lightweight Turbojet Engine Geometry

Engine Lubrication System. Basic high T/W engines will have a total-loss oil system. The orbiter must supply a pressurized oil tank and oil quantities consistent with design mission time.

Engine Fuel System. Engine and fuel system must be enclosed in a protective environment. Pressure must be sufficient to insure retention of lubricants. Temperature must be under 160 F.

8.7.3 Propulsion System Conceptual Definition

Propulsion system analysis was conducted for the baseline 50,000-pound-payload shuttle vehicle to define conceptual system designs for the main rocket propulsion, RCS and turbojet systems. These conceptual designs were used in preparing the detail vehicle weight and cost predictions.

Main Rocket Propulsion

Engine System. The baseline booster configuration uses ten high-chamber-pressure bell engines with fixed nozzles. The baseline orbiter configuration uses two of the same basic bell engines with a two-position nozzle. The characteristics of the rocket engine are given in Figure 8.7-21. The booster engine produces 500,000-pound sea-level-thrust engines with a fixed 35:1-expansion-ratio nozzle and the orbiter engine produces 576,000-pound vacuum-thrust engines with two-position 120:1-expansion-ratio nozzles. The booster and orbiter engines are identical to an expansion ratio of approximately 5:1, where either the booster or orbiter nozzle can be attached. The booster and orbiter engines are required to throttle to 75 and 73 percent of maximum thrust, respectively, to limit the ascent acceleration to 3 g. In addition, the orbiter engine is required to throttle to 10 percent of maximum thrust when used for on-orbit velocity increments down to 50 feet per second. The orbiter two-position nozzle separation line is at an expansion ratio of 58:1, which provides minimum stowed length nozzle. The operating mixture ratio selected as a result of vehicle performance optimization is 6:1. The engine dimensions and weight are shown in the figure. The gimbal angle requirement for vehicle control and CG excursion is ±7 degrees.

Bell engine interface requirements are:

LO_2 NPSH, 16 feet

LH_2 NPSH, 60 feet

LO_2 feed line interface diameter, 16 inches

- COMMON POWER PACK FOR BOOSTER & ORBITER, TWO NOZZLES

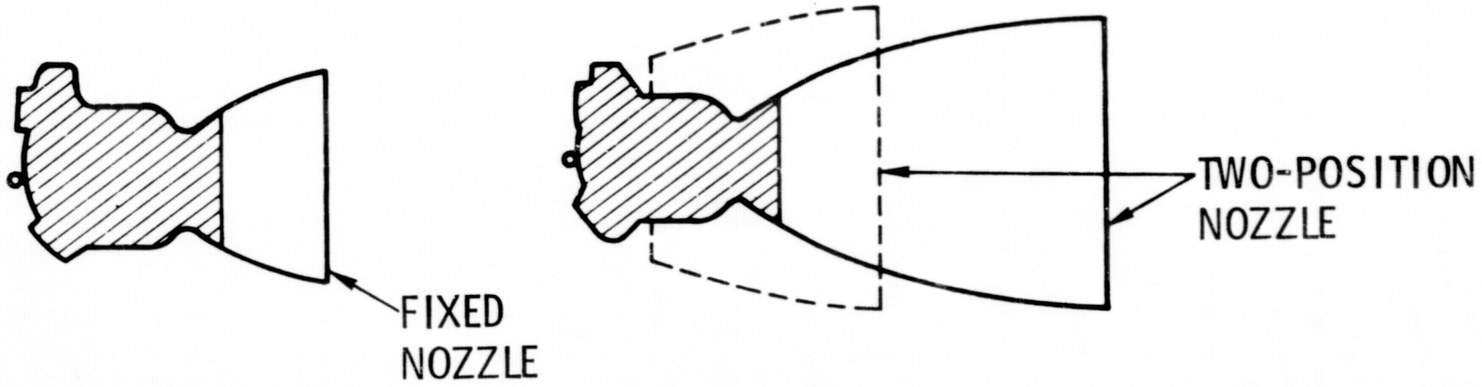

CHARACTERISTIC		BOOSTER	ORBITER
THRUST, SL	(KLB)	500	
VAC		550	576
THROTTLE	(% F_{MAX})	75	10
EXPANSION RATIO		35:1	58:1/120:1
MIXTURE RATIO		6:1	6:1
EXIT DIAMETER	(IN.)	67	122
OVERALL/STOWED LENGTH	(IN.)	124	220/127
DRY WEIGHT	(LB)	5000	5400
GIMBAL ANGLE	(DEG)	±7	±7

Figure 8.7-21. Main Rocket Engine Characteristics

Space Division
North American Rockwell

LH_2 feed line interface diameter, 16 inches

GO_2 for pressurant

GH_2 for pressurant

Note: Final schedule vehicle sizing increased the engine thrust requirement to 510,000 pounds for the booster and 590,000 pounds for the orbiter.

Propellant Feed and Pressurization System. The propellant tank pressurization system regulated pressure requirements were established to satisfy the engine NPSH requirements. The vent valve settings were also established. These values are shown in Table 8.7-14.

The booster propellant and pressurization system is illustrated in Figure 8.7-22. The booster LO_2 propellant tank is located forward of the LH_2 tank with a common bulkhead separating the propellants. The LO_2 tank contains two feed lines, 30 inches in diameter, to the engine compartment, where each line forms a semicircular manifold of the same diameter feeding 5 engines. The 30-inch LO_2 lines provide approximately 15-foot-per-second fluid velocity. The large LO_2 head provided by this configuration provides an engine inlet pressure considerably in excess of NPSH requirements. High internal pressures (near 200 psi) will be encountered at the engine/stage LO_2 interface during the end-boost maximum acceleration period. Some reduction in the diameter of the 30-inch ducts may also be possible; however, higher fluid velocities in the long LO_2 feed system may pose a serious surge problem at engine cutoff. Surge pressures may become a significant factor in the design of the LO_2 feed system, possibly more critical than the steady-state acceleration loads. The engine inlet lines from the 30-inch manifold will be 16 inches in diameter, which will reduce engine inlet fluid velocity to approximately 12 feet per second. The LH_2 feed system will consist of ten, 16-inch lines from the LH_2 tank to the engines. Normally, open 16-inch prevalves (LO_2 and LH_2) will be supplied in each of the engine inlet lines.

LO_2 and LH_2 filling and draining can be accomplished through two 8-inch systems (shutoff valve and disconnect). To preclude leaving large quantities of undrainable LO_2, it will be necessary to locate a fill and drain system at each of the 30-inch feed lines in the engine compartment. Two 8-inch systems should also be provided at the LH_2 tank in the engine compartment. Two LH_2 fill and drain systems are recommended for redundancy to assure detanking capability in case of malfunction of one system. Two 8-inch fill and drain systems for each propellant is capable of providing a 10,000-gpm LO_2 filling rate and a 20,000-gpm LH_2 filling rate based on the Saturn V Launch Complex 39 criteria. Initial evaluation indicates this loading system would be compatible with the two-hour countdown requirements for the booster and orbiter.

Table 8.7-14. Ascent Propellant Tank Pressure Requirements

Stage	Prelaunch Pressure (psia)	Regulated Pressure (psia)	Vent Valve Pressure Setting (psia)
Booster			
LO_2 tank	18-20	18-20	20-22
LH_2 tank	30-32	30-32	33-35
Orbiter			
LO_2 tank	30-32	20-22	30-32
LH_2 tank	30-32	30-32	33-35

The booster pressurization system is also illustrated in Figure 8.7-22. The LOX tank is prepressurized to 20 psia with helium from a ground supply before launch. During main-engine operation, the LO_2 tank will be pressurized by gasified oxygen (GO_2) generated by a heat exchanger on each engine.

Evaporated hydrogen is used for the LH_2 tank pressurant. The gaseous hydrogen for the LH_2 tank is taken from the engine cooling jacket supply at approximately 200 R. Tank ullage pressure was determined as follows:

LO_2 Tank. Assuming an initial LOX vapor pressure of 15 psia and a 10 F temperature rise, the end-boost LO_2 vapor pressure is estimated at 25 psia. For an NPSH of 16 feet, the engine inlet pressure must be 33 psia. Assuming an ullage pressure of 20 psia, a line pressure drop of 3 psi, and an end-boost load factor of 3.0 g, the engine inlet requirement can be met with approximately 11 feet of fluid head. This 11-foot head is estimated to be less than the available head from the end of the main feed ducts (manifold inlet) to the engine inlets. The 20-psia level is dictated primarily by structural reasons, but it will permit utilization of the LO_2 in the main feedlines.

LH_2 Tank. The sum of the NPSH and vapor pressure (assuming a 2 R temperature rise in the LH_2) at end boost is 24.5 psia. This sum at launch is 18.5 psia. The static head at launch is slightly over 2 psi and essentially zero at end boost. Assuming a 3-psi line loss and a regulation tolerance with some margin (30 to 32 psia) nominal pressure was selected for the fuel tank ullage pressure.

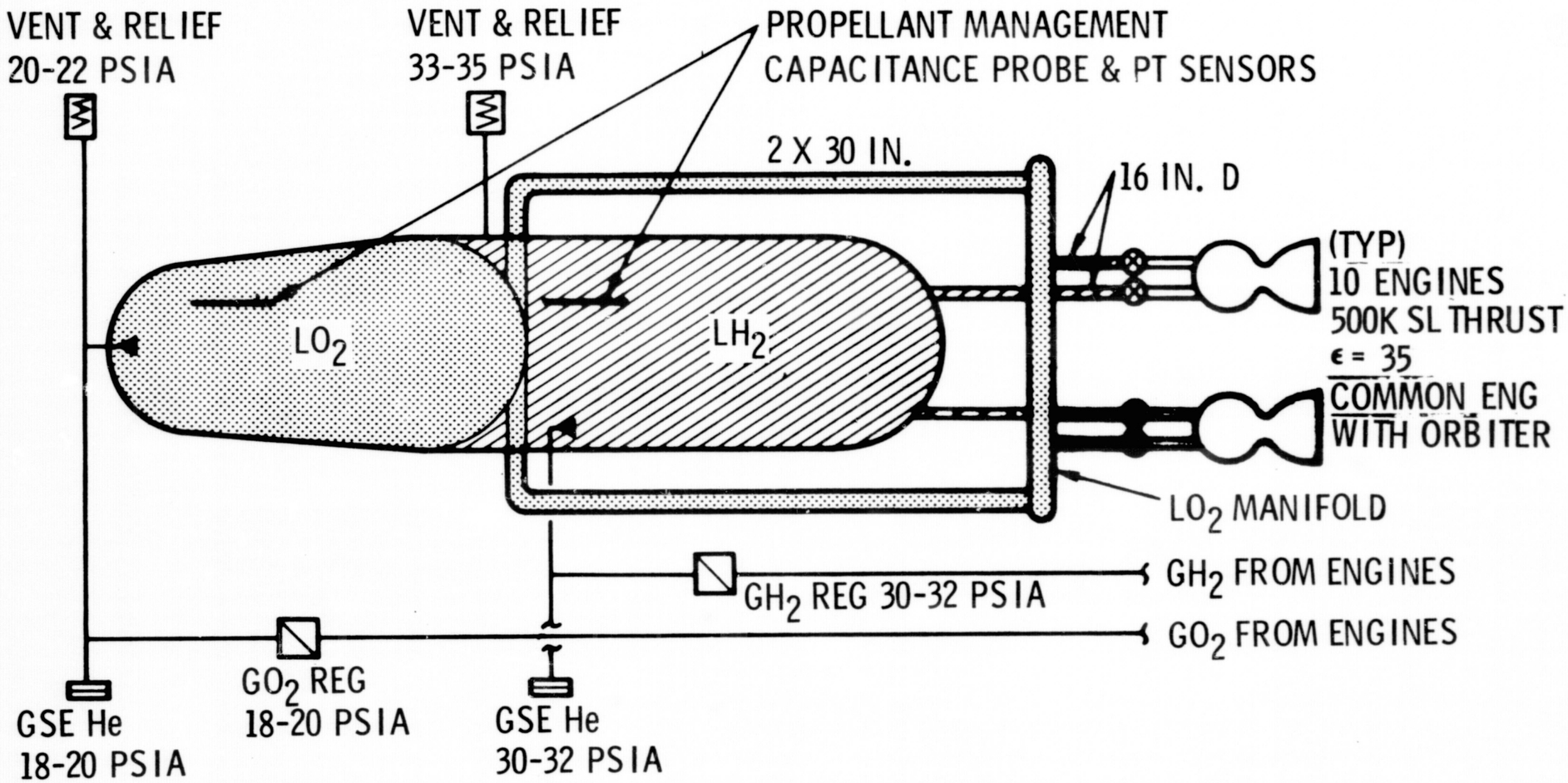

Figure 8.7-22. Booster Main Propulsion System

Space Divis.on
North American Rockwell

The mean gas space temperature at end boost was assumed to be 350 R and 160 R for the LO_2 and LH_2 tanks, respectively, to calculate pressurant weights. Prepressurization is assumed to be provided by ground supply. The fuel tank pressure will be raised from approximately 16.5 psia to (30 to 32 psia) and the oxidizer tank pressure will be raised from 15 to 18-20 psia immediately prior to launch. Pressure venting systems are required for both tanks to allow propellant loading and to protect against over-pressurization during boost.

	LH_2 Tank (psia)	LO_2 Tank (psia)
Pressurization	30-32	18-20
Venting	33-35	20-22

The LO_2 tank pressure level of 20 psia versus 32 psia for the LH_2 tank poses a possible significant structural problem. The common bulkhead will, under these conditions, be compression loaded and must be designed against collapsing. Evaluation of the additional structural weights to protect against this was considered in the tank structure analysis.

The orbiter propellant and pressurization system is illustrated in Figure 8.7-23. The orbiter main LO_2 tank is located forward with the main fuel tank located aft and separated by the cargo bay as shown. The LO_2 tank contains two feedlines 14 inches in diameter to the engine compartment and to each engine. The 14-inch lines provide approximately 15-foot-per-second fluid velocity. The same potential problems exist in the LO_2 feed system on the orbiter as on the booster, although less severe. Two 16-inch LH_2 feed ducts from the LH_2 tank connect directly to each engine inlet. The same prevalves (16 inch) are to be used on the orbiter as on the booster.

The on-orbit tanks (2-LH_2 and 1-LO_2) will be connected to the main feedlines and filling and draining of the orbiter tanks will be accomplished simultaneously with the main propellant tanks by use of the orbiter tank shutoff valves. The orbiter shutoff valves will be used for maneuvering, RCS and deorbiting operation. During these operational periods, the main propellant tanks will be isolated by prevalves which are actuated closed at the end of the main burn period. Preliminary sizing indicates a LO_2 tank volume of 450 cubic feet and the LH_2 tankage of 1,200 cubic feet. The sizing of the tank shutoff valves are estimated to be 3 inches in diameter.

The orbiter pressurization system is also illustrated on Figure 8.7-23. The ascent tank pressurization system is the same as for the booster.

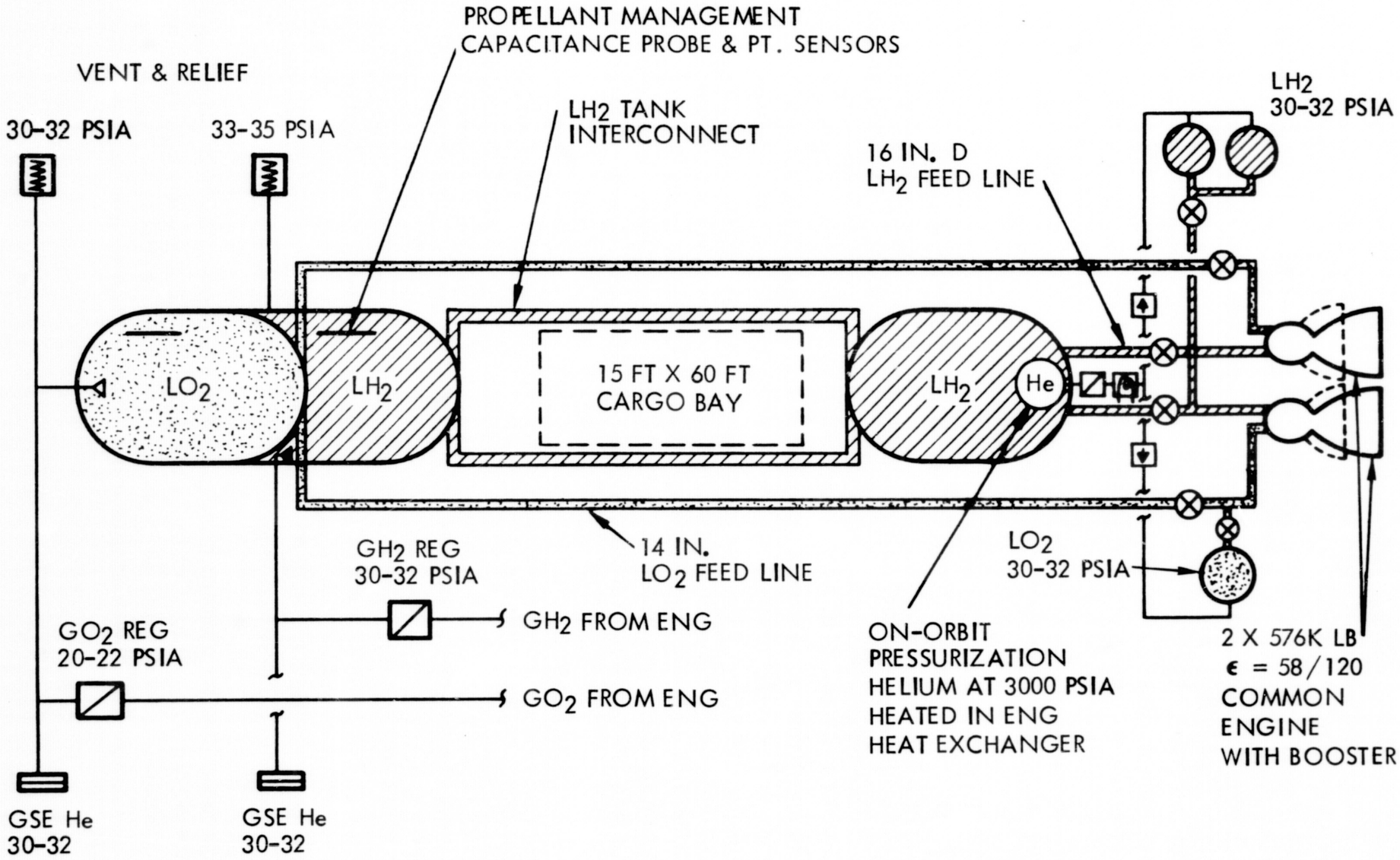

Figure 8.7-23. Orbiter Main Propulsion System

Space Division
North American Rockwell

At orbiter ignition, the load factor is essentially zero. Assuming a LO_2 vapor pressure of 16 psia, 24 psia minimum ullage pressure is required to supply 60 feet NPSH at start. To compensate for some pressure decay during first stage boost, the LO_2 tank will be prepressurized on the ground to 30 to 32 psia. After ignition, the engine inlet pressure requirement is more than satisfied by the hydrostatic head. As is the case of the booster, the orbiter LO_2 tank will be pressurized with heated GO_2 to reduce total pressurant weight. The GO_2 regulated pressure will be 20 to 22 psia. Normally the orbiter engines will be shut down as a function of velocity rather than propellant depletion; thereby causing considerable propellant residual in the tanks; however, if the need arises, LO_2 could be used down to approximately 11 feet from the engine inlet.

Evaporated hydrogen is used as the LH_2 tank pressurant. The gaseous hydrogen for the LH_2 tank is taken from the cooling jacket supply at approximately 200 F. Similar to the case with the booster fuel tank where the fluid head values are small, 30 to 32 psia is required in the orbiter main fuel tank. For engine start, the prepressurization level of helium to 30 to 32 psia will be adequate for NPSH requirements. The predicted sum of the NPSH and vapor pressure at end boost is 25 psia based on a 2 R temperature rise in the LH_2. Allowing some margin with a 3-psi line loss, 30 to 32 psia is selected as the regulated tank pressure band. Venting band will be 34 to 35 psia. Prelaunch pressurization of the LH_2 ullage with chilled helium will be adequate through the engine start transient until the vaporized LH_2 supplies regulated pressure at 30 to 32 psia to the tank. A similar system concept has been proven on the Saturn S-II LH_2 tank pressurization system.

The orbiter on-orbit system will be used over the mission period. Although definition of the total pressurant requirements cannot be defined until on-orbit venting losses are determined, it is expected that several short burns will be required for maneuvering and deorbit. It is expected that a pressure level in both oxidizer and fuel tanks will be 30 to 32 psia, the same as in the orbiter main tanks for main engine start. More exact pressurant requirements will be determined based on heat-up of the tanked propellants. Limiting propellant temperatures; e.g., (17 psia saturation) may be provided by controlled venting during non-engine operation. Then during operation, the ullage pressures would be raised to 30 to 32 psia.

The pressurization system configuration consideration and calculated pressurant weights are presented in Table 8.7-15. The booster propellant and pressurization system hardware weight is shown in Table 8.7-16. The orbiter propellant and pressurization system hardware weight is shown in Table 8.7-17.

Table 8.7-15. Pressurization System Data and Pressurant Weight

Description	Oxidizer	Fuel
Booster		
Total tankage volume (ft^3)	35,400	95,600
Propellant weight (lb)	2,228,570	371,430
Pressurant weight (lb)	6,960 (GO_2)	3,365 (H_2)
Ullage volume (ft^3)	1,770	4,780
Propellant flow rate per engine (ft^3/sec)	15	41
Orbiter (ascent burn)		
Total tankage volume (ft^3)	7,500	20,000
Propellant weight (lb)	475,700	79,300
Pressurant weight (lb)	1,485 (GO_2)	718 (H_2)
Ullage volume (ft^3)	375	845
Propellant flow rate per engine (ft^3/sec)	15	41
Orbiter (on-orbit)		
Total tankage volume (ft^3)	450	1,200
Propellant weight (lb)	30,000	5,000
Pressurization weight (lb)	90	400
Ullage and residual volume (ft^3)	22	60

Table 8.7-16. Booster Propellant and Pressurization System Hardware Weight

Description	Quantity	Weight (lb)	
		Each	Total
Prevalves, 16-in.	20	150	3,000
(VJ) LH_2 line, 16-in. D x 12 ft (10 lb/ft)	10	120	1,200
(VJ) LO_2 line, 16-in. D x 10 ft (10 lb/ft)	10	100	1,000
(VJ) LO_2 line 30-in. D x 150 ft (25 lb/ft)	2	3,750	7,500
Fill and drain valve, 8-in.	4	50	200
Fill and drain disconnect (airborne)	4	50	200
LO_2 fill and drain line, 8-in. D x 5 ft (5 lb/ft)	2	25	50
LH_2 fill and drain line 8-in. D x 15 ft (5 lb/ft)	2	75	150
Pressure manifold (engine to LH_2 tank) 5-in. D x 150 ft (3 lb/ft)	1	450	450
Pressure lines (LH_2) engine to manifold 2-in. D x 10 ft (1 lb/ft)	10	10	100
Pressure regulator (LH_2) tank)	1	50	50
Pressure check valves, 2-in.	10	10	100
LO_2 heat exchanger	10	40	400

Table 8.7-17. Orbiter ILRV Propellant and Pressurization System Hardware Weight (Main Tank)

Description	Quantity	Weight (lb)	
		Each	Total
Ascent system			
Prevalves	4	150	600
(VJ) LH_2 lines, 16-in. D x 12 ft (10 lb/ft)	2	120	240
(VJ) LO_2 lines 14-in. D x 120 ft (8 lb/ft)	2	960	1,920
Fill and drain valve, 8 lin.	2	50	100
Fill and drain disconnect, 8-in.	2	50	100
LO_2 fill and drain line, 8-in. D x 5 ft (5 lb/ft)	1	25	25
LH_2 fill and drain line 8-in. D x 15 ft (5 lb/ft)	1	75	75
Pressure manifold (engine to LH_2 tank) 3-in. D x 125 ft (1.5 lb/ft)	1	185	185
Pressure lines (LH_2) engine to manifold 2-in. D x 10 ft (1 lb/ft)	2	10	20
Pressure regulator (LH_2) tank)	1	50	50
Pressure check valves	2	10	20
Main tank vent valves	4	50	200
LO_2 heat exchanger	2	40	80
On-orbit system			
Tank shutoff valves	3	15	45
Vent valves	3	20	60
Pressure regulators	2	10	20
Helium supply tank	1	1,000	1,000
Miscellaneous lines (helium)	-	-	100

Propellant Management System. The propellant management system is used for propellant loading and engine cutoff.

The booster propellant gauging system is illustrated in Figure 8.7-24. The figure is typical for the booster and orbiter, although it shows the divided LH_2 tank as in the orbiter. The system consists of a short linear capacitance probe in the upper part of each tank and a series of point sensors located at selected levels through the length of the tank. Engine cutoff will be normally accomplished at LO_2 depletion by a pressure switch signal from the main engine thrust chamber. Secondary engine cutoff mode is by LH_2 low level point sensors at the bottom of the tank. The system operation is discussed in the following paragraphs:

The propellant gauging system (short-capacitance probes and point sensors) provide signals to the facility loading control system. Initial loading at some reduced flow rate is maintained to the 5-point sensor level. The Number-5 sensor initiates the fast fill mode (20,000 gpm LH_2 and 10,000 gpm LO_2) which is maintained into the capacitance probe range (approximately 98 percent of mission load). At the 98-percent level, flow rate is reduced and cutoff is provided at the 100-percent level by the capacitance probe signal. Topping flow (boiloff) is maintained around the 100-percent level signal.

Point sensors for the fast-fill cutoff (FFCO) and overfill cutoff (OFCO) are provided as backup to the capacitance probe system. The levels of these sensors are slightly above the maximum planned fast-fill cutoff and full load level.

Engine cutoff on the booster will not occur until propellant depletion. To achieve minimum average residuals, engine cutoff is planned as a result of LO_2 depletion. The cutoff signal is provided by engine main chamber pressure (P_c) switch dropout. This condition occurs near LOX exhaustion when LOX pump cavitation results in dropoff of discharge pressure. The first engine to indicate P_c dropout signals engine cluster shutdown.

The backup engine cutoff system is provided as a result of LH_2 liquid-level sensor signal. This cutoff mode only occurs as a result of propellant loading inaccuracy or an abnormal in-flight mixture ratio shift resulting in LH_2 depletion prior to LO_2 depletion.

It is estimated that average propellant residuals at engine cutoff are as follows:

LO_2—1/3 percent of initial total load

LH_2—1-1/2 percent of initial total load

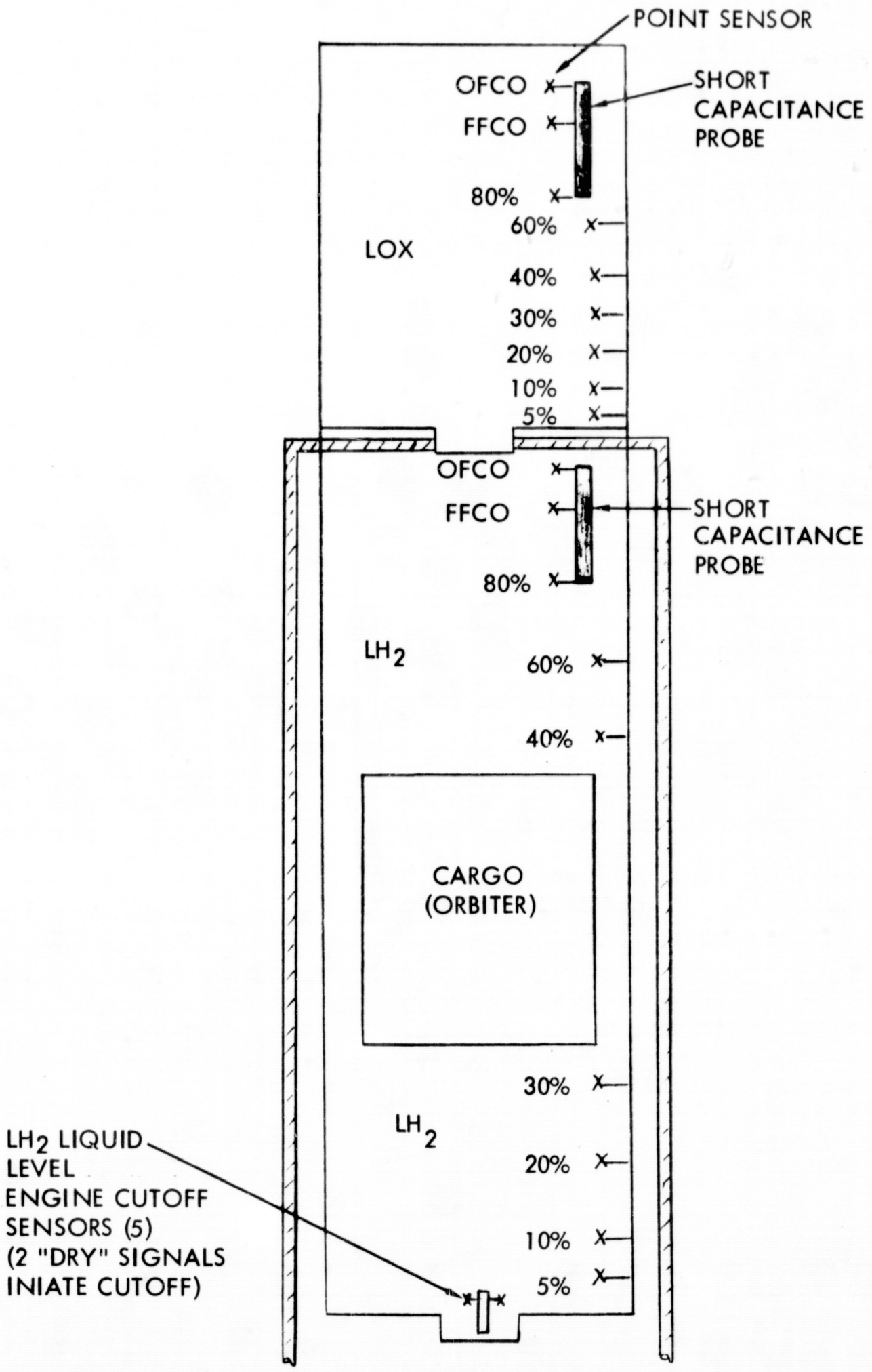

Figure 8.7-24. Preliminary Propellant Gauging System (Typical for Booster or Orbiter)

These residuals result in liquid hydrogen remaining in the bottom of the tank, but the remaining LO_2 is well down into the feed lines.

If engine cutoff (ECO) by P_c dropout near LO_2 exhaustion cannot be tolerated by the engine, it will be necessary to provide a liquid-level cutoff system (point sensor) in the LO_2 ducts. This system may increase LO_2 residuals considerably, depending on the safety margin to be provided to meet engine LO_2 pump NPSH requirements.

The orbiter propellant management system for the ascent tanks is basically the same configuration as the booster system (Figure 8.7-24).

The orbiter main tank propellant loading approach is accomplished similar to that of the booster, except that maximum filling rates are 10,000 gpm LH_2 and 5000 gpm LO_2. Filling of the on-orbit tanks is accomplished concurrently with the main tank filling.

Engine cutoff on the orbiter is normally provided by a velocity cutoff signal. (Not a part of the propellant management system.) If orbit velocity is not achieved before LO_2 depletion, the engines cut off under the same conditions as on the booster.

Preliminary evaluation indicates that an in-flight propellant utilization (PU) system is not required for either the booster or orbiter. Adequate propellant utilization to achieve minimum residuals at cutoff can be achieved by the open-loop approach. The efficiency of the open-loop concept is predicated on propellant mass loading accuracy and ability to predict in-flight engine propellant flow rates.

The closed-loop PU system is an in-flight operating system, which will control the engine mixture ratio as a function of the remaining propellants. The Saturn S-II stage, although containing a closed-loop PU system, has shown excellent results in flights where the closed loop system has been deactivated. S-II PU performance is indicated below where the PU residual is the variation from the predicted quantity of LH_2 to be remaining at engine shutdown.

Flight	PU System	PU Residuals (lb LH_2)
S-II (AS-501)	Closed-loop	+255
S-II (AS-502)	Closed-loop	+822
S-II (AS-503)	Open-loop	+186
S-II (AS-504)	Closed-loop	- 46
S-II (AS-505)	Open-loop	- 70
S-II (AS-506)	Open-loop	+385

The ILRV booster and orbiter will have an additional advantage over the Saturn as a result of multiple flights. Progressive system calibration can be obtained and refined loading masses used for each subsequent flight.

The propellant management system hardware weight is shown in Table 8.7-18. The on-orbit system was not defined, but a weight allocation is provided.

Reaction Control System

The reaction control system analysis conducted for this study was based on the use of an O_2/H_2 system as agreed upon with NASA MSC. Other candidate propellant combinations may provide attractive alternatives and should be the subject of further studies. The O_2/H_2 does provide a system with high performance, good reuse capability, and clean exhaust products; however, propellant storage and conditioning present formidable problems and considerable technology advancement is required.

The reaction control system design requirements are:

1. All subsystems shall be designed to fail operational after the failure of the most critical component without loss of design capability and fail safe after the second failure.

2. A three-axis translation system and a three-axis attitude control system will be provided for the orbiter; however, in the case of X-axis translation, it is assumed that safe operation will permit rotation of the vehicle and translation by other thrusters in the desired direction. Three-axis attitude control, only, will be provided for the booster.

Based upon the design requirements and physical properties of the selected configurations, the RCS design data are shown in Table 8.7-19. It can readily be seen that extensive moment arms or large size RCS thrusters will be required to meet the requirements. Booster RCS thrusters were located in the forward portion of the fuselage approximately 15 feet aft of the nose and on the inside of the engine nacelle as shown in Figure 8.7-25. By proper selection of moment arms and redundancy requirements a reasonable RCS thrust level was determined, and a single thrust level is compatible with all RCS requirements. A total of twenty-four 1,800-pound-thrust motors will meet the booster RCS requirements.

Table 8.7-18. Propellant Management System Weight

Component	Weight (lb)
Booster	
Capacitance probes	100
Capacitance probe electronics	60
Point sensors	20
Point sensor electronics	20
Wiring	75
Total	275
Orbiter	
Ascent Tanks	
Capacitance probes	100
Capacitance probe electronics	60
Point sensors	20
Point sensor electronics	20
Wiring	75
On-orbit tanks	
Gaging system (undefined)	100
Wiring	25
Total	400

Table 8.7-19. RCS Design Data

Vehicle	Flight Condition	Weight (lb)	Moment of Inertia (slug - ft^2 x 10^{-6})	Critical Condition	Flight Axis	Condition Torque (ft lb x 10^{-3})	Design Acceleration Rates
Booster	Post-separation	550,000	Ixx 16.7	Reentry and	Roll	147	Angular -0.5°/sec^2
	Rocket Fuel		Iyy 85.0	Coast	Pitch	750	
	Expended		Izz 94.5	Activity	Yaw	830	Translation- 0.1 ft/sec^2
Orbiter	Post-separation	835,000	Ixx 2.9	In orbit,	Roll	240	Same as above
	Rocket fuel		Iyy 29.0	one main		---	
	on board		Izz 30.9	engine out		---	
	Reentry	245,000	Ixx 2.9	----		---	Same as above
			Iyy 15.8	Reentry	Pitch	162	
			Izz 17.8	Reentry	Yaw	176	

Design of the orbiter RCS system was more complex, since pure couples are required to meet space station docking requirements. A configuration consisting of ten motors mounted forward, eight motors on the wing tips, and ten aft-mounted motors was developed as shown on Figure 8.7-26. Both booster and orbiter RCS data for thruster sizing are summarized in Table 8.7-20. Thruster geometry is tabulated below:

System Parameters	Booster	Orbiter
Thrust, lb	1800	800
P_c, psi	300	300
ϵ	20:1	30:1
De, in.	9	6.6
Le, in.	17	13.2
Wt, lb	10	6

Typical thrusters are shown on Figure 8.7-27 where both regenerative and film-cooled configurations are shown. Specific selection of either configuration will be predicated on duty cycle and installation requirements such as permissible black-wall and nozzle temperature levels.

Reaction control system propellant storage, conditioning, feed system, and thrust-chamber-pressure selection are so closely interrelated that they cannot be considered separately. Three RCS concepts identified are:

1. Low P_c thruster system with thrusters fed by residual gases remaining in the ascent propellant tanks: This system is simple and makes use of normally unusable propellant. Unfortunately, the residual propellant quantity and quality cannot be predicted accurately. For this reason and the low performance of the low P_c system for reasonable thruster sizes, this concept was not selected for study. This concept, however, should be the subject of future study trades.

2. High P_c thruster system with propellant stored as a low-pressure liquid, conditioned (pumped and vaporized) and stored as a gas in high-pressure accumulators for subsequent distribution to the

REQUIREMENT
● 0.5°/SEC^2 ROTATION ● FULL CONTROL - ONE FAILURE ● SAFETY - TWO FAILURES
CONFIGURATION
● O_2/H_2 ● 24 THRUSTERS (1800 LB/300 PSIA P_C) ● MODULAR INSTAL ● LIQ SUPPLY/PROP. COND/GAS STOR
WEIGHT
● 2230 LB HARDWARE ● 1800 LB PROPELLANT

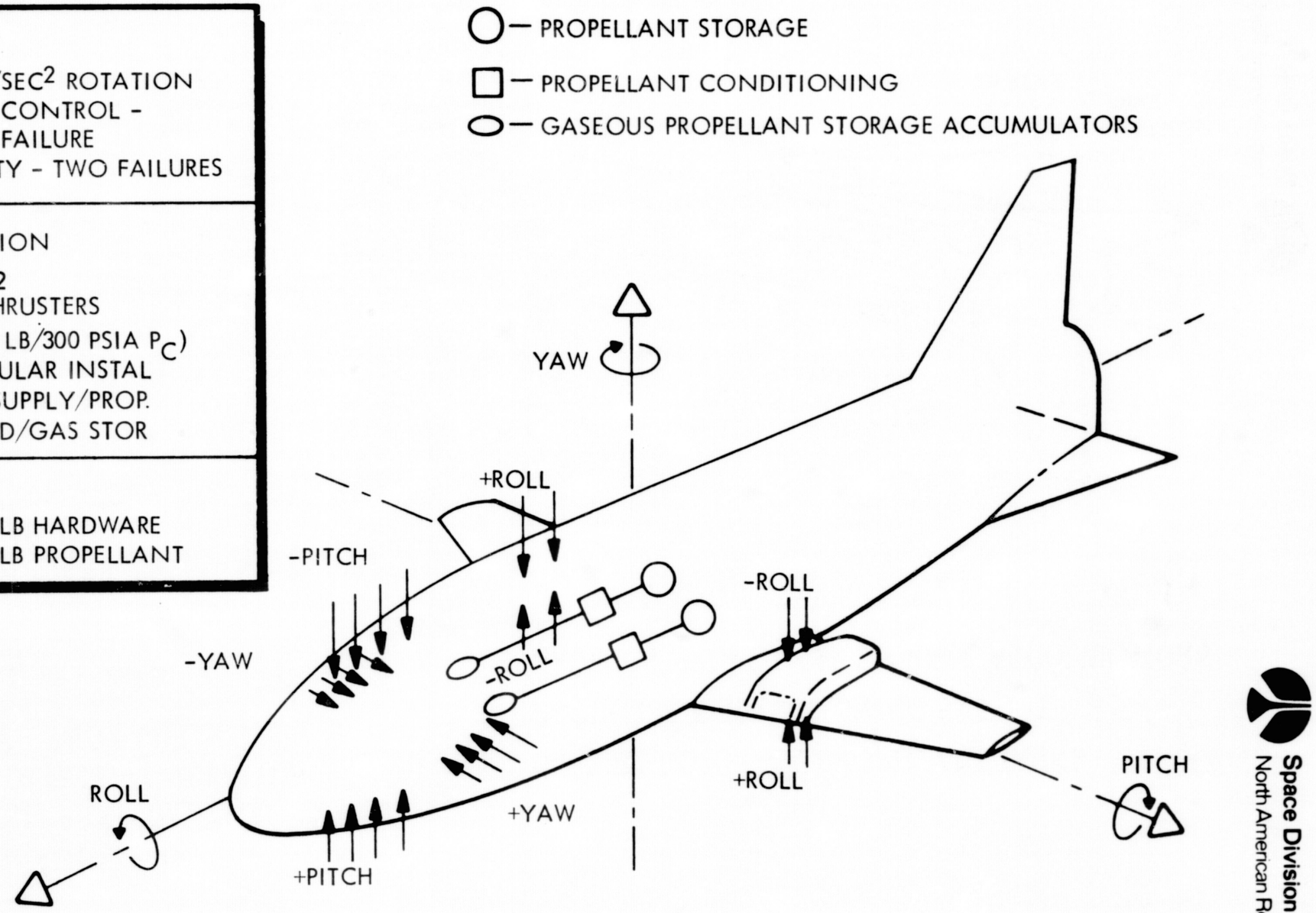

Figure 8.7-25. Booster RCS Configuration

Space Division
North American Rockwell

REQUIREMENT

- 0.5°/SEC^2 ROTATION
- 0.1 FT/SEC^2 TRANSLATION
- FULL CONTROL - ONE FAILURE
- SAFETY - TWO FAILURES

CONFIGURATION

- O_2/H_2
- 28 THRUSTERS (800 LB/300 PSIA-PC) MODULAR INSTAL
- LIQ SUPPLY/PROP.COND/GAS STOR

WEIGHT

- 4000 LB HARDWARE
- 4000 LB PROPELLANT

○ ON-ORBIT STORAGE PROPELLANT TANKS

□ PROPELLANT CONDITIONING SYSTEM

⬭ GASEOUS PROPELLANT STORAGE ACCUMULATORS

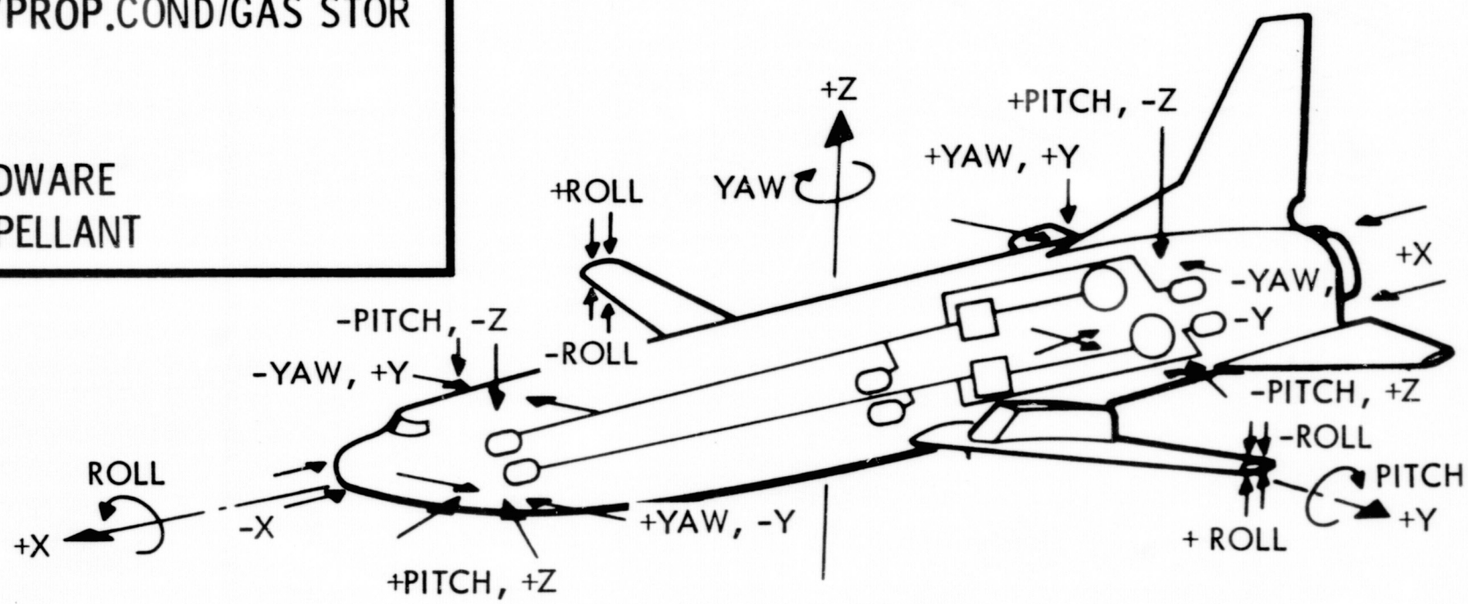

Figure 8.7-26. Orbiter RCS Configuration

Space Division
North American Rockwell

Table 8.7-20. RCS Thruster Sizing

Vehicle	Axis	Moment Arm (ft)	Thrust Level (lb)	Resulting Thruster Complement and Moment Arm	Remarks
Booster	Roll	30	5,000	8 - 1800 lb @30 ft	Meet engine-out requirements. However, will not produce pure couples.
	Pitch	155	4,850	8 - 1800 lb @155 ft	
	Yaw	155	5,350	8 - 1800 lb @155 ft	
Orbiter	Roll	135	2,400	8 - 800 lb @135 ft	Four motors canted to avoid heat shield penetration.
	Pitch	150	2,160	8 - 800 lb @150 ft	
	Yaw	150	2,340	8 - 800 lb @150 ft	
	Y-axis Translation	---	--	4 - 800 lb ---	

Note: The critical roll torque level is based upon a single main engine failure, the second engine operating at maximum thrust and gimbal angle. Obviously, this condition was not met by the selected system; however, a maximum thrust and gimbal angle of four degrees can be controlled by the selected system.

REGENERATIVE COOLED

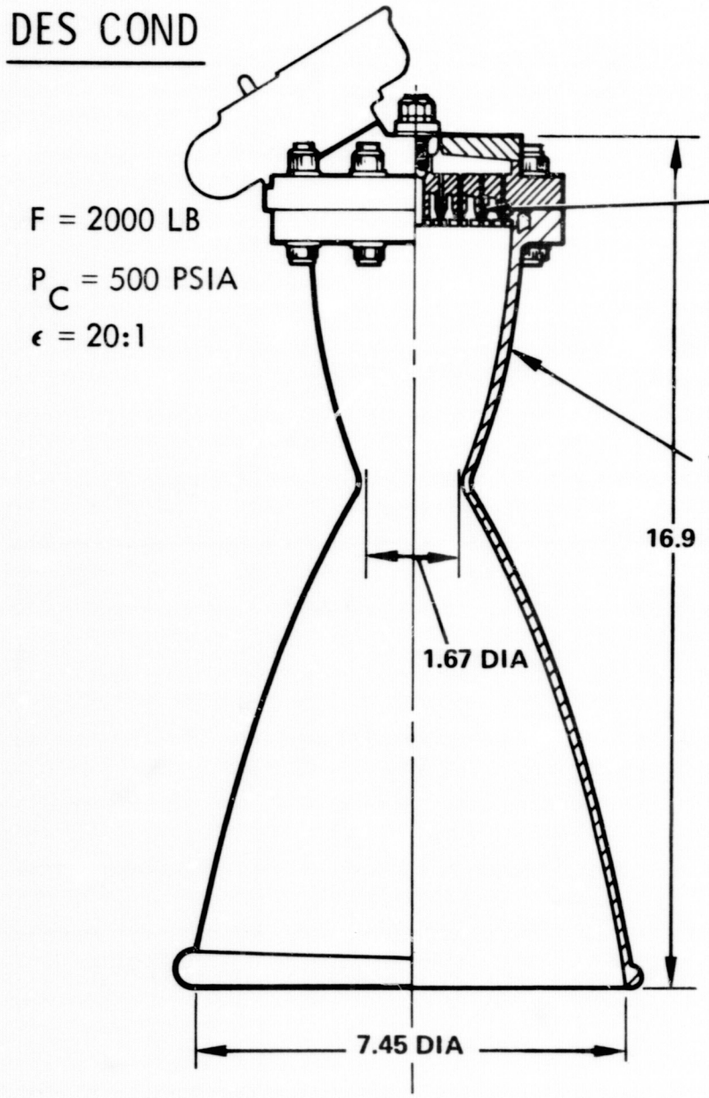

RADIATION COOLED

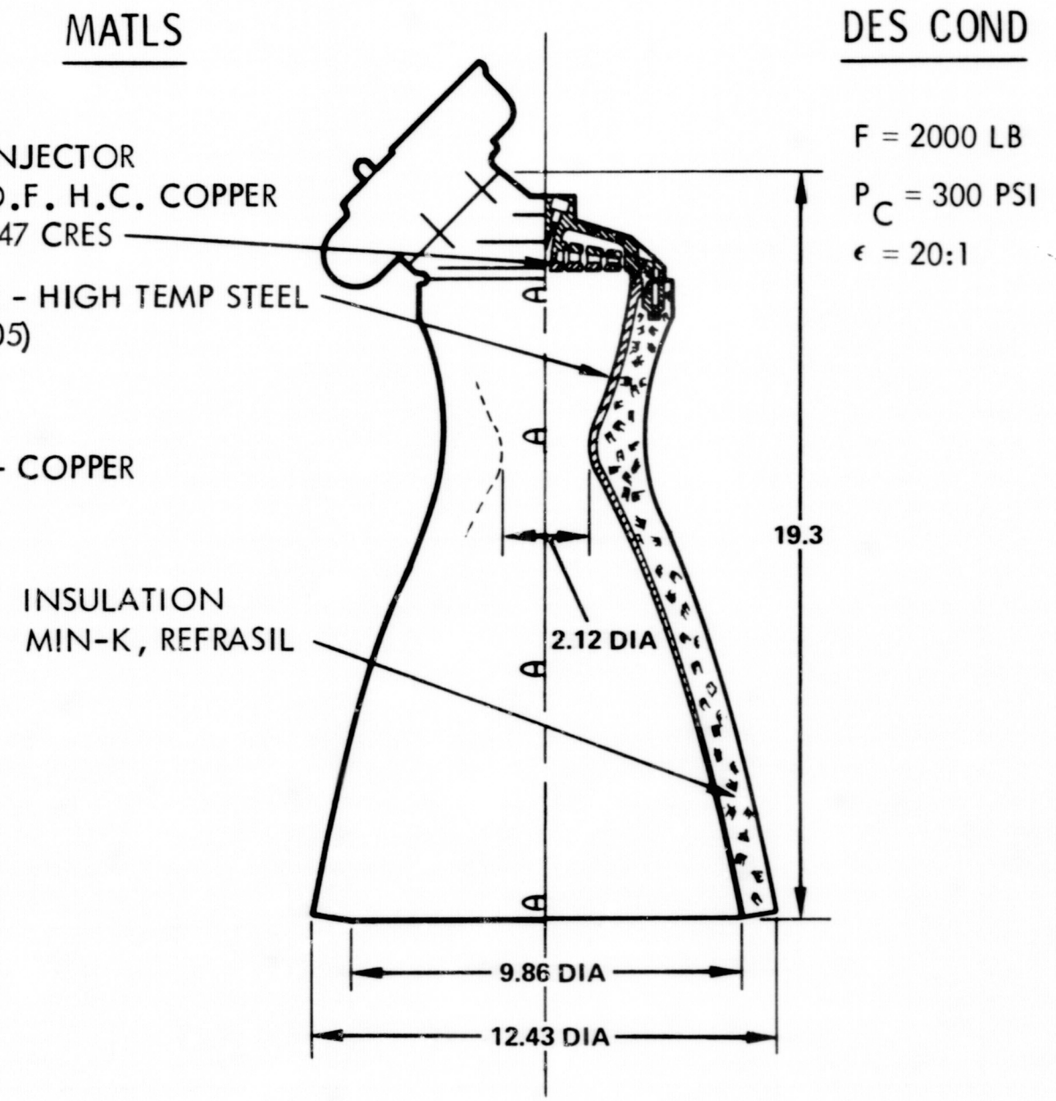

Figure 8.7-27. Candidate Thruster Configurations and Materials

Space Division
North American Rockwell

various thrusters: This is a feasible system for both the orbiter and booster. Orbiter propellant storage can be in the on-orbit propellant tankage. Propellant orientation control is required for zero g operation. This concept, which was selected for further study, is illustrated in Figure 8.7-28.

3. High P_c thruster system using gaseous propellant from the ascent propellant tanks: The gases are compressed and stored in high-pressure accumulators for subsequent distribution to the various thrusters. This system is illustrated in Figure 8.7-29. This concept was not analyzed because it was identified late in the study; however, it should be considered in further studies.

A pump fed GO_2/GH_2 RCS system schematic for the orbiter is shown in Figure 8.7-30. Accumulators store high-pressure gaseous propellants for distribution to the thrusters. The accumulators are sized to contain 150 pounds of propellant. This quantity of propellant is selected to meet the RCS entry requirement in the event of a dual pump failure. The accumulators are recharged by the propellant conditioning system. Accumulator gases are supplied to gas generators (GG). The GG gases are the working fluid to drive the turbine pumps that pressurize the liquid propellant. The high-pressure liquid propellants are vaporized in heat exchangers which use GG gases as the heat source. The vaporized propellants are then stored in the accumulators.

The orbiter on-orbit propellant tanks will be used to store the RCS propellant. For this vehicle, 4000 pounds of propellant is needed. Use of this particular tankage will provide RCS propellant throughout the duration of a normal mission. A capillary screen propellant retention system is used as shown on Figure 8.7-30 to locate propellant at the feedout ports.

Optimization of RCS engine chamber pressure (P_c) was primarily based upon its impact on system installation factors and weight. Typical engine geometry and weight variation with engine P_c is shown on Figure 8.7-31. It can readily be seen that low P_c (20 psi) yields a substantial weight penalty over a higher P_c (300 psi) by a factor of two for a 3000-pound-thrust engine; and when 28 engines are used, this penalty becones excessive. Similarly, engine exit diameters and lengths vary by a factor approaching 2.25 for similar P_c and $\epsilon = 20$ engines.

A specific RCS propulsion module was optimized as illustrated by the following example. Consider a module of ten 500-pound-thrust engines serviced by a single set of high-pressure accumulators. These two components provide the major contribution to the RCS system weight.

- ASSUMPTIONS:
  - PROPELLANT STORED IN ON-ORBIT TANK (LIQUID STATE)
- PROBLEM AREAS:
  - LIQUID LOCATION CONTROL IN ON-ORBIT TANKS
  - CONDITION OF PROPELLANT AT PUMP INLET
  - ENERGY SOURCE FOR H-X & PUMP DRIVE

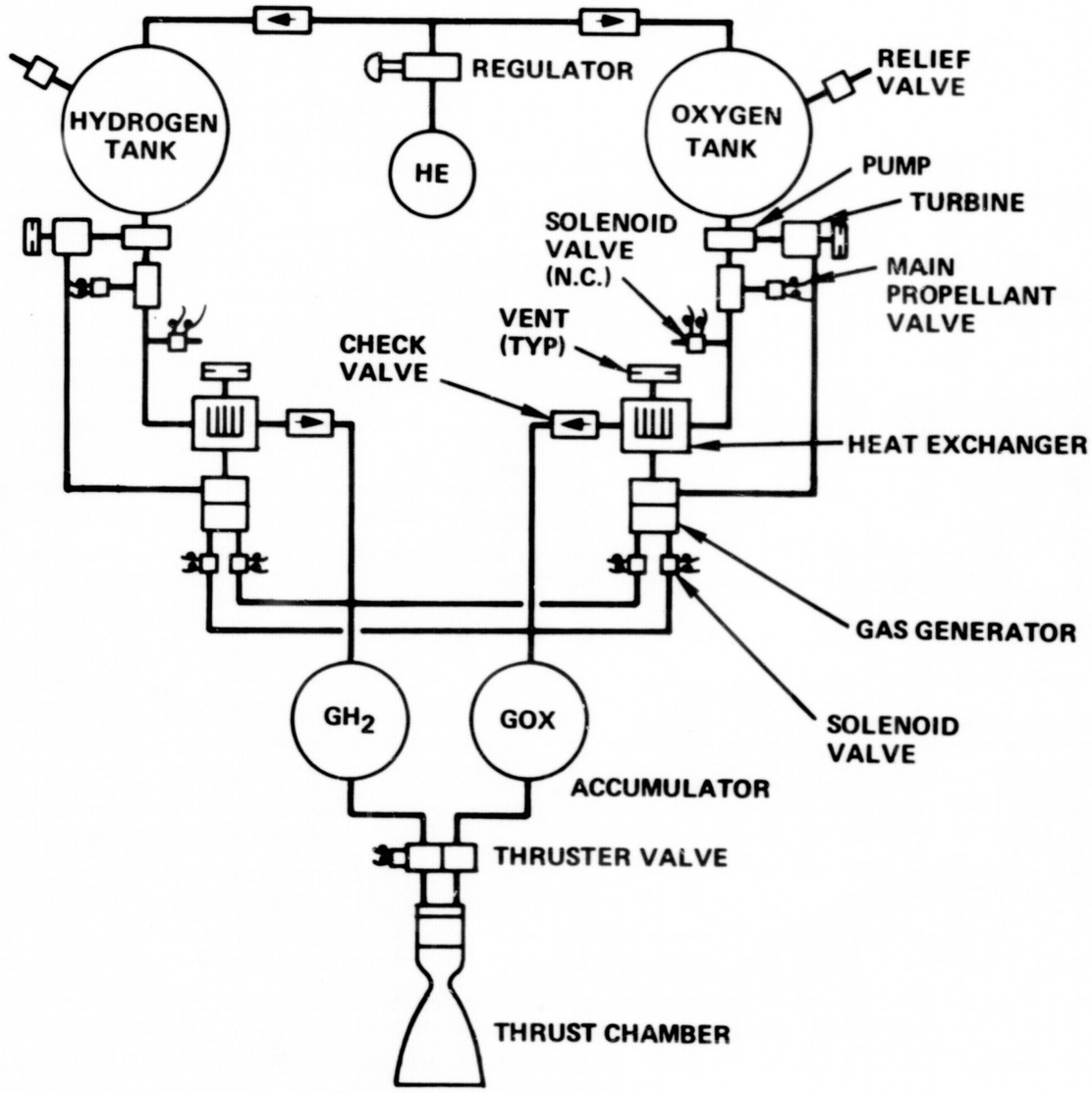

Figure 8.7-28. Typical Liquid- and Pump-Fed Propellant Conditioning System

- ASSUME:
  - PROPELLANT STORED IN MAIN TANKS (GASEOUS STATE)
- PROBLEM AREAS:
  - LIQUID LOCATION CONTROL IN MAIN TANKS (RESIDUALS)
  - PRESSURANT DILUTION OF PROPELLANT
  - PROPELLANT CONDITION AT COMPRESSOR INLET
  - ENERGY SOURCE TO DRIVE COMPRESSOR
  - MAIN PROPELLANT SYSTEM LEAKAGE
  - LONG TERM PROPELLANT STORAGE & THERMAL CONTROL

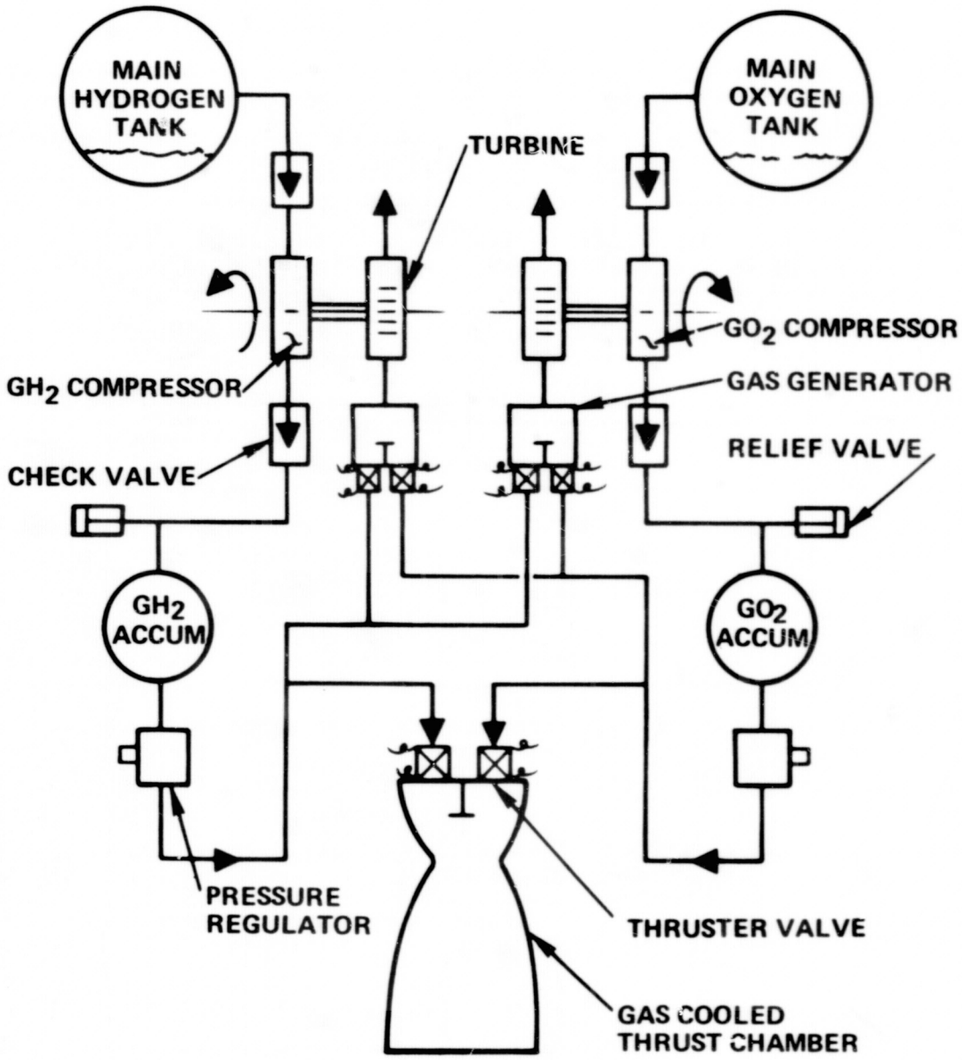

Figure 8.7-29. Typical Gas and Turbo-Compressor Propellant Conditioning System

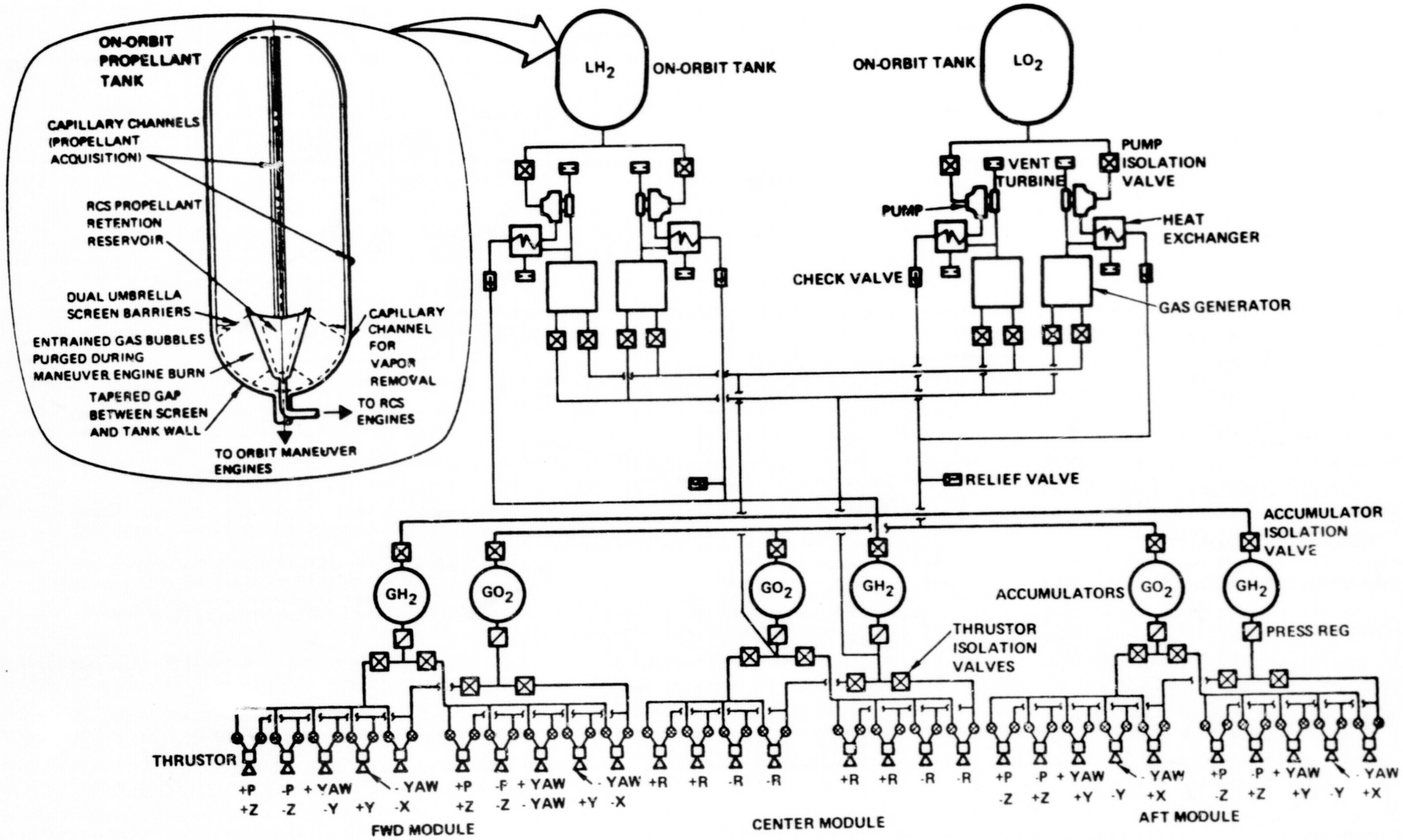

Figure 8.7-30. RCS System Definition

Space Division
North American Rockwell

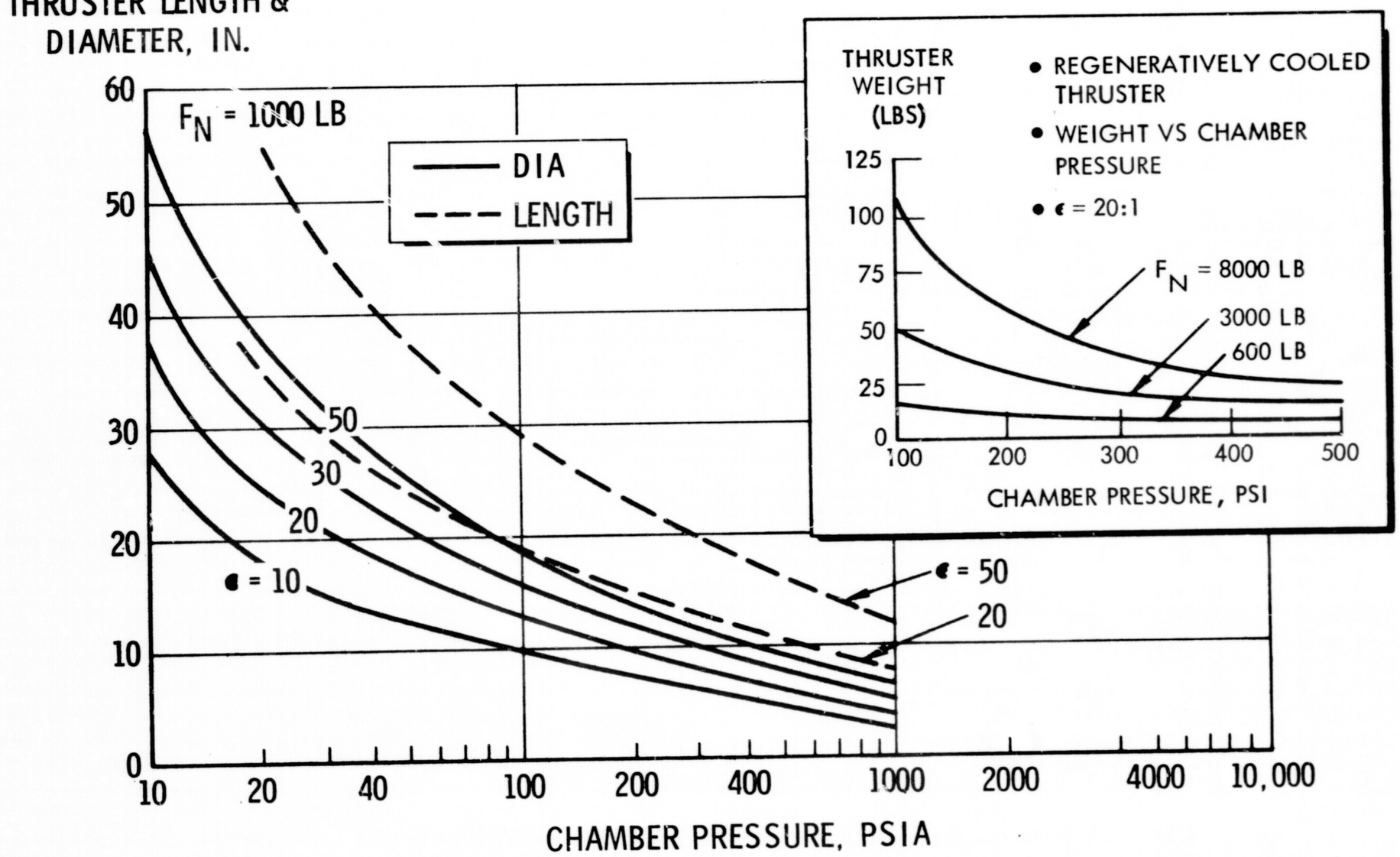

Figure 8.7-31. Effect of Chamber Pressure on Engine Characteristics

Figure 8.7-32 shows the variation of RCS module weight with chamber pressure for a fixed size accumulator. The selected system uses steel and aluminum for oxygen and hydrogen tanks, respectively, and optimizes at engine chamber pressure slightly in excess of 300 psi.

The minimum permissible accumulator tank pressure was determined by estimating losses for the injector, regulator, and line as shown by the following relationship.

$$P_{min} = 1.3\ P_c + \Delta P_{reg} + \Delta P_{lines}$$

$$P_{min} = 1.3\ (300) + 60 + 50 = 500\ psi$$

The maximum storage tank pressure was initially set at three times the accumulator minimum pressure level; hence, P_{max} = 1500 psia. Subsequently, a separate study indicated optimization of RCS system weight and accumulator maximum gas pressure to occur at slightly over P_{max} = 1000 psia as shown on Figure 8.7-33. Since the total system weight is not affected, the accumulator maximum pressure was maintained at 1500 psia.

The RCS systems weights are presented in Tables 8.7-21 and 8.7-22.

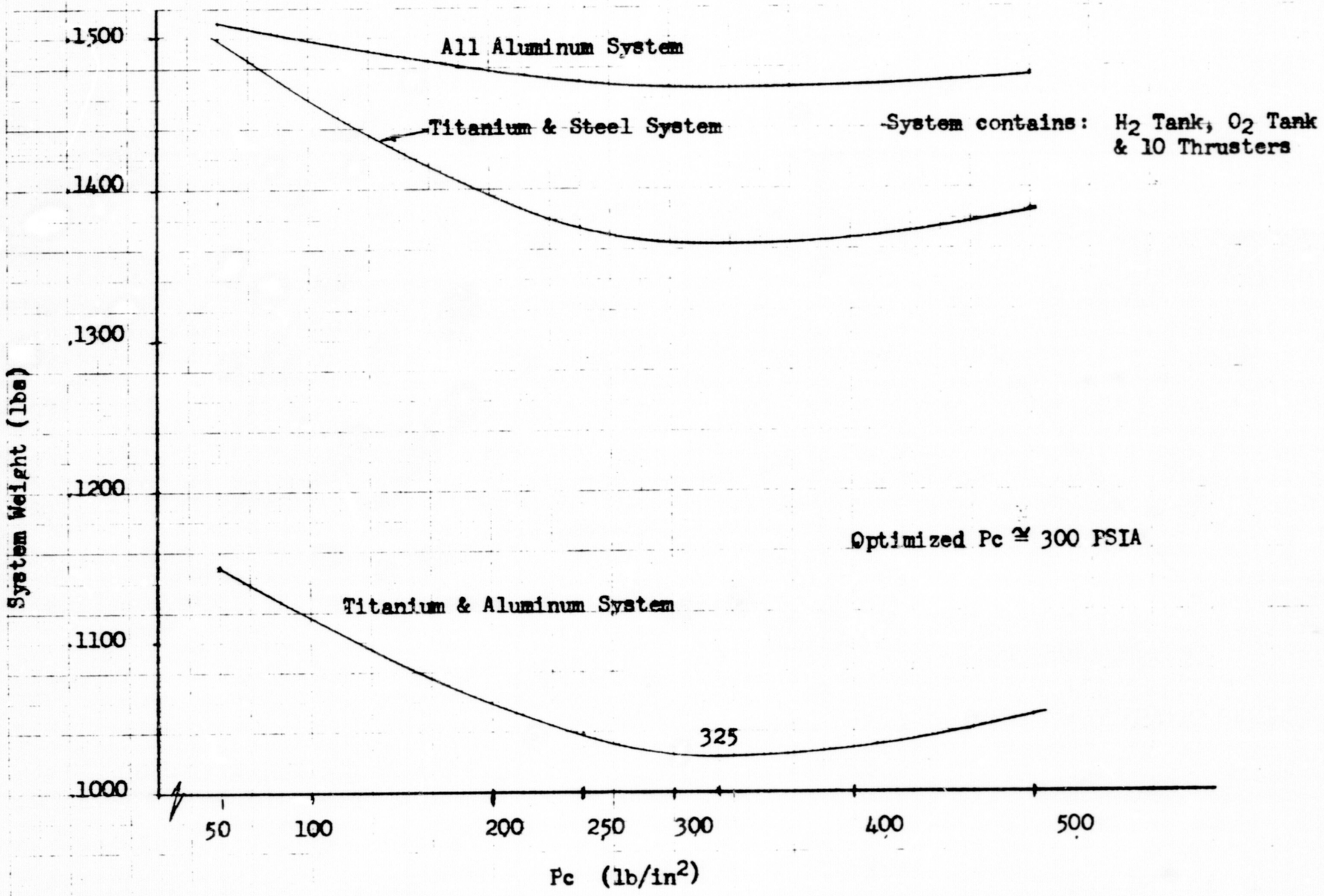

Figure 8.7-32. Optimization of Chamber Pressure

ACCUM SIZING CRITERIA
GH_2 = 64.5 LB IN 3 TI TANKS AT 300°R
GO_2 = 257.5 LB IN 3 AL TANKS AT 400°R,
(DELIVERABLE QUANTITIES~ TOT REQ'D FOR RCS DURING DEORBIT)

WTS INCLUDE
1. COMPONENTS
2. ACCU RESIDUALS
3. I_{SP} DEGRADATION

PROPELLANT DELTAS

P_C	I_{SP} DEL	I_{SP} EFF
PSIA	SEC	SEC
100	414	383
300	423	393
500	432	401

F_N = 2000 LB

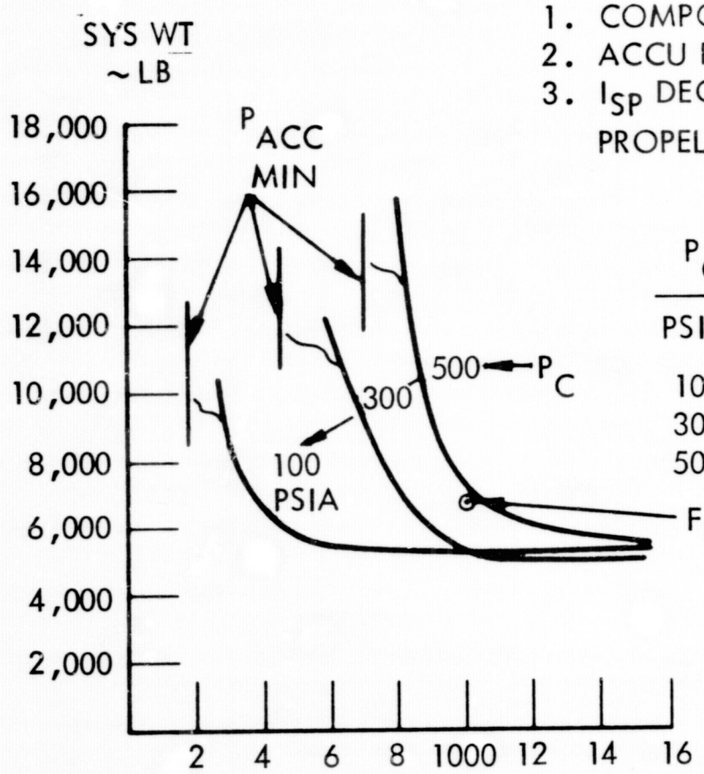

PUMP INLET TEMP
T_{O_2} = 167°R
T_{H_2} = 40°R

ROT MACH SIZING CRITERIA
4 ENG FLOW RATE
PER PUMP/TURB/GG

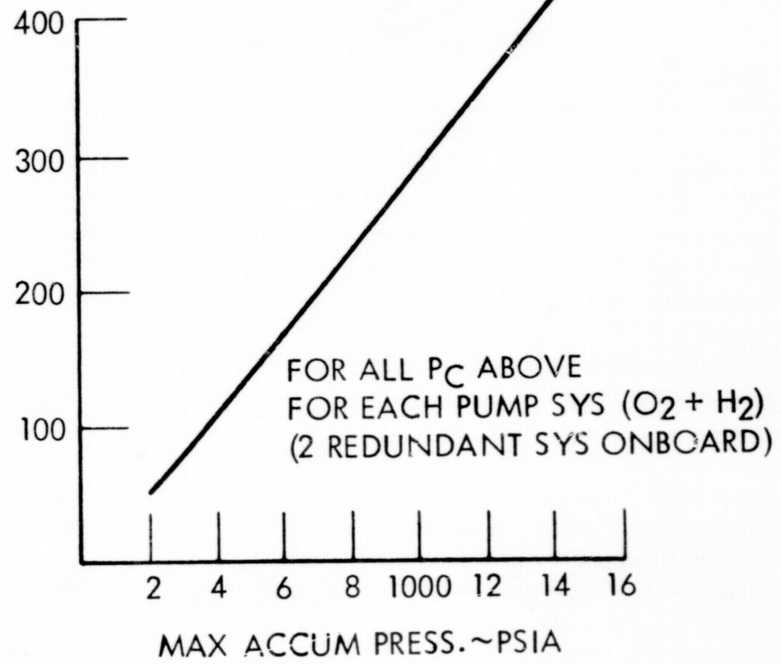

Figure 8.7-33. Orbiter Accumulator Pressure Optimization

Space Division
North American Rockwell

Table 8.7-21. Orbiter RCS System Weight

Item Description	Wt/Item (lb)	No. of Items	Total Item Wt/Vehicle (lb)
Engines (incl. valves)	6	28	(168)
Propellant storage (accumulators)			(3039)
O_2 tanks	721 Steel	3	2163
H_2 tanks	262 Al	3	786
Valves (O_2 & H_2)	15	6	90
Propellant feed & conditioning			(453)
Turbine, O_2	15	2	30
H_2	10	2	20
Pumps, O_2	10	2	20
H_2	7	2	14
Isolation valves O_2	3.9	6	24
H_2	3.4	6	20
Pressure regs O_2	41	3	123
H_2	34	3	102
H-X	20	2	40
Gas generator	6	2	12
Check valves O_2	8.3	3	25
H_2	7.7	3	23
Total			3660

Table 8.7-22. Booster RCS System Weight Estimate

Item Description	Wt/Item (lb)	No. of Items	Total Weight of Items
Engines (incl. valves)	10	24	(240)
Propellant storage (cryo)			(177)
O_2	49	1	49
H_2	124	1	124
Vent	2	2	4
Propellant feed & conditioning			(574)
Turbine, O_2	25	2	50
H_2	17	2	34
Pumps O_2	17	2	34
H_2	12	2	24
Isolation valves O_2	6.5	6	39
H_2	6.5	6	39
Pressure regs O_2	60	2	120
H_2	50	2	100
H-X	35	2	70
Gas generator	10	2	20
Check valves O_2	12	2	24
H_2	10	2	20
Accumulators (Hi Pc gas) (200 lb)			(632)
O_2	165	1	165
H_2	467	1	467
Total			1623

Turbojet System

Turbojet Engines. The booster has airbreathing propulsion for cruise back to landing site, go-around, and landing. The orbiter has airbreathing propulsion for go-around and landing. Airbreathing propulsion systems will provide ferry capability for both the booster and orbiter.

The booster uses four JT9D-15 turbofan engines, as illustrated in Figure 8.7-34A. The JT9D-15 is currently being produced for use on the Boeing 747 commercial transport. A pair of turbojets are installed in a nacelle on each top side of the wing. Inlet doors are provided for ascent protection. To provide a 310-n.m. cruise capability and two go-arounds, 57,800 pounds of JP-type fuel is provided. The payload growth potential of using H_2 fuel is shown in Figure 8.7-34A. Estimated engine performance for maximum continuous power, pressure recovery of 0.98, and ΔSFC accounting for power extraction is shown in Figures 8.7-35 and 8.7-36.

The orbiter uses four JT3D-7 turbofan engines, as illustrated in Figure 8.7-34B. The JT3D-7 is currently being used in the Boeing 707 and 720B and Douglas DC-8 commercial transports. Similar to the booster, a pair of engines is installed in a nacelle on the top side of each wing. Inlet doors are provided for ascent protection. Engine compartment environmental control is provided for orbital stay time. To provide for engine-idle to landing and two go-arounds (12 minutes at go-around power) 4650 pounds of JP type fuel is provided. The payload growth potential of high T/W engine on the orbiter is shown in Figure 8.7-34B.

Estimated JT3D-7 installed engine data for maximum continuous and maximum cruise power settings versus Mach number and altitude are shown in Figures 8.7-37 through -39. The engine performance presented here were developed for use by the aerodynamics and flight mechanics personnel to establish the cruise back altitude, performance, and vehicle propellant weight requirement. Typical turbojet start envelope is shown in Figure 8.7-40.

Fuel System. The following basic design criteria and assumptions were the basis for synthesis of fuel systems to accommodate launches and orbiter vehicle airbreathing propulsion systems.

1. Booster pump pressure feed operation shall provide minimum pressure at the engine inlet of fuel true vapor pressure plus 5 psi.

2. If fuel booster pumps are inoperative, suction feed operation shall provide emergency fuel delivery throughout normal propulsion operating envelope.

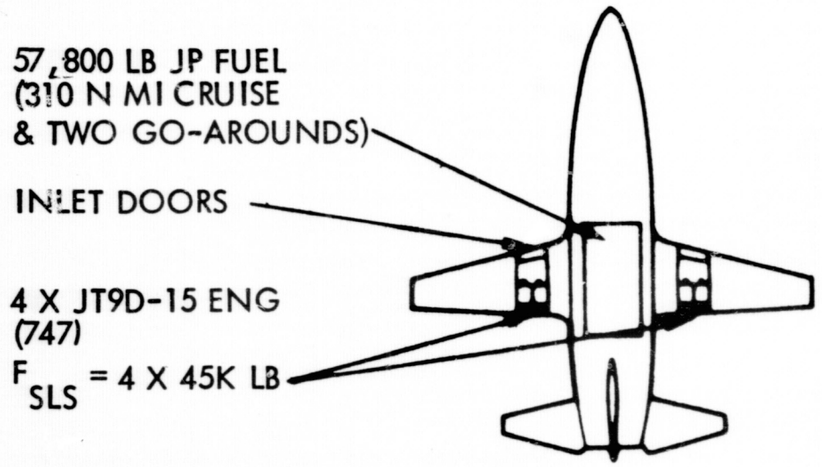

GROWTH POTENTIAL -
H_2 FUEL REQ'D APPROX 28% OF JP
PAYLOAD INCREASE ≈ 5500 LB

A. BOOSTER

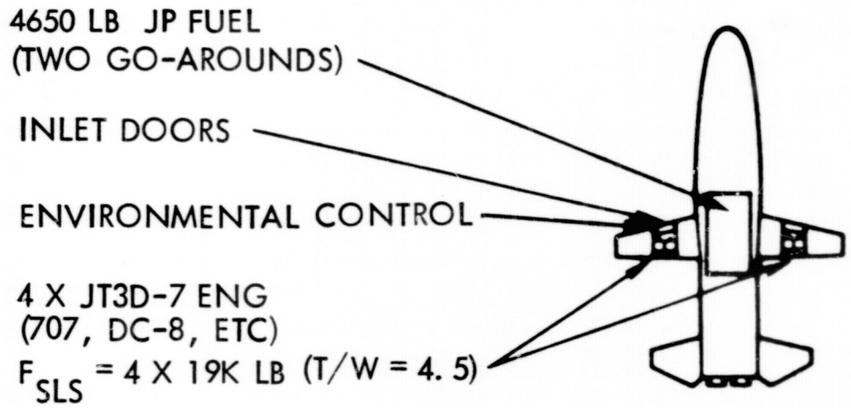

GROWTH POTENTIAL -
HIGH THRUST/ENG WT (T/W ≈ 15)
PAYLOAD INCREASE APPROX 10,500 LB

B. ORBITER

Figure 8.7-34. Turbojet Propulsion System

JT9D-15 Turbofan

We = 8370 lbs

Max. Cont. Pwr.
H_2/Ho = .98%
Hpx = SFC = .03
Fuel = JP4

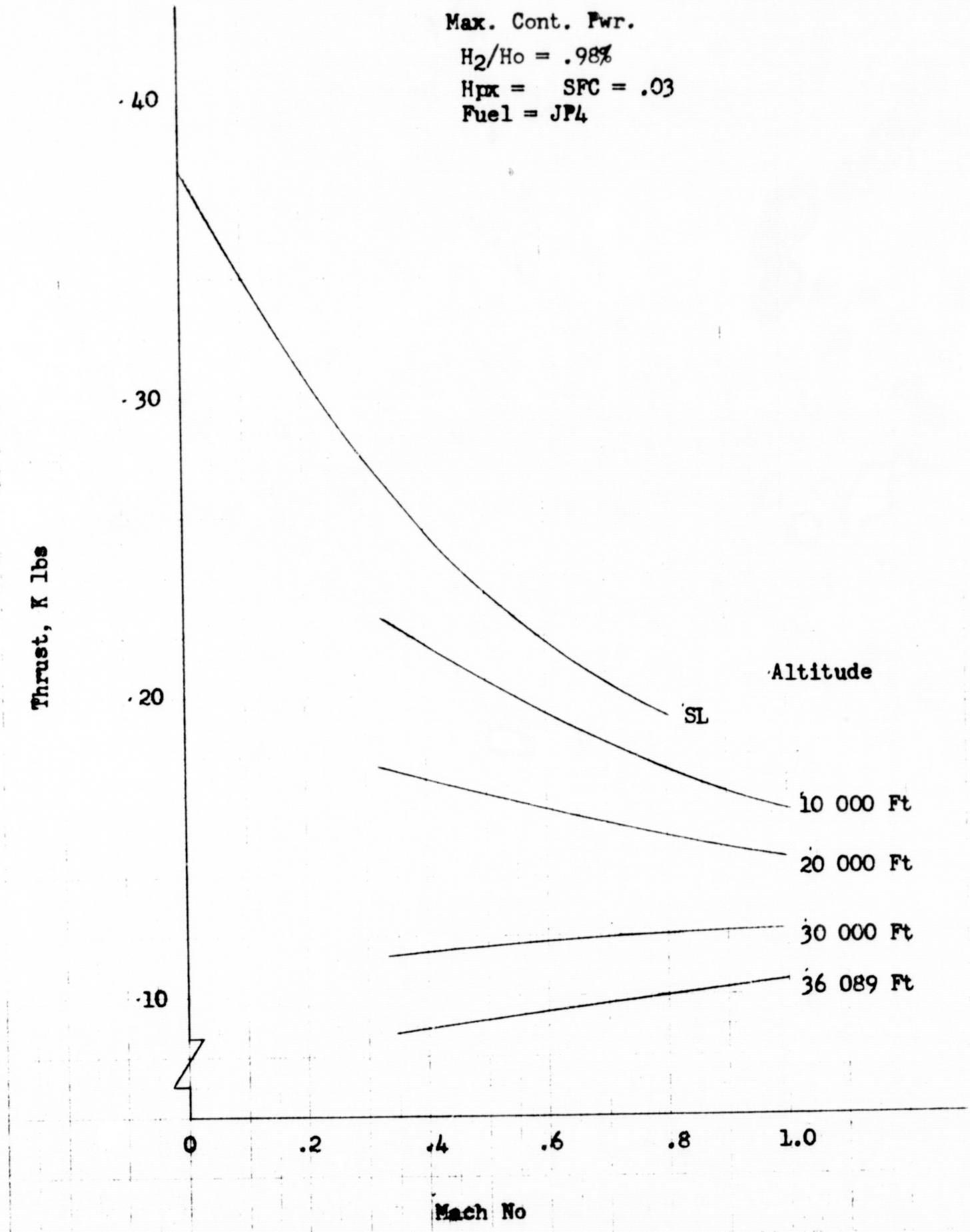

Figure 8.7-35. Estimated JT9D-15 Turbofan Engine Performance, Thrust Versus Mach Number

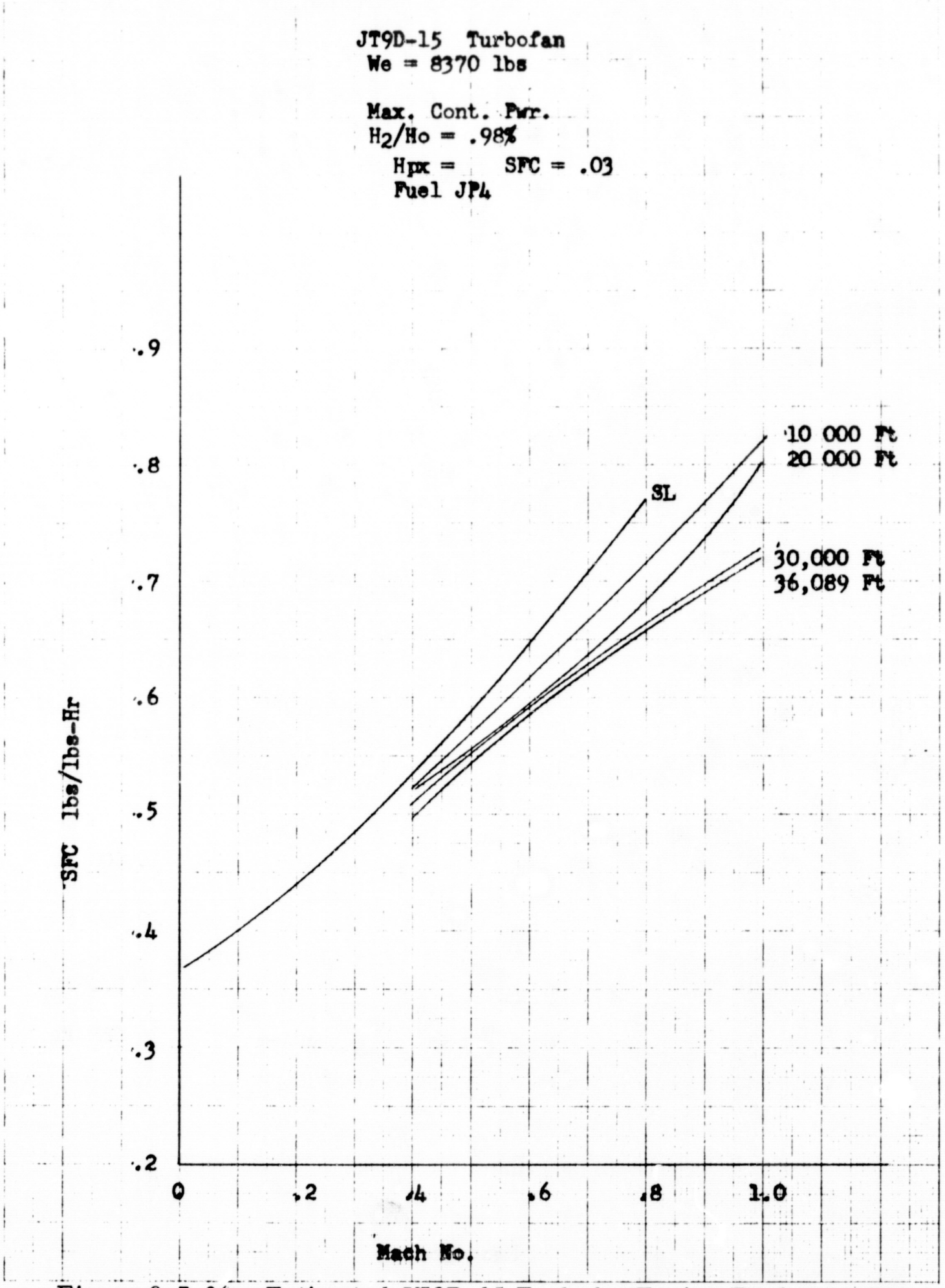

Figure 8.7-36. Estimated JT9D-15 Turbofan Engine Performance, SFC Versus Mach Number

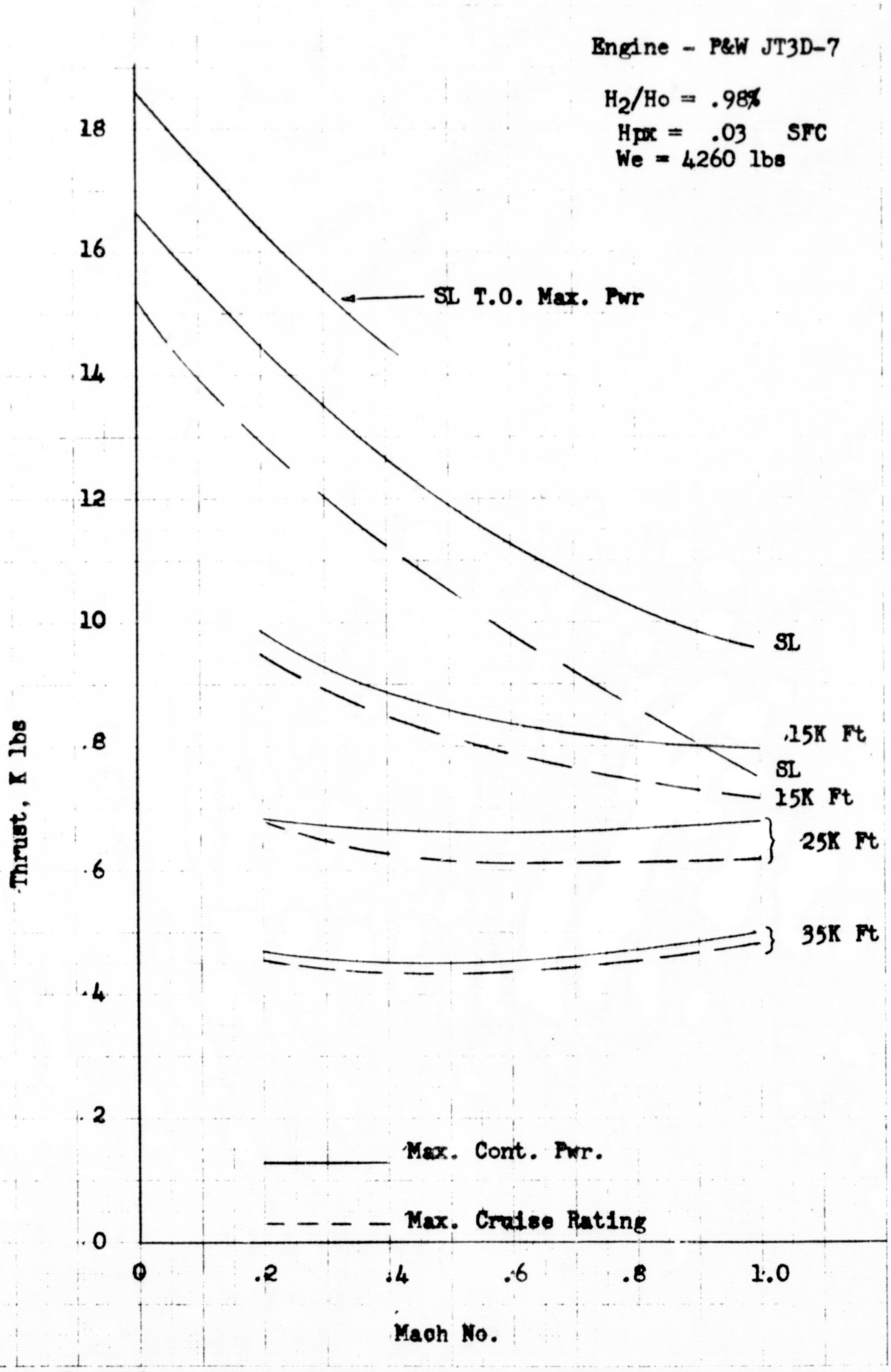

Figure 8.7-37. Estimated Pratt & Whitney JT3D-7 Engine Performance, Thrust Versus Mach Number

Engine - P&W JT3D-7

H_2/Ho = .98%
Hpx = .03 SFC
We = 4260 lbs

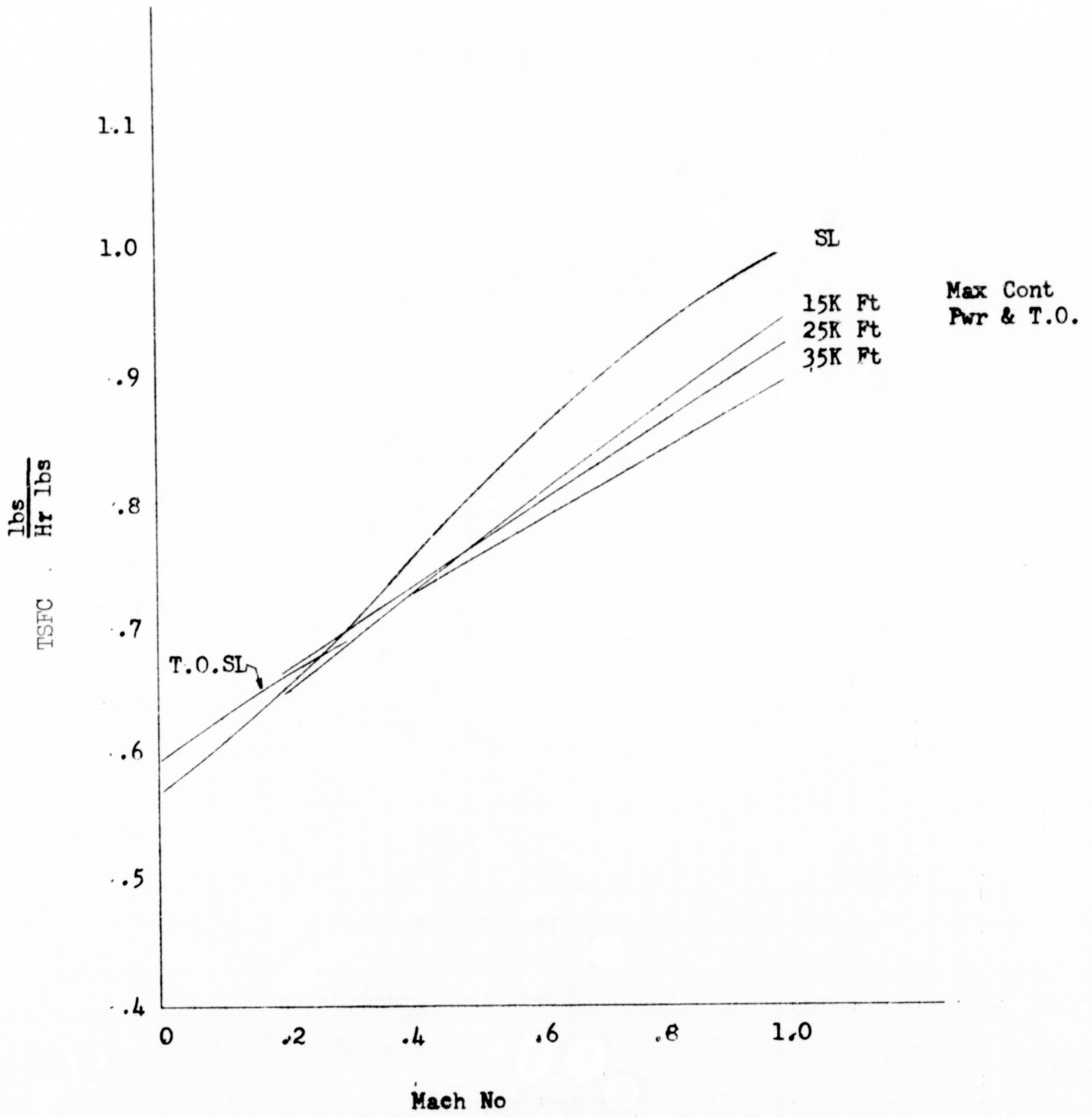

Figure 8.7-38. Estimated Pratt & Whitney JT3D-7 Engine Performance, TSFC Versus Mach Number

Space Division
North American Rockwell

Engine - P&W JT3D-7

H_2/H_o = .98
H_{px} = .03 SFC
We = 4260 lbs

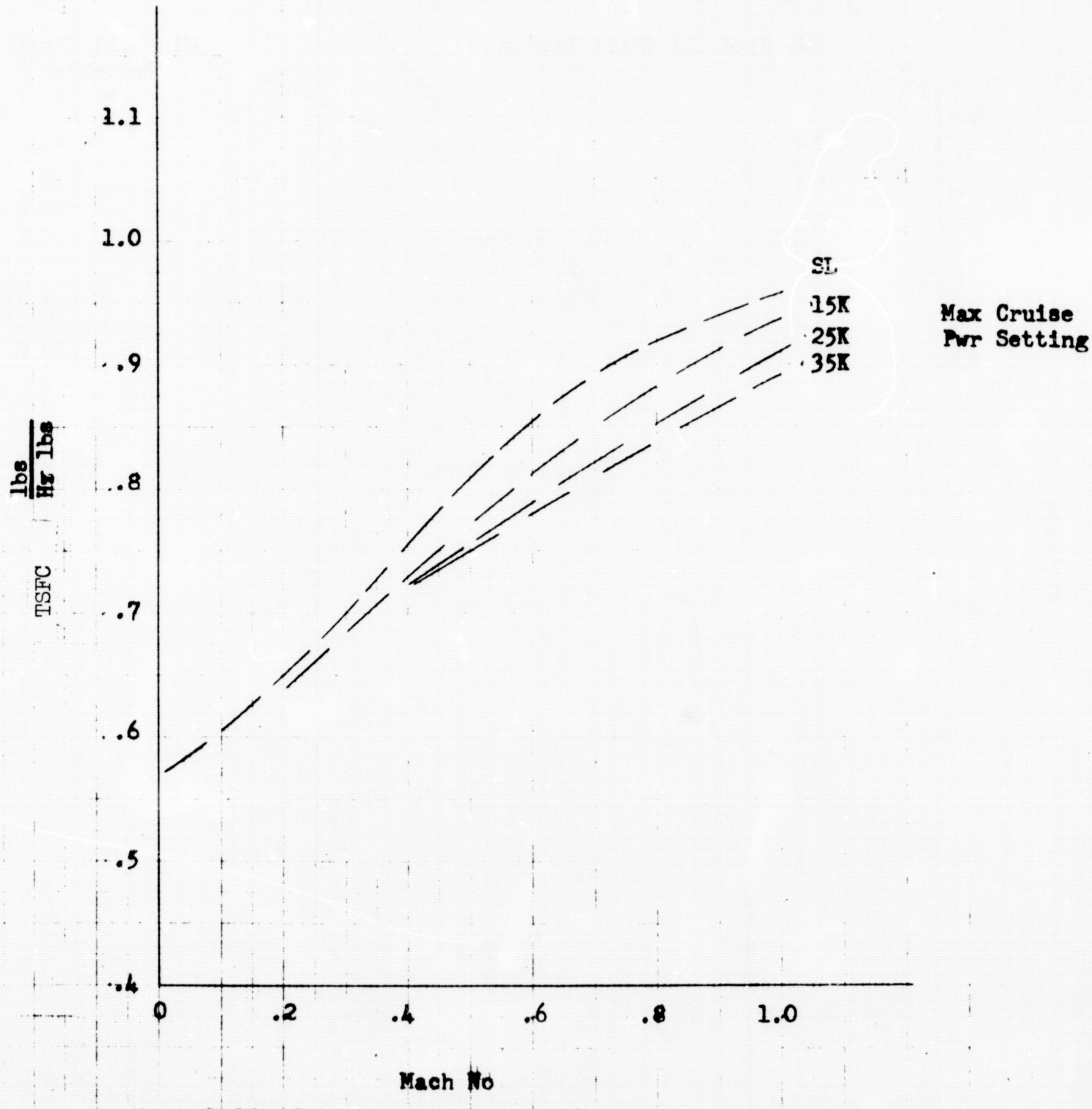

Figure 8.7-39. Estimated Pratt & Whitney JT3D-7 Engine Performance, TSFC Versus Mach Number

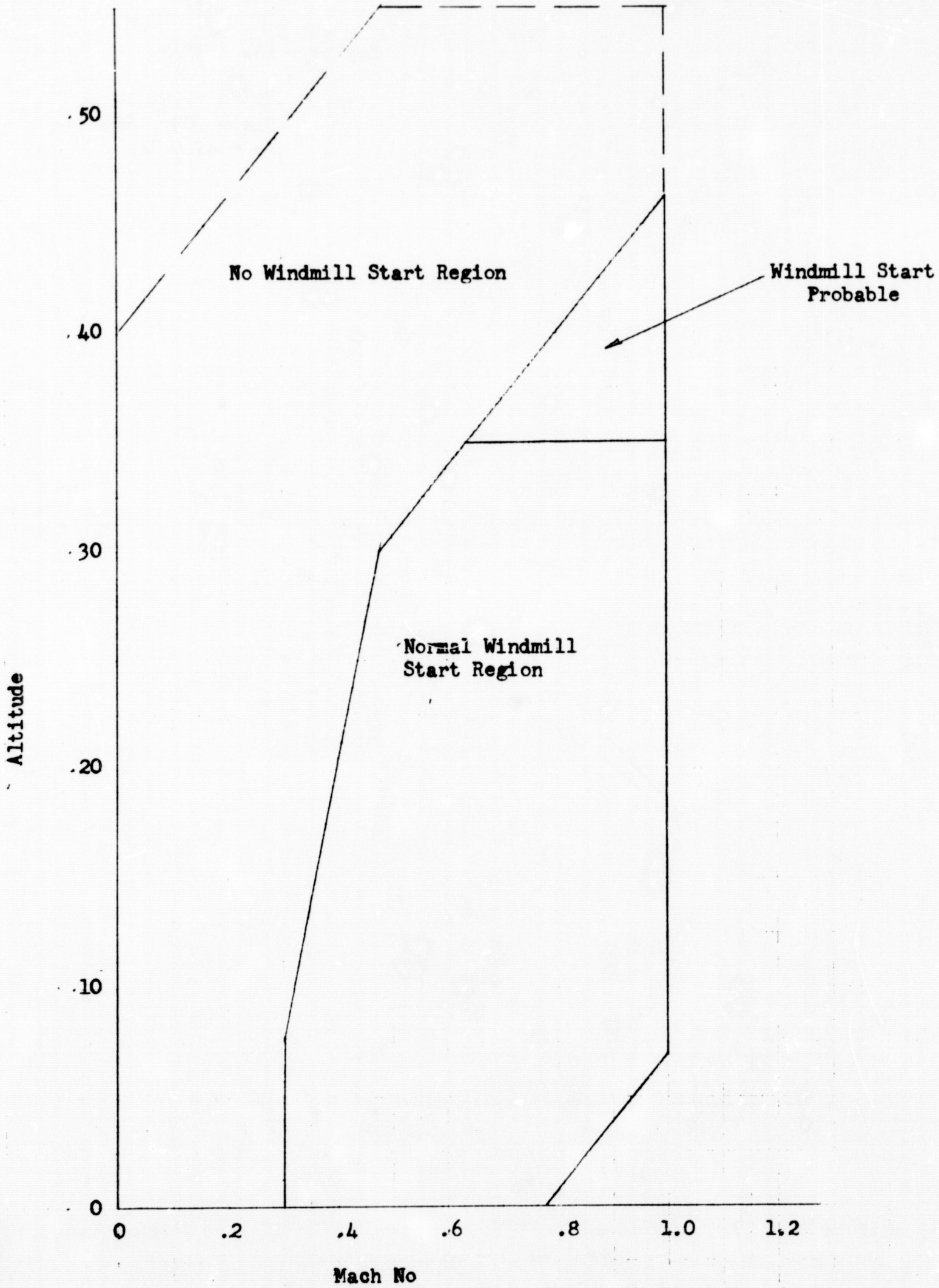

Figure 8.7-40. Typical Turbojet Windmill Start Envelope

3. Fuel temperature may vary from fuel freeze point (approximately -60 F) to assumed maximum engine inlet temperature of 200 F.

4. System shall be functionally operational with single failure.

5. System shall be operationally safe with multiple failures.

Note: This preliminary study assumes above failure criteria does not apply to structural components such as a fuel tank.

6. System shall be designed for maximum simplicity.

A relatively low volatility fuel is required to allow for a possible large bulk fuel temperature change caused by the external environment and to achieve emergency suction feed operational design objectives. Therefore, aviation kerosene "Jet A-1" in accordance with ASTM Specification D1655-67 has been selected as the preliminary choice for the design fuel. Jet A-1 fuel was selected rather than grade Jet A aviation kerosene because of lower freeze point (-58 F maximum versus -40 F maximum). A military kerosene fuel, MIL-T-5624G, Grade JP-5, is slightly less volatile than Jet A-1 and is also a good fuel candidate. Final selection of the fuel must wait until fuel temperature history data are available to assess fuel vapor pressure variation.

Fuel system design is based on a fuel with the following properties:

1. Fuel freeze point -58 F maximum.

2. Fuel true vapor pressure 1 psia or less at the assumed 200 F maximum allowable fuel inlet temperature.

These requirements control density and heat of combustion values as presented in Table 8.7-23. Fuel vapor pressure data are presented on Figure 8.7-41, and general hydrocarbon fuel reference data are presented on Figure 8.7-42.

The booster air breathing propulsion fuel system is designed for a storage capacity of 57,800 pounds of Jet A-1 aviation kerosene. The engine feed system is based on fuel delivery to four JT9D-15 engines which have maximum power flow demand requirements as shown on Figure 8.7-43. Figure 8.7-44 presents a schematic diagram of the booster fuel system.

Table 8.7-23. Turbojet Fuel Properties

Property	JET A-1 Fuel		JP-5 Fuel	
	Spec	*Actual	Spec	*Actual
Density (lb/ft^3)	51.7 max 48.4 min	50.5	52.7 max 49.2 min	51.1
Heat of combustion (Btu/lb)	18,400 min	18,558	18,300 min	18,513
Freezing point (°F)	-58 max	-61.6	-51	-58.3
*Based on Bureau of Mines survey, "Aviation Turbine Fuels, 1968"				

Basic refuel and defuel system design criteria are as follows:

1. Provide a single-point pressure refuel inlet connection that allows refueling in either horizontal or vertical launcher position.

2. Defueling will be accomplished through refueling system by inclusion of a defuel gravity and suction inlet.

3. The tank bottom fill will be used to minimize system plumbing weight and to minimize generation of electrostatic charge.

The schematic system shown on Figure 8.7-44 meets the above design criteria. The refuel shutoff valve is controlled by remote fuel level sensors. One level sensor functions for vertical position fill, and the other sensor functions for horizontal position fill. Defueling is accomplished through a check-valved inlet.

The pumping system consists of individual feed lines to each engine feeding from a single 57,800-pound capacity tank. Within the tank, booster pumps feeding the left engines are interconnected, and similarly, pumps feeding the right engines are interconnected. The system is designed in such a way that with an inoperative pump, the parallel pump can meet the pressure feed requirements of both engines.

Booster pump sizing requirements for the booster pumps are listed in Table 8.7-24.

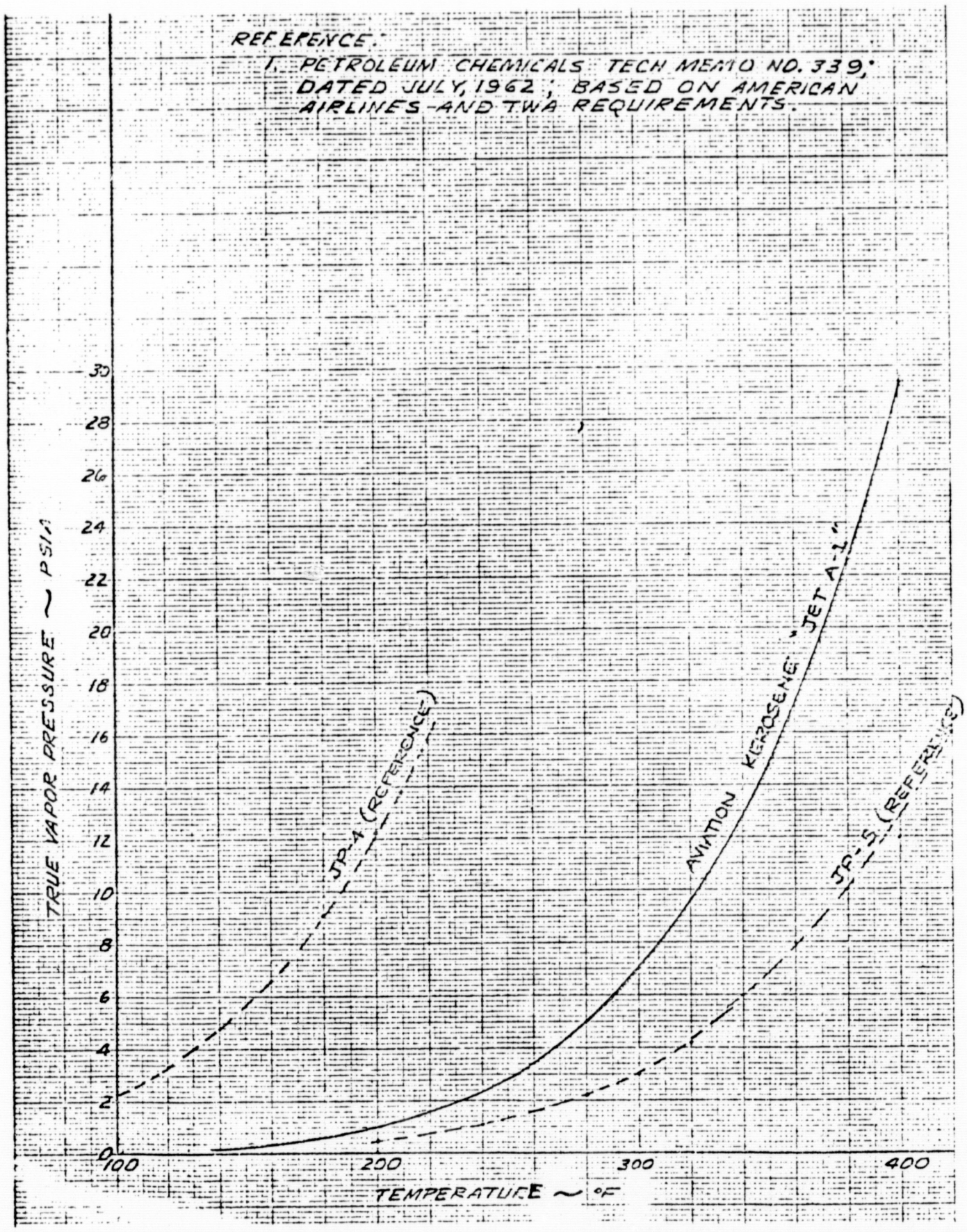

Figure 8.7-41. True Vapor Pressure of Aviation Kerosene, Maximum Volatility

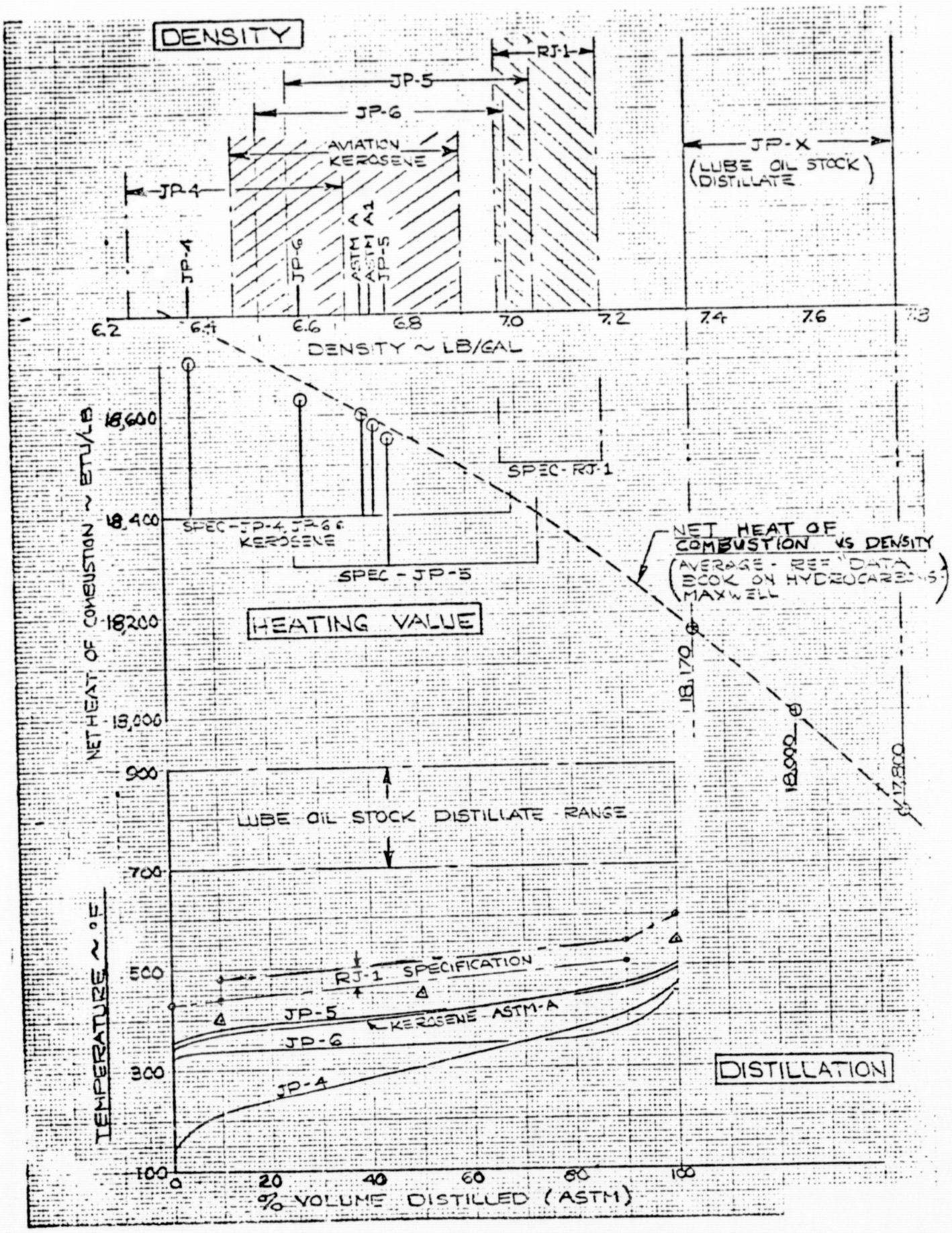

Figure 8. 7-42. Fuel Data, Aviation Hydrocarbons

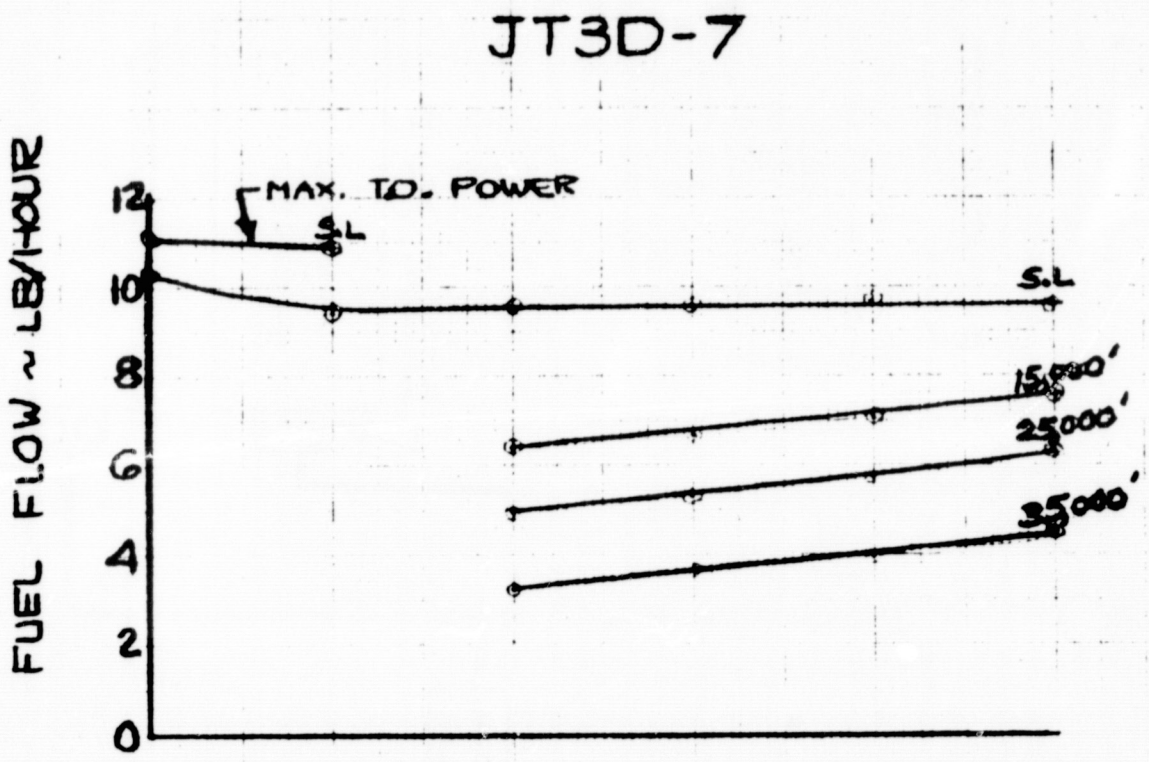

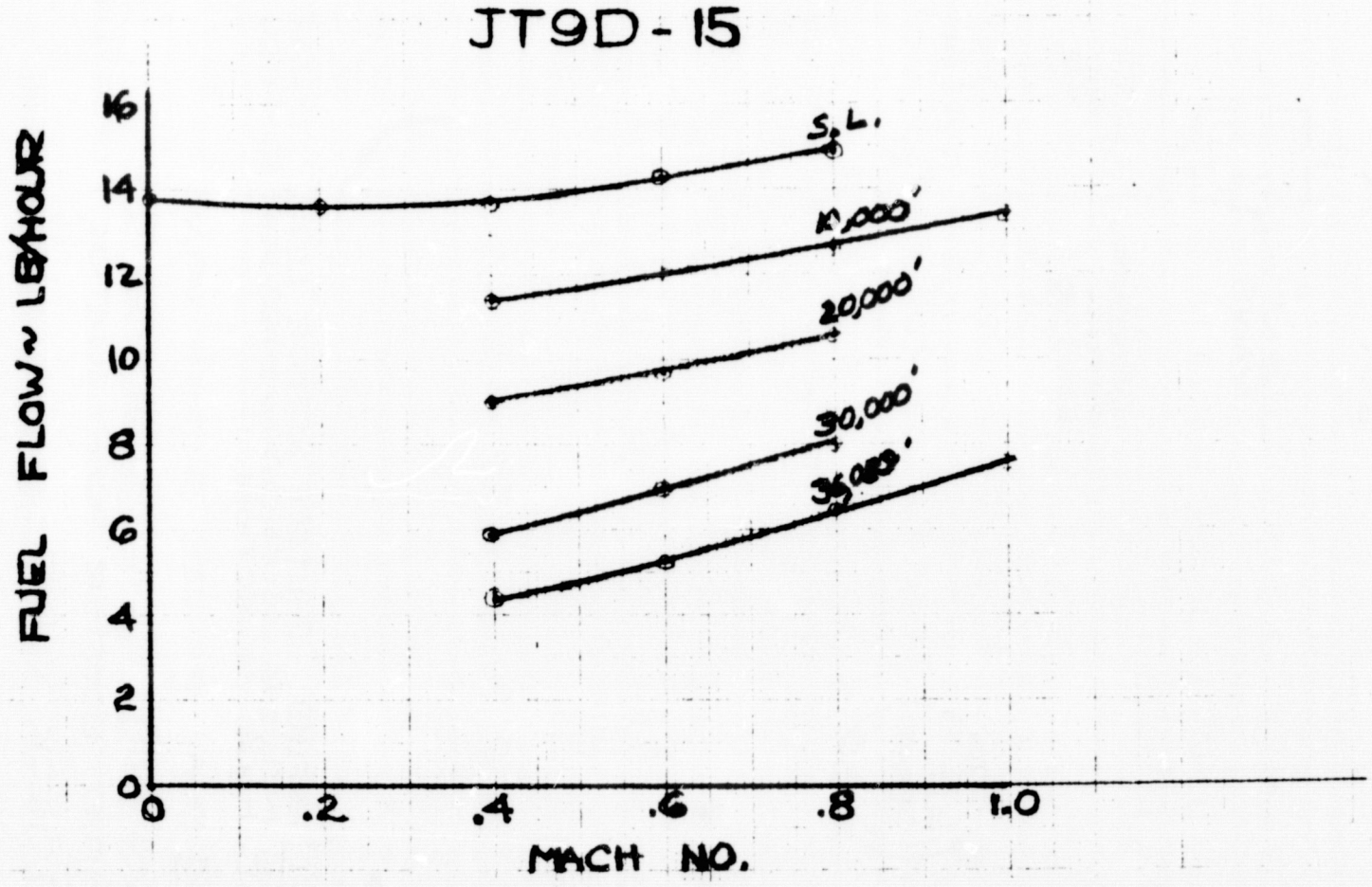

Figure 8.7-43. Fuel Flow Versus Mach Number for JT3D-7 and JT9D-15 Engines

FUEL QUANT.

Figure 8.7-44. Fuel-System Schematic for Air-Breathing Propulsion Booster With Jet A-1 Aviation Kerosene or JP-5 Fuel

Space Division
North American Rockwell

Table 8.7-24. Booster Pump Sizing

Evaluation Parameter	Orbiter Booster Pumps	Launcher Booster Pumps
Design point flow rate	22,000 (2 X max engine flow rate)	28,000 (2 X max engine flow rate)
Engine inlet pressure requirement	5.0 psi	5.0 psi
Line ΔP	1.5 max psi	1.5 max psi
Fuel head	1.0 psi	1.0 psi
Pump pressure rise required	7.5 psi	7.5 psi

The fuel pumps selected are state-of-the-art electrical motor drive centrifugal impeller-type pumps, and pump performance data are presented on Figure 8.7-45. Motor drives are 400 H_Z, 200-volt, three-phase ac power units. Table 8.7-17 presents trade study data for electrical motor drives versus a hydraulic motor drive, and weight data only include the basic pump and motor unit. Installation items such as electrical provisions, hydraulic lines, and hydraulic fluid and not listed included in Table 8.7-25. Electrical motor drives were selected primarily on the basis of the high reliability that can be achieved with this non-complex machine.

A primary system design objective is to provide emergency suction feed operation with booster pumps inoperative. During emergency operation, it is required that the vapor liquid ratio at the engine inlet not exceed 0.45. A suction feed, check-valved inlet is provided to furnish fuel to left and right engine pairs (refer to schematic diagram).

Engine feed lines were sized to achieve suction feed requirement, and a 2.0-inch-diameter line is required. The feed line pressure drop is approximately 1.2 psi at 15,000 pph. Suction feed operation at engine start altitudes will be assured by providing positive tank pressurization as described in next paragraphs.

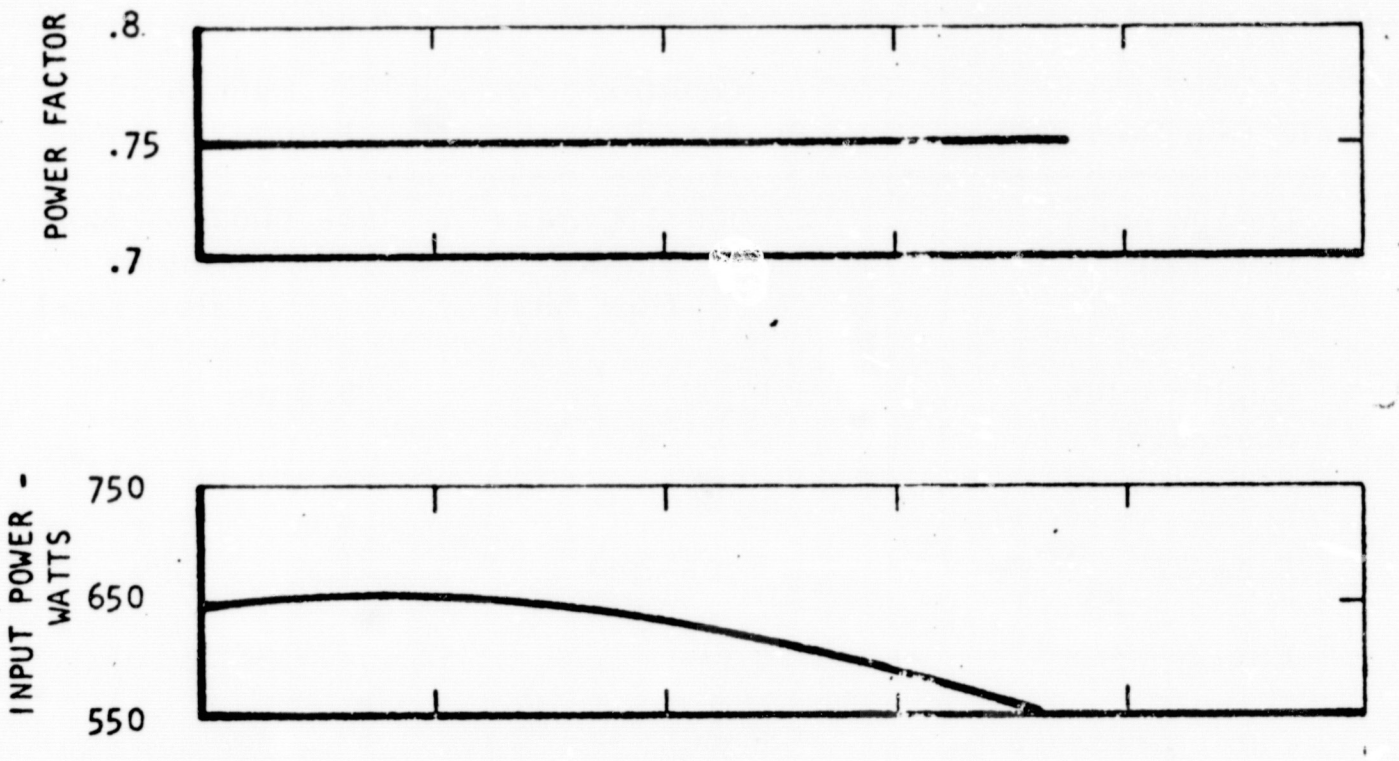

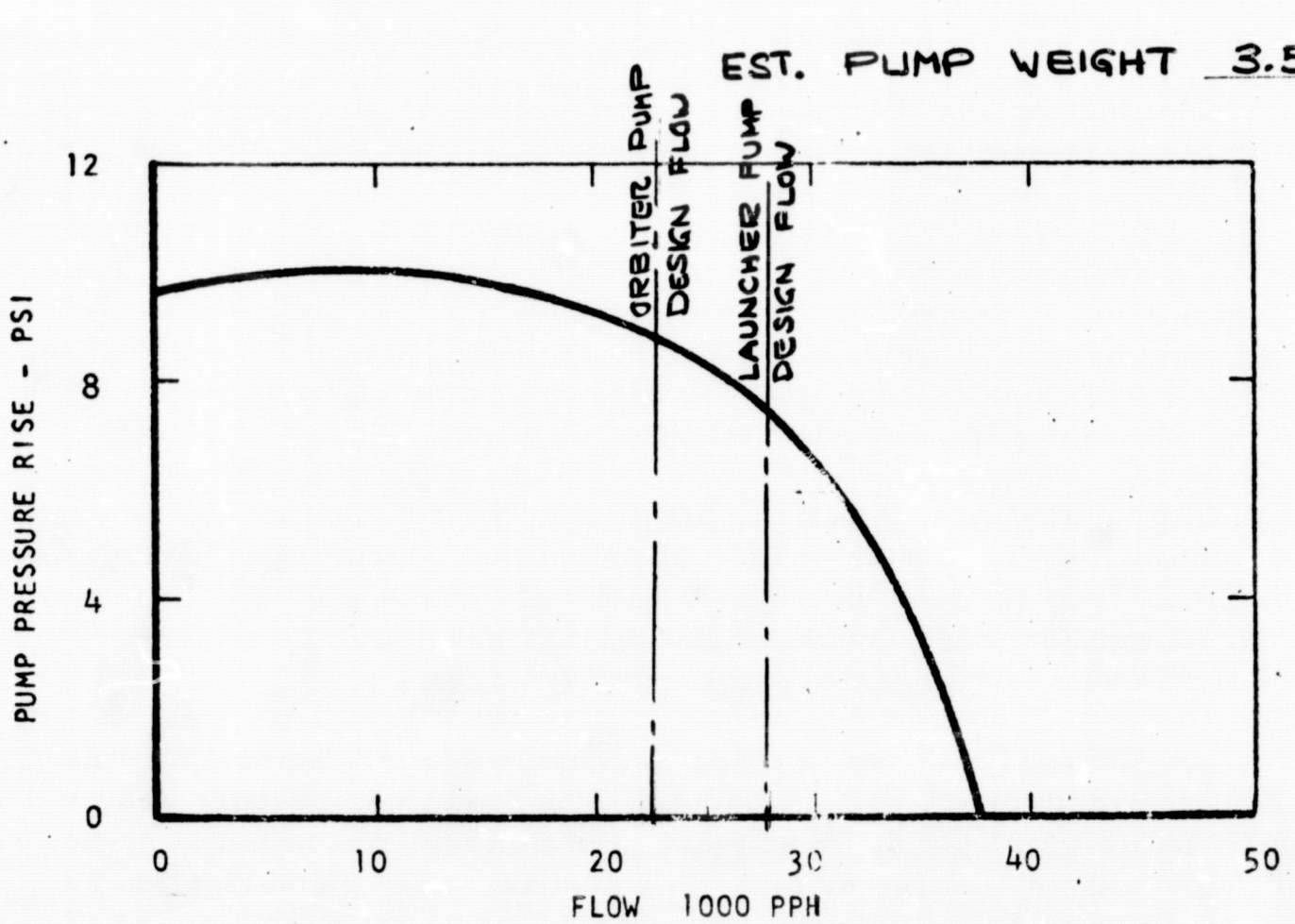

Figure 8.7-45. Predicted Sea-Level Performance of TRW Model 376800 Fuel Booster Pump; Fuel, MIL-T-5624, Grade JP-4, at 60 F (Performance Approximately the Same for Jet A-1 Kerosene)

Table 8.7-25. Fuel Pump Drive Trade Study Summary

Evaluation Parameter	Concept Evaluation	Concept A - AC Electrical Motor	Concept B - Hydraulic Motor
Performance	Equal	Fuel pump performance independent of drive	
Reliability	A, B	Very simple machine. Does not require overspeed protection.	Less reliable based on complexity and maintainability data.
Weight	B, A	Four booster pumps 14.0 lb Total 14.0 lb	Four booster pumps 13.6 lb Pump solenoid valves 2.0 lb Total 15.6 lb
Producibility	A, B	Less complex.	
Maintainability	A, B		2.89 times MMH/FH of electric motor.
Cost	A, B		Pump and motor unit cost 2 to 3 times electrical drive.

The venting and pressurization subsystem must perform the following functions:

1. Vent tank during refueling and during boost to 50,000-ft altitude.
2. Close tank vent line above 50,000-ft altitude.
3. Provide small positive ram air tank pressurization during fuel usage.

Redundant vent valves are installed in parallel, as shown in the schematic diagram, Figure 8.7-44. The vent line overboard exit configuration will be designed with suitable scarf angle to provide approximately 1.5 to 2 psi pressure recovery. This small positive pressure will maintain tank at a positive pressure during vehicle descent and will assure emergency suction feed operation.

It is essential that the vent valves perform the safety-critical function of closing off the tank at 50,000 feet and thus prevent fuel boil-off. Therefore, the valve should be a failed-close design with the overboard flow path restricted to the maximum extent possible while still achieving refuel and climb venting.

The orbiter fuel system is designed for a storage capacity of 3,000 pounds of Jet A-1 and delivery of fuel to four engines of the JT3D-7 engine class. A system schematic diagram is presented on Figure 8.7-46. The orbiter system is basically the same as the launcher system. Additional features are a bulk fuel temperature control system for 30 day orbit operation and provisions on the engine feed lines for gas bleed and fuel precharge during reentry.

The orbiter basic pumping system (Figure 8.7-46) is the same as the launcher fuel system (Figure 8.7-44). A new feature required for the orbiter system is the gas-bleed/fuel-precharge valve installed at the engine inlet pump. It would be impractical to attempt to maintain fuel feed lines full of fuel and in a liquid state throughout orbital flight; therefore, the system will be launched with the lines empty of fuel. During entry, prior to engine start, the valves will be opened to bleed gas from the lines and precharge with fuel.

Orbiter fuel system booster pump data are listed in Table 8.7-25. Engine maximum design flow is approximately 11,000 pph (Figure 8.7-43), which requires a booster pump design flow rate of 22,000 pph in accordance with single-pump-failure sizing criteria. The orbiter booster pump is only 20 percent smaller than the launcher booster pump; therefore, during this preliminary sizing study, the launcher pump data of Figure 8.7-45 should be used for the orbiter booster pump.

Suction Feed is the same as in the booster fuel system.

The orbiter vent and pressurization subsystem is identical with that of the booster. Consideration should be given to the inclusion of an additional vent-valve control feature. It may be desirable to provide a switch-operated shutoff valve in the cockpit as a backup to the automatic vent valve closure at 50,000 foot altitude.

A tank-fuel temperature control system is required for the orbiter to maintain the bulk fuel above freezing during the possible 30-day orbital flight. This system is based on the assumption that the tank is located with the heat leak toward the external environment; i.e., fuel cooling. An external heat leak direction appears desirable in devising a system for bulk fuel temperature control.

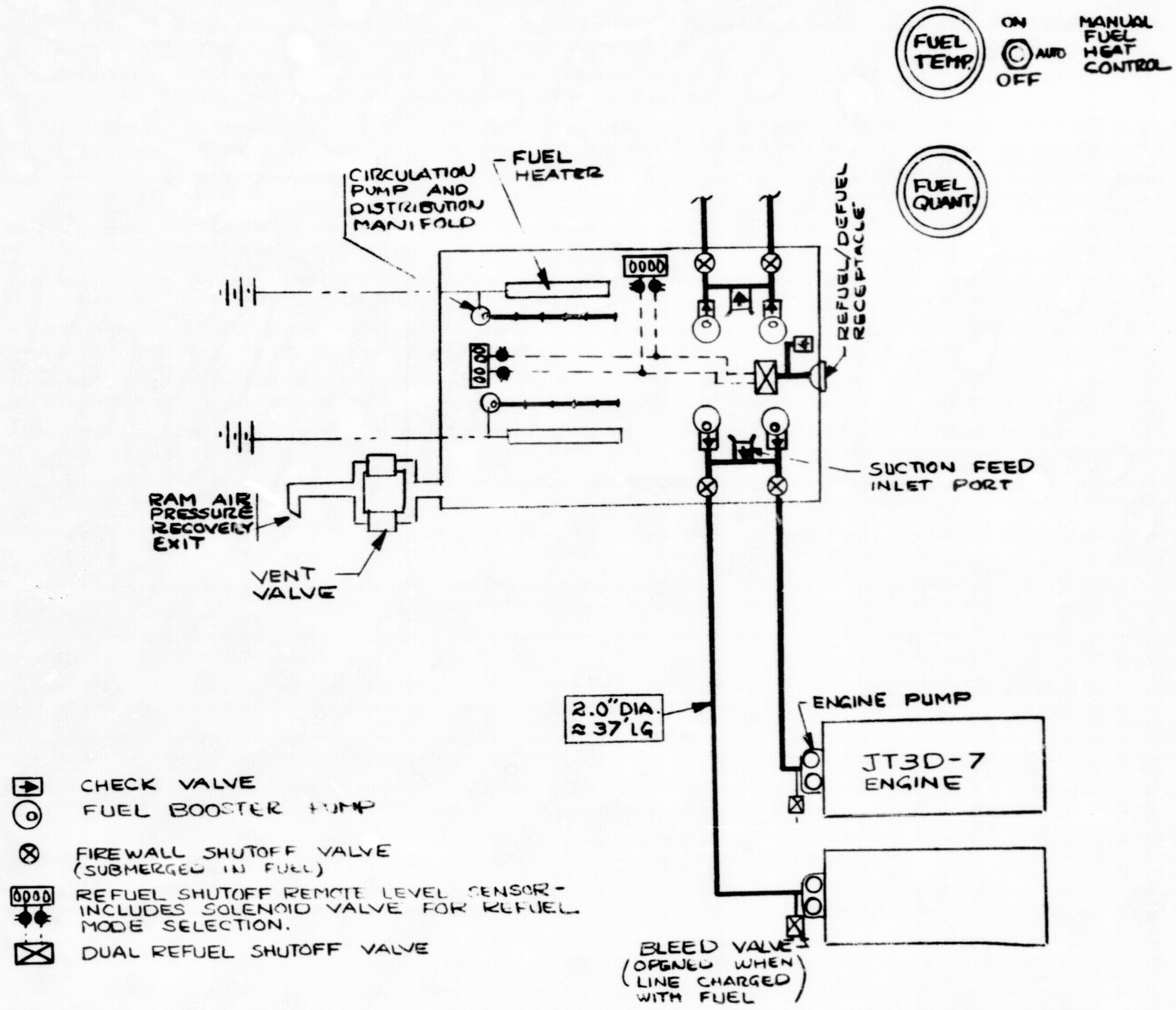

Figure 8.7-46. Fuel-System Schematic for Air-Breathing Propulsion Orbiter With Jet A-1 Aviation Kerosene or JP-5 Fuel

Space Division
North American Rockwell

As shown on the schematic diagram (Figure 8.7-46), redundant temperature control systems are provided. Each system consists of a small fuel-circulation pump and a heater with its associated control. The circulation pumps prevent excessive temperature gradients within the bulk fuel and prevent hazardous solidification of fuel. These submerged small pumps are a centrifugal-type designed to handle a combination of gas and liquid, which could exist at zero-g conditions.

The temperature control will be normally automatic and control heater output to maintain fuel temperature at approximately -30 F. This minimum temperature is based on an assumed tolerance of 30 F above the fuel freezing point, which is nominally -60 F. Flight safety considerations dictate the need for a fuel temperature-monitoring gage and a manual heater backup control.

8.8 HYDRAULIC SYSTEM

Both the booster and orbiter have significant power requirements for normal air vehicle functions and rocket engine gimbal. A hydraulic system was selected to provide powered actuation for ailerons, elevator, rudder, flaps, gear, brakes, and rocket engine gimbal (Figure 8.8-1). The hydraulic system includes hydraulic power generation, distribution, control, and conversion to mechanical energy. The objectives of the hydraulic system studies were to develop conceptual system design to meet projected functional, reliability, and safety requirements; estimate system weight; and provide system definition for cost analysis.

8.8.1 Hydraulic System Requirements

The aerodynamic controls deflection rate requirements and control surface hinge moments established for the hydraulic system design are given in Tables 8.8-1, 8.8-2, and 8.8-3.

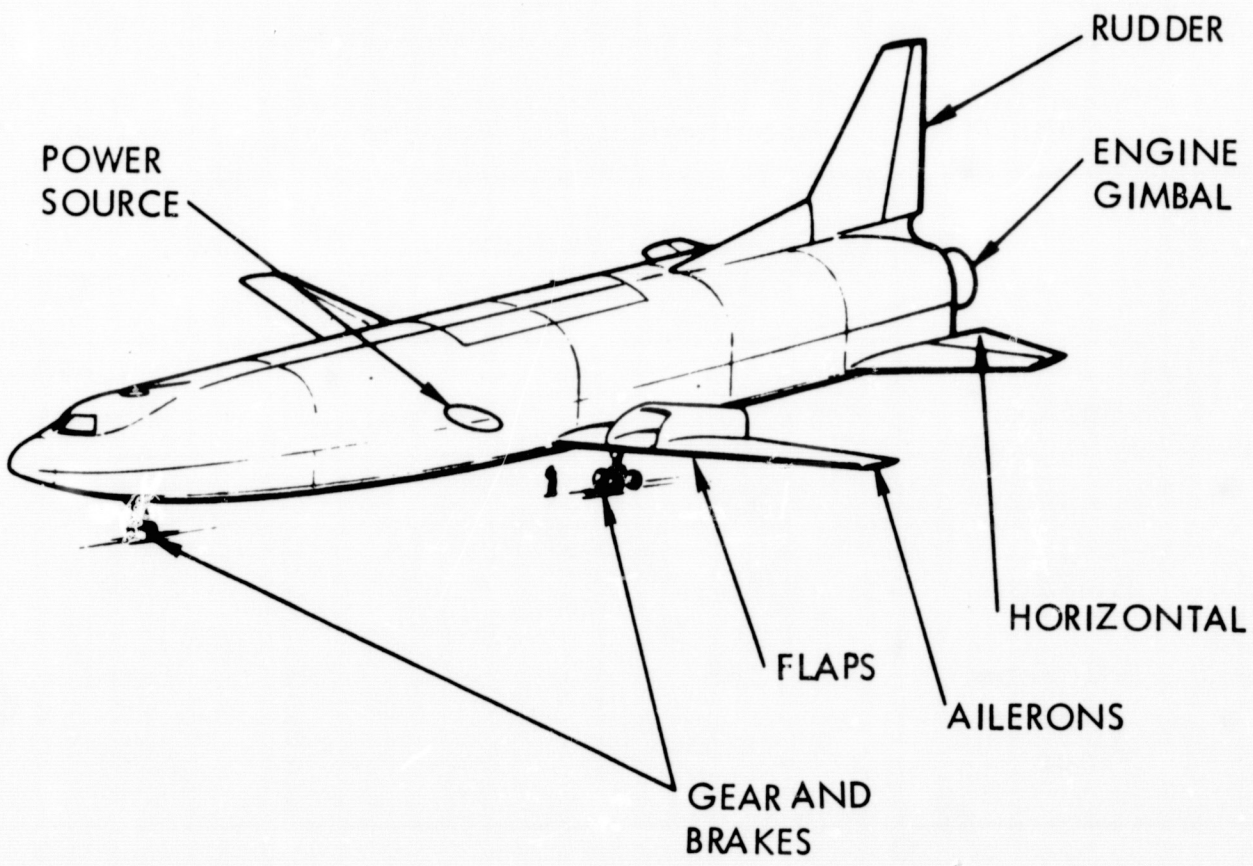

Figure 8.8-1. Hydraulic System Functions

Table 8.8-1. Aerodynamic Control Deflection Rates

Surface	Area Deflected (ft^2)	Range (deg)	Deflection Rate (deg/sec)
Booster			
Rudder	422	±15	12
Elevator	900	+45 to -60	25
Ailerons	334	±40	20
Flaps	695	-30	3
Orbiter			
Rudder	213	±15	12
Elevator	585	+45 to -60	25
Ailerons	137	±40	20
Flaps	265	-30	3

Table 8.8-2. Booster Control Surface Hinge Moments

Surface	Hinge Moment (10^6 in.-lb)		
	Flight Conditions		
	Transition (at 65 psf)	Cruise (at 98 psf)	Approach (at 48 psf)
Rudder	1.135	--	0.839
Elevator	3.1	4.69	2.29
Ailerons	0.355	--	0.262
Flaps	--	--	1.89

Table 8.8-3. Orbiter Control Surface Hinge Moments

Surface	Hinge Moment (10^6 in. -lb)	
	Flight Conditions	
	Transition (at 44 psf)	Approach (at 65 psf)
Rudder	0.215	0.319
Elevator	1.235	1.825
Ailerons	0.064	0.094
Flaps	--	0.69

Based on the deflection rates and hinge moments, the hydraulic system flow requirements were established. The requirements for the booster and orbiter are listed in Table 8.8-4. The landing gear requirement is based on a 10-second operating period.

Table 8.8-4. Hydraulic Flow Requirements

Condition	Component	Flow Rate (gpm)	
		Booster	Orbiter
Transition maneuvers	Rudder	6.43	1.33
	Elevator	29.20	11.63
	Ailerons	5.36	0.97
		40.99	13.93
Cruise	Elevator	44.3	--
Landing approach	Rudder	4.80	1.47
	Elevator	21.70	17.20
	Ailerons	3.94	1.43
	Flaps	4.26	1.56
		34.70	21.66
Landing	Gear	55	33
Taxi	Steering	7	7
	Brakes	22	22
		29	29
Rocket engine gimbal	Gimbal Actuators	64	16

8.8.2 Hydraulic System Description

The hydraulic system includes hydraulic power generation, distribution, control, and conversion to mechanical energy. The mechanical shaft power for the hydraulic pumps is provided by APU's (see Section 8.10). High pressure (4000 psi) fluid is distributed through pressure lines to control valves, distributed from control valves to actuators, and returned to the reservoirs. Conversion of hydraulic power to mechanical energy is accomplished by linear actuators and hydraulic motors. A typical hydraulic system schematic is shown in Figure 8.8-2. The system classification is as follows:

Type: -65 F to 450 F bulk fluid temperature

Class: 4000-psi, closed-center, in which the normal cutout pressure at the main pressure controlling device is 4000 psi

The hydraulic systems consist of four independent subsystems to provide mission capability after a single failure and provide for safe flight and landing in the event of a second failure regardless of the maneuver at the time of the second occurrence. A major contributing factor is the use of the four equal status hydraulic systems, which optimizes a combination of high system reliability and low weight. The system arrangement shown in Figure 8.8-3 provides for retention of all hydraulic functions and satisfactory flow rates in the event of an APU failure, and safe operation in the event of two APU failures.

Actuation functions are served by arrangements in three general categories:

1. The actuation function is supplied by two hydraulic systems but has a third source of power: accumulator, or gravity freefall. Functions which are supplied from three hydraulic systems may also be placed in this category.

2. The actuation function is supplied by two systems. These functions are required for full mission completion, but do not endanger safe flight. Either hydraulic system can supply adequate flow to permit mission completion without the other system. A double failure of the supplying systems would be mission-limiting, but safe flight would not be adversely affected.

3. Power to the actuation function is supplied from all four systems. This arrangement is applicable when the function is mandatory for safe flight and/or has high power requirements. A minimum of weight results since failure conditions combined with high power

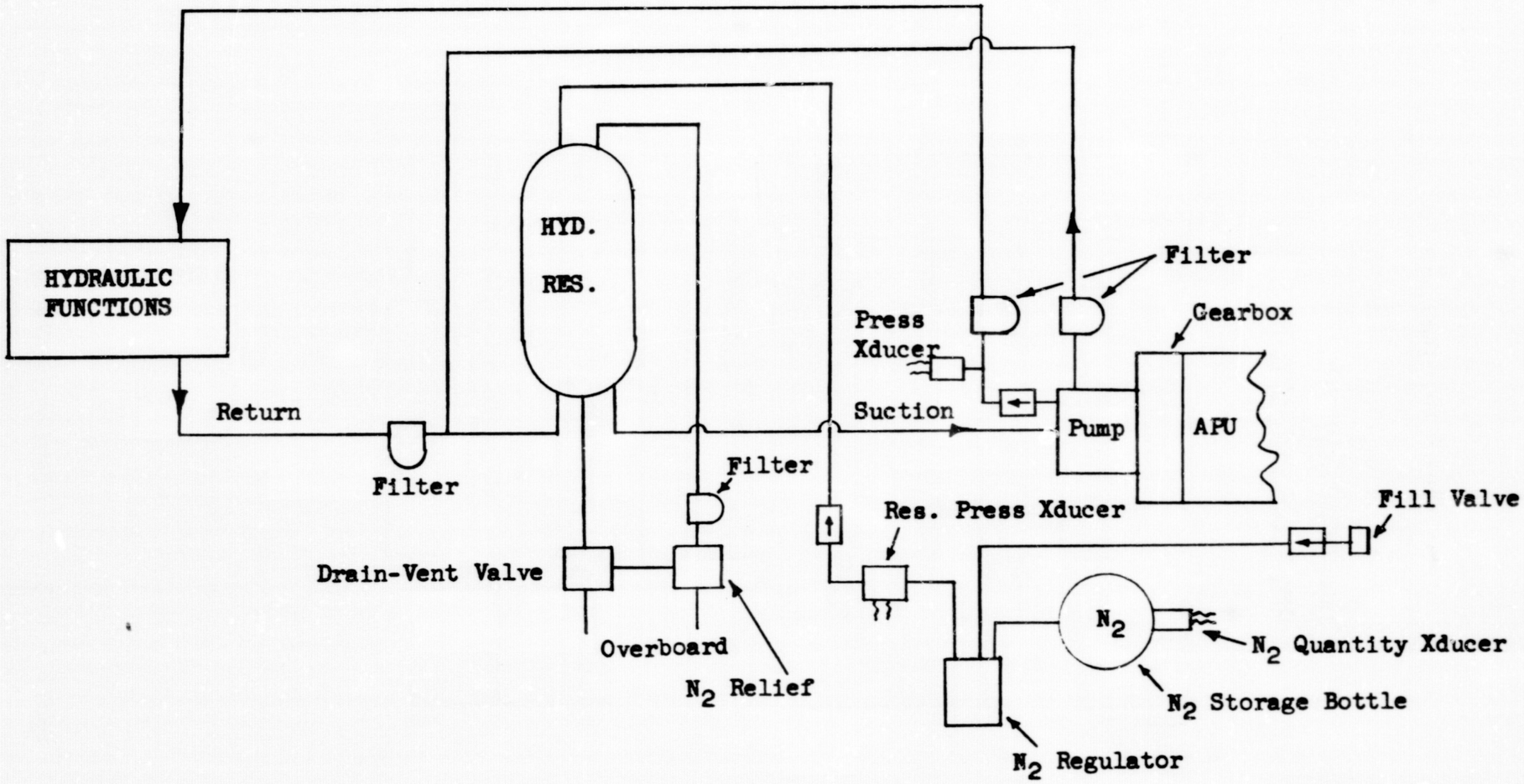

Figure 8.8-2. Typical Hydraulic Subsystem

INTERFACE WITH
POWER SYSTEM APU'S.

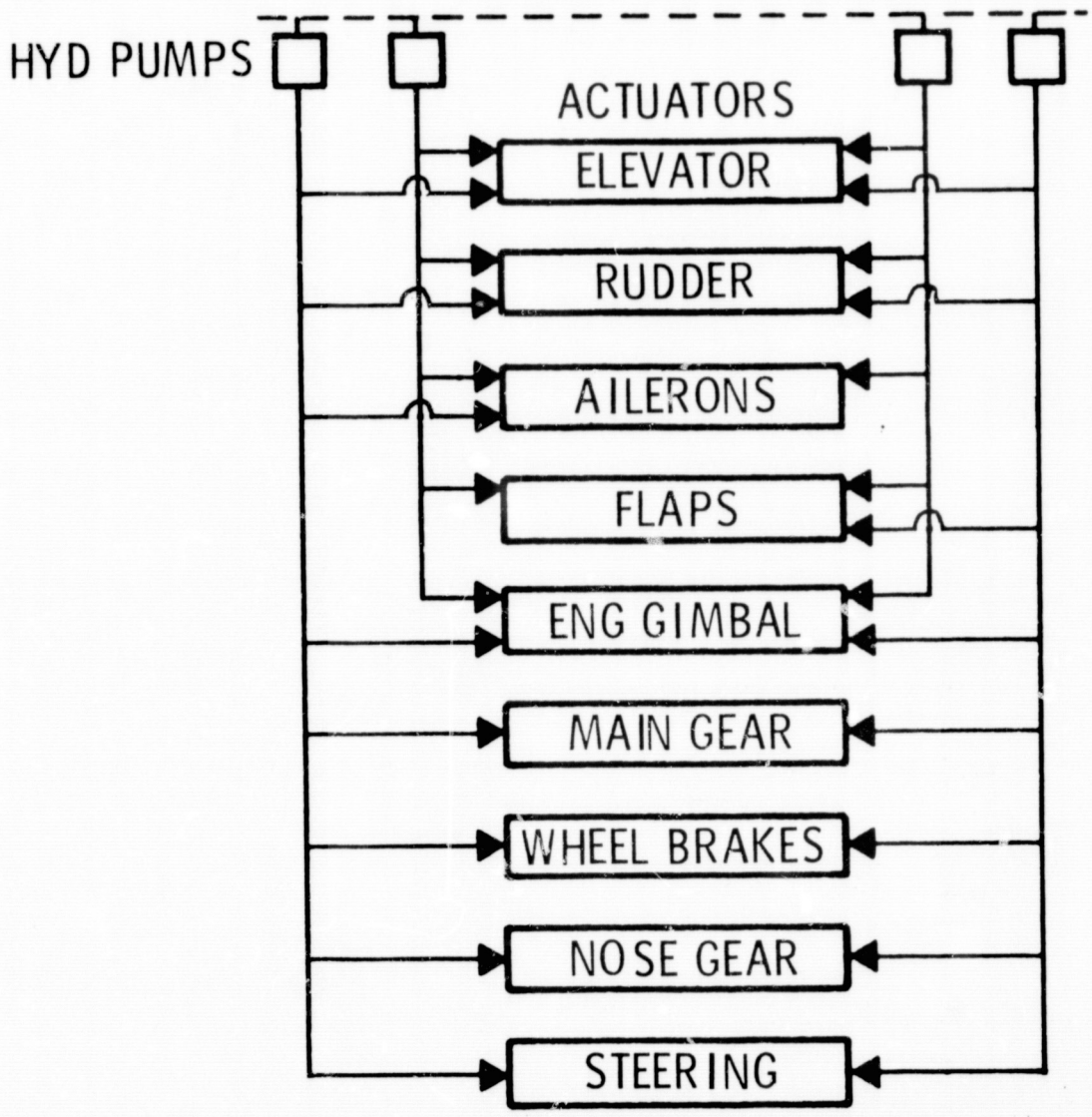

Figure 8.8-3. Hydraulic System Arrangement

requirement allow the functions to be shared by two or more hydraulic systems.

The choise of titanium for mechanical and metallurgical tubing and tubing connections was based on tradeoff studies and testing performed by NR for the F-15 and AMSA proposals. A weight saving of 15 to 18 percent was realized on those vehicles over other materials.

To maintain system reliability and minimize weight through avoiding the need for excessive fluid supply, leakage must be kept to a minimum. Metallurgical tubing joints will be used to provide permanently leak-proof connections which are not used for maintenance or operating component replacement. The metallurgical joint is lighter than the mechanical connector.

The hydraulic system and components are to be designed for maximum life with minimum maintenance and recycle time for high operational capability. Minimum hydraulic system maintenance is ensured by application of design principles verified in severe environments such as those afforded by the XB-70 and X-15 programs and in similar environments afforded by the F-107 and A3J.

Checkout will consist basically of structural integrity testing (system leakage), of individual testing of each of the pumps and reservoirs, and of testing the failure indication measurements.

The servicing requirement will consist of periodic replacement of filters, checking fluid level, and replenishing fluid if necessary.

Hydraulic Pump and Reservoir Subsystem

The pumping system provides hydraulic power for each of the four independent subsystems. Each orbiter subsystem receives its power from one 40-gpm pump at 4000 psi; each booster subsystem receives its power from two 40-gpm pumps at 4000 psi. Each unit is a positive displacement, variable output pump. Fluid is supplied to the pump inlet port at a minimum pressure as supplied by the reservoir subsystem. The use of a 1.7-cubic-inch-per-revolution pump, which when driven at 5700 rpm supplies 40 gpm at 4000 psi, is assumed. The pump is of a configuration similar to that of the pump qualified for, and presently being used on, the Concorde. The booster system delivery of 80 gpm will adequately meet the maximum system demand of 64 gpm. The orbiter system delivery of 40 gpm will adequately meet the maximum system demand of 33 gpm. For commonality and logistics purposes, the booster and orbiter pumps will be of the same size and type.

In addition to meeting the requirement of safe flight and landing after a second failure, the choice of four systems over three systems for the elevator and rudder hydraulic subsystems is based on the fact that a minimum weight results from sharing power between the maximum number of systems. To meet the requirement of two-thirds power after the second failure--when three subsystems are in use, each must provide 66 2/3 percent power for a total of 3 x 66 2/3 percent or 200 percent requirement. When four systems are in use, each subsystem supplies 33 1/3 percent for a total of 4 x 33 1/3 or 133 1/3 percent. The total actuator capacity and power of the four systems are therefore less than the total actuator capacity and power of three systems. The three-system configuration for the flaps and aileron is lighter because of the low flow requirements for these two subsystems.

Each of the four independent hydraulic subsystems has a separate supply reservoir. The function of the reservoir is to contain the fluid supply at an acceptable temperature and pressure in order to maintain efficient pump operation. The reservoir also provides for separation of entrained gas bubbles from the circulating fluid.

Each reservoir is pressurized by an on-board nitrogen storage bottle, as shown in the following:

1. Reservoir Volume (70 F)

Booster

Space (N_2) = 3822 $in.^3$

Fluid = 646 $in.^3$

4468 $in.^3$/19.3 gallons

Orbiter

Space (N_2) = 2486 $in.^3$

Fluid = 479 $in.^3$

2565 $in.^3$/11.1 gallons

2. N_2 Pressurization Bottle

Booster

Volume 500 $in.^3$

Pressure = 2500 psi

Orbiter

Volume = 500 $in.^3$

Pressure = 2500 psi

Booster Hydraulic System Reservoir Requirements are as follows:

1. Fluid Volume -- Inasmuch as flight control duty cycle is not yet available, it is estimated that there will be a continuous flow demand of 10 percent of maximum flow demand:
0.10 x 44 gpm = 4.4 gpm

An estimated 4 gpm of continuous leakage is added for the total fluid volume required.

4.4 gallons

4.0 gallons

8.4 gallons

By using the fluid exchange of three times per minute,

$\frac{8.4}{3}$ = 2.8 gallons (646 $in.^3$)

2. Space -- Space above the fluid is required in the reservoir for thermal expansion of the fluid.

Fluid volume

Actuators	1722 $in.^3$
Pumps, filters, etc.	270 $in.^3$
Reservoir	646 $in.^3$
Hydraulic lines	12,545 $in.^3$
	15,183 $in.^3$

By assuming the use of Orinite 8200 hydraulic fluid, 20 percent of the systems total volume is required for thermal expansion over a temperature range of 70 to 450 F.

$0.20 \times 15293 = 3058 \text{ in.}^3$

Additional space for 5 percent of the systems total volume of fluid is provided for nitrogen space and system growth.

$0.05 \times 15293 = 764 \text{ in.}^3$

3. Total Volume

Thermal expansion	=	3058
Space (N_2)	=	764
Fluid	=	646
		4468 in.^{3}/19.3 gallons

4. Reservoir Pressurization Nitrogen Bottles (4)

Pressure = 2500 psi

Volume = 500 in.^{3}

5. Booster Weight -- Pumping and Reservoir System

Pumps (8) 40 gpm pump	192 lb
Reservoirs	160 lb
Relief valves, filters, check valves	340 lb
Plumbing	434 lb
Fluid	360 lb
N_2 pressurization system	126 lb
	1612 lb

Orbiter Hydraulic System Reservoir Requirements are as follows:

1. Fluid Volume -- Inasmuch as a flight control duty cycle is not yet available, it is estimated that there will be a continuous flow demand of 10 percent maximum flow demand: $0.10 \times 22 = 2.2$ gpm

   An estimated 4 gpm of continuous leakage is added for the total fluid volume required.

   $$2.2 + 4 = 6.2 \text{ gpm}$$

   By using the fluid exchange of three times per minute,

   $$\frac{6.2}{3} = 2.07 \text{ gallons } (479 \text{ in.}^3)$$

2. Space -- Space above the fluid is required in the reservoir for thermal expansion of the systems fluid.

   Fluid volume

Actuators	689 $in.^3$
Pumps, filters, etc	180 $in.^3$
Reservoir (fluid)	479 $in.^3$
Hydraulic lines	7000 $in.^3$
	8348 $in.^3$

   Assuming the use of Orinite 8200 hydraulic fluid, 20 percent of the systems total volume is required for thermal expansion over a temperature range of 70 to 450 F: $0.20 \times 8348 = 1669 \text{ in.}^3$

   Additional space for 5 percent of the systems total fluid volume is provided for nitrogen space and system growth.

   $$0.05 \times 8348 = 417 \text{ in.}^3$$

3. Total Volume

Thermal expansion	1669 $in.^3$
Space (N_2)	417 $in.^3$
Fluid	479 $in.^3$
	2565 $in.^3$ / 11.1 gallons

4. Hydraulic Pump and Reservoir System Weight (Orbiter)

Pump (4)	96 lb
Reservoirs (4)	110 lb
Relief valves, filters, check valves,	210 lb
Plumbing	237 lb
Fluid	280 lb
N_2 pressurization	126 lb
	1059 lb

Hydraulic Flight Control Subsystem

The hydraulically operated functions are the actuators for the aileron, rudder, elevator and flap; and the pitch, roll and yaw servos. The position and rate of movement are controlled by electro-mechanically operated servo valves through an electrical signal.

Four independent hydraulic systems supply power to the rudder and elevator subsystems. Three independent hydraulic systems supply power to the flaps and ailerons. Two-thirds hinge moment power capability, adequate for safe flight, is provided after a second failure, regardless of flight maneuver.

Weights are as follows:

Vehicle	System	Weight (lb)
Booster	Rudder actuators and controls	856
	Aileron actuators and controls	592
	Elevator actuators and controls	1600
	Flaps actuator and controls	702
	Plumbing	1586
	Hydraulic fluid	780

Vehicle	System	Weight (lb)
Orbiter	Rudder actuators and controls	210
	Aileron actuators and controls	205
	Elevator actuators and controls	1200
	Flaps actuators and controls	532
	Plumbing	948
	Hydraulic fluid	500

Landing Gear and Door Hydraulic System

The landing gear control system consists of nose gear and main gear subsystems that are supplied power simultaneously by two systems. A third source of power can be supplied by accumulation or gravity free fall.

Weights are as follows:

Vehicle	System	Weight (lb)
Booster	Actuators and controls	705
	Plumbing	428
	Hydraulic fluid	200
Orbiter	Actuators and controls	465
	Plumbing	188
	Hydraulic fluid	88

Nose Wheel Steering Subsystem

Nose wheel steering is accomplished by a hydraulically powered actuator, electrically controlled by the pilot's pedals. Pressure is supplied by the nose gear shut off valve from System 1 for normal operation and System 4 for emergency operation. The weight of the actuator, shuttle valve, shut off valve, servo valve, lines and fluid is 33 pounds.

Wheel Brake Hydraulic System

The wheel brakes are powered by Systems 1 and 4, both working simultaneously. An automatic system modulates the brake control valve to provide maximum effective braking within the demand level.

Brake pressure applied by one system is reacted by the other system. There is no change in braking or in pedal position if one of the dual hydraulic brake systems should fail.

The system weight is 25 pounds.

Rocket Engine Gimbaling

Each rocket engine will be gimbaled by two servo actuators which will provide pitch, yaw, and roll control. Each actuator will be a tandem configuration with each section of the tandems powered by an independent hydraulic system. Each actuator section will be controlled by an electro-hydraulic servo valve. The feedback loop will be closed mechanically within the actuator. The area of each tandem section will be designed for the full engine gimbal load. Interspersing of four independent hydraulic systems among the tandem actuators of the controlling engines will fulfill the reliability requirement of second-order fail safe. A first order servo valve hardover condition can also be averted by the chosen tandem arrangement as the unaffected section will oppose and cancel this condition.

Weights are as follows:

Vehicle	System	Weight (lb)
Booster	Actuator and controls	672
	Plumbing	730
	Oil	400
Orbiter	Actuator and controls	224
	Plumbing	100
	Oil	64

8.9 ENVIRONMENTAL CONTROL/LIFE SUPPORT SYSTEMS

Environmental control/life support systems (EC/LSS) analysis was conducted to develop conceptual system design to meet projected functional, reliability, and safety requirements, estimate system weight, and provide system definition for cost analysis. Determination of EC/LSS for the booster and the orbiter was accomplished by:

1. Definition of requirements and constraints
2. Selection of concept and description of systems
3. Determination of system and crew equipment weight, power, volume, and location
4. Study of possible space station interfaces
5. Determination of recommended electronic interface requirements
6. Preparation of a brief timeline in narrative form

The following paragraphs provide detailed information concerning these efforts. Sizing information for the system concept selected is shown in Table 8.9-1.

Table 8.9-1 EC/LSS Requirements

Requirement	Orbiter	Booster
Weight EC/LSS (lb)	1093	278
Weight consumables (lb)	779	-
Power required EC/LSS (watts) (ground)	414	200
Power required EC/LSS (watts) (space flight)	305	200
Crew/personnel equipment weight (lb)	2509	-
Crew/personnel equipment volume (cu ft)	110	-

The study indicated that in follow-on contracts additional work should be directed to:

1. Location of space radiator
2. Crew emergency operations

3. Definition of system and subsystem performance parameters

8.9.1 EC/LSS Requirements and Assumption

The orbiter EC/LSS must provide a shirtsleeve environment for the crew and passengers. The booster is unmanned for the space shuttle mission, but provisions must be provided for manned ferry flights. The EC/LSS subsystem requirements for the orbiter and booster (as applicable) are:

1. Thermal Control System. Remove excess heat from selected areas of the vehicle and reject to space

2. Atmosphere Circulation and Control System. Provide adequate circulation of the crew/passenger compartment gases

3. Pressure Control System. Provide cabin pressure control and supply makeup gas as required to support other EC/LSS systems

4. Emergency Oxygen Supply. Provide capability for face-mask operation under emergency conditions

5. Contaminant Control System. Provide control of crew/passenger compartment humidity, carbon dioxide and trace contaminants

6. Water Management System. Provide for storage of portable and waste water. Supply to other systems as required

7. Food Management System. Provide for storage and reconstitution and distribution of food for boost and entry phases

8. Waste Management. Provide system for urine and fecal reception and storage or dump

The following vehicle definition and assumptions were used in the EC/LSS analysis and are reflected in the equipment sizing:

Definition/Assumption	Orbiter	Booster
1. Vehicle pressurized crew/passenger compartment free volume	1300 cu ft	350 cu ft
Compartment wall area crew compartment	625 cu ft	350 cu ft

Definition/Assumption	Orbiter	Booster
2. Vehicle leakage	5.0 lb/day/ 1000 ft of wall area	Same
3. Vehicle repressurization	None	
4. Gases and liquids may be vented to space		
5. Solids shall not be dumped to space		
6. Vehicle pressure flight	Nominal: 5 psia Range: 0-16.5 psia	Same
7. Heat rejection	Space, ground, and atmosphere	Ground
8. Vehicle heat gain/loss	Ferry/space flight	Atmosphere, ferry

Prelaunch environment - orbiter

Maximum heat gain = 5 Btu/ft^2/hr of wall area

Conditions:

1. Compartment atmosphere temperature = 75 F
2. Environment (ambient temperature) = 100 F
3. Solar load
4. Air velocity at wall = natural convection

Atmosphere Flight Environment/Ferry - Booster and Orbiter

Maximum heat gain = 5 Btu/ft^2/hr

Conditions:

1. Compartment atmosphere temperature = 75 F
2. Ambient temperature = 70 F

3. Altitude = 5000 ft to 15,000 ft

4. Speed = 240 kn

Space Flight - Orbiter

Maximum heat gain = 3.0 Btu/ft^2/hr

Maximum heat loss = no condensation

Conditions:

1. Earth orbit

2. Cabin atmosphere dew point = 60 F

3. Cabin atmosphere temperature = 75 F

4. Air velocity at wall = 20 ft/min

Entry/Landing/Post Landing - Booster and Orbiter

Maximum inner wall temperature = 200 F maximum local with 130 F maximum average inner wall temperature

Conditions:

1. Inner wall temperature = 80 F maximum at start of entry

2. Air velocity at wall = natural convection

3. Air temperature at start of entry = 80 F maximum

4. Air temperature at postlanding = 100 F maximum

5. Crew compartment inner wall conditioned to minimize radiative heat transfer between crew/equipment and wall

The life support subsystems crew/passenger requirements and subsystem definition considered in system sizing are given below:

Crew/Passenger Requirements	Orbiter
1. Metabolic load (total)	Nominal: 11,200 Btu/man-day Range: 10,300-13,600 Btu/man-day Design maximum: 650 Btu/man-hr
2. Latent load	Nominal: 4,110 Btu/man-day Range: 2,320-7,640 Btu/man-day Design maximum: 360 Btu/man-hr
3. Sensible load	Nominal: 7,090 Btu/man-day Range: 4,920-9,680 Btu/man-day
4. Oxygen consumption	Nominal: 1.84 lb/man-day Range: 1.67-2.45 lb/man-day
5. Carbon dioxide production	Nominal: 2.12 lb/man-day Range: 1.98-3.0 lb/man-day
6. Food consumption	1.68 lb/man-day
7. Water consumption (not docked)	Nominal: (6.6) lb/man-day Range: 5.89-12.0 lb/man-day
8. Wash water	None (excess fuel cell water may be used)
9. Latent water loss	Nominal: 3.97 lb/man-day Range: 2.78-8.5 lb/man-day
Respiration	2.65 lb/man-day
Perspiration	1.32 lb/man-day

Crew/Passenger Requirements	Orbiter
10. Urine water	Nominal: 2.65 lb/man-day Range: 2.54-4.48 lb/man-day
11. Fecal water	Nominal: 0.25 lb/man-day Range: 0.22-0.33 lb/man-day
Water	0.25 lb/man-day
Solids	0.08 lb/man-day

Subsystems Definition	Orbiter
Atmosphere Control	
1. Total pressure	Nominal: 5 psia Range: 0-14.7 psia
O_2 partial pressure	Nominal: 4.8 psia Range: 3.1-5.0 psia (flight) 3.1-10 psia (ground)
2. N_2 partial pressure	40 percent of total pressure at launch 2 psia max at 5 psia total cabin pressure
3. CO_2 partial pressure	
Normal	5.0 mmHg
Maximum	7.6 mmHg
Emergency maximum	15 mmHg
4. Quiescent-pressure	Up to 10 psia supplied by space station
5. Cabin trace contaminants	0.1 of threshold limit value in NASA CR-612
6. Atmosphere temperature	Nominal: 75 ± 2 F Range: 65-80 F Emergency/atmospheric flight; no reduction in crew performance

Subsystems Definition	Orbiter
7. Cabin relative humidity	Nominal: 50 percent Range: 35-70 percent
8. Atmospheric dew point	Maximum: 60 F Except postlanding; no reduction in crew performance
9. H_2O partial pressure	Approximately 8 mm Hg minimum
10. Cabin ventilation rate	
Maximum velocity	300 ft^3/min
Minimum velocity	10 ft^3/min
Water Management	
1. Waste	Stored to waste tank capacity 24-hr boiler operations
2. Potable	Stored at launch/fuel cell makeup
3. Fecal	Stored
4. Food preparation	
Hot water	154 ± 4 F (1 oz/min)
Cold water	55 F (1 oz/min)
5. Potable water reserve	4 hr

8.9.2 Concept Selection and Description

Concept Options

Various options to perform the EC/LSS functional requirements were grossly assessed for the shuttle vehicle mission. The functional requirements and the most likely conceptual options that could be used are shown in Figure 8.9-1. These do not include all the possibilities: for example, further definition of the mission may indicate a long quiescent period with a

EC/LSS

- CO_2 and Trace Contaminant Control
  - Gas Purge
    1. 83 CFH/crew required = 2.3 lb/hr/man 0_2 at 5 psia = 470 lb/man for 7 day
  - Cabin Storage
    1. 83 cu ft/crew/hr = good for approximately two hr
  - Mol Sieve
    1. 48 lb/man/mission X 12= 575 lb (for fail operational - fail safe = 1100 lb)
  - Lioh/activated charcoal
    1. 6 lb/man/mission and 0.16 lb/man/hr x 168 hr = (6 lb x 12 =) 72 + 322 = 394 lb
    2. Can be off loaded for short missions
    3. Power required about same as per mol sieve
- Humidity Control
  - Gas Purge
    1. 160 lb/day/crew
  - Condenser
    - Integral to Cabin Hx
      1. Higher air flow through cabin Hx than needed (increase Power - Regen Hx required large condenser)
    - Integral to CO_2 ABS
      1. Air flow rate required about the same. 2. Will pick up heat of reaction. 3. Smaller condenser required.
    - Independent Condenser
      1. Adds need for additional fans. 2. In integral systems, fans are larger.

Figure 8.9-1. EC/LSS Systems Concept Options, Orbiter (Sheet 1 of 9)

Space Division
North American Rockwell

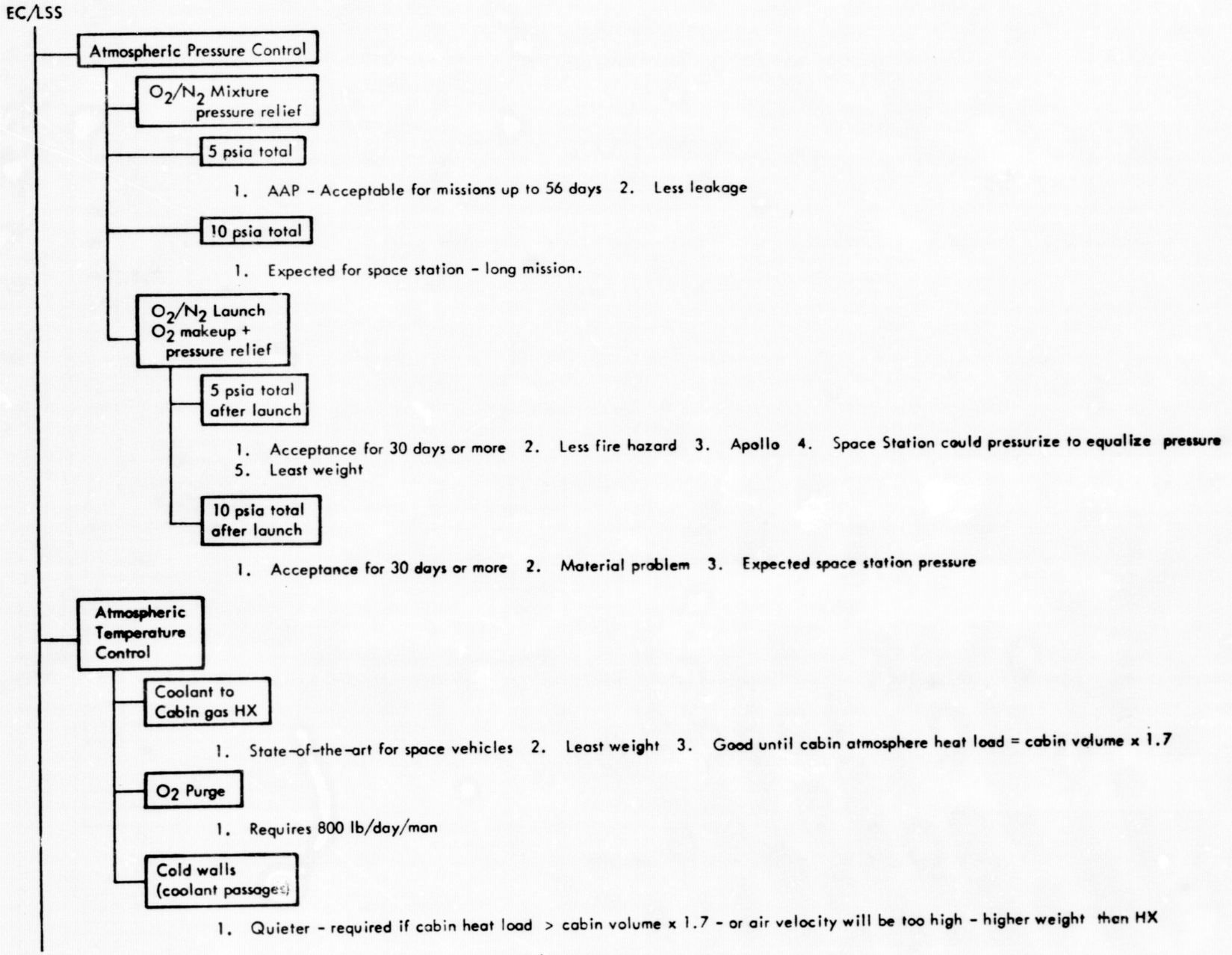

Figure 8.9-1. EC/LSS Systems Concept Options, Orbiter (Sheet 2 of 9)

EC/LSS

- Electronic Cooling
  - Air
    1. High flow rates required 2. Must exchange heat at low temperatures or cabin will be too hot for crew comfort
    3. Low temperature (50 to 70 F) 4. Low efficiency
  - Coldplate
    1. Most ideal from standpoint of heat transfer 2. Will be difficult to get heat from lights and displays - IR losses
  - Air and coldplates
    1. Most practical 2. Lights, displays, IR losses, small low load electronic boxes, and some instrumentation by air, major portion of electronic boxes by coldplates
- Coolant Loop
  - Coolant
    - Water
      1. Radiator surface coating is such that water could freeze and not thaw
      2. Water will be acceptable for use in evaporators
      3. Will freeze out of GSE HX
    - Glycol
      1. No freeze problem
      2. Lower specific heat and water of water/glycol
      3. High viscosity 4. Possible fire hazard
    - Water/Glycol
      1. If freeze, easy to thaw 2. Good specific heat 3. Acceptable viscosity 4. No exceptional fire hazard 5. Most experience.
    - Freon
      1. Low viscosity 2. No freeze 3. No fire
      4. Bigger contamination problem 5. Low specific heat requires high flow rates
      6. Freon heavy 90 + lb versus 60 + lb

Figure 8.9-1. EC/LSS Systems Concept Options, Orbiter (Sheet 3 of 9)

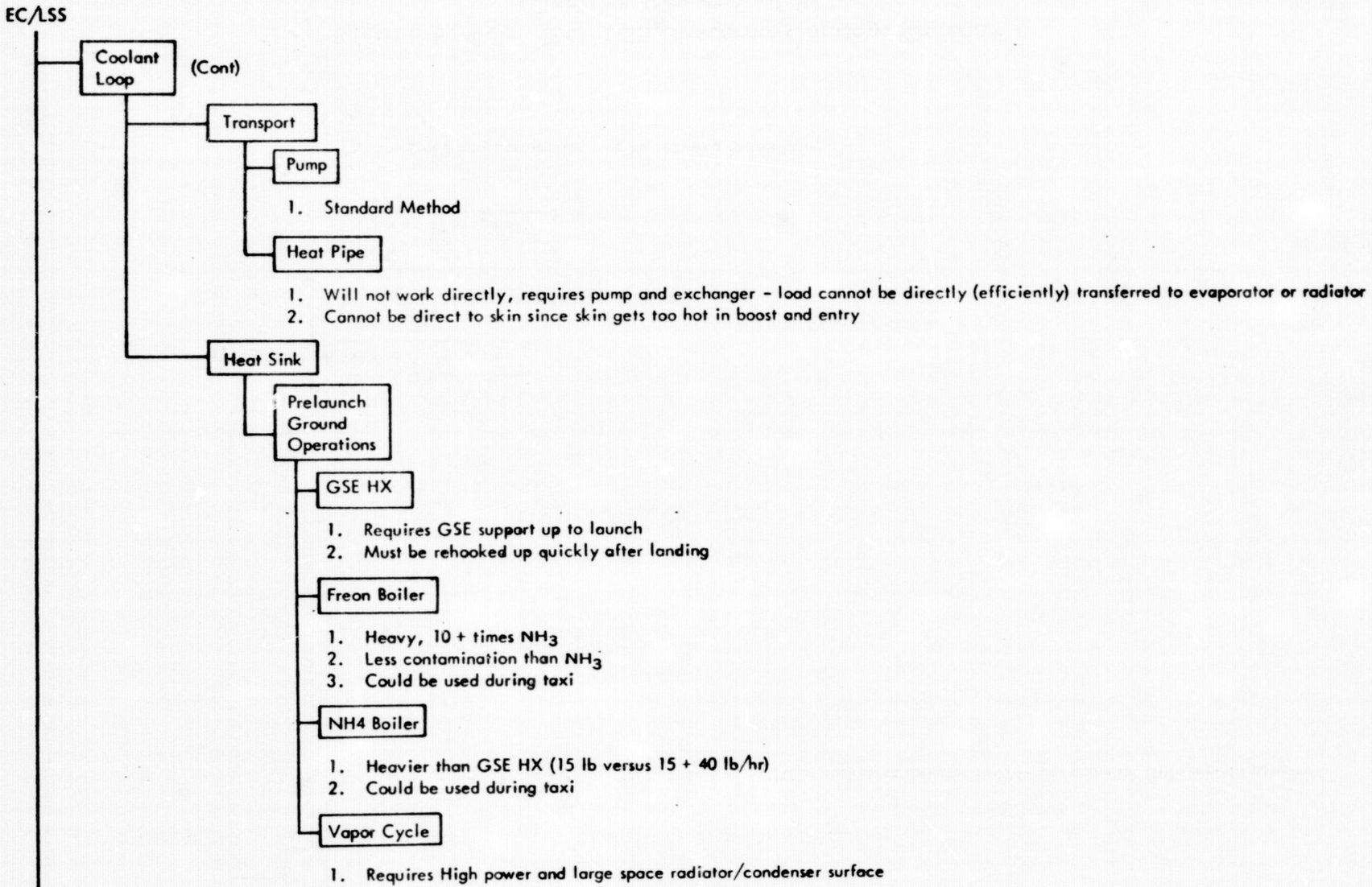

Figure 8.9-1. EC/LSS Systems Concept Options, Orbiter (Sheet 4 of 9)

Space Division
North American Rockwell

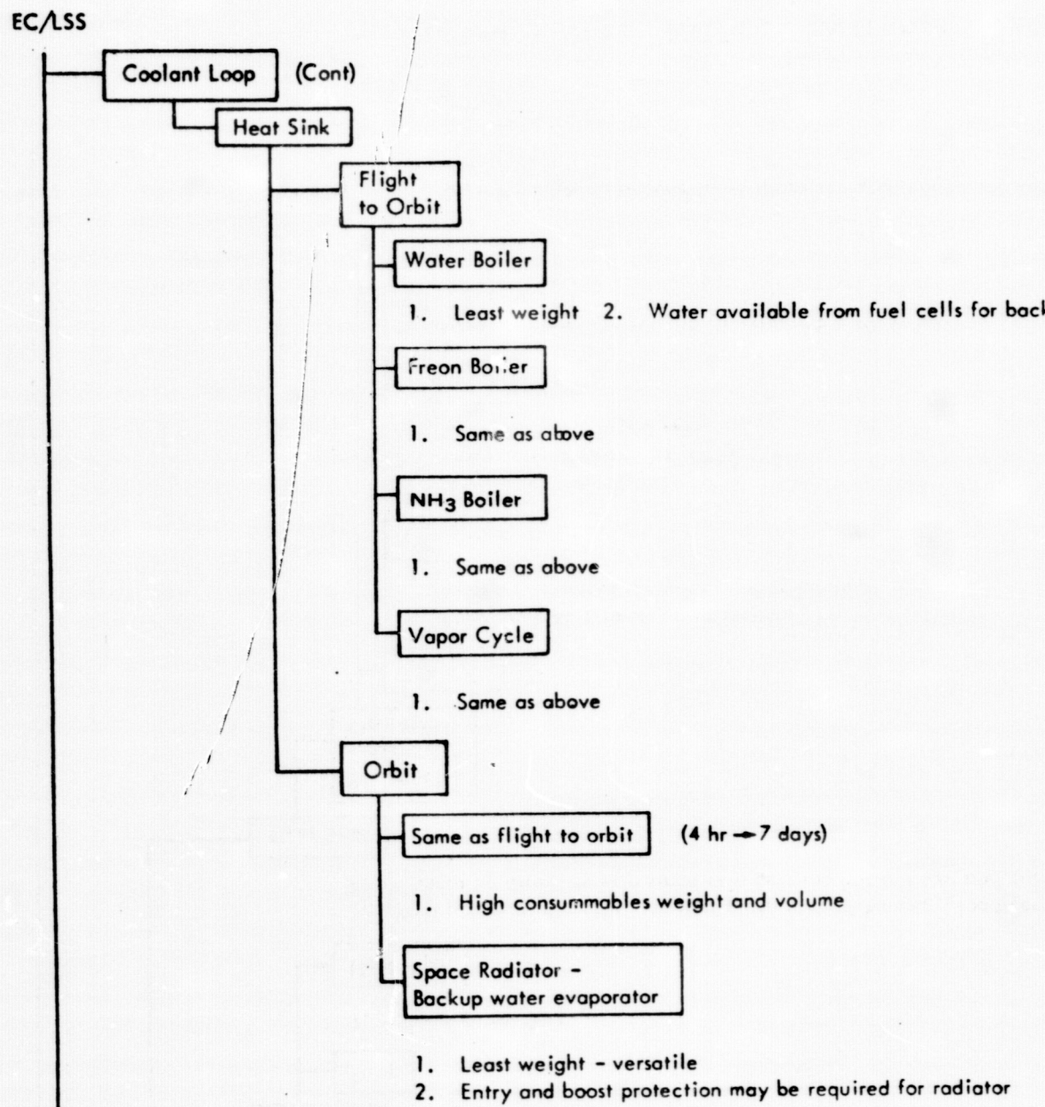

Figure 8.9-1. EC/LSS Systems Concept Options, Orbiter (Sheet 5 of 9)

Space Division
North American Rockwell

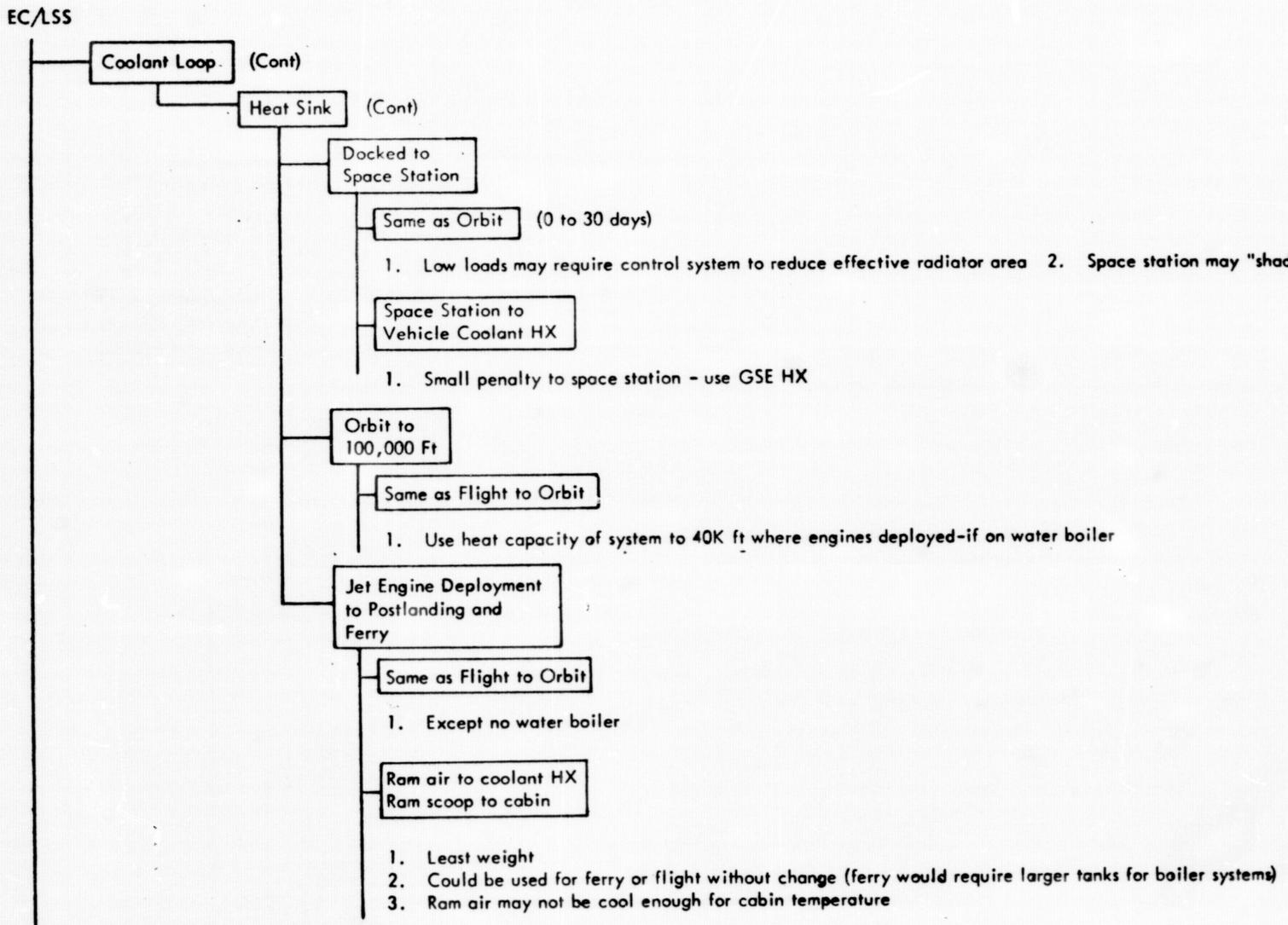

Figure 8.9-1. EC/LSS Systems Concept Options, Orbiter (Sheet 6 of 9)

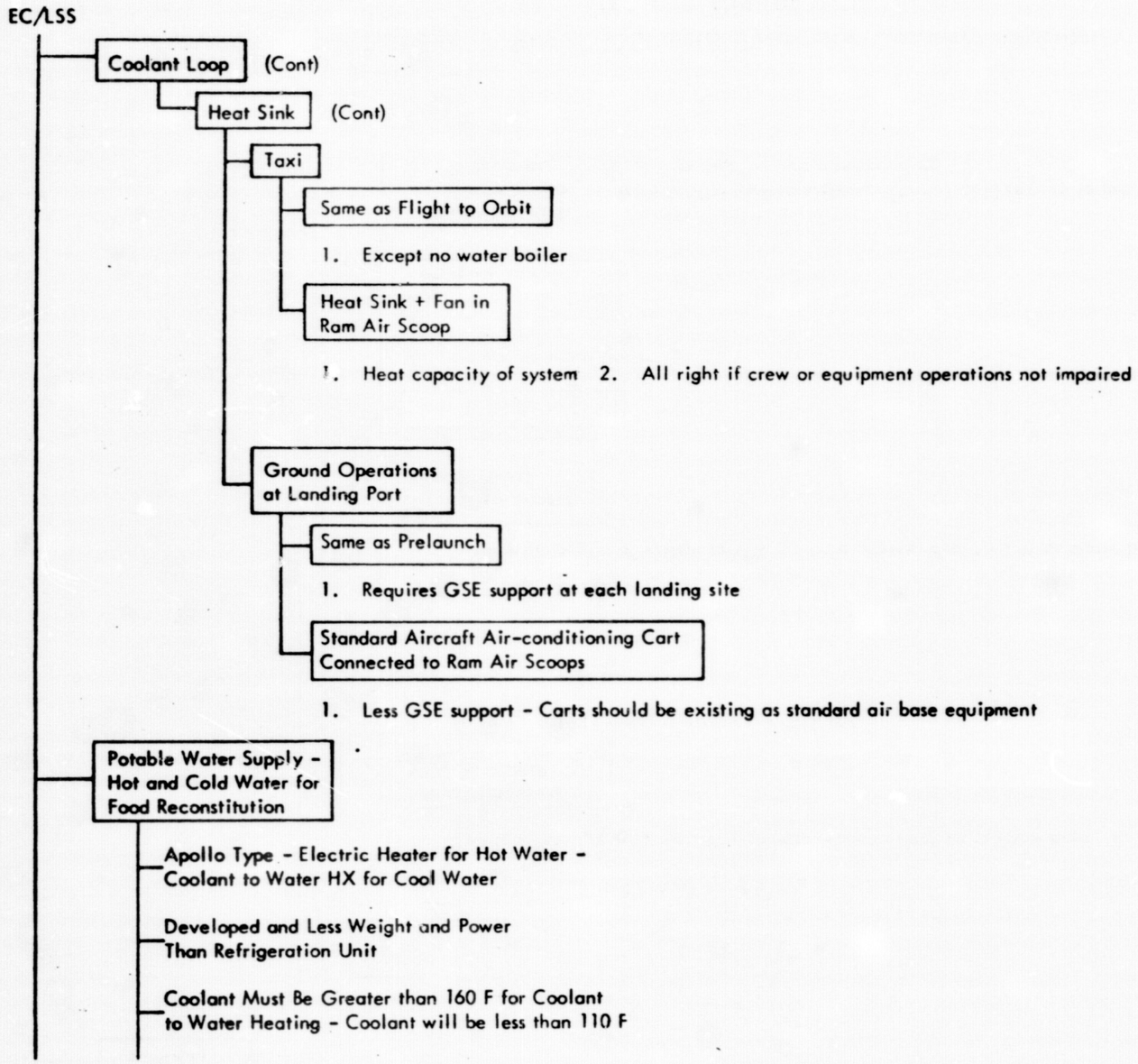

Figure 8.9-1. EC/LSS Systems Concept Options, Orbiter (Sheet 7 of 9)

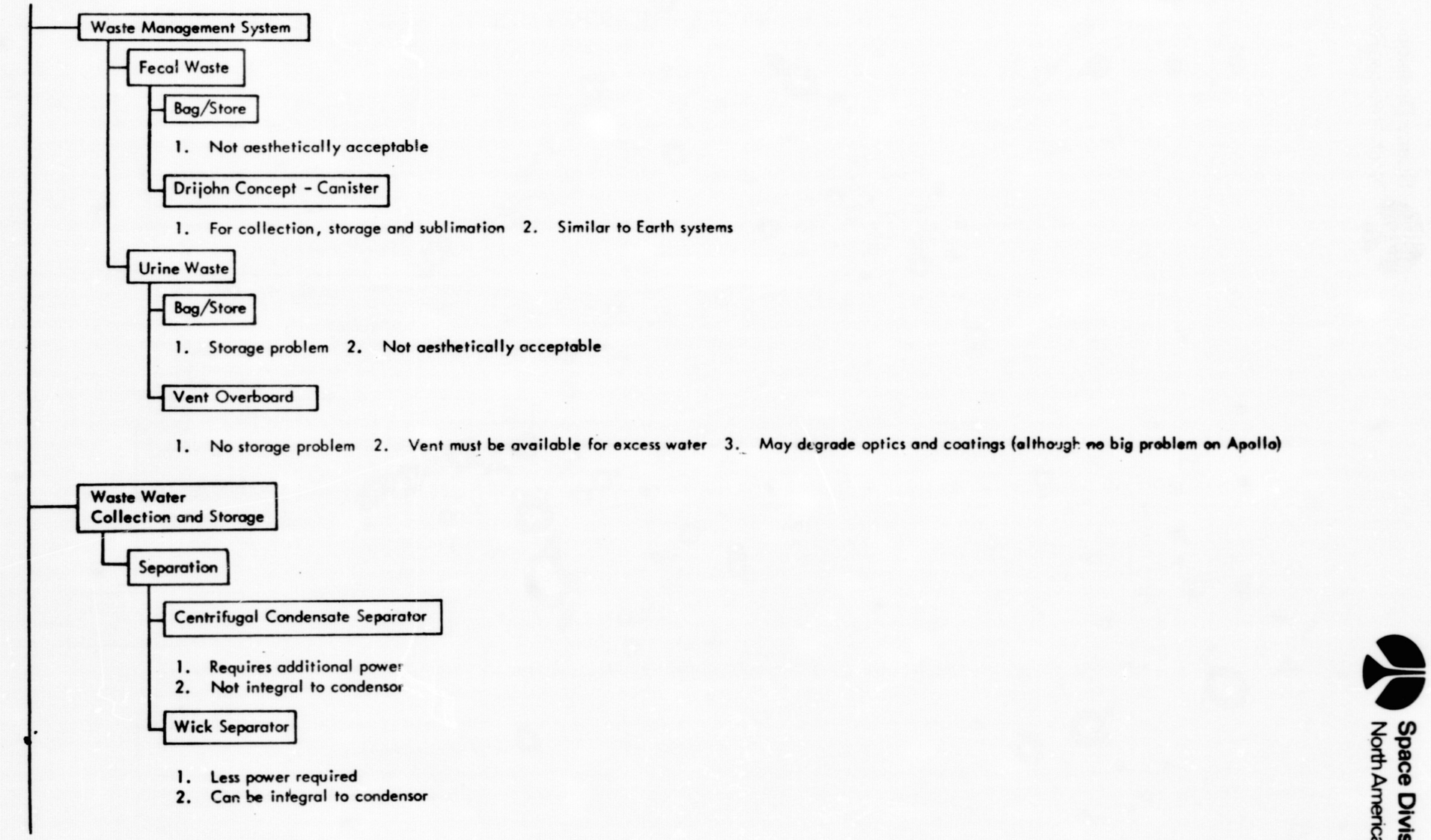

Figure 8.9-1. EC/LSS Systems Concept Options, Orbiter (Sheet 8 of 9)

Space Division
North American Rockwell

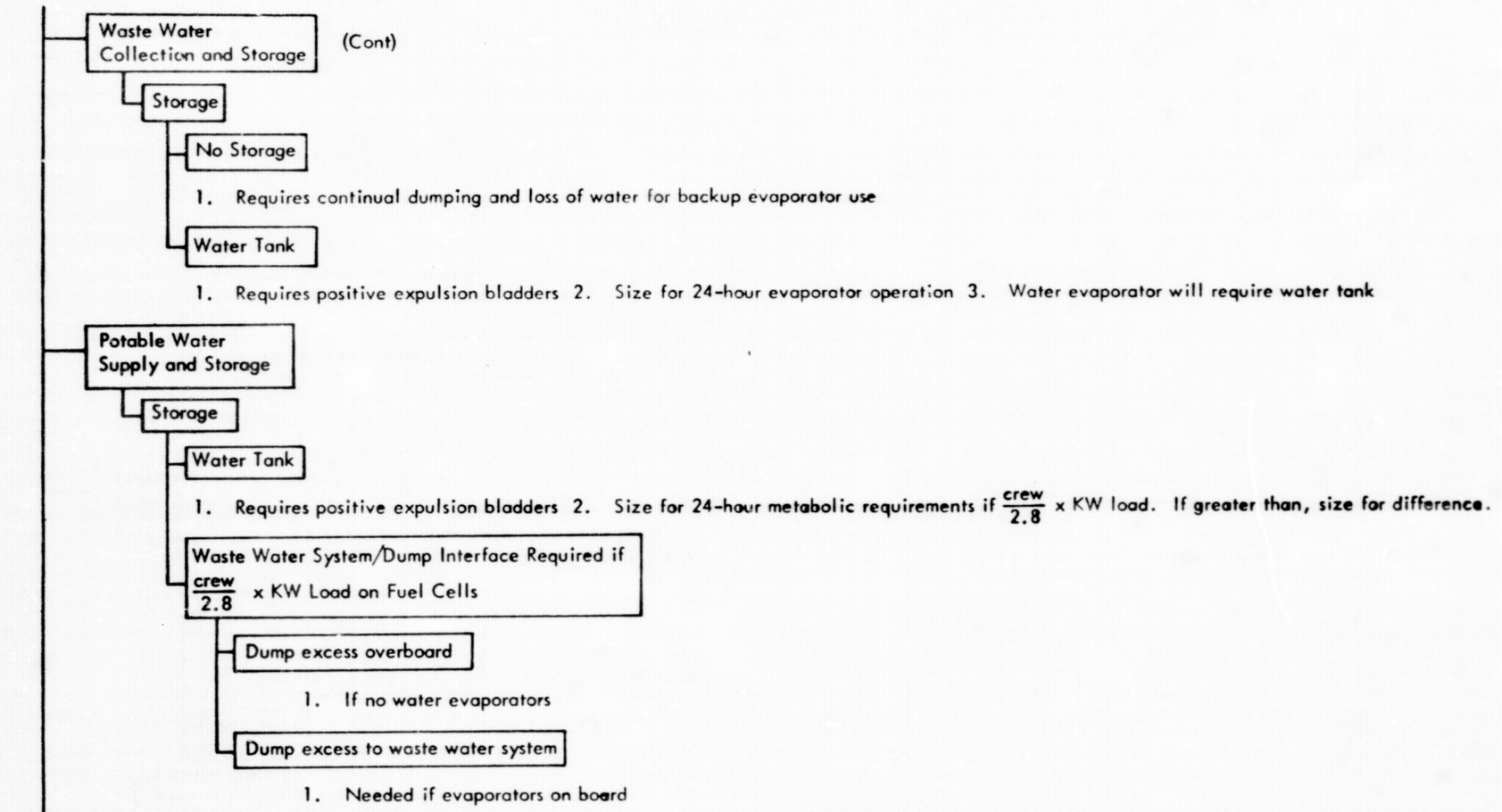

Figure 8.9-1. EC/LSS Systems Concept Options, Orbiter (Sheet 9 of 9)

very low load. In this case, it may be advisable to consider a Freon coolant in the radiator system with water coolant in the cabin and a Freon-to-water heat exchanger. The chart was developed for the orbiter since the system is more complex. The booster is unmanned for the shuttle mission application. Therefore, provisions are only required for environmental control of equipment during the short duration out of the atmosphere, atmospheric cruise back, and ferry. Provisions will be added for two crew members to perform a ferry mission.

Systems Description

The Shuttle vehicle EC/LSS is made up of a group of subsystems which performs the functions of thermal control of the crew, passengers crew/passenger compartment and electrical equipment; pressure control of the cabin; contaminant control of the cabin atmosphere, and metabolic provisions for crew and passengers.

Because of the orbiter's longer space flight requirements, the orbiter system is more complex. The booster's primary mission requires only two to six minutes in which cooling cannot be provided by either a GSE heat sink or a ram air heat sink. For this flight phase, a heat sink is not provided and the system heat capacity will be used as the sink. Other significant differences are noted in the description. The proposed orbiter system includes equipment for wheel well temperature control, and engine compartment environment control. The requirements and constraints for such a system were not well defined in this phase. It is recommended that further investigations be conducted in this area.

The EC/LSS concept for the orbiter and booster was developed so that systems would be common to both with space flight support equipment deleted from the booster. Crew equipment items are also briefly described. System redundancy is provided to meet the fail operational or fail safe requirements of mechanical equipment. This requirement was not considered to apply to structural integrity. For example, two coolant loops have been provided. If a hard line failure or passage failure in common heat exchangers should occur, the system would fail from operational to fail safe since a second failure in some particular flight phase, (in a flight phase where earth landing or space station rendezvous is more than eight hours away), may cause loss of crew or equipment. The only other recourse would be to incorporate a third coolant loop and isolate each loop in separate heat exchangers.

Schematic diagrams of the selected system for the orbiter is shown in Figure 8.9-2. Equipment location is illustrated in Figure 8.9-3. A description of the selected system is given below.

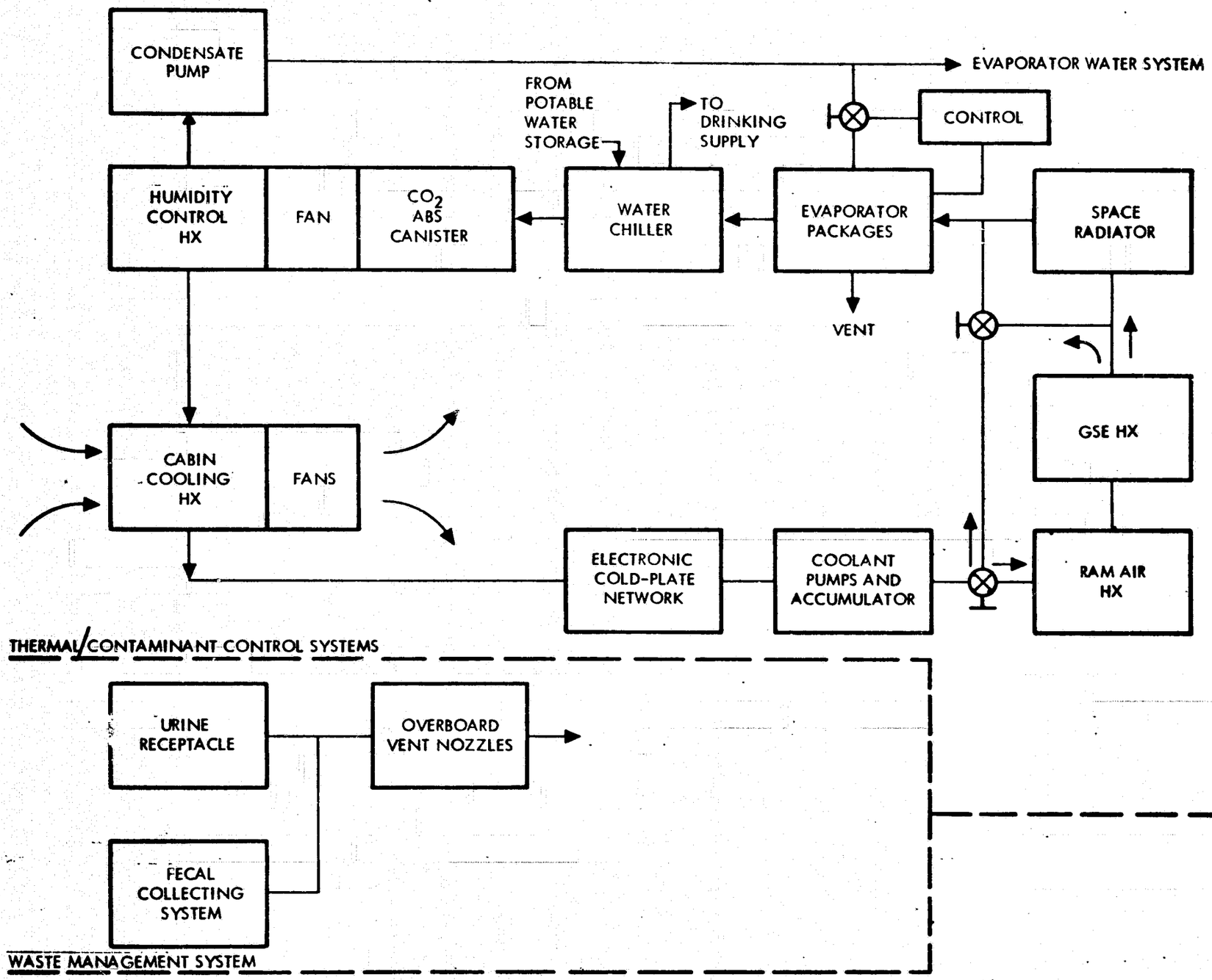

Figure 8.9-2. Orbiter EC/LSS Schematic (Sheet 1 of 2)

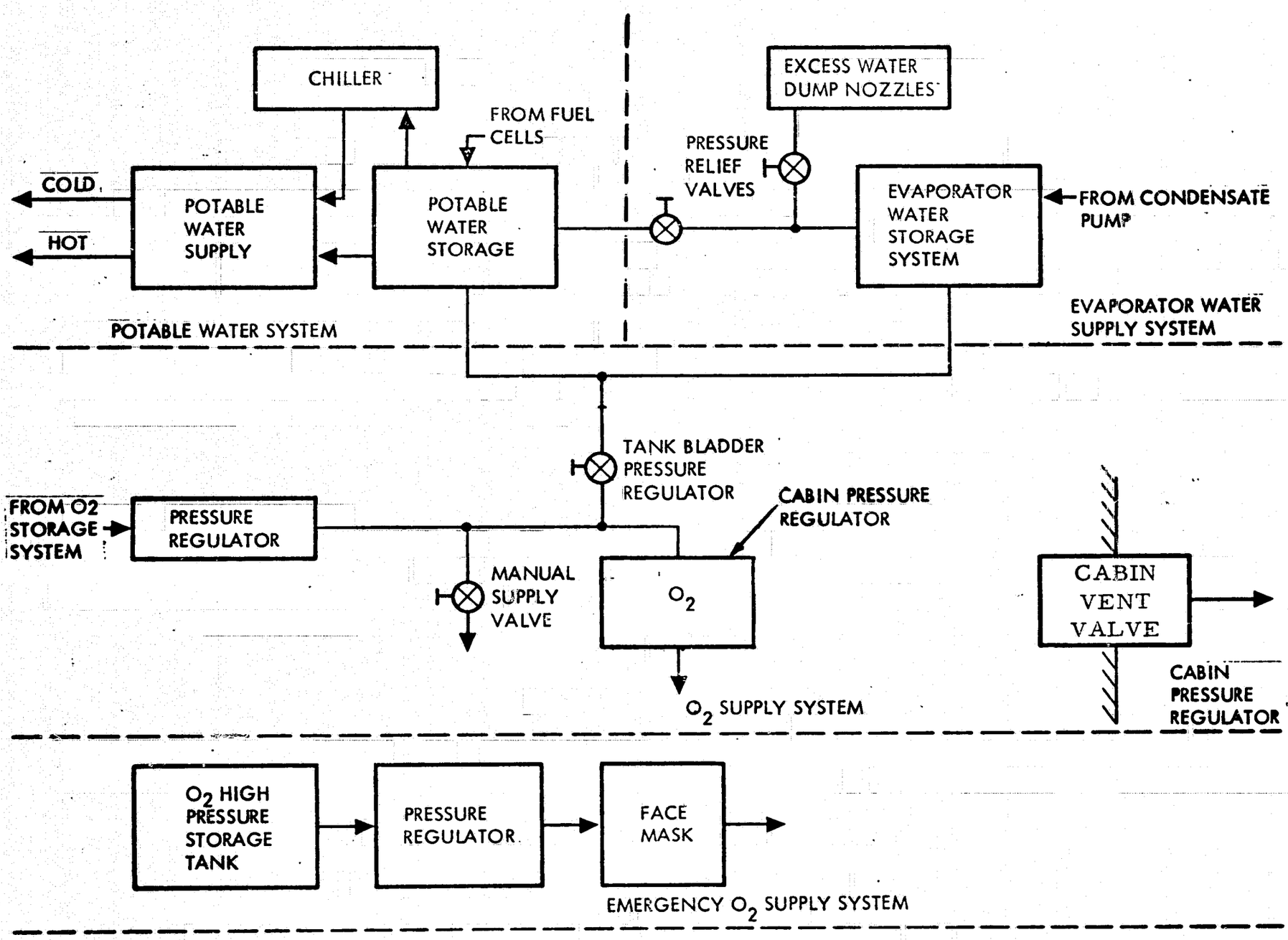

Figure 8.9-2. Orbiter EC/LSS Schematic (Sheet 2 of 2)

Space Division
North American Rockwell

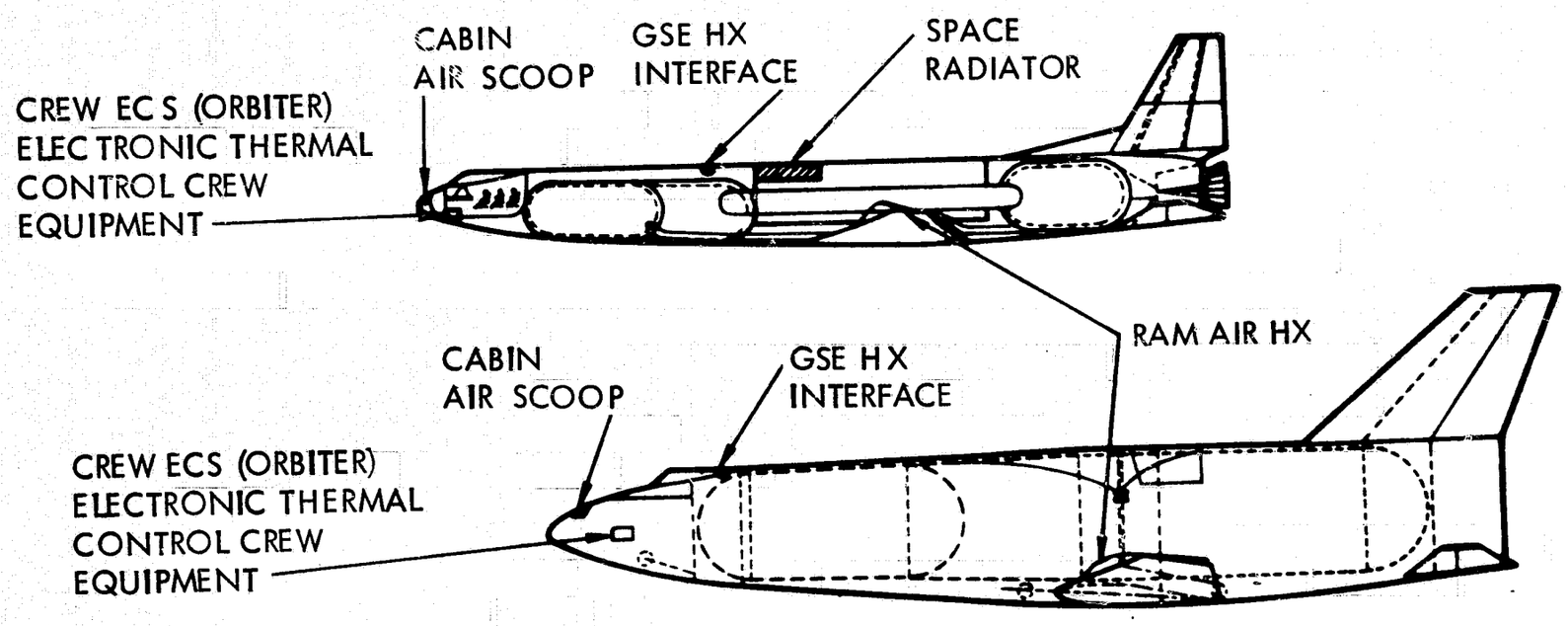

Figure 8.9-3. EC/LSS Equipment Locations

Space Division
North American Rockwell

The humidity control - atmospheric contaminant control system consists of:

1. A heat exchanger incorporating an air passage, two coolant loop passages, and wicks in the air passages to collect the humidity condensate.

2. Two condensate pumps, either electrically or pneumatically operated, to pump the condensate into the evaporator water storage system.

3. Two fans, one for redundancy, to circulate the cabin gas through the system.

4. A carbon dioxide and trace contaminant absorber canister to hold the absorber elements.

5. Absorber elements consisting of filters, activated charcoal charges, and a LiOH charge. Each element will be sized for one man-day use. One element will control the atmosphere to a safe, operational carbon dioxide level. However, one element will be changed every 12 hours.

The system will be sized to control the carbon dioxide to a level of zero to 7.6-mm pressure and the moisture dew point to approximately 50 to 65 F (relative humidity 30 to 70 percent) for a twelve-man load. Redundant cooling passages, fans, canisters, elements, and water pumps will provide fail-operational, fail-safe requirements. For example, should both fans fail, moisture will collect on the cabin heat exchanger and can be vacuumed off by the urine hose. The carbon dioxide will build up to the maximum constant exposure limit of 16 mmHg in nine hours. If this is not sufficient time, dumping the cabin to 3 psia and repressurizing will extend the time.

The cabin pressure control system consists of plumbing and regulators to:

1. Control the cabin pressure to 5 psia oxygen atmosphere by make up with pure O_2.

2. Reduce the oxygen pressure from the vehicle oxygen supply system to a usable pressure. Two sources are planned.

3. Control the bladder pressure of the water tanks to provide for positive expulsion of the water.

4. Provide for pressure relief during boost, entry, and flight to prevent excessive positive or negative pressure. To allow for minimum size valving to prevent sudden cabin pressure loss should a relief valve fail open, it is planned to provide for positive relief at 12 psig and negative relief at 2 psig. The valves will be provided with three positions: one closed; one boost/entry, which will allow the valves to go full open if required; and one for space flight, limiting the valve opening in case of failure.

The energency oxygen supply consists of face masks, regulators, and a ten-minute supply of oxygen. Ten minutes should be sufficient to purge the cabin of any trace contaminants or close a cabin pressure relief valve should one fail open. Provisions could be provided to refill the system from the vehicle oxygen storage system if the system pressure is high enough.

The cabin pressure relief system and the emergency oxygen system are all that are required on the booster.

The cabin temperature control system incorporates dual fans and dual coolant loop passages in the heat exchanger. Provisions will be provided to bypass coolant around the heat exchanger to control cooling capacity. No heating provisions are planned. Both fans will be required to provide sufficient cabin cooling on hot days on the pad and ferry flights. For space flight, one fan will be turned off and capped.

The electronic thermal control network (coldplate circuit) coldplates will be fixed to the structure, with the electronic equipment bolted or clamped to the coldplates.

The coolant circuit pump package includes two pumps and an accumulator for one coolant loop and one pump and an accumulator for the other system. The accumulators can be isolated from the system in case of failure so that the total system is not lost. The coolant will probably be a glycol/water mixture.

The ram air-to-coolant heat exchanger is provided as the heat sink during flyback and ferry flight. The altitude of the flyback and ferry is low - from 5000 to 15,000 feet. In this case, the ram air temperature is warm (70 F) and the cabin temperature is expected to be 75 to 90 F. The cabin would be ventilated by opening a ram scoop and exiting the air through cabin pressure relief valve. Because of the short duration of the orbiter atmospheric flight phase, the cabin ventilation may not be required. If the orbiter or the booster land at an airport that is not equipped with ILRV GSE, a cooling

air duct from a ground cart would be slipped over the face of the ram air heat exchanger to provide the heat sink before the ferry flight back to the launch base.

A GSE liquid-to-liquid heat exchanger is incorporated into the heat transport loops to provide heat sink during ground checkout and prelaunch, while the orbiter is docked to the space station (if desired), and after landing.

A radiator system with supplementary evaporators is provided that incorporates passages for both heat-transport loops and two evaporators, one for each transport loop. The evaporators will be used to reject heat during boost and entry and in case of failure of both radiators. Each evaporator is sized to reject the boost and entry loads, while the space radiator is sized to reject the space flight load. The radiator and evaporators are not required for the booster.

The evaporator water system supply consists of a water tank with a pressurized bladder and valving. The bladder is pressurized by the oxygen supply system. Sufficient water is carried at launch to provide for heat rejection by means of the water evaporators until the radiator system can reject the load. The evaporator water tank will have isolation capability in case of failure. Fuel cell water will first fill the potable water system. The excess will then flow through a pressure relief valve into the evaporator water tank. Condensate water is also fed to this system. In case of failure of the evaporator water tank, the tank will be isolated and water will be supplied from the potable tank. The evaporator water system capacity is sized for 24-hour operation of the evaporator with flight loads.

The potable water system for the orbiter consists of a water tank with a pressurized bladder, valving, plumbing, water chiller, and a potable water supply which incorporates a heater and provides hot and cool water for drinking and food reconstitution. The tank is sized for a 24-hour supply. Fuel cell water provides the source for the extended stay period. The potable water system for the booster consists of a pressurized tank, water chiller, and a water supply valve. The system is sized for 4 pounds available water.

The waste management system for the orbiter consists of a urine relief tube which is vented overboard through heated nozzles to prevent freezing. Collapsible bags are provided should the crew wish to store the urine for some time before dumping the full amount overboard. The fecal collection system consists of the collection device which has sufficient air flow through the system to provide for positive bolus detachment and entrainment. The odors would be dumped overboard through the urine dump nozzles. Between uses, the canister will be evacuated to sublime the feces.

A ram air scoop, fan, and filter have been added to the system to provide for cabin humidity, carbon dioxide, and, to some extent, temperature control. This system will provide for cabin ventilation during ground operations, ferry flight, taxi, and atmospheric flight.

Although a definite requirement has not been established for pressure and temperature control of the wheel well and turbojet engine compartments, a gross analysis was conducted to assess the effect of this requirement. It was assumed that the ILRV orbiter wheel wells and engine compartment temperatures will be maintained at 30 to 120 F, and the pressure maintained at or above 0.5 psia.

The following configuration and estimates were used for calculations.

Configuration	Estimates
2 Wheel wells	
Dimensions	17.7 x 6.8 x 7.3 (ft)
Internal wall area	695 ft^2 (each)
Volume	880 ft^3 (each)
2 Engine compartments	
Dimensions	20.5 x 12.5 x 7.3 (ft)
Internal wall area	995 ft^2
Volume	1870 ft^2
Pressure leak rate	5 psia/day/1000 ft^2/at 5 psia compartment pressure
	0.5 psia/day/1000 ft^2/at 0.5 psia compartment pressure
Thermal heat load	3.0 Btu/ht/ft^2 wall area
Compartment ambient temperature	30 to 120 F

Calculations were made to determine the heat load, the time after boost before nitrogen gas makeup is required to maintain compartment pressure at 0.5 psia, and the rate of makeup gas required at this time.

The wheel wells and engine compartments will vent down to 5 psia during boost, and will then slowly leak down to 0.5 psia during orbit. When the 0.5 psia pressure level is reached, nitrogen will be supplied from a gas supply system to regulate the pressure at 0.5 psia until reentry. The results are shown in Table 8.9-2. The data show that no makeup gas or pressure regulation systems will be required for orbiter missions less than 12 days.

Table 8.9-2. Compartment Pressure Requirements

Compartment	Heat Load (Btu/hr)	Time to Make Up Gas Required (days)	Make Up Nitrogen Required (lb/day)
2 Wheel wells	5270	12.8	0.35
2 Engine compartment	5960	19.0	0.50

The crew equipment used to determine the weight and volume requirements included seats, head sets, coveralls, medical kit, survival kits, containers, retainers, cushions, tool kit, flight data file, constant wear garments, towels, tissue, urine hose, filters, transfer units, seat shock absorbers, and structure support.

The EC/LSS system equipment and consumable weight are listed in Table 8.9-3; electrical power requirements are summarized in Table 8.9-4.

8.9.3 Space Station Interfaces Requirements

In further studies, configurations and missions of both the space station and the ILRV will become better defined. This will allow better definition of the interfaces. Also, as space station processing depth is established and tradeoffs are concluded, interfaces will define the responsible vehicle for emergency equipment storage, pressure control, and waste products disposal. Additional functional and physical interfaces will be required to identify instrumentation monitoring requirements of active equipment and pressure and temperature of critical areas in the quiescent logistics vehicle.

The interfaces required will be of two modes: functional and physical hardware. The functional interfaces will concern the following:

1. Equalization of logistics vehicle/and space station pressure after docking

2. Changeover of atmosphere control and equipment thermal control after docking

3. Transfer and storage of such perishable items as food and medicines

Table 8.9-3. EC/LSS Weights

System Description	Orbiter		Booster	
	Weight (lb)	Volume (cu ft)	Weight (lb)	Volume (cu ft)
Equipment				
Humidity and CO_2 control system	190	5.9	0	0
Electronic coldplate network	85	1.2	85	1.2
Cabin cooling system	149.4	3.0	58.7	1.2
Coolant pump package	91.3	2.7	62.8	1.9
Radiator system[1]	187	18.7	0	0
Evaporators	91.3	4.6	0	0
Ramair heat exchanger	42.9	2.1	35.4	1.8
GSE heat exchanger	42.9	2.1	35.4	1.8
Emergency O_2 system and O_2 pressure control	56.4	6.0	0	0
Potable water system	73.0	1.5	0	0
Evaporator water system	56.2	6.9	0	0
Urine and fecal system	26.0	2.0	0	0
Crew equipment	2509	109.7	0	0
Consumables				
Evaporator water	98.6	—	—	—
Oxygen	170.4	—	—	—
Food	185.5	—	—	—
CO_2 absorber elements	322.6	10.8	—	—

[1]Assumes 236.6 ft^2 radiator area.

Table 8.9-4. EC/LSS Electrical Power Requirements

Condition	Power (watts)	
	Orbiter	Booster
Ground power	414	200
Flight power	305	200

4. Adjustment and preparation of the systems for the quiescent stage, which will probably include deactivating pressure controls, humidity and carbon dioxide controls, and reduction of coolant loop flow

5. Occasional maintenance, operation, and first-level repair or replacement during the quiescent period

6. Pressurization and activation of the vehicles before separation

7. Storage procedures for equipment and perishable items returned to the vehicle

8. Other functional procedures that would provide options for emergency and unscheduled use of the vehicle

Many of the functional procedures will not require a hardware interface but may affect the makeup and configuration of tool kits and checkout equipment used on board the space station.

The hardware interface requirements will result from decisions made in optimization studies. These would include whether to use vehicle electrical power or space station power after docking; use of the vehicle as sleep/rest quarters; which vehicle should provide pressurization gas after docking and before separation; and if electrical equipment is required in the quiescent stage, the operation of the coolant circuit. Hardware interfaces that must be considered include the following:

1. Coolant transport loop. During start-up and shutdown periods, coolant from the space station may be required. This could interface with a liquid-to-liquid heat exchanger location in the logistic vehicle. No fluid interchange will probably occur. Coolant temperature will be on the order of 35 to 70 F and a flow of 100 to 400 pounds per hour, depending on the load and mission phase.

2. Electrical power. Electrical power will be required to operate the EC/LSS during the start-up and shutdown periods. The 30 to 200 watts that will probably be required may be provided by the space station.

3. Cargo and crew compartment pressurization. The space station may be required to provide gas and controls for pressurizing the logistics vehicle after docking.

8.9.4 Mission Time Line as Applied to Environmental Control and Life Support Systems

A mission time line was generated in narrative form to provide a clearer understanding of the systems and systems operations. Unless otherwise noted, the following information applies to both vehicles.

Ground Operations - Systems Checkout and Maintenance

1. When electrical or electronic equipment located on coldplates is operated, ground cooling must be provided. This is accomplished through interface of the GSE ground cooling and the vehicle GSE heat exchanger. The GSE coolant will be on the order of 10 to 30 F; flow rates will be on the order of 500 pounds per hour. The vehicle system one or two coolant pump would be operating.

2. Cabin cooling fans may be on if required.

3. The humidity control system will be operating if personnel are in the cabin and condensation is evident. Carbon dioxide elements will not be installed.

4. The cabin pressure relief valve and the cabin ram air scoop will be open. A fan/filter assembly will draw in outside air. The flow will be in the order of 100 cubic feet per minute, although a minimum of 11 cubic feet per minute is required.

5. The radiator (in the orbiter) and ram-air heat exchanger are being bypassed by the coolant.

6. Ground personnel will:

   Drain and clean the urine receptacle and urine storage system.

   Remove and replace the waste canister in the orbiter.

   Clean and service potable and evaporator water systems and test for microbe count.

   Replace crew equipment such as tissue, towels, and clothing.

7. The onboard checkout system will have evaluated the systems performance from the previous mission. Redundant systems will be operated by ground personnel, and the onboard checkout system will evaluate these data. The onboard checkout system information and crew log will be used by ground crews to repair or replace equipment as required. All equipment will have a minimum life of 2500 operating hours and a shelf life of five years.

T-2 Hours to T-5 Minutes

1. Crew and passengers will be inserted.

2. Crew or onboard checkout system will verify that:

   Coolant pump (System 1) is on, and coolant temperature to humidity control system is 35 to 45 F.

   Cabin air dew point is +50 F maximum out of humidity control system.

   Cabin fans are on and in full cooling or in partial bypass of coolant if crew is cold. (Desired prelaunch cabin temperature is 50 to 70 F.)

   Ram air heat exchanger and space radiator are in bypass.

   Cabin pressure relief valve is open and fan is operating.

   Ground crew has signed off ship's log indicating vehicle is ready for flight.

3. LiOH elements will be installed.

4. The cabin ram air scoop will be closed.

5. Cabin will be purged to 60-percent oxygen.

6. Cabin pressure relief valve will be set to boost/entry position.

T-5 Minutes to Liftoff

GSE will disconnect coolant lines.

Orbiter - Liftoff to Orbit, Orbit

1. During boost, cabin pressure will vent to 12.0 psia. Through metabolic use and cabin leakage, cabin pressure will drop to 5.0 psia where cabin pressure regulator will maintain cabin pressure at 5 psia with 100 percent oxygen makeup.

2. After cabin pressure has dropped to 5 psia, the crew at some convenient time will set cabin pressure relief valve to normal position.

3. Crew will change one LiOH element at end of 12 hours and then replace one element every 12 hours. (Element size can be adjusted for any other schedule.)

4. Approximately one-half hour after launch, the space radiator will be activated and the water evaporators will be deactivated.

5. Crew can drink cool water (40 to 60 F) from the water supply.

6. Meals can be prepared using hot water (130 to 150 F), from the hot water supply.

7. Urination is accomplished through a tube into a holding bag, or the urine is dumped overboard through the urine dump nozzles (orbiter only).

8. For defecation, the toilet is opened to the cabin. With the overboard vent through the dump nozzles still activated to entrain the bolus, the bolus is moved to the bottom of the container. After completion, waste tissue and toweling are inserted. The seat cover is closed, the cabin pressure vent valve is closed, and the shredder is activated for 30 seconds. With the overboard vent valve still open, the feces will sublimate.

Space Station Rendezvous and Docked Operation

If the orbiter is docked to a space station, the following operations may occur:

1. Space station will pressurize the access tunnel.

2. Crew will open vent valve between tunnel and equalize pressure.

3. Interface with the coolant system may be made through the GSE coolant-to-coolant heat exchanger.

4. Waste material and excess water is offloaded to the space station for processing and use.

5. If the orbiter cabin is depressurized during the stay time, the space station will repressurize before crew ingress.

Orbiter Entry to Jet Engine Operation

Approximately one hour before the orbiter enters earth atmosphere, the following occurs:

1. The water evaporator is activated.

2. The cabin pressure relief valve is set to the boost entry position.

3. If located on the vehicle skin, the space radiator is vented overboard. If protected, it will not be vented.

Jet Engine Flight Phase to Touchdown

The jet engines will be deployed. The ram air heat exchanger becomes effective after transition to cruise altitude and the water evaporation will be turned off. On a warm day, the ram air temperature will be able to control the cabin air temperature below 90 F. The crew may open the ram air scoop and the cabin pressure relief valve to provide additional cooling and control humidity.

Landing to Crew Egress

On touchdown and until GSE can be connected to the system, structure heat capacity and fan air pulled in the ram air scoop will control the cabin temperature to a livable condition.

If the cabin is warm, the crew will egress as soon as possible, and electronics equipment will be turned off. The GSE coolant will be connected to the GSE heat exchanger as soon as convenient.

If the vehicle lands at a facility that does not have the ground cooling cart, a conventional ground air-conditioning cart will flow cold air through the ram air heat exchanger.

Ferry Flight

For ground operations, the GSE coolant-to-coolant heat exchanger will be used until taxi is started, or cold air will be flowed through the ram air heat exchanger. System heat capacity will be used until the vehicle is airborne and ram air can be used.

8.10 POWER SYSTEM

The booster and orbiter require electrical and mechanical power to perform the shuttle vehicle mission. The electrical power subsystem must generate, condition, and distribute electrical energy to the using subsystems throughout the mission cycle. Internal energy sources are required to deliver power from prelaunch transfer to internal power until reconnection of GSE supplies after vehicle landing. Internal power generation is also required for ferry operations from the manufacturing site and from alternate landing sites to the launch site.

The auxiliary power subsystem must supply mechanical energy to the hydraulic and electrical power subsystems, as required, during the same periods.

The objectives of the power system analysis were to develop conceptual system design to meet projected functional, reliability, and safety requirement; estimate system weight; provide system definition for cost analysis; and identify technology requirements.

8.10.1 Power System Requirements

The following requirements are considered applicable for the shuttle vehicle:

1. Seven day self-sufficient period from liftoff until touchdown for orbiter stage
2. Thirty-day maximum quiescent period while docked to space station
3. Two-week turnaround period
4. Two-hour launch response
5. Minimum of 100 missions
6. Fail-operational with full mission capability after first subsystems failure and fail-safe after second subsystems failure
7. Capability to supply energy to all required loads for 24 hours after second failure
8. Minimize or eliminate undesirable transients caused by equipment failures

9. Integration of distribution and control with multiplexed data system

10. Aircraft maintenance practices

11. Flexibility for technology growth

The orbiter has the most significant electrical power requirement because of orbital operations and mission duration. Table 8.10-1 contains the results of electrical load analyses for the orbiter. The maximum continuous load is about 4600 watts; peak loads (including engine ignition, water heaters, and teleprinter) will approach 7000 watts. A 30/70 percent ac-dc split and 5 percent line losses were assumed.

The peak and continuous shaft loads for each auxiliary power unit on the orbiter and booster are presented in Table 8.10-2. The continuous loads include hydraulic system leakage losses and electrical power to supply boost pumps, landing lights, navigation lights and other cruise or landing loads. Peak loads include control surface actuation, engine gimbaling, engine nozzle extension and retraction, gear steering, and wheel brakes. Periodic operation of this system will be required during boost and on-orbit operations for engine gimbaling, during reentry to landing phases, and possibly for hydraulic system heating or peak load operation during orbital operations. The estimated energy requirements are summarized in Table 8.10-3.

Based on a 7 day mission, 2 week turnaround, a 100 missions, the minimum subsystem life requirements are 16,800 hours flight time and 5.8 years total life from first flight until end of life. Quiescent mode operation, ground checkout, prelaunch operation, installation time, and launch delays must be considered in addition to these minimum subsystem life figures. Surveys of current and projected equipment lifetimes indicate that these time durations are in excess of the expected lifetimes of such candidate equipment as fuel cells and most battery types.

8.10.2 Power Source Selection

Candidate energy source, conversion, heat rejection, conditioning and distribution approaches are presented in Table 8.10-4. Weight tradeoffs for likely candidates on the orbiter stage are presented in Figure 8.10-1. For a 168-hour powered mission duration, fuel cells have been selected since they represent a space proven power source, exhibit relatively long life characteristics, and have a low specific weight, as shown in the comparison Table 8.10-5.

Table 8.10-1. Typical Orbiter Electrical Power Requirements

Subsystem	Continuous Power Requirements (watts) — Mission Phase: Prelaunch	Boost	Coast and Parking Orbit	On-Orbit Operations	Gross Rendezvous	Terminal Rendezvous and Docking	Docked (Active)	Docked (Inactive)	Quiescent Mode Operation	Preparation Checkout and Undocking	Return Phasing	ΔV Operations	Deorbit Coast	Entry and Recovery	Transition	Descent and Landing
Maximum Duration (hr)	5	0.12	20	-	1.6	1.6	54	54	30 Days	12	24	-	0.4	0.3	0.03	0.1
GN&C	900	900	1170	970	1170	1170	900	150	--	1010	1170	900	990	990	990	990
Data System	950	950	950	950	950	950	950	550	--	950	950	950	950	950	950	950
Communications	500	500	850	850	1050	1050	350	350	--	600	850	850	850	1000	1000	1000
EC/LSS	415	415	415	415	415	415	305	305	--	415	415	415	415	415	415	415
Propulsion	80	480	--	480	--	--	--	--	--	--	--	480	--	--	--	--
Electrical Power	250	250	250	250	250	250	220	210	--	250	250	250	250	250	250	250
Sub-Total	2995	3395	3635	3915	3835	3835	2725	1565	--	3225	3635	3845	3455	3605	3605	3605
Losses*	465	525	565	605	595	595	425	245	--	500	565	595	535	560	560	560
Totals	3460	3920	4200	4520	4430	4430	3150	1810	--	3725	4200	4440	3990	4165	4165	4165

*Assumes 30/70 percent ac-dc split, 75 percent inverter efficiency, and 5 percent line losses.

Table 8.10-2. Auxiliary Power Subsystem Loads

Stage	Peak Power (hp)	Continuous Power (hp)
Orbiter	111	37
Booster	195	55

Table 8.10-3. Energy Requirements

System	Orbiter Requirement	Booster Requirement
Electrical power subsystem	540 kw/hr	
Auxiliary power subsystem	36 hp/hr	90 hp/hr

For the hydraulic system loads on both the orbiter and booster, the open-cycle, hydrogen/oxygen dynamic APU has been selected. Power from this source is required during boost, on-orbit operations, reentry, cruise, and landing. All booster loads from liftoff until landing are supplied from the APU.

All power for ferry operations with both booster and orbiter are supplied from the APU's.

8.10.3 Subsystem Concept Description and Weight

The subsystem concept for the booster and orbiter is illustrated in Figures 8.10-2 and 8.10-3 (certain equipment is identified as orbiter only). Major equipment descriptions and characteristics are as follows:

1. Fuel cell cryogenic storage: Six storage tanks are used for each reactant, with three tanks per reactant used during ascent and early mission phase and three tanks per reactant used during descent. Supercritical storage of high-purity reactants at 250 psia for liquid hydrogen and 900 psia for liquid oxygen is assumed for the ascent and early mission phase tankage. Each tank contains 50 percent of the requirements for the ascent and early mission phase. Each tank contains sufficient reactants to supply the orbiter requirements for at least 24 hours for

Table 8.10-4. Candidate Power System Approaches and Equipment

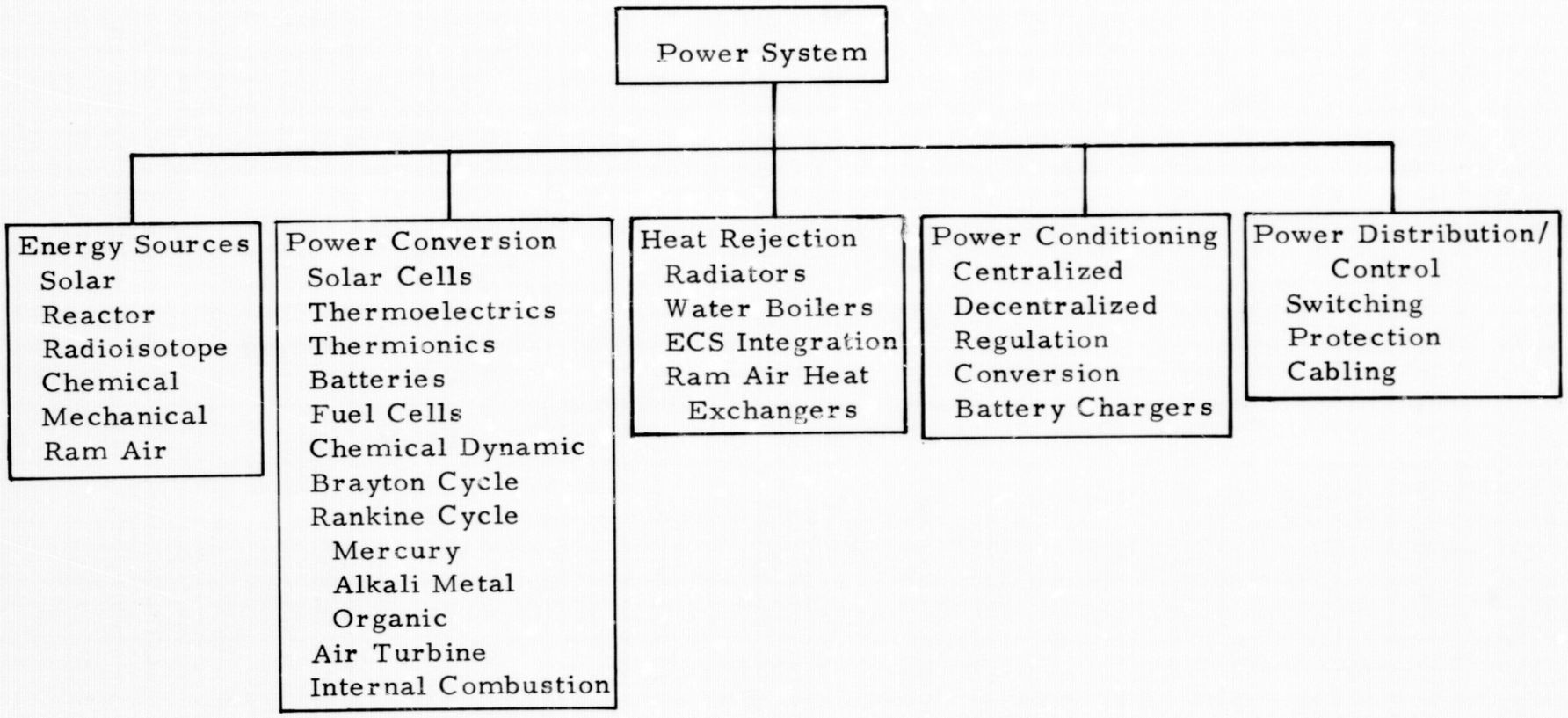

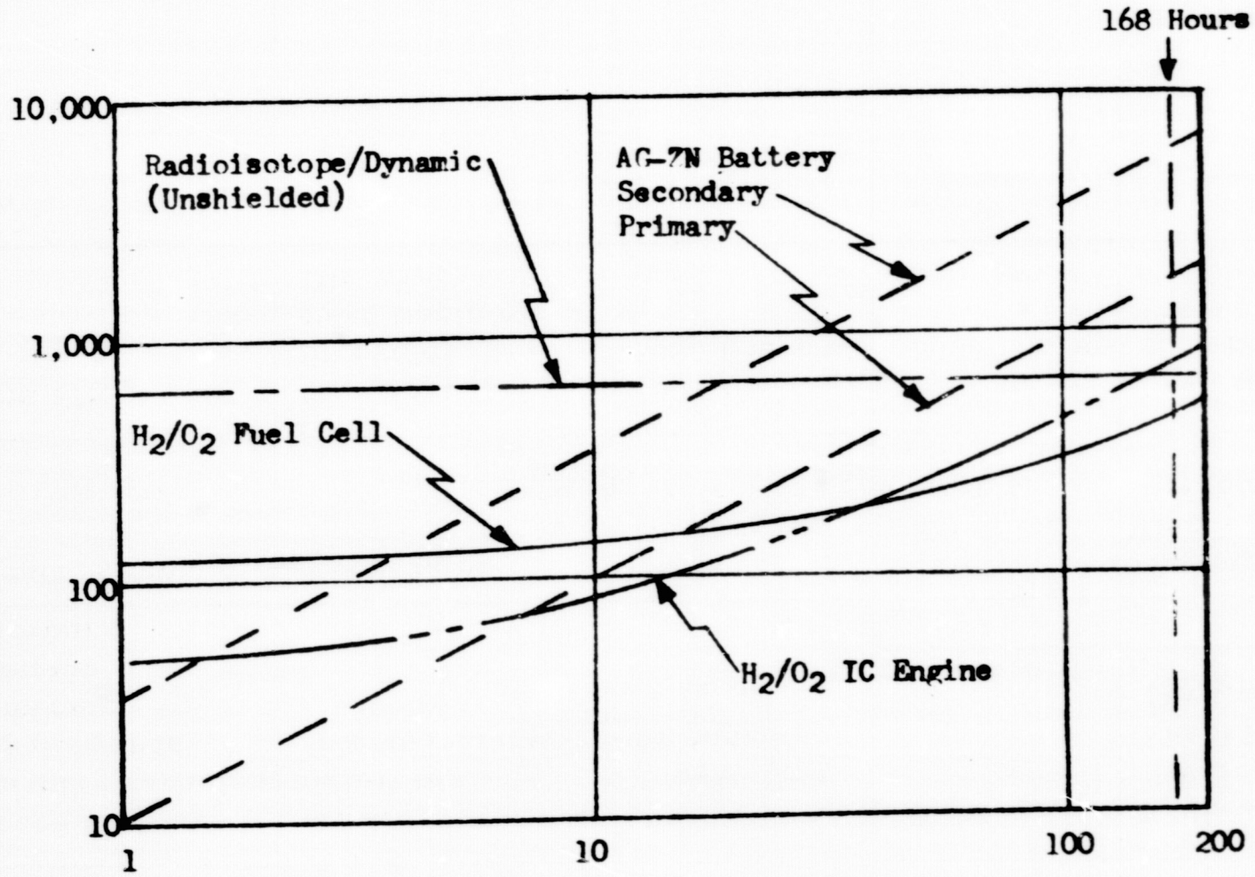

Notes: 1. Does not include redundancy considerations.
2. Includes separate tankage.

Figure 8.10-1. Comparison of Energy Source Specific Weights

Table 8.10-5. Comparison of Candidate Power Sources

	AG-ZN Primary Batteries	AG-ZN Secondary Batteries	H_2/O_2 Fuel Cells	Radioisotope Dynamic	Chemical Dynamic
Specific weight at 168 hours	1700 lb/kw	5600 lb/kw	430 lb/kw	630 lb/kw	710 lb/kw for H_2/O_2 IC engine
Flight experience (space vehicles)	Space boosters Reentry capsules Apollo lunar module Gemini Mercury	Apollo Satellites Interplanetary probes	Apollo Biosatellite Gemini	None	X-15 (Hydrogen Peroxide Turbine)
Major integration considerations	Replacement	Recharging	Tankage Heat rejection	Safety Shielding Heat rejection	Tankage Heat rejection
Life (Current to 1975)	One Flight	One Year, 50 cycles (50% Depth of Discharge)	2000 to 5000 hours	2000 to 5000 hours	Less than 1000 hours
Produces Water for human consumption or evaporative cooling	No	No	Yes	No	No

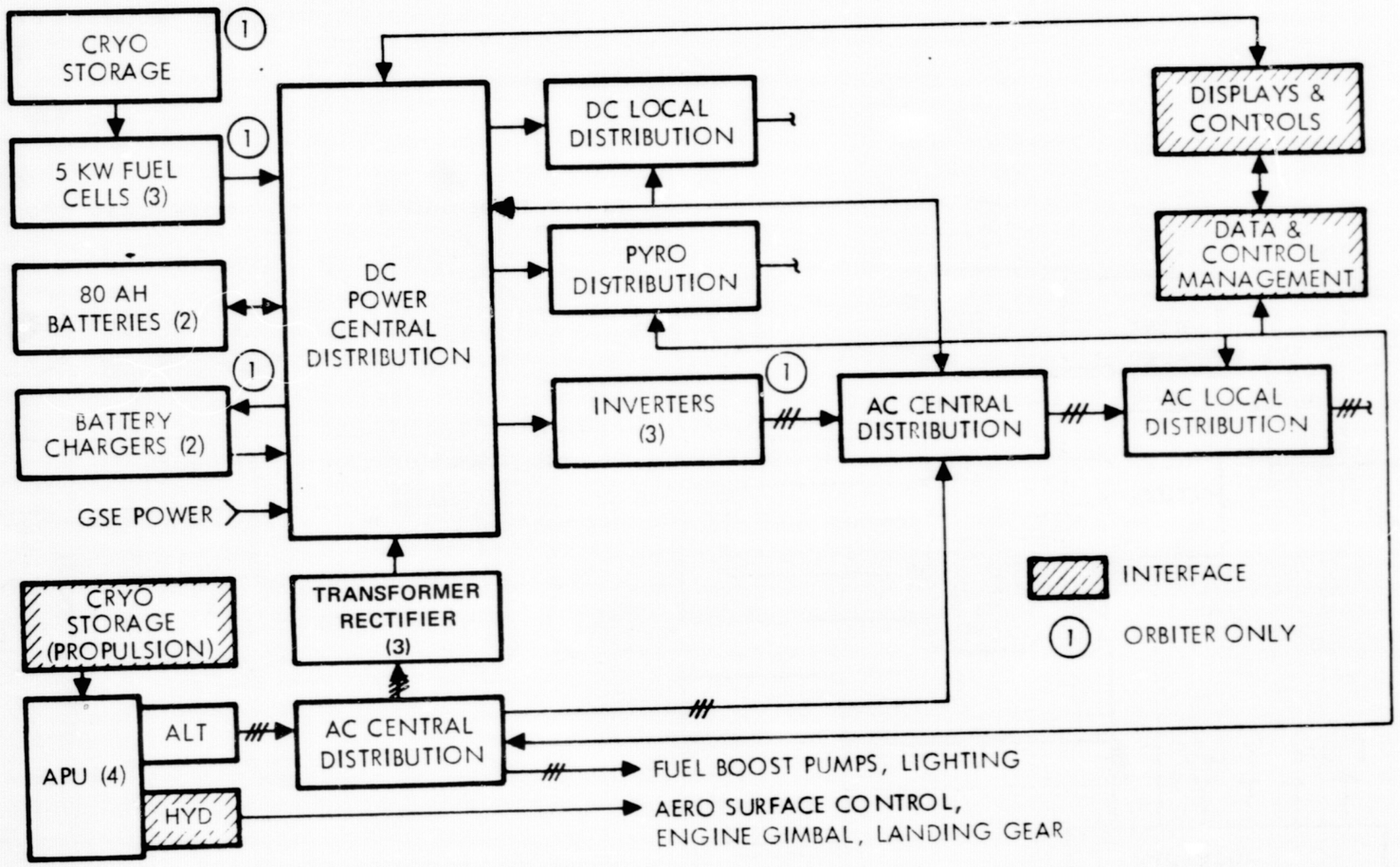

Figure 8.10-2. Electrical Power Subsystem Block Diagram

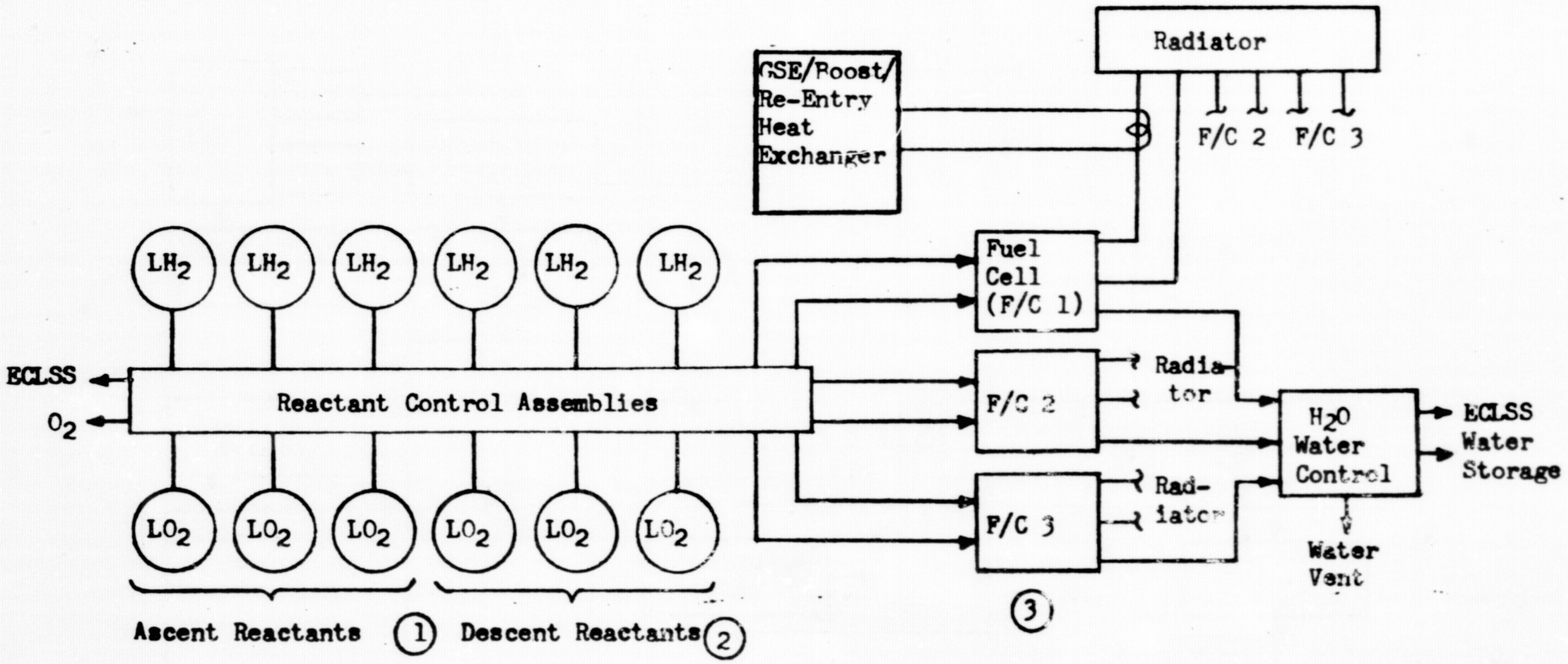

Notes:
(1) Each tank contains 50 percent of ascent and early mission requirements.
(2) Each tank contains 100 percent of descent requirements.
(3) Each fuel cell is capable of supplying average load requirements.
4 Fill relief and purge lines not shown for clarity.

Figure 8.10-3. Baseline Fuel Cell System

Space Division
North American Rockwell

emergency return. Supercritical storage of high-purity reactants is assumed for the descent tankage when in operation; but the reactants are in the subcritical state at liftoff. Heat leaks must be minimized through struts, feed and vent lines, and electrical cables. This systems applies only to the orbiter.

2. Fuel cells: Three five-kilowatt fuel cell modules are required. The fuel cells can be either the low temperature asbestos matrix units manufactured by Allis-Chalmers or Pratt & Whitney, or the solid polymer (R-membrane) unit manufactured by General Electric. Each module contains the required valves, temperature control pumps, water pumps, controls and instrumentation. A typical subsystem schematic is shown in Figure 8.10-3. Fuel cells are used only in the orbiter.

3. Batteries: Eighty ampere-hour silver/zinc batteries are required for peak loads and transient loads, such as hot wire pyrotechnic devices and engine ignition. Plate separator systems similar to those developed and under development for the Mariner series interplanetary probes are assumed to achieve a one year wet life. These separator systems may include multiple layers of SWRI-GX irradiated polyethylene and/or fibrous sausage casing. Two battery chargers are required for battery recharging in the orbiter.

4. Auxiliary power unit (APU): Four APU's having peak shaft power of 150 horsepower are used in the orbiter and 250 horsepower are used in the booster. The selected baseline APU concept uses are open-cycle, hydrogen/oxygen fueled, multiple-entry turbine, such as the unit which was under development for the DynaSoar program. To maintain a suitable pressure ratio across the turbine during both atmospheric and space flight, use of a feed system common with the RCS propellant supply is assumed. This system will supply at least 250 psia gases to the combustor and turbine. The largest hydrogen/oxygen fueled unit to reach the advanced development phase was the DynaSoar unit (Sunstrand Model 876). This unit had a design requirement of 36 horsepower (peak) and 25 horsepower (continuous).

5. Conversion and distribution equipment: A centralized ac inverter system is assumed for the baseline concept. A distributed ac and dc bus system is assumed for optimum integration with the data bus system. All discrete functions (on-off controls and measurements, circuit breaker reset, remote control, and position indicators) will be routed through the data bus system.

Direct displays and controls will be minimized by optimum use of self-check circuitry, computer control, and caution and warning indicators.

The power subsystem hardware quantities, sizes, and weights and fluid weights are shown in Table 8.10-6. The total orbiter hardware weight is 3,339 pounds and the H_2 and O_2 requirements are 275 pounds and 1,573 pounds respectively. The total booster hardware weight is 2,565 pounds and the H_2 and O_2 requirements are 366 pounds and 293 pounds respectively.

8.10.4 Maintenance Concepts

Equipment life characteristics and projections for the power systems equipment are:

1. Fuel cells. The life of a fuel cell system may be expressed in terms of degradation of cell performance with reactants supplied, cell shutdown/restart cycles, storage life between missions or during quiescent periods, and life of accessories. The Allis-Chalmers hydrogen/oxygen fuel cells which were under development for the Air Force and the NASA have required lifetimes of 1500 hours and design goals of 2500 to 3000 hours. Similar effort by Pratt and Whitney has resulted in lifetimes of approximately 2000 hours. These characteristics are based on average degradation rates of 10 to 20 microvolts/cell-hour. Allis-Chalmers and Pratt and Whitney are projecting an improvement to approximately 5 microvolts/cell-hour degradation and a design goal life of 10,000 hours before the technology baseline for this program. General Electric is projecting an average lifetime of about 10,000 hours at 180 F operating temperature for their solid polymer (R-membrane) fuel cell with no voltage degradation. These projections are based primarily on single-cell laboratory tests. A more conservative projection of 5,000 hours life is appropriate at this time.

   Methods to extend life include the performance of an electrolyte flush operation on asbestos matrix fuel cells when the terminal voltage approaches a minimum acceptable value. The electrolyte flush operation has been demonstrated on laboratory cell stacks at Allis-Chalmers and Pratt and Whitney, with indications that field service gear can be designed to accomplish this task on installed fuel cell modules.

Table 8.10-6. Power Subsystem Equipment Size and Weight

Equipment	Quantities		Size (each) (in.)	Weight (each) (lb)
	Orbiter	Booster		
Fuel Cells, 5 Kw	3	0	12 x 12 x 55	210
H_2 Cryo Tanks - Ascent	3	0	30.8 O.D.	62 + 27 H_2
- Descent	3	0	28.7 O.D.	51 + 17 H_2
O_2 Cryo Tanks - Ascent	3	0	26.2 O.D.	70 + 291 O_2
- Descent	3	0	25 O.D.	61 + 195 O_2
Plumbing	1	0	-	120
Batteries, 80AH	2	2	10 x 20 x 7	65
Inverters, 1250 VA	3	0	7 x 15 x 15	52
Power Contr/Distribution	1	1	6 x 20 x 36	125
Battery Charger	2	0	4 x 5 x 7	8
Distribution Wiring	240 lb	320 lb	-	See Qty
Remote Distr.	8	8	-	40
Radiator	1	0	-	100
APU - Chemical Dynamic				
150 hp (orbiter)	4	0	20 x 20 x 36	150
250 hp (booster)	0	4	24 x 24 x 39	230
H_2: Orbiter	-	-	-	143
Booster	-	-	-	366
O_2: Orbiter	-	-	-	115
Booster	-	-	-	293
Plumbing	60 lb	100 lb	-	See Quantity
Power Contr/Distribution	1	1	-	50
Distribution Wiring	80 lb	120 lb	-	See Quantity

Operation at lower stack temperatures will also extend lifetime significantly with a sacrifice in voltage performance and radiator area. Alkaline fuel cell operation using commercial purity reactants results in more rapid deterioration indicating that CO_2 absorbers or molecular sieves may be of use in extending life.

Forty to 150 shutdown/restart cycles, depending on the manufacturer's experience, have been demonstrated with no evidence that cycle life cannot be extended significantly further. Tests have also indicated that standby storage (reactants not supplied to the cells and temperatures up to normal operating temperature) does not seem to cause significant degradation.

Such accessories as coolant pumps, filters, and CO_2 absorbers will require replacement at more frequent intervals, suggesting the use of replaceable pump modules.

2. Batteries. The life of silver-zinc batteries may be expressed in terms of activated life and cycle life for a particular depth of discharge. Sealed batteries developed and under development for the Mariner series, Mars Orbiter and Mars Lander have lifetimes of 9 to 18 months and a cycle life of approximately 100 cycles at 50 percent depth of discharge (DOD). Up to 9 months life has been flight demonstrated during the Mariner series. Vented batteries developed for the Signal Corps exhibit one year life and 100 cycles at 60 percent DOD. A vented battery developed for a classified satellite has achieved one-year orbital life at 3 to 4 percent DOD and 90 minute cycles. It is estimated that the silver-zinc batteries should be replaced at one-year intervals.

3. Dynamic APU's. The most suitable APU type which had reached the advanced development state was the Sunstrand Model 876 which was under development for the DynaSoar program. This unit had a design life of 250 hours and a peak power output of 36 horsepower. Propellants were hydrogen and oxygen. A 250-hour life is compatible with the vehicle usage during reentry, cruise and landing periods for 100 missions. The peak power requirement for an APU will approach 250 horsepower indicating the need for a major development program in this area. A conservative replacement interval of 100 hours is considered to be appropriate at this time.

4. Solid State Equipment. Both solid state equipment and electromechanical switching should be capable of meeting vehicle life characteristics without replacement. Replacement would, therefore, be based on failures and degradation trends.

Servicing and checkout considerations for the power system are:

1. Fuel cells. After landing, reactants will be drained and the system will be purged and/or allowed to consume residual reactants. Checkout will consist of leakage tests, a hydrogen diffusion test to detect fuel cell cross-leakage, and an electrical resistance test in addition to the normal on-board checkout and self-check features. Servicing before liftoff will require loading of reactants and electrical heating to operating temperature (180 to 200 F).

2. Batteries. Recharging or top-charging will be required to achieve maximum capacity before liftoff. A permanent capacity loss of 20 percent can be assumed over a one-year period with periodic recharging in-flight and during ground operations.

3. Dynamic APU. After landing, propellants will be drained and the system will be purged. The development program will indicate the replacement cycle for gear box lubricant and catalytic or other ignition components. Checkout will consist of leakage tests and gaseous nitrogen turbine operation.

8.10.5 Technology Advancements

The following technology advancements are necessary or desirable for the power subsystem:

1. Auxiliary power units capable of peak shaft horsepower requirements of up to 250 hp and a total operating life of 250 hours

2. Fuel cells capable of 5000 hours of operation at 180 to 200 F including 150 restarts.

3. High energy density batteries capable of 50 to 100 cycles at 50 percent depth of discharge within a one-year period

4. Low heat leak cryogenic storage

5. Solid state switching and circuit protection equipment

8.10.6 Follow-On Study Recommendations

Only limited tradeoffs were conducted during this study phase. Several areas of investigation should be pursued to identify the best power system to provide minimum weight and reuse cost. The following major tradeoffs have been identified for future and more detail studies:

1. Cryogenic tankage. Combining tankage for fuel cells and APU's. This will probably result in reduced tankage size and weight, but will require study of equipment location to minimize plumbing weights and complexities. Since fuel cells generally require high-purity reactants to prolong life, the combined tankage must either contain high-purity reactants or absorbers (or sieves) must be used to remove contaminants from the fuel cell reactants. Combining tankage for power subsystem and propulsion subsystem. The same comments apply as outlined above. The necessity for separate emergency tankage must also be identified. Tankage arrangements for ferry operations. Evaluation of subcritical tankage for the descent period. Trades with high-pressure gas and other storage systems.

2. Evaluation of the life characteristics of fuel cells for the mid 1970's. This evaluation should include type of fuel cell, maintenance between flights, reactant purity, and operating temperature.

3. Evaluation of the life characteristics of dynamic APU's for the mid 1970's. This evaluation should include number of turbine stages, turbine inlet temperatures, materials and maintenance between flights. Tradeoffs between hydrazine, hydrogen perioxide, and hydrogen/oxygen fuel APU's should be conducted when using separate tankage.

4. Evaluation of the use of chemical APU's augmented by ram-air turbines. Study requires detailed determination of aerodynamic and flight requirements during reentry and cruise flight modes.

5. Tradeoffs for the use of the turbofan accessory drives to supply power after turbofan deployment and during ferry operations.

6. Evaluation of the integration of power system with the environmental control system (heat rejection and absorption).

7. Evaluation of the effects of long-term quiescent docked mode on subsystem configuration.

8. Centralized versus decentralized power conversion and distribution systems.

9. Tradeoffs between existing voltage standards and higher voltages and frequencies.

10. Evaluation of the degree of interface between the power control and protection equipment with the multiplexed data bus system.

11. Evaluation of the use of boost switching regulators in voltage critical areas to minimize cable weights.

8.11 INTEGRATED ELECTRONICS SYSTEMS

To minimize the weight and cost of space vehicle electronics and to provide a reusable vehicle that is capable of rapid turnaround, an integrated electronic system (IES) with inherent checkout capability is desirable.

The mid-1970 technology will be applied in the design of the IES where the application will result in the meeting of the mission and system requirements and provide weight and cost savings. The technology will be evaluated not only technically, but from the producibility point of view.

Highly reliable equipment operation well within design tolerances will be used. In areas where failure of critical components or assemblies would result in a situation where the crew, passengers, and vehicle could not be recovered safely, redundant systems will be employed to meet a fail-operational/fail-safe criteria.

The subsystems included in the integrated electronics system are described below with their associated functions.

Central Computer - The central computer is a partitioned multiprocessor which works in on-line, real-time mode, interfacing with all other subsystems and providing all details of timing, sequencing, and mission profile.

Guidance and Navigation - The guidance and navigation subsystem includes redundant IMU's, stellar trackers, infrared horizon sensors, a satellite navigation unit, a multimode laser tracker, biomodal LORAN, TACAN, radar altimeters, and an air data computer with necessary inputs. The subsystem, working in conjunction with the flight controls subsystem, provides automatic attitude control, trajectory control, present position information, targeting information (in conjunction with radars), orbital information, landing site information, and such detailed information as guide path angle, ETA, etc. Working in conjunction with the central computer, the subsystem performs complete self-test, calibration, and alignment. Backup modes of operation provide for complete man-in-the-loop use.

Displays and Controls - The displays and crew information subsystem makes extensive use of general-purpose electronic displays to present all aspects of mission and vehicle operation. Crew interface with the displays is provided through multipurpose keysets which interface with the central computer. Both keysets and displays are capable of working through their associated input/output (I/O) buffers in man-in-the-loop mode, even if all processors of the central computer are out of service. The formats of display include horizontal mapping, contrast analogs, manometer graphs,

TV monitors, Q-ball, world mapping, orbital plane sections, and various navigation aids. Various warning and failure lights are provided to augment visual graphics. An on-board printer logs messages which require crew hardcopy retention, or nonvolatile format.

Record and Playback - This system will record voice and predetermined data to permit postflight evaluation of vehicle performance for the purpose of maintenance and detection of incipient failures.

Communication - This system will provide the RF external data/voice link required for rendezvous, docking, approach, and landing operations. It will also provide the voice intercom system.

Onboard Performance Monitoring and Checkout - The system will perform flight and preflight subsystem checkout.

Onboard Performance Monitoring and Checkout - The system will perform preflight checkout, inflight performance monitoring, and post-flight checkout of vehicle subsystems.

Signal Distribution (Multiplexing) - This subsystem provides a signal distribution network for all subsystems. It includes signal conditioning, analog-to-digital conversions, and multiplexing. Data and control signals are transmitted to and from the computer system by serial bit transmission over coaxial lines. This will minimize the interface problems, reduce design change impact, and increase system accuracy.

Subsystems Instrumentation/Data Interfaces, Subsystems Control Signal Interfaces, and External Interfaces are extensions of the signal distribution system providing a standard approach to vehicle interfacing.

8.11.1 Central Computer System

The heart of the IES subsystem is the Central Computer System which performs (with its software) the following mission management functions:

Vehicle subsystem configuration control (hardware)

Onboard checkout

Performance monitoring and display

Data (information) management

Control management

Guidance, navigation, and control

Aircraft and space vehicle electronics have to date tended to be heterogenous collections of spare parts; air data converters are added as later developments to pitot-static tubes and flux gate compasses. But with the availability of small, light, high-performance digital computers capable of performing reliably in the operational environment of aircraft and spacecraft, a single, coherent electronic system becomes feasible. The digital computer is capable of functioning as any definable system, so long as that system can be programmed and defined in logical mathematical terms. The essentials of all the electronic tasks can be so defined.

Assignment as the central processing unit of an integrated electronic system imposes a requirement on the computer that is not always found in ground-based systems. Since the vehicle is a dynamic device operating in an environment containing important operational constraints, there is a manifest set of time boundaries imposed upon the computer. The computer must make its results available when they are needed. In brief, it must be a "real-time" computer.

In working with ground-based computers, it is always possible to trade space and time within the machine. Thus, a machine with smaller memory may take more time to solve a problem. But such a tradeoff is not possible in the dedicated electronic computer, since the time allotted is bounded by the task needs.

Further, the operational regimes of the ILRV are such that the crew often will not be able to schedule the computer's tasks. The computer must perform many of its functions on demand, must interface with the crew by means of displays and query switches, must interface with sensing devices and vehicle equipment by means of probes, and so forth. In short, the electronics computer operates in an on-line environment.

Most on-board computers to date have been of three general types: (1) the special-purpose machine which performs a single function or solves a given problem repeatedly or continually (air data computers are often of this type); (2) the digital differential analyzer (DDA) which is customarily used to solve differential equations of a specified dynamic system with time as the independent variable; and (3) the general-purpose machine which, except for its physical characteristics, could as well be ground based.

General-purpose machines in use on aircraft and space vehicles have tended to be normal in their logical organization; that is, except for their interrupt and input/output structures, which permit them to operate in real time, they make use of a rather standard set of instructions and standard internal organization. For the job of integrated electronics on the vehicle, a different computer organization should be considered. A multiprocessor, for example, can run two and more programs simultaneously by time-sharing

parts of the machine through such techniques as logically blocking memory or overlapping memory cycles. Yet a multiprocessor can retain the features of priority interrupts which permit it to work effectively in real time.

The computer, in view of its internal organization, is called a "partitioned multiprocessor." The central units are three complete and independent processors, each with its own power supply and capable of functioning alone with the others shut off.

Processors

All processors are full-parallel machines. All have the same clock rate. Built-in string manipulation capabilities let the processors readily handle 4-, 6-, 8-, 10-, and 12-bit characters.

Extensive interrupt capabilities permit MAP (the Master Avionics Program) to intervene for resource allocation and error detection. Each processor can handle its own interrupts without disturbing other processors. Processors can also share processing of external interrupts from any device in the avionics system. The command and stacking structure provides for automatic implementation of string notation and automatic subroutine linkage.

Each processor can operate in either of two states: CONTROL state under MAP, and NORM state for executing operational programs. More than one processor may be in CONTROL state at one time, as when the computer is processing a fast sequence.

Entry of a processor into CONTROL state occurs when the processor is started originally, or as a result of certain internal interrupts, a procedure, or I/O entry or exit, or a disable interrupt condition. In CONTROL state, the processor can execute certain privileged instructions not available for execution in NORM state. Various classes of interrupts can be inhibited in CONTROL state. The processor switches to NORM state whenever it starts execution of an operational program or returns to such execution after processing an interrupt. The processor may return to a different program execution after processing an interrupt.

Operation in NORM state excludes the use of the privileged operators, permits hardware detection of invalid operators, and enforces memory protection. Exit from NORM state will occur as a result of an interrupt, or by a call to a CONTROL state program, such as an I/O.

Interrupts

Each processor has a private, internal interrupt system. Interrupts internal to the processor are fed into this system and stacked in order if they overlap.

Each processor also has an external interrupt system. External interrupts may be handled by the first processor which services them.

Each processor responds to an interrupt as though it were entering a subroutine. The following actions take place.

1. The program place is marked and the essential register contents are stored.

2. A record of the interrupt definition is written.

3. The processor switches to CONTROL state.

4. The interrupt is processed.

Stacks

A stack is an area in a memory segment which is assigned to a particular operational program while that program is being executed. It provides basic program and data references, as well as temporary storage of data and dynamic program history. When a program is executed, certain of the high-speed registers of the executing processor are linked to the stack memory area. Each register so linked serves as a "top of stack" register.

Since the stack is a working area, its absolute address is irrelevant. An assigned processor register continually keeps track of the location of stack top. Stacks are always filled and emptied from the top and are preserved until execution of the using program is complete, even if interrupts intervene. Stack memory areas are defined by a stack base address and a stack limit register.

I/O

Communication through any I/O buffer to any device in the avionics system is memory-to-device, or device-to-memory. Processors communicate directly only with memory. They communicate with devices through the interrupt system.

Any processor can initiate an I/O operation through any I/O device or multiplexer at any time by executing an I/O INITIATE command. This command transmits the essential information to start the I/O to the cognizant I/O buffer. When the buffer completes an assignment, it sets an I/O COMPLETE interrupt.

Data Communications Processor

This small, special-purpose computer has sufficient logic to carry out the basic functions required to transmit and format telemetry data.

MAP

The Master Avionics Program controls various computer functions, automatic system assignment, and multiprocessing coordination. It controls all computer functions except the man-machine interface where there are man-generated interrupts. It analyzes error conditions, and provides a standard course of action (i.e., shut down faulty I/O buffer and continue). It assigns memory areas and labels I/O files. It determines the optimum sequence for processing a batch of programs, adjusting the schedule for new or higher-priority jobs. It initiates all I/O operations.

MAP contains an executive program, a scheduling routine, an environmental control routine, and an exception condition routine (see Figure 8.11-1).

Bulk storage has its own I/O processor which, loaded with instructions by any processor, is capable of simultaneously loading any memory segment and unloading any other memory segment.

An I/O buffer may have access to a number of parallel-word data common lines, each of which serves a number of device interface units. Interface units are of two kinds: the sensor interface, which takes a single word of information from an external sensor and sends it to the acquiring processor on properly addressed command, and the actuator interface, which takes a single word of information provided by the computer and makes it available to an external device in the proper form (i.e., analog signal, etc.). Since interfaces are of two kinds, data common trunks are of two kinds, input and output (Figure 8.11-2).

I/O buffers typically contain small processors. The buffers are actuated by an I/O INITIATE command from a processor, after which each buffer may load its own instructions from memory and proceed to execute them. A buffer, having completed its work, sets an I/O interrupt, but it may continue working indefinitely on an assigned task (e.g., regenerate

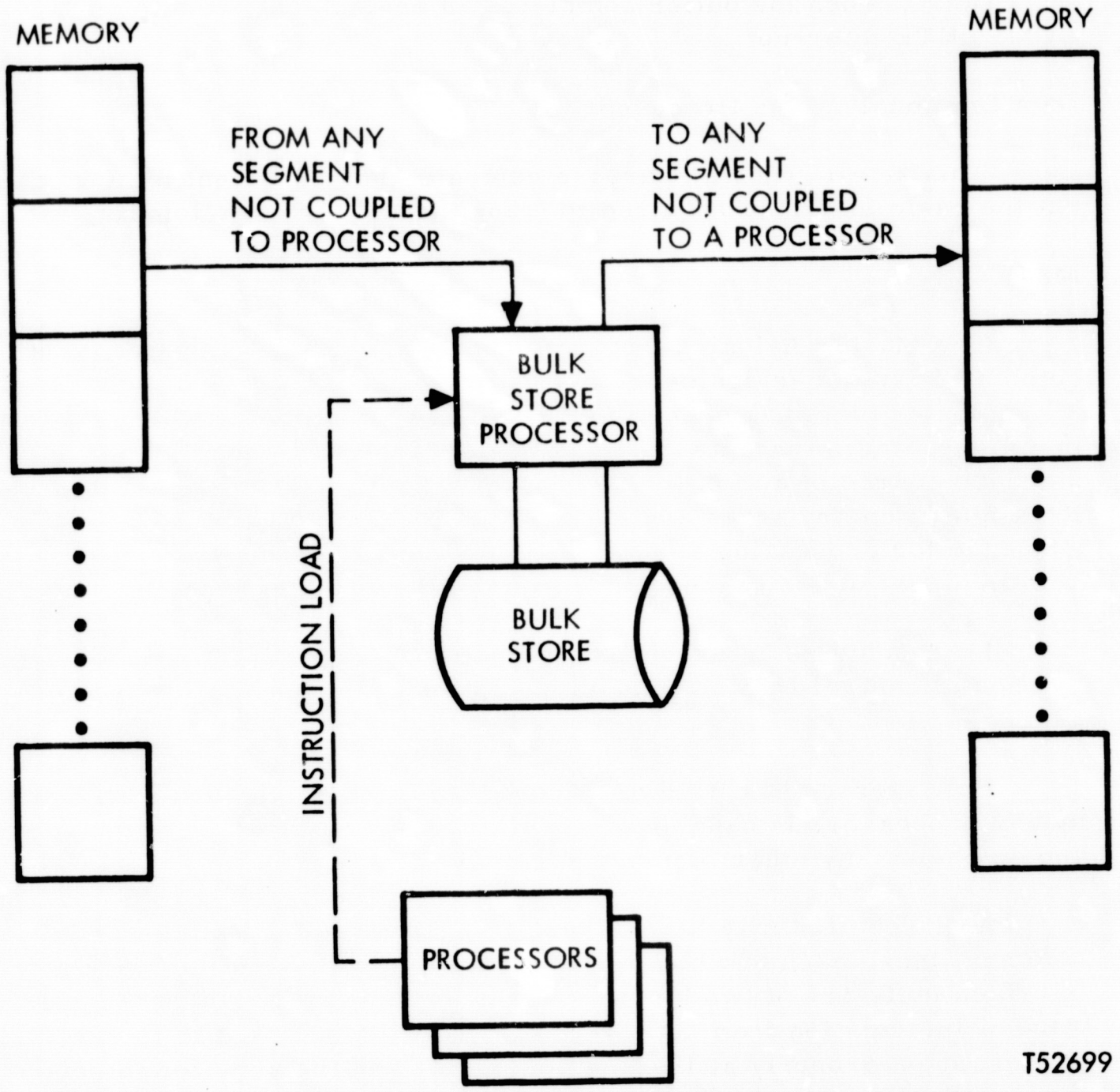

Figure 8.11-1. Master Avionics Program Control

display) without setting this interrupt. I/O buffers keyed to man-in-the-loop operation of the vehicle may have their INITIATE commands set from the keyboard, and hence may continue operation even in the unlikely event of outage of all processors, (Figure 8.11-3).

Depending on the traffic requirements for I/O buffers, they need not couple directly into the processor-memory data exchange but may work in teams, time-sharing a data trunk through an I/O multiplexer which, together with a data switching channel, directs traffic on the trunk.

Internal Organization of the Central Computer

The central control function of the computer is disbursed throughout the system. This permits component outage without destruction of the system's ability to perform. Such an approach is known as "graceful degradation" and is found in such ground-based systems as the NTDS.

The key to the organization of the computer is found in MAP. This program is resident at all times in two physically and logically separate regions of bulk store. From bulk store it can be loaded through Store I/O into any memory segments, where it is available for use by any processor. The system cannot access the primary MAP except to read it. It cannot rewrite or destroy MAP.

MAP maintains continual cognizance of the hardware configuration of the vehicle, as viewed from the central computer, and reallocates resources to the operational programs accordingly.

The central computer contains three processors operating independently and in parallel. Among the features of processor design are:

1. An operational program which cannot be modified while it is in residence (being executed).

2. A stacking scheme which provides for efficient handling of temporary storage and subroutine requirements.

3. Control bits associated with every word which identify its type and actuate appropriate MAP or hardware action.

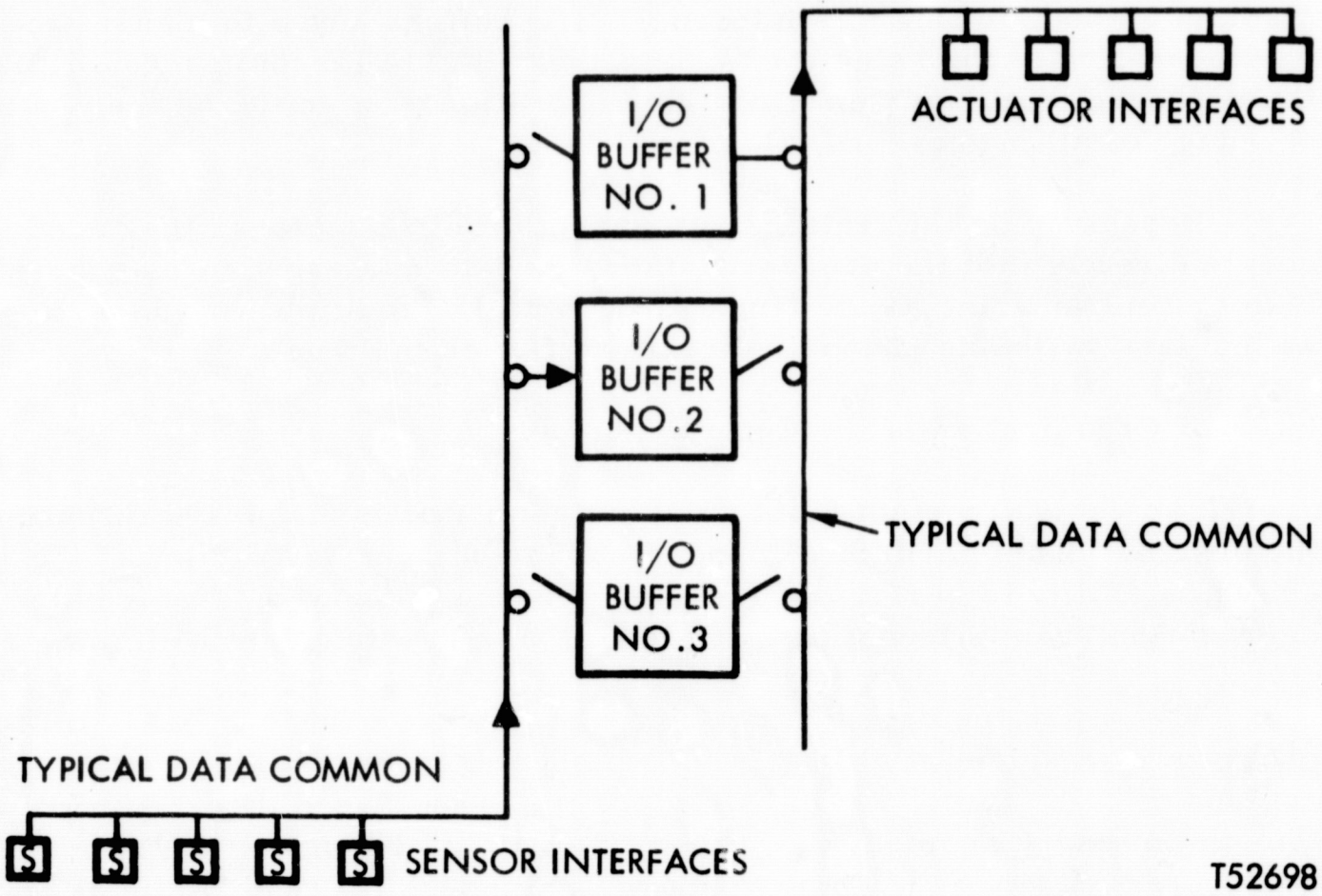

Figure 8.11-2. Interface Units

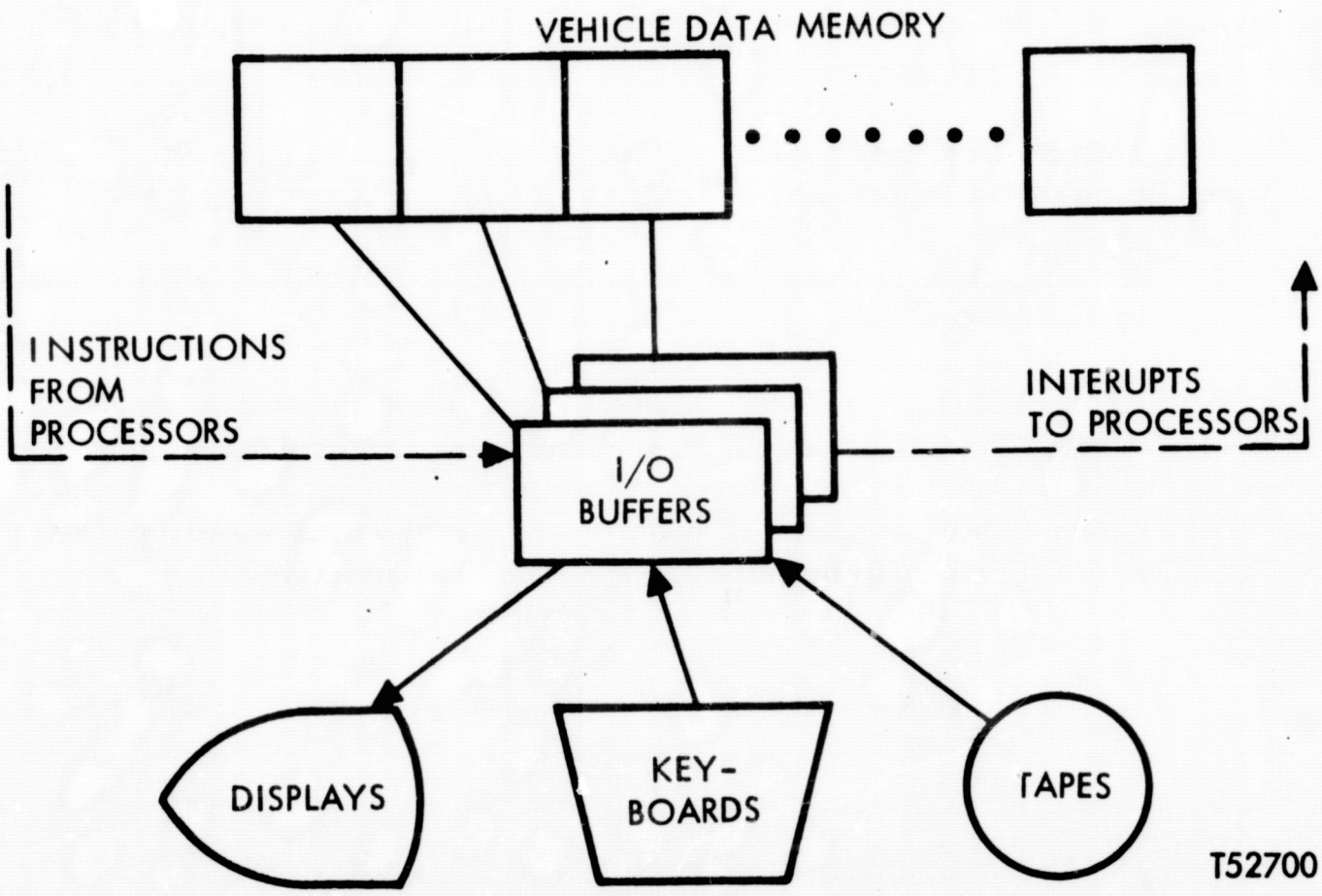

Figure 8.11-3. Manual Interface

4. Memory protection which is carried out by a combination of hardware and software features and prevents one program from affecting another. For example, hardware provides automatic detection of a program attempt to index beyond a defined area. Each word contains a control bit. The control bits of the words prevent an operational program from changing program segments, data descriptors, segment descriptors, memory links, MAP tables, etc. MAP software sets the control bits of those words which are not available to the object program.

5. Selected registers and control flip-flops which in each processor contribute to the system multiprocessing capabilities.

Memory

Memory is divided into segments and is organized so that any segment can send information to any processors, any stand-alone I/O units, and any data trunks.

As a word transfers along any buss in the main memory switch, it is inspected by circuitry in each module to see if it is addressed to that particular module. Thus, there is no need to establish module linkage. All information transfers in word parallel. Operation of any memory segment is independent of the operation of others, and memory cycles can occur simultaneously in all.

Processors work with a partitioned memory. Each processor may connect, through a triply redundant switching scheme, to any memory segment. The processor acquiring a memory segment has control of that segment until it releases it, at which time another processor may acquire it. Processors have their own, dedicated scratchpad memory so that such things as bootstraps, interrupt processing, and internal housekeeping are always present, whether the processor is connected to a program memory segment or not.

Memory is also accessible in segments by any I/O buffer. The memory assigned to vehicle data contains the current essential information during any mission phase. It may be unloaded during any time that its particular segment is not accessed by a processor through an I/O buffer for purposes of, for instance, writing the mission log (Figure 3. 11-4).

Figure 8. 11-5 shows central computer organization.

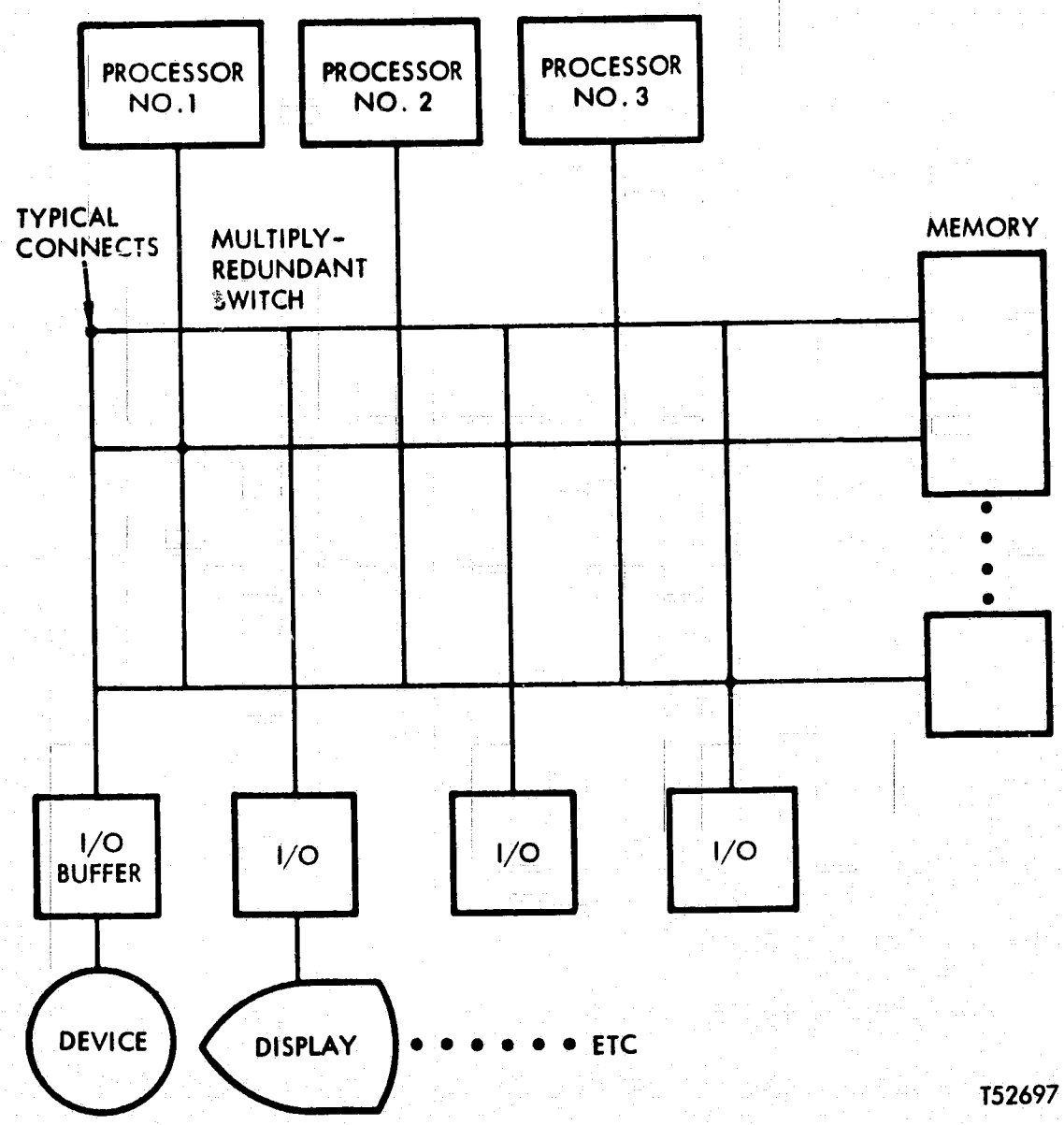

Figure 8.11-4. Memory Access

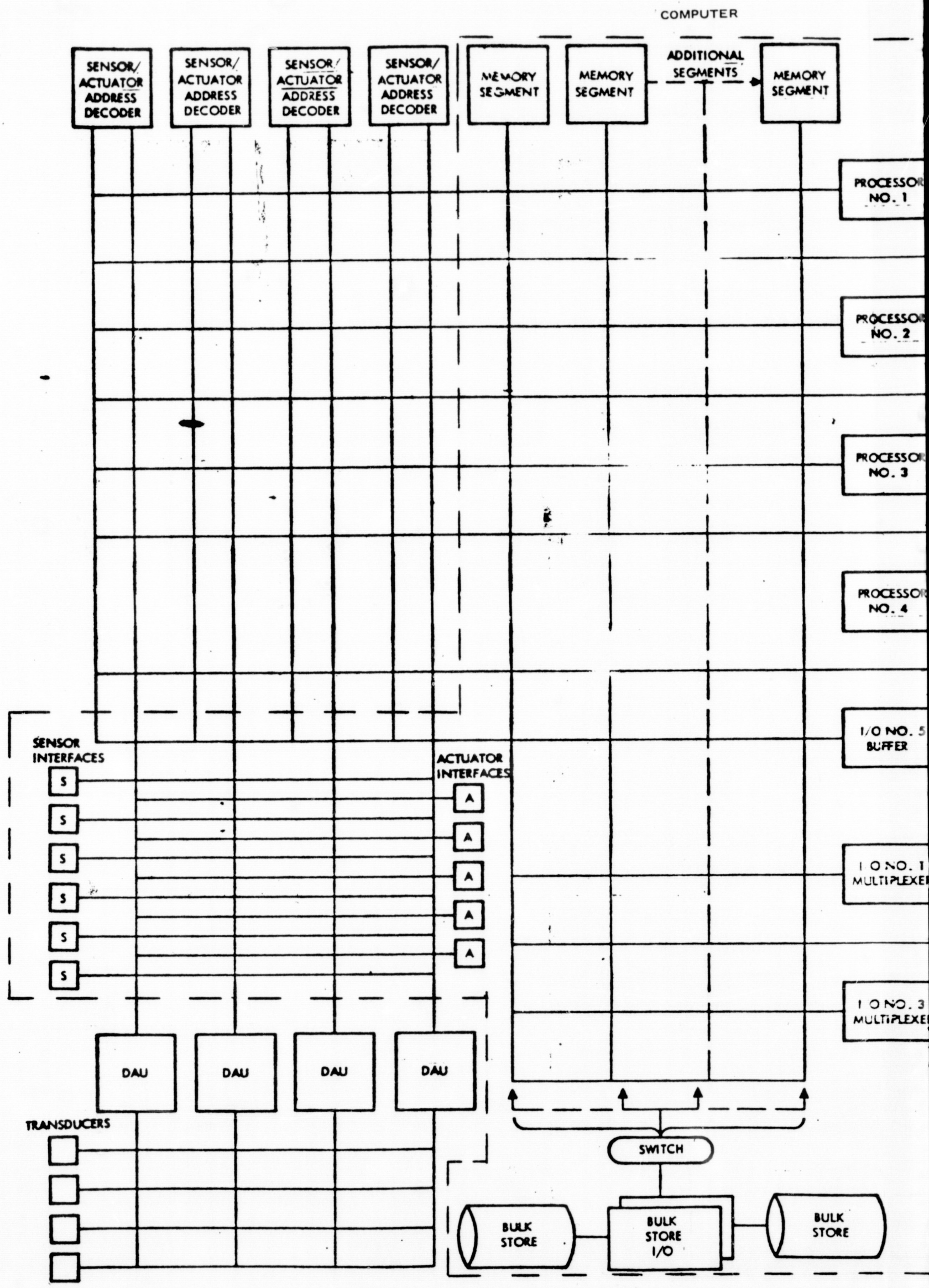

FOLDOUT FRAME 1

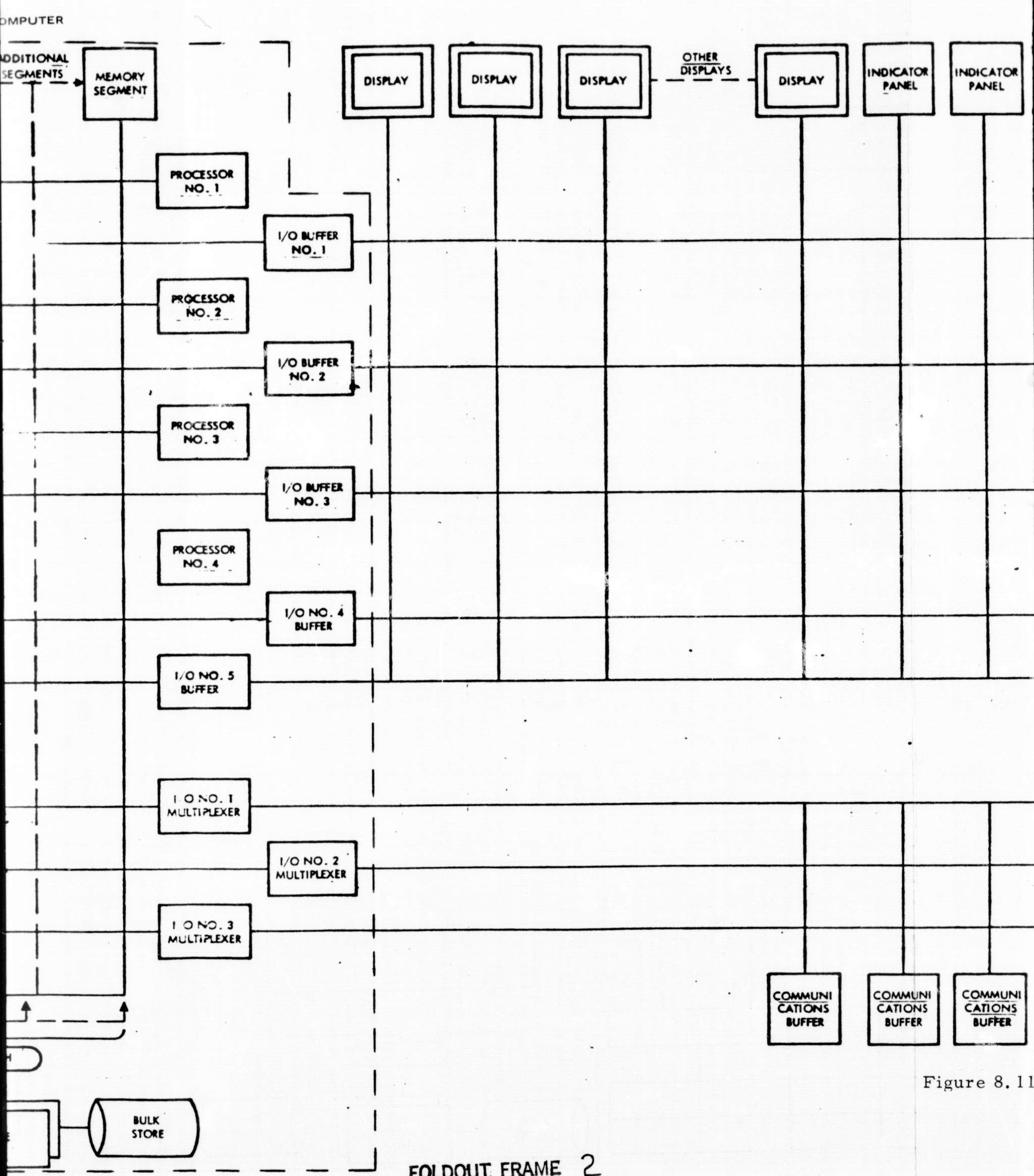

Figure 8.11

FOLDOUT FRAME 2

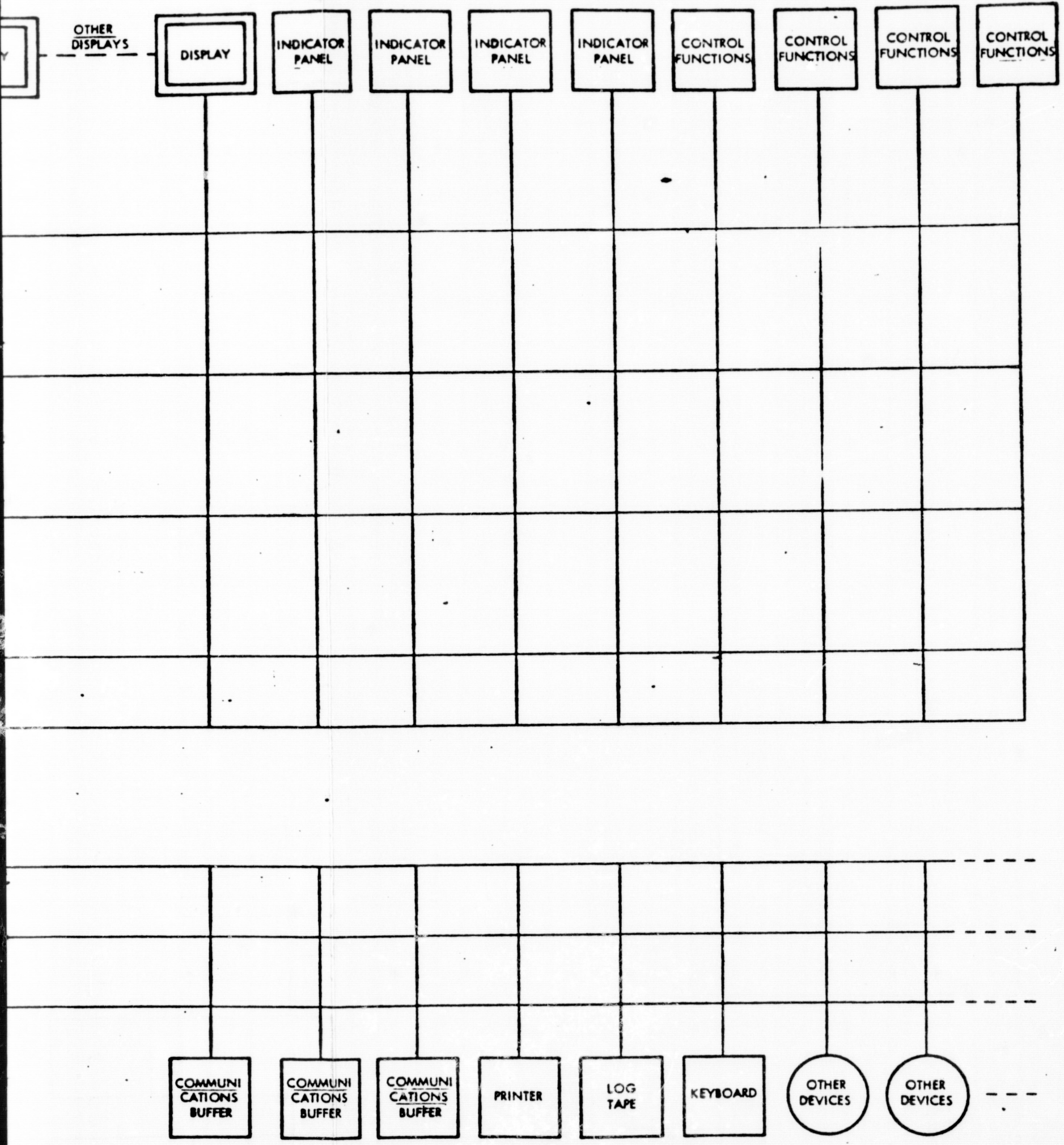

Figure 8.11-5. Central Computer Organization

FOLDOUT FRAME 3

8.11.2 Guidance, Navigation, and Control

Requirements imposed upon the ILRV guidance, navigation, and control (GN&C) system are defined in Section 7.5 of Volume III.

This section of the report defines GN&C functional and performance requirements, hardware necessary to perform the function, and the subsystem interfaces.

GN&C Functional and Performance Requirements

The requirements are presented here according to flight phase, starting with prelaunch. Operational requirements are listed first, followed by performance and hardware requirements. Displays and controls are listed for purposes of cabin design. Finally, anticipated unresolved problem areas are delineated.

Prelaunch Phase. This phase begins with firm launch order, includes system initialization, checkout and alignment, and ends at liftoff.

Operational Requirements. The system must be capable of two-hour reaction time from launch order to liftoff.

G&C Functions

1. Awake system from standby/alert status.
2. Perform computer(s) self check.
3. Perform computer check of systems readiness.
4. Calibrate and align IRU.
5. Accept mission and initialization data and perform necessary launch time, boost trajectory, and mission profile computations.
6. Downlink systems data to Launch Control Center (LCC).

Computer Functions

1. Perform computer self check and systems readiness monitoring programs.
2. Perform IRU calibration sequencing and computations and IRU attitude determination from alignment measurements. Control

platform torqueing and fine align sequence (if a platform is used).

3. Accept targeting and other uplink data, manual computer input data, digital autopilot load, etc., and compute (as required, in orbital vehicle only) mission profile parameters to satisfy mission constraints:

   a. Rendezvous with space station/satellite

   b. Return to base flight plan

   (Mission profile parameters probably will be supplied by the ground for many missions.)

4. Transfer launch time and end boost constraints from orbital vehicle to booster computer(s).

5. Compute (as required, in booster) boost trajectory parameters.

6. Transfer (if required) boost safety limits to orbital vehicle computer.

System Hardware

1. Computer and clock

2. IRU and telescope or autocollimator mounted on common navigation base.

3. Hard wires to system monitoring instruments, system selection switch, voltage analog-to-digital converter (if computer systems monitoring used).

4. Hard wires between orbital vehicle, booster(s), and LCC.

Performance Requirements

1. IRU local level determination to 1 $\widehat{\text{min}}$ (3σ); IRU azimuth determination to 1 $\widehat{\text{min}}$ (preferably better; 3σ). These errors correspond to insertion $\delta\mathring{r} \approx 8$ ft/sec, $\delta\mathring{y} \approx 8$ ft/sec, which are acceptable dispersions for a rendezvous transfer.

2. Compute end boost conditions to 1 ft/sec accuracy, or comparable accuracy of other boost parameters.

3. Computer time reference should be initialized to 20 millisecond accuracy (~500-ft phasing error for rendezvous or surveillance target location error); one part in 10^5 time accoracy (for 24-hr supply and return mission ~1 sec error ~4-nm navigation error).

4. Optics should be aligned with the IRU base within 20 $\widehat{\text{sec}}$ maximum.

5. Accuracy (3σ) and resolution of optics angle resolvers should be 20 $\widehat{\text{sec}}$ or better.

6. Platform gimbal angle resolvers should have a granularity of no more than 20 $\widehat{\text{sec}}$.

Controls and Displays

Computer input keyboard and computer display. Power switches for computer/clock, IRU, and optics. Systems readiness and computer check go/no-go lights.

Problem Areas

1. IRU azimuth alignment can be performed by gyrocompassing (with platform), earth rate measurement (with strapdown IRU, relatively inaccurate), telescope/autocollimator sighting of azimuth target (weather limitations and launch facility requirements) or by star sighting on clear nights. In-flight azimuth refinement after boost cutoff by star sighting is worth considering.

2. Choice of ground or on-board mission profile computation TBD when range of missions and probable mission constraints and situations are better defined.

Ascent Phase. Phase begins at lift-off and includes atmospheric boost, staging, vacuum boost and coast, and orbit insertion.

Operational Requirements. Safe return to base of manned booster vehicles (where used) and the orbiter after a boost abort is required.

G&C Functions

1. Perform inertial navigation during thrusting and/or atmospheric flight periods, and compute the orbit during exo-atmospheric coasting portions of boost.

2. Perform powered flight guidance to achieve near optimum powered ascent trajectories which satisfy the orbit or suborbit conditions at thrust cutoff, and satisfy $q\alpha$, attitude rate, and other vehicle constraints. Modify vehicle guidance and trajectory parameters if engine failure is detected.

3. Issue discretes for engine ignition, liftoff, staging ullage and thrust cutoff, and any other required discretes during boost. These discretes will be issued when appropriate criteria (time, fuel depletion, orbit attained, etc.) are met.

4. Perform autopilot functions of executing guidance attitude commands and stabilizing the vehicle(s) by issuing flight and thrust vector control signals during atmospheric and/or powered portions of ascent. Satisfactory maneuver response and stability must be provided for varying Mach number, q, engine thrust, and vehicle configuration.

5. Perform attitude control and stabilization by issuing reaction control commands during exo-atmospheric coasting flight portions of ascent.

6. Monitor vehicle systems and flight conditions during all portions of ascent for malfunctions and possible boost abort situations. Generate vehicle status, malfunction, or possible abort displays for pilot evaluation and decision (orbiter) or automatic thrust cutoff and/or staging (booster).

7. After pilot or automatic abort decision (orbiter), issue staging and/or thrust cutoff discretes, and compute and display the landing sites which can be reached, time to reach each site, and possibly other pertinent factors (max g's, reentry heat load, etc.) for pilot evaluation. Upon receipt of landing site choice, compute required atmospheric turns and exit conditions (V, γ, location) for exo-atmospheric skips, etc.

8. Perform IRU gyro bias torquing or attitude computation.

9. Display position, velocity, and attitude information to the pilot, as required or requested.

10. Incorporate ground tracking navigation updates.

11. Refine IRU azimuth alignment by star sighting (optional).

Computer Functions

1. IRU bias compensation, attitude computation, inertial navigation or orbit computation; output position, velocity, and attitude signals for pilot displays.

2. Compute optimum powered flight trajectory, within vehicle limitations, and desired thrust direction. Compute required attitude change and attitude rate for optimum thrust direction program. Perform autopilot computations to generate thrust vector control signals.

3. Test discrete command criteria against existing conditions and issue discretes when the appropriate criteria are satisfied.

4. Monitor vehicle attitude and rates during exo-atmospheric coasting flight, compare with desired deadbands and issue commands to the reaction jets or momentum control devices.

5. Compute and issue pilot display signals.

6. Monitor vehicle systems and flight condition status, and issue abort situation warning and/or alarm display signals.

7. Compute flight attitude (lift acceleration, bank angle) during atmospheric turns following boost abort. Compute required bank angle change. Perform autopilot computations to generate flight control signals.

8. After a boost abort, compute and display reachable landing sites and trajectory parameters to reach the selected site.

9. Incorporate ground-based navigation updates into the state vector estimate.

System Hardware

1. IRU, computer(s), pilot displays, computer uplind/downlink coupler.

2. Signal distributor for flight and engine control commands, staging discretes, etc.

3. Attitude rate gyros for stabilization.

4. Vehicle systems status signal A/D converter(s) and switching box.

5. Telescope mounted on a common base with the IRU(s).

Performance Requirements

1. Flight and thrust vector control sampling and command issuance rate will be 25 to 50 times/sec (20-to-40 millisec interval for adequate vehicle stability).

2. Navigation update rate during powered flight will be 25 to 50 times/sec. Navigation computations should be to 20-bit (1 in 10^5) accuracy, which corresponds to granularities on the order of 30 ft and 0.03 fps. This computation accuracy and rate will limit orbit insertion computation errors to less than 1 ft/sec.

3. Orbit insertion accuracies, including both navigation and thrust cutoff errors, should be less than 10 ft/sec and 1 nm in the cross range and radial directions, and 8 ft/sec and 1 nm in the downrange direction (all accuracies are 3σ values). Better accuracies are desirable but not critical for rendezvous. The stated accuracies can be achieved approximately with 1σ inertial component errors on the order of 10^{-4} scale factor error and 0.5×10^{-4}g bias for accelerometers, 0.05 deg/hr overall gyro drift rate, 20 $\widehat{\text{sec}}$ levelling, and 20 $\widehat{\text{sec}}$ azimuth alignment (with in-flight refinement, if required). With the stated gyro drift uncertainty of 0.05 deg/hr, strapdown IRU azimuth alignment by earth rate sensing would be accurate to only about 1 deg (3σ) creating insertion cross plane errors as large as 450 ft/sec, and 10 nm. These errors are unacceptable. Consequently, either much more accurate gyros or prelaunch gyro drift calibration procedures must be used with strapdown IRU's to reduce the 3σ drift uncertainty to less than 0.01 deg/hr, or an optical azimuth alignment must be performed, either prelaunch or in flight after booster separation. All the other stated hardware accuracies are well within the state of the art for inertial components.

4. Vehicle steering accuracy requirements have not been precisely defined for the powered and/or atmospheric flight phases, but a maximum steering error of 1 deg (actual-desired vehicle attitude) is probably adequate and achievable.

5. The boost trajectory guidance software should be no more than 25 ft/sec off optimum from liftoff or orbit insertion.

6. The thrust cutoff signal will be issued with a time granularity no greater than 0.02 sec.

Controls and Displays

1. Systems status and abort warning lights

2. Position, velocity, and attitude displays

3. Angle of attack indicator

4. Manual flight controls

5. Computer entry keyboard and data readout (DSKY)

Problem Areas

1. On-board computation of reachable alternate landing sites and trajectories to reach those sites, are relatively unexplored areas that will require some development effort.

Cooperative Rendezvous and Docking Phase. This phase begins after insertion into the target orbit or into intermediate orbit a few miles lower, and 30 to 70 miles away from the target. After taking rendezvous navigation sightings for an estimated 1/4 to 1/2 orbit to determine the orbit plane, eccentricity, deviations, etc., the rendezvous maneuver will be computed and executed with two to four thrusting maneuvers (probably three) over a period of one to two orbits. The location of final rendezvous will be fixed to allow docking in daylight. The ΔV's generally will be less than 50 feet per second. Additional navigation sightings will be taken between burns. A midcourse correction may be made between the last two burns (with RCS jets) on the basis of the postburn navigation sightings. The final velocity matching maneuver time can be modified by the additional navigation data to achieve a closer gross rendezvous.

At gross rendezvous, the two vehicles will be 1/4 to 1/2 mile apart with a small relative velocity and within the cone of acquisition of the docking sensor. Docking sensor acquisition may require a manual optical sighting to establish the line-of-sight direction to the space station followed by a shuttle attitude maneuver. The shuttle then will be properly aligned in attitude for docking and guided in by the docking sensor, using RCS translation thrusting to control relative velocity. The closing velocity will be

about two to give feet per second from the initial standoff distance (1/4 to 1/2 mile) to within a few hundred feet of the space station. The closure rate then will be reduced to a final closing velocity of about 0.5 feet per second.

Operational Requirements. Automatic docking is a system requirement.

Guidance and Control Functions

1. Perform rendezvous navigation by computing line-of-sight inertial direction from vehicle attitude, telescope shaft, trunnion angles (with optical sightings), or rendezvous radar gimbal angles during sightings of the space station. Determine shuttle orbit deviations by processing optical or radar sighting and radio range measurements.

2. Compute efficient or near optimum two- to four impulse rendezvous transfers, with rendezvous to occur at a fixed location within one or two orbits.

3. Compute and control economical attitude maneuvers to align the shuttle vehicle for thrust maneuvers.

4. Perform attitude control and stabilization functions (attitude and attitude-error computation, rate sensing, RCS jet selection and jet firing command issuance) for attitude hold, automatic maneuvers to computer specified attitudes, or manually controlled maneuvers. Hold attitude within specified rate and attitude deadbands, and execute maneuvers at pilot-selected maneuver rates.

5. Perform main engine thrust maneuver guidance: control steering with thrust vector control and roll axis RCS, and terminate thrust when the desired ΔV has been attained.

6. Perform inertial navigation to obtain revised orbit parameters during thrusting maneuvers.

7. Compute midcourse corrections from rendezvous navigation measurements to minimize position dispersions at gross rendezvous.

8. Perform RCS translation maneuver guidance: steering and attitude control, thrust initiation, and termination at the desired ΔV.

9. Perform docking sensor acquisition: control attitude maneuver to center the sensor scan field on the optically determined line of sight to the docking face, initiate sensor operation, acquire return signal, and perform range, range rate and angle lock on.

10. Accept and store space station orientation data via radio link from the station.

11. Perform terminal closure and docking guidance and control utilizing docking sensor data. Using the RCS in a translation mode, establish a relative velocity to place the shuttle about 500 feet away from the space station and along the docking axis within ten minutes time. At that point, null the line-of-sight angular rates and reduce the closure rate to 2 feet per second. Orient the shuttle so the docking faces of the shuttle and space station are properly aligned. Maintain the shuttle docking hatch on the space station docking axis by RCS corrections. As range decreases, reduce the closure rate until, at a distance of 10 to 20 feet, the closure rate is 0.5 feet per second. Final docking can be accomplished automatically by allowing the 0.5-foot-per-second closure rate to continue to impact, but probably will be manually controlled in most instances. Redundant RCS jets for translation along the shuttle docking axis must be provided. Windows on the shuttle docking hatch door or adjacent to the docking face should be provided for visual inspection of the docking-face alignment before docking.

12. Manual control override of the automatic terminal closure and docking will be provided.

13. Perform normal systems, monitoring, and orbit navigation functions.

14. Issue main engine ignition and shutdown discretes.

15. Provide for manual thrust vector control takeover.

Computer Functions.

1. Computer orbit position and velocity.
2. Continuously update position and velocity from inertial sensor inputs during thrusting maneuvers.
3. Compute vehicle attitude continuously. Process sensor data and guidance inputs to generate RCS jet firing commands for attitude control and RCS translation maneuvers.

4. Generate thrust vector control commands from steering error and rate inputs for main engine thrusting maneuvers.
5. Compute thrust maneuver steering errors.
6. Provide guidance and control mode switching, when appropriate switching criteria are met, for coasting flight, RCS and main engine thrust maneuvers, terminal closure guidance, etc.
7. Provide discretes, at appropriate times, for dockingsensor turnon, docking, engine ignition and shutdown, radio range mark, etc.
8. Accept and process optical or radar angle and radio range navigation data.
9. Accept and store space station attitude data.
10. Compute terminal closure guidance commands from docking sensor data.
11. Compute and generate display and indicator signals.
12. Compute a near optimum rendezvous transfer profile and associated thrusting maneuvers.
13. Monitor vehicle systems status.
14. Accept manual control inputs and generate display and indicator signals.
15. Perform IRU bias compensation.

System Hardware.

1. Basic inertial, optical, computer (w/I/O provisions) control system.
2. Docking sensor to measure range, range rate, angles, and angular rates. Corner reflector is required on the space station.
3. VHF or other radio range, with transponder on the space station.
4. Radio data link with the space station.

Performance Requirements.

1. Thrust maneuvers shall be measured within 0.1-foot-per-second accuracy (3) with the primary system.
2. Docking sensor range measurement should be accurate to 2 feet or 1 percent (3). Range rate should be accurate to 0.3 feet per second, or 10 percent (3). Angles should be accurate to 1 degree (3), and angular rates should be accurate to 0.05 degree per

second (3) for docking. Maximum acquisition range of the docking sensor should be 1.5 nautical miles. Minimum range of operation should be less than 10 feet. The 3σ angular rate error times the minimum operating range squared should be less than 0.1 feet squared per second. Measurement resolution should be equal to, or better than, the measurement accuracies. These accuracy requirements are currently achievable with laser and perhaps radar sensors, and will insure docking with less than 1-foot misalignment.

3. Thrust maneuver steering errors (taken for the maneuver as a whole) should be less than 1 degree, 3σ, to attain gross rendezvous.

4. Thrust vector pointing resolution should be accurate to 0.1 degree, 3σ, for adequate vehicle control.

5. Telescope point accuracy and 1σ resolution should be 40 arc seconds or better.

6. Attitude control accuracy for docking should be 5 degrees or better.

7. Maneuver initiation times should be accurate to 1 second and thrust cutoff granularity should be 0.1 second or less.

8. Thrust maneuver ΔV's should be computed to within 0.1 foot per second in each direction.

9. Attitude for ΔV maneuvers should be computed and the orientation maneuver initiated 5 to 10 minutes before the maneuver.

Displays and Controls.

1. Manual attitude and RCS translation controls.

2. Manual thrust vector control.

3. Pilot approval of each thrusting maneuver and of initiation of terminal closure guidance should be obtained through key depression.

4. Quantities to be displayed during various phases or on request are orbit position and altitude, range, range rate, and angle to the space station, ΔV maneuver data (time to go, ΔV), and alignment and relative position for docking.

5. Telescope controls (for optical sightings) are pointing control, power, reticle brightness(?), and mark button.

Problem Areas. The laser docking sensor requires additional evaluation.

Orbital Stay and Startup Phase. The orbital stay and startup phase includes system shutdown after docking, hibernation during the orbital stay time, and system reinitialization for return.

Operational Requirements. It is desirable to not require environmental control (temperature and atmosphere) during the orbital stay period of up to one week. Constraints on orbital checkout time have not been specified.

Guidance and Control Functions

1. Perform final vehicle systems check.
2. Power-down guidance, navigation, and control system.
3. Power-up guidance, navigation, and control system.
4. Perform vehicle systems check.
5. Accept orbital navigation data from the space station or ground.
6. Issue undock discrete.
7. Control separation maneuver.
8. Reinitialize IRU.

Computer Functions

1. Monitor systems status.
2. Issue power-down and power-up discretes and undocking discrete.
3. Perform attitude control and stabilization computations, and issue RCS jet firing signals.
4. Generate display and indicator signals.
5. Accept and execute manned control inputs.
6. Accept and store orbital navigation update from the space stations or ground.
7. Perform orbital navigation computations.

8. Accept line-of-sight direction data from sun, local vertical or known (stored) stars and process to determine vehicle attitude and inertial platform orientation (if a platform is used).

9. Generate platform gyro torquing signals for platform alignment.

System Hardware

1. Basic IRU-computer system.

2. Telescope mounted on common base with IRU's.

3. Sun sensor and/or horizon sensor.

4. Radio or hardwire data link with the space station or ground (radio link appears preferable).

Performance Requirements

1. Inertial platform gimbal angle or strapdown IRU initialization resolution should be 30 arc seconds or better.

Displays and Controls

1. Keyboard callup of IRU alignment program.

2. RCS attitude and translation manual controls.

3. System power switches.

4. Optics controls.

Problem Areas. System environment during orbital stay and system component compatibility with that environment remains to be determined.

Deorbit and Reentry Phase. Phase begins with deorbit ΔV maneuver, and continues through a half-orbit coast, entry alignment, reentry meneuvering to control g's and heating, and glide toward the landing site. A turn or skipout to achieve greater out-of-plane range capability may be used.

Operational Requirements. Cross-range capability is required to facilitate landing at a selected site within 74 hours of recall.

G&C Functions.

1. Compute entry and cruise heading to reach the landing site.

2. Compute deorbit time and ΔV to achieve desired entry conditions. Iterate with entry parameters as required.

3. Execute deorbit ΔV and preentry alignment maneuvers.

4. Perform deorbit ΔV guidance.

5. Perform entry guidance to achieve desired terminal or skipout conditions (location, heading, velocity, altitude or γ) within vehicle g, heating, and attitude-rate limitations.

6. Perform inertial navigation during atmospheric flight and during deorbit ΔV.

7. Perform exoatmospheric attitude control and stabilization, and issue RCS jet command to the signal distributor.

8. Perform flight control and stabilization functions at 60 degrees angle of attack from entry velocity down to M = 0.4. Issue flight control commands to the signal distributor.

Computer Functions.

1. Perform orbit navigation and monitor systems status.

2. Perform deorbit ΔV alignment, steering error, and Vg computations; and issue engine ignition and shutdown discretes.

3. Compute desired attitude and attitude errors (guidance function) during reentry.

4. Perform autopilot computations for space attitude control and stabilization, and for reentry flight control and stabilization; and generate RCS and flight control commands.

5. Monitor flight conditions and perform guidance, navigation, and flight control mode switching at appropriate times.

6. Perform inertial navigation computations during atmospheric flight.

7. Generate IRU bias compensation signals and/or gyro torquing commands during all flight modes.

8. Generate pilot display and indicator signals.

9. Perform deorbit maneuver and reentry phase targeting computations.

10. Accept and execute manual flight and attitude control commands.

Performance Requirements.

1. Deorbit ΔV maneuver targeting computation accuracy, steering, ΔV errors, and meansurement should be the same as for the rendezvous phase ΔV maneuvers.

2. Reentry and skipout targeting computations should be accurate to 10 feet per second in the downrange and cross range directions, 5 feet per second in vertical direction, and 2 nautical miles in location. These errors are compatible with the desired navigation accuracy for cruise.

3. Inertial navigation computation accuracy requirements are the same as for the ascent phase.

4. Preentry vehicle alignment accuracy, including both IRU attitude reference errors and attitude control errors, should be 1 degree.

5. Allowable entry guidance terminal condition errors remain to be determined.

6. Flight control commands should be issued 25 to 50 times per second during reentry.

7. Inertial navigation errors during reentry (from initial entry to cruise configuration transition) should be less than 15 feet per second and 2 nautical miles (3σ). These accuracies are achievable with the inertial sensor errors specified for the ascent phase.

8. Reentry attitude error (actual-guidance command) in bank angle should be less than 5 degrees.

System Hardware. Only the basic IRU-computer system, with appropriate software is required for this phase. Ground navaid receivers could be employed toward the end of the phase (subsonic glide) for a navigation update, but these are considered in the following phase.

Displays and Controls.

1. Manual attitude and flight controls.

2. Earth location display.

3. Attitude and attitude rate display.

4. Velocity-to-be-gained counter.

5. Velocity altitude, bank angle, flight path angle, g, heading, angle and angle-of-attack displays. (May require different displays during reentry through hypersonic, and supersonic-subsonic glide portions).

Transition to Cruise Configuration and Return to Base Cruise Phase. Transition to the cruise configuration and return to the base cruise phase begins with pitch down to a low angle of attack. After the cruise configuration is attained, the engines are started and the vehicle cruises back to the landing site. The phase ends with acquisition of landing approach signals.

Operational Requirements. No special requirement as yet identified.

Guidance and Control Functions

1. Sequence deployment of air data sensors (α, β, q, p), engines, wings, antennas, etc.

2. Control α and β (angles of attack and sideslip) to specified values during the vehicle metamorphosis and jet engine startup.

3. Sequence jet engine startup.

4. Provide maneuver guidance to reach cruise attitude, altitude, airspeed, and heading.

5. Perform autopilot functions (determine attitude, altitude and velocity errors, compute required flight and engine control settings from flight-condition errors and settings from flight-condition errors and rates; and issue engine/flight control command signals) during pitch down, configuration change, cruise configuration flight maneuvers, and return to base cruise.

6. Provide return-to-base cruise guidance (may be the same guidance mode as for the transition maneuver).

7. Accept pilot or ground issued command and data (for unmanned booster flight) to fly to an alternative base. Perform necessary computations (heading change, fuel available check, flight time, etc.) and execute maneuver to new heading and altitude.

8. Perform inertial navigation.

9. Control ground navaid receiver radio frequencies and use acquired data to update the inertial navigation estimate.

10. Provide manual control mode, and execute manual flight and engine control commands.

Computer Functions.

1. Issue discrete commands for configuration change sequencing and cruise engine startup.

2. Issue discretes for gound navaid receiver frequency/channel change based on stored station location and frequency.

3. Issue IRU bias compensation and gyro torquing signals.

4. Perform inertial navigation computations, and update the inertial navigation state vector estimate by processing ground navoid measurements and barometric altimeter readings.

5. Perform guidance and control mode switching when appropriate criteria are met.

6. Perform cruise guidance mode computations.

7. Perform autopilot computations and issue flight and engine control signals during transition, flight maneuvers, and cruise.

8. Monitor systems status.

9. Generate pilot display and indicator signals.

10. Perform cruise range capability computations.

System Hardware

1. Basic IRU - computer system.

2. Air data sensors (angle of attack, sideslip, q, altitude).

3. Ground navaid receivers and A/D converter.

4. Manual flight and engine controls.

5. Ground-air uplink data buffer/decoder.

Performance Requirements.

1. Control angle of attack, sideslip, and roll angles during configuration transition.

2. Inertial navigation computations should be accurate to one nautical mile per hour or better. Twenty-bit computation accuracy will exceed this requirement.

3. Altitude measurement should be accurate to ±500 feet (3σ). This restriction is less stringent than given current ARINC specifications.

4. Inertial navigation accuracy for cruise should be three nautical miles per hour or better (one sigma). This requirement is estimated to be compatible with, and no more stringent than, the ascent accuracy requirements.

5. Autopilot sampling and computation rate may have to be as high as 50 times per second for adequate stability.

Displays and Controls

1. Manual flight and engine controls, and auto/manual mode switches.

2. Computer keyboard for entering alternate landing sites, additional VOR station data, requesting data display, etc.

3. Manual ground navaid receiver controls.

4. Attitude indicator/display.

5. Heading, altitude, airspeed angle-of-attack instruments, or displays.

6. Location, readout/display, preferably map display.

7. Fuel gages.

8. Computer data display.

9. Flight control trim and feel system, and limiter.

10. Stall avoidance and warning.

Terminal Approach and Landing Phase. The terminal approach and landing phase begins approximately 50 miles from the landing facility and ends with engine shutdown after taxiing to the parking ramp. The sequence of flight events may include maneuvers to acquire the ground-based landing approach aids (advanced ILS localizer and glide slop beams, or airport tracking radar, or ?), flight along the glide path, phasing maneuvers to modify arrival time (speed variation, S-turns, or breakoff into a holding pattern in designated area), landing go-arounds on ground command or by on-board decision, landing flare, touchdown, rollout and braking, and taxiing to the parking area.

Operational Requirements. The vehicle must be able to execute all flight maneuvers unmanned. Safe landing must be possible under zero-visibility, weather conditions and with one turbojet engine out.

Guidance and Control Functions

1. Command flight maneuvers to acquire glide-path signals or to issue discrete for approach radar transponder turn-on as required.

2. Monitor forward hemisphere of airspace for other vehicles; determine if a collision hazard exists; and if so, take appropriate evasive action.

3. Control heading and glide slope automatically in response to glide path signals or ground commands.

4. Reduce speed or perform S turns as appropriate to maintain safe separation from other aircraft in the glide path, in response to collision avoidance sensor data, pilot command, or ground command.

5. Perform programmed holding patterns in preassigned areas in response to pilot or ground command.

6. Command landing gear deployment, flaps, and/or other variable geometry devices at the desired points during approach.

7. Initiate and control landing flare to touchdown. Sense yaw angle during flare, and execute decrab yaw and roll maneuver before touchdown.

8. Execute landing go-arounds within the airframe and engine limitations, in response to pilot or automatic on-board decisions or ground command. This activity will include automatic engine power-up control, landing gear and flap retraction, and flying a programmed flight path to reacquire the ground landing aids and glide path.

9. Provide mode-switching capability for manual or automatic piloting and systems control. Manual takeover of flight and engine controls must be possible at all times.

10. At touchdown, initiate and control runway braking sequence: flap retraction, engine throttle-back, brakes, braking chute deployment, etc.

11. Control vehicle heading to stay on the runway centerline during braking.

12. Provide stability augmentation and perform autopilot functions (command flight and engine controls) during the approach and landing phases in all flight configurations (flaps, gear down/up, one engine out, etc.).

13. Control, in response to radio-transmitted commands, wheel brakes, engine thrust (individually), and rudder for taxiing to the parking area.

14. Monitor braking effectiveness during landing rollout and taxiing, and transmit warning signal in event of brake overheating or poor tire traction.

15. Provide suitable pilot displays of vehicle position, altitude, and attitude relative to the assigned runway during approach, landing, and runway braking. Provide display mode switching at specified flight points or at pilot request.

Computer Functions.

1. Inertial navigation, IRU bias compensation, attitude compensation (strapdown torquing impulses or platform gimbal angles).

2. Output state vecotr and attitude signals for flight displays.

3. Store desired flight path to acquisition of landing aid signals, and programmed alternate maneuvers (S-turns, landing approach holds, landing go-arounds). Provide logic for executing programmed maneuvers (initiate and end-turns).

4. Compute stability-augmentation control commands and flight control and engine commands based on desired versus actual flight path error signals. Output these commands to the signal distributor.

5. Provide logic for guidance mode switching (cruise, programmed maneuver, flare, rollout, remote control taxiing, etc.)

6. Provide logic for issuing discretes (gear, flap deployment, engine throttle-back, brakes, etc.).

7. Provide logic for on-board decisions: collision avoidance, approach-path phasing (speed reduction or S-turns), landing go-arounds, etc.

8. Compute relative flight path of other aircraft from collision-avoidance sensor data.

9. Compute landing decrab maneuver steering commands.

10. Compute landing flare control signals.

11. Generate braking engine control, flap, rudder, etc., commands during landing rollout.

12. Execute ground commands for flight maneuvers (holding pattern, landing go-arounds) and taxiing after landing rollout.

13. Provide control mode switching and manual control override logic.

14. Process state vector and attitude signals for pilot displays.

15. Monitor systems status and issue crew warning display signals.

System Hardware.

1. Basic IRU-computer system, plus air data sensors.

2. Landing radar altimeters (two, probably one in each wheel well)

3. ILS-type signal receivers or ground radar transponders.

4. Flight maneuver/taxiing control command receivers and decoders.

5. Airborne navid receivers (VOR, DME, etc.)

6. Landing-gear brake temperature and locked brake sensors.

Performance Requirements. The critical accuracy requirements are to be lined up on the runway centerline at the start of flare, to initiate and control flare to achieve touchdown within the sink-rate limitations of

the vehicle, to remove yaw (decrab) prior to touchdown, and to keep the vehicle near the runway centerline during landing rollout and braking.

1. Inertial navigation accuracy of 2 to 3 nautical miles per hour (1σ) would limit maximum total position error after a 300-nautical mile cruise to base to within about 10 miles. Even these errors would not prevent approach navaid signal acquisition; consequently 2- to 3-natuical-mile-per hour inertial navigation accuracy (1σ) is adequate.

2. Flight control sampling and command rate may have to be as high as 50 times per second (20-millisecond intervals)for adequate vehicle control.

3. Alignment with the runway centerline must be within 10 feet (1σ) and 1.4 degree maximum yaw angle at touchdown. The yaw angle error is essentially a control requirement, as the vehicle heading can be sensed to 0.1 degree or better. These accuracies will give 4σ confidence of keeping all wheels on the runway during rollout, with a 150-foot-wide runway.

4. Runway centerline displacement at the start of flare should be within 5 feet (1σ) and flight path heading error (with respect to runway heading) should be within 0.5 degree (1σ) assuming approximately a one to two second vehicle yaw-roll response time lag, and the touchdown lateral accuracy requirements.

5. Displacement from the runway centerline should be sensed within 3 feet and 3 feet per second (1σ) after the vehicle crosses the end of the runway.

6. Vehicle sink rate at touchdown should be less than 10 feet per second. For a 1.15-g load factor during flare and a one second vehicle response time, maximum radar altimeter errors of 2 feet and 2 feet per second are required. Radar altimeter maximum detection height should be 150 feet or more to initiate flare soon enough with slightly higher than normal descent rate.

Displays and Controls

1. Manual flight and engine controls, manual guidance and control mode switches.

2. Flight control trim and feel and g limiting system.

3. Stall avoidance and warning.

4. Pilot display(s) showing distance, altitude and attitude with respect to the runway.

Problem Areas. Achieving position and velocity accuracies (with respect to the runway) during terminal approach, flare, and landing roll is considered to be one of the most difficult technical requirements.

Guidance, Navigation, and Control Hardware Utilization List

A preliminary hardware survey has been conducted to select suitable guidance and control equipment for the shuttle mission. Most of the components considered reflect the present state of the art. As such, the weight, volume, and power listed represent the upper bound for any corresponding items that will be designed for 1975-1976 initial operational capability.

Reliability requirements for each item have not yet been generated; hence, the selection of specific vendor's hardware cannot be made at this time. The examination of weight, power, and volume data for each hardware type, however, does allow projection of probable 1976 values. This projection is shown in Table 8.11-1. This table, therefore, represents the estimation of hardware physical characteristics applicable for the shuttle mission.

Based on the requirement for fail-operational/fail-safe, the number of required redundant units for each of the hardware components is shown. In flight phases, such as rendezvous, docking, and oribital operations, wherein crew safety is relatively high, the needed hardware redundancy levels are reduced. The most critical reliability design requirements are in the control signal distributor and the sensor signal coupler. These two components, respectively, receive control commands from the guidance and control computers for routing to control actuators and receives sensor signals for routing to the guidance and control computer. It is expected that built-in circuit redundancy and/or voting circuits are needed for their implementation.

Figure 8.11-6 presents a preliminary proposed hardware installation. An obvious anticipated problem area is the rendezvous radar antenna efficiency through an ablative radome. Most of the locations for the various sensors are based on criteria used for the supersonic transport. During the cruise back to base phase, use of all radio navigation aids are required.

Table 8.11-1. Projected Guidance and Control Hardware Characteristics (ILRV)

Hardware Components	Number of Units		Per Unit Physicals		
	Booster	Orbiter	Weight (lb)	Volume (ft^3)	Power (watts)
Guidance and control digital computer	3	3	40	0.8	60
Inertial reference unit	3	3	30	0.9	100
Inertial reference electronics	3	3	30	0.5	100
Horizon sensor	0	2	10	0.1	10
Star telescope with mounting plate	0	1	35	0.25	50
Air-data sensor (subsonic, supersonic, hypersonic)	2	2	12	0.2	20
Radar altimeter	2	2	10	0.2	50
Control signal distributor	1*	1*	30	0.9	200
Sensor signal coupler	1*	1*	20	0.5	50
Rendezvous radar	0	1	55	9.0	400
Laser radar	0	1	35	1.0	100
Laser transponder	0	1	10	0.7	100
Landing data receiver	3	3	5	0.1	10
Landing radar transponder	3	3	3	0.35	400
VHF navigation receiver	2	2	15	0.1	10
Distance measurement equipment	2	2	30	0.25	75
Automatic direction finder	2	2	6	0.1	5
ATC transponder	2	2	5	0.1	5

*S. S. Steady State Power - Does not reflect peak power which is defined by mission reqmts. (equip. duty cycle).

Space Division
North American Rockwell

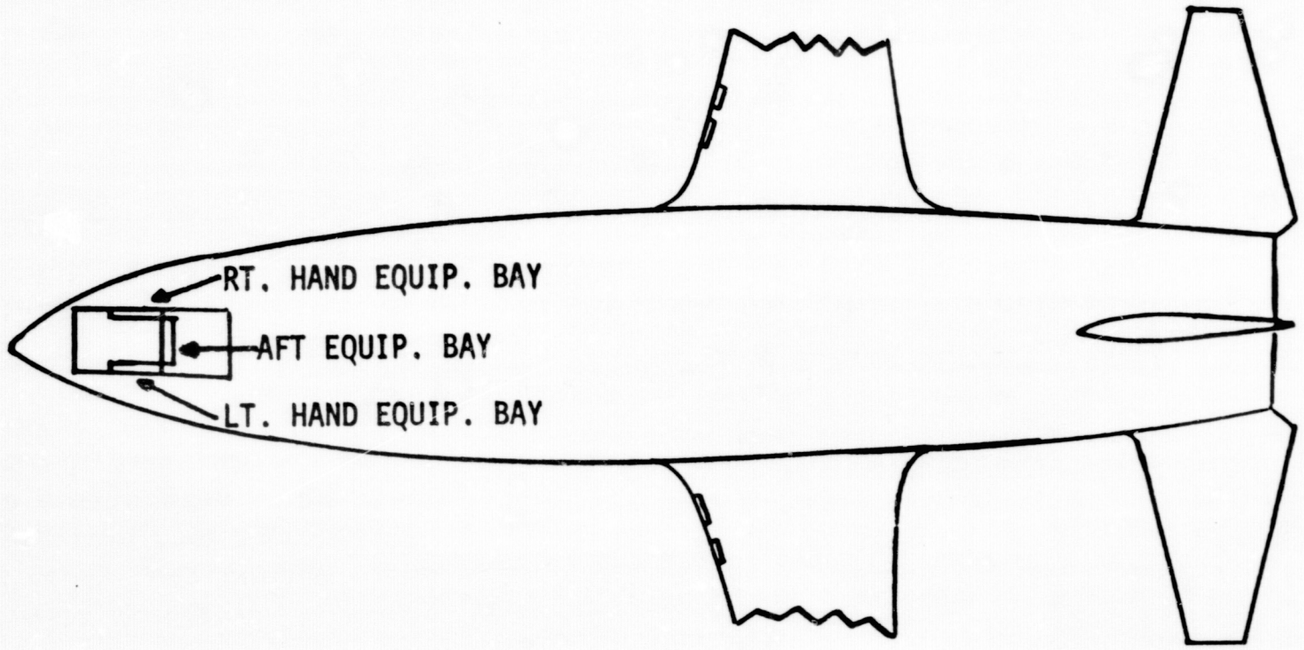

VOR ANTENNA (5"x5")

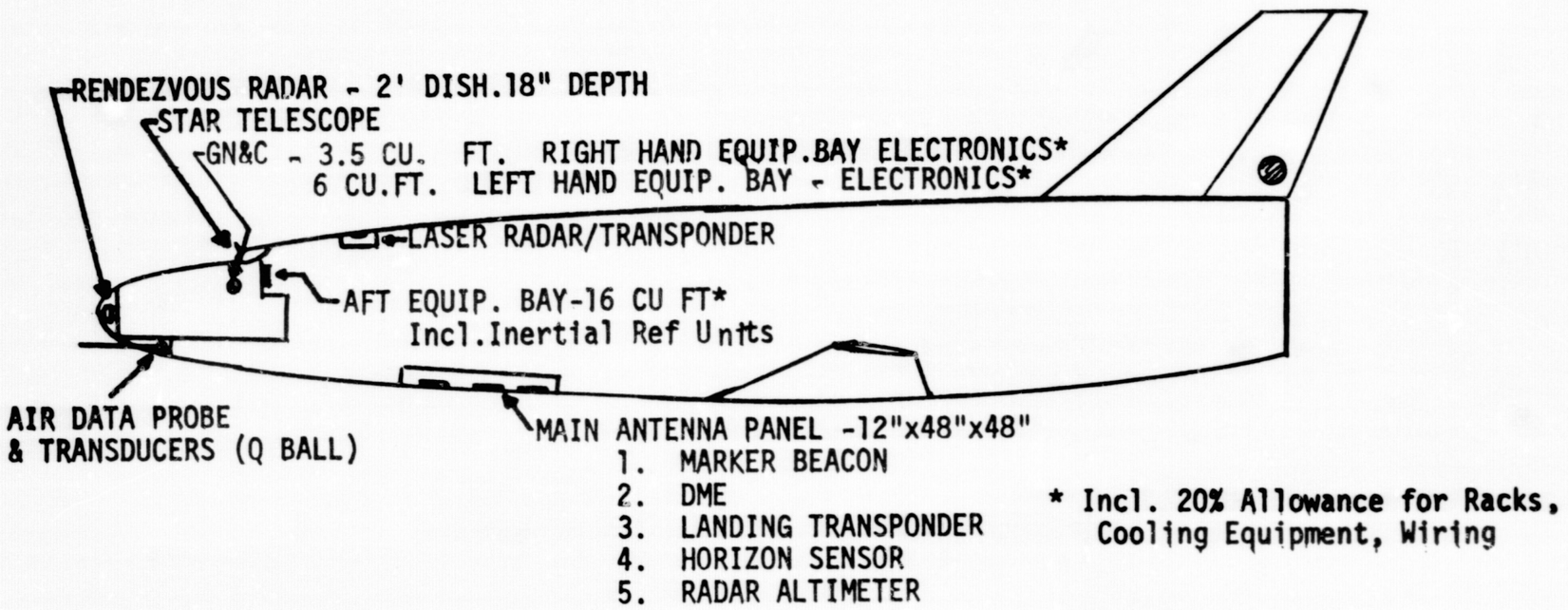

* Incl. 20% Allowance for Racks, Cooling Equipment, Wiring

Figure 8.11-6. G&C Hardware and Sensor Locations on Orbiter and Booster

Concurrently, fuselage temperatures and integrated heat built up are probably still severe. Adequate heat protection and equipment cooling are required to assure that electronics are not damaged or degraded over the 100 reuse cycles.

GN&C Method of In-Flight Malfunction Detection and Testing of Signals to the Performance Monitor

For the GN&C subsystem, the redundancy requirement is that more than one set of common hardware will be used. This configuration allows performances of redundant hardware to be checked one against another. The most logical signals for checking purposes are those of the GN&C computer output. This approach minimizes both built-in test equipment (BITE) and the needed number of signals. The rationale for this approach is described in the following paragraphs.

During the critical phases of boost, entry, and landing, all redundant navigators are operating simultaneously with one navigator designated as the master. The master navigator's outputs are connected to the control elements by means of the control distributor, whereas the outputs from the other navigators are dead-ended there. Even though these navigators are not controlling the vehicle, their outputs ought to be nearly identical to those of the master navigator under normal circumstances. Now, with the use of a performance monitor, some of the more meaningful GN&C computer's outputs can be monitored and compared. For instance, at a given instance of time, the velocity and position data as computed should all agree within some tolerance limits. If this condition is satisfied, the implication is that all affected inertial reference units (IRU's) and computers are operating normally. Further, if three or more navigators are used, the one that is marginally degrading in performance can be isolated readily. The speed of isolation depends on the degree of degradation. For instance, if one gyro of one IRU malfunctions, the velocity data error can be detected almost within the immediate next velocity computation interval. Since high accuracy is not required, an erratic gyro may not be detected. But there is no cause to be alarmed and the operational objectives will still be met. The above arguments also hold for the case of velocity meter performances.

Consider next the possible failure of IRU electronics. The most dramatic failure would be that connected with the IRU servo loops. In this case, the monitor would pick up a very large difference in the comparisons of both velocity and flight-control commands. Conversely, if the temperature-control loops are degrading or nonoperative, the output differences will not be detected quickly, but then all operational objectives will be met.

Next, consider possible computer failure situations. Since digital computers are proposed, their malfunctions are easily detected by the monitor when three or more computers are supposed to provide nearly identical outputs throughout the critical flight phases. Additionally, before launch and return from orbit, each computer has performed its own parity bit check, preprogrammed routines, IRU calibration and alignment, and has calculated the required boost or reentry nominal trajectory. These computations exercise a large percentage of each computer's memory and almost all of its arithmetic sections so that its performance is well verified before its flight commitment.

In regard to the control elements, it is proposed that quadruple redundancy be provided in the sensor and actuating areas. This approach is completely within the state of the art since these types of hardware have been developed and proven in many operational vehicles. The in-flight performance checking of these elements can be effected by signal recording of control sensors and actuator or valve motions for a few short, separate flight phases. Upon landing, these records will be processed by a ground computer and the degraded or malfunctional item will be isolated with computer programmed logics.

There appears to be a need to consider the imposed reliability for the monitor. Since the monitor passes judgment on computer outputs, its own decision outputs ought to be highly reliable during critical flight phases. It is envisioned that switching of the master computer should be performed automatically by the monitor so that speed of control-signals switching can be achieved. When any such event has taken place, the crew should be informed with visual and audio alarm signals. At the same time, a hard copy of computer output comparisons ought to be printed for the crew so that confirmation is possible for crew confidence. Alternatively, a display of outputs might be considered. Also, both automatic and manual switching of the control signal distributor should be required so that crew override of the monitor's decision is possible. Additional signals not checkable in flight could be provided with BITE.

To facilitate the implementation of in-flight performance monitoring and to provide sufficient data base for in-flight switching of control signals, the performance monitor must possess some processing capability. The various signals proposed for processing by the performance monitor are tabulated in Table 8.1.1-2. These signals are chosen with the criterion that they be sufficient for assuring flight readiness and detecting impending vehicle unsafe conditions. They can also be used to detect gradual degrading navigation/computers performance if these signals are compared among the computer channels over longer time intervals.

Table 8.11-2. GN&C Signals to Performance Monitor

1. Prelaunch Phase		
Signal Names	Data Format	Frequency of Output
1st Stage Burnout V_x, V_y, V_z, P_x, P_y, P_z, Time	24-bit Digital	One-Time Output
2nd Stage Burnout V_x, V_y, V_z, P_x, P_y, P_z, Time		
Phasing Orbit Parameters (24) (Specific Parameters TBD)		
Launch Azimuth		
IRU/Computer Calibration Status		
Flight Control Hardware Status		

Table 8.11-2. GN&C Signals to Performance Monitor (Continued)

Signals	Data Format	Output Frequency	Source of Output
2. Orbiter Boost Phase			
V_x V_y V_z t	24-bit	each 1/2 sec	each of 4 Computers
Large Gyro Angle and Status			
TVC and Ignition Commands	Analog	✓	✓
3. Rendezvous and Docking Phases			
ΔV and Time Range to Go Time to Go Δθ Δψ Δϕ			
12 Reaction Jet Commands	Discretes	As Occurred	✓
4. On-Orbit Alignment			
Gimbal θ Gimbal ψ Gimbal ϕ			

Table 8.11-2. GN&C Signals to Performance Monitor (Continued)

Signals	Data Format	Output Frequency	Source of Output
Time in Alignment	↓	↓	↓
Gimbal Difference			
$\Delta\theta$			
$\Delta\psi$			
$\Delta\phi$			
Star Identification Readiness Status			
Star Tracker Angles σ			
Star Tracker Angles μ			
5. Orbiter Entry Phase			
V_x	24-bit Digital	every 1/2 sec	each of 4 Computers
V_y	↓	↓	↓
V_z			
Latitude			
Longitude			
Altitude			
Heading			
Status			
Flight Path			
Angle of Attack			
6 Reaction Jet Commands	Discretes	As occurred	
12 Control Surface Commands	Analog	As occurred	

Table 8.11-2. GN&C Signals to Performance Monitor (Continued)

6. Orbiter Cruise and Landing Phases			
Signals	Data Format	Output Frequency	Source of Output
V_x V_y Alt. Rate Latitude Longitude Heading Status Angle of Attack Air Speed Sink Rate Altitude Time to Touch Down	24-bit Digital	every 1/2 sec	each of 3 Computers
12 Control Surface Commands	Analog	As Occurred	each of 3 Computers
Flap and Landing Gear Status	Discrete	As Occurred	each of 3 Computers
7. Signals for the booster will be identical as for the orbiter during similar flight phases			

Interfaces of the individual components are directly into the computer complex with very few interfaces between components. Almost all interfaces are in parallel digital format and are always present at the computer input buffers. Status and command data are interfaced in serial word format and presented to the computer upon command or at discrete times. Discrete inputs are also used and are usually equipment on commands and built-in test equipment (BITE) signals. A breakdown of the types of interface and data is presented in Table 8.11-3.

Table 8.11-3. Data Breakdown

Data words (parallel)	Computed pointing angles Aided track Biases Torquing Signals Velocities TDA TDB
Command words (serial)	Slew Search Align Self test Stellar magnitudes
Status words (serial)	Slew Search Track Fail signals
Discretes	ON command BITE failures

Some analog interfacing is done but this is primarily in the area of video signals from TV and I. R. that go to the displays. All computations for vertical reference, stability augmentation, altitude control, trajectory control, position determination, computed command angles, aided track, and sequencing is done by the computer complex.

Signal Flow Block Diagrams

This section presents a preliminary set of subsystem flow diagrams (Figures 8.11-7 through 8.11-9) and explanatory notes for the various mission phases. The diagrams reflect the explicit requirement of fail-operational and fail-safe for the GN&C electronics. Preliminary interpretation of this requirement led to the use of triple redundancy, especially for critical equipment during boost, entry, and landing phases. Because of this redundancy level, highly reliable signal distributors and signal couplers are needed to interface with the redundant hardware. To plan for their reliability compliance, both parallel elements and voting approaches must be considered.

Targeting and Mission Planning (Orbiter)

Before alignment and temperature stabilization of inertial instruments, the GN&C computers can individually proceed to calculate a nominal trajectory. This is done with the targeting data as received from the command data link (pilot input or uplink). Essentially, all three computers are programmed to perform an identical task. The required stored parameters are the density table, the gravity model, trajectory constraints, the vehicle mass, and propellant characteristics. At the completion of this task, each computer will have determined and stored in memory various criteria for the impending flight sequence. A few selected trajectory parameters can be sent to the performance monitor for comparison. When all three computers have provided identical outputs, the status will be displayed and a hard copy of flight events can be provided automatically to the crew. If one computer sends flight events different from the other two, a mission rule is required to determine whether to continue with launch or to replace hardware. This function is not required of the booster computer (Figure 8.11-10).

Prelaunch Calibration and Alignment

With local gravity received from the data link, the computer can then command IRU's to be calibrated as soon as temperatures have been stabilized. This is done individually by the three independent inertial navigation systems simultaneously. With the present state of the art, the calibration and alignment process probably will require an hour of undisturbed launch pad condition.

Techniques for strap-down system calibration by gyro compassing have not been proven as of this writing. For this reason, the following will pertain to a gimbaled IRU. It is further assumed that an alignment block, with level detectors mounted on different faces, is an integral part of the

Figure 8.11-7. Relationship of Control Signal Distributor and Signal Coupler

Space Division
North American Rockwell

Figure 8.11-8. Control Signal Distributor With Voting Logic

Space Division
North American Rockwell

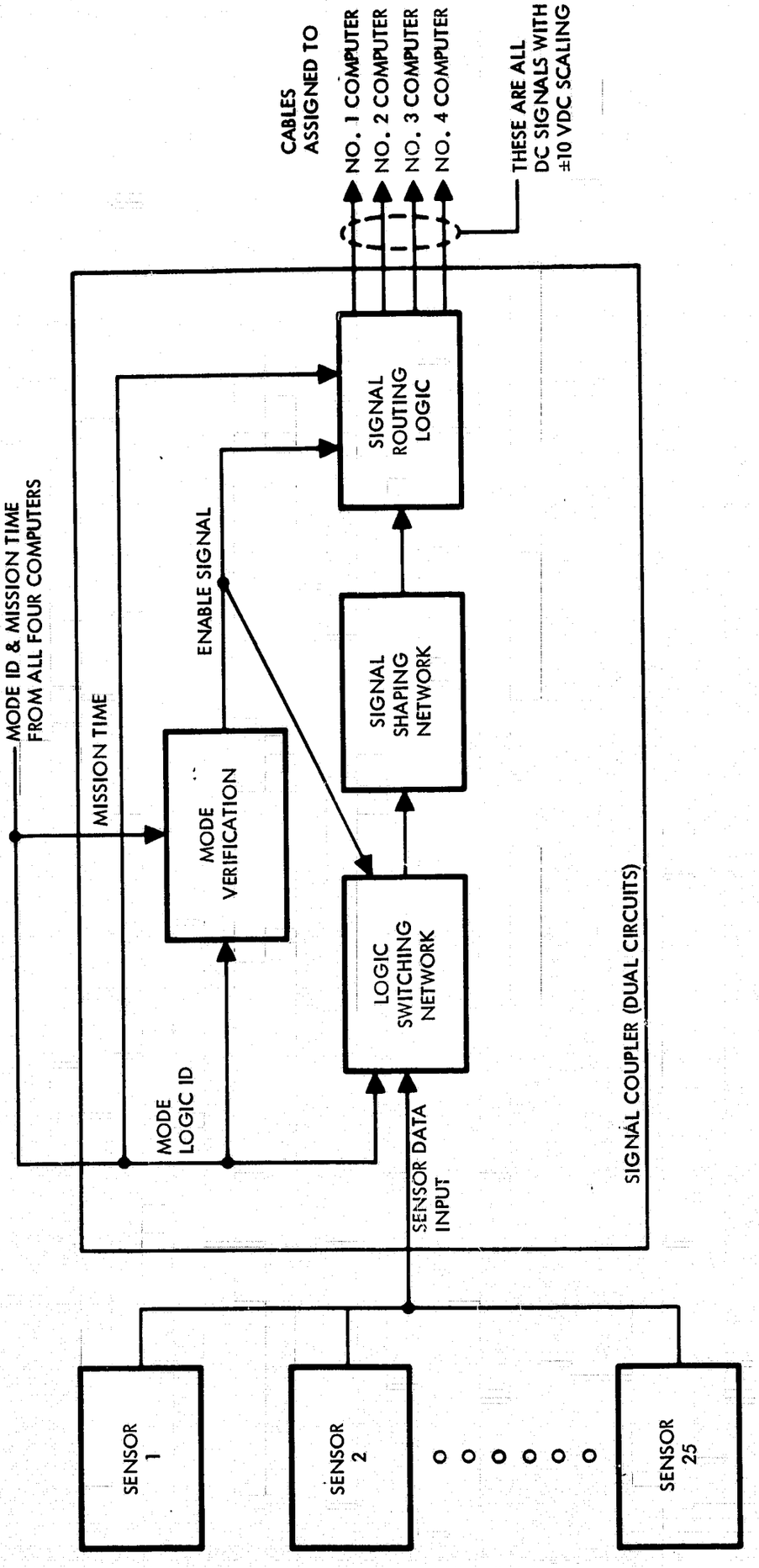

Figure 8.11.9. Input Signal Coupler (Mode-Switching Approach)

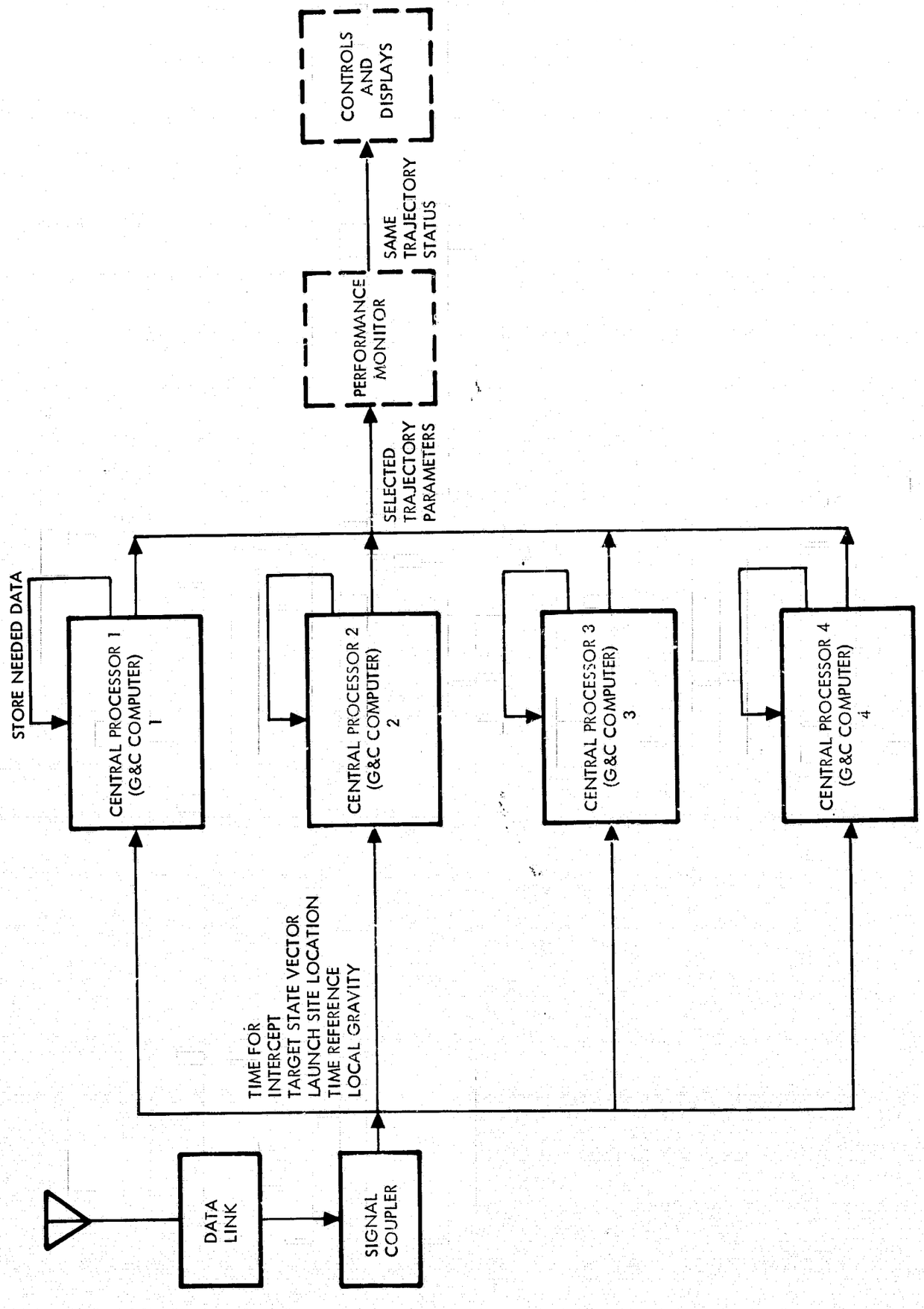

Figure 8.11-10. Targeting and Mission Planning

stable member (SM) which houses the gyroscopes and velocity meters (VM's). The computer can then command the SM to a given orientation and collect VM pulses.

After a predetermined amount of time in the first orientation and with VM pulses stored in memory, the next SM orientation is acquired and the process is repeated for four orientations. The computer, makine use of alignment block angular relationships and VM pulse data, will determine instrument (or IRU) biases and scale factors.

When calibration is completed, gyrocompassing can provide azimuth alignment. It is expected that Kalman filtering will be used to obtain faster gyrocompassing and more accurate IRU parameter estimates.

The performance monitor will compare azimuth estimations from all three computers. When all three inputs are within tolerance, then all IRU's and computers are operational to the extent that a large portion of each computer has been exercised and nearly all parts of the IRU have been operating properly. If the gyro pickoff large angle indication prevails, then the IRU is defective and calibration has to be halted and mission rule must be applied. (See Figure 8.11-11.)

Boost Navigation

During boost, all GN&C computers perform identical functions, but only one set of outputs is used for actual vehicle control. All of the navigators are kept operating to monitor the primary navigator performance and to preserve navigation and attitude data if the primary system fails. Since the orbiter must have all navigation data to continue with the orbital phases, its navigation must be initiated at liftoff. It is presently planned to have booster control during boost performed in the orbiter.

The scheme, as shown in Figure 8.11-12, dictates that the control signal distributer must be designed for reliability levels of 0.9999 or so. Criteria for switching need to be incorporated in the performance monitor. This is easily mechanized since it is receiving identical information from all GN&C computers and majority voting can be implemented.

Engine-out conditions can be detected by each computer from acceleration differences, with verification provided by engine-chamber pressure measurements. When the failed engine is identified, each computer can modify guidance and control commands accordingly and optimize the boost trajectory for one-engine-out propulsion performance.

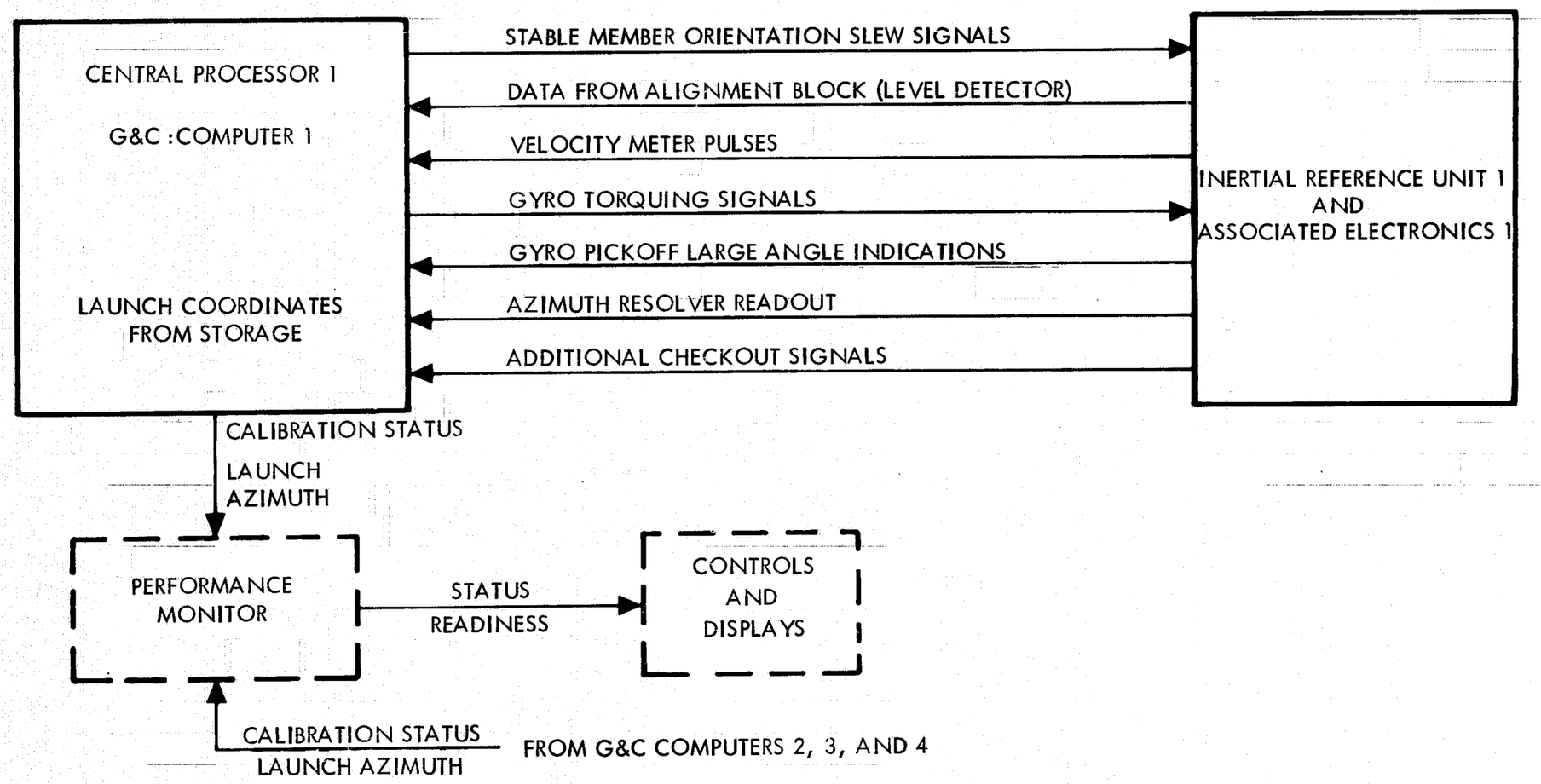

Figure 8.11-11. Prelaunch Calibration and Alignment and Self-Test

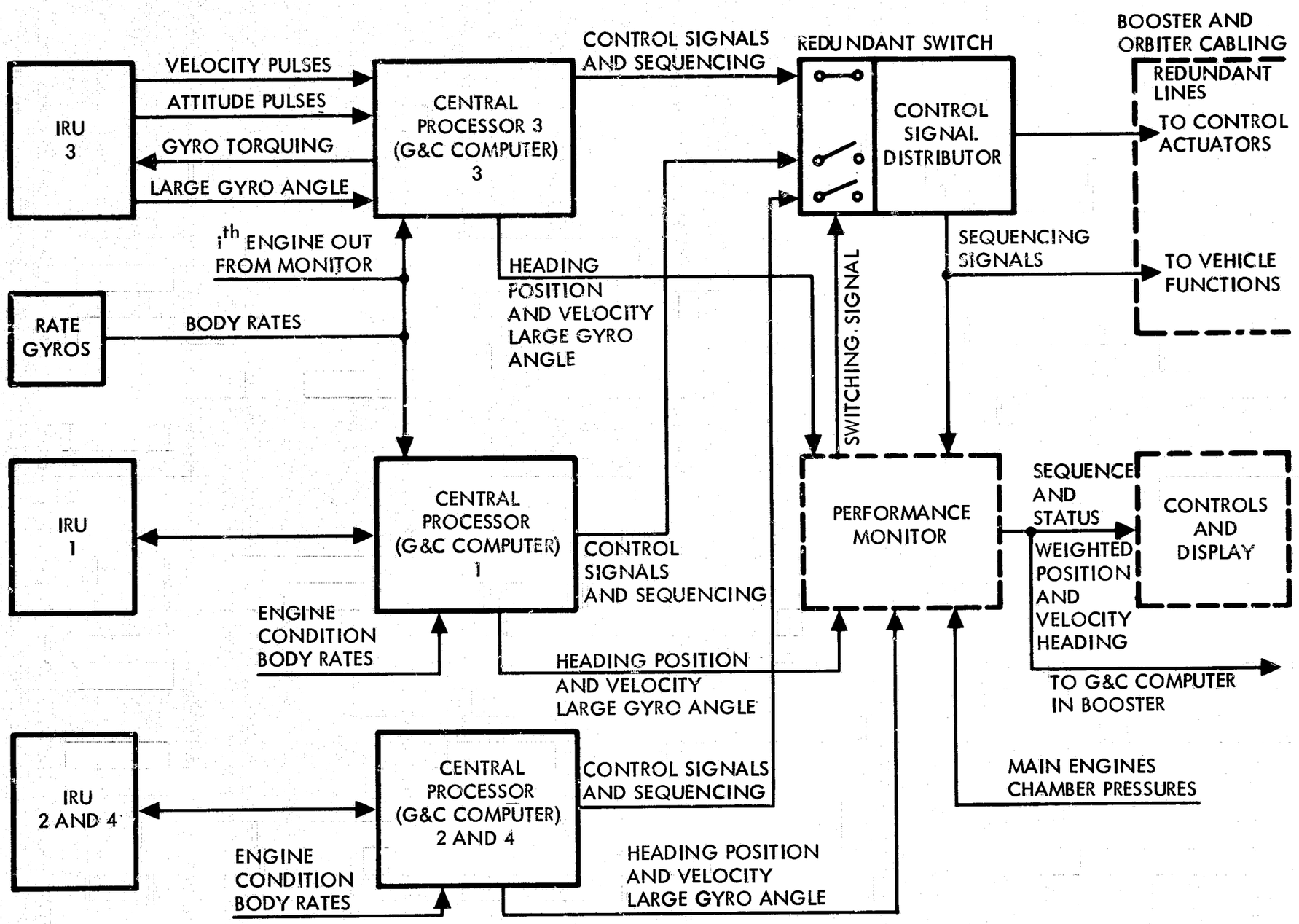

Figure 8.11-12. Boost Navigation, Steering, and Control for Orbiter

During the boost phase, rate gyros and angle of attack signals are needed to compensate for body bending modes and to minimize structural (aerodynamic) loads. The location for these sensors can only be determined from detailed vehicle design data (bending modes, etc.). Likewise, the sequencing signals for the vehicle cannot be ascertained until more detailed design is performed.

Phasing and Parking Orbit

In addition to functions performed during boost, the parking-orbit phase may require the determination and execution of delta V maneuvers. If an extended-duration parking orbit is required, the telescope may be used for periodic IRU alignment update by star sightings. During this and the subsequent orbital phases, pilot monitoring and manual takeover of the vehicle control is possible to a large extent in place of redundant system operation, since failures are generally not time critical. (A separate signal flow diagram is not shown for this phase.)

Rendezvous and Docking

At 120 nautical miles out, the rendezvous radar is used to obtain ranges to go data until about five nautical miles out. At this point, the laser radar will be used until docked. For docking, the space station is required to be holding attitude to an inertial reference. Since automatic docking is a requirement, attitude and range data must be accurate. For range and range-rate data, the laser radar has inherently better resolution than the microwave radar. Since the docking port is mechanically fixed and the station is holding inertial attitude, the shuttle vehicle can negotiate appropriate attitude maneuvers to engage the docking port. The gimbal angle readouts from the laser radar can be used to drive translation jets until the two vehicles are properly lined up.

Because of the use of multiple GN&C computers, the interface with both the rendezvous radar and the laser radar must have a central distributor so that any GN&C computer can operate these sensors and read data from them (Figure 8.11-13).

On-Orbit Alignment of IRU

Once the state vector and time are received, the GN&C computers can start updating and the shuttle can back off from the station. With the horizon sensor signal transmitted to the signal distributor and thence to the computer, the vehicle can be commanded to hold to local vertical. An initial star or sun sighting then establishes a coarse IRU alignment which enables automatic star acquisition with the telescope. If the horizon

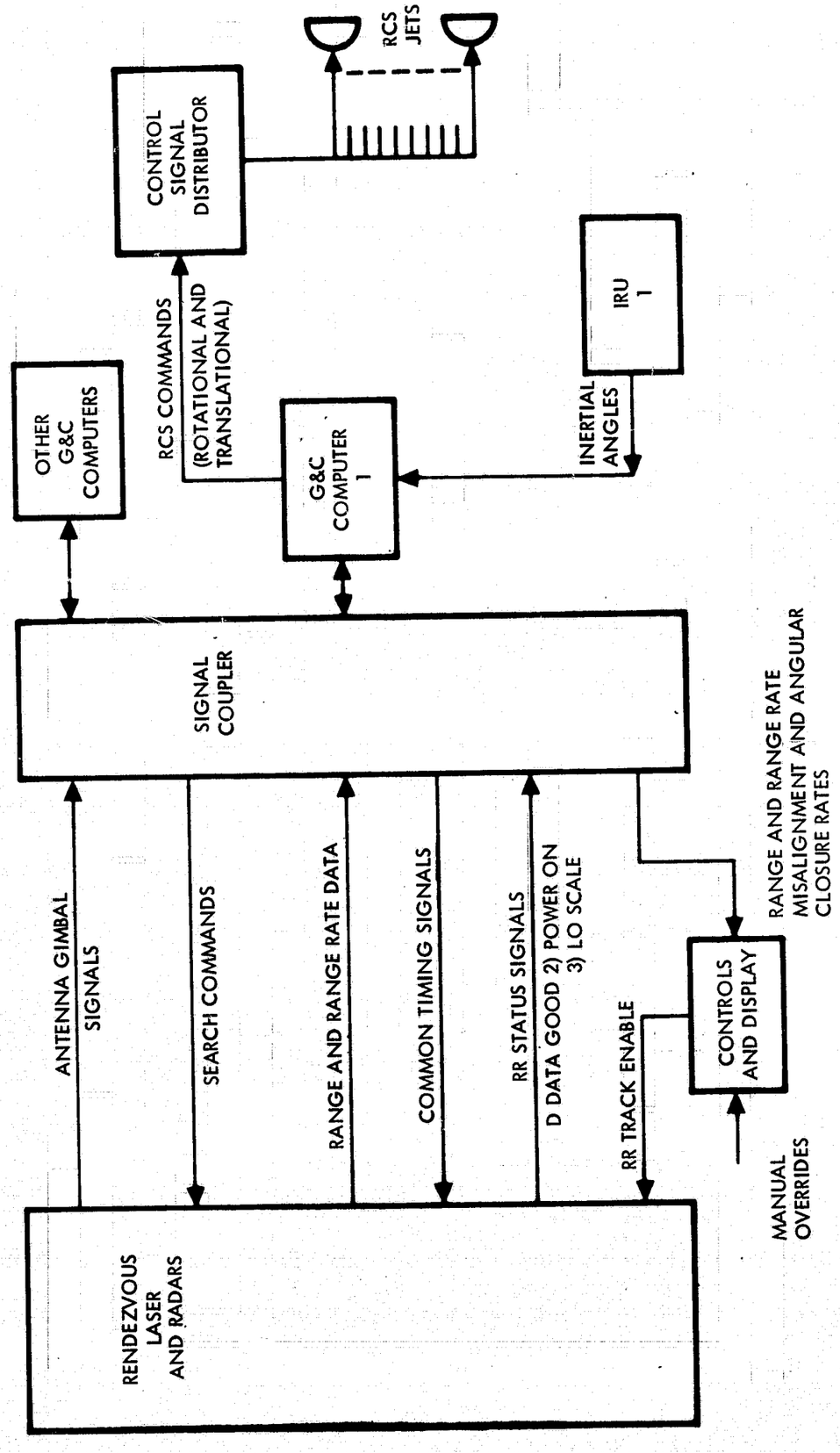

Figure 8.11-13. Rendezvous and Docking

sensor is nonoperative, then manual star search and acquisition must be used (as is done in the Apollo CM). In this case, the crew must identify the star being sighted. Redundant horizon sensors could also be used. Polaris can be easily acquired for the initial star sighting with a gross heading from a magnetic compass. Sighting of two additional stars after coarse alignment will allow the fine alignment of the IRU's.

When all gimbal angles from all IRU's are within tolerance, the performance monitor then turns on readiness status crew display. It is important during design to plan for telescope field-of-view and for mechanical alignment between the IRU's, horizon sensor, and telescope. (See Figure 8.11-14.)

Entry Guidance and Control

Once the landing site has been selected and stored in the GN&C computers, the deorbit location and delta V requirements will be calculated and displayed to the crew. The manner in which landing-site coordinates will be provided has not been determined at this time. It is probable that both manual loading and automatic loading via the data link will be required. Since the delta V for de-orbit is a function of landing site and orbital state, the computer automatically will correct down the time to delta V and command the vehicle altitude maneuver before ignition.

As the vehicle approaches the entry interface (400,000 feet altitude), a preprogrammed entry alignment maneuver will be performed while navigation and control functions are maintained. (See Figure 8.11-15.)

Cruise and Landing Phases

The onboard navigation system is designed for entry accuracy of approximately two nautical miles. The navigation aids will be used to perform area navigation according to FAA regulations. Since automatic blind terminal approach and landing is a requirement, a high accuracy runway fix is needed. It is proposed here that an SPN-42 carrier-landing type of system be installed at the landing site. In this way, the only airborne hardware would be the landing receiver, the transponders, and the GN&C computers. The SPN-42 uses tracking radars and can provide 10-by-40-foot runway accuracy. Other landing parameters such as path deviation, heading errors, and sink rates are also available from the ground transmission if desired for comparison with airborne autopilot-furnished data.

If self-contained automatic blind landing is to be implemented (which is not likely), the vehicle would have to carry multiple search-and-track radar for pinpointing runway touchdown location. The weight penalty of this approach is not attractive. (See Figure 8.11-16.)

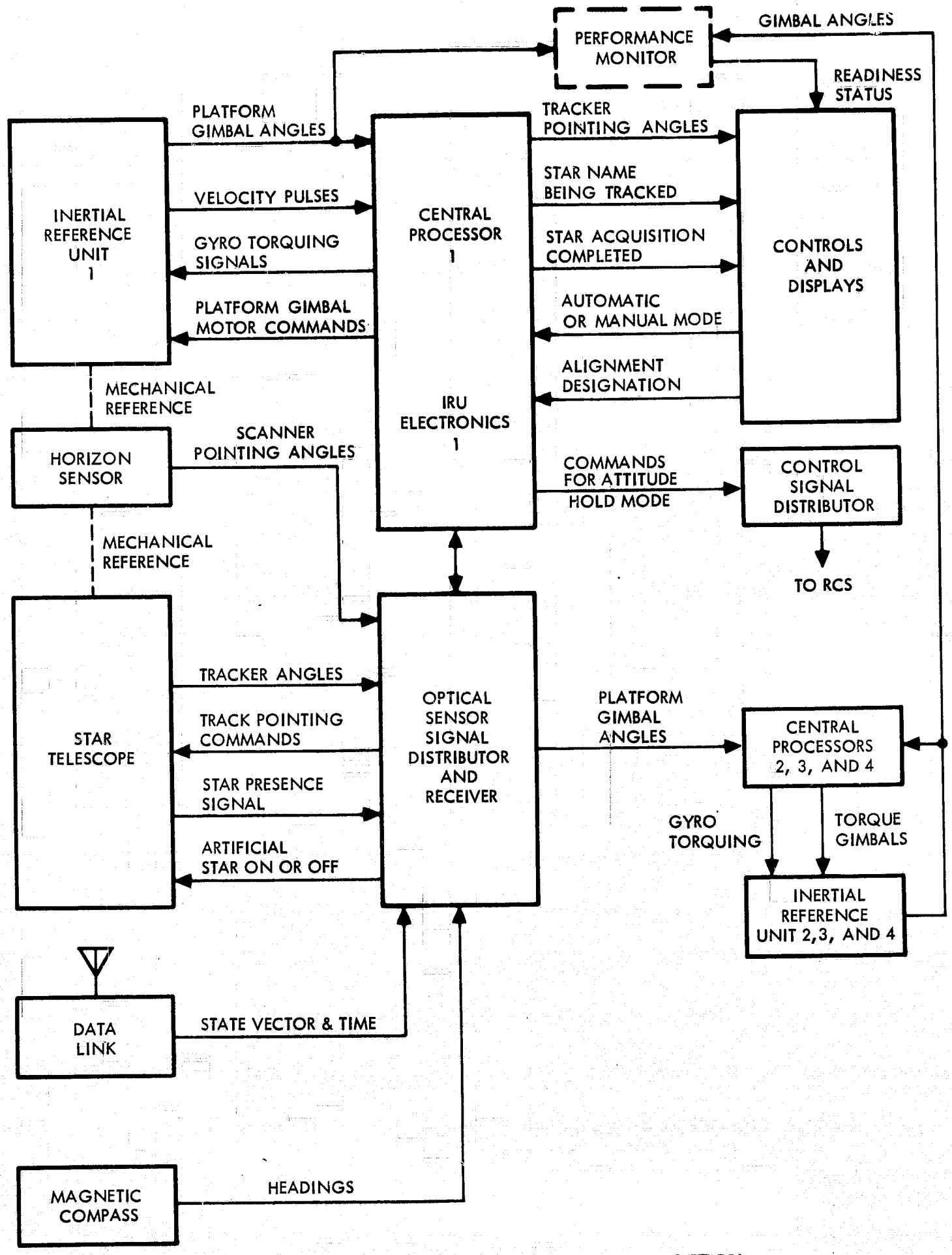

Figure 8.11-14. On-Orbit Alignment of IRU's

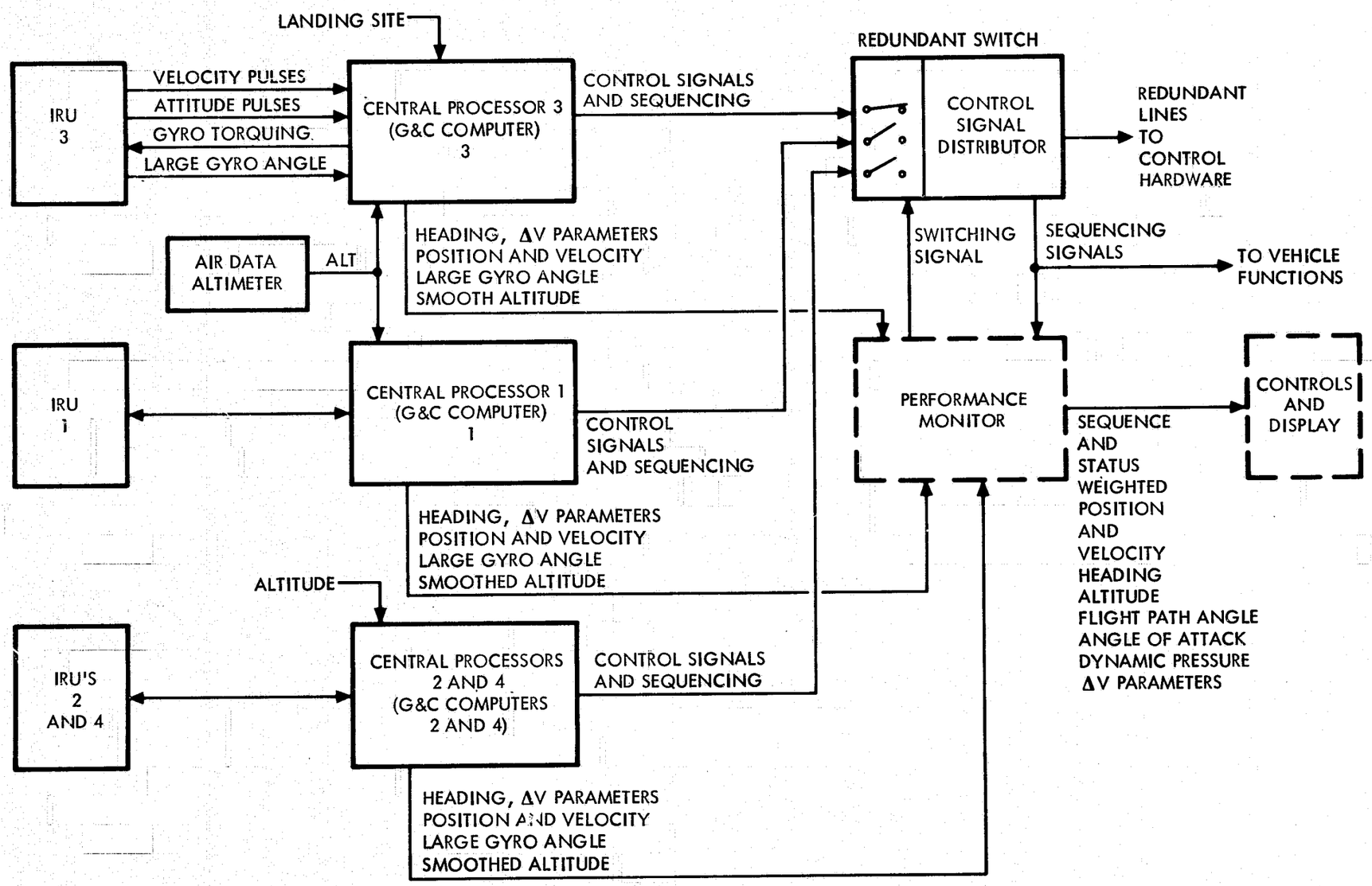

Figure 8.11-15. Entry Navigation, Steering and Control

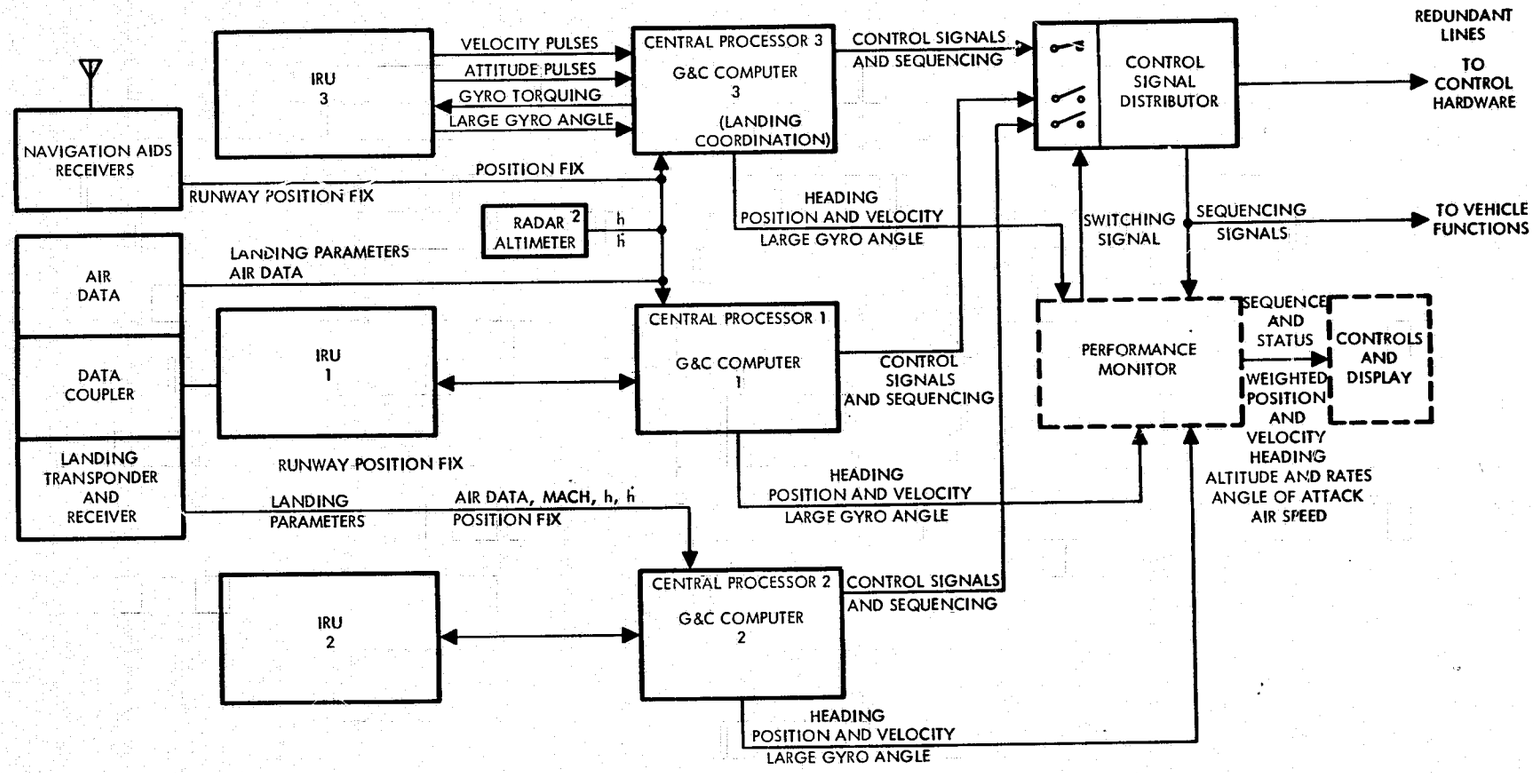

Figure 8.11-16 Cruise and Landing Navigation, Steering, and Control for Orbiter and Booster

Space Division
North American Rockwell

Booster Guidance and Control After Separation

Since the booster must perform the GN&C functions only after separation, it is possible to synthesize a simple set of guidance hardware that may be different from that carried by the orbiter. Certainly the software requirements for the booster GN&C would be less extensive than those of the orbiter.

It is expected that a total operational time of less than an hour is required of the booster.

8.11-3 Displays

The checkout and monitoring of the operational status of large-complex equipment systems, such as space vehicles and high-performance aircraft, has traditionally been performed by crewmen scanning large numbers of separate quantitative indicators or go-no-go lights. With the increased number of parameters to be monitored, the reduction in crew members, and limited panel space; the multi-instrument approach appears to be complex, expensive, and requires an excess of time to scan. The go-no-go light matrices simplify the monitoring problem, but deprive the crew of quantitative data required for the decision-making process after a fault is detected.

A review of the mission timeline reveals that not all indicators would be used throughout the mission. A detailed study would probably reveal that very few indicators located on prime panel space are required during a normal mission. The logical conclusion which can be derived is that a departure from fixed multi-instrument approach is required.

The need for fixed instruments for crewman checking the vehicle normal operation status is practically eliminated as subsystem performance monitoring and operational verification are accomplished automatically (see IES section on Performance Monitoring and Checkout). As long as the mission is proceding in a normal manner, the information displayed to the crew is of an operational nature. The subsystem operational status is displayed to the crew when it is (1) pre-programmed, (2) crewman requested (on-demand), and (3) if an out-of-tolerance condition or trend is detected by the monitoring or checkout system.

Display Concept, Elements, and Examples

The basic display concept is to employ versatile and flexible electro-optical systems which can be programmed to display information. The

concept will provide an effective interaction between the systems management by the crew and subsystem equipment in the formation of decisions regarding system performance.

Figure 8.11-17 depicts the bar graph data display. On the left side, an alpha-numeric generator provides the legend for the particular bar. This can be done with a symbol generator if large numbers of parameters are involved, or an optical projector if only a few parameters are to be displayed.

In operation, a bar is generated on a cathode ray tube (CRT) for each quantity which is to be monitored. The length of the bar is proportional to the quantitative status of each monitored condition. The data to be displayed are normalized so that a high-normal-low scaling results. When system equipment is operating normally, all bars will fall within the center segment. When an out-of-tolerance condition occurs, the bar changes length and activates an alarm. The system is designed in such a way that a number of data frames can be displayed sequentially. These can be selected manually, item by item, for initial checkout, or cycled automatically at a selected rate for routine monitoring.

The monitoring function is normally performed in an automatic mode with a typical cycle rate of one frame per second. The result is a changing bar legend as well as the bar graph data. The operator merely watches the center section to determine that all bars are within the central normal area. If a trend toward an abnormal condition develops, he can switch to the manual mode and select the frame in which the malfunction is contained.

The device would have a preempt mode which would automatically return to the frame displaying the out-of-tolerance condition. An override control is provided so that the operator can continue to monitor other functions after noting that an out-of-tolerance condition exists. The malfunction indication (warning light) would continue to be displayed until the underlying disturbance is corrected.

In those areas of application where time to detect and react is critical, instrumentation could be supplied to store and display the instructions and procedures to be followed to correct the malfunction or alleviate the effects incurred by the condition. The instruction mode would be of particular importance where a large number of critical conditions are being monitored and where access to written instruction and procedures is limited or is too time consuming to be useful. It would be particularly useful where a central computer provides computation for adaptive response to an out-of-tolerance condition. The alpha-numeric printing unit could be used to present either stored instructions or volatile, adaptive instructions.

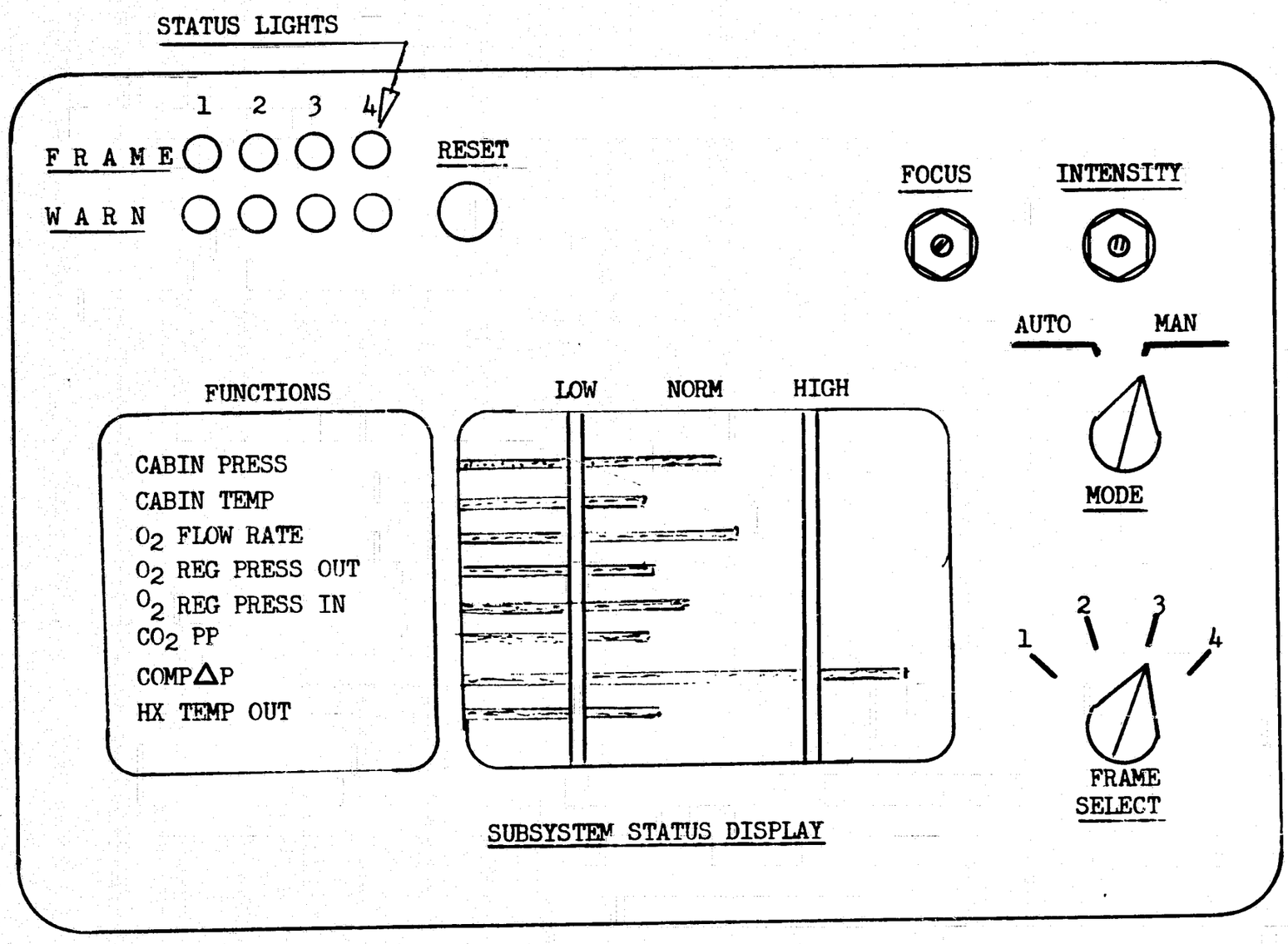

Figure 8.11-17. Electronically Generated Bar Graph (CRT)

Space Division
North American Rockwell

The indicating instruments are replaced by tapes on the face of a CRT as shown in Figure 8.11-18 which is a typical contact analog image of the IHAS display. The tapes in this case indicate altitude and indicated airspeed. Here the index against which the tapes are read are fixed while the tapes themselves move up and down the screen. If the range of the variable is not prohibitively large, then the index could be made to move with the tape left stationary. Any value of a desired variable could be presented along such a linear scale on the screen at a CRT. The crewman can call up any variable by the push of a button. Several variables that are likely to be of interest to the crewman at the same time could be called simultaneously by operating a single push button. This idea is conveyed pictorially in Figure 8.11-19. The resolution of such electro-optical indicators would not fall below that of conventional instruments and, depending on the type of raster used, may even exceed it.

The other use of the CRT is in the realm of rough schematic representations of subsystems to the level of a flow diagram as depicted in Figure 8.11-20. A template of the fixed part of the diagram can be stored on a photographic slide, magnetic tape, or digitally in a computer memory. The variables there and other rates can be superimposed electrically as a function of the subsystem status that is being monitored. All subsystems thus monitored can be displayed on the same CRT by actuation of a button. The CRT can double as a quantitative instrument and a qualitative status monitor. It can thus occupy the most favored and convenient position on the cockpit instrument panel and exhibit prominently the information a particular crewman is interested in at the time.

The scheme should not convey the impression that a single CRT is proposed. Aside from redundant screens for emergency cases, multiple sensors are proposed, as Figure 8.11-21 suggests. Not only may one pilot have to look back and forth from one screen to another as the information of interest may be too numerous to be projected for comfortable viewing on a single screen, but more than one pilot may desire to monitor data simultaneously. With multiple screens, not only can several crewmen view different information without interference with each other, but they can also view the same data simultaneously.

Aside from the quantitative and the schematic presentations, the screen can also serve as visual transducers of signals from a regular TV camera, a low light TV camera radar, in sensors (directly or through scan converters), and other devices whose signals lend themselves to visual presentation. This approach could also be regarded as an extension of the multisensor display.

Figures 8.11-22 through 8.11-24 indicate the conceptual uses which the CRT can serve as a visual transducer.

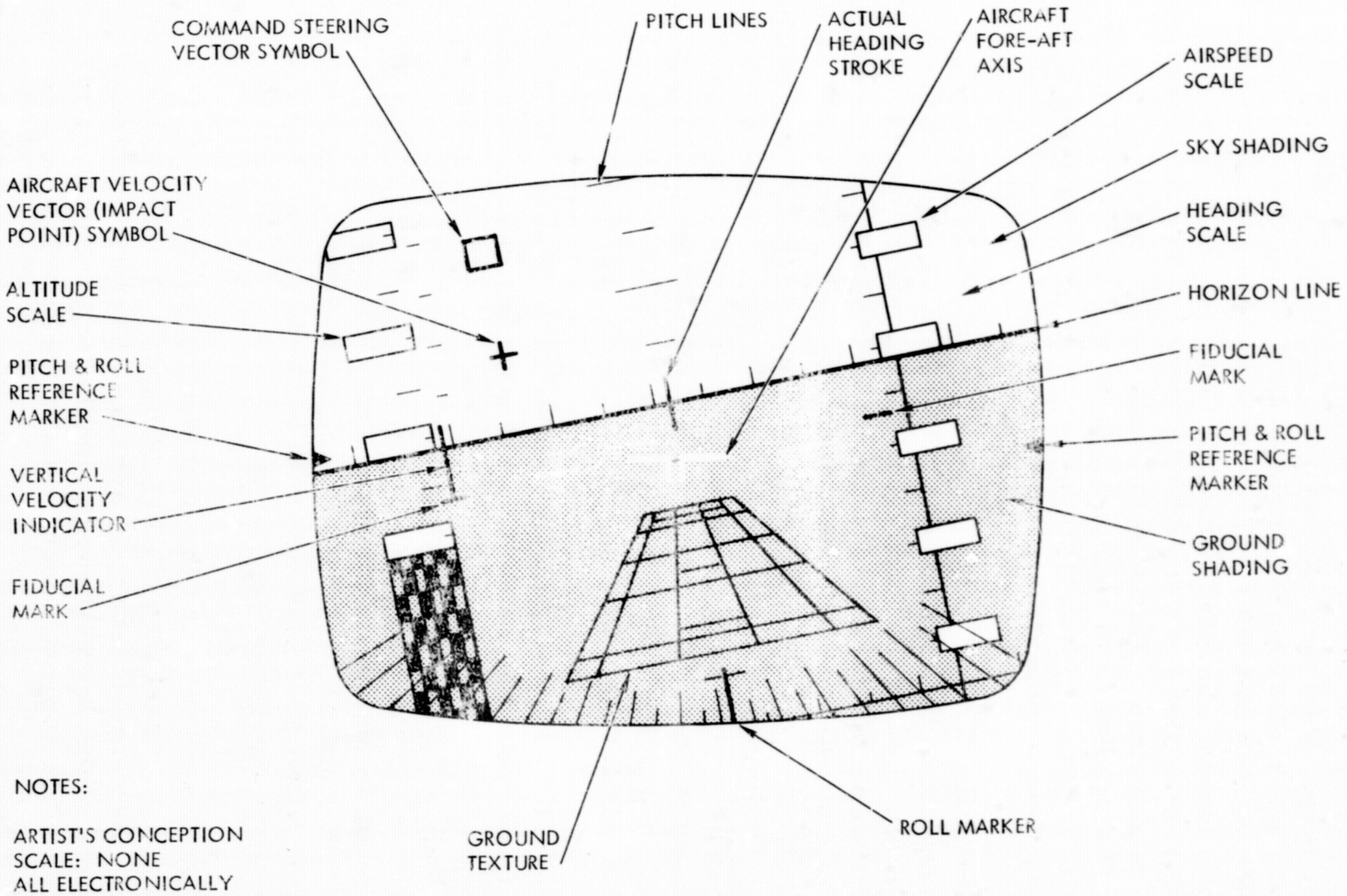

NOTES:

ARTIST'S CONCEPTION
SCALE: NONE
ALL ELECTRONICALLY GENERATED BRIGHT LINES ARE SHOWN BLACK

Figure 8.11-18. Contact Analog Display

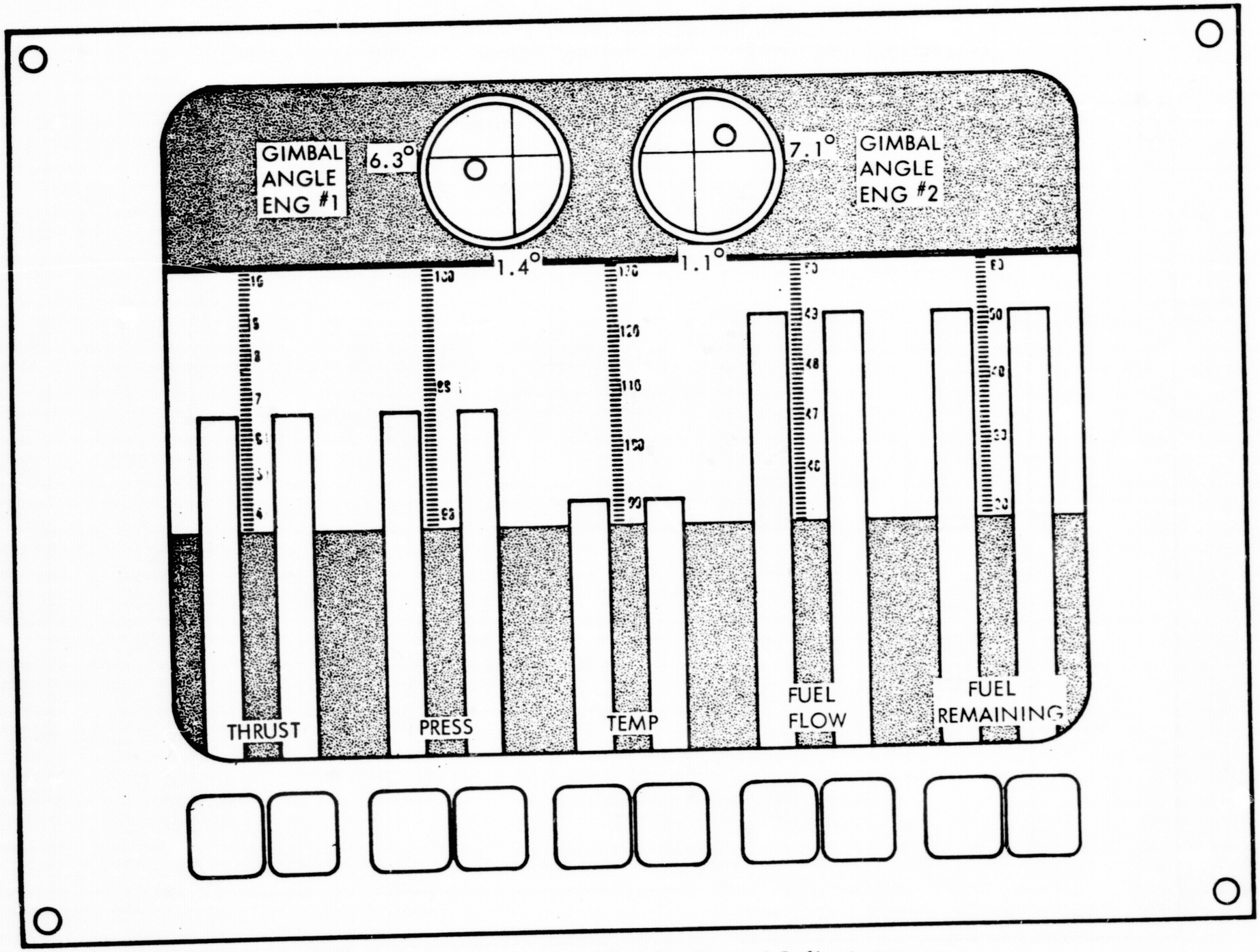

Figure 8.11-19. Electro-Optical Indicators

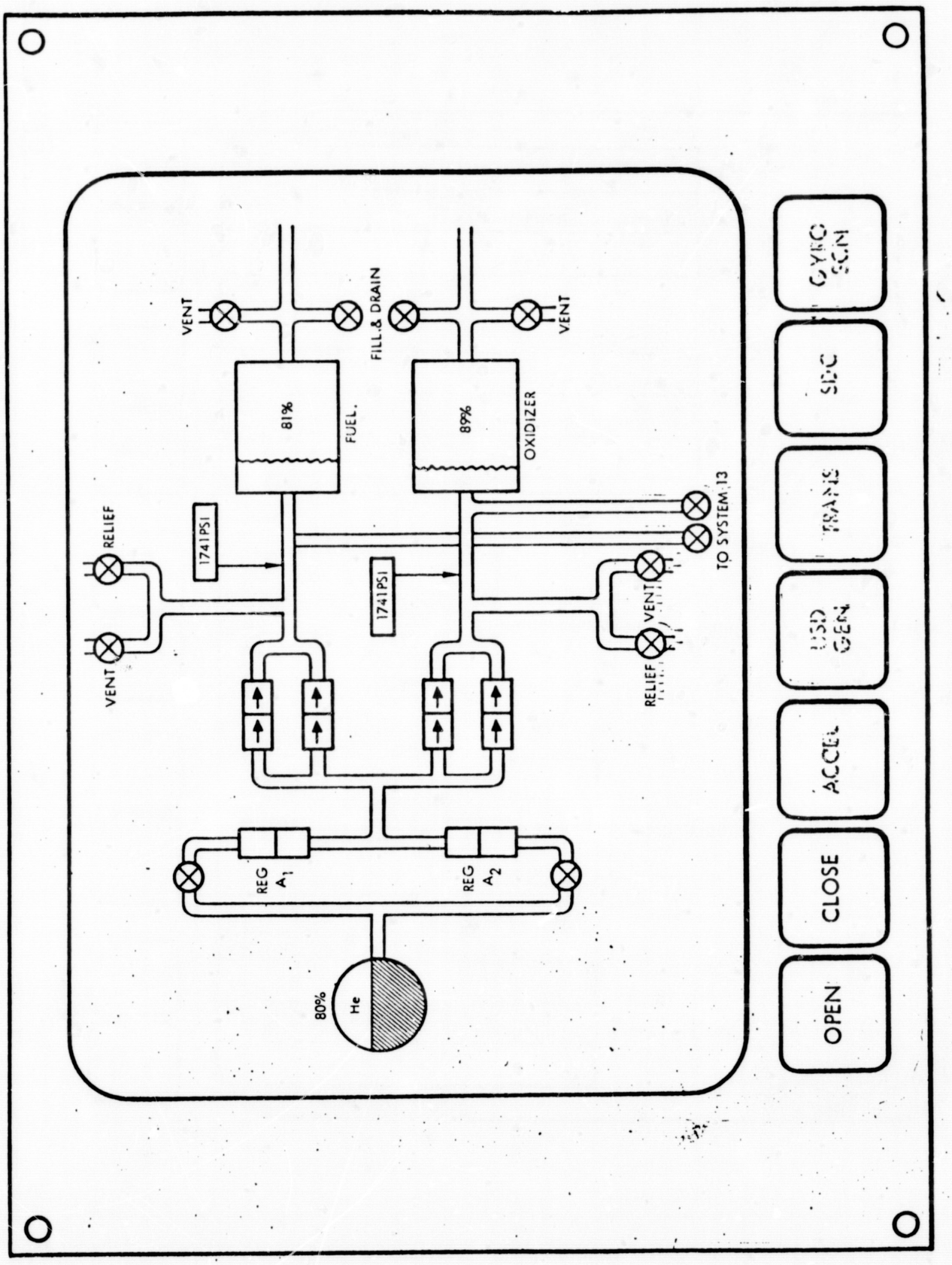

Figure 8.11-20. Schematic System Flow Diagram (With Variables)

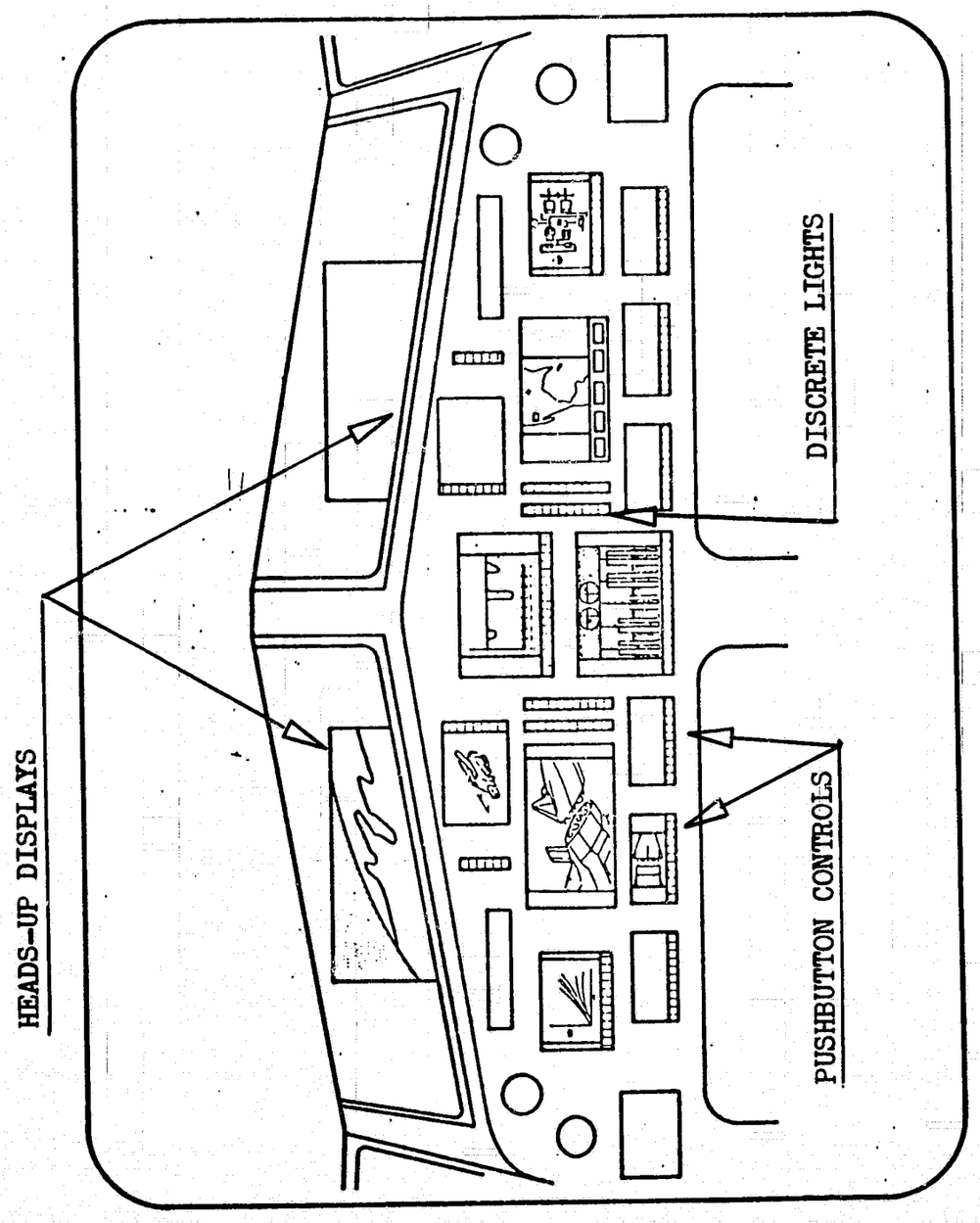

Figure 8.11-21. Crew Compartment Display Concept

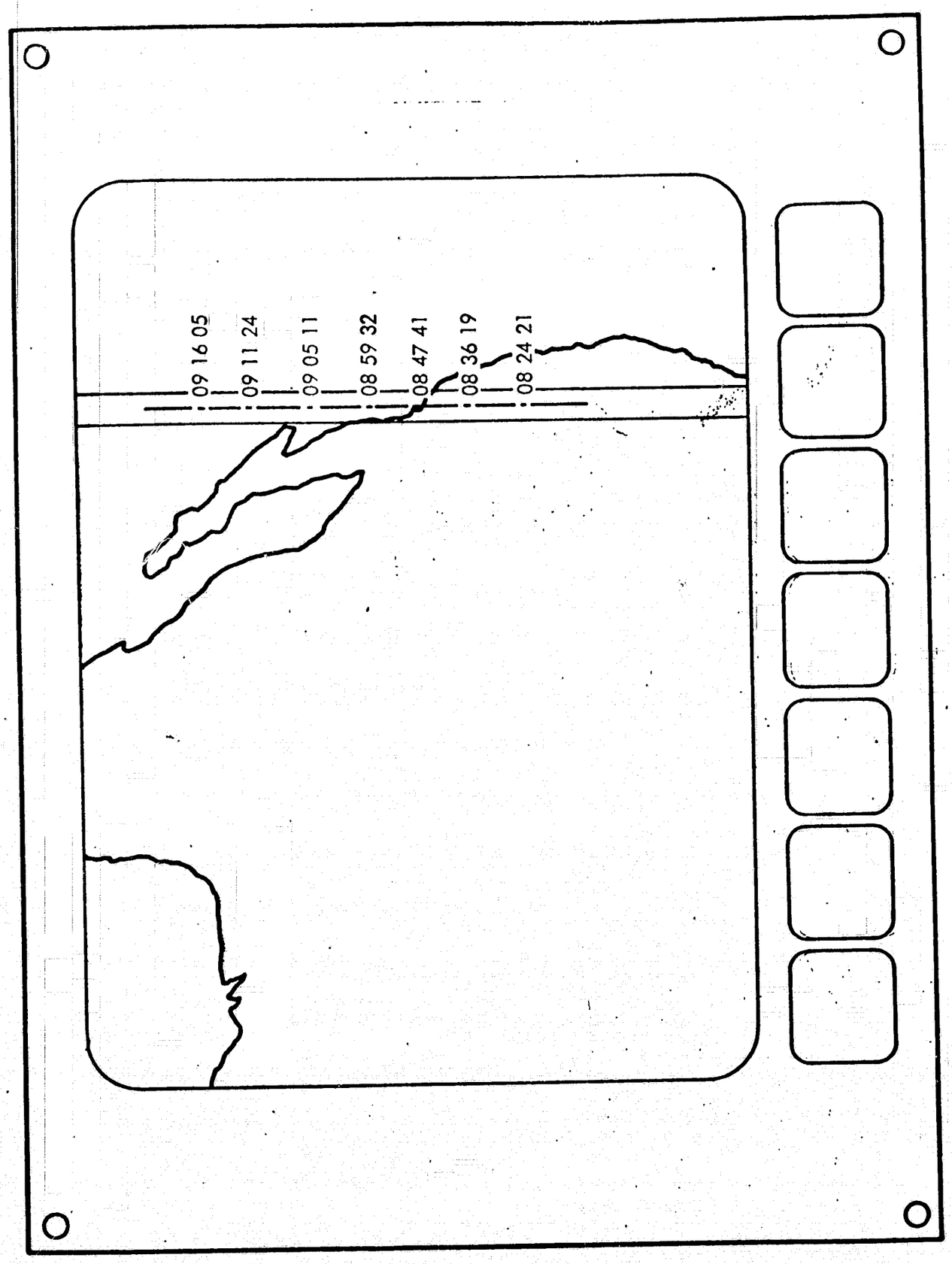

Figure 8.11-22. Time Lines in Orbital Planes

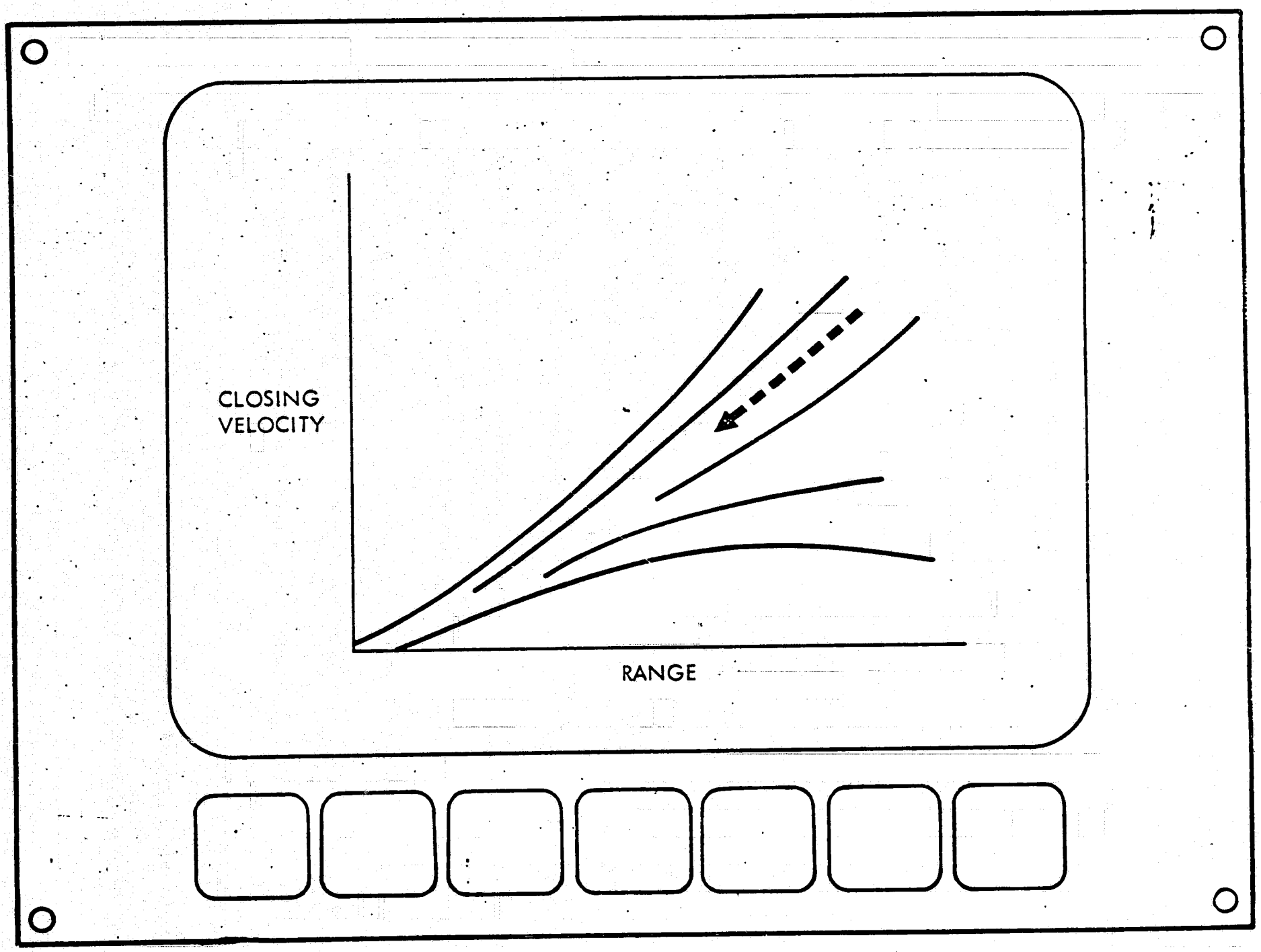

Figure 8.11-23. Docking Display of Range and Velocity

Space Division
North American Rockwell

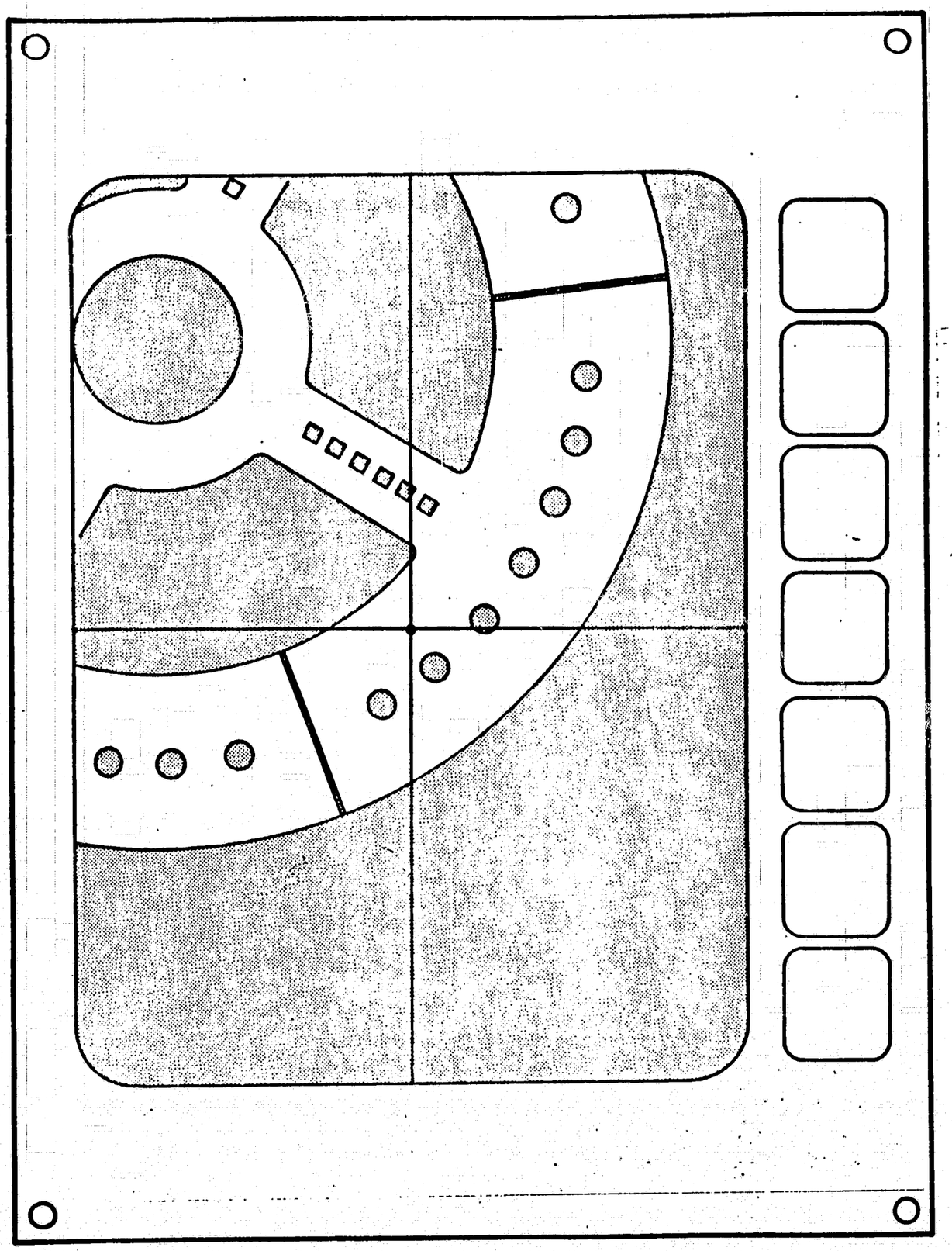

Figure 8.11-24. Docking Display of Azimuth, Elevation, and Roll

The philosophy behind the proposed scheme of display can be summarized as trading the space and hardware of the various indicating instruments for the space occupied by some form of storage device. The CRT's can be located in almost any corner and the instrument panel which the pilots have to face during critical period of flight can thus be tailored to the best advantage of the personnel who use it.

Display and Manual Control Buffering

Figure 8.11-25 illustrates the integration of the crew into the vehicle control and operation function. All data concerning the spacecraft status are obtained through a sensor. The sensor signal is converted to a digital form by an interface. Similarly, every physical action involved in the control and functioning of the spacecraft is achieved through an actuator, a device which actuates according to a digital message placed in its interface.

To achieve any desired degree of automation, each of the several processors in the central computer can address the sensor and actuator interfaces and obtain full information on the vehicle's condition, and thus control its activities. The integration of the crew into the vehicle control loop is made in a fully redundant manner. Hence, anything a processor can do, the man can do and vice versa. In the automatic modes, the crew will observe the displays and confirm that the operation is as desired. In most manual modes, the processors will modify the manual control instructions (adding such things as smoothing, cross coupling, etc.) and will embellish the displays with more thoroughly digested and filtered information. In the fully manual-backup-only mode, the processor will be completely out of the loop. Raw sensor data will appear on the displays and direct control will be exercised over vehicle functions.

For both the crew and the processors to independently access sensors and actuators, the interfaces are treated as addressable memory locations. Hence, a program in a processor or I/O buffer will incorporate the sensor (or actuator) to identity in the address portion of an instruction. This is similar to a memory or address decoder needed to convert this address to a sensor (or actuator) selection. To obtain a high confidence of sensor and actuator access, redundancy in the address decoders is used so that a processor or I/O buffer can address a sensor through one of several routes.

This basic philosophy of treating sensors and actuators as addressable memory locations where data may be obtained or placed is a cornerstone of the redundant design. If one considers that the output data generation of a sensor (such as a code wheel) or the input command storage of an actuator is actually an intrinsic part of that sensor or actuator, then the failure of the

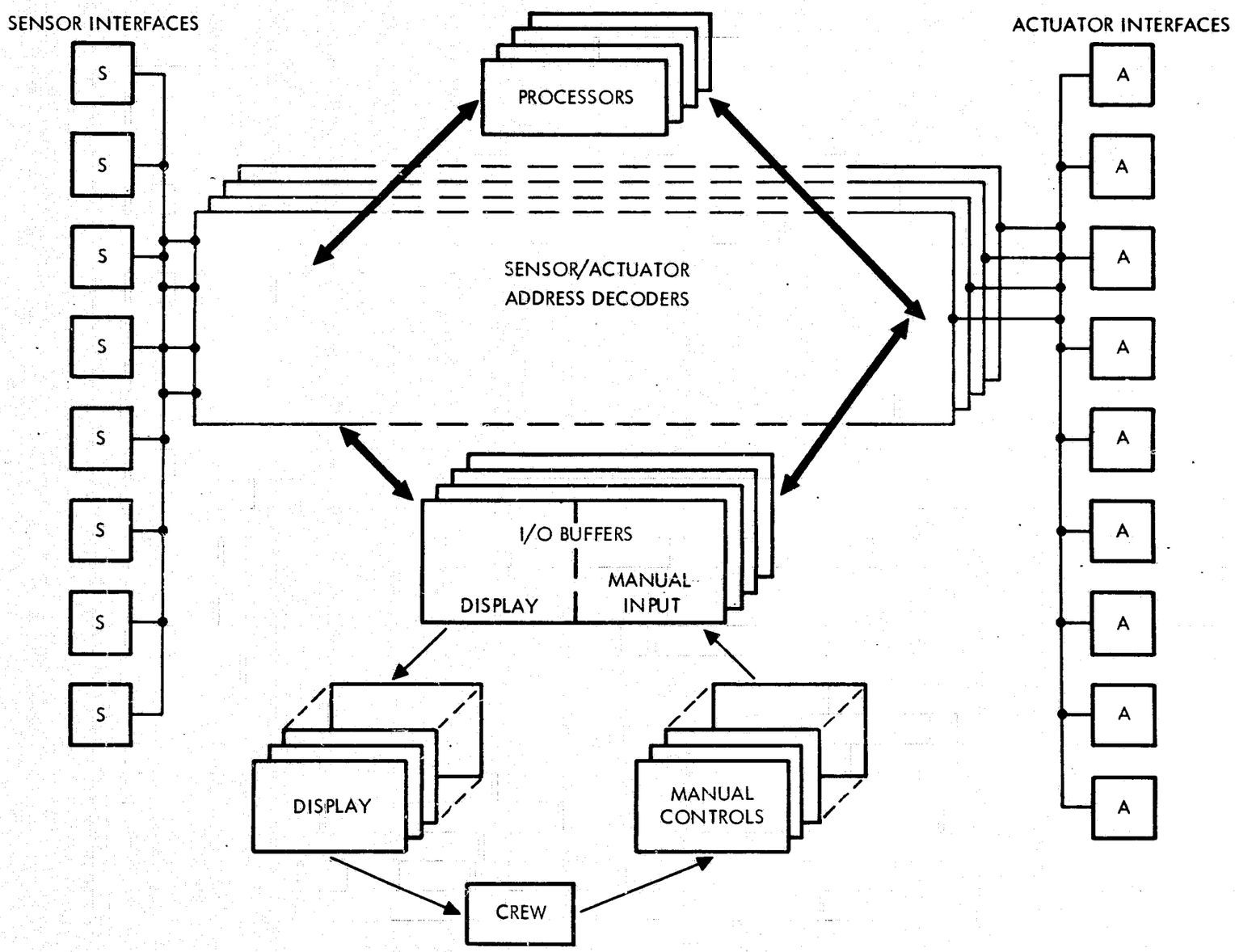

Figure 8.11-25. Integration of Crew Into Vehicle Control

data generation or acceptance mechanism is in effect the failure of the sensor or actuator. Hence, the sensing and control functions must obtain their requisite reliability through redundancy in not only the sensors and actuators but also their interfaces.

Sensor outputs and actuator inputs are addressable by any of the processors just as if they were ordinary memory locations. Any and all processors can address them subject to restrictions included in the computer program. The I/O buffers can similarly address the sensor and actuator interfaces. The crewman thus has independent access to the sensor data and control of the actuators and can, to the extent of his physical abilities, duplicate the functions of a processor in controlling the spacecraft.

Sensor Data Interfaces. The latest data output from any particular sensor is treated as if it were available at a certain digital memory location. In many cases, a small special-purpose interface may be necessary to ensure that the sensor output is in fact available in binary form. In the majority of cases, however, a sensor output will be directly available to an addressing memory I/O cycle. For example, on startrackers and inertial platforms, angular outputs will be available from code wheels (digital shaft encoders). The outputs from these code wheels can be interfaced to data busses as if they were in a core memory block. The I/O buffer or processor simply addresses a sensor, the address decoder selects it, and the output (an angle, for instance) is received on the data buss.

Besides shaft angles, many other sensor outputs lend themselves to digital representation. For example, the accelerometer outputs from an inertial platform are currents which are normally bucked out by corresponding equal and opposite currents. The object is to prevent the pendulous sensing element from moving and to actually measure the current required to prevent its motion. One can anticipate that the next generation of accelerometer circuitry will produce these bucking voltages through an D to A converter. The bucking voltage will be available in a statis flip-flop register, the content of which can be obtained as if it were a memory location.

A few special sensors have their outputs available only at particular times. An example is the radar. The instantaneous range of the radar is the number in this digital counter, and it can be accessed any time an I/O buffer wishes the information. The range of a particular target, however, is available only when the echo from that target is received. There are two ways in which real-time information can be transferred digitally to the display. One is in the mode in which a display cathode ray tube presents live video information. There are a number of modes in which the cathode

ray tubes can present live video from the radar TV camera, infrared scanners, laser, and other video devices. Navigation and communication signals can also be displayed in their raw form. In these video modes, the digital outputs of the sensor parameter, such as the radar range from the range counter, or the pointing angles from code wheels, are switched directly to the D to A converters.

A more common and automatic mode of handling data from video sensors is tracking. In tracking, the video output is examined by certain threshold circuits. When the video signal exceeds this threshold, the digital contents of the range register (or code wheels for IR or television) are transferred to static flip-flop registers which hold the data until the buffer or processor can service the interrupt. Where precision is required, a beam splitting operation in which the recorded range or angle data is adjusted to find the point of peak video or the center of gravity of the video spike takes place in special hybrid circuits. The conclusion of this operation will result in a computer interrupt. During automatic operation, many objects in the same video can be tracked simultaneously, provided the processor picks up the information from the static register with sufficient speed. The computer can then do a number of useful things like smoothing and extrapolating the motion of tracked objects.

In a manual mode, the requirement for threshold circuits and beam splitting is obviated by the human's ability to perceive target images in display. To take advantage of this skill, some sort of cursor or slew spot with which a crewman can convert the visually observed information to digital range or angle information is needed. Since a cursor is controlled by the crew, it is an actuator output.

Sensor/Actuator Address Decoding. In order to be able to suffer two critical failures and still operate safely, it is necessary to have triple redundancy in accessing the critical sensors and actuators. If an I/O buffer for display or control purposes or a processor, wishes to address a sensor, it will, by transmitting an address, identify which of the sensors from which data are required. It is necessary to implement a function within the computer system which generates a select signal on a wire leading to the particular sensor addressed. The sensor/actuator address decoder will itself be selected by the processor or I/O buffer by the more significant bits in the memory location address in its program. The least significant bits will specify which sensor or actuator it is desired to select. There are three sensor/actuator address decoders, so that there can be two failures and the system will still operate satisfactorily. Part of the design also takes account of the fact that if a sensor or actuator should fail, it has no failure mode in which it can also cause the failure of an address decoder.

Figure 8.11-26 illustrates a sensor/actuator address decoder interface showing how the address decoder picks up data from a sensor. The selected address decoder (and a processor or I/O buffer can select any one of the three which is operative at random) decodes the least significant bits of the memory address to decide which sensor interface is to be selected. Since a given sensor can be selected by any one of the three address decoders, the select input is through an OR gate, the output of which becomes the strobe telling the sensor to transmit the data. It does this in parallel by placing signals on its data lines, there being one data line for each bit of resolution in the sensor parameter transmitted. When the data has stabilized, a "data present" line is raised indicating the data is present on the lines and can be sensed.

The address decoder must be able to receive "data" and "data present" signals from each sensor to ensure that the data sensed is only from the sensor selected. It uses the "select" line to open AND gates through which the sensor data word must pass before it is sensed. The sensing actually is done by the I/O buffer or processor in the same way that they noremally sense the contents of a word selected from memory. When a processor or buffer addresses a sensor/actuator address decider, it connects its data receiving lines to that decoder so that in effect, with the decoder's help, it is connected directly to the sensor interface.

Display Buffer Operation

An I/O buffer essentially is a display buffer in its output mode and a manual control buffer in its input mode. Its operation is essentially to transfer data out of storage or into storage. These buffers have a modest arithmetic capability. In display, the buffer operates as follows: it essentially has control of the beam of a cathode ray tube; it has the opportunity to address more than one cathode ray tube, and, in general, can address any cathode ray tube in the vehicle. When the display buffer transmits a word to a display, the effect on the addressed cathode ray tube depends upon the mode of operation of that display unit. There are six basic modes of operation. These are:

1. Dots
2. Independent vectors
3. Head to toe vectors
4. Random characters

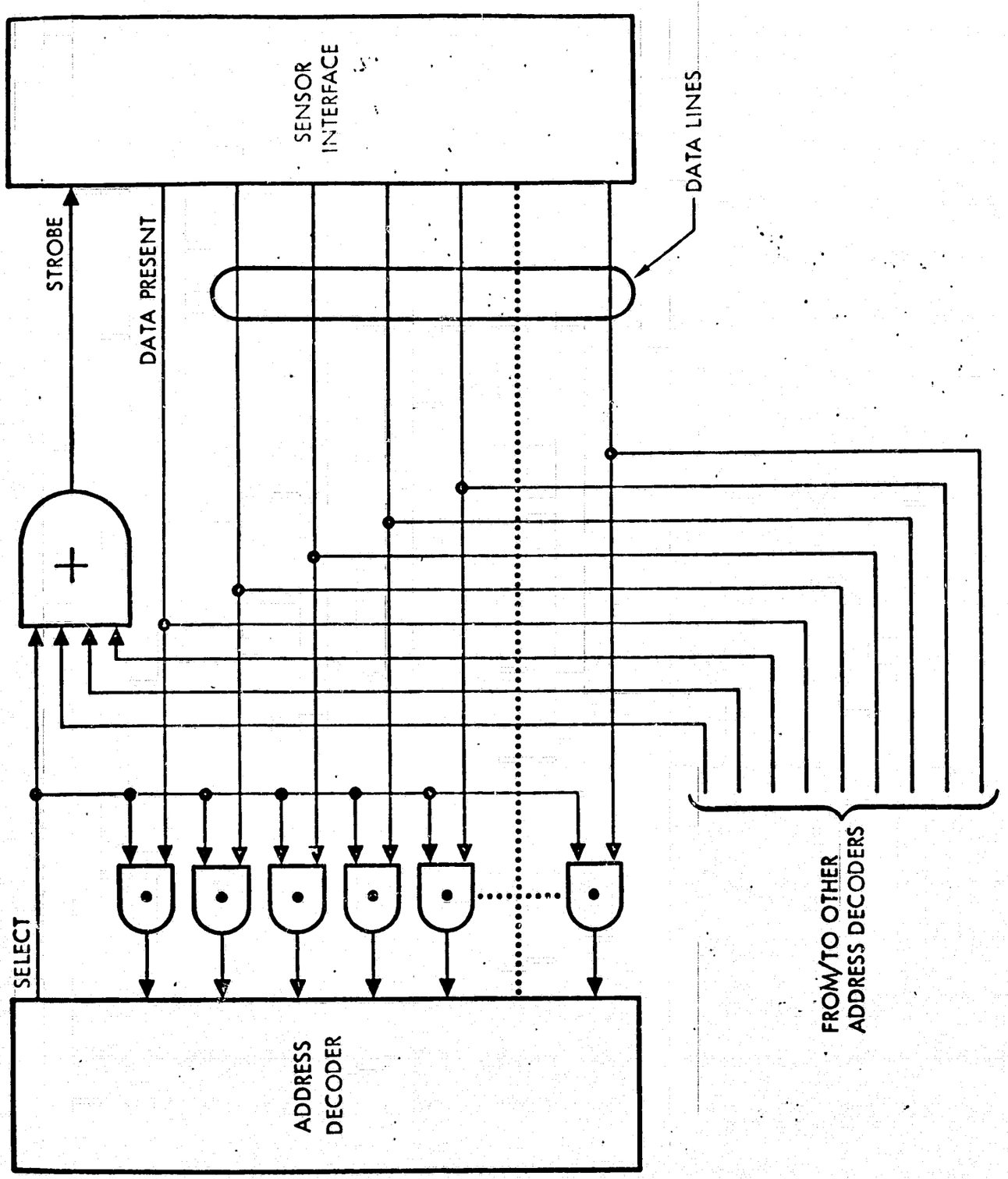

Figure 8.11-26. Sensor and Actuator Address Decoder Interface

5. Textural characters

6. Tabular characters

The I/O buffer output word is divided into several cells, one of which is used to change modes, another is used to designate intensity, and a third is used in the character mode to indicate the size of the character. Two large cells indicate X and Y coordinates on the cathode-ray tube surface. In the Dot mode, the cathode-ray tube beam is aimed at a certain direction on the screen and a dot of the specified intensity is painted. Given a sufficient number of dots spaced sufficiently close, any picture or character can be drawn on the cathode-ray screen. It is, however, basically inefficient to do too much with just dots. Instead, vectors or line segments are drawn on a cathode ray tube to make diagrams and pictures. There are two vector modes: the independent vector mode requires two computer words per segment, the first one designating the origin of the vector or line segment and the second one designating the terminus of the segment. Most pictures of interest, however, consist of connected vectors in which case the head to toe vector mode is used. Here it is understood that the origin of each vector is the terminus of the previous one. When the computer wishes to stop drawing a continuous line segment, it must exist from the head to toe vector mode. Needless to say, the first character upon entry into the head to toe mode is the origin of the first line segment.

There are three character modes; the simplest is one in which the location of a character is contained in the coordinate cells of the computer word and the character is designated by six other bits in the computer word. It is useful to also have a textual mode in which characters are written down as they would be with a typewriter. Normally, each character is, of course, one character space to the right of the preceding one; however, spacings, carriage returns, and line feeds are used as special kinds of characters to appropriately modify the origin of each succeeding character. Using the textual mode, one can pack four characters into a single computer word. A third character mode is tabular. In the tabular mode, each successive 6-bit cell of a computer word represents a new character which is written to the right of the preceding character; however, a special character meaning "tab," causes the writing position to move to the right a larger distance. This spacing is indicated by the next character giving 1 of 64 possible spacings. Carriage return and line feed characters are also used in the tabular mode. The tabular mode is most useful for presenting tables.

With the above capabilities, it is clear that almost any type of format or picture can be drawn on the face of the cathode-ray tube. Data from the computer can be presented in a great many ways. The computer has control

over the intensity, the size of characters, and, if desired, can make certain portions of the picture or certain words blink, thereby drawing the crew's attention to them.

An important function of I/O buffers is the activation of indicators. Indicators are lamps telling the crew about the condition of various discrete functions and, in many cases, giving warning of important events, such as malfunctions. The display buffer selects an indicator the same way it selects a part of a cathode ray tube. It essentially treats each latch which drives a lamp as a separate coordinate on a cathode-ray tube screen.

The discrete parameters which are indicated by lights are formed into a sensor word, there being one discrete for each bit in a data word. The I/O buffer's program, therefore, specifies the display of a particular set of discrete data on a particular set of indicators. Several sensor data words will be necessary to drive all of the indications. The buffer thus goes out through a sensor/actuator address decoder and picks up the discretes as if they were single sensor data words and displays them on indicators by setting the appropriate latches. Because these indicator display words are part of the 1000-word cycle, the latches are reset 60 times per second.

Manual Control Buffer

The manual control buffer function of an I/O buffer is used to link crew controls to actuators or to enter crew-inserted information into the computer. It works in just the reverse of the display buffer and it is part of the 1024-word cycle of an I/O buffer. An assigned I/O buffer has as part of its routine a control pickup sequence or program. Under this program, it picks up the states of pushbuttons or control at levers and transfers them to appropriate places in computer memory or to actuators. A simple example might serve to explain the operation. The control buffer, cycling at 60 times per second, senses the state of a pushbutton which is programmed to control the state of a valve. The fact that this pushbutton is now in control of that particular valve is indicated by illuminating the pushbutton. The pilot desiring to close the valve depresses the pushbutton. The manual control buffer senses that this pushbutton is activated the next time it cycles through.

In the case of continuous controls (rotation control), the position of the control stick would be sensed by the manual control buffer. It would transfer, on each of its cycles, that position to the input of an actuator. If the control stick has not moved, the actuator input would simply receive the same position that it had received before. Unlike the display buffer, the manual control buffering function does not perform any arithmetic

operations. The control stick activates only the ailerons or reaction controls and the scaling and/or biasing is appropriately accomplished by the way in which the code wheel, position, or angle sensing function is implemented on the stick and by the significance of the bits transferred to the actuator. This built-in scaling and biasing obviates the necessity of using computer arithmetic.

When the astronaut has control of the spacecraft, he may directly effect the actuators; however, during normal conditions, he may wish to have the assistance of an automatic pilot. Certainly, during atmospheric flights, he will want such conveniences as yaw damping or stabilizing functions. Since the destination of the control functions inputs are under software control, the usual case is for it to be placed into computer memory rather than into actuator output. The processors then operate on the data and calculate modified actuator commands data to be transferred to the actuator interfaces.

A particular type of manual output of considerable interest has to do with coordination through the display. For this purpose, two devices are available. One is a light pen which a pilot or copilot can point to an item displayed and designate to the computer that he is referring to it. For example, in the video display mode discussed above, the pilot may wish the computer to lock-on and track a particular target which he sees in the video. He can simply point the light pen at this target. An alternative to the light pen is a cursor which tends to be a more precise designator of position. Movement of the cursor can be accomplished through the rotation control stick, and it can be endowed with rate or proportional controls by including the computer in the loop. Its sensitivity can also be expanded to give it a great deal of precision. Thus, the pilot may wish to measure the range to a particular object seen in his radar display. He could position the cursor over that target and that cursor's position would then be proportional to range. He can then, by pushing on enter button, transfer the cursor coordinates to computer storage.

The cursor X-Y coordinates are two words in the display buffer program. When the cursor is not desired, these words have zero intensity. However, when the cursor is selected, it will appear on a particular cathode-ray tube. The cursor coordinates are modified by transferring the control stick (rotation control stick) position either directly or as modified by the computer program to the coordinates in the cursor words.

In emergency situations, the crew can transfer cursor coordinates directly to an actuator. One could thus directly point the laser ranger or a startracker in a certain direction.

Actuator Outputs

An actuator output is essentially the setting of a flip-flop register to a particular state. The actuator then tries to match the commanded state by positioning whatever it is that it controls. Continuously variable controlled devices (such as control surfaces) will be positioned under feedback control in which the device's position is compared with the analog meaning of the digital input word. Many actuator outputs are, however, discretes. There is a flip-flop which will control a solenoid or otherwise operates a discrete action.

A third category of actuator outputs involves timed or compared control functions. Specifically, the firing of engines must be very carefully controlled. The computer will come up with a burn time for a reaction control motor that will impart just the right amount of rotation or translation required to accomplish a desired maneuver. The actuator output will be a digital word which will be stored in a flip-flop register; however, the flip-flop register will count down to zero. The motor will be on while it is counting down and will go off as soon as it reaches zero. Hence, just the right amount of thrust will occur. Main engine thrusting would be based upon the velocity increment achieved and hence there would be a comparison between a commanded velocity increment and the achieved increment observed by integrating an accelerometer output.

Some actuators must necessarily be coupled. For example, flaps and spoilers, in which case, there is only one output but two elements are actuated. Any assymetry in the followup response is cause for the generation of an alarm and deactivation of the spoiler or flap deployment.

8.11.4 Record and Playback

The recording and playback system will provide the capability to record data and voice similar to that of the present-day aircraft crash recorder. Examples of data which would be recorded are results of preflight checkout, computer self-check, and subsystem performance monitoring. This data is logged for later ground processing and evaluation. If immediate information is required on the ground, the recorded data may be transmitted to the ground by the telemetry link. Such an operation may be conducted to shorten the maintenance and refurbishment time.

Because of the recording system's intimate interface with the computer, the basic functions of the computer in data processing are re-stated as follows:

1. Control of signal acquisition sequence and timing.

2. All data processing for scaling, filtering, and combining signal values.

3. Testing of measured signal values against stored limits.

4. Initiation of trend recording.

5. Printout and recording of failure advisory when failure monitoring.

6. Maintenance of current status information: clock (GNT) time, operating time, fuel remaining, oxygen remaining, magnetic tape remaining, etc.

7. Printout of status information on request.

8. Formatting of data for printout and recording, including formulation of maintenance advisories on the printer.

9. Control of the printer and recorders pertaining to live steps on the printer, character steps, rewind, transfer, playback (on recorders), and proper record termination.

10. Continuous self-test of the monitor and recording system.

Tape Recorder and Playback Unit

Two tape recorder and playback units will be used onboard the orbiter vehicle. Each will be an incremental tape recorder, which will provide tapes from either asynchronous or continuous data sources and will have the ability to re-play these tapes to the computer upon request. To be computer-compatible, tapes must be generated with data evenly spaced at fixed packing densities. The tape will be contained in cassettes which can be easily removed and reloaded in flight without requiring the use of any tools.

The recorders will be completely under the control of the computer program, which provides the following features:

1. Recording of all required checkout and performance data.

2. Recording of all time/history and trending data.

3. Recording of all malfunction data.

4. Automatic transfer of recording responsibility to the alternate recorder when either end of tape is noted or playback is requested.

If playback is requested, for either a summation of flight or transmission to ground, the alternate recorder is energized and the first recorder rewinds. These actions and actual playback to the computer will be under programmed control.

After the tape has been rewound, an automatic interlock is set to prevent the loss of data by recording over the data.

BITE will assure equipment readiness and performance. Significant parameters such as read or write error, end of tape, over temperature, and tape movement error will be monitored and presented at the BITE output.

Printout Unit

The printout unit for the recording system will provide a hard copy record for inflight reference, as well as for ground maintenance and preflight purposes.

The printout unit will be operated completely under the control of the computer and prints out character by character as programmed.

Voice Recording Unit

Voice recording will be accomplished on a separate recorder. Timing signals will be recorded at the same time to provide correlation with other data records.

8.11.5 Communication

The communication portion of the IES will differ in concept between the orbiter and the booster. If the booster is unmanned, the criticality of this system is increased, hence, the reliability factor increases. The booster will not require the equipment needed for target acquisition, tracking, automatic approach, and docking. Therefore, the orbiter communication system will be covered as it contains all the elements of the booster communication system.

The ILRV communication requirements are depicted in Figure 8.11-27. To meet these requirements, the communication concept depicted in Figure 8.11-28 was conceived. This flow diagram shows the major elements of the communication network and indicates the system's internal and external interfaces.

Several alternative approaches should be considered in implementing the concept depicted in Figure 8.11-28 and tradeoffs performed considering performance, weight, volume, reliability, cost, availability, and cost. The alternative approaches are:

Voice, Data and Command RF Link

Unified S-band equipment (USBE)

VHF

X-band

Combination of the above for redundancy

Tracking, Ranging and Docking Communication Link

USBE

Multi-mode radar

VHF/AM

Laser

TV

IR and optical trackers

Combinations of the above for redundancy

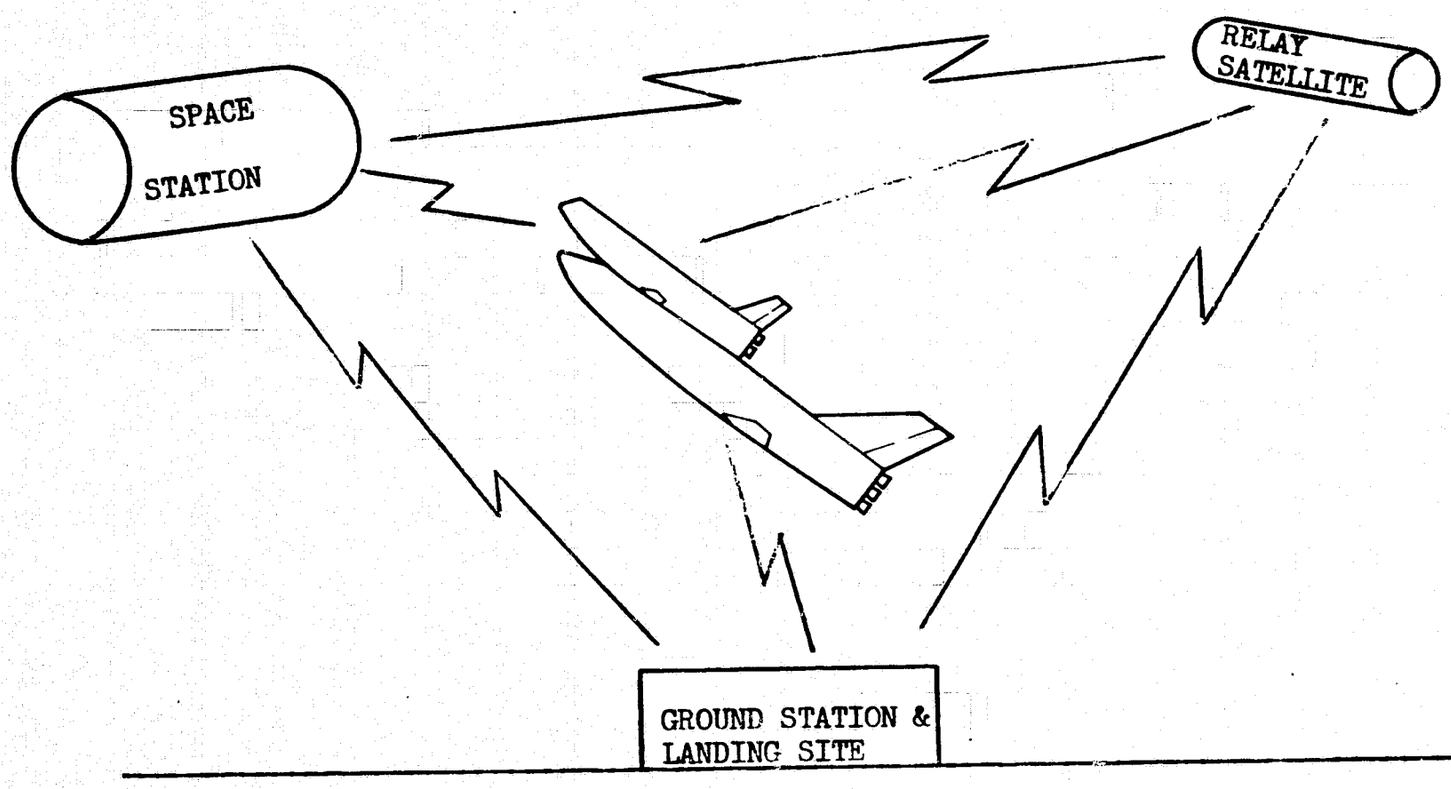

VOICE, DATA & COMMAND

RECEIVE & TRANSMIT VOICE
RECEIVE UP-DATA COMMANDS
TRANSMIT RECORDED VOICE AND DATA
TRANSMIT REAL TIME T.V. & DATA
VOICE INTERCOM - CREW, PASSENGERS, PAD & SPACE STATION

TRACKING & DOCKING

TRACKING FROM LAUNCH SITE
COOPERATIVE TARGET TRACKING
PASSIVE TARGET TRACKING
TERMINAL TRACKING

APPROACH & LANDING

DISTANCE MEASURING EQUIP
LATERAL & VERTICAL GUIDANCE
OMNI DIRECTIONAL RANGE
MARKER BEACON
WEATHER PENETRATION

Figure 8.11-27. Communication Requirements

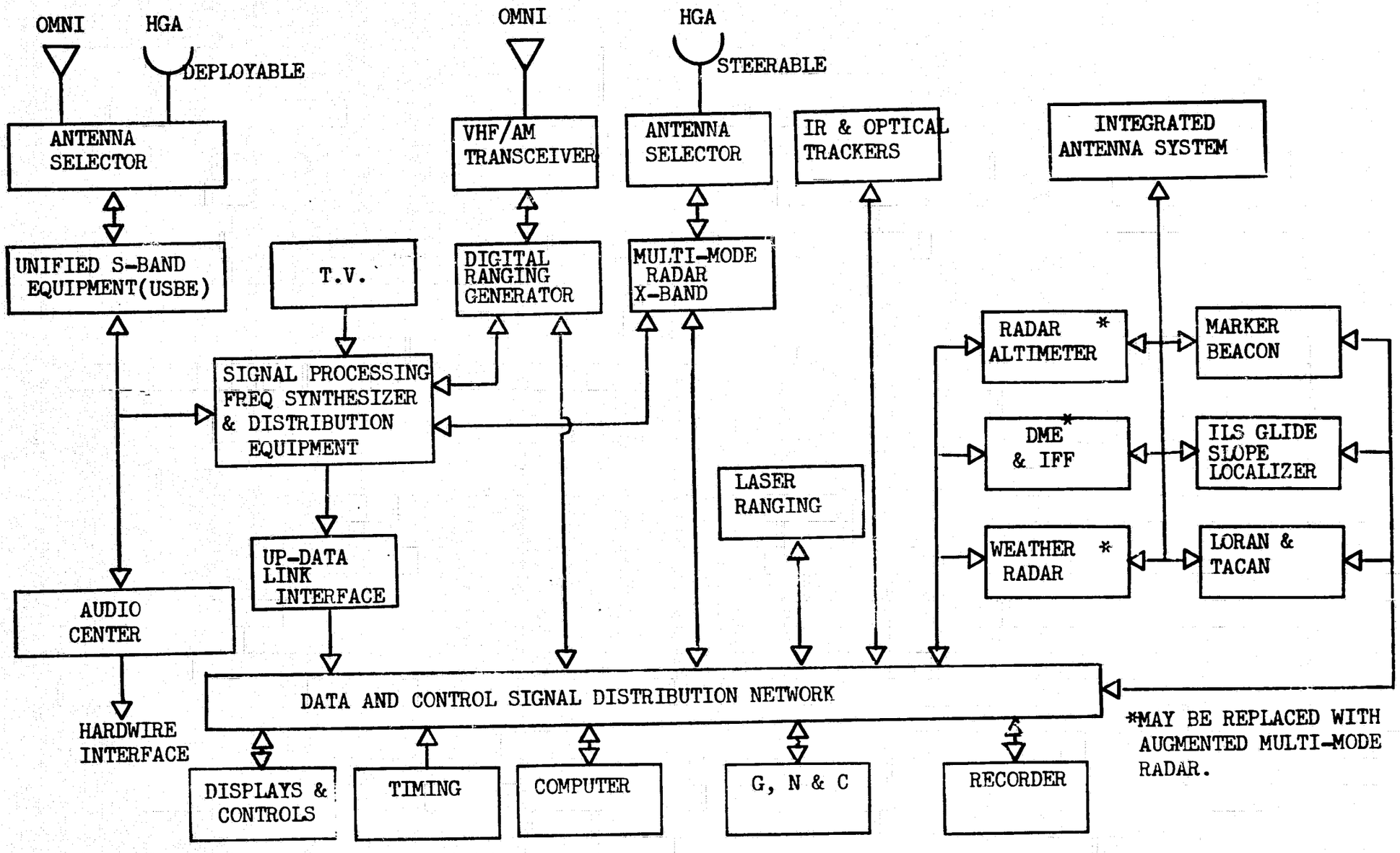

Figure 8.11-28. Communications System Concept

Approach and Landing

Instrument landing system (ILS)

Weather radar

Distance measuring equipment (DME)

Augmented multi-mode radar

Loran and Tacan

Combinations of the above for redundancy

The environment of the vehicle in respect to surface temperature encountered versus placement of antennas is very close to the upper limit on the vehicle's upper surface, and exceeds the upper limit on the lower surfaces and the leading edges. A tradeoff should be performed in this area considering the development of high-temperature exposed antennas versus deployable ones.

8.11.6 Onboard Performance Monitoring and Checkout

The IES concept for operational subsystem performance monitoring, verification, and display is extended to include the function of onboard checkout. This is a natural and logical integration as the measurement systems required for performance monitoring are identical, in the majority of cases, to those required for the checkout function.

Onboard performance monitoring and checkout is one of the major functions which will promote onboard autonomy; minimize ground base checkout, facilities, and equipment; and simplify launch and refurbishment operations.

The major functions performed by the IES are defined as follows:

Preflight Checkout. This is defined as the programmed-automatic checkout operation performed in sufficient depth to determine that all subsystem (flight and flight-associated subsystems) are operational or flight-ready. Preflight in the mission profile is the time before any maneuver or concurrent series of maneuvers such as prelaunch or pre-entry.

Inflight Checkout. This is defined as any checkout performed on a subsystem, during flight, to verify its operational readiness before being put into active service.

Postflight Checkout. This is defined as checkout operations which integrate the IES checkout system with ground checkout operations to perform the required vehicle maintenance and refurbishment. Postflight checkout would be similar to the preflight checkout operation if all subsystems were "go". If any subsystem is "no-go" or trend data indicates that an incipient failure may occur, indepth onboard testing will be initiated to isolate the malfunction to a predetermined line replaceable unit (LRU).

Inflight Performance Monitoring and Display

The IES will perform the following functions in the execution of inflight performance monitoring and display during the active use of any vehicle subsystem.

1. Automatically make the required measurements at rates necessary to compare subsystem's actual performance to predetermine acceptable limits of operation.

2. Automatically provide actual and predicted values of data to the crew via the display system.

3. Automatically activate subsystem performance monitoring with subsystem activation.

4. Automatically provide vehicle configuration operational status and data required for automatic or manual corrective action.

5. Automatically perform the Caution and Warning function. Parameters identified as critical are flagged as an actual or potential subsystem failure by the checkout program and displayed to the crew as a critical function requiring crew alert or action.

6. Automatically perform data reduction, data compression, and data storage required for historical data, incipient failure detection, and fault isolation.

Onboard Performance Monitoring and Checkout Concept

The major concept to be implemented in the onboard performance monitoring and checkout system is decentralization of the decision-making function and centralization of the data and control management function.

Figure 8.11-29 shows the basic elements of the IES used in implementing performance monitoring and checkout functions. The figure illustrates use of common equipment, standardization of interfaces with all subsystems, indtroduction of built-in-test-equipment (BITE) and stimuli for checkout and monitoring, and the two-way data and control signal distribution network.

Decentralization of the decision-making function is delegated to the subsystem, at the lowest level, whenever it is possible and practical. It is implemented by maximizing the use of self-test BITE in the design of subsystem hardware. The monitoring of the subsystem's health is accomplished completely within the subsystem. The dissemination of data from the subsystem occurs when it is interrogated by the central control system (computer) or whenever a subsystem function goes out-of-tolerance, BITE interrogated the central control system through the computer interrupt input. The performance monitoring operational sequence (with BITE) is shown in Figure 8.11-30. One of the major benefits of this concept is the reduction realized in software programming which would be required if this function was centralized.

Centralization of the data and control management function provides capability of interrogating and obtaining all data which are available in and from the subsystem. This permits checkout operations of control, stimuli, and data retrieval to be conducted from a central control location. The checkout operational sequence is depicted in Figure 8.11-31.

8.11.7 Data and Control Signal Distribution Network (Multiplexing)

The data and control signal distribution network (multiplexing) provides an effective-common signal processing and distribution network for all subsystems. It provides the necessary two-way data and control communication link between subsystems and the integrated electronics subsystem, and it is also the internal communication link between major elements of the IES. Multiplexing stations are located throughout the vehicle and provide the digital interface between vehicles and subsystems.

Figure 8.11-32 illustrates a typical multiplexing network with the three basic classifications of input signal being analog, discrete, and digital. The top row in the block diagram depicts the signal processing required to convert all signals into a specific digital format before digital transmission. The second row shows the long line coaxial serial transmission of pulse-code-modulated (PCM) signals throughout the vehicle from multiplexing station to station. The last two rows depict the digital signals being converted back to the required classification (analog, discrete, or digital) for inputing into the using hardware.

Figure 8.11-29. On-Board Performance Monitoring and Checkout System

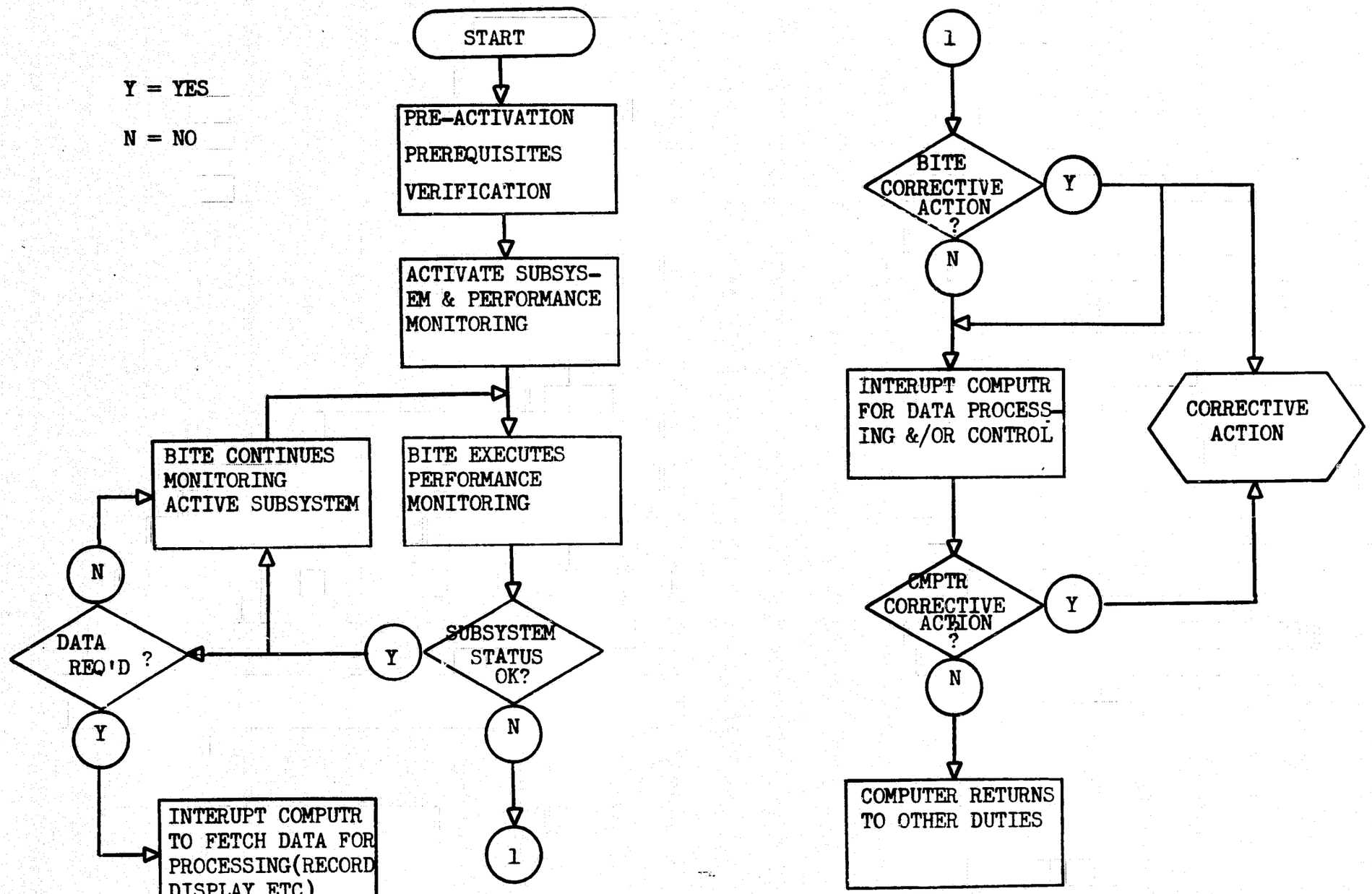

Figure 8.11-30. Systems Flow Diagram of Performance Monitoring Sequence (With BITE)

Space Division
North American Rockwell

Figure 8.11-31. On-Board Checkout Sequence Systems Flow Diagram (Sheet 1 of 2)

Space Division
North American Rockwell

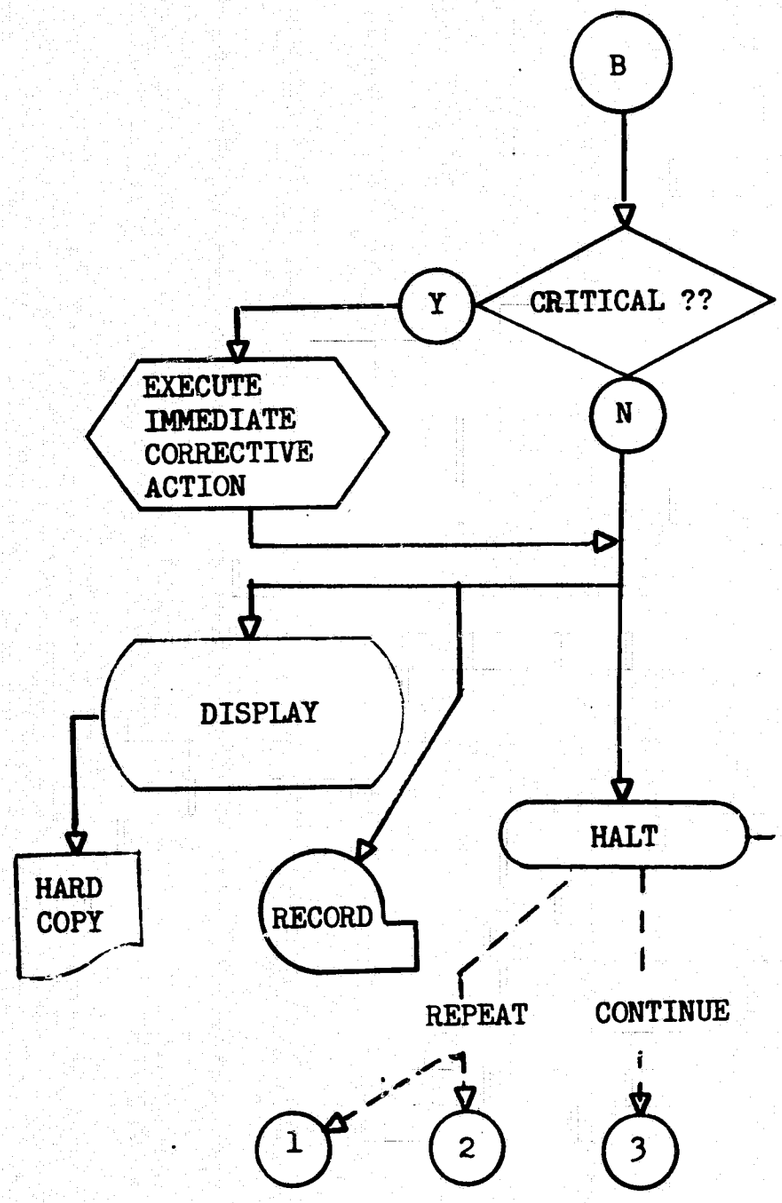

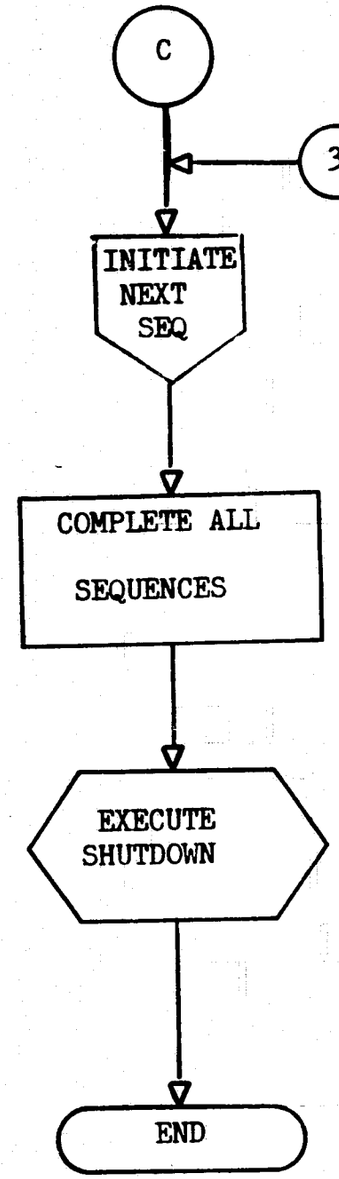

Figure 8.11-31. On-Board Checkout Sequence Systems Flow Diagram (Sheet 2 of 2)

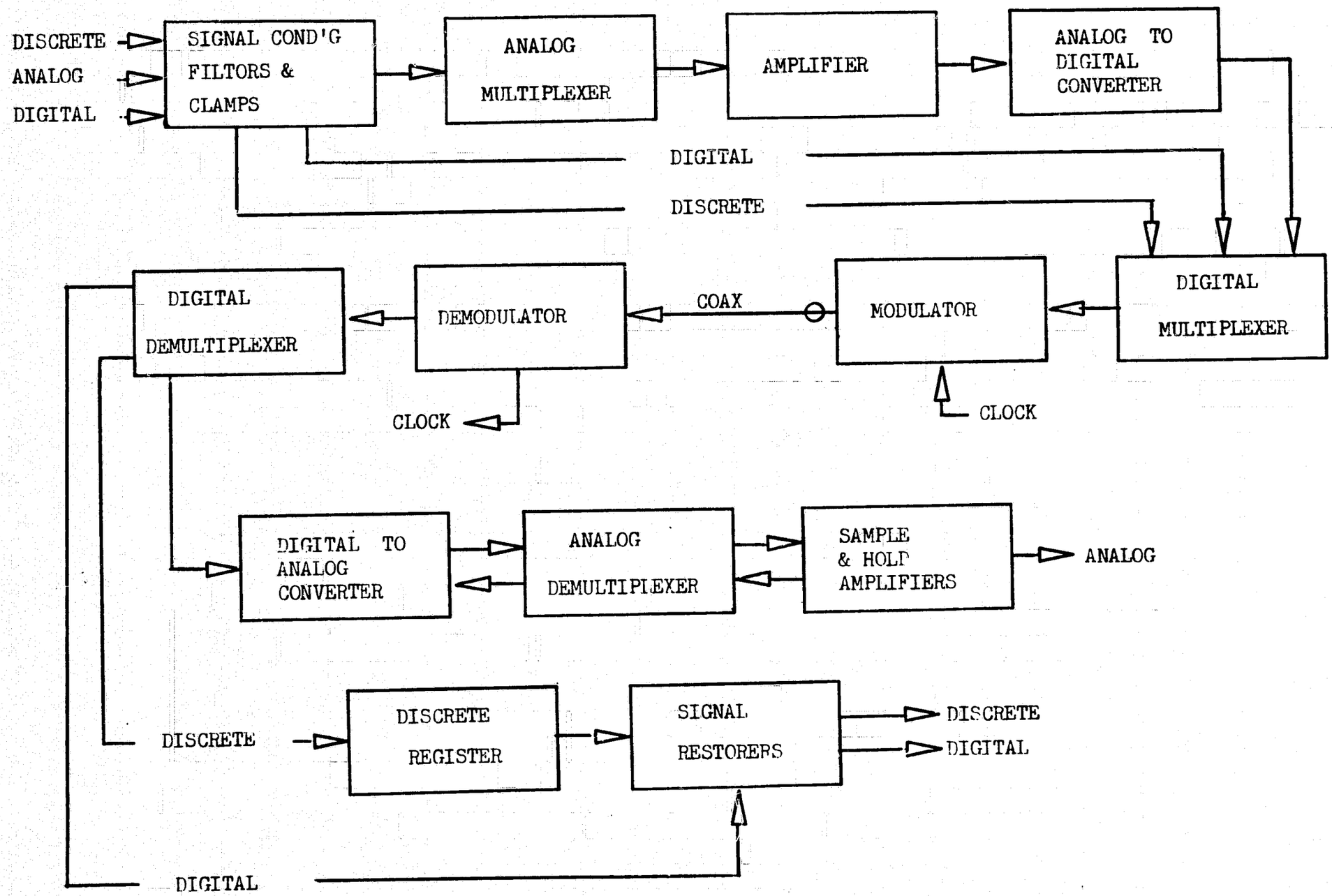

Figure 8.11-32. Typical Multiplexing Network

Space Division
North American Rockwell

The multiplexing concept is not limited to the IES or its interfaces with the subsystems, but it is extended into each subsystem as a design requirement. Figure 8.11-33 illustrates the extension of the multiplexing system concept from the subsystem sensor/transducer input to the IES interface, and the digital input from the IES interface to the using hardware.

Interfaces - Special and Standard

There are many problems associated with interfaces, ranging from the management of functions which cross the interface to the hardware selection, to meet the stringent requirements of the disconnect type of interface.

The standard interfaces would be of the type which join different subsystems, such as the main propulsion engine interface with the multiplexing system. Once connected, it would remain connected until scheduled or non-scheduled maintenance required it to be disconnected.

The special interface would be of the type in which special requirements are imposed upon the system, such as the orbiter and booster interface. This interface must meet the critical reliability requirements of more than 100 error-free, deadfacing/disconnect and re-mating operations.

Special Interface - Orbiter/Booster. This interface is probably the most critical one in the vehicle. All booster commands, control, and data cross this interface during the launch, boost, and separation phases of the mission. It must be deadfaced just before vehicle separation, and must be mechanically and electrically perfect to reliably withstand disconnects and re-mating without degradation in its capability to perform.

To date, no two-wire per function interfacing hardware has been developed which would meet the above requirements. With multiplexing, the problem is reduced by minimizing the number of wires crossing the interface. Further development of different interfacing techniques should be investigated such as the following:

Fibre Optics - multiplexing and modulating a light beam interface. Deadface would be accomplished by extinguishing the light source.

Laser Communication - see Fibre Optics.

RF Communication - space link.

Special Interfaces - Orbiter or Booster to Ground. This interface is similar to the orbiter and booster interface as control and data signals

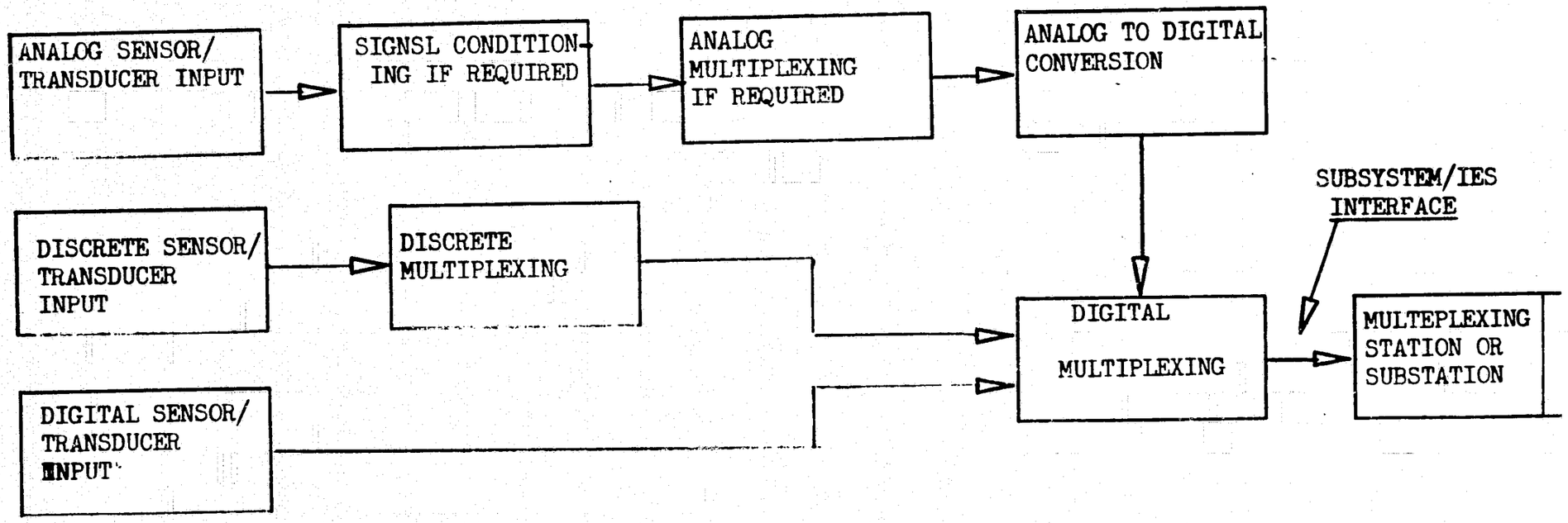

Figure 8.11-33. Subsystem Multiplexing Concept

cross this interface to control launch ground support operations. Examples of these functions would be propellant loading, topping, and disconnect operations, or the vehicle holddown release after lift off thrust is attained.

The interfacing techniques of the Orbiter/Booster would apply, except in the area where hardwire connections must be used for functions, such as power distribution. The hardwire interface in disconnect applications should be limited to noncritical functions.

Special Interface - Cargo. Although no specific requirements for the cargo interface are known at this time, it can be assumed that an IES interface will exist even though the cargo is supposed to be completely self-contained and self-sustaining. This interface, as a minimum, would probably consist of (1) an ac/dc, two-way power interface, (2) a two-way control and display function hardwire interface, and (3) an intercom station.

Standard Interface - Subsystem Digital. In using a multiplexing system, the data and control signal interfaces with the subsystems are digital in the majority of cases. This digital interface will be standardized in digital format when the computer's digital word structure and format are finalized. It will be implemented by design directives detailing the compatibility requirements of signal format and characteristics, as well as standard hardware requirements.

Standard Interfaces - Hardwire Functions. These interfaces are general in nature and cover the entire area of electrical distribution. Within this area there are common electrical functions which can be categorized, and the wiring and electrical connector pin versus function standardized. This would reduce the quantity of different types of connectors, reduce the logistics problem, and decrease maintenance time.

8.11.8 Integrated Electronic System Technology Advancement Requirement

The electronic subsystem technology advancement requirements are summarized below and are also defined in Volume V of this

Non Volatile High Speed Mass Memory

The basic techniques and hardware for a non-volatile mass memory with a fast read/write capability and memory array optimized for mass memories and space applications must be developed.

Computer Reliability Through Redundant Techniques

Reliability improvements for a computer system for advanced space missions is desirable. Redundancy through systems, modules, or circuits will enable the design computer systems to achieve reliability goals exceeding those presently achievable.

Computer Organization, Design and Software

The hardware technology and manufacturing techniques have been developed to an extent that it is known that relatively low cost hardware can be produced. The major effort attendant to the development of a special purpose computer complex is the systems engineering and therefore the hardware and software design and organization.

Crew Station Integration (Displays and Controls)

Highly integrated displays and controls systems are being developed for the F111, F-14, and F-15 high performance aircraft. Large displays are or have been developed for the C-5A and 747 aircraft. Further development of the display system will be necessary for the ILRV and simulators and development mockups will be required.

9.0 CONCLUSIONS

Based on the design and subsystem investigations, the following may be concluded:

1. The two-stage shuttle vehicle configured with a 15-foot-diameter by 60-foot-long cargo bay and a payload delivery capability of 50,000 pounds has a gross weight of approximately 4.5 million pounds.

2. The shuttle system gross weight and payload capability are very sensitive to predicted subsystem weight, rocket engine performance, and on-orbit mission velocity requirement.

   a. Structure/thermal protection system weight is the most significant subsystem weight item; a 10-percent reduction in projected orbiter weights increases the payload by 23 percent.

   b. High rocket engine performance is essential to obtain predicted vehicle weight; a 1-percent decrease in predicted value decreases the payload by 15 percent.

   c. A common rocket engine was used in the study; optimized engines for each stage can increase the payload by 12 percent.

   d. Current transport turbojet engines can be used with modification for the space environment; but (1) use of hydrogen fuel in the booster turbojets can increase payload by 10 percent, and (2) use of a high-thrust-to-weight (15:1) turbojet in the orbiter can increase payload by 20 percent.

   e. The on-orbit velocity increment provided is 2000 feet per second. This value can probably be reduced by 500 feet per second for most missions and provide a 20-percent payload gain.

3. Analyses of the structure and thermal protection system indicate that suspended tanks and external load-carrying structure is desirable in the orbiter to minimize weight. The use of densified quartz as the external thermal protection also minimizes system

weight and provides a safe system. The safety aspect associated with the use of densified quartz is attributable to the capability of the thermal protection to ablate under more severe reentry thermal environments than projected, thus preventing catastrophic vehicle failure. It is projected that, for the booster element, integral load-carrying tanks should be used to minimize system weight.

4. For the vehicle configured to deliver a 50,000-pound payload, eleven 510,000-pound-sea-level-thrust rocket engines are desirable on the booster. Two 590,000-pound-vacuum-thrust rocket engines are desirable for the orbiter. The booster and orbiter engines are basically the same with two different nozzles.

5. Existing turbojets may be used on orbiter and booster elements for cruise and go-around, but these systems would require requalification for the space environment. The use of hydrogen fuel and high T/W engines has significant benefit as discussed above.

6. O_2/H_2 was selected for the reaction control system as a desirable goal; however, considerably more study is required to identify the best system.

7. To provide low weight, flexibility, and a system with automatic checkout capability, an integrated electronic system is desirable.